6th International Conference and Postgraduate Colloquium for Environmental Research 2022 (POCER 2022) 9 - 11 June 2022
Langkawi, Kedah, Malaysia

PROCEEDINGS OF THE 6TH INTERNATIONAL CONFERENCE AND POSTGRADUATE COLLOQUIUM FOR ENVIRONMENTAL RESEARCH (POCER 2022) 9-11 JUNE 2022

"THE GREEN INDUSTRIAL REVOLUTION OF THE NEXT DECADE"

Edited by:

Angela Paul Peter, Doris Tang Ying Ying, Azalea Dyah Maysarah Satya, Foo Wei Han, Sherlyn Koay Sze Ning, Tham Pei En, Ng Yan Jer, Lim Hooi Ren, Nurul Syahirah Mat Aron, Chew Kit Wayne, Khoo Kuan Shiong, Show Pau Loke

Organiser: University of Nottingham, Malaysia

Organiser Partner:

- Xiamen University Malaysia
- UCSI University
- International Bioprocessing Society
- Human Life Advancement Foundation
- Centre of Excellence for Green Technologies

Supported by:

- Malaysia Convention & Exhibition Bureau
- Malaysia Truly Asia Campaign
- Malaysia Airlines
- Atmosphere 360
- Langkawi Development Authority (LADA)
- Advaspire Sdn. Bhd.
- Biocare
- Biolina
- Biotek Abadi Sdn. Bhd.
- CAIQ Intelligent Technology
- Donewell Resources
- Evergreen Engineering & Resources
- Global Water Consultants Sdn. Bhd.
- IChemE's Biochemical Engineering Special Interest Group
- JetPro Technology Sdn. Bhd.
- KLK OLEO
- Nanyang Global Scientific Research Center Sdn. Bhd.
- Novozymes
- Pharma Plus Pharmacy

Published by

University of Nottingham Malaysia

Jalan Broga

43500, Semenyih Selangor, Malaysia.

Proceedings of the 6th International Conference and Postgraduate Colloquium for Environmental Research (POCER 2022)

9 – 11 June 2022

Resort World Langkawi, Kedah, Malaysia

eISSN 2948-5223

9 772948 522005

Copyright © 2022 University of Nottingham Malaysia. All rights reserved. No part of this publication may be reproduced or distributed in any form or by any means, or stored in a database or retrieval system, without the prior written permission of the copyright holder. The proceedings contain information from recognized sources and reasonable efforts are made to ensure their reliability. However, the authors, editors and publisher do not assume any responsibility for the validity of all the materials or for the consequences of their use.

Organising Committee

POCER 2022 Conference

Organising Committee

Chairman	**Prof. Ir. Ts. Dr. Show Pau-Loke (University of Nottingham Malaysia)**
Co-Organising Chairs	Asst. Prof. Dr. Chew Kit Wayne (Xiamen University Malaysia) ChM. Dr. Khoo Kuan Shiong (UCSI University) Assoc. Prof. Dr. Edward Ooi Chien Wei (International Bioprocessing Society) Ts. Noor Azmi bin Mat Said (Human Life Advancement Foundation)
Programme Book	Ms. Tham Pei En
Event Managements & Logistics	Ms. Chia Wen Yi Ms. Chan Sook Sin Ms. Tham Pei En
Registration	Ms. Doris Tang Ying Ying Ms. Angela Paul Peter
IT & Media	Mr. Lim Hooi Ren Mr. Chong Jun Wei Roy Ms. Azalea Dyah Maysarah Satya Mr. Cai Yong Qiu
Design & Public Relations	Ms. Chung Shei Li Ms. Tee Wan Ting Mr. Ng Yan Jer
Finance & Sponsorship	Ms. Nurul Syahirah Mat Aron Ms. Doris Tang Ying Ying
Itinerary & Prize	Mr. Chong Jun Wei Roy Ms. Silvanir
Photographer	Mr. Aaronn Avit Ajeng
Ushers	Mr. Abdul Azim bin Azmi Mr. Vishno Vardhan Ms. Zhuang Dingling Ms. Sherlyn Koay Sze Ning Mr. Foo Wei Han Mr. Zhao Dehua

International Advisory Board

- Acd. Prof. Dr. Alvin B. Culaba (De La Salle University, Philippines)
- Prof. Dr. Akihiko Kondo (Kobe University, Japan)
- Prof. Dr. Ao Xia (Chongqing University, China)
- Prof. Dr. Aydin Berenjian (The University of Waikato, New Zealand)
- Prof. Dr. Chongqing Wang (Zhengzhou University, China)
- Prof. Dr. Dai-Viet N. Vo (Nguyen Tat Thanh University, Vietnam)
- Prof. Dr. Daniel C.W. Tsang (The Hong Kong Polytechnic University, Hong Kong)
- Prof. Dr. Eric Leroy (Université de Nantes, France)
- Prof. Dr. Fawzi Banat (Khalifa University, United Arab Emirates)
- Prof. Dr. Francesco Gentili (Swedish University of Agricultural Sciences, Sweden)
- Prof. Dr. Gopalakrishnan Kumar (University of Stavanger, Norway)
- Prof. Dr. Heli Siti Halimatul Munawaroh (Universitas Pendidikan Indonesia, Indonesia)
- Prof. Dr. Heriberto Hernández Cocoletzi (Facultad de Ingeniería Química, BUAP, Mexico)
- Prof. Dr. Ioannis Anastopoulos (Hellenic Mediterranean University, Greece)
- Prof. Dr. Jörg Rinklebe (University of Wuppertal, Germany)
- Prof. Dr. Jo-Shu Chang (Tunghai University, National Cheng Kung University, Taiwan)
- Prof. Dr. Malinee Sriariyanun (King Mongkut's University of Technology North Bangkok, Thailand)
- Prof. Dr. Masahiro Takagi (Japan Advanced Institute of Science and Technology Asahidai, Japan)
- Prof. Dr. Md. Mofijur Rahman (University of Technology Sydney, Australia)
- Prof. Dr. Mohammad Taherzadeh (University of Borås, Sweden)
- Prof. Dr. Mukesh Kumar Awasthi (Northwest A&F University, China)
- Prof. Dr. Nashiru Billa (Qatar University, Qatar)
- Prof. Dr. P. Senthil Kumar (Sri Sivasubramaniya Nadar College of Engineering, India)
- Prof. Dr. Petar Sabev Varbanov (Brno University of Technology, Czech Republic)
- Prof. Dr. Sakhon Ratchahat (Mahidol University, Thailand)
- Prof. Dr. Shih-Hsin Ho (Harbin Institute of Technology, China)
- Prof. Dr. Sivakumar Manickam (Universiti Teknologi Brunei, Brunei Darussalam)
- Prof. Dr. Sonil Nanda (York University, Canada)
- Prof. Dr. Tejraj M. Aminabhavi (KLE Technological University, India)
- Prof. Dr. Vijai Kumar Gupta (Scotland’s Rural College (SRUC), UK)
- Prof. Dr. Xiaoting Fu (Ocean University of China, Qingdao, China)
- Prof. Dr. Yang Tao (Nanjing Agricultural University, China)
- Prof. Dr. Young-Kwon Park (University of Seoul, Korea)
- Prof. Dr. Zengqiang Zhang (Northwest A&F University, China)

Local Scientific Committee

- Assoc. Prof. Dr. Derek Chan Juinn Chieh (Universiti Sains Malaysia)
- Assoc. Prof. Dr. Grrace Ng Hui Suan (Xiamen University Malaysia)
- Assoc. Prof. Dr. Joon Ching Juan (Universiti of Malaya)
- Assoc. Prof. Dr. Mohamad Faizal Bin Ibrahim (Universiti Putra Malaysia)
- Assoc. Prof. Dr. Ng Eng Poh (Universiti Sains Malaysia)
- Assoc. Prof. Dr. Nyuk Ling Ma (Universiti Malaysia Terengganu)
- Assoc. Prof. Dr. Wee Jun Ong (Xiamen University Malaysia)
- Assoc. Prof. Ir. Dr. Fang Yenn Teo (University of Nottingham Malaysia)
- Assoc. Prof. Ir. Dr. Leo Choe Peng (Universiti Sains Malaysia)
- Asst. Prof. Dr Steven Lim (Universiti Tunku Abdul Rahman)
- Asst. Prof. Dr. Ayu Haslija Binti Abu Bakar (UCSI University)
- Dr. Ang Wei Lun (Universiti Kebangsaan Malaysia)
- Dr. Chow Yin Hui (Taylor University)
- Dr. Hayyiratul Fatimah Binti Mohd. Zaid (Universiti Teknologi Petronas)
- Dr. Ho Yeek Chia (Universiti Teknologi Petronas)
- Dr. How Bing Shen (Swinburne University of Technology Sarawak Campus)
- Dr. Kua Yin Leng (Xiamen University Malaysia)
- Dr. Lam Man Kee (Universiti Teknologi Petronas)
- Dr. Lim Jun Wei (Universiti Teknologi Petronas)
- Dr. Mohd Zuhair Mohd Nor (Universiti Putra Malaysia)
- Dr. Muhammad Hazwan B. Hamzah (Universiti Putra Malaysia)
- Dr. Muhammad Mubashir (Asia Pacific University of Technology & Innovation)
- Dr. Ng Lik Yin (UCSI University)
- Dr. Zakry Fitri Ab. Aziz (Universiti Putra Malaysia Bintulu Campus)
- Dr. Zatul Iffah Bte Mohd Arshad (Universiti Malaysia Pahang)
- Prof. Dr. Lee Keat Teong (Universiti Sains Malaysia)
- Prof. Dr. Ling Tau Chuan (Universiti of Malaya)
- Prof. Dr. Luqman Chuah Bin Abdullah (Universiti Putra Malaysia)
- Prof. Dr. Meisam Tabatabaei (Universiti Malaysia Terengganu)
- Prof. Dr. Norhamidi Muhamad (Universiti Kebangsaan Malaysia)
- Prof. Dr. Rosnah Shamsudin (Universiti Putra Malaysia)
- Prof. Ir. Dr. Chin Nyuk Ling (Universiti Putra Malaysia)
- Prof. Ir. Dr. Denny K. S. Ng (Heriot-Watt University Malaysia)
- Prof. Ir. Dr. Siti Mazlina Mustapa Kamal (Universiti Putra Malaysia)
- Prof. Ir. Dr. Yus Aniza Yusof (Universiti Putra Malaysia)
- Prof. Madya Dr. Ing. Mohd Noriznan Bin Mokhtar (Universiti Putra Malaysia)
- Prof. Ts. Dr. Lam Su Shuing (Universiti Malaysia Terengganu)
- Senior Prof. Phang Siew Moi (Universiti of Malaya, UCSI University)
- Ts. ChM. Dr. Khalisanni Bin Khalid (MARDI)
- Ts. Dr. Alan Ting Huong Yong (University of Technology Sarawak)

Preface

Postgraduate Colloquium for Environmental Research (POCER) was first initiated in 2011 by the University of Nottingham Malaysia (UNM), it has since expanded to a wider pool of local and international participants. POCER aims to provide the opportunity and impact between undergraduate and postgraduate students to engage with fellow researchers locally and internationally, for the discussion of their research work-related project with a community of experts. POCER conference is held every 2 years and it has been a success since the 1st POCER, commenced in 2011. The 6th POCER was supposing held in the year of 2021. However, due to COVID-19 pandemic, the conference was delay to 2022.

In this 6th POCER 2022, the theme is "The Green Industrial Revolution of the Next Decade". The purpose of this theme is to enlighten world-class researchers and project leaders for the need in addressing issues related to Green-Industrial Revolution research. The 6th POCER will take place from 9th to 11th June 2022 at Langkawi Island here in Malaysia.

POCER 2022 is also working together with Langkawi Development Authority (LADA) for the "One Tourist, One Tree Campaign", under the 'Penanaman 100 Juta Pokok - Program Penghijauan Malaysia' campaign coordinated by The Ministry of Energy and Natural Resources (KeTSA) Malaysia in which all the participants will be planting a tree as a symbol of conservation to enhance the natural environment quality in Langkawi. This event will be held on the last day of the conference. On top of that, LADA will also be rendering its on-site support via MICE (Meeting, Incentive, Conference, Exhibition) incentives that are made available to eligible event's organiser.

Table of Contents

PCR 27122021 – 02: Achieving the necessary environmental-compatibility scale and technology to promote the green health industry.....22

PCR 07122021 – 03: Characteristic of bacterial cellulose nanocrystal as drug delivery system candidate .23

PCR 07122021 – 04: In Silico activity of collagen peptide derived from Salmon salar as Anti SARS-CoV-2 26

PCR 01012022 – 05: Carbon credits from Windrow composting of Municipal solid waste –A solution to climate change 29

PCR 13122021 – 06: Biosynthesis of Adansonia digitata leaves' Mediated TiO_2 Nanoparticles 31

PCR 25012022 – 07: Layup sequence and interfacial bonding of addictively manufactured polymeric composite.....32

PCR 13012022 – 08: Kinetic Study on Subcritical Water Pre-treatment Prior to Co-digestion of Pineapple Waste and Cow Dung 34

PCR 20012022 – 09: Exploiting Continuous Photochemical Processes for the Greener Preparation of Complex Drug-Like Entities.....37

PCR 26012022 – 10: Effects of roller speed on the structural and electrochemical properties of $LiCo_{0.6}Sr_{0.4}O_2$ cathode for intermediate temperature solid oxide fuel cell application 40

PCR 27012022 – 11: Performance analysis of PEMFC with single-channel and multi-channels on the impact of the geometrical model.....44

PCR 28022022 – 13: Performance Evaluation Of A Novel And Environment-Friendly Biodiesel-Based Drilling Fluid Using Non-Edible Vegetable Oil 52

PCR 04032022 – 14: Microalgae biorefinery concepts: Multiphase separation and extraction processes...55

PCR 08032022 – 15: Establishment of preliminary frameworks for beneficial uses of dredged materials including contaminated marine sediments in Colombia 58

PCR 08032022 – 16: Morphological Effects on Catalytic Performance of LTL Zeolites in Acylation of 2-Methylfuran Enhanced by Non-Microwave Instant Heating 65

PCR 08032022 – 17: SAPO-34 crystallized using novel pyridinium template as highly active catalyst for synthesis of ethyl levulinate biofuel 66

PCR 10032022 – 18: Biodegradable Dual-Layer Polyhydroxyalkanoate (PHA)/Polycaprolactone (PCL) Mulch Film For Agriculture: Preparation And Characterization.....69

PCR 10032022 – 19: Electrochemical evaluation of nickel oxide addition toward lanthanum strontium cobalt ferrite cathode for intermediate temperature solid oxide fuel cell (IT-SOFCs) 77

PCR 10032022 – 20: Design of microbial cell factories for sustainable production of biofuels.....80

PCR 12032022 – 21: Optimization of Screening Media for The Identification and Isolation of Waste Edible Oil-Degrading Lipolytic Microorganisms from Food Wastes.....82

PCR 12032022 – 22: Electrocoagulation Process For the Treament of Soaked Pepper Berries: Kinetic Modeling and Some Physical Properties 84

PCR 14032022 – 23: Modification and characterization of plant-based natural coagulants (PBNC) for application in drinking water treatment – A review.....87

PCR 11042022 – 24: Recycling of Spent Primary Batteries as Catalysts for VOCs Removal.....91

PCR15032022 – 26: How Effective are Consumers' Perceived Value? Using Behavioural Insightto Promote Solar Energy Adoption in Urban Households 94

PCR18032022 – 27: Kinect-Based Handedness-Invariant Badminton Movement Analysis and Recognition System.....97

PCR18032022 – 28: Vision-Based Monitoring of Microalgae Growth and Analysis of its Bioactive Compounds: A Preliminary Results.....99

PCR18032022 – 29: The Experience of Developing UTS Experimental Smart Home.....101

PCR10042022 – 30: A Generic Framework for the Evaluation of Visual Network Algorithms on Documents 104

PCR10042022 – 31: Investigating Neutral Face Reconstruction for Improving Face Identification using Nonlinear Approach.....107

PCR10042022 – 32: Phytomicrobiomes for the Sustenance of Agro-ecosystem 109

PCR18032022-33: Correlative modeling of algal biodiesel units using statistical algorithms and artificial neural networks.....110

PCR11042022 – 34: Micro Computerized Tomography: Potential Applications of Polychromatic and Monochromatic X-ray Source in Unconventional Gas Reservoirs 111

PCR18032022-35: Simultaneous capture of H_2S and CO_2 from high sour Saudi natural gas using cryogenic packed bed 114

PCR18032022-36: Multiobjective optimization, simulation, and modeling of biodiesel synthesis from used cooking using response surface methodology 115

PCR18032022-37: Modeling and Optimization of Dynamic Viscosity of Titania Nanotubes Dispersions in Ethylene Glycol/Water-Based Nanofluids using Response Surface Methodology 116

PCR19032022 – 40: Optimization of natural gas dehydration using low-temperature techniques 117

PCR20032022 – 42: Adsorption of Methylene Blue Dye onto Graphene Composite.....118

PCR22032022 – 43: A Comprehensive Review on the Production Methods and Effect of Parameters for Glycerol-Free Biodiesel Production 119

PCR22032022 – 44: Recovery of microalgae biodiesel using liquid biphasic flotation system.....122

PCR23032022 – 45: Purification of Phycocyanin by using Ionic Liquid Based Biphasic Flotation.....124

PCR13042022 – 46: An efficient method of heavy metal removal from wastewater using symbiosis of microalgae and bacterial consortium 126

PCR24032022 – 47: Cloud-based residential façade analysis system: mobile application development using machine learning algorithms 128

Tag 130

PCR26032022 – 49: Structure characterisation for Hydroxypropyl Bispalmitamide MEA and Ceramide 3 131

PCR28032022 – 50: Critical Review of the Various Reaction Mechanisms For Glycerol Etherification .132

PCR28032022 – 51: Simultaneous Extraction of Low-gluten Flour and Gum from Durian Seed for Food Applications 136

PCR28032022 – 52: Biomass waste-based mesoporous silica 140

PCR29032022 – 54: Stabilization of Protein-Fortified Pineapple Jam Using Natural Deep Eutectic Solvents (NADES).....142

PCR29032022 – 55: Intensification of Biodiesel production by hydrodynamic cavitation: A critical review 144

PCR30032022 – 58: Some Physical Properties and Relationship Between Fractions of Dabai Fruit (*Canarium Odontophyllum Miq.*) Variety '*Ngemah'*.....147

PCR01042022 – 59: Substrate-enzyme mixing characteristics in a bio-inspired reactor for saccharification 155

PCR01042022 – 60: Mixing Performance of Soft-elastic Bionic Reactor with 160

PCR01042022 – 61: Simultaneous mechanical and biological pretreatment of lignocellulose for enhancing the efficiency of enzymatic hydrolysis 165

PCR01042022 – 62: Continuous photoenzymatic decarboxylation of free fatty acids from waste oil for hydrocarbon fuels production in a microfluidic photobioreactor.....170

PCR10042022 – 63: ISOLATION AND SCREENING OF DETERGENT DEGRADING MICROBES FROM DETERGENT WASTEWATER.....175

PCR01042022 – 64: Is it necessary to adopt a two-step catalytic transesterification for producing black soldier fly larvae biodiesel? 177

PCR01042022 – 65: Characterization of Lignocellulosic Biomass and Synthesis of Low Transition Temperature Mixture (LTTM) as Green Delignification Approach.....180

PCR01042022 – 66: Effect of Different Iron Percentage in Sulphonated Activated Carbon Catalyst for Microwave-Assisted Acetylation of Glycerol.....183

PCR01042022 – 67: Co-pyrolysis of plastics and food waste mixture under flue gas condition for bio-oil production 186

PCR01042022 – 68: Role of Supercritical Fluid Extraction in Biorefinery Application: A Perspective from Malaysia.....189

PCR01042022 – 69: Parametric Study and Energy Analysis of the Progressive Freeze Concentration of Cucumber Juice.....193

PCR04042022 – 70: Comparison Study on Sunway BRT's Terminus Stations' 198

PCR01042022 – 71: Reduction of Anaerobic Pretreated Sewage Sludge via Assimilation by Black Soldier Fly Larvae for Growth 201

PCR01042022 – 72: Utilization of Lignocellulosic Solid Waste for Attached Microalgal Growth and its Lipid Accumulation in Relation to pH of Cultivation Medium 204

PCR01042022 – 73: The Effect of Temperature on Anaerobic Co-Digestion of Chicken Manure and Empty Fruit Bunch at Optimized C/N Ratio 208

PCR01042022 – 74: Overview on Potential of Biogas Generation: A Case Study of Poultry Industry in The Manjung Region 212

PCR 10032022 – 75: Characterization of Lithium Doped Calcium Oxide from Organic Waste for Biodiesel Production 216

PCR01042022 – 76: A Short Review on the Enhancement of Biogas Production from Anerobic Digestion of Animal Manure 220

PCR04042022 – 77: Development of Ridership Forecasting Model for 224

PCR04042022 – 78: Optimization of Deep Eutectic Solvent Pretreatment for Bioethanol Production from Napier Grass 227

PCR04042022 – 79: Physiochemical Properties of Choline Chloride Based Green Solvents in Water 230

PCR04042022 – 80: Improvement of Enzymatic Saccharification and Ethanol production from Organic Acid-Pretreated Coffee Shells 233

PCR04042022 – 81: Bioethanol and Biogas Production From Organic and Mineral Acid Pretreated Sugarcane Bagasse**:** Comparative and Optimization Studies 236

PCR04042022 – 82: Towards the Enhancement of Microalgae Cultivation as Biofertilizer for Sustainable Agriculture 239

PCR05042022 – 83: Investigation of nondamaging mud filtration properties in high-pressure, high-temperature conditions 242

PCR06042022 – 84: Adhesion of Bacillus consortium on Sago Starch-Oil Palm Kernel Shell Biochar as Soil Organic Amendment: Optimization and Kinetic Analysis 245

PCR06042022 – 85: The Influence of Biochar on Plant-Soil Metabolites in Shaping the Rhizosphere 247

PCR06042022 – 86: A Review on the Life Cycle Assessment of Different Advanced Wastewater Treatment Systems 250

PCR06042022 – 87: Activated carbon monoliths, from eucalyptus and patula pine biomass and their mixtures with residual tires and polystyrene, for CO_2 capture 254

PCR06042022 – 88: Evaluation of pyrolysis in CO_2 atmosphere for obtaining liquid fuel through the waste compact disc (CDs) 257

PCR07042022 – 89: Impacts of different sparger designs for micro-sized bubbles generation on mixing performances in flat panel photobioreactors to improve microalgae growth and carbon capture 260

PCR07042022 – 90: E-waste recycling using dimethylacetamide: Organic swelling mechanisms of coarse waste printed circuit boards 263

PCR07042022 – 91: Microalgal Extract as Bio-coating to Enhance Biofilm Growth of Marine Microalgae on Microporous Membranes 267

PCR07042022 – 92: Real-time biomonitoring of Spirodela polyrhiza for the detection of heavy metals via image analysis approach 268

PCR07042022 – 93: A Novel Cultivation of Giant Duckweed via Application of Superhydrophobic Coatings 272

PCR08042022 – 94: Antioxidant potential of herbal extracts from sea buckthorn seeds oil 275

PCR08042022 – 95: Research on the Intelligent System Construction of Street Landscape for Smart City 277

PCR08042022 – 96: Research on Carbon System Measurement Model of Rural Landscape Based on Emission Factor Method: A Case Study of Paifang Village 281

PCR11042022 – 98: Bio Conversion of Biomasses for Enhancing Food Security in Changing Climatic Scenario 284

PCR11042022 – 99: Technical and environmental analysis of a product produced by additive manufacturing from recycled PET 286

PCR11042022 – 100: Verifying the effect of alternative NH_3 and CO_2 production routes on 290

PCR11042022 – 101: Heavy Metal effect on seed of *C. comosum*: morphological and molecular study .. 294

PCR11042022 – 102: Estimating ammonium changes in pilot and full - scale constructed wetlands using kinetic model, linear regression and machine learning 295

PCR12042022 – 103: Utilization of Biomass Wastes as Sustainable Electrocatalyst Precursors in Metal-Air Batteries: A Review 297

PCR12042022 – 104: Comparative growth inhibitory activities of resin cyanoacrylate nanoparticles 301

PCR12042022 – 105: Screening and Benchmarking of Commercial Corrosion Inhibitors for Organic Acid Corrosion Mitigations 302

PCR12042022 – 106: Theoretical Studies of Quaternary Ammonium Surfactant Corrosion Inhibitors on FE (110) in Acetic Acid Media via DFT Calculation and MD Simulation 304

PCR13042022 – 108: Quantification of Leachate Using Material Flow Analysis and Transport of Leachate Using Water Quality Modelling 306

PCR13042022 – 110: A Short Review on Recent $NiCo_2O_4$-based Composite Materials for Fuel Cell Applications 308

PCR13042022 – 111: Effect of Cellulose Passivator on Enhancing Power Conversion Efficiency of Perovskite Solar Cell in High Humidity Condition 310

PCR13042022 – 112: Degradation of Polyethylene Microplastic by Plasma in Liquid Process 314

PCR13042022 – 113: Solar-mediated phase-changing materials: Design and innovations on solar energy conversion and storage 317

PCR13042022 – 115: Ecotoxicology of moxifloxacin on freshwater microalgae: growth, photosynthesis and antioxidant responses 320

PCR13042022 – 116: Simulation of acid gas removal unit using ternary amine mixture of MDEA, sulfolane, and AMP 321

PCR14042022 – 117: Technical and environmental evaluation of a Biogas Power Plant operating in Amazon.....324

PCR14042022 – 118: Tunable nanochannels of NiAl-LDH/SiO_2 for power generation performance by natural water evaporation.....328

PCR14042022 – 119: In-situ synthesised hydroxyapatite coated on wood powder for efficient copper(II) removal from wastewater.....329

PCR14042022 – 120: Bionanocomposite of chitosan and ZnO and its functionality in the preservation of strawberries.....332

PCR14042022 – 121: Conductivity and Crystallinity Correlation Study Of MnO2/3D-G Nanocatalyst for MAFC Application 334

PCR14042022 – 122: Synthesis of Novel Adsorbents on Commercial Activated Carbon for H_2S Adsorption Capability Using the Core Shell Technique.....336

PCR14042022 – 123: Hydrogen Production via Electrolysis Unit: Mathematical Modelling and Simulation on Parametric Towards PEM Electrolysis Performance.....338

PCR14042022 – 124: Polymer-Encapsulated Crystalline Zirconium Phosphates as NH_4^+ and K^+ Ion Exchangers for Application in Sorbent Dialysis Cartridges 339

PCR14042022 – 125: Pretreatment of secondary sludge with bacteriophage T4, T7 or λ lysozyme to increase hydrolysis efficiency and biogas production 343

PCR14042022 – 126: Mechanochemical Synthesis of Highly Crystalline Magneisum Zirconium Phosphate for Fast Sorption of Scandium.....346

PCR14042022 – 127: EFFECT OF MAGNETIC FIELD ON THE PREPARATION OF Fe-COATED CELULLOSE/PLA NANOCOMPOSITE.....348

PCR15042022 – 128: Peptides purified from jellyfish wastewater with antimicrobial activity against *Propiobacterium acnes*.....352

PCR15042022 – 129: The ammonium based ionic liquids for gas hydrate mitigation 355

PCR15042022 – 130: Synthesis and characterization of MIL-101(Cr) and ZnO@MIL-101(Cr) nanocomposites for photocatalytic degradation of phenanthrene.....356

PCR15042022 – 131: Acceleration the recalcitrant synthetic dyes biodegradation processing by modification culture conditions: A case study by *Fusarium oxysporum*.....359

PCR15042022 – 132: Identification and analysis of short peptides derived from wastewater in pre-salted jellyfish (*Lobonema smithii*) processing.....361

PCR15042022 – 133: The Reliance on Zirconate for the Production of Proton-conducting Solid Oxide Fuel Cell Electrolyte: A Short Review 364

PCR15042022 – 134: Optimum hole-depth of porous anodes for electrically active microorganisms at specific apertures 367

PCR15042022 – 137: Modelling of Oxygen Diffusion Mechanism at SOFC Cathode using AdlerLane-Steele Mathematical Method: Applied to 5% wt $SrFe_{0.9}Ti_{0.1}O_{3-\delta}$ and 5% wt SDC 369

PCR15042022 – 138: Bibliometric Analysis of Research Trends in Plant Ageing Management and Application of Industry 4.0 Technologies.....371

PCR15042022 – 139: Effects of the current collector on the microstructural and electrochemical performance of modified lithiated nickel based electrode 375

PCR15042022 – 140: A Review on Glass Fiber Reinforced Polymer Composites in Marine Water Applications.....378

PCR15042022 – 141: Effects of rice straw and gabage enzyme (GE) addition on soil and rice plant growth at early vegetative stage.....380

PCR15042022 – 142: Potential of Nata de Coco as Pectinase Immobilization Support for Guava Juice Clarification and Techno-Economic Analysis of Its Process Design 383

PCR15042022 – 143: Rice Husks as Carrier for Lipase Immobilization and Its Application in Continuous Monoacylglycerol Production Using a Packed Bed Bioreactor.....386

PCR15042022 – 144: Techo-Economic Analysis of Palm Oil Mill After Addition of Unit Procedures for 3-Monochloropropane-1,2-diol (3-MCPD) Mitigation.....389

PCR15042022 – 147: A biorefinery approach of two different Marine macroalgae *Sargassum polycystum* and *Rosenvingea intricata*: extraction and characterization of fucoxanthin, fucoidan and bioethanol.....392

PCR15042022 – 149: Gastrointestinal digestion stability and zinc absorption mechanism of casein peptide-zinc chelate 395

PCR15042022 – 150: Lichen as the Biological Indicator for Environment Tobacco Smoke (ETS) Detection in Malaysia.....398

PCR15042022 – 153: Indoor Pollutants and Its Impact on Respiratory Health Symptoms and Lung Functions among School Children Exposed to Bauxite Mining.....408

PCR15042022 – 154: Two-stage Ultrafiltration for the Separation of α-Amylase from Red Pitaya Peel..411

PCR15042022 – 155: Utilisation of palm kernel shell biochar for supplementary cementitious replacement 415

PCR15042022 – 157: From strain improvement to lutein extraction: Attempts to CO_2 Capture And Utilization by Microalgae 418

PCR15042022 – 158: Clogging detection in anaerobic co-digestion continuous system using machine learning approach.....421

PCR15042022 – 159: Reduction of polycyclic compounds and biphenyls generated by pyrolysis of polyethylene terephthalate by using supported metal catalysts 424

PCR15042022 – 160: Valorization of waste tea bags via CO_2-assisted pyrolysis.....425

PCR15042022 – 161: Thermochemical conversion of mulching film waste via pyrolysis with the 426

PCR15042022 – 162: Quarry Respirable Dust Pollutant Impact on Fractional Exhaled Nitric Oxide (FENO) and Interleukin-8 (IL-8) Concentration 427

PCR15042022 – 164: Single-Use Disposable Waste Upcycling via Thermochemical Conversion Pathway 429

PCR15042022 – 165: The assessment of the ability of urban parks to self-sustain the GHG emissions in densely populated cities through carbon sequestration.....430

PCR15042022 – 166: Dehydration of apple slices and black chokeberries by sequential drying pretreatments and ultrasound-assisted air drying: Study on mass transfer, profiles of phenolics and PPO activity 432

PCR15042022 – 167: Hydrodynamic Modelling of an Idealised Coastal Reservoir with Consideration of Algal Bloom Occurrence 435

PCR15042022 – 168: Effects of Palm Oil Ash on Hydration, Development, and Strength of Cement 438

PCR15042022 – 169: A Study on the Current Status and Issues of Integrated River Basin.....440

PCR15042022 – 170: Hydro-Environmental Modelling of Putrajaya Lake.....443

PCR21042022 – 171: Multiple Solutions For Consideration? A P-graph Model For Heat Integrated Hydrogen Regeneration Networks Generation.....446

PCR15042022 – 172: Phase Equilibrium Measurements of Acetonitrile and Benzene with EMIM-based Ionic Liquid 449

PCR15042022 – 173: Optimising Cost in Production of Green and Clean Hydrogen Systems.....452

PCR15042022 – 174: Bioelectrochemical auxiliary reactor improving the performance of horizontal anaerobic digesters.....453

PCR15042022 – 175: Potential role of catechins in Indonesian seaweed for their anticancer activity against melanoma cell line 456

PCR15042022 – 176: Environmental and economic analysis of renewable heating and cooling sources in Chongqing.....457

PCR15042022 – 177: Nuclear Trigeneration System: A Promising Sustainable Technology for Generating Simultaneous Power, Heating and Cooling Energy.....458

PCR15042022 – 178: Impact of Biomass Burning Haze on Precipitation in Malaysia.....462

PCR16042022 – 179: Improved defluoridation and energy production using dimethyl sulfoxide modified carbon cloth as bioanode in microbial desalination cell 465

PCR04052022 – 180: Thermodynamic solubility modelling evaluation for the supercritical carbon dioxide extraction of palmitic and oleic acid from papaya seed oil.....468

PCR16042022 – 181: Mathematical Optimisation of Hydrogen Supply Chain based on Cost.....470

PCR16042022 – 182: Optimal Blue Hydrogen Process with Carbon Capture, Utilisation and Storage 471

PCR16042022 – 183: Life Cycle Assessment of Organic Citrus Orchard Carbon Footprint: The Case Study of Central Taiwan 472

PCR16042022 – 184: Effects of coil density in a solenoid magnetic field microbial fuel cell 475

PCR16042022 – 185: The Effect of Non-Thermal Plasma Towards Waste Cooking Oil and Pyrolysis Oil 477

PCR17042022 – 186: SIMULATION OF EMPTY FRUIT BUNCH PELLET HEATING IN MICROWAVE REACTOR....481

PCR17042022 – 187: Solvothermal liquefaction of Kariba weed into value-added products....483

PCR17042022 – 188: Conversion of shellfish waste into high value-added products by microwave pyrolysis....484

PCR17042022 – 189: Conversion of shrimp shell waste into high value-added products by microwave pyrolysis....486

PCR17042022 – 190: Microwave-assisted chemical extraction of chitosan from shellfish wastes 487

PCR17042022 – 193: Catalytic thermal conversion of organic solid wastes to energy 488

PCR17042022 – 194: Effect of Nb_2O_5 and NiO/Nb_2O_5 catalyst on the degradation of polystyrene....490

PCR17042022 – 195: Kinetic analysis for the catalytic degradation of polyethylene terephthalate 493

PCR17042022 – 196: Selective solvent extraction and quantification of synthetic microfibers in textile laundry wastewater 496

PCR17042022 – 197: Effects of different Al_2O_3 support on HDPE thermal degradation using Ni-based catalysts....499

PCR17042022 – 198: Catalytic degradation of polypropylene over Ga loaded HZSM-5....502

PCR17042022 – 199: Effect of Nb_2O_5 on NH_4HSO_4 poisoning and thermal degradation over V_2O_5-WO_3/TiO_2 SCR Catalyst....505

PCR17042022 – 201: Recycling and characterization of carbon fibers from waste CFRP with a different amine curing agent....511

PCR17042022 – 202: Effects of hybrid stabilization methods on textural properties of HDPE-based activated carbon fibers....514

PCR17042022 – 203: Effects of electron beam irradiation on DMMP adsorption behaviors of activated carbon fibers 517

PCR17042022 – 204: Effect of oxygen-containing functional groups on elctrochemical performance of activated carbon for EDLC....520

PCR17042022 – 205: Fabrication of Ni/TiO_2 visible light responsive photocatalyst for decomposition of Oxytetracycline....523

PCR17042022 – 206: Hydrogen production from hydrocarbons by catalytic decomposition using liquid-phase plasma....527

PCR17042022 – 207: Sweat electrolyte functioning on Textile supercapacitors from PEDOT:TREN/MnO_2@$MnCO_3$ composite for wearable approach 531

PCR19042022 – 208: Actual operation of direct urea fuel cells and their role in achieving the sustainable development goals 534

PCR21042022 – 209: Glycol-based Deep Eutectic Solvent for Extractive Desulfurization of Fuel Oil....537

PCR01042022 – 210: Microfluidic synthesis of hollow microfibers for photocatalytic reduction of NOx from flue gas....538

PCR23042022 – 211: Application of LCA-WQI Approach for River Conservation....540

PCR23042022 – 212: Thermal, Physical and Acid Pretreatment Of Napier Grass For Lignin Extraction 543

PCR25042022 – 213: Energy and exergy analysis of R-134a operated large scale vapor compression refrigeration (VCR) cycle for district cooling (DC) application....546

PCR25042022 – 214: An estimation method of watershed-scale water environmental capacity supported by machine learning....549

PCR26042022 – 215: The adsorption of antibiotics by the solid particles in the aquifer by intraparticle diffusion....551

PCR27042022 - 216 : [Bmim]acetate Pretreatment of Giant Reed Triggering Yield Improvement of Biohydrogen Production via Photo-fermentation....554

PCR27042022 – 217: Effects of AM Fungi on Selenium Accumulation and Utilization Efficiency in Winter Wheat (*Triticum aestivum* L.) under Different Fertilization Time....555

PCR27042022 – 218: Enhancing Performance of a Groove-type Flat Panel Bio-reactor using Immobilized Photosynthetic Bacteria for Continuous Photo-fermentative Hydrogen Production....556

PCR27042022 – 219: Effect of Biochar Supplement on the Dynamics of Antibiotic Resistant Fungi during Pig Manure Composting....557

PCR27042022 – 220: Enhancement of anaerobic fermentation with corn straw by sludge-corn stalk mixed biochar....558

PCR27042022 – 221: Effect of Polyethylene Glycol 4000 and Ammonium Polyphosphate on Photo-fermentative Hydrogen Production of Corncob....560

PCR27042022 – 222: Determination of Physicochemical Properties of Stingless Bee (*Geniotrigona thoracica* and *Heterotrigona itama*) Honey....562

PCR27042022 – 223: Co-pyrolysis of food waste and wood bark to produce hydrogen with minimizing pollutant emissions....566

PCR29042022 – 224: Biochemical Compositions and Prediction of Chlorophyll Content in Microalgae for Potential Therapeutic Applications....568

PCR29042022 – 225: Inhibition Effect of Pure Diethylene Glycol , Glycine and their mixture on CO_2 Gas Hydrate: An Experimental Study....570

PCR29042022 – 226: Modification and innovative utilization of straw biomass....572

PCR29042022 – 227: Treatment of oily wastewater from gas condensate field by chemical demulsification approach....575

PCR30042022 – 228: Extraction and separation of lipids from municipal sewage sludge for biodiesel production: A sustainable approach....578

PCR30042022 – 229: Effect of quorum sensing molecules on bio-hydrogen production in an anaerobic CSTR 579

PCR30042022 – 230: Effect of quorum quenching in anaerobic digestion for biomethane recovery.....582

PCR30042022 – 231: Optimization of Deep Eutectic Solvent Pretreatment for Bioethanol Production from Napier Grass 584

PCR30042022 – 234: In-situ Condensation of Furans to Diesel Precursors during the Acidic Saccharification of Lignocellulose 586

PCR30042022 – 237: Enhancing the production of fermentative bioH_2 from lignocellulosic biomass through manipulated photo nanocatalysts.....589

PCR30042022 – 238: AI-autonomous ventilation control for smart indoor air quality and energy management in a subway station: Offline reinforcement learning approach.....591

PCR30042022 – 239: Interpretable Soft Sensor Development for Total Nitrogen and Total Phosphorus Concentrations Using eXplainable Deep AI Models with Hybrid Feature Selection.....594

PCR30042022 – 240: Spatial-temporal pattern analysis of long-term particulate matter distributions with land use information and an optimum sensor network placement in Mega-city urban environments.....597

PCR30042022 – 241: Development of a biowaste-driven carbon-negative multigeneration system using a circular integration approach 600

PCR30042022 – 242: An effectiveness guidance of deploying solar and wind energy alongside with microalgae-based biofuel in a nationwide scale: A case study of South Korea.....603

PCR30042022 – 243: Artificial Neural Network modeling for prediction of weight average molecular weight, number average molecular weight and the Polydispersity Index of Polycaprolactone synthesized using enzymatic polymerization 606

PCR30042022 – 244: Cultivation of Chlorella vulgaris using food waste compost as an organic nutrient source.....609

PCR30042022 – 245: Biorefinery of *Chlorella vulgaris* via Ultrasound-Assisted Three Phase Partitioning 612

PCR30042022 – 247: Semi-batch *Chlorella vulgaris* cultivation: Artificial Intelligence model for biomass growth monitoring 615

PCR30042022 – 248: Polyhedral Oligomeric Silsesquioxane as hydrophobic support for heterogenous catalysis: CO_2 hydrogenation to methanol.....618

PCR03052022 – 249: Enhancement of anaerobic fermentation with corn straw by sludge-corn stalk mixed biochar 621

PCR03052022 – 250: Structure-performance correlation of high surface area and hierarchical porous biochars as chloramphenicol adsorbents.....623

PCR03052022 – 251: Effects of biochar and biogas slurry reflux on methane production by mixed anaerobic digestion of cow dung and corn straw.....625

PCR03052022 – 252: Remediation of Cd and Zn contaminated soil by zero valent iron (Fe^0): a field trial 627

PCR03052022 – 253: The application of mineral additive in mitigating pollutant during the composting process 629

PCR03052022 – 254: Enhancing the performance of microbial fuel cells with a Fe-CN catalyst modified bioanode.....630

PCR03052022 – 255: Caproic acid production from anaerobic fermentation of organic waste – Pathways and microbial perspective 633

PCR03052022 – 256: Effect of water regime on the emission of free ammonia during high solid anaerobic digestion of pig manure 634

PCR03052022 – 257: Interfacing Biosyntheic CdS with Engineered *Rhodopseudomonas palustris* for Efficient Visible Light-Driven CO_2-CH_4 Conversion 635

PCR10052022 – 258: Waste biorefinery for renewable energy and valuable bioproducts production 637

PCR11052022 – 259: Resource recovery and biorefinery potential of apple orchard waste in the circular bioeconomy.....639

PCR14052022 – 260: Graphene Oxide-based Dendritic Thin Film Nanocomposite Membrane for Improved Flux and Antifouling Properties 640

PCR16052022 – 261: Novel Carbon Aerogel from Pineapple Leaf-based Microfibrillated Cellulose for Removal of Oil and Organic Solvent.....643

PCR17052022 – 262: Al-impregnated biochar derived from Korean pine residue and Alum sludge for phosphorus removal.....646

PCR17052022 – 263: Evalution of Waste Oxy-fuel Combustion with Indirect Supercritical Carbon Dioxide Cycle 649

PCR18052022 – 264: Evaluation of gut microbiome community in Jeju-Black Swine under the effect of *Rhodobacter sphaeroides using* longitudinal dynamics 652

PCR20052022 – 265: Binding Sites Interaction between MOF and Ionic Liquids from Molecular Docking Simulation.....654

PCR22052022 – 266: Bioremediation Potential of *Chlorella Vulgaris* in the treatment of Restaurant Wastewater: An approach contributing towards Green Circular Bioeconomy.....657

PCR26052022 – 267: Hydrogen-Rich Gas Production from Steam Reforming of Ethanol over Ni-Based Catalysts: Effect of Re Addition.....661

PCR30052022 – 268: Response Surface Methodology and Docking Simulation for Optimization of MCPA Removal onto MIL-101(Cr) Metal-organic Framework.....669

PCR31052022 – 269: Structural, Electrical and Magnetic Properties in $Pr_{0.67}Ba_{0.33}MnO_3$.....672

PCR31052022 – 270: Structural, Optical and Electronic Studies of Sr_2NiTeO_6 and Sr_2ZnTeO_6 Double Perovskite by Experimental and First-Principle DFT–LDA+U Calculation 673

PCR31052022 – 271: Investigating the magnetic structures of LiM1-xZnxPO4 (M= Fe, Mn) cathode materials for lithium-ion batteries by neutron powder diffraction Preparation.....675

PCR31052022 – 272: Synthesis and Study on the Effect of Ca^{2+} Doping on the Structural, Optical and Dielectric Properties of Tungstate Based Double Perovskite 677

PCR31052022 – 273: Influence of Ag Substitution on Electrical Properties of $NdMnO_3$ 678

PCR 27122021 – 02: Achieving the necessary environmental-compatibility scale and technology to promote the green health industry

Sami Sarabadani[a*]

- Corresponding Author E-mail: sami@trumk7.co.nz

Extended Abstract

In TRU MK7TM, we care deeply about the environment and so strive constantly not only to improve human health in compliance with local rules and regulations but also to minimise our global carbon footprint. Studies has shown that the TRU MK7TM nutraceutical complex improves the viability of chondrocyte cells through acting as a mineralisation inhibitor and increases the expression of MGP to support joint health. Moreover, TRU MK7TM is proud to design and create a novel dietary supplement system that is inclusive, efficient, and sustainable. TRU MK7TM has simply transformed the current dietary production methods through microbial fermentation during which microorganisms transform one type of product to another. Microbial fermentation has been used for many years to produce ingredients such as enzymes, vaccines, and drugs in the biopharma industry. This biotechnology is now being applied to enable the creation of animal-free products to preserve our natural resources worldwide and produce a new generation of supplements with functional ingredients. It is critical to drive innovation and investment towards achieving the necessary environmental-compatibility scale and technology to promote the green health industry.

6th International Conference and Postgraduate Colloquium for Environmental Research 2022 (POCER 2022) 9 - 11 June 2022
Langkawi, Kedah, Malaysia

PCR 07122021 – 03: Characteristic of bacterial cellulose nanocrystal as drug delivery system candidate

Heli Siti Halimatul Munawaroh[a*], Budiman Anwar[a], Galuh Yuliani[a], Gun Gun Gumilar[a], Intan Cahaya Murni[a], Larasati Martha[b], Nur Akmalia Hidayati[c], Apurav Krishna Koyand[d], Pau-Loke Show[d]

[a]Study Program of Chemistry, Universitas Pendidikan Indonesia, Indonesia.
[b]Department of Clinical Laboratory Medicine, Gunma University, Japan.
[c]Department of Chemistry, Institut Teknologi Bandung, Indonesia.
[d]Department of Chemical and Environmental Engineering, University of Nottingham Malaysia, Malaysia.

- Corrensponsing Author E-mail: heli@upi.edu

Keywords: Bacterial cellulose; BCNC; Nanocellulose; pineapple waste valorization; drug delivery system.

Extended Abstract

A large amount of pineapple waste is annually disposed of, and by utilizing it into useful materials the concept of sustainable development can also be implemented. Pineapple peel waste contains sugar which is useful as a medium for Bacterial cellulose (BC) biosynthesis by gram-negative bacteria, such as *Gluconacetobacter xylinus* [1] to gram positive bacteria, such as *Sarcina ventriculi* [2]. Transformation of BC into cellulose nanocrystals (CNCs) through hydrolysis with strong acids was carried out to gain nanocellulose (BCNC) with nanoscale dimension. This structure possesses great compaction properties, such as high degree polymerization, high crystallinity, high loading and holding-capacity, high mechanical stability, non-toxic, biodegradable, and biocompatible [3] which fulfil the criteria for consideration as drug delivery systems. The negative charge and large surface area of CNC enable binding to the drug molecule, improving the loading efficiency [4]. In the present study, GTA was used to reinforced the polymer networking of BCNC in order to improve its mechanical properties, swelling ratio, and release behavior. This study also systematically investigated, for the first time, the applicability of BCNC as drug delivery system for phycocyanin as model drug for the treatment of type-2 diabetic mellitus.

Production of BC was performed according to a previous study [1] Isolation of BCNC includes the processes of sulfuric acid hydrolysis, centrifugation, dialysis and sonication. The optimum conditions, according to a previous study [1]. Synthesis of cross-linked BCNC with GTA was performed using a previous method [5]. Characteristics of BCNC-GTA, BCNC, and BC were evaluated

by using SEM and TEM, Fourier Transform Infrared (FTIR), XRD analysis, and thermogravimetric analysis [6]. Drug loading efficiency and drug release profiles of the BCNC-GTA were evaluated by referring to previous method [7].

The XRD patterns of BC and BCNC were shown in **Figure 1**. The XRD peaks of BC and BCNC at around 2θ = 22.6° showed sharper peaks for BCNC compared to BC. The sharper diffraction peak indicates the higher degree of crystallinity of BCNC compared to BC [8]. The FTIR spectrum in **Figure 1b** showed that the spectrum of BCNC is similar to BC, suggesting that the hydrolysis process did not significantly affect the chemical composition. There was a slight shift found at the peaks around 2900 cm^{-1} and 1430 cm^{-1} which indicates that the two substances have different crystallinities [6]. Glutaraldehyde was used as a crosslinking agent for chemical crosslinking of cellulose chains. The FTIR spectra of BCNC-GTA was shown in **Figure 1c**, where the intensity of the absorption peak at around 1647 cm^{-1} was increased compared to BCNC, respectively, indicated that the cellulose chains successfully cross-linked with glutaraldehyde.

The swelling ratio analysis shown that where the rate of expansion and water absorption in BC were very low, whereas the highest rate of 2% was shown in BCNC-GTA. Swelling and water absorption rate were increased to 81.87% and 66.40, mainly due to the fact that the surface of BCNC contains plenty of hydrophilic groups -OH which causes high hydrophilicity. The results demonstrated that the cellulose as drug delivery of C-PC extract can prevent from gastric fluid that can make C-PC extract released on the target.

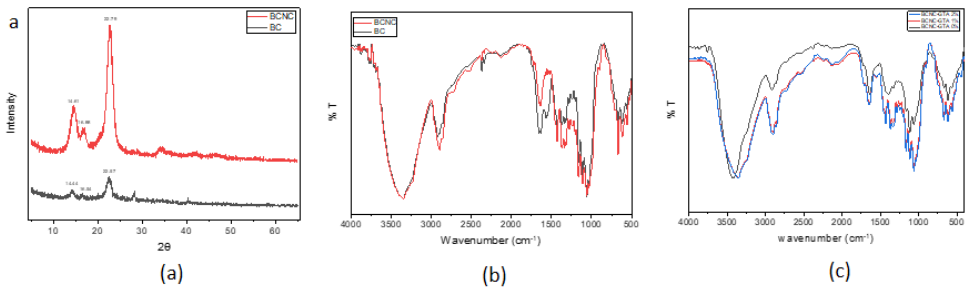

Figure 1. a) XRD Pattern Spectrum of Bacterial Cellulose (black) and Bacterial Cellulose Nanocrystals (red); b) BC and BCNC; c) BCNC at various concentration of GTA

The present work is to explore the potential of crosslinked BCNC as a candidate for DDS Phycocyanin. The BCNC has a needle-like structure, with an average diameter and length of 25±10 nm and 626±172, respectively, and an average aspect ratio (L/D) of 25±1. The BCNC has a crystallinity index of 87.8%. The The optimum adsorption of phycocyanin has reach on crosslinked BCNC at 65.3% in 3 h. Release study show that the crosslinked BCNC as drug delivery of phycocyanins can prevent from gastric fluid that can make phycocyanins released on the target.

Acknowledgements: The authors thank the Ministry Ministry of Research and Technology/National Research and Innovation Agency through the University Basic Research scheme (PDUPT) for the fiscal year of 2021 (Contract Number: 10/E1/KP.PTNBH/2021 and 280/UN.40.LP/ PT.01.03/2021) and Universitas Pendidikan Indonesia.

References

1. Anwar, B.; Bundjali, B.; Arcana, I.M. Isolation of Cellulose Nanocrystals from Bacterial Cellulose Produced from Pineapple Peel Waste Juice as Culture Medium. *Procedia Chem.* **2015**, *16*, 279–284, doi:10.1016/j.proche.2015.12.051.
2. Lin, S.P.; Loira Calvar, I.; Catchmark, J.M.; Liu, J.R.; Demirci, A.; Cheng, K.C. Biosynthesis, production and applications of bacterial cellulose. *Cellulose* **2013**, *20*, 2191–2219, doi:10.1007/s10570-013-9994-3.
3. Tomé, L.C.; Brandão, L.; Mendes, A.M.; Silvestre, A.J.D.; Neto, C.P.; Gandini, A.; Freire, C.S.R.; Marrucho, I.M. Preparation and characterization of bacterial cellulose membranes with tailored surface and barrier properties. *Cellulose* **2010**, *17*, 1203–1211, doi:10.1007/s10570-010-9457-z.
4. Thomas, D.; Latha, M.S.; Thomas, K.K. Synthesis and in vitro evaluation of alginate-cellulose nanocrystal hybrid nanoparticles for the controlled oral delivery of rifampicin. *J. Drug Deliv. Sci. Technol.* **2018**, *46*, 392–399, doi:10.1016/j.jddst.2018.06.004.
5. Yang, L.; Yang, Q.; Lu, D.N. Effect of chemical crosslinking degree on mechanical properties of bacterial cellulose/poly(vinyl alcohol) composite membranes. *Monatshefte fur Chemie* **2014**, *145*, 91–95, doi:10.1007/s00706-013-0968-9.
6. Anwar, B.; Bundjali, B.; Sunarya, Y.; Arcana, I.M. Properties of Bacterial Cellulose and Its Nanocrystalline Obtained from Pineapple Peel Waste Juice. *Fibers Polym.* **2021**, *22*, 1228–1236, doi:10.1007/s12221-021-0765-8.
7. Wang, Y.P.; Liang, Y.; Chen, J.C.; Yan, X.D.; Li, C.L.; Wang, X.P. Utilisation of potato leaves and organophilic montmorillonite for the preparation of superabsorbent composite under microwave irradiation. *Polym. Polym. Compos.* **2009**, *17*, 423–430, doi:10.1177/096739110901700704.
8. Wijaya, C.J.; Saputra, S.N.; Soetaredjo, F.E.; Putro, J.N.; Lin, C.X.; Kurniawan, A.; Ju, Y.; Ismadji, S. Cellulose nanocrystals from passion fruit peels waste as antibiotic drug carrier. *Carbohydr. Polym.* **2017**, doi:10.1016/j.carbpol.2017.08.004.

PCR 07122021 – 04: In Silico activity of collagen peptide derived from Salmon salar as Anti SARS-CoV-2

Heli Siti Halimatul Munawaroh[a*], Gun Gun Gumilar[a], Anisa Nurjanah[a], Siti Aisyah[a], Andriati Ningrum[b], Eko Susanto[c], Larasati Martha[d], Nur Akmalia Hidayati[e], Apurav Krishna Koyand[f], Pau-Loke Show[f]

[a] Study Program of Chemistry, Universitas Pendidikan Indonesia, Indonesia.
[b] Department of Food Science and Agricultural Product Technology, Faculty of Agricultural Technology, Gadjah Mada University, Indonesia.
[c] Faculty of Fisheries and Marine Science, Universitas Dipenogoro, Indonesia.
[d] Department of Clinical Laboratory Medicine, Gunma University, Japan.
[e] Badan Riset dan Inovasi Nasional RI, Indonesia.
[f] Department of Chemical and Environmental Engineering, University of Nottingham Malaysia, Malaysia.

- Corrensponsing Author E-mail: heli@upi.edu

Keywords: hydrolysate collagen; peptide-based antivirals; SARS-CoV-2; Mpro; RBD.

Extended Abstract

Peptide are natural compound which can be obtained from both enzymatic hydrolysis in the digestive system, and fermentation process by microorganisms (Jakubczyk *et al.*, 2020). One of the most common sources of peptide is collagen, which is the main structural of white connective tissue. Utilization of collagen derived from marine fish can be a promising alternative. Recent study reporting, there are about 25 types of collagens that have been identified, namely type I to XXV (Olsen *et al.*, 2003). The most commonly identified types of collagens in fish are type I and type V. Type I collagen can be found in the fish skin, bones, and scale, while type V collagen is found in connective tissue in the fish skin, tendons, and the muscle of the fish which also contains type I collagen (Nagai and Suzuki, 2000). In This study, we employed an *in-silico* method to stimulate collagen degradation by gastrointestinal enzymes and produced a large number of active peptides. Then, the binding abilities of these active peptides to SARS-CoV-2 Mpro and RBD were evaluated.

The result for the *in silico* hydrolysis of collagen hydrolysate from *Salmon salar* using three gastrointestinal enzymes (pepsin, trypsin, and chymotrypsin) giving the TDH value in range 6%-60%; the majority of hydrolysates were amino acids and oligopeptides ($2 \leq$ peptide length ≤ 6), and a few were polypeptides (peptides length > 6). *In silico* hydrolysis produced 31 fragments length 3-6 amino acids or 31.96% from type I collagen and 162 fragments or 33.89% from type V collagen. The binding affinity of salmon type I and type V collagen against SARS-CoV-2 Mpro and RBD is shown in Figure 1. Hydrolysate GTQGIR (Gly-Thr-Gln-Gly-Ile-Arg) and AWPEK (Ala-Trp-Pro-Glu-lys) derived from type V collagen show highest binding affinity toward Mpro and RBD with free energy of -167,677 *kcal/mole* and -158,621 *kcal/mole*, respectively.

Hydrolysate derived from type I and type V collagen showed high affinity against SARS-CoV-2 Mpro. Molecular interaction between Mpro and hydrolysate involved hydrogen bonds and hydrophobic interactions with moderate strength. Hydrogen bonding is one of the most important non-covalent interactions where the interaction occurs when a hydrogen atom is covalently bonded to an electronegative atom, such as oxygen or nitrogen (acceptor) (Cardoso *et al.*, 2014). The presence of hydrogen bonds and hydrophobic interactions shows the stability of the complexes formed between peptide and protein. Hydrogen bond is one of the most important interactions between molecules, where the three-dimensional structure of proteins and nucleic acids is stabilized by hydrogen bonds (Basak *et al.*, 2021). Hydrolysate derived from type I and type V collagen *Salmon salar* showed moderate strength hydrogen bonding towards SARS-CoV-2 Mpro. Enzymes have evolved to perform reaction in aqueous solutions and thus require water to maintain their native conformation (Chong *et al.*, 2019), the presence of hydrogen bonds between the hydrolysate and SARS-CoV-2 main protease is likely to distort conformation, causing enzyme instability and consequent poor performance.

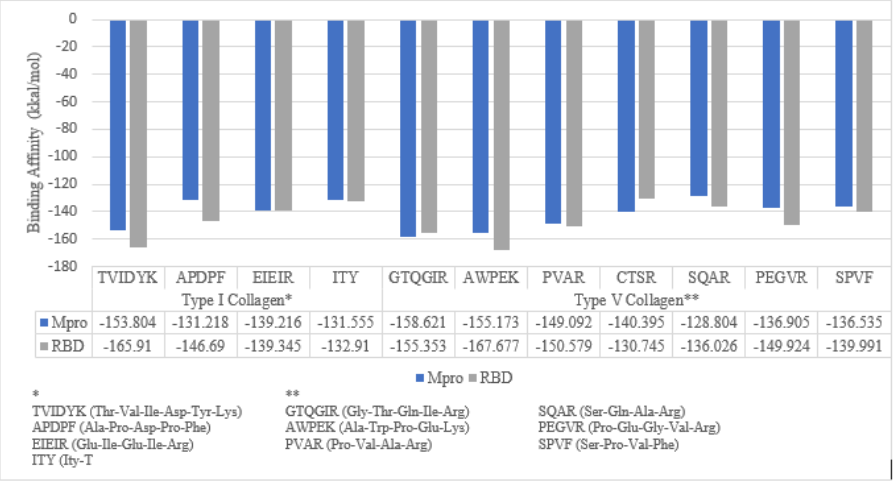

Figure 1. Binding affinity of hydrolysate collagen type I and type V Salmon salar against SARS-CoV-2 Mpro and RBD

Toxicity and allergenicity test showed that all active hydrolysates are non-toxic and non-allergenic. The sensory evaluation resulted in 27.3% short peptides which has a bitter taste. In conclusion, our results demonstrated that collagen hydrolysates derived from salmon have potential as anti-SARS-CoV-2 candidate.

Acknowledgements: The authors would like to thanks Universitas Pendidikan Indonesia for providing a research fund through Indonesian Research Collaboration Program (PPKI) for fiscal year of 2021 (No.: 163/UN40.D/PT.01.03/2021).

References

Basak, T. *et al.* (2021) "Hydrogen bond mediated intermolecular magnetic coupling in mononuclear high spin iron(iii) Schiff base complexes: synthesis, structure and magnetic study with theoretical insight," *RSC Advances*, 11(6), pp. 3315–3323. doi:10.1039/d0ra09425k.

Cardoso, V.S. *et al.* (2014) "Collagen-based silver nanoparticles for biological applications : synthesis and characterization," pp. 1–9. doi:10.1186/s12951-014-0036-6.

Chong, S.L. *et al.* (2019) "Immobilization of bacterial feruloyl esterase on mesoporous silica particles and enhancement of synthetic activity by hydrophobic-modified surface," *Bioresource Technology*, 293, p. 122009. doi:10.1016/j.biortech.2019.122009.

Jakubczyk, A. *et al.* (2020) "Current trends of bioactive peptides - New sources and therapeutic effect," *Foods*, 9(7). doi:10.3390/foods9070846.

Nagai, T. and Suzuki, N. (2000) "Isolation of collagen from fish waste material - Skin, bone and fins," *Food Chemistry*, 68(3), pp. 277–281. doi:10.1016/S0308-8146(99)00188-0.

Olsen, D. *et al.* (2003) "Recombinant collagen and gelatin for drug delivery," *Advanced Drug Delivery Reviews*, 55(12), pp. 1547–1567. doi:10.1016/j.addr.2003.08.008.

PCR 01012022 – 05: Carbon credits from Windrow composting of Municipal solid waste –A solution to climate change

Vishal Sharma [a]

[a] Department of Botany, Post Graduate Government College for Girls,
Sector-11,Chandigarh (India)

Extended Abstract

In the present era, the accumulation of solid waste was the main global environmental challenge in cities with high population density. The paradigm of 'waste to energy, mitigation of carbon and its sequestration is relegated to a secondary level which conversely results in India discarding 68.8 million tonnes, which would increase to 300 million tons by the year 2047,however, only 19.36 was treated and rest 80.64% of municipal solid waste were used for unscientific land filling ,hence India comes third after China and US in total GHGs emission.The objective of the present study was to discuss the adept schemes for successful co-composting of green waste and kitchen waste (food & fruit waste),its designing aspects, composting area sizing, capital and operational cost, to develop prototype of composting facility to achieve zero waste sustainable future.In this direction the windrow composting plant of 0.5 TPD capacity was established at campus premises to evaluate the physico-chemical parameters(temperature, moisture content, pH, electrical conductivity and C/N ratio) of municipal solid waste to produce safe, stabilized and nutrient enriched soil conditioner, which minimize the negative environmental impact of traditional underground pit composting. The micro positive pressures windrows makes the piles aerobic and organoleptic, which resulted in carbon dioxide avoidance and sequestration, preventing 346.7 million tons of carbon dioxide emissions, generating 346 carbon credits and 564 quintals organic compost which results in eco-restoration and micro-climatic moderation. The present study agrees that carbon footprint of landfilling organic waste is higher relative to windrow composting by factor 8.3 .The objective of present study was to produce compatible compost in 110 days in TSC, an operational modifications of single stage composting (SSC),a prototype of composting facility to achieve sustainable zero waste future. Presently, a pilot-scale investigation is the pioneer attempt to study the both technologies; single windrow composting and two stage(mechanical-manual) composting strategy to produce bio-stable, organoleptic and compatible evaluating the physicochemical parameters (temperature, moisture content, pH, electrical conductivity, C:N ratio).The two treatment has the same mixture of materials:50% green waste (60% leaves, 35% grass clippings and 5% tree

branches) 25% food waste and 25% fruit and vegetable waste of total 300 per day including scalability at 2 more institutes.

In this direction, the present project aimed in using windrow composting to manage their solid waste generated. The main objective/aim of the present project is the monitoring of the windrow composting plant through the evaluation of the important parameters are temperature, moisture content, pH and C/N ratio:

(i) Temperature: Temperature is the most important parameter that controls microbial activity during the windrow composting process. The temperature change is directly dependent on the biological activities of micro-organisms.

(ii) Moisture content: The moisture content of the mixed waste at the beginning of the process is measure and in the subsequent weeks .The moisture content in windrow to be maintained optimum, as the reduction in the moisture i.e the lower moisture content, reduces the growth of micro-organisms, thus the biological process slows down, however, the higher moisture content, hampered oxygen movement, resulting in anaerobic conditions and an unpleasant smell.

(iii) pH and Electrical conductivity(EC):The pH and EC measurements to be done at regular intervals for the composting time for effective management of the compost conversion in single stage composting and two stage composting(TSC).

(iv) Carbon to nitrogen ratio (C/N): C: N is an important parameter in defining the maturity of the compost, the C:N ratio is done with the optimization of the amount of dry, wet layers

6th International Conference and
Postgraduate Colloquium for
Environmental Research 2022 (POCER
2022) 9 - 11 June 2022
Langkawi, Kedah, Malaysia

PCR 13122021 – 06: Biosynthesis of Adansonia digitata leaves' Mediated TiO_2 Nanoparticles

A. Fall[a,b,c], Elsayed Ahmed Mohamed Hamza[a,b], J. Sackey[a,b], B.D. Ngom[a,b,c], Malik Maaza[a,b]

[a]UNESCO-UNISA Africa Chair in Nanosciences-Nanotechnology, College of Graduate Studies, Muckleneuk Ridge, PO Box 392, Pretoria, South Africa

[b]Nanosciences African Network (NANOAFNET), iThemba LABS-National Research Foundation, 1 Old Faure Road, Somerset West, Western Cape 7129, PO Box 722, South Africa

[c]Quantum Photonics, Energy and Nano-Fabrication Laboratory, Faculty of Sciences and Technics, University Cheikh Anta Diop of Dakar (UCAD) B.P. 5005 Dakar-Fann Dakar, Senegal

•Adama Fall: fallmokhtada@gmail.com

Keywords: Photocatalytic Activity; Biosynthesis; Titanium Dioxide Nanoparticles; Adansonia Digitata; Leaves Extract

Abstract

High purity Titanium dioxide TiO_2 nanoparticles are bio-synthesized for the first time via a natural extract of the African indigenous *Adansonia digitata* leaves. The nanoparticles are thermally oxidized in the air for 2 hours at annealing temperatures of 700, 800, and 900°C. Subsequently, the nanoparticles are characterized for their functional group's identification, morphological and optical properties. The XRD patterns showed well-defined peaks of anatase and rutile phases, while the FTIR revealed peaks at 498 and 753 cm-1 assigned to vibrational modes of the Ti-O and the Ti-O-Ti groups respectively. TEM analysis revealed spherical shape nanoparticles with averaged grain sizes estimated as 3.94, 29.15, and 45.4 nm for TiO_2_700, TiO_2_800, and TiO_2_900°C respectively. Furthermore, the *Adansonia digitata* leaves assisted TiO2 nanoparticles showed an excellent photodegradation ability of 92 % towards methylene blue dye within120 minutes.

PCR 25012022 – 07: Layup sequence and interfacial bonding of addictively manufactured polymeric composite

Nabilah Afiqah Mohd Radzuan[a] , Abu Bakar Sulong[a] , Norhamidi Muhamad[a]

a Department of Mechanical and Manufacturing, Faculty Engineering and Built Environment, Universiti Kebangsaan Malaysia, 43600 Bangi, Selangor, Malaysia

Corrensponsing Author E-mail: afiqah@ukm.edu.my

Keywords: fused deposition modelling, polymer composite, mechanical properties, interfacial bonding

Extended Abstract

Additively manufactured polymeric composites exhibit customized properties beyond those offered by conventionally fabricated ones. However, in many cases, the mechanical performance mainly depends on the processing parameters, tools, and material selection. Yet, one of the issues on additive manufacturing process especially in the material extrusion process is the inability to control the printing layups hence, causing interlaminar damage. Thus far, literature and research have focused on improving the mechanical performance of such polymeric composites by focusing on the interlaminar shear strength under a transverse load transfer. Polymeric composites prepared using material extrusion technique namely fused deposition modelling are discussed upon its layup sequence, and orientation. This paper proposes that, by realizing a homogenous distribution of the transverse load, the orientation and the printing direction can maximize the printed load bearing. Moreover, the layup sequence and the interlayer diffusion are key for controlling the mechanical properties of polymeric composites. This brief review presents a comprehensive elucidation of polymeric composites manufactured using fused deposition modelling that interpreter the needs of having greater load bearing in each layup printing sequence of polymeric composites. In such, by able to control the layup sequence one can control the mechanical performance based on specific functionality.

Four-dimensional printing

Based on the importance of oriented and aligned structures by printing in additive manufacturing, fourdimensional (4D) printing must be considered to ensure best desired output. Until now, studies have focused on 4D printing because of its ability to control the magnitude of and dynamically vary each input (169–171). However, 4D printing is frequently associated with swelling dynamics, as elucidated in composites 4D printed using a morphing nozzle. This phenomenon, in turn, promotes a minimum proportion of oriented fibres as the filaments shift from anisotropic to isotropic swelling properties ($p < 0.001$) (169,172). These fundamental modifications occur in 4D printing as the swelling effect alters the filler arrangement without reorientation as well as minimises the effect of misalignment (173,174). Hence, this allows better control and manipulation of the printing shapes and customization of the functionalities of the end product (53,174). Although 4D printing is currently a future direction, the manipulation of the fibres in

the printing process has received attention in terms of its void formation, poor adhesion, method and parameter application, blockage issues, and material selection (53,169– 171,174). Clearly, detailed findings and progressive research are required to fully fill the gap related to 4D printing.

Acknowledgements: The authors wish to express their gratitude and appreciation for the Ministry of Higher Education (MOHE) Malaysia and the Center for Research and Instrumentation Management (CRIM), UKM for their financial support under Grant Number FRGS/1/2020/TK0/UKM/02/18, which enabled them to complete this study

References

Armstrong CD, Todd N, Alsharhan AT, Bigio DI, Sochol RD. A 3D Printed Morphing Nozzle to Control Fiber Orientation during Composite Additive Manufacturing. Adv Mater Technol. 2021;6(1):1–10.

Daminabo SC, Goel S, Grammatikos SA, Nezhad HY, Thakur VK. Fused deposition modeling-based additive manufacturing (3D printing): techniques for polymer material systems. Mater Today Chem. 2020;16(January):100248.

Agarwala S, Goh GL, Goh GD, Dikshit V, Yeong WY. 3D and 4D printing of polymer/CNTs-based conductive composites. In: 3D and 4D Printing of Polymer Nanocomposite Materials. Elsevier; 2020. p. 297–324.

Joshi A, Goh JK, Goh KEJ. Polymer-based conductive composites for 3D and 4D printing of electrical circuits. 3D and 4D Printing of Polymer Nanocomposite Materials: Processes, Applications, and Challenges. Elsevier Inc.; 2019. 45–83 p.

Burela RG, Kamineni JN, Harursampath D. Multifunctional polymer composites for 3D and 4D printing. In: 3D and 4D Printing of Polymer Nanocomposite Materials. Elsevier; 2020. p. 231–57.

González-Henríquez CM, Sarabia-Vallejos MA, Rodriguez-Hernandez J. Polymers for additive manufacturing and 4D-printing: Materials, methodologies, and biomedical applications. Prog Polym Sci. 2019;94:57–116.

6th International Conference and Postgraduate Colloquium for Environmental Research 2022 (POCER 2022) 9 - 11 June 2022
Langkawi, Kedah, Malaysia

PCR 13012022 – 08: Kinetic Study on Subcritical Water Pre-treatment Prior to Co-digestion of Pineapple Waste and Cow Dung

Aili Hamzah, A. F.[a], Hamzah, M. H. [a, b*], Mazlan, N. I.[a], Che Man, H. [a, b], Jamali, N.S.[c], Siajam, S. I. [c], Show, P.L.[d]

[a] Department of Biological and Agricultural Engineering, Faculty of Engineering, Universiti Putra Malaysia, Serdang, Selangor, Malaysia

[b] Smart Farming Technology Research Centre, Faculty of Engineering, Universiti Putra Malaysia, Serdang, Selangor, Malaysia

[c]Department of Chemical and Environmental Engineering, Faculty of Engineering, Universiti Putra Malaysia, Serdang, Selangor, Malaysia

[d]Department of Chemical and Environmental Engineering, Faculty of Science and Engineering, University of Nottingham Malaysia, Semenyih, Malaysia.

- Corresponding Author E-mail: hazwanhamzah@upm.edu.my

Keywords: Biogas; Co-digestion; Gompertz; Pineapple waste: Pre-treatment; Subcritical Water

Extended Abstract

Anaerobic co-digestion of pineapple waste with cow dung appears to be an effective method for biogas production. Still, the lignocellulosic structure of pineapple waste due to linkage between cellulose, lignin and hemicellulose is one of the major difficulties to achieving high biogas production. In this study, pineapple waste was pre-treated with subcritical water (SCW) pre-treatment to enhance the biogas production before co-digestion with cow dung. The pre-treatment was conducted in two temperature modes (120ºC and 200ºC). The highest biogas production was observed at combination pre-treatment of 120ºC for 5 minutes at the water to solid ratio of 10 with 32% improvement compared to untreated. However, pre-treatment at 200ºC for 25 minutes at 5:1 water to solid ratio reduced the biogas production by 9%. Moreover, kinetic study of anaerobic co-digestion of pre-treated pineapple waste and cow dung using the modified Gompertz model showed that the pre-treatment had improved the lag phase, and the highest biogas production rate was observed at 14.41 mL/day. The compositional analysis found that the pre-treated pineapple waste reduced lignin, hemicellulose, and cellulose contents. Compared to untreated pineapple waste, the co-digestion of pre-treated pineapple waste improved the process stability in terms of total ammonia nitrogen, VS removal, and pH. Subcritical water pre-

treatment, especially at higher temperatures and prolonged, did not improve anaerobic digestion, thereby not recommended.

Result and Discussion

The cumulative biogas production data were kinetically analyzed by modified Gompertz model Equation 1 to obtain a better understanding of the process of the SCW pre-treatment.

$$B = B_0 \exp\left\{-\exp\left[\frac{\mu.e}{B_0}(\lambda - t) + 1\right]\right\} \quad (1)$$

where B is the cumulative biogas production, e is exp (1), μ is the maximum biogas production rate, B_0 is the maximum biogas production, λ is the lag phase time and e is a Euler's function.

Table 1: List of SCW pre-treatment conducted prior to anaaerobic co-digestion

Run	**1**	**2**	**3**	**4**	**5**	**6**	**7**	**8**
Temperature	120	120	120	120	200	200	200	200
Water to solid ratio	10	10	5	5	10	10	5	5
Time	5	25	5	25	5	25	5	25

The SCW pre-treatment was conducted based on **Table 1**. According to **Figure 1 (a)** the cumulative biogas production for the pre-treated pineapple waste at 120ºC for 5 minutes was higher than untreated with 32% improvement. Previously, biogas production of SCW pre-treated rice straw, Napier grass, municipal solid waste, and rice straw reported an increase of 9.2% (Chandra et al., 2012), 32% (Dasgupta and Chandel, 2019) and 3% (Wang et al. 2018), respectively. Kim et al. (2015) reported that cumulative biogas production was increased due to the enhancement of anaerobic biodegradability by subcritical water pre-treatment resulting from the disintegration of substrates due to pre-treatment.

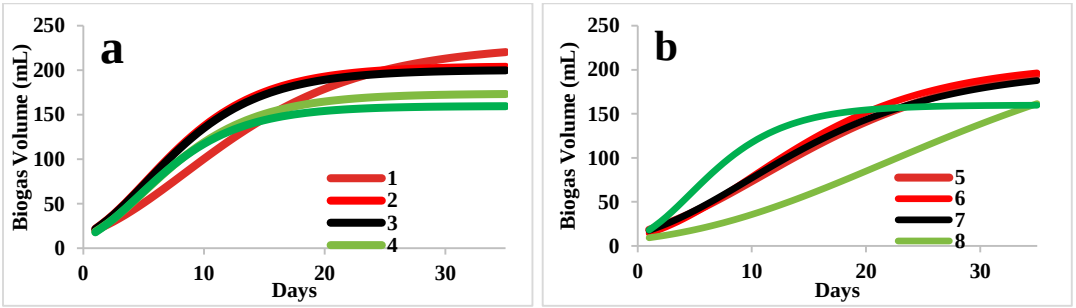

Figure 1: Cumulative biogas production based on Gompertz Model Equation at (a) 120ºC (b) 200ºC

According to **Table 2**, the maximum biogas production rate (μ) reduced from 12.77 to 5.464 mL/day after pre-treatment at high temperature was applied. The R^2 values of pre-treated pineapple waste with cow dung also higher in comparison with untreated materials. Thus, the pre-treated pineapple waste prior to the co-digestion with cow dung showed good feasibility and reliability between the experimental results and model prediction.

Table 2: Modified Gompertz on SCW pre-treated pineapple waste at high temperature mode

Run	5	6	7	8	Untreated
Experimental Biogas (mL)	199	194	189	155	171
Predicted Biogas (mL)	194.430	196.300	187.701	161.373	159.56
μ (mL/d)	7.330	8.592	7.696	5.464	12.77
B_0 (mL)	216.822	208.314	201.737	257.827	159.78
R^2	0.9878	0.9980	0.9928	0.9816	0.9619
Deviation (%)	2.35	-1.17	0.69	-3.95	7.17

Acknowledgements: This study was supported by the *Geran Inisiatif Putra Berkumpulan* (Ref. No: GP-IPB/2020/9687803) awarded by the Universiti Putra Malaysia.

References

Chandra, R., Takeuchi, H., Hasegawa, T., 2012. Hydrothermal pre-treatment of rice straw biomass: A potential and promising method for enhanced methane production. Appl. Energy 94, 129–140. https://doi.org/10.1016/j.apenergy.2012.01.027

Dasgupta, A., Chandel, M.K., 2019. Enhancement of biogas production from organic fraction of municipal solid waste using hydrothermal pre-treatment. Bioresour. Technol. Reports 7, 100281. https://doi.org/10.1016/j.biteb.2019.100281

Kim, D., Lee, K., Park, K.Y., 2015. Enhancement of biogas production from anaerobic digestion of waste activated sludge by hydrothermal pre-treatment. Int. Biodeterior. Biodegrad. 101, 42–46. https://doi.org/10.1016/j.ibiod.2015.03.025

Wang, D., Shen, F., Yang, G., Zhang, Y., Deng, S., Zhang, J., Zeng, Y., Luo, T., Mei, Z., 2018. Can hydrothermal pre-treatment improve anaerobic digestion for biogas from lignocellulosic biomass? Bioresour. Technol. 249, 117–124. https://doi.org/10.1016/j.biortech.2017.09.197

6th International Conference and
Postgraduate Colloquium for
Environmental Research 2022 (POCER
2022) 9 - 11 June 2022
Langkawi, Kedah, Malaysia

PCR 20012022 – 09: Exploiting Continuous Photochemical Processes for the Greener Preparation of Complex Drug-Like Entities

M. Baumann[a]*, M. Di Filippo[1], S. Bonciolini[1], C. Trujilo[b], G. Sánchez-Sanz[c], and A. S. Batsanov[d]

[a] School of Chemistry, University College Dublin, Science Centre South, Belfield, Dublin, Ireland

[b] **Trinity Biomedical Sciences Institute, School of Chemistry, Trinity College, Dublin, Ireland**

[c] Irish Centre for High-End Computing (ICHEC), Grand Canal Quay, Dublin 2, Ireland

[d] Department of Chemistry, Durham University, DH1 3LE, South Road, Durham, UK

- Corresponding Author E-mail: marcus.baumann@ucd.ie

Keywords: Sustainable chemistry; Photochemistry; Flow chemistry.

Extended Abstract

Introduction

Photochemical reactions, whether via photoexcitation or photocatalysis, are becoming important chemical transformations for the rapid generation of various important scaffolds. Specifically, these can contribute to more sustainable synthesis as photons are perceived as renewable and tunable reagents devoid of generating stoichiometric by-products. To overcome limitations with non-uniform irradiation (Beer's law) and thus scalability, our group and others have exploited continuous flow processing to realise powerful methods to forge strategic C-C bonds and harness complex drug-like entities with high efficiency and reproducibility.[1] As demonstrated in this presentation, continuous flow photochemistry is effectively exploited for the greener synthesis of important drug-like structures minimising waste whilst optimising different synthetic transformations in a scalable manner.

Materials and Methods

A commercially available Vapourtec E-series flow reactor was exploited in combination with its UV-150 photo-module allowing for superb control over residence time and temperature. The reactor coil is made of transparent PFA tubing (perfluoroalkoxy alkane, 10 ml volume, i.d. 1/16'') and can be used with suitable low-pass filters when paired with a medium-pressure Hg-lamp (variable 75-150 W). To provide for more energy-efficient and wavelength-selective irradiation a high-power LED lamp

emitting at 365 nm (50-100 W) was favoured. Tetrabutylammonium decatungstate (TBADT) was prepared by literature known methods and used in low catalyst loadings (1 mol%) for effective continuous HAT processes to forge important C-C bonds.

Results and Discussion

The photocatalysed synthesis of γ-aminopropylsulfones[2] (**1**, Figure 1), which are underrepresented entities in medicinal chemistry, was achieved using TBADT as a HAT catalyst in combination with vinyl sulfones and a variety of different formamide and acetamide building blocks. Stock solutions were successfully processed through the flow reactor (t_{Res} = 15-50 min) where irradiation with the high-power UV-LED light source (365 nm, 50-100 W) facilitated formation of a new C-C bond in high chemical yields. Crucially, the throughput of this process reached multi-gram quantities (20 mmol/h) for a variety of substrates which is testament to the excellent irradiation profile in flow which allows for high concentrations of up to 0.5 M to be processed with high efficiency.

The same UV-LED was subsequently trialed in a photochemical quinoline synthesis (**2**).[3] Comparing its performance to a traditional medium-pressure Hg-lamp clearly showed its superiority with respect to higher purity and increased chemical yield for all substrates tested. This flow approach allowed for a scalable process reaching a 100-fold higher productivity than analogous batch processes. Due to the excellent purity of the resulting quinoline solution, a telescoped flow hydrogenation using a packed-bed reactor filled with a heterogeneous Pd-catalyst was possible giving rise to a series of drug-like tetrahydroquinolines, including the antimalaria natural product galipinine.

Taking inspiration from this quinoline forming process that exploits a photo-catalysed alkene isomerisation step, we next evaluated an unprecedented process whereby the adjacent amino group was replaced by an alkyne species. Irradiation in flow mode used short residence times (5-8 min) within the UV-LED reactor (70 W, 365 nm) providing access to complex polycyclic scaffolds (**3**) with exquisite efficiency.[4] These novel materials were fully characterised by spectroscopic techniques including single crystal X-ray diffraction. Computational work supported an intricate mechanism whereby the alkyne intercepts the isomerising alkene thus triggering a novel photocascade. The cascade products were isolated in high yields and the flow process enabled provision of gram quantities for further studies that are currently underway in our laboratory.

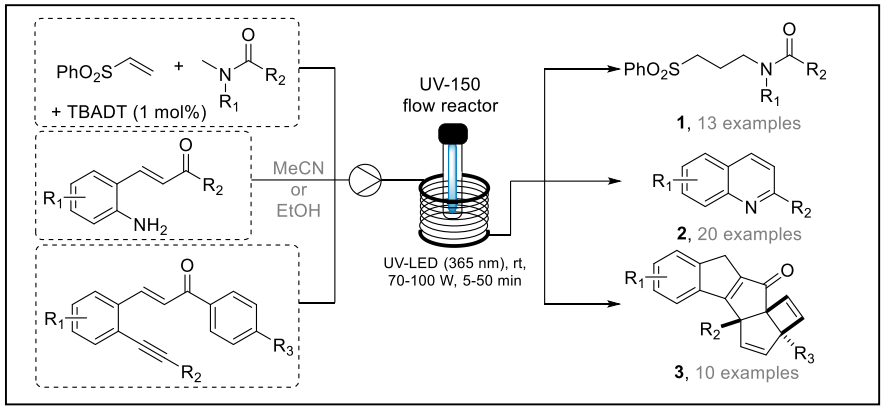

Figure 2: Overview of continuous photocatalysed processes achieved.

Significance

Photochemical processes towards various drug-like entities were developed using a new energy efficient high-power LED lamp. These processes utilise continuous flow reactor technology to harness excellent reaction control, safety, and scalability. The photochemical processes exploit either direct excitation of substrates or readily available photocatalysts (e.g. TBADT) that can be used in low loadings (1 mol%). In addition, the telescoping of further transformations, for instance Pd-catalysed hydrogenations, was demonstrated to access bioactive molecules such as the antimalarial galipinine in an uninterrupted process. In view of sustainability, the presented reactions are devoid of stoichiometric reagents as well as halogenated solvents and can be performed at high concentrations of up to 0.5 M.

Acknowledgements: The authors thank the Science Foundation Ireland as well as the School of Chemistry at University College Dublin for generous support of our research programmes.

References

1. Buglioni, L., Raymenants, F., Slattery, A., Zondag, S.D.A., Noël, T. 2021. *Chem. Rev.* (doi.org/10.1021/acs.chemrev.1c00332)

2. Bonciolini, S., Di Filippo, M. Baumann, M. 2020. *Org. Biomol. Chem.* 18 (46): 9428-9432.

3. Di Filippo, M., Baumann, M. 2020. *Eur. J. Org. Chem.* 6199-6211.

4. Di Filippo, M., Trujillo, C., Sánchez-Sanz, G., Batsanov, A.S., Baumann, M. 2021. *Chem. Sci.* 12 (29), 9895-9901.

PCR 26012022 – 10: Effects of roller speed on the structural and electrochemical properties of $LiCo_{0.6}Sr_{0.4}O_2$ cathode for intermediate temperature solid oxide fuel cell application

Nur Nadhihah Mohd Tahir[-a], Nurul Akidah Baharuddin[a*], Mahendra Rao Somalu[a], Andanastuti Muchtar [a,b], Lai Jian Wei[c]

[a] Fuel Cell Institute, Universiti Kebangsaan Malaysia, 43600, UKM Bangi, Selangor, Malaysia

[b] Department of Mechanical and Manufacturing Engineering, Faculty of Engineering and Built Environment, Universiti Kebangsaan Malaysia, Bangi, Malaysia

[c]Orbiting Scientific & Technology Sdn. Bhd
35-1 Jalan Radin Anum 1, Bandar Baru Seri Petaling, 57000 Kuala Lumpur, Malaysia

- Corresponding Author E-mail: akidah@ukm.edu.my

Keywords: Cathode; Ink; Triple-roll Mill; Lithium; Solid Oxide Fuel Cell.

Extended Abstract

A solid oxide fuel cell (SOFC) is a high-efficiency device that can convert chemical energy to electrical energy (Lina et al. 2019). Nowadays, the demand for lowering the operating temperature of SOFC has become a major issue amongst scientists. One of the new alternatives is to develop proper and reliable cathode ink materials for intermediate temperature SOFC (IT-SOFC) (Shirani-Faradonbeh et al. 2019).Choosing the suitable and compatible cathode materials for making ink that is used with the ionic and protonic electrolyte is crucial in achieving good performance of IT-SOFC. A study has discovered that LiCoO doped with Sr shows good electrochemical performance in IT-SOFC cathode applications (Wan Yusoff et al. 2020). In this work, the potential of $LiCo_{0.6}Sr_{0.4}O_2$ (LCSO) cathode was further investigated via the fabrication-related parameter; the roller speed of the triple-roll mill (TRM) process. The main purpose of roller speed evaluation is to produce a homogeneous cathode ink that can yield better performance (Somalu et al. 2017). The LCSO cathode ink composition and roller speed values evaluated in this study are shown in Table 1. The working principle of TRM is shown in Figure 1. The prepared sampled powder of LCSO was initially characterized using X-Ray diffraction (XRD), followed by a scanning electron microscope (SEM) to analyze the structural properties and surface morphologies. Then, the inks were produced using the TRM process at different speeds of 300 m/s, 350

m/s, 400 m/s, 450 m/s, and 500 m/s. The LCSO high-quality inks produced were then layered on both sides of the SDC electrolyte to produce an LCSO | SDC | LCSO symmetrical cell with 1cm^2 active site at the centre of the cell (Baharuddin et al. 2019). The electrochemical performance and structural properties of the symmetrical cell were measured by electrochemical impedance spectroscopy (EIS) to calculate the area-specific resistance (ASR) value at a temperature of 500 ℃ to 800 ℃ and by the field emmision scanning electron microscope (FESEM) method. The best roller speed to produce a high quality LCSO cathode ink was determined by referring to the lowest ASR value of 16.17 Ωcm^2 at 300 rpm. In conclusion, this study confirmed the influence of TRM's roller speed on the performance of the cathode for IT-SOFC application.

Table 1: Parameters for LCSO cathode ink formation

Solid content	Weight % (wt%)
LCSO powder (ball milled)	67.33 %
Solvent (Terpineol)	29.98 %
Binder (Ethylcelulose N7 grade (0.25-0.5wt%)	1.35 %
Dispersant (Hypermer KD15)	1.35 %

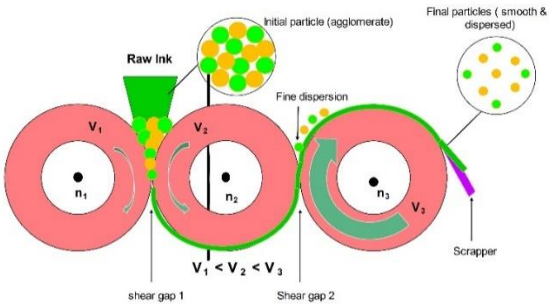

Figure 1: Triple roll mill machine working principle

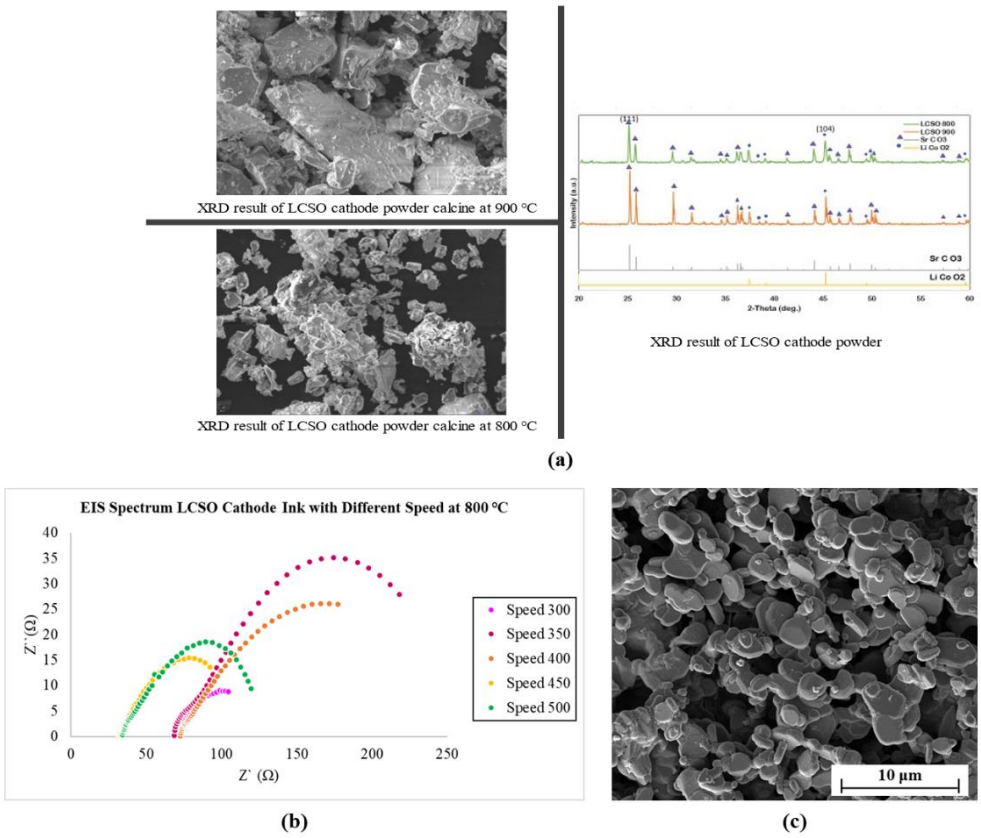

Figure 2: (a) XRD and SEM results for LCSO powders, (b) Nyquist plots for LCSO cathode produced at different speeds and (c) FESEM morphology of LCSO cathode (ink produced at roller speed of 300 rpm)

Acknowledgements: The authors gratefully acknowledge the financial support provided for this work by the Ministry of Higher Education, Malaysia for the funding support via the research sponsorship under Fundamental Research Grant Scheme grant number FRGS/1/2019/TK07/UKM/02/1 and Universiti Kebangsaan Malaysia through the Research Grants DIP-2010-011.

References

Baharuddin, N.A., Muchtar, A., Somalu, M.R., Kalib, N.S. & Raduwan, N.F.Synthesis and characterization of cobalt-free $SrFe_{0.8}Ti_{0.2}O_{3-\delta}$ cathode powders synthesized through combustion method for solid oxide fuel cells. *International Journal of Hydrogen Energy* 44(58): 30682–30691.

Lina, N., Mohd, R., Abdul, A. & Azim, A.Review on zirconate-cerate-based electrolytes for proton-conducting solid oxide fuel cell. *Ceramics International* 45(6): 6605–6615.

Shirani-Faradonbeh, H., Paydar, M.H., Paydar, S., Gholaminezhad, I. & Bazargan-Lari, R.Synthesis

and Electrochemical Studies of Novel Cobalt Free $(Nd_{0.9}La_{0.1})_{1.6}Sr_{0.4}Ni_{0.75}Cu_{0.25}O_{3.8}$ (NLSNC4) Cathode Material for IT-SOFCs. *Fuel Cells* 19(5): 578–586.

Somalu, M.R., Muchtar, A., Ramli, W., Daud, W. & Brandon, N.P.Screen-printing inks for the fabrication of solid oxide fuel cell films : A review. *Renewable and Sustainable Energy Reviews* 75(October 2016): 426–439.

Wan Yusoff, W.N.A., Somalu, M.R., Baharuddin, N.A., Muchtar, A. & Wei, L.J.Enhanced performance of lithiated cathode materials of $LiCo_{0.6}X_{0.4}O_2$ (X = Mn, Sr, Zn) for proton-conducting solid oxide fuel cell applications. *International Journal of Energy Research* 44(14): 11783–11793.

6th International Conference and
Postgraduate Colloquium for
Environmental Research 2022 (POCER
2022) 9 - 11 June 2022
Langkawi, Kedah, Malaysia

PCR 27012022 – 11: Performance analysis of PEMFC with single-channel and multi-channels on the impact of the geometrical model

B.H. Lim[a,*], M.I. Rosli[a,b], E.H. Majlan[a] , T. Husaini[a] , W.R.W. Daud[a,b] and S.F. Lim[c]

a Fuel Cell Institute Universiti Kebangsaan Malaysia, Selangor, Malaysia.

b Department of Chemical and Process Engineering, Faculty of Engineering and Built Environment, Universiti Kebangsaan Malaysia, Selangor, Malaysia

c Faculty of Engineering Universiti Malaysia Sarawak, Sarawak, Malaysia

• Corresponding Author E-mail: beehuah@ukm.edu.my

Keywords: PEMFC; modelling geometry; channels; performance.

Extended Abstract

An underperformance fuel cell significantly hinders the fuel cell technology application and commercialization. Conventionally, a prototype is built to test the performance of a fuel cell, nevertheless, this approach is excessively high-priced and labour intensive. Prediction of Proton Exchange Membrane Fuel Cell (PEMFC) performance using numerical investigation are widely used over several decades. The computational fluid dynamic modelling method could predict and evaluate the performance of a PEMFC using less time consumption and cost-effectiveness. This study is aimed to predict the different modelling dimensions on fuel cell performance. Two contrasting 3D model dimensions particularly single-channel and small-scale 7-channel models are configured. Both 3D models are correlated with a multi-channel model to assess the effect of the modelling dimension on the PEMFC performance. The simulated findings show that the single-channel model has an elevated current density generation. A uniformly distributed pressure produces an even fluid dynamic of the reactant and water in both the anode and cathode. The extensive effect of PEMFC performance in the cell is the distribution of the reactant as well as the pressure, which directly affects the water and current density distribution.

Modeling and simulation

Figure 1 displays the 3D models of single-channel and small-scale 7-channel models developed for this study. Models have different active area geometry where the study aims to consider the effects of simplification of 3D PEMFC models geometry on the predicted performance.

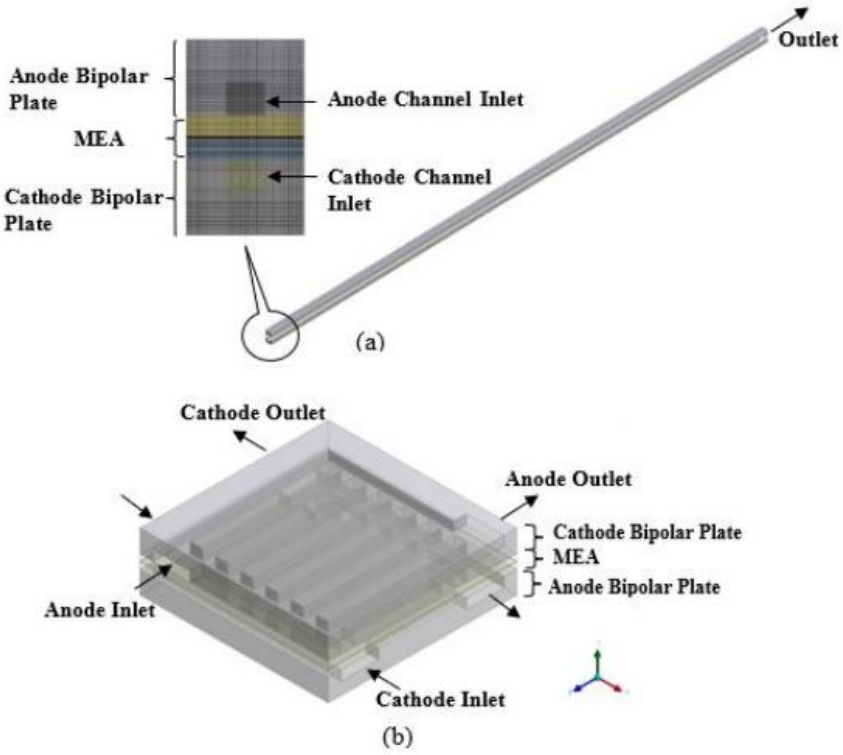

Figure 1: The 3D models: (a) single-channel model and (b) small-scale 7-channel model. The singe-channel model will represent the simplest simulation model which only consists of a single inlet-outlet channel for anode and cathode. It has a long channel flow with no flow distribution in the models. The second 3D model developed for this study is the small-scale 7-channel models. It has 7 parallel channels for both anode and cathode. The anode flow field has the conventional parallel flow field with single inlet and outlet. On the cathode, it has a bend C-shape parallel flow field with 2 inlet and 2 outlets. The model has a small active area with flow distribution being considered in the model. The multi-channel model has the largest active area with multiple flow field as reported in the previous literature. The model has similar configuration as the small-scale 7-channel model. The difference between both model are the sizing of the active area and the channel length.

Results and Discussion

The 3D modelling of single-channel and small-scale 7-channel models was performed to determine the effect of geometry on predicted PEMFC performance. The fuel cell performance of the largest scale was simulated

in the previous work (Lim et al., 2020) using a multi-channel model for comparison purposes. Figure 2 shows the comparison of polarization curves on the model developed for this study (single-channel, small-scale 7-channel) and multi-channel models from the previous study. The singlechannel model had the highest performance, followed by the small-scale 7-channel model. The underperformance model was demonstrated by the multi-channel model. As reported in a foregoing study, the multi-channel model had the largest active area along with numerous channels. The cell performance was greatly affected by the large area and a high number of channels. At a cell capacity of 0.6 V, the current density generated by the single-channel model was 0.9 A/cm2. As for the small-scale 7-channel model, the current density was marked at 0.76 A/cm^2, and the multi-channel model had 0.71 A/cm^2.

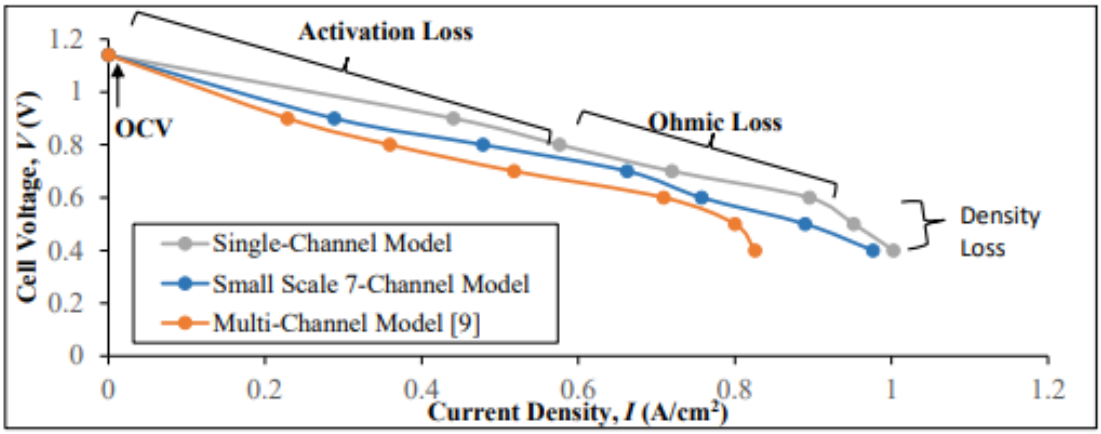

Figure 2: Polarization curves of single-channel, small-scale 7-channel, and multi-channel models.

Acknowledgments: This work was supported by the Ministry of Higher Education grant FRGS/1/2021/TKO/UKM/02/27 and Universiti Kebangsaan Malaysia Dana Pecutan Penerbitan (PPSELFUEL-2021).

6th International Conference and Postgraduate Colloquium for Environmental Research 2022 (POCER 2022) 9 - 11 June 2022
Langkawi, Kedah, Malaysia

PCR 21022022 – 12: ALCOHOL/SALT AQUEOUS BIPHASIC SYSTEM FOR DIRECT RECOVERY OF MICROBIAL PROTEASE

Hui Suan Ng [a,*], Pher Er Kee [a], Kai Ting Foo[a], Po-Ting Chen[b], John Chi-Wei Lan[c,d], Kuan Shiong Khoo[a]

[a]Faculty of Applied Sciences, UCSI University, UCSI Heights, 56000 Cheras, Kuala Lumpur, Malaysia.
[b]Department of Biotechnology and Food Technology, Southern Taiwan University of Science and Technology, Tainan, 710, Taiwan.
[c]Biorefinery and Bioprocess Engineering Laboratory, Department of Chemical Engineering and Materials Science, Yuan Ze University, Chungli, Taoyuan, 320, Taiwan.
[d]Graduate School of Biotechnology and Bioengineering, Yuan Ze University, No. 135 Yuan-Tung Road, Chungli, Taoyuan, 320, Taiwan.

Corresponding authors: Dr. Ng Hui Suan GrraceNg@ucsiuniversity.edu.my

Keywords: *aqueous biphasic system; protease; recovery; alcohol; salt*

EXTENDED ABSTRACT

Protease enzyme dominates the global enzyme market with a broad range of applications in food and feed, detergent, leather and pharmaceutical industries. Microbial protease is gaining much attention over the plant and animal protease due to its sustainability and productivity. Aqueous biphasic system (ABS) is recommended as a potential technology for single-step recovery of protease from microbial crude feedstock with desirable recovery efficiency. Hence, alcohol/salt ABS was employed in the present study for the direct recovery of protease from recombinant *Bacillus subtilis* crude feedstock. Protease was recovered in the alcohol-rich phase of ABS of pH 7 comprising 20% (w/w) 2-propanol and 22% (w/w) phosphate salt, loaded with 25% (w/w) crude feedstock with a partition coefficient of 3.14 ± 0.09. The highest recovery yield of 86.25% ± 0.32, purification fold of 2.32 ± 0.06 and selectivity of 2.61 ± 0.08 were achieved with the optimum alcohol/salt ABS. The findings suggested that alcohol/salt ABS could be employed as an effective approach for the recovery of microbial protease in single-step operation.

INTRODUCTION

Protease enzyme accounts for nearly 60% of the global enzyme market, of which microbial protease contributes to approximately 40% of the total worldwide enzyme sales because of the strong organic solvents and a broad range of pH and temperature tolerance [1, 2]. The *Bacillus* sp. emerges as the attractive source of bacterial protease due to the excellent fermentation characteristics with the capability to synthesize a high yield of protease enzyme and a small amount of toxic by-product [2, 3]. Among all, *Bacillus subtilis*, a GRAS (Generally Recognized as Safe) bacterial strain, is a promising workhorse to synthesize recombinant protease owing to the simple genetic manipulation and cultivation process [4]. To date, the industrial applications of protease enzyme have been broadened from food and feed industries to detergent, leather and pharmaceutical industries. However, the conventional downstream

processing methods for the recovery of microbial protease generally require multi-step operations which lead to high investment cost, long processing time and difficulty in scaling up.

Aqueous biphasic system (ABS) is introduced as a potential replacement to circumvent the limitation of the traditional approaches for the recovery of microbial enzyme. ABS has been widely employed for the separation and purification of target biomolecules due to the technical simplicity, scaling-up and continuous operation capability, cost-effective and eco-friendly properties [5]. ABS featuring high water content and low interfacial tension provides a biocompatible environment for the biomolecules recovery process, leading to the high recovery yield of target biomolecules in a one-step process [6]. In this study, alcohol/salt ABS was selected for the recovery and purification of recombinant *Bacillus subtilis* protease. Alcohol/salt ABS exhibits low viscosity and shorter phase separation time, and the alcohol can be easily recycled through evaporation and reused for the consecutive recovery process [7]. Several parameters including types and concentration of phase-forming alcohol and salt, concentration of crude feedstock load and system pH were investigated.

MATERIALS AND METHODS

Materials

The alcohols (1-propanol, 2-propanol and ethanol) were obtained from R&M Chemicals, Malaysia. Ammonium sulphate was acquired from Sigma-Aldrich, USA, sodium citrate from Chemiz, Malaysia, whereas potassium dihydrogen phosphate and dipotassium hydrogen phosphate from Merck, Germany. Bicinchoninic acid (BCA) protein assay kit was purchased from Nacalai Tesque, Japan.

Methods

Experimental procedure:

ABS of 5 g was prepared by adding alcohol, salt stock solution, crude enzyme and ultrapure water into a 15 mL falcon tube. After mixing, the mixture was subjected to centrifugation (4000 rpm, 10 min) and the phase volume was measured. The phase sample was collected for the evaluation of total protein concentration and protease activity.

Analytical procedure:

The total protein concentration was determined by adding 50 µL of protein sample to 200 µL of BCA working reagent. After incubation (37 ℃, 10 min), the absorbance was measured at 562 nm. [8]. To determine the protease activity, 250 µL of sample was mixed with 250 µL of 0.25% (w/v) casein substrate dissolved in Tris-HCl (10 mM, pH 9) and incubated (40 ℃, 10 min). Then, 500 µL of 0.4 M TCA solution was added into the mixture and centrifuged, followed by the measurement of absorbance at 280 nm [9].

Calculations:

The recovery yield of protease in top phase (Y_T) was calculated using Eq. (1) [10]:

$$Y_T, \% = \frac{100}{1+(\frac{1}{V_r * K_e})} \quad (1)$$

Where V_r is the volume ratio of top and bottom phases.

The partition coefficient of protease (K_e) and total protein (K_p) were calculated using Eq. (2) and (3), respectively [10]:

$$K_e = \frac{Protease\ activity\ in\ top\ phase}{Protease\ activity\ in\ bottom\ phase} \quad (2)$$

$$K_p = \frac{Total\ protein\ content\ in\ top\ phase}{Total\ protein\ content\ in\ bottom\ phase} \quad (3)$$

The purification fold (PF) was calculated using Eq. (4) [11]:

$$PF = \frac{SA\ of\ top\ phase}{SA\ of\ crude\ feedstock} \quad (4)$$

Where SA denotes the specific enzyme activity which defines as the ratio of protease activity (U) to total protein content (mg).

The selectivity (S) was calculated using Eq. (5) [8]:

$$S = \frac{K_e}{K_p} \quad (5)$$

RESULTS AND DISCUSSION

In the selection of types of phase-forming components, the highest recovery of protease was achieved in the in 2-propanol/phosphate ABS with greatest K_e of 3.03 ± 0.12 and Y_T of 86.75% ± 0.44 obtained. Protease was preferentially migrated towards the hydrophobic alcohol-rich top phase (K_e > 1) due to the low hydrophilicity of protease enzyme, leading to the formation of hydrophobic interaction among the protease and 2-propanol in ABS [12].

Following this, the recovery efficiency of 2-propanol/phosphate ABS at different concentration was studied. ABS comprising of 20% (w/w) 2-propanol and 22% (w/w) phosphate resulted in the highest Y_T of 89.62% ± 0.11 and PF of 2.55 ± 0.06 when compared to the other systems.

Fig. 1 demonstrates the effect of concentration of crude feedstock loaded into the ABS on protease recovery. Increase of crude feedstock concentration enhanced the recovery efficiency as more of the protease enzyme are loaded into the systems, thus enhanced the recovery yield [8]. The highest recovery efficiency was attained in the biphasic system loaded with 25% (w/w) crude feedstock (Y_T = 89.42% ± 0.82, S = 2.19 ± 0.15).

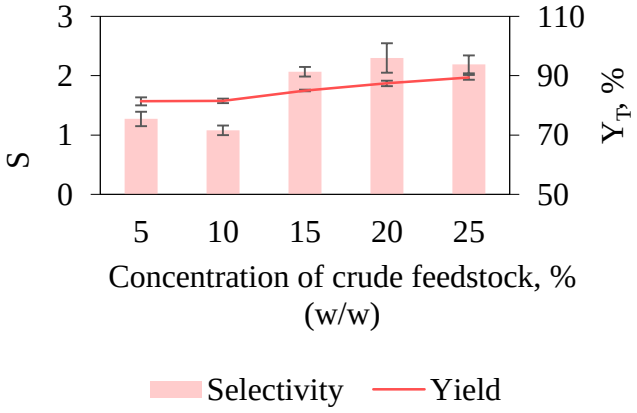

Fig. 1 Effect of concentration of crude feedstock on protease recovery.

The effect of system pH on protease recovery is shown in Fig. 2 whereby ABS of pH 7 resulted in the highest recovery efficiency with K_e of 3.22 ± 0.06, PF of 2.36 ± 0.06 and Y_T of 86.55% ± 0.22 recorded. Majority of the protease enzyme exhibits an isoelectric point (pI) of around 7. Hence, ABS with pH closer to the pI of proteins tends to strengthen the hydrophobic interactions, thereby improves the protease recovery in alcohol-rich top phase [13].

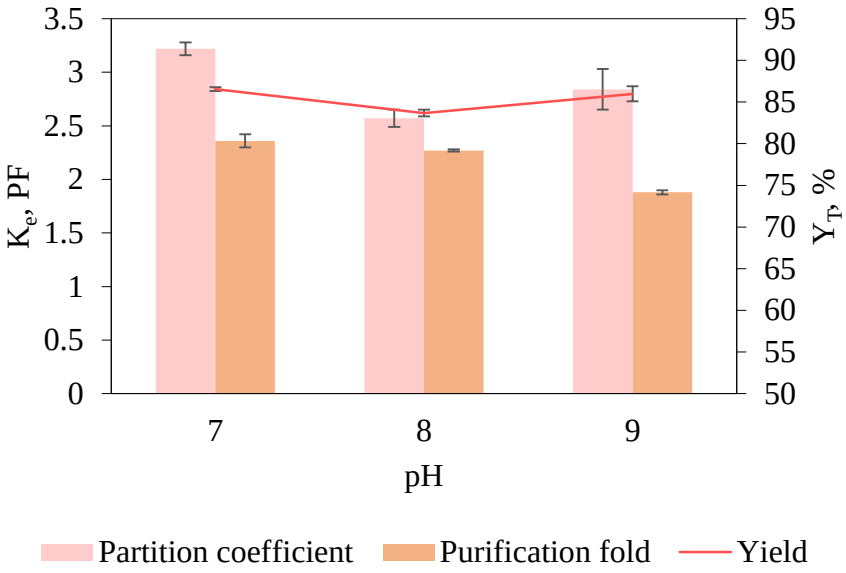

Fig. 2 Effect of system pH on protease recovery.

CONCLUSION

The direct recovery of protease from recombinant *B. subtilis* crude feedstock was successfully performed in alcohol/salt ABS. ABS comprised of 20% (w/w) 2-propanol and 22% (w/w) potassium phosphate of pH 7, loaded with 25% (w/w) of crude load was the ideal system for protease recovery. Highest K_e of 3.14 ± 0.09, Y_T of 86.25% ± 0.32, PF of 2.32 ± 0.06 and S of 2.61 ± 0.08 were achieved in the optimum ABS. Alcohol/salt ABS could be the useful technique for the one-step recovery of microbial protease with minimal investment cost and processing time.

ACKNOWLEDGEMENT

The work was financially supported by Fundamental Research Grant Scheme under grant number [FRGS/1/2020/TK0/UCSI/02/6] from Ministry of Higher Education.

REFERENCES

[1] M. Sharma, M. Gat, S. Arya, V. Kumar, A. Panghal, A. Kumar, A review on microbial alkaline protease: An essential tool for various industrial approaches, Ind Biotechnol, 15 (2019) 69-78.
[2] S. Singh, B.K. Bajaj, Potential application spectrum of microbial proteases for clean and green industrial production, Energy Ecol Environ, 2 (2017) 370-386.
[3] F.J. Contesini, R.R. Melo, H.H. Sato, An overview of *Bacillus* proteases: From production to application, Crit Rev Biotechnol, 38 (2018) 321-334.
[4] E.B. Drejer, S. Hakvåg, M. Irla, T. Brautaset, Genetic tools and techniques for recombinant expression in Thermophilic *Bacillaceae*, Microorganisms, 6 (2018) 42.
[5] S. Ketnawa, N. Rungraeng, S. Rawdkuen, Phase partitioning for enzyme separation: An overview and recent applications, Int Food Res J, 24 (2017) 1-24.
[6] A.M. Ferreira, V.F.M. Faustino, D. Mondal, J.A.P. Coutinho, M.G. Freire, Improving the extraction and purification of immunoglobulin G by the use of ionic liquids as adjuvants in aqueous biphasic systems, J Biotechnol, 236 (2016) 166-175.
[7] K.-W. Lee, C.W. How, L. Chen, P.T. Chen, J.C.-W. Lan, H.-S. Ng, Integrated extractive disruption of *Gordonia terrae* cells with direct recovery of carotenoids using alcohol/salt aqueous biphasic system, Sep Purif Technol, 223 (2019) 107-112.
[8] P.E. Kee, L.S. Cheah, P.K. Wan, P.L. Show, J.C.-W. Lan, Y.H. Chow, H.S. Ng, Primary capture of *Bacillus subtilis* xylanase from crude feedstock using alcohol/salt liquid biphasic flotation, Biochem Eng J, 165 (2021) 107835.
[9] N. Lộc, H. Lien, G. Do, H. Quang, Purification of recombinant neutral protease (NPRC10) by partitioning in aqueous two-phase systems, Eur J Exp Biol, 3 (2013) 252-257.
[10] C.W. Ooi, B.T. Tey, S.L. Hii, S.M.M. Kamal, J.C.W. Lan, A. Ariff, T.C. Ling, Purification of lipase derived from *Burkholderia pseudomallei* with alcohol/salt-based aqueous two-phase systems, Process Biochem, 44 (2009) 1083-1087.
[11] M. Amid, M. Shuhaimi, M.Z. Islam Sarker, M.Y. Abdul Manap, Purification of serine protease from mango (*Mangifera Indica Cv. Chokanan*) peel using an alcohol/salt aqueous two phase system, Food Chem, 132 (2012) 1382-1386.
[12] M.O. Toledo, F.O. Farias, L. Igarashi-Mafra, M.R. Mafra, Salt effect on ethanol-based aqueous biphasic systems applied to alkaloids partition: An experimental and theoretical approach, J Chem Eng Data, 64 (2019) 2018-2026.
[13] H.S. Mohamadi, E. Omidinia, R. Dinarvand, Evaluation of recombinant phenylalanine dehydrogenase behavior in aqueous two-phase partitioning, Process Biochem, 42 (2007) 1296-1301.

6th International Conference and
Postgraduate Colloquium for
Environmental Research 2022 (POCER
2022) 9 - 11 June 2022
Langkawi, Kedah, Malaysia

PCR 28022022 – 13: Performance Evaluation Of A Novel And Environment-Friendly Biodiesel-Based Drilling Fluid Using Non-Edible Vegetable Oil

Aftab Hussain Arain[a*], Syahrir Ridha[a,b], Mysara Eissa Mohyaldinn Elhaj[a], and Raja Rajeswary Suppiah[a]

[a] Petroleum Engineering Department
Universiti Teknologi PETRONAS, Seri Iskandar, Perak Darul Ridzuan, Malaysia

[b] Institute of Hydrocarbon Recovery
Universiti Teknologi PETRONAS, Seri Iskandar, Perak Darul Ridzuan, Malaysia

- Corresponding Author E-mail: aftab_17005015@utp.edu.my

Keywords: Ester-based Drilling Fluid, Non-Edible Vegetable Oil, Biodiesel, Calophyllum Inophyllum, Rheology

Extended Abstract

Drilling fluid plays an essential role in the success of any drilling operation. A high-performance drilling fluid is crucial to drill the highly challenging formations such as highly deviated, ultra-deep, and extended reach wells. Oil-based mud (OBM) is preferred over other drilling fluids due to its superior performance to drill highly technical and challenging formations. OBM offers less formation damage with fewer hole problems, excellent lubricity, corrosion inhibition, decreased differential sucking, increased rate of penetration (ROP), and superior wellbore stability [1]. However, there are significant challenges that restrict its application, including environmental issues, high cost, and elastomer incompatibility. The biggest problem related to the use of OBM is its toxicity, which has the potential to damage the ecosystem. OBM uses diesel or mineral oil as a continuous phase in the formulation, which is refined from crude oil and contains a high concentration of hazardous and non-biodegradable aromatic components. Therefore, the stringent environmental regulations imposed by the environmental regulatory agencies have limited the use of oil-based mud around the world due to its detrimental effect on the environment [2]. To maintain and preserve the environment, an eco-friendly, biodegradable, and chemically stable drilling fluid created from alternative sources is necessary. This situation makes ester-based drilling fluid an attractive alternative to oil-based drilling fluid.

The ester-based drilling fluid used biodiesel as a base fluid for the formulation of drilling fluid. It is generally derived from vegetable oil and considered environment-friendly and biodegradable, as it does not contain any aromatic compounds [3]. The performance characteristics of ester-based drilling fluid are very much similar to the oil-based drilling fluid but with significantly reduced environmental impact. Biodiesel production from second-generation feedstock (non-edible vegetable oil) is gaining worldwide attention as they are more environment-friendly, efficient, economical compared to edible vegetable oils. Calophyllum inophyllum has been emerging as a potential source of non-edible feedstock for the production of biodiesel. This plant is native to southeast Asia, east Africa, the southern coast of India, Australia, and the south pacific [4]. Calophyllum inophyllum oil is non-toxic, environmentally friendly, efficient, and economical, which makes it a suitable candidate for the development of an ester-based drilling fluid.

The objective of this research study is to develop and evaluate the performance of an ester-based drilling fluid using Calophyllum inophyllum oil as base fluid. The crude Calophyllum inophyllum oil is extracted and synthesized to produce biodiesel by two-step esterification and transesterification process at optimum conditions. The produced biodiesel is used as a base oil for the formulation of ester-based drilling fluid. A comprehensive experimental study is carried out to evaluate the performance of formulated ester-based drilling fluid. The rheological and filtration tests are performed at ambient and reservoir conditions along with electrical stability and barite sagging and viscoelastic properties. The formulated drilling fluid demonstrates efficient performance and meets the API recommendations. The drilling fluid shows superior rheological characteristics, improved filtration properties, high electrical stability and enhanced viscoelastic properties. The rheological modelling recommends the non-Newtonian shear-thinning behaviour which is correlated with the Herschel–Bulkley model as shown in Fig 1. The performance of the ester-based drilling fluid is evaluated by comparing the rheological and filtration properties with commercially available oil-based drilling fluids. The test results exhibit that the newly developed ester-based drilling fluid has improved rheological and filtration properties with better emulsion stability and barite sagging tendency. It is anticipated from the results that the Calophyllum inophyllum ester-based drilling fluid has the potential to overcome the technical and environmental challenges of oil-based drilling fluid for drilling shale formation.

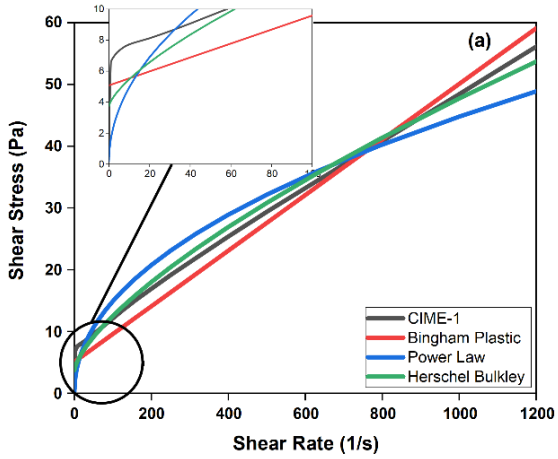

Figure 3: Rheological model showing a relationship between shear stress and shear rate of CIME-based drilling fluid

Acknowledgements: The authors thank the Petroleum Engineering Department and Institute of hydrocarbon recovery at Universiti Teknologi PETRONAS for providing financial assistance for this research work through the YUTP015LC0-101 grant.

References

Said, M.M. and A.-A.H. El-Sayed, The use of palm oil fatty acid methyl ester as a base fluid for a flat rheology high-performance drilling fluid. Journal of Petroleum Science and Engineering, 2018. 166: p. 969-983.

Peixoto, R.D., Bicudo, T.C., Heloise, O.D.A., Sousa, A.S. and de Carvalho, L.S., 2021. Synthesis of decyl methyl carbonate and a comparative assessment of its performance as the continuous phase of synthetic-based drilling fluids. Journal of Petroleum Science and Engineering, 199, p.108301.

Sulaimon, A.A., Adeyemi, B.J. and Rahimi, M., 2017. Performance enhancement of selected vegetable oil as base fluid for drilling HPHT formation. Journal of Petroleum Science and Engineering, 152, pp.49-59.

Atabani, A. and A. da Silva César, Calophyllum inophyllum L.–A prospective non-edible biodiesel feedstock. Study of biodiesel production, properties, fatty acid composition, blending and engine performance. Renewable and Sustainable Energy Reviews, 2014. 37: p. 644-655.

6th International Conference and Postgraduate Colloquium for Environmental Research 2022 (POCER 2022) 9 - 11 June 2022
Langkawi, Kedah, Malaysia

PCR 04032022 – 14: Microalgae biorefinery concepts: Multiphase separation and extraction processes

Kit Wayne Chew[a,b]

[a] School of Energy and Chemical Engineering, Xiamen University Malaysia, Jalan Sunsuria, Bandar Sunsuria, 43900 Sepang, Selangor Darul Ehsan, Malaysia

[b] College of Chemistry and Chemical Engineering, Xiamen University, Xiamen 361005, Fujian, China

- Correnspoding Author E-mail: kitwayne.chew@xmu.edu.my

Keywords: Biorefinery; Extraction; Microalgae; Multiphase; Separation

Extended Abstract

Microalgae have received much interest as a biofuel feedstock in response to the uprising energy crisis, climate change and depletion of natural sources. Development of biofuels alone from microalgae does not satisfy the economic feasibility of overwhelming capital investments and operations. Hence, high-value co-products have been produced through the extraction of a fraction of algae to improve the economics of a microalgae biorefinery [Chew *et al.*, 2017]. Examples of these high-value products are pigments, proteins, lipids, carbohydrates, vitamins and anti-oxidants, with applications in cosmetics, nutritional and pharmaceuticals industries [Zhuang *et al.*, 2021]. To promote the sustainability of this process, an innovative microalgae biorefinery structure needs to be implemented through the production of multiple products in the form of high value products and biofuel.

Many research works have successfully used microalgae for various bioproducts generation. This involves the upstream processing and downstream processing, which consists of the main stages in microalgae biorefineries. The efficiency of the upstream processing involves four important factors, namely: microalgae strain, supply of carbon dioxide (CO2), nutrient source such as nitrogen and phosphorus, and source of illumination [Peter *et al.*, 2022]. While the downstream processing involves the coagulation, harvesting, extraction, separation and purification technologies. Adequate nutrient sources are significant for microalgae growth as it provides the necessary conditions to enhance the productivity of microalgae [Chia *et al.*, 2018]. Different light sources can influence the photosynthesis rate of microalgae, which will directly impact its growth rate. As for downstream processing, the

selection of appropriate technologies for biorefineries depends on several factors: energy input required, availability of current technology, economic feasibility, simplicity of process, number of processing steps and others [Chew *et al.*, 2017]. These factor play a major role in optimizing the process to enable better efficiency and higher profits from the products generated. Hence, the development of multiphase separation technologies can serve as an uprising method to promote the biorefinery of biomass.

Multiphase separation techniques like three phase partitioning (TPP) or liquid triphasic system (LTS) is an emerging separation process that could overcome the associated limitations of the conventional processes [Chew *et al.*, 2019b]. LTS is a multiphase system that comprises of three phases as a result of two immiscible liquid mixtures consisting of a combination of alcohol and salt phase, where lipids are separated to the top, proteins present in the intermediate and the remaining carbohydrates and contaminants in the bottom phase. Each layer holds a desired product that can be purified and processed for further applications (Figure 1). The LTS represents a simple and quick method for extraction, purifying and concentrating biomolecules and can be used directly with crude suspensions. Integrating the technology with pretreatment procedure have also established higher quality products with better desired compound recovery [Chew *et al.*, 2019a]. The incorporation of pretreatment steps with LTS can contribute to cell disruption of microalgae, leading to the rapid release of valuable biomolecules. This shows the prospects of LTS as a potential rapid downstream processing for the extraction and purification of multiple products from microalgae.

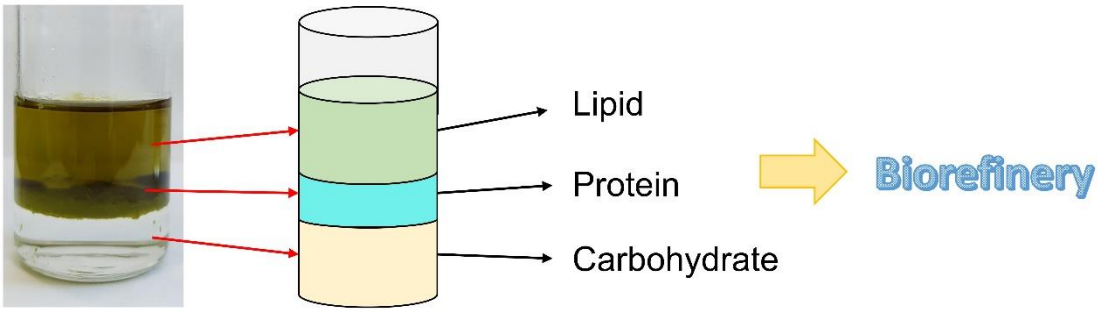

Figure 4: Schematic representation of biorefinery system using multiphase separation.

Acknowledgements: The author would like to acknowledge Xiamen University Malaysia (XMUM) under the XMUM Research Fund (Grant number: XMUMRF/2021-C7/IENG/0033).

References

Chew, K.W., Yap, J. Y., Show, P. L., Suan, N. H., Juan, J. C., Ling, T. C., Lee, D. J. and Chang, J. S., 2017. Microalgae biorefinery: high value products perspectives. *Bioresource technology*, 229: 53-62.

Chew, K.W. , Chia, S.R. , Lee, S.Y. , Zhu, L. and Show, P. L., 2019a. Enhanced microalgal protein extraction and purification using sustainable microwave-assisted multiphase partitioning technique. *Chemical Engineering Journal*, 367: 1-8.

Chew, K. W., Ling, T. C. and Show, P. L., 2019b. Recent developments and applications of three-phase partitioning for the recovery of proteins. *Separation & Purification Reviews*, 48 (1): 52-64.

Chia, S. R., Chew, K. W., Show, P. L., Yap, Y. J., Ong, H. C., Ling, T. C. and Chang, J. S., 2018. Analysis of economic and environmental aspects of microalgae biorefinery for biofuels production: a review. *Biotechnology journal*, 13 (6): 1700618.

Peter, A. P., Koyande, A. K., Chew, K. W., Ho, S. H., Chen, W. H., Chang, J. S., Krishnamoorthy, R., Banat, F. and Show, P. L., 2022. Continuous cultivation of microalgae in photobioreactors as a source of renewable energy: Current status and future challenges. *Renewable and Sustainable Energy Reviews*, 154: 111852.

Zhuang, D., He, N., Khoo, K. S., Ng, E. P., Chew, K. W. and Ling, T. C., 2021. Application progress of bioactive compounds in microalgae on pharmaceutical and cosmetics. *Chemosphere*, 291 (2): 132932.

6th International Conference and
Postgraduate Colloquium for
Environmental Research 2022 (POCER
2022) 9 - 11 June 2022
Langkawi, Kedah, Malaysia

PCR 08032022 – 15: Establishment of preliminary frameworks for beneficial uses of dredged materials including contaminated marine sediments in Colombia

Wendy Tatiana Gonzalez Cano[a,b,c] and Kyoungrean Kim[b,c*]

[a] The Colombian Navy (ARC, Spanish: Armada República de Colombia), Colombia
[b] KIOST School, University of Science and Technology (UST), Busan, Republic of Korea
[c] **Marine Environmental Research Center,** Korea Institute of Ocean Science & Technology (KIOST), Busan, Republic of Korea

*Corresponding Author E-mail: kyoungrean@kiost.ac.kr

Abstract

Qualities of marine sediments along Colombia's Caribbean Coast were mainly investigated, including ex-situ pollutants treatment technologies. This research aims to establish preliminary frameworks to improve environmental assessment for beneficial uses of dredged materials (DM), including contaminated marine sediments (CMS) in Colombia, where such studies have not been reported until now. This research proposed using solidification-stabilization as sustainable remediation technologies along with complex methods. Low values of harmful heavy metals and organic pollutants were found in the literature reviewed. However, cadmium (Cd) and chromium (Cr) concentrations were above the international environmental standards. For those reasons, remediation strategies should be considered to control pollutants. Finally, future research should focus on the potential benefits of combining multiple technologies to improve outcomes. More detailed studies should be continuously conducted in Colombia to formulate marine sediments' environmental standards and enhance dredged materials sustainability.

Keywords: dredged materials; contaminated marine sediments; beneficial use; remediation; sustainability.

1. Introduction

Contaminated marine sediments denote a potential risk for human health and the marine environment due to their long-term detrimental consequences [1]. Thus, strategies for sustainable remediation are required. Remediation treatments are critical because their management and disposal involve significant monetary resources, time, and space [2]. Also, due to the high water contents and

particle size distribution in DM, pre-treatment processes are necessary before beneficial uses. The London Protocol 1996; LP [3] has established guidelines for adequately disposing of DM, avoiding the perception of contaminated materials as waste, and considering them commercially exploitable resources [4]. Therefore, their usage for beneficial uses should be viewed as a priority.

Aside from these factors, cost-effectiveness, treatability per unit time, and life cycle assessment (LCA) are significant to determine treatments methods [5]. In DM, the removal efficiency of contaminants is exacerbated by the large fraction of fine particles and pollutants. [6] provides a well-developed guide on selecting feasible remediation technologies to treat DM and CMS. With an extensive coastline and the absence of normativity to properly manage dredged processes, Colombia faces an urgent need to set up national environmental standards of marine sediments to evaluate their contamination level and reduce decision-making uncertainty during dredging activities. Therefore, specific assessment guidelines are needed to meet sustainability and better management practices. This research is intended to provide preliminary frameworks for increasing beneficial uses of DM and CMS in Colombia through remediation technologies that may reduce disposal dredged volume, cost-saving in dredging work, and controlling contaminants from the environment.

2. Methodology

Theoretical review concerning the state of marine sediments in Colombia [7], [8], [9], [10], [11],[12] was developed, including normativity of dredged process. Next, results of sediment quality reported in the Colombia's Caribbean Cost were compared with Sediments Quality Guidelines (SQGs) of developed countries to assess contamination levels. Ex-situ technologies to treat pollutants were investigated due to the ease of environmental parameters control compared to in-situ methods. Finally, this research provided preliminary frameworks for beneficial uses of DM, recognizing them as valuable resources different than wastes.

3. Results

International SQGs with specific pollutants and Action Levels with Upper (AL1) and Lower (AL2) limits were collected to assess acceptable values of contaminants because there is no current legislation for sediment qualities in Colombia. In Table 1, Cd and Cr concentrations exceeded international AL1 and AL2 in cities with a strong influence of anthropogenic contaminants, representing a potential risk to the coastal ecosystem. In contrast, inorganic and organic pollutants were low in regions with inferior industrialization. Preliminary studies have not been proposed recovery methods to obtain beneficial uses of DM and CMS in Colombia until now. In that sense, solidification and/or stabilization combined with complex alternative methods promise to remediate contaminated materials. The mobility of

harmful heavy metals is reduced by mixing agents that solidify and then immobilize the target pollutants. The average cost is 90 USD per tonne (cost range from 30 to 250 USD per tonne) [1]. Compared with other technologies, this method is relatively low cost and easy to process. Numerous studies have investigated the application of this remediation technology [2][13][14].

Table 1: Comparison of sediment quality reported in Colombia with international sediments quality criteria [1]. Exceeding concentrations values are stated in italics

Specification	Republic of Korea	Hong Kong	Belgium		Florida, USA	Colombia	References
Action Level	AL1	AL1	AL1	AL2	AL1		
Unit	AL2 mg/kg	AL2 mg/kg-µg/kg*	mg/kg-µg/goc*		AL2 mg/kg	mg/kg, dw	
Hg	1.2 0.3	1 0.5	1.5	0.3	0.696 0.13	0.099 ± 0.0886	[7]
Cd	10 2.5	4 1.5	7	2.5	4.21 0.676	0.3328 ± 0.4266 0.12 ± 0.15 1.1 ± 0.72 *9 ± 14*	[7] [10] [11] [12]
Zn	410 200	270 200	500	160	271 124	80.7 ± 55 32.33 ± 12.549	[10] [8]
Ni	52 35	40 40	280	70	-	-	24.97 ± 7.52 19.5 ± 6.47	[7] [10]
Pb			350	70		8.214 ± 5.247	[7] [10] [8]

	220 50	110 75			112 30.2	2.36 ± 2.3 1.194 ± 0.059 18.95 ± 8.5023 22 ± 46	[11] [12]
Cr	370 80	160 80	220	60	160 52.3	34.129 ± 19 60.1 ± 31.16 *179 ± 360*	[7] [11] [12]
Cu	270 65	110 65	100	20	108 18.7	21 ± 13.20 83.2 ± 122 20 ± 30	[7] [11] [12]
PAHs	45 4	3160* 550*	180*	70*	1442 312	0.188 ± 0.249	[9]
PCBs	0.180 0.023	180* 23*	2*	2*	189 21.6	0.0025 ± 0.0045	[9]

3.1 Preliminary Framework for Beneficial uses of Dredged Materials and CMS in Colombia

Followed by determining the contamination level of DM, suitable remediation technologies should be applied to reduce concentrations of contaminants and obtain beneficial uses. Figure 1 provides schematic frameworks for the sustainable management of DM. Generally, more than one technology should be considered. In addition, pre-treatment technics might be required depending on the types of pollutants to remediate [6].

For instance, particle separation pre-treatment is crucial in reducing the volume of DM to be treated for beneficial uses or disposed of in confined facilities [1], while the dewatering process will reduce the volume of fine particles remaining. Final products will generate worth construction materials and several engineering applications. Various researchers have further investigated the beneficial uses of DM and CMS.

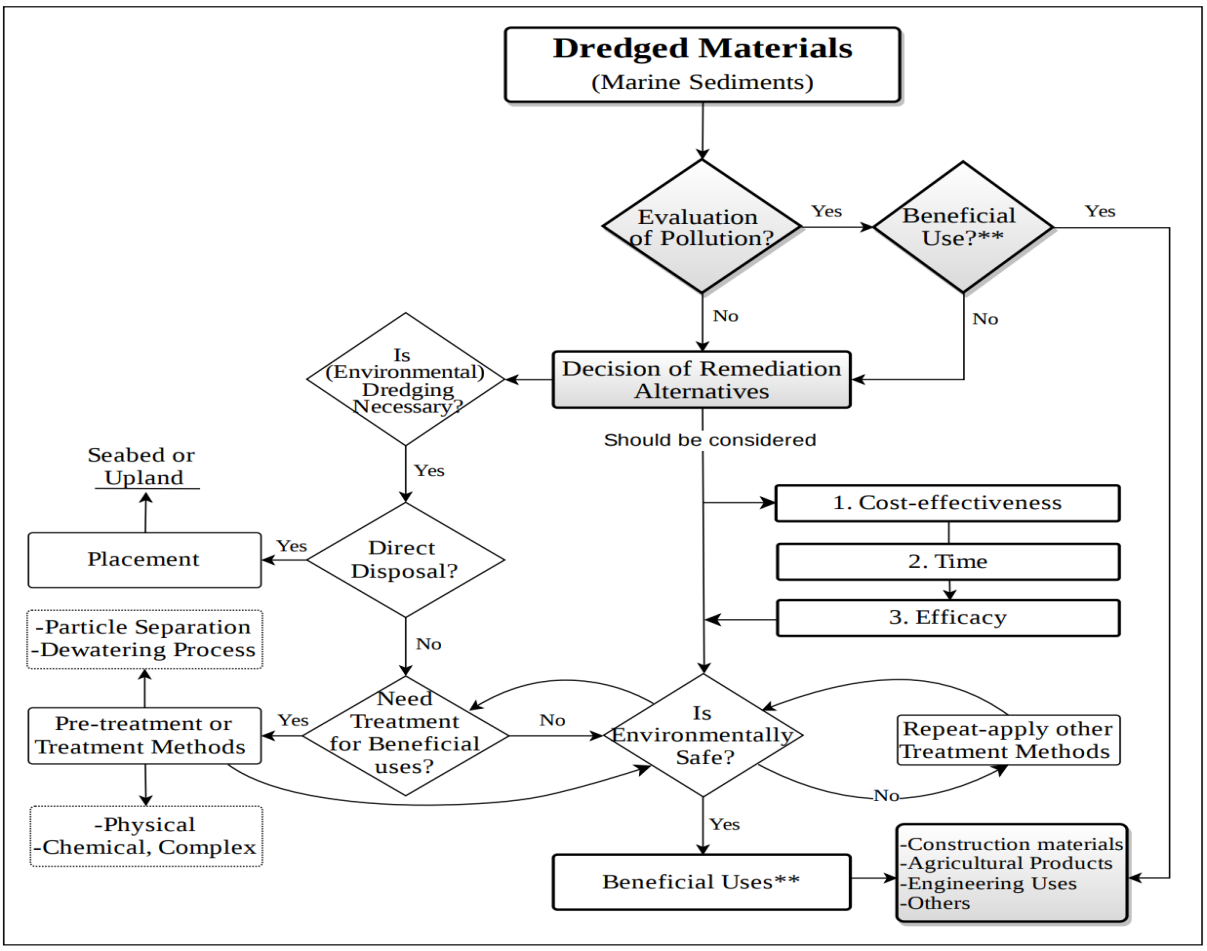

Figure 2: Preliminary Framework for Beneficial uses of Dredged Materials and CMS in Colombia

**As a result, enhancing the sustainability management of dredged materials and marine sediments will be reached

4. Discussion

Qualities of marine sediments in Colombia and proposals for remediation alternatives of DM and CMS were investigated. Few studies regarding this topic were found during the review. Table 1 showed relatively non-contaminated materials, suitable for multiple beneficial uses without additional pollutant control technologies. Remediation technologies have advantages and limitations; thus, risk management and critical aspects discussed before should be evaluated, including community participation. Beneficial uses of DM are not usually considered in treatment processes, however it may reduce the volume of dredged, which is often very large, providing valuable commercialized products and improving the implementation of circular economy strategies [1].

5. Conclusions

1. Particle separation or dewatering pre-treatments are critical before beneficial uses of DM. The findings in this study offer solidification and/or stabilization combined with other alternative technologies as a suitable, cost-effective remediation method to treat harmful heavy metals.
2. The preliminary frameworks developed during this study may improve the decision-making of national and environmental authorities in Colombia regarding sustainable management of DM, increasing their beneficial uses.
3. Colombia needs to consider being a contracting party of LP, which plays an essential role adequately managing of DM and preventing pollution from harmful pollutants at sea.
4. The potential effects of two or more technologies concerning remediation treatments to enhance results may be considered in future research.
5. Further studies should be constantly developed in Colombia to formulate national environmental standards of marine sediments based on appropriated environmental regulations and referencing the experiences of other countries' international standards.

Acknowledgements: This research was supported by The Korea Institute of Ocean Science and Technology (PO01418), Republic of Korea.

References

[1] C. N. Mulligan, M. Fukue, and Y. Sato, "Sediments Contamination and Sustainable Remediation.pdf." CRC Press, Boca Raton, FL, pp. 19–289, 2010.

[2] Y. Gang, E. J. Won, K. Ra, J. Y. Choi, K. W. Lee, and K. Kim, "Environmental assessment of contaminated marine sediments treated with solidification agents: Directions for improving environmental assessment guidelines," *Mar. Environ. Res.*, vol. 139, no. April, pp. 193–200, 2018, doi: 10.1016/j.marenvres.2018.05.011.

[3] U. S. Environmental Protection Agency, "Ocean Dumping: International Treaties," 2021. https://www.epa.gov/ocean-dumping/ocean-dumping-international-treaties.

[4] F. Todaro, S. De Gisi, and M. Notarnicola, "Contaminated Marine Sediments: Waste or Resource? An Overview of Treatment Technologies," *Procedia Environ. Sci. Eng. Manag.*, vol. 3, no. 3–4, pp. 157–164, 2016.

[5] Y. Zhang *et al.*, "Sustainable ex-situ remediation of contaminated sediment: A review," *Environ. Pollut.*, vol. 287, no. April, p. 117333, 2021, doi: 10.1016/j.envpol.2021.117333.

[6] United States Environmental Protection Agency, *Selecting Remediation Techinques For Contaminated Sediment (U.S. EPA, 1993).*, EPA-823-B9. Washington D.C: Office of Science and Technology Standards and Applied Science Division U.S EPA, 1993.

[7] M. Tosic, J. D. Restrepo, S. Lonin, A. Izquierdo, and F. Martins, "Water and sediment quality

in Cartagena Bay, Colombia: Seasonal variability and potential impacts of pollution," *Estuar. Coast. Shelf Sci.*, vol. 216, pp. 187–203, 2019, doi: 10.1016/j.ecss.2017.08.013.

[8] A. C. Torregroza-Espinosa, E. Martínez-Mera, D. Castañeda-Valbuena, L. C. González-Márquez, and F. Torres-Bejarano, "Contamination Level and Spatial Distribution of Heavy Metals in Water and Sediments of El Guájaro Reservoir, Colombia," *Bull. Environ. Contam. Toxicol.*, vol. 101, no. 1, pp. 61–67, 2018, doi: 10.1007/s00128-018-2365-x.

[9] K. Caballero-Gallardo, J. Olivero-Verbel, C. Corada-Fernández, P. A. Lara-Martín, and A. Juan-García, "Emerging contaminants and priority substances in marine sediments from Cartagena Bay and the Grand Marsh of Santa Marta (Ramsar site), Colombia," *Environ. Monit. Assess.*, vol. 193, no. 9, p. 596, 2021, doi: 10.1007/s10661-021-09392-5.

[10] R. Fernandez-Maestre, B. Johnson-Restrepo, and J. Olivero-Verbel, "Heavy Metals in Sediments and Fish in the Caribbean Coast of Colombia: Assessing the Environmental Risk," *Int. J. Environ. Res.*, vol. 12, no. 3, pp. 289–301, 2018, doi: 10.1007/s41742-018-0091-1.

[11] E. Duarte-Restrepo, K. Noguera-Oviedo, D. Butryn, J. S. Wallace, D. S. Aga, and B. E. Jaramillo-Colorado, "Spatial distribution of pesticides, organochlorine compounds, PBDEs, and metals in surface marine sediments from Cartagena Bay, Colombia," *Environ. Sci. Pollut. Res.*, vol. 28, no. 12, pp. 14632–14653, 2021, doi: 10.1007/s11356-020-11504-6.

[12] O. Bayona-Arenas, M. y Garcés-Ordóñez, "Diagnostico y evaluacion de la calidad de las aguas marinas y costeras del caribe y pacifico colombianos," *REDCAM: INVEMAR, MinAmbiente, CORALINA*, vol. 4, p. 336, 2018.

[13] C. N. Mulligan, R. N. Yong, and B. F. Gibbs, "An evaluation of technologies for the heavy metal remediation of dredged sediments," *J. Hazard. Mater.*, vol. 85, no. 1–2, pp. 145–163, 2001, doi: 10.1016/S0304-3894(01)00226-6.

[14] Jesse R. Conner & Steve L. Hoeffner, "A Critical Review of Stabilization/Solidification Technology," *Crit. Rev. Environ. Sci. Technol.*, vol. 28:4, no. 397–462, 1998, doi: 10.1080/10643389891254250.

PCR 08032022 – 16: Morphological Effects on Catalytic Performance of LTL Zeolites in Acylation of 2-Methylfuran Enhanced by Non-Microwave Instant Heating

Eng-Poh Ng[a,*] Nur Hidayahni Ahmad,[a] T. Jean Daou,[b] Pedro Maireles-Torres,[d] Tau-Chuan Ling,[e]

[a]School of Chemical Sciences, Universiti Sains Malaysia, 11800 USM, Penang, Malaysia.

[b]Université de Haute-Alsace, Axe Matériaux à Porosités Contrôlées, Institut de Science de Matériaux de Mulhouse UMR 7361, ENSCMu, 3b rue Alfred Werner, 68093 Mulhouse, France.

[c]Université de Strasbourg, 67000 Strasbourg, France.

[d]Departamento de Quimica Inorganica Cristalografia y Mineralogia (Unidad Asociada al ICP-CSIC) Facultad de Ciencias Campus de Teatinos, Universidad de Mlaga, 29071 Malaga, Spain.

[e]Institute of Biological Sciences, Faculty of Science, University of Malaya, 50603 Kuala Lumpur, Malaysia.

[*]Corresponding author. E-mail address: epng@usm.my

Abstract

Morphological characteristics of zeolites can have significant effects on the catalytic reactions. However, the roles of zeolite morphology on catalytic reactions, particularly Friedel-Crafts acylation of 2-methylfuran, are still not clear. Hence, LTL-type zeolites with different morphologies are prepared by using bamboo leaf bio-silica source where the zeolites are used to elucidate the morphological properties in this acylation reaction. The results show that LTL zeolites with short-rod, cylindrical, stick-like and nanosized shapes can be prepared by simply tuning the water content of the precursor hydrogels and the crystallization time. The morphological properties of LTL zeolites are also found to have pronounced influences on their surface properties (surface areas, pore volumes, number of micropore channels, textural properties) and acidity (amount, strength and type) where these properties affect their catalytic activity in acylation of 2-methylfuran under non-microwave instant heating condition. Furthermore, the influence of temperature and heating time on the kinetics of catalytic acylation of 2-methylfuran, and the catalytic comparative study between nanosized LTL zeolite and several homogeneous and heterogeneous catalysts are also discussed.

6th International Conference and Postgraduate Colloquium for Environmental Research 2022 (POCER 2022) 9 - 11 June 2022
Langkawi, Kedah, Malaysia

PCR 08032022 – 17: SAPO-34 crystallized using novel pyridinium template as highly active catalyst for synthesis of ethyl levulinate biofuel

Yik-Ken Ma,[a] Stephen Chia,[b] T. Jean Daou,[c,d] Fitri Khoerunnisa,[e] Salah M. El-Bahy,[f] Zeinhom M. El-Bahy,[g] Tau Chuan Ling,[h] Eng-Poh Ng[a,*]

[a]*School of Chemical Sciences, Universiti Sains Malaysia, 11800 USM, Penang, Malaysia.*
[b]*Centre for Global Archaeological Research, Universiti Sains Malaysia, 11800 USM, Penang, Malaysia*
[c]*Université de Haute-Alsace, Axe Matériaux à Porosités Contrôlées, Institut de Science de Matériaux de Mulhouse UMR 7361, ENSCMu, 3b rue Alfred Werner, 68093 Mulhouse, France.*
[d]*Université de Strasbourg, 67000 Strasbourg, France.*
[e]*Chemistry Education Department, Universitas Pendidikan Indonesia, Jl. Setiabudhi 258, Bandung 40514, Indonesia.*
[f]*Department of Chemistry, Turabah University College, Taif University, P.O.Box 11099, Taif 21944, Saudi Arabia.*
[g]*Department of Chemistry, Faculty of Science, Al-Azhar University, Nasr City 11884, Cairo, Egypt.*
[h]*Institute of Biological Sciences, Faculty of Science, University of Malaya, 50603 Kuala Lumpur, Malaysia.*

*Corresponding author. E-mail address: epng@usm.my

Keywords: SAPO-34; 1-Propylpyridinium hydroxide; Levulinic acid; Ethy levulinate; Biofuel; Non-microwave instant heating

Extended Abstract

Silicoaluminophosphate Number 34 (SAPO-34) crystallized using novel *N*-heterocyclic organic template—1-propylpyridinium hydroxide ([PPy]OH)—as an excellent catalyst for the production of ethyl levulinate biofuel is reported. First, the time-dependent crystallization study of SAPO-34 using various spectroscopy, microscopy and analytical techniques is performed. As shown in "Figure 1", the precursor undergoes several important crystallization steps, namely dissolution of reactants (induction), nucleation and crystal growth of SAPO-34, before it transforms into a more metastable SAPO-36 crystalline phase. The resulting cubic-shaped SAPO-34 solid ($Si_{0.198}Al_{0.475}P_{0.327}O_2$) exhibits high porosity (S_{BET} = 673 m^2/g, V_{Tot} = 0.27 cm^3/g) and high Si content

(Si/(Si+Al+P) = 0.198) which contribute to high surface acidity (2.52 mmol/g) as confirmed by the NH_3-TPD analysis as shown in "Table 1". The SAPO-34 catalyst shows 93.4% conversion to ethyl levulinate *via* esterification of levulinic acid with ethanol just within 20 min at 190 °C under non-microwave instant heating "Figure 2A", which is considered very fast as compared to other systems. In addition, high catalyst recyclability is observed even after fifth cycle of reaction "Figure 2B", thus offering another promising pathway for crystallizing zeolites using this new class of template that are beneficial for catalytic biofuel upgrading process.

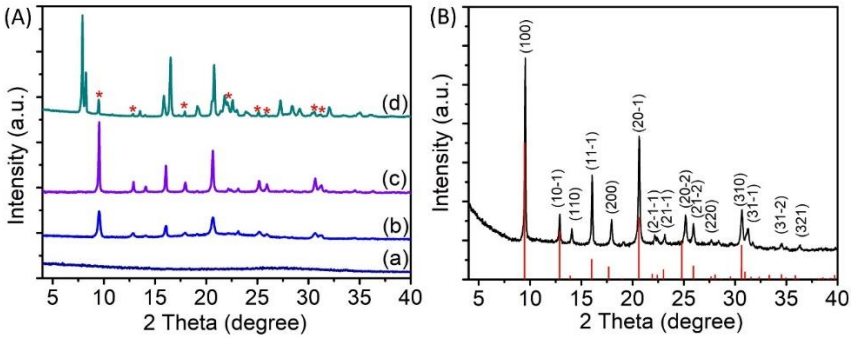

Figure 1: (A) XRD patterns of samples after (a) 0 h (amorphous), (b) 16 h (amorphous + SAPO-34), (c) 19 h (SAPO-34) and (d) 30 h (SAPO-34 + SAPO-36) of hydrothermal treatment. The asterisks in (d) show the presence of SAPO-34 as a minor competing phase for SAPO-36. (B) XRD pattern of A(c) after indexing and comparing with the theoretical CHA simulated pattern.

Table 1: Crystalline phase, chemical composition, porous and acid properties of solid samples treated at various times.

Sample	Product composition[a]	S_{BET} (m^2/g)[b]	S_{Mic} (m^2/g)[c]	V_{Tot} (cm^3/g)[d]	Acidity (mmol/g)[e]		
					100-300 °C	300-600 °C	Total
0 h	$Si_{0.018}Al_{0.424}P_{0.558}O_2$	87	0	0.07	0.01	0	0.01
16 h	$Si_{0.145}Al_{0.479}P_{0.376}O_2$	241	121	0.29	1.03	0.25	1.28
19 h	$Si_{0.198}Al_{0.475}P_{0.327}O_2$	673	661	0.27	1.26	1.26	2.52
30 h	$Si_{0.194}Al_{0.470}P_{0.335}O_2$	587	582	0.26	1.16	1.14	2.30

[a]Determined from ICP-OES; [b]Specific surface area; [c]micropore surface area; [d]total pore volume; [e]determined from NH_3-TPD

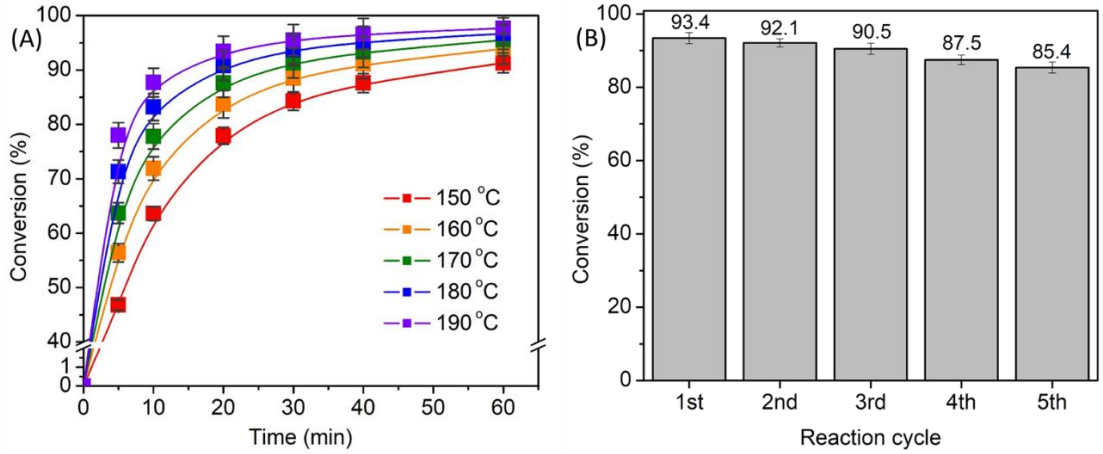

Figure 2. (A) Effect of temperature and time on the conversion of LA into ethyl levulinate biofuel additive in the presence of SAPO-34 and (B) catalyst recyclability test of SAPO-34.

Acknowledgements: The financial support from RUI (1001/PKIMIA/8011128) and Taif University Researchers Supporting Project (TURSP-2020/135) (Taif University, Saudi Arabia) is gratefully acknowledged.

PCR 10032022 – 18: Biodegradable Dual-Layer Polyhydroxyalkanoate (PHA)/Polycaprolactone (PCL) Mulch Film For Agriculture: Preparation And Characterization

Nor Azillah Fatimah Othman[1], Sarala Selambakkannu[1]*, Noriaki Seko[2]

[1]Radiation Processing Technology Division, Malaysia Nuclear Agency, Bangi, 43000 Kajang, Malaysia

[2]Takasaki Advanced Radiation Research Institute, Quantum Beam Science Research Directorate, 1233,Watanuki-machi, Takasaki 370-1292, Gunma, Japan

Abstract

This study focused on the preparation of biodegradable dual-layer mulch film based on polyhydroxyalkanoate (PHA) and polycaprolactone (PCL). The main aim of this study is to prepare mulch film which is completely biodegradable without generating any micro-plastics. The dual-layer mulch film is made of PHA as the first layer and a mixture of PHA and PCL at different ratios as the second layer. The ratio of PHA/PCL used was 90:10, 70:30, and 50:50. The dual-mulch film was prepared by using the hot-press technique and later was cross-linked by using electron beam irradiation in order to ensure the strong adherence between the two layers. The mixture of PHA/PCL films with different ratios, PHA and PCL virgin film were subjected to a soil burial bio-degradability test. The PHA and PCL virgin film had shown the highest degradation percentage. Therefore, further characterization was performed on dual-layer PHA/PCL (100%) based on their higher degradability tendency. The apparent properties, morphology, thermal stability, chemical composition, and mechanical properties of dual-layer PHA/PCL (100%) were tested thoroughly.

Keywords: Biodegradable mulch film, Polyhydroxyalkanoate, Polycaprolactone, Hot-press, Crosslinking.

1. Introduction

This study aims to investigate the biodegradability of PHA-based mulch film layered with polycaprolactone (PCL). Generally, the use of PHA solely for the formulation of plastic is unsuitable as the PHA is very inflexible. Thus, PCL was introduced in the formulation of biodegradable film since

PCL capable to act as plasticizer. The PHA-based mulch film with PCL was prepared in dual layers specifically to control the rapid UV degradation on the surface of the mulch film due to sunlight which usually shortens the life span and also to avoid the uneven degradation due to microbe decomposition at only one side that comes in contact with soil. The PCL possess the tendency to withstand rapid UV degradation. Meantime, PCL shows a much slower decomposition rate with microbial activities in soil. Thus, the dual-layer of PHA/PCL based mulch film is expected to own higher biodegradability at a slower rate. At first, the PHA was hot-pressed that followed by the second layer of PCL. However, as for the second layer, the melt compounding of PHA and PCL was performed at different ratios as well. The prepared film was further subjected to radiation crosslinking. The crosslinking yield was measured by gel content analysis. The biodegradability of the prepared film was investigated by performing soil burial test. The chemical composition, morphology, thermal, and mechanical properties of prepared PHA/PCL mulch film were investigated thoroughly.

2. Experimental

2.1. Melt-compounding

The PHA and PCL granules were pre-dried at 40°C for 24 hours in a vacuum oven prior to processing. The PHA was blended with PCL by mixing LABO Plastomill Model 50C150 (Toyoseki, Japan), with the total mass of 50 g for every batch. The formulations and compounding conditions are as shown in the Table 1.

Table 3. Formulations and compounding conditions

Sample (blends for second layer)	PHA (wt%)	PCL (wt%)	Rotor speed (rpm)	Temperature (ºC)	Time (min)
B1	100	0	-	190	10
B2	90	10	20	190	10
B3	70	30	20	190	10
B4	50	50	20	190	10
B5	0	100	-	190	10

2.2. Hot-press

The granules were placed in a mould, with thickness of 0.1 mm. Silicon mat was used as a protective layer on both sides. The sample was then placed in the hot-press which was set at predetermined temperature (185 ºC for 100 wt% PHA, 75 ºC for 100 wt% PCL, and 185 ºC for the mix-compound). The sample was pre-heated for 10 minutes before pressure was applied. The pressure was increased to 150 kg/cm^2 (=15 MPa) for 5 minutes and then cooled down to room temperature. The dual-layer film was prepared by melting the first layer (100 wt% PHA) at 185 ºC for 5 minutes, followed by layering the second layer (blend compound as shown in Table 1) and press it with 150 kg/cm^2 pressure for 5 minutes. The sample was then cooled down to room temperature.

2.3 Radiation Crosslinking

The radiation crosslinking was performed on PHA/PCL mulch film in batch by using EPS 3000 electron beam accelerator machine. The prepared mulch film was placed on petri dish with the dimension of 10 cm x 10 cm and been transported into irradiation chamber via conveyor system. The mulch film were irradiated with 30 kGy of irradiation dose, 2 MeV voltage, and 10mA current.

2.4 Soil Burial Test

The soil burial test was carried out in an open area with realistic conditions. The specimens of PHA/PCL mulch film with different ratios, virgin PHA and PCL were placed on a wire mesh and buried in soil shallowly. The final weight of the film after the burial was recorded on weekly basis. The degree of degradation was evaluated by weight loss (WL) by using the following equation (1) (La Mantia, Ascione, Mistretta, Rapisarda, & Rizzarelli, 2020).

$$\boldsymbol{WL}\ (\%) = {\left(\boldsymbol{W_{before} - W_{after}}\right)}/{\boldsymbol{W_{before}}} \times \mathbf{100} \qquad \textbf{(1)}$$

Where, W is the weight of the film before and after the established time of burial test.

2.4 Characterizations

Apparent and Morphological Properties: The thickness of the film obtained was measured using a hand-held dial thickness micrometer (Mitutoyo, Japan). The transparency of the film were determined using UV-Visible spectrophotometer Model (UV-1800, Shimadzu). Detailed observation of the two

layers were confirmed by Scanning Electron Microscopy (SEM). SEM SU350 (Hitachi, Japan) was performed at the voltage of 15.0 kV and current of 0.2 mA.

Thermal Analysis: The Differential Scanning Calorimetry (DSC) measurements were performed using approximately 5 mg of sample placed in sealed aluminium pans and loaded into the sampler on Thermo Plus DSC 8320 (Rigaku, Japan). The samples were analyzed for its thermal stability with Thermogravimetric Analyzer (Pyris 1 TGA, Perkin Elmer). The samples were heated from room temperature to 700 °C, with heating rate of 10 °Cmin^{-1}. Nitrogen flow was maintained at a rate of 50 ml min^{-1}.

Mechanical Analysis: Universal Testing Machine Model (Instron, USA) 2.5 kN was used to determine the tensile strength and elongation at break for each samples. Samples were cut into 50 mm × 12.7 mm at the gauge length according to ASTM D882. The tests were conducted with crosshead speed of 50 mm/min. Elongation at break, EL was calculated according to the equation (2) below.

$$\boldsymbol{EL = \left(d_{after} - d_{before}\right) / d_{before} \times 100} \quad \textbf{(2)}$$

Where, $\boldsymbol{d}$ is the distance between grips holding the sample before and after the sample breaks.

3. Results and Discussion

3.1 Apparent Test

The thickness and transparency of both single-layer PHA and PCL films along with double-layered PHA/PCL films with different blending ratios were reported in Table 2. According to the results obtained, the thickness of the single-layered film are much lower in comparison to dual-layered film. On the other hand, the transparency of single-layered film is much higher than doubled-layered film.

Table 2. Thickness and transparency of the single and double layer PHA/PCL mulch film

Film Type	**Thickness[b] (µm)**	**Transparency[c] (%T)**
Single-layer 100 wt% PHA (B1)	73.35	78.85
Single-layer	100.30	95.50

100 wt% PCL (B5)

Dual-layer[a]		
B1 + B5	175.25	78.45
B1 + B2	151.35	67.58
B1 + B3	168.75	70.25
B1 + B4	159.85	61.25

3.2 Biodegradability Test

In this study, the biodegradability of PHA/PCL film with different ratios, PHA and PCL films were investigated via a soil burial test. The result obtained on the soil burial degradation test is displayed in Figure 2. The appearance of the PHA/PCL film with the mixed ratio of 90/10, 70/30 and 50/50 remains almost intact. The mulch film with 100 % of PHA and PCL had shown some visual defects in terms of appearance.

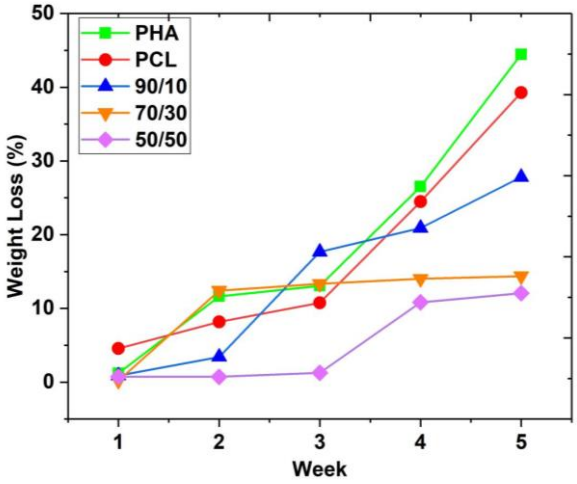

Figure 2. Weight loss values (%) vs. degradation time for double layered mulch film

3.3 Characterization of the PHA/PCL Double Layered Mulch Film

Further characterization was performed on the single layer of PHA (100%), the single layer of PCL (100%) and the dual-layer of PHA/PCL (100%).

3.3.1 Morphology

The surface morphology of a single layer of PHA (100%), single layer of PCL (100%), and dual-layer of PHA/PCL (100%) was shown in Figure 1.

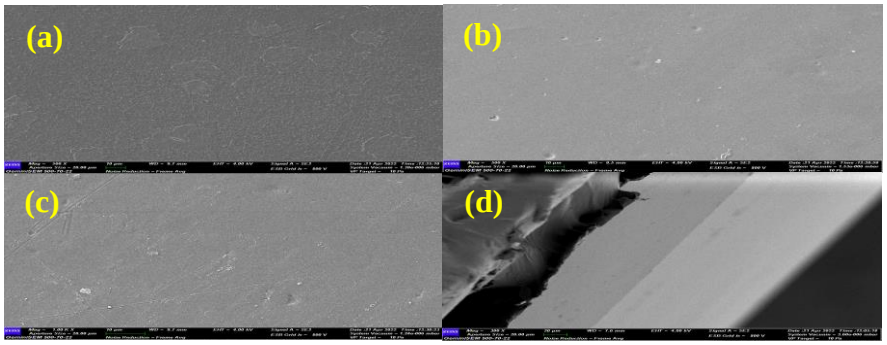

Figure 1. SEM images for (a) single-layer 100 wt% PHA film, (b) single-layer 100 wt% PCL film, (c) dual-layered film consisting PHA/PLA (100%) and (d) cross-section of dual-layered PHA/PLA (100%)

3.3.2 Thermal Properties

The thermogravimetric curves for single-layered PHA, single-layered PCL, and double-layered PHA/PCL (100%) are shown in Figure 2. Single-layered PHA film exhibits only single-step thermal degradation with good thermal stability. Meanwhile, single-layered PCL had shown two-step thermal degradation with good thermal stability, too. On the other hand, the double-layered PHA/PCL (100%) had shown three-steps degradation with poor thermal stability.

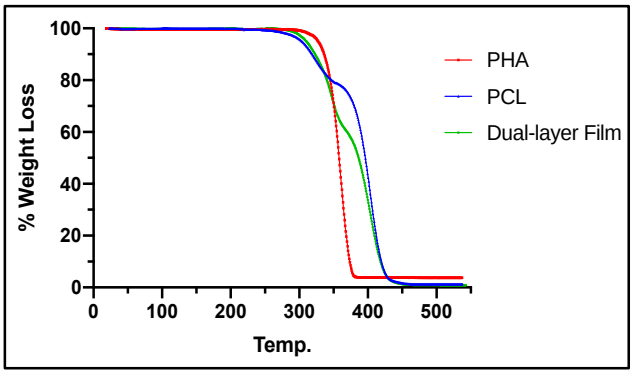

Figure 2. TGA for single-layer 100 wt% PHA film, single-layer 100 wt% PCL film and dual-layered film consisting PHA/PLA (100%)

Figure 3 shows the DSC thermograms of single-layered PHA, single-layered PCL, and double-layered PHA/PCL (100%). There was one endothermic peak on the thermogram of both single-layered PHA and single-layered PCL, respectively. On the other hand, two endothermic peaks were found on the thermogram of double-layered PHA/PCL (100%). The one endothermic peak of single-layered PHA described the melting behavior of PHA at the temperature of 170.2°C. Meanwhile, the melting behavior of PCL was detected at a temperature of 59.6°C. The hot-pressed and radiation cross-linked double-layered PHA/PCL (100%) demonstrated the shifting of the endothermic peak of PHA to 168.6 °C and PLA to 57.1 °C with a decrease in the area and intensity of the melting peak.

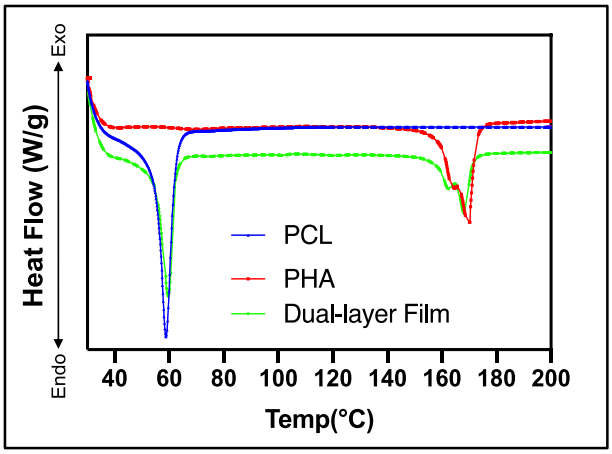

Figure 3. DSC thermogram for single-layer 100 wt% PHA film, single-layer 100 wt% PCL film and dual-layered film consisting PHA/PLA (100%)

3.3.3 Mechanical Analysis

The mechanical stability of single-layered PCL, and double-layered PHA/PCL (100%) was analyzed in this study and the result is reported in Table 3. The mechanical analysis on single-layered PHA film is unable to be performed due to its extreme brittleness. The single-layered PHA film with greater brittleness is unsuitable to be analyzed universal testing machine. The tensile strength and modulus of single-layered PCL are slightly higher in comparison to double-layered PHA/PCL (100%).

Table 3. Mechanical properties of single-layer 100 wt% PCL film and dual-layered film consisting PHA/PLA (100%)

Material	Young Modulus (MPa)	Ratio	Yield Stress (MPa)	Ratio	Stress at Break (MPa)	Ratio	Strain at Break (%)	Ratio	Toughness (kJ/m^3)	Ratio
PCL	330±10	1.0	12.0±0.4	1.0	24.0±0.4	1.0	334±10	1.0	40.4±0.8	1.0
PHA/PCL	306±15	0.9	11.4±0.5	0.9	20.5±0.4	0.8	357±10	1.1	42.4±1.2	1.0

4. Conclusion

The preparation of degradable mulch by using both PHA and PCL in different ratios was investigated in this study. The mulch film was prepared in dual-layer whereby the first layer was made of PHA and the second layer was made of a mixture of PHA/PCL at different ratios. The dual-layer mulch film was prepared via the hot-press technique and further cross-linked by electron beam irradiation. The soil burial biodegradability test had shown that dual-layered mulch film made of PHA/PCL (100%) possesses a higher degradability percentage.

Acknowledgement

This research was partially supported by Malaysia Nuclear Agency, Bangi.

Reference

La Mantia, F. P., Ascione, L., Mistretta, M. C., Rapisarda, M., & Rizzarelli, P. (2020). Comparative investigation on the soil burial degradation behaviour of polymer films for agriculture before and after photo-oxidation. *Polymers*, *12*(4), 753.

6th International Conference and
Postgraduate Colloquium for
Environmental Research 2022 (POCER
2022) 9 - 11 June 2022
Langkawi, Kedah, Malaysia

PCR 10032022 – 19: Electrochemical evaluation of nickel oxide addition toward lanthanum strontium cobalt ferrite cathode for intermediate temperature solid oxide fuel cell (IT-SOFCs)

Ahmad Fuzamy Mohd Abd Fatah[a], Ahmad Zaki Rosli [a], Ahmad Azmin Mohamad,[b*] Andanastuti Muchtar,[c] Muhammed Ali,[c] Noorashrina Abdul Hamid[a*]

[a] School of Chemical Engineering, Engineering Campus, Universiti Sains Malaysia, 14300 Nibong Tebal Penang, Malaysia

[b] School of Materials & Mineral Resources, Engineering Campus, Universiti Sains Malaysia, 14300 Nibong Tebal Penang, Malaysia

[c] Fuel Cell Institute, Universiti Kebangsaan Malaysia, UKM, 43600 Bangi, Selangor, Malaysia

- Corrensponsing Author E-mail: chrina@usm.my*

Keywords: Solid oxide fuel cell, Oxygen reduction reaction, Optimization, LSCF, Nickel oxide

Extended Abstract

Research towards lanthanum, strontium, cobalt, ferrite (LSCF) has gained much attention towards SOFC type cathode lately and various work has been done to improve the catalytic activity of the cathode which mainly revolves around the oxygen reduction reaction (ORR) process **(Ahmad et al., 2022; Tahir et al., 2022; Zarabi Golkhatmi et al., 2022)**. Several suggest that addition of nickel oxide (NiO) capable to improve the catalytic activity of LSCF cathode primarily at intermediate temperature operation **(Guo et al., 2015; Nadeem et al., 2018; Wang et al., 2016)**. Previous work also suggest that addition of nickel oxide toward LSCF capable to sustain nanosize particle even after calcined at 800 ^{o}C **(Rosli et al., 2021)**. However, in detail explanation regarding the oxygen reduction reaction process occurred in low frequency and high frequency was not discussed in previous work. In this work, addition of nickel oxide towards LSCF is primarily investigated in term of optimization ratio LSCF:NiO, bode phase peak of low frequency and high frequency of bare LSCF and LSCF-NiO together with several characterization to support the result. Phase analysis revealed that two-phase LSCF and NiO was succesfully be synthesized via enhanced modified sol gel method at 800 ^{o}C calcination temperature. Thermal and bonding anlysis further support the result from phase analysis

where LSCF-NiO synthesize via enhanced modified sol gel method indeed suitable to be synthesized aslow as 800 ^{o}C calcination temperature. Comparison specific surface area towards LSCF with addition of 3 wt%, 5 wt%, 7 wt% and 9 wt% of NiO was done and it is revealed that addition 5 wt% of NiO gives the highest value of specific surface area among candidates. Electrochemical analysis suggested addition 5 wt% of NiO toward LSCF cathode capable to reduce the area specific resistacne (ASR) from 0.088 Ω cm^2 to 0.055 Ω cm^2 at 800 ^{o}C operating temprature. Bode phase plot further confirmed the improvement of ORR process as low frequency area specific resistance (ASR) was reduce significantly from 0.070 Ω cm^2 to 0.030 Ω cm^2 as same working temperature. Even at 600°C operating temperatures, adding 5% nickel oxide to LSCF improves peak power density and allows it to perform better than bare LSCF. Surface morphology and specific surface area analyses agrees that the LSCF-NiO effectively produces nanosized particles which much lower that previous work. Elemental analysis verifies the presence of NiO on the cathode surface, showing a uniform distribution of NiO on the cathode layer.

Acknowledgements: This work was financially supported by Ministry of Higher Education (MOHE) Malaysia under Fundamental Research Grant Scheme (Grant No: 203/PJKIMIA/6071482).

References

Ahmad, M. Z., Ahmad, S. H., Chen, R. S., Ismail, A. F., Hazan, R., & Baharuddin, N. A. (2022). Review on recent advancement in cathode material for lower and intermediate temperature solid oxide fuel cells application. *International Journal of Hydrogen Energy*, *47*(2), 1103-1120. https://doi.org/10.1016/j.ijhydene.2021.10.094

Guo, S., Wu, H., Puleo, F., & Liotta, L. (2015). B-Site Metal (Pd, Pt, Ag, Cu, Zn, Ni) Promoted La1−xSrxCo1−yFeyO3–δ Perovskite Oxides as Cathodes for IT-SOFCs. *Catalysts*, *5*(1), 366-391. https://doi.org/10.3390/catal5010366

Nadeem, M., Hu, B., & Xia, C. (2018). Effect of NiO addition on oxygen reduction reaction at lanthanum strontium cobalt ferrite cathode for solid oxide fuel cell. *International Journal of Hydrogen Energy*, *43*(16), 8079-8087. https://doi.org/10.1016/j.ijhydene.2018.03.053

Rosli, A. Z., Somalu, M. R., Osman, N., & Hamid, N. A. (2021). Physical characterization of LSCF-NiO as cathode material for intermediate temperature solid oxide fuel cell (IT-SOFCs). *Materials Today: Proceedings*. https://doi.org/10.1016/j.matpr.2021.01.778

Tahir, N. N. M., Baharuddin, N. A., Samat, A. A., Osman, N., & Somalu, M. R. (2022). A review on cathode materials for conventional and proton-conducting solid oxide fuel cells. *Journal of Alloys and Compounds*, *894*. https://doi.org/10.1016/j.jallcom.2021.162458

Wang, Y.-P., Xu, Q., Huang, D.-P., Zhao, K., Chen, M., & Kim, B.-H. (2016). Evaluation of La 1.8 Sr 0.2 NiO 4+δ as cathode for intermediate temperature solid oxide fuel cells. *International Journal of Hydrogen Energy*, *41*(15), 6476-6485. https://doi.org/10.1016/j.ijhydene.2016.03.019

Zarabi Golkhatmi, S., Asghar, M. I., & Lund, P. D. (2022). A review on solid oxide fuel cell durability: Latest progress, mechanisms, and study tools. *Renewable and Sustainable Energy Reviews*, *161*. https://doi.org/10.1016/j.rser.2022.112339

PCR 10032022 – 20: Design of microbial cell factories for sustainable production of biofuels

Rupesh Maurya [a], Nisarg Gohil [a], Iqra Mariam [b] , Mukul Suresh Kareya [b] , Asha Arumugam Nesamma [b] , Pannaga Pavan Jutur [b] , Snovia Nixon [c], Nilesh Kumar [d,e] , Shriya Hans [d] , Shalini S. Deb [e] , Santosh B. Noronha [c] , Shamlan M. S. Reshamwala [e] , Debarun Dhali [f] , Heykel Trabelsi [g] , Gargi Bhattacharjee [a] , Khushal Khambhati [a] , Khalid J. Alzahrani [h] , Janardhan Keshav Karapurkar [i] , Suresh Ramakrshna [i,j]* , Vijai Singh [a]*

[a] Department of Biosciences, School of Science,
Indrashil University, Rajpur, Mehsana-382715, Gujarat, India

[b] Omics of Algae Group, Industrial Biotechnology,
International Centre for Genetic Engineering and Biotechnology, Aruna Asaf Ali Marg, New Delhi

[c] Department of Chemical Engineering,
Indian Institute of Technology Bombay, Mumbai, India

[d] M.Tech. programme in Bioprocess Engineering,
Institute of Chemical Technology, Mumbai, India

[e] DBT-ICT Centre for Energy Biosciences,
Institute of Chemical Technology, Mumbai, India

[f] EV Biotech BV, Zernikelaan 8, 9747 AA Groningen, The Netherlands

[g] Carbocode GmbH, Byk-Gulden-Strasse 2, 78467 Konstanz, Germany

[h] Department of Clinical Laboratories Sciences, College of Applied Medical Sciences,
Taif University, P.O. Box 11099, Taif 21944, Saudi Arabia

[i] College of Medicine,
Hanyang University, Seoul, South Korea

[j] Graduate School of Biomedical Science and Engineering,

Hanyang University, Seoul, South Korea

- Correnspondsing Author E-mail: SR: suri28@hanyang.ac.kr

VS: vijaisingh15@gmail.com / vijai.singh@indrashiluniversity.edu.in

Keywords: Biofuels; microbial cell factories; metabolic pathways; microorganisms; scale up; optimization; genome editing

Extended Abstract

Currently increasing the oil price and the long term energy security have increased the demands for design of microbial cell factories for biofuels production in a renewable and sustainable manner. Biofuels are cleaner, safer and economical source of energy. Number of microorganisms have been engineered successfully with the help of synthetic biology, metabolic engineering and genome editing for large scale production of biofuels and advanced biofuels. Number of fermentation optimization conditions and used for large scale up of biofuels production in designed microorganisms have been mentioned. In this review, we highlight recent development of design of number of MCFs and their challenge and opportunities for production of biofuels for industrial scale with economical prices.

6th International Conference and
Postgraduate Colloquium for
Environmental Research 2022 (POCER
2022) 9 - 11 June 2022
Langkawi, Kedah, Malaysia

PCR 12032022 – 21: Optimization of Screening Media for The Identification and Isolation of Waste Edible Oil-Degrading Lipolytic Microorganisms from Food Wastes

Sook Sin Chan[a,b], Arun Suria Karnan Mahendran[b], Yin Sze Lim[b], Cheng Foh Le[b], Tau Chuan Ling[a]

[a] Institut Biologi Sains, Fakulti Sains, Universiti Malaya, Kuala Lumpur, Malaysia.
[b] School of Biosciences, Faculty of Science and Engineering, University of Nottingham Malaysia, Semenyih, Malaysia.

Corresponding Author E-mail: chengfoh.le@nottingham.edu.my

Keywords: Waste Edible Oil; Food Waste; Copper Soap Test; Lipolytic Bacteria; Bioremediation

Extended Abstract

Municipal solid waste is a major issue globally as a result of urban migration, population expansion, variable consumption modes and abilities, and rapid development. According to Wah and Osman, the generation of daily waste in Peninsular Malaysia was estimated to be 0.8kg per capita per day (Wah and Osman, 2014). Daily wastes are generally made up of food wastes (45%), plastics wastes (24%), glasses (18%), papers (7%), and metals (6%) (Wong et al., 2019). Fat, starch and protein are the three main constituents of kitchen waste, which account for about 80% of dry kitchen waste (Wang et al., 2016). Cooking oil is one of the essential ingredients in almost all types of food preparation. Waste edible oil (WEO) is an oil-based substance comprising of animal and vegetable matter that has been utilized in cooking or preparation of foods and is no longer appropriate for human consumption (Gui et al., 2008). The presence of fats, oils, and greases (FOGs) and WEO in kitchen waste and wastewater is imposing severe environmental problems due to foul odours, blockage of sewer lines, difficulty to be degraded, and highly toxic to the aquatic organisms (Ferronato and Torretta, 2019). Lipolytic microorganisms are capable of degrading lipid-based macromolecules and are highly valuable in the biodegradation and bioremediation of WEOs contamination. A simple and effective screening media would further enhance the isolation and identification of lipolytic microorganisms. In this study, different types of screening media comprising phenol-red and peptone-yeast media supplemented with specific lipid components (olive oil, butter, ghee) were tested for their efficiency. Inoculation was introduced by spread plate, drop a plate or well diffusion methods. The assay endpoint was determined using a copper soap test. Peptone yeast agar (PYA) was then utilised to screen for the presence of lipolytic bacteria and the corresponding lipid degrading activity on various food wastes and soil-incubated food wastes used as the direct substrates. It is highly applicable with the WEOs instead of using a lipid surrogate such as tributyrin or Tween-20. The assay can also be applied for the screening of lipolytic fungi. We have isolated a total of three highly potent lipolytic bacteria which were identified to be *Klebsiella pneumoniae* (isolate A9), *Acinetobacter nosocomialis*/*Acinetobacter seifertii* (isolate A10), and *Klebsiella aerogenes* (isolate B2) using the 16s rRNA sequencing method. From the results, the copper soap test using the spread plate method on PYA produced the ideal screening outcome (in terms of visualisation) for the future identification and isolation of lipolytic microorganisms. Future studies shall focus on enhanced expression and purification of lipases from these strains for potential applications in WEO bioremediation and food waste management.

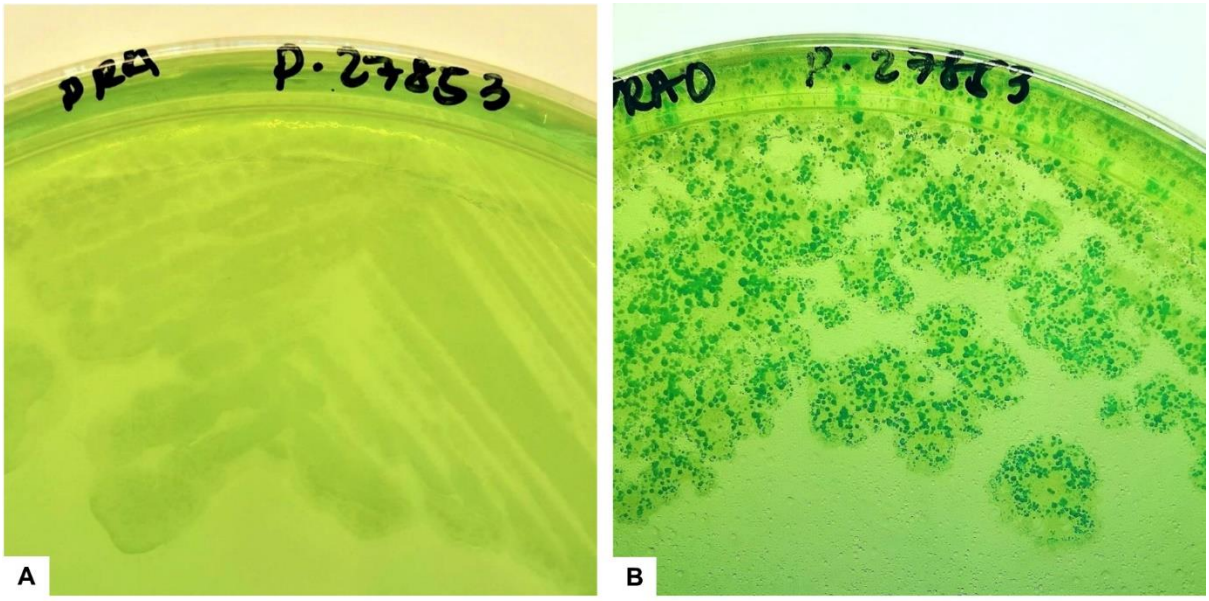

Figure 5: Copper soap test showing dense depositions of green precipitates with *Pseudomonas aeruginosa* ATCC 27853 on a phenol-red agar with olive oil (PRAO) spread plate. (A) *P. aeruginosa* ATCC 27853 on PRA (without oil supplementation) showed normal colony morphology and no formation of precipitation was seen. (B) The same strain on PRAO showed deposition of dense green precipitates surrounding individual colonies due to the breakdown of oil and formation of the green fatty acids-copper compound.

Acknowledgements: This work was supported by the School of Biosciences Research Project Fund 2019/20, University of Nottingham Malaysia.

References

Ferronato, N., and Torretta, V. (2019). Waste mismanagement in developing countries: A review of global issues. In International Journal of Environmental Research and Public Health. Vol. 16, Issue 6. https://doi.org/10.3390/ijerph16061060

Gui, M. M., Lee, K. T., and Bhatia, S. (2008). Feasibility of edible oil vs. non-edible oil vs. waste edible oil as biodiesel feedstock. Energy, 33(11), 1646–1653. https://doi.org/10.1016/j.energy.2008.06.002

Wah, C. K., and Osman, S. (2014). Current Patterns Of Waste Segregation Behaviour At Source Among Households In Putrajaya. Jurnal Pengguna Malaysia, 1–12.

Wang, Zhou, C., He, W., Zhu, H., Huang, J., and Li, G. (2016). The Content Variation of Fat, Protein and Starch in Kitchen Waste Under Microwave Radiation. Procedia Environmental Sciences, 31, 530 – 534. https://doi.org/10.1016/j.proenv.2016.02.075

Wong, D., Mun, H. H., Tuan, J., Poh, M., and Lee, M. (2019). Zero Waste Event Handbook 2019. Zero Waste Malaysia.

6th International Conference and
Postgraduate Colloquium for
Environmental Research 2022 (POCER
2022) 9 - 11 June 2022
Langkawi, Kedah, Malaysia

PCR 12032022 – 22: Electrocoagulation Process For the Treament of Soaked Pepper Berries: Kinetic Modeling and Some Physical Properties

Puteri Nurain Megat Ahmad Azman[a], Rosnah Shamsudin[ab*], Hasfalina Che Man[c] and Mohammad Effendy Ya'acob[a]

[a] Department of Process and Food Engineering, Faculty of Engineering,
Universiti Putra Malaysia, 43400 Serdang, Selangor, Malaysia

[b] Institute of Nanoscience and Nanotechnology,
Universiti Putra Malaysia, 43400 Serdang, Selangor, Malaysia

[c] Department of Biological and Agricultural Engineering, Faculty of Engineering,
Universiti Putra Malaysia, 43400 Serdang, Selangor, Malaysia

- Corresponding Author E-mail: rosnahs@upm.edu.my

Extended Abstract

The focus of this study is to evaluate the performance of the electrocoagulation process on some physical properties for treating soaked pepper berries using stainless steel and aluminium electrodes and develop kinetic models. The retting process using electrocoagulation was conducted by having pepper berries soaked in 1000 ml of water for 7 days. The findings indicate that the soaked pepper berries for stainless steel electrodes have the highest reduction of diameter, 22.07%. Both stainless steel and aluminium electrodes have the same reduction difference of 35.29% and 3.88% in weight and volume of soaked pepper berries. The soaked pepper berries for aluminium electrodes have the highest total colour change (87.76%). Additionally, some physical properties of the soaked pepper berries were adequately expressed by zero, first and second-order kinetic models. Therefore, these findings are useful information and provide novel insights into the acceleration of the retting process of pepper berries to produce white pepper.

Keywords: Pepper berries; physical; retting; electrocoagulation; kinetics

Equations

$$\Delta E = \sqrt{(L^t - L_o)^2 + (a^t - a_o)^2 + (b^t - b_o)^2} \quad (1)$$

Where, ΔE = total colour change; L^t, a^t, b^t = the measured colour values at certain time; L_o, a_o, b_o = the initial measured colour values.

$$Zero\ order = C = -kt + C_0 \quad (2)$$

$$First\ order = \ln C = -kt + \ln C_0 \quad (3)$$

$$Second\ order = \frac{1}{C} = kt + \frac{1}{C_0} \quad (4)$$

Where, C = the measured value for each parameter of water quality; C_0 = the initial value of the measured parameter of water quality; k = the rate constant; t = the retting time.

Table

Table 1. Kinetics of the effect of electrocoagulation on some physical properties of soaked pepper berries

Properties	**Electrode**	**Zero-Order Model**		**First-Order Model**		**Second-Order Model**	
		k (mm day^{-1})	R^2	k (day^{-1})	R^2	k (mm^{-1}day^{-1})	R^2
Diameter	SS	0.160	0.964	0.032	0.956	0.006	0.977
	Al	0.179	0.985	0.036	0.982	0.007	0.946
Properties	**Electrode**	**Zero-Order Model**		**First-Order Model**		**Second-Order Model**	
		k (g day^{-1})	R^2	k (day^{-1})	R^2	k (g^{-1} day^{-1})	R^2
Weight	SS	0.009	0.932	0.065	0.920	0.464	0.900
	Al	0.009	0.960	0.064	0.962	0.462	0.957
Properties	**Electrode**	**Zero-Order Model**		**First-Order Model**		**Second-Order Model**	
		k (m^3 day^{-1})	R^2	k (day^{-1})	R^2	k (m^{-3} day^{-1})	R^2

Volume	SS	1.00×10^{-8}	0.955	0.079	0.972	6.450×10^{5}	0.976
	Al	9.00×10^{-9}	0.969	0.071	0.967	5.753×10^{5}	0.957

Properties	**Electrode**	**Zero-Order Model**		**First-Order Model**		**Second-Order Model**	
		k (day^{-1})	R^2	k (day^{-1})	R^2	k (day^{-1})	R^2
ΔE	SS	0.572	0.779	0.292	0.729	0.187	0.672
	Al	0.490	0.880	0.333	0.804	0.311	0.687

Data are expressed SS, stainless steel electrodes; Al, aluminium electrodes; ΔE, total colour change; k, rate constant (day^{-1}); R^2, coefficient.

Figure

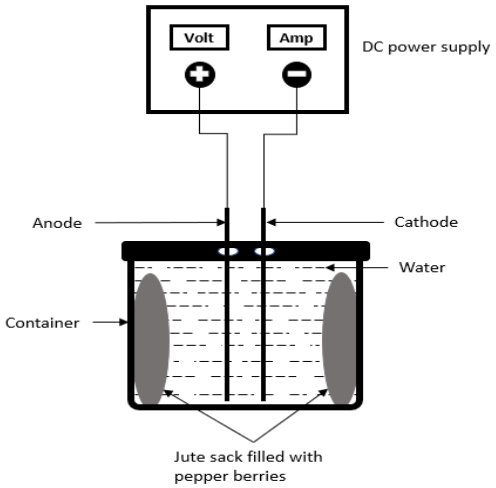

Figure 1. A schematic representation of the experimental set-up

Acknowledgement: The authors would like to express their appreciation to Universiti Putra Malaysia for the financial and technical support given during conducting this research work.

6th International Conference and
Postgraduate Colloquium for
Environmental Research 2022 (POCER
2022) 9 - 11 June 2022
Langkawi, Kedah, Malaysia

PCR 14032022 – 23: Modification and characterization of plant-based natural coagulants (PBNC) for application in drinking water treatment – A review

Ibrahim-Muntaqa Tijjani-Usman[a,d], Lavania Baloo[a], Lam Man Kee[b,c], and Yeek-Chia Ho[a*]

[a] Department of Civil and Environmental Engineering, Centre of Urban Resource Sustainability, Institute of Self-Sustainable Building, Universiti Teknologi PETRONAS, 32610, Seri Iskandar, Perak Darul Ridzuan, Malaysia.

[b] Department of Chemical Engineering, Universiti Teknologi PETRONAS, 32610, Seri Iskandar, Perak Darul Ridzuan, Malaysia.

[c] HICoE-Centre for Biofuel and Biochemical Research, Institute of Self-Sustainable Building, Universiti Teknologi PETRONAS, 32610, Seri Iskandar, Perak, Malaysia.

[d] Department of Agricultural and Environmental Engineering
Bayero Univeristy, Kano, Nigeria

- Corrensponding Author E-mail: yeekchia.ho@utp.edu.my

Keywords: Plant-based natural coagulants; modification; characterization; coagulation; water treatment.

Extended Abstract

1.0. Introduction

The use of conventional chemical coagulants in drinking water treatment has been found to leave traces of chemical residues in the water filtrate, which have been linked to the cause of some neurogenerative and neurotoxic diseases. Although plant-based natural coagulants (PBNC) are promising, but their biological instability has rendered them unsuitable for application. Therefore, the need to modify these PBNC to suit their application is necessary, since an alternative to the chemical-based coagulants is inevitable. The mini review paper investigates modification via microwave-assisted grafting copolymerization in the production of new products as coagulants, and the use of some characterization techniques to verify the new product physiochemical properties.

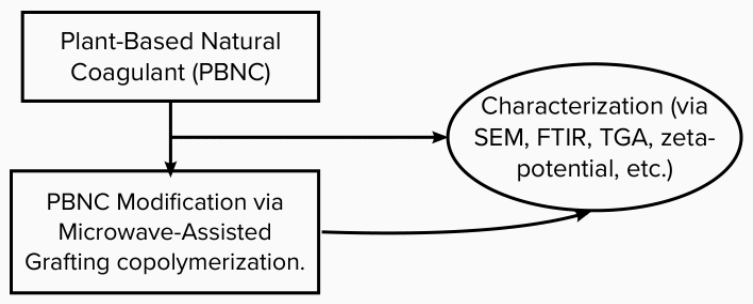

Figure 1: A graphical presentation of the mini review

2.0. Modification Methods

Three methods for modification of polymer properties include blending, curing, and grafting. 'Grafting' is a method of modification where monomers are modified by being covalently bonded onto the polymer chain. In plant polysaccharides modification, grafting copolymerization is the most used method in which high-energy-initiated grafting copolymerization is preferred, also refered to as radiation induced grafting copolymerization. Types of radiation-induced grafting copolymerization include photochemical radiation, gamma radiation, UV radiation, and microwave radiation grafting copolymerization (Nayak et al., 2018; Setia, 2018). Among the types of radiation-induced methods, microwave radiation is often use which is further sub-divided into microwave-initiated, microwave-assisted, and microwave grafting using solid media. The microwave-assisted grafting copolymerization is found to be the most used method because it involves the use of initiators which major advantage is the production of initial radical in a quick and very efficient time with the effect of the microwave radiation, and an improvement in grafting efficeincy is attained. Table 1 gives some examples of plant polysaccharides modified using microwave-assisted grafting copolymerization and their usage as potential flocculants in water treatment.

Table 1: Examples of PBNC-g-copolymers use as flocculants in water treatment

PBNC	Initiator	PBNC-g-copolymer	Effluent treated	Reference
Lentil extract (LE)	DMC	LE-g-DMC	Kaolin suspension and Agricultural wastewater	(Chua, Chong, et al., 2020; Chua, Show, et al., 2020)

Gum Ghatti (GGt)	PAM	GGt-g-PAM	Kaolin suspension and municipal wastewater	(Rani et al., 2012)
Etc.				

DMC - 2-methacryloyloxyethyl trimethyl ammonium chloride; PAM - polyacrylamide

3.0. Characterization Techniques

Physiochemical properties of PBNC and its modified products are evaluated to confirm the modification process. Scanning electron microscopy (SEM) indicates surface morphology and particle distribution of material; Fourier transform infra-red spectroscopy (FTIR) identifies functional groups of materials; Thermogravimetric Analysis (TGA) shows physical properties of materials; Energy dispersive X-ray (EDX) indicates elemental composition of material, etc.

4.0. Conclusions

This mini review provides an overview of the use of microwave-assisted grafting copolymerization of PBNC for their application in drinking water treatment. The initial characterization gives the existing properties of the PBNC, and after modification, the new product is characterised to confirm the modification process by identifying new properties that are not present in the native PBNC. The major aim of the modification is to enhance the water treatment efficiency of the PBNC.

Acknowledgements: The authors would like to acknowledge the Ministry of Higher Education Malaysia for the funding under the Fundamental Research Grant Scheme grant with project code 015MA0-106 (Ref: FRGS/1/2020/TK0/UTP/02/18). Also, the authors would also like to thank Universiti Teknologi PETRONAS for providing all the necessary facilities for this research. Lastly, the technical advice and assistance from Madam Norhayama Bt Ramli from Environmental Engineering Laboratory, UTP.

References

Chua, Chong, Mustafa, Mohamed-Kutty, Sujarwo, AbdulMalek, Show, & Ho. (2020). Microwave radiation-induced grafting of 2-methacryloyloxyethyl trimethyl ammonium chloride onto lentil extract (LE-g-DMC) as an emerging high-performance plant-based grafted coagulant. *Sci Rep*, *10*(1), 3959. https://doi.org/10.1038/s41598-020-60119-x

Chua, Show, Chong, & Ho. (2020). Lentil waste as novel natural coagulant for agricultural wastewater treatment. *Water Sci Technol*, *82*(9), 1833-1847. https://doi.org/10.2166/wst.2020.409

Nayak, A. K., Bera, H., Hasnain, M. S., & Pal, D. (2018). Synthesis and Characterization of Graft Copolymers of Plant Polysaccharides. In *Biopolymer Grafting: Synthesis and Properties* (pp. 1-62). https://doi.org/10.1016/b978-0-323-48104-5.00001-9

Rani, P., Sen, G., Mishra, S., & Jha, U. (2012). Microwave assisted synthesis of polyacrylamide grafted gum ghatti and its application as flocculant. *Carbohydrate Polymers*, *89*(1), 275-281. https://doi.org/10.1016/j.carbpol.2012.03.009

Setia, A. (2018). Applications of Graft Copolymerization. In *Biopolymer Grafting: Applications* (pp. 1-44). https://doi.org/10.1016/b978-0-12-810462-0.00001-6

6th International Conference and
Postgraduate Colloquium for
Environmental Research 2022 (POCER
2022) 9 - 11 June 2022
Langkawi, Kedah, Malaysia

PCR 11042022 – 24: Recycling of Spent Primary Batteries as Catalysts for VOCs Removal

Young-Kwon Park[a], and Sang-Chul Jung[b], Sang Chai Kim[c*]

[a] School of Environmental Engineering
University of Seoul, Seoul, Republic of Korea

[b]Department of Environmental Engineering
Sunchon National University, Sunchon, Republic of Korea

[c] Department of Environmental Education
Mokpo National University, Muan, Republic of Korea

- Corrensponsing Author E-mail: gikim@mnu.ac.kr

Keywords: Spent primary battery; Catalyst; VOCs; Recycle; Oxidation

Extended Abstract

Because a large amount of spent primary batteries is generated and cause environmental problems, recycling or disposal of spent primary batteries are necessary. In this work, a spent primary battery-based (SB) catalyst was prepared from the black mass (BM) of the spent primary batteries of R and D companies and tested in the complete oxidation of volatile organic compounds (VOCs) to examine whether the BM of spent primary batteries can be used as catalyst materials.

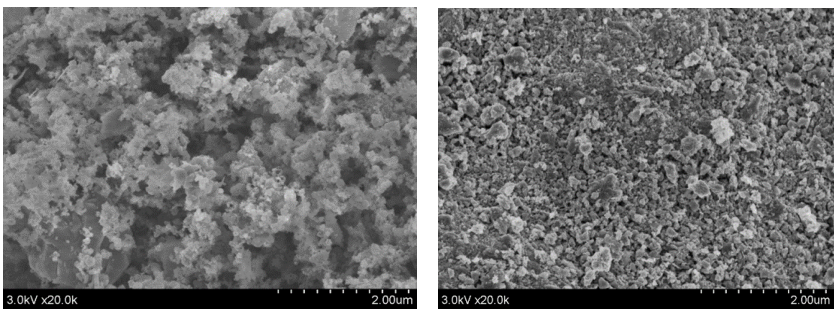

(a) (b)

Figure 1. SEM images (a) RSB and (b) DSB catalysts

The SEM images of the RSB catalyst show that the catalyst surface looks like swollen blossoms (Fig. 1 (a)). On the other hand, the surface of DSB seems to have melted or spread small particles (Fig. 1(b)). From these morphologies, it could be inferred that the surface area of the RSB catalyst may be larger than that of DSB catalyst.

Table 1. Components of RSB and DSB catalyst measured by SEM/EDX.

The surface elements of the RSB catalyst were composed of manganese, iron, zinc, oxygen, carbon, chlorine, aluminum, sodium, silica and potassium, while those of the DSB catalyst consisted of manganese, zinc, oxygen, carbon and potassium. The main transition metal components of the RSB catalyst were manganese, iron, and zinc, while that of the DSB catalyst was manganese.

Table 2. Textual properties of the RSB and DSB catalysts.

Catalyst	BET surface area (m^2/g)	Mean pore diameter (nm)	Total pore volume (cm^3/g)
RSB	45.1	16.0	0.18
DSB	31.1	15.1	0.11

The BET surface areas of the RSB and DSB catalysts were 45.1 m^2/g and 31.1 m^2/g, respectively. In addition, their mean pore diameters and total pore volumes were 16.0 nm and 0.18 cm^3/g, and 15.1 nm and 0.11 cm^3/g, respectively. The RSB catalyst had a larger BET surface area, mean pore diameter and total pore volume than the DSB catalyst.

Elements (wt. %)	Mn	Zn	Fe	O	C	Cl	Al	Na	Si	K
RSB	24.1	7.0	8.2	28.8	24.6	0.1	1.5	0.4	5.0	0.2
DSB	50.4	0.4	-	29.7	19.0	-	-	-	-	0.5

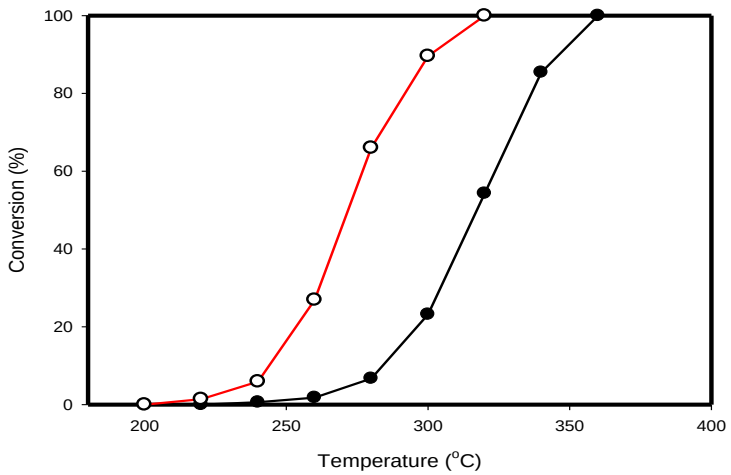

Figure 2. Toluene conversion according to reaction temperature.
(Reaction conditions: reactant concentration = 1,000 ppm, GHSV = 50,000 h^{-1}).
● RSB catalyst ○ DSB catalyst

Toluene was completely oxidized at 360℃ on the RSB catalyst and at 320℃ on theDSB catalyst.

Acknowledgements: The authors thank the the Basic Science Research Program the National Research Foundation of Korea (NRF) funded by the Ministry of Science and ICT (2022R1A2C1006391).

References

De Souza, C.C.B.M., De Oliveira, D.C., Tenorio, J.A.S., 2001. Characterization of used alkaline batteries powder and analysis of zinc recovery by acid leaching. J.Power Sources 103 (1), 120–126.

Kierkegaard, S., 2007. EU battery directive, charging up the batteries: squeezing more capacity and power into the new EU battery directive. Comput. Law Secur.Rep. 23, 357–364

Li, Y., Xi, G., 2005. The dissolution mechanism of cathodic active materials of spent Zn–Mn batteries in HCl. J. Hazard. Mater. B127, 244–248

Sayilgan, E., Kukrer, T., Civelekoglu, G., Ferella, F., Akcil, A., Veglio, F., Kitis, M., 2009. A review of technologies for the recovery of metals from spent alkaline andzinc–carbon batteries. Hydrometallurgy 97, 158–166.

6th International Conference and
Postgraduate Colloquium for
Environmental Research 2022 (POCER
2022) 9 - 11 June 2022
Langkawi, Kedah, Malaysia

PCR15032022 – 26: How Effective are Consumers' Perceived Value? Using Behavioural Insightto Promote Solar Energy Adoption in Urban Households

Norzalina Zainudin [a,*] , Shazleen Ilyana Sharifuddin [a] , Syuhaily Osman [a,b] , Zuroni Md Jusoh [a,b] , Husniyah Abd Rahim[a,b] , and Nurnaddia Nordin [c]

a Department of Resource Management and Consumer Studies, Faculty of Human Ecology, UniversityPutra Malaysia, Serdang, MALAYSIA
b Sustainable Consumption Research Group, Faculty of Human Ecology, University Putra Malaysia, Serdang, MALAYSIA
c Faculty of Entrepreneurship and Business, University Malaysia Kelantan, MALAYSIA

*Corresponding author: norzalina@upm.edu.my

Keywords: Solar Photovoltaic; Green Energy; Perceived Value: Behavioural; Urban Households; Extended Theory of Planned Behaviour.

Extended Abstract

The aim of this study is to test whether the perceived values intervention, designed basedonbehavioural theories can be effective in promoting solar energy adoption in urban Malaysia. Theeffect of the intervention was estimated through a survey questionnaires in Klang Valley. The studyproposed two comparison frameworks which the first is from the original Theory of PlannedBehaviour (TPB) and the second model is an Extended Theory of Planned Behaviour (ETPB). TheETPB model consists of eight variables namely as attitude, subjective norms, perceived behavioural control, perceived benefit, perceived compatibility, perceived cost, perceived complexity, andperceived performance. The data were evaluated using regression analysis. The model of ETPBconfirmed that subjective norm, perceived behavioural control, perceived compatibility, perceivedbenefit and perceived performance of solar PV affected the consumers' behavioral intention toinstall solar PV at home. The second model is also shown to have a better explanation of intention toinstall solar PV with the r-value of 0.605 compared to 0.467 for the TPB model. Based on what emergedfrom the analysis, the work could be understood as a useful tool for scholars and practitioners. Infact, it contributes to the scientific literature to the factor triggering consumer choices of green energy, andit also helps maximize the success of the government program by pointing out the levers tobeactionable for more to improve green business performance.

Introduction: Households' energy consumption is increasing in trend. The unsustainable energy supply of electricitygeneration from fossil fuel by most of the countries contributes to the increment of carbon dioxideinthe air which will cause global warming. Taking action on this issue, many of the countries have madeproactive action in utilizing the technical development of photovoltaic (PV) as an opportunityinproducing electricity at home. Net Energy Metering scheme has been implemented in Malaysiainpromoting green and sustainable energy production through solar PV (SEDA, 2016). This schemeaims to attract the involvement of Malaysian households in generating clean electricity throughtheinstallation of solar PV on their rooftop. Despite the government's effort to promote solar PVanddevelop this industry, several issues have been discovered to be the barriers to acceptance of greeninnovation products in Malaysia. Studies in most countries show consumer acceptance as a major challenge for manufacturers to develop and market green innovation products such as solar PV(Galarraga

et al. 2010). As a result, many countries that implement green innovation productsexperience difficulties and often rely on government policy support in the form of subsidies andtaxincentives (Sijm, 2002). Thus, this study uses the behavioral aspect in order to investigatetheinfluence factors of household intention to install solar PV. There are many studies that have beenused the Theory of Planned Behavior in analyzing the green behavioral aspect. This studythenextends the knowledge of this theory by adding the perceived value of consumers to the TPBmodel. Individual perceived value is an important aspect in marketing products, especially when the products are considered new in the market. They are many factors like convenience, cost, and performanceof the product that can contribute to the individual perceived value of a product. Since Solar PVisconsidered new to the Malaysian market, therefore, it is worth identifying how consumers perceivedthe value of solar PV which then may influence the adoption rate of solar PV in Malaysia. Marketingprofessionals may need to learn more about consumer perceived value and how it can affect businessprofits.

Methodology: Malaysian urban dwellers residing in the Klang Valley of Malaysia were surveyed using a face-to-facequestionnaire within 6 months of 2018 and 2019. Data was collected through a structured refinedresearch instrument that comprised scales to measure consumer behaviour using five Likert scales. The research instrument also included questions for generating the demographic profile of respondents. Analysis from Exploratory factor analysis (EFA) revealed the existence of eight underlyingfactorsnamely attitude, subjective norm, perceived behavioral control, perceived benefit, perceivedcompatibility, perceived cost, perceived complexity, and perceived performance that affects solar PVusage intention of urban households in Malaysia. Multiple linear regression analyses were usedtoexamine which variables were influencing factors for solar PV installation intention.

Findings: A total of 416 consumers completed the study. The theory of Planned Behaviour explained 46.7%of the variance in intention, with perceived behavioural control shows as the most dominant predictor. The additional perceived values variables (perceived benefit, perceived compatibility, perceivedcost, perceived complexity, and perceived performance) increased the amount of explained varianceinintention by 13.8%. The significant predictors of solar PV installation intention were the subjectivenorm, perceived behavioural control, perceived benefits, perceived compatibility and perceivedproduct performance. Results from the analysis confirm the importance of consumer perceivedvalueof solar PV product, which three predictors namely perceived compatibility (b=0.300), perceivedsolar PV performance (b=0.171), and perceived benefit (b=0.150).

Conclusion The extended theory of planned behaviour had a good predictive ability in explaining solar PVinstallation intention. The consumers' intention to install solar PV may be improved by improvingconsumers' perceived values on the solar PV product itself. The more positive value consumer put onsolar the higher the intention level to install solar in the future. The element of product performance, compatibility, and benefit of installing solar should be more highlighted in any promotionandinformation sharing in the future. Providing correct information about solar PV will improve their perception of the benefits and many other advantages of this green energy to household energymanagement. This paper is expected to provide valuable insight into the area of solar PVusageintention of urban consumers which can be an immense help to domestic and international marketersin dovetailing their marketing strategies and developing appropriate promotions messages. This paper also attempts to provide a glimpse into the nature of green energy purchasing behaviour of urbanMalaysian consumers under the Net Energy Metering

Program which has been scantily researched. Also, the roles of perceived values contribute to the worth of literature.

Acknowledgements: The authors thank the Universiti Putra Malaysia for the Fund project of IPM9562100.

References

Galarraga, I., González-Eguino, M., & Markandya, A. (2010). Evaluating the role of energy efficiencylabels: the case of Dish Washers.

SEDA. 2016. Annual Report 2018. Sustainable Energy Development Authority Malaysia. Putrajaya. www.seda.gov.my

Sijm, J. P. M. (2002). The performance of feed-in tarif s to promote renewable electricity in Europeancountries (Vol. 7). Energy research Centre of the Netherlands ECN.

6th International Conference and
Postgraduate Colloquium for
Environmental Research 2022 (POCER
2022) 9 - 11 June 2022
Langkawi, Kedah, Malaysia

PCR18032022 – 27: Kinect-Based Handedness-Invariant Badminton Movement Analysis and Recognition System

Jackie-Tiew-Wei Ting[a*], Huong-Yong Ting[a], Marcella Peter[a], Khairunnisa Ibrahim[b] and Keh-Kim Kee[c]

aDrone Research and Application Centre,
University of Technology Sarawak, Sarawak, Malaysia
bAdvanced Centre for Sustainable Socio-Economic and Technological Development,
University of Technology Sarawak, Sarawak, Malaysia
cSchool of Engineering and Technology
University of Technology Sarawak, Sibu, Sarawak, Malaysia

*Corrensponsing Author E-mail: jackie@uts.edu.my

Keywords: Badminton; Movement Analysis; FastDTW; Handedness Invariant; Kinect.

Extended Abstract

Badminton is one of the most popular sports in Malaysia. In training, there is still lack of movement recognition and analysis research for badminton. The common way for badminton coach to analyse badminton performance thus far has always been using their naked eyes and qualitative measurement. The inconsistency of judgements increases the difficulties of performance justification, for example, an assessment of performance between a right-handed coach and a left-handed player. Besides that, the coach can barely benchmark the player's performance even with considerable expertise in coaching career. Specifically, they are not able to perform measurement consistently among themselves and may be clueless on progressive improvement for badminton players. As such, badminton movement analysis system is crucial to be introduced and proposed to analyse or assess badminton performance quantitatively.

Currently, there are two popular methods utilized to perform movement analysis, the first is to video record and providing feedbacks via the footage manually (Tahan et al., 2018; Archana and Ayyasamy, 2018; Kobayashi, Kaseda and Miyamoto, 2018), and the other method being attaching marker-based tracker onto a badminton player's body (Shu et al., 2018; Zhang et al., 2018). These methods are rather cumbersome and had become inconvenient and inefficient to badminton players and coaches.

To address these problems, Microsoft Kinect v2 sensor is adopted in this research. Microsoft Kinect v2 is a camera that can generate depth map sequence and provide human body silhouette in real time. The previous version of Microsoft Kinect sensor only capable to track up to 20 body joints, while the newer version, Microsoft Kinect v2 sensor can track up to 25 joints as illustrated in Figure 1. Moreover, a new handedness invariant lossless compression technique, namely dominant range of movement index (D-RoMI) is also proposed by combining with embedded intelligent handedness adaptive module and FastDTW time-series algorithm in the Kinect-based badminton movement analysis system. The dataset of the study consists of total 800 badminton movements, in which collected from subject group that

consists of 40 left and right-handed male and female badminton players that have different body size, clothes, and skin color.

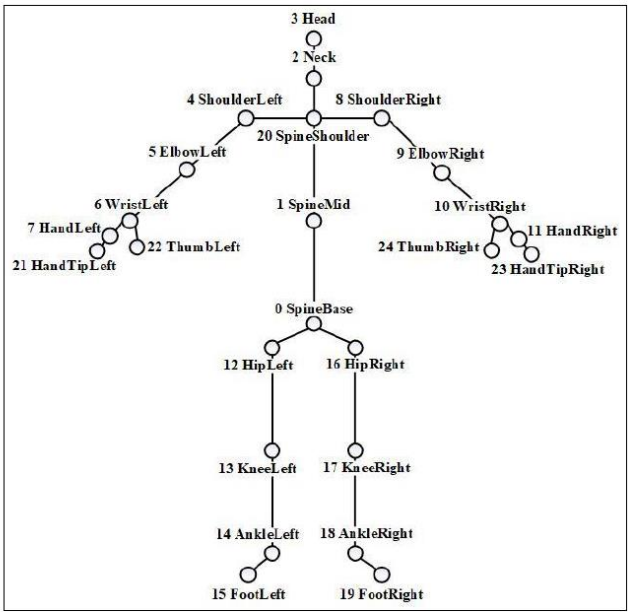

Figure 1. Skeleton Model

Experimental results revealed 96.13% of badminton movement recognition accuracy, while the framework also allows badminton players or coaches to analyze and benchmark badminton movement invariantly with shorter processing time regardless of different handedness. In addition, an open source three-dimensional framework is also employed in order to provide three-dimensional scenes for better illustration of badminton movement comparison.

References

Archana, M. and Ayyasamy, A. (2018). Tracking based Event Detection of Singles Broadcast Tennis Video. 2018 3rd International Conference on Communication and Electronics Systems (ICCES).

Kobayashi, S., Kaseda, H. and Miyamoto, R. (2018). Robust Localization of Body Parts Based on Interframe Failure Correction. 2018 IEEE International Conference on Systems, Man, and Cybernetics (SMC).

Shu, Y., Chen, C., Shu, K. and Zhang, H. (2018). Research on Human Motion Recognition Based on Wi-Fi and Inertial Sensor Signal Fusion. 2018 IEEE SmartWorld, Ubiquitous Intelligence & Computing, Advanced & Trusted Computing, Scalable Computing & Communications, Cloud & Big Data Computing, Internet of People and Smart City Innovation (SmartWorld/SCALCOM/UIC/ATC/CBDCom/IOP/SCI).

Tahan, O., Rady, M., Sleiman, N., Ghantous, M. and Merhi, Z. (2018). A computer vision driven squash players tracking system. 2018 19th IEEE Mediterranean Electrotechnical Conference (MELECON).

Zhang, C., Yang, F., Li, G., Zhai, Q., Jiang, Y. and Xuan, D. (2018). MV-Sports: A Motion and Vision Sensor Integration-Based Sports Analysis System. IEEE INFOCOM 2018 - IEEE Conference on Computer Communications.

6th International Conference and
Postgraduate Colloquium for
Environmental Research 2022 (POCER
2022) 9 - 11 June 2022
Langkawi, Kedah, Malaysia

PCR18032022 – 28: Vision-Based Monitoring of Microalgae Growth and Analysis of its Bioactive Compounds: A Preliminary Results

Yuk-Heng Siaa, Huong-Yong Tinga*, Siew-Ling Hiib, Pau-Loke Showc, Jackie-Tiew-Wei Tinga, Marcella Petera, Khairunnisa Ibrahimb and Keh-Kim Keed
aDrone Research and Application Centre,
University of Technology Sarawak, Sarawak, Malaysia
bAdvanced Centre for Sustainable Socio-Economic and Technological Development,
University of Technology Sarawak, Sarawak, Malaysia
cDepartment of Chemical and Environmental Engineering, Faculty of Science and Engineering,
University of Nottingham Malaysia, Selangor Darul Ehsan, Malaysia
dSchool of Engineering and Technology
University of Technology Sarawak, Sibu, Sarawak, Malaysia

*Corrensponsing Author E-mail: alan.ting@uts.edu.my

Keywords: Microalgae; Image Processing; Machine Learning

Extended Abstract

Microalgae have many potentials such as to be used as nutrition, biofuel and the manufacture of pharmaceutical products. Therefore, the cultivation of microalgae for commercial purposes is getting popular in recent days. The growth monitoring of microalgae is important to ensure the microalgae grow optimally under suitable environment and nutrition level and thus the most suitable harvesting time could be decided.

Currently, the monitoring approach of microalgae growth including direct measurements of optical density by UV-Vis's spectrophotometer, measurement of the dry weight cell of biomass and spectrophotometric analysis of chlorophylls (Aris Hosikian, 2010). The spectrophotometric analysis of chlorophylls requires the spectrophotometer to be set up in spectrum mode and scan between a range of wavelength, ranging from 220 to 800nm and use the absorbance information to calculate the concentration of chlorophylls. Although this approach can offer highly precise readings, the main disadvantage of utilising a UV–vis spectrophotometer is the time required to dilute the culture samples because it can only detect a certain maximum value with great precision. As such, this method is generally time-consuming, labour intensive and expensive (Winata et. al, 2021).

Therefore, in this study, a vision-based monitoring of microalgae growth and analysis of its bioactive compounds, such as the concentration of chlorophylls is proposed. The study includes the different colour models, such as RGB, HSL and CMYK with different type of machine learning algorithms, such as Fast Tree Regression and LightGBM Regression. In the experiment, around 700 images of microalgae were captured and adopted to train the machine learning model. Figure 1(a) to 1(c) demonstrate the concentration of microalgae biomass against colour index using different solvents. Moreover, Table 1 shows the correlation between microalgae biomass concentration with different colour models and machine learning algorithms. CMYK colour model produced best accuracy with R_2 equals to 0.88 by using

LightGBM Regression machine learning algorithm. Moving forward, more colour spaces, for example CIE LAB, and other machine learning algorithms, i.e., Fast Forest Regression algorithm will be adopted into the study for comparison.

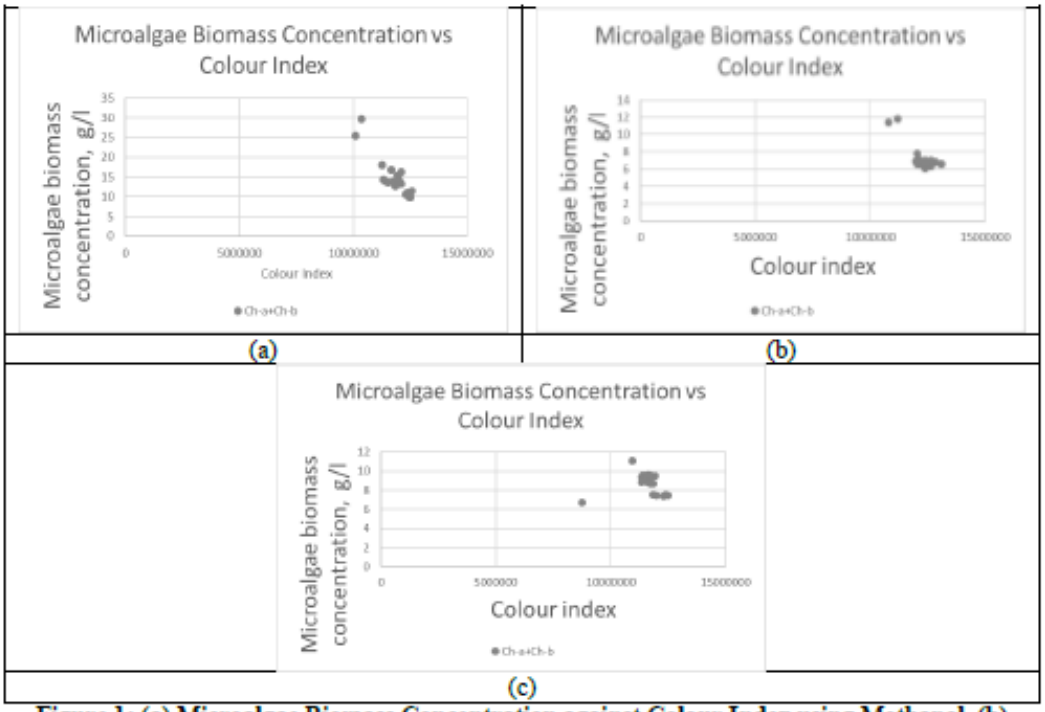

Figure 1: (a) Microalgae Biomass Concentration against Colour Index using Methanol, (b) Microalgae Biomass Concentration against Colour Index using Dimethyl Sulfoxide and (c) Microalgae Biomass Concentration against Colour Index using Ethanol.

Table 1: Correlation between Microalgae Biomass Concentration and Different Colour Models

Colour Model	R^2	Machine Learning Algorithm with Best Performance
RGB	0.77	Fast Tree Regression
HSL	0.81	LightGBM Regression
CMYK	0.88	LightGBM Regression

References

Hosikian, A., Lim, S., Halim, R., Danquah, M. K., 2010. Chlorophyll Extraction from Microalgae: A Review on the Process Engineering Aspects. *International Journal of Chemical Engineering*. 2010: 1-11.

Winata, H. N., Nasution, M. A., Ahamed, T., 2021 Prediction of Concentration for Microalgae using Image Analysis. *Multimedia Tools Application*. 80:8541–8561.

6th International Conference and
Postgraduate Colloquium for
Environmental Research 2022 (POCER
2022) 9 - 11 June 2022
Langkawi, Kedah, Malaysia

PCR18032022 – 29: The Experience of Developing UTS Experimental Smart Home

Keh-Kim Kee[a*], Huong-Yong Ting[b], Jackie-Tiew-Wei Ting[b], Marcella Peter[b] and Khairunnisa Ibrahim[c]
[a] School of Engineering and Technology
University of Technology Sarawak, Sibu, Sarawak, Malaysia
[b]Drone Research and Application Centre,
University of Technology Sarawak, Sarawak, Malaysia
[c]Advanced Centre for Sustainable Socio-Economic and Technological Development,
University of Technology Sarawak, Sarawak, Malaysia

*Corrensponsing Author E-mail: kkkee@uts.edu.my

Keywords: Smart Home; Energy Management System; Smart Devices; IoT Platform; Cloud Computing; Decision Support System

Extended Abstract

Introduction

Smart Home (SH) is essentially an extension of building automation with smart features in the monitoring, analysing, controlling and cloud computing of all its embedded technologies [Li *et al.*, 2018]. It is typically equipped with devices or appliances or so-called Smart Things due to their abilities of sensing, decision-making, and actuating the SH environment [Li *et al.*, 2017]. These smart devices are intelligently interconnected via the internet and applied in different aspects in SH, namely lighting, heating and cooling, computers, entertainment systems, security, surveillance systems, and home appliances such as TVs, washers, dryers, refrigerators and others. SH plays a vital role in the building sector with the green and sustainable buildings provide a healthier, more productive and comfortable space for the people staying in an eco-friendly environment.

The escalating trend of electricity demand causes environmental degradation. Both residential and commercial buildings contribute 53% of electricity consumption in Malaysia. The combustion of fossil fuels in power plants causes the emissions of greenhouse gases (GHGs), and accelerates environmental degradation. As pledged to UNFCCC, Malaysia needs to reduce 45% GHG emissions in terms of carbon intensity by 2030, relative to the 2005 level. Although numerous measures of energy efficiency (EE) and renewable energy (RE) are implemented, the effectiveness remains questionable due to the lack of facilities and end-user awareness for conscious consumption, energy inefficiency and low adoption of renewable energy. Smart Home mitigates the stated challenges by load monitoring, demand-side management (DSM), and energy management system (EMS) with control algorithms for savings of energy and bills, comfort and safety [Peruzzini *et al.*, 2013]. On the other hand, there is a need of an SH platform with real settings for the research community, for instance, the validation of SH control algorithms of EMS. This type of research is not commonly supported by adequate experimental validation, and the results are not directly comparable with different experimental settings [Cordopatri *et al.*, 2015].

This paper aims to present our experience in establishing a holistic and multi-functional experimental SH at the University of Technology Sarawak (UTS) campus in Malaysia. The actual environment settings of SH with hardware and software is used for different purposes, namely exhibition, teaching & learning, and R&D activities, which ultimately beneficial to university, students, researchers and industrial partners.

A holistic SH framework is proposed, consisting of hardware (smart devices, communication devices and smart appliances) and software (cloud IoT Platform and DSS System) with actual SH environment settings. Based on the 7-layered architecture supported by Representational of State Transfer (REST) and Application Programming Interface (API) for communication between physical and cyberspace, SH indeed a cyber-physical system (CPS) applied in residence with a holistic monitoring and controlling of SH for safety, human comfort, and energy efficiency. In terms of SH hardware, SH is equipped with various smart sensors and actuators, so-called smart devices or smart appliances. It is divided into different zones to demonstrate smart features such as smart lighting, smart energy, smart living, smart kitchen and smart access control. On the other hand, SH software comprises (1) IoT Cloud platform, which collects IoT data acquired from SH for cloud storage, computation and visualisation, and (2) DSS System, which has smart features embedded with AI/ML algorithms. For a showcase of SH smart features in the energy domain, optimisation of lighting energy and realisation of building energy sustainability were demonstrated as use cases. Figure 1 depicts the exterior and interior view of the UTS Experimental Smart Home.

(a) the exterior view (b) the interior view

Figure 1. UTS Experimental Smart Home

As a proof of concept, the preliminary results of SH smart features are collected to demonstrate SH effectiveness and functionality. An SH control algorithm has shown a 20% lighting energy cutting compared to a conventional house in the intelligent lighting system. Furthermore, an intelligent SH energy system with a hybrid PV and grid supply has shown a total match of PV generation and load demand for building energy sustainability with zero GHG emissions.
UTS SH is a multi-functional SH with actual settings for different purposes presented. It can be beneficial to the students, researchers and industrial partners. The preliminary results from the use cases exhibit the potentials of SH in the energy domain, i.e., energy savings with SH and its control strategies applied to counteract the current environmental issue.

Acknowledgements: This work is fully funded by UTS Research Grant (Project ID: UCTS/RESEARCH/2/2020/06) of the University of Technology Sarawak

References

A. Cordopatri, R. De Rose, C. Felicetti, M. Lanuzza, and G. Cocorullo, “Hardware implementation of a Test Lab for Smart Home environments,” *2015 AEIT Int. Annu. Conf. AEIT 2015*, 2015.

M. Li, W. Gu, W. Chen, Y. He, Y. Wu, and Y. Zhang, "Smart home：architecture, technologies and systems," *Procedia Comput. Sci.*, vol. 131, pp. 393–400, 2018.
M. Peruzzini, M. Germani, A. Papetti, and A. Capitanelli, "Smart Home Information Management System for Energy-Efficient Networks," *IFIP Adv. Inf. Commun. Technol.*, vol. AICT-408, pp. 393–401, Sep. 2013.
Z. Li, H. Shen, W. Ligon, and J. Denton, "An Exploration of Designing a Hybrid Scale-Up/Out Hadoop Architecture Based on Performance Measurements," *IEEE Trans. Parallel Distrib. Syst.*, vol. 28, no. 2, pp. 386–400, Feb. 2017.

6th International Conference and
Postgraduate Colloquium for
Environmental Research 2022 (POCER
2022) 9 - 11 June 2022
Langkawi, Kedah, Malaysia

PCR10042022 – 30: A Generic Framework for the Evaluation of Visual Network Algorithms on Documents

Khairunnisa Ibrahim[a], Stephanie Chua[b], Huong-Yong Ting[c], Marcella Peter[c], Jackie-Tiew-Wei Ting[c] and Keh-Kim Kee[d]

[a] Advanced Centre for Sustainable Socio-Economic and Technological Development,
University of Technology Sarawak, Sarawak, Malaysia
[b] Faculty of Computer Science and Information Technology
University Sarawak Malaysia, Sarawak, Malaysia
[c] Drone Research and Application Centre,
University of Technology Sarawak, Sarawak, Malaysia
[d] School of Engineering and Technology,
University of Technology Sarawak, Sarawak, Malaysia

• Corresponding Author E-mail: khairunnisa.ibrahim@uts.edu.my

Keywords: Generic Evaluation Framework; Graph Visualisation; Graph Algorithms Evaluation; Named Entities Network, Layout Algorithms Evaluation, Clustering Algorithms Evaluation.

Extended Abstract

Visual network is a special type of graph representing real life systems where the vertices are accompanied with attributes and the edges represent relationships between them. Network visualisation facilitate document analysts, to understand and explain complex data (Yoghourdjian et al., 2021), especially for documents where important events, facts and relationships are recorded. Varieties of visual network algorithms have been devised to ease network visualisation task. Each of the algorithms has a different mechanism, which may result in a different network representation. The large choice of algorithms therefore, made it hard for researchers to determine which algorithm is proper to be used and that can appropriately represent their documents. Hence, this study proposed a generic framework to perform evaluation of visual network algorithms to find the best network representation of a document.

The proposed framework is modular in characteristic where each part is able to be modified or removed according to situations or preferences. The proposed framework is divided into six parts namely document filtering process, annotation process, data transformation process, graph tool input formatting process, graph generation process and evaluation process. In the document filtering process, the document is determined to undergo through annotation or not. If required, the document will go through annotation process. Data transformation process is then required to generate information on the relations between NEs in the annotated data. In the evaluation part, the framework suggests to evaluate both graph layout and clustering algorithm in order to produce a good network. The graph layout algorithm for instance, generate automatic placement of vertices and edges in a network following certain rules. The rules applied aim for the network to be drawn in a way so that they are easy to read and understood.

The graph clustering algorithms make use of the vertices attributes to produce a clustered view of the visual network (Gibson et al., 2014). Graph clustering algorithms improve representation of the data in the network by revealing implicit relationships between them through their clusters, if exist.

In this study, the proposed framework has been applied to several documents, namely the historical Sarawak Gazette (SAGA), Biotext Corpus and dBPedia-Sarawak. Each of the documents have different structures. In the evaluation, the metrics used to evaluate graph layout algorithms include running time, edge crossings, and cluttered vertices. On the other hand, the metrics used to evaluate graph cluster algorithms are running time, modularity, relative density, conductance and CPL metrics. In total, three graph layout algorithms are evaluated, namely Force Atlas 2 (FA2), Hu's multilevel (HU) and OpenORD (OO) algorithm. The mentioned algorithms can be categorised as force-directed methods, which has been agreed by many researchers to produce good graph outputs (Hua et al., 2018; Kobourov, 2013; Gibson et al., 2014). Another three graph clustering algorithms, namely Chinese Whispers (CW), Markov Clustering (MC) and Girvan-Newman (GN).

The evaluation conducted on SAGA found that FA2 algorithm when combined with MC algorithm produce the best network representation for SAGA. The proposed evaluation framework has been further used on Biotext Corpus and dBPedia which are of different structure in order to investigate whether the combination of the algorithms selected to perform best on SAGA (FA2+MC) can produce the same good layout and good cluster division again. The results showed that FA2 generates the network of Biotext slightly faster than the network of SAGA and dBPedia. This is expected since the Biotext network is the simplest network among the three with the smallest number of vertices and edges (185 vertices and 255 relations). Compared to SAGA, FA2 produce network which is pleasant to the eyes on Biotext data, where the vertices and edges are easily differentiated from each other, with very few edge crossings. This is due to the simple structure of the data itself. The evaluation of the clustering algorithms showed great changes in the metric scores for different documents. This is because all cluster metric scores changes depending on the aspects that they measured. Documents with different structure have different characteristics that affect certain score. Thus, the results of each score varied based on the structure of the documents.

From the conducted evaluation, it is found that using the same selected algorithms on SAGA does not necessarily produce the same results on other datasets. This is because the performance of a layout or a clustering algorithm actually depends on the structure of the document itself. Therefore, evaluations of algorithms on documents are ineluctable whenever we want to represent a new document in the form of a network. Hence, there is a significance in the proposed generic framework so that it can be reused in future researchs regardless of the type of documents that are worked on. Since evaluations are ineluctable, it is also important to ensure that the evaluation metrics used are reliable and at the same time, simple. This can be the center of focus for possible future work.

Acknowledgement: The authors thank the Ministry of Higher Education (MoHE), Malaysia, for the financial support of this research under the grant RACE/b(5)/1097/2013(05).

References

Yoghourdjian, V., Yang, Y., Dwyer, T., Lawrence, L., Wybrow, M., & Marriott, K., 2021. Scalability of Network Visualisation from a Cognitive Load Perspective. *IEEE Transactions on Visualization and Computer Graphics*. 27 (2): 1677-1687.

Gibson, H., Faith, J., & Vickers, P., 2014. A Survey of Two-Dimensional Graph Layout Techniques for Information Visualisation. *Information Visualisation*. 12 (3-4): 324-357.

Hua, J., Huang, M. L., & Wang, G., 2018. Graph Layout Performance Comparisons of Force-Directed Algorithms. *International Journal of Performability Engineering*. 14 (1): 67-76.

Kobourov, S. G. (Tamassia, R., Ed.), 2013. *Force-Directed Drawing Algorithms*. In *Handbook of Graph Drawing and Visualisation.* pp. 383-408. CRC Press.

6th International Conference and
Postgraduate Colloquium for
Environmental Research 2022 (POCER
2022) 9 - 11 June 2022
Langkawi, Kedah, Malaysia

PCR10042022 – 31: Investigating Neutral Face Reconstruction for Improving Face Identification using Nonlinear Approach

Marcella Peter[a*], Jacey-Lynn Minoi[b], Huong-Yong Ting[a], Khairunnisa Ibrahim[c], Jackie-Tiew-Wei Ting[a] and Keh-Kim Kee[d]

[a]Drone Research and Application Centre,
University of Technology Sarawak, Sarawak, Malaysia

[b] Faculty of Computer Science and Information Technology
Universiti Malaysia Sarawak, Sarawak, Malaysia

[c]Advanced Centre for Sustainable Socio-Economic and Technological Development,
University of Technology Sarawak, Sarawak, Malaysia

[d]School of Engineering and Technology
University of Technology Sarawak, Sarawak, Malaysia

*Corresponding Author E-mail: marcella@uts.edu.my

Keywords: Neutral Face Reconstruction; modified Kernel Active Shape Model; Nonlinear Approach; 3D face

Extended Abstract

Face recognition is particularly important in various professions. Our reliance on images to prove our identity in driver's licenses and passports is based on facial recognition. A recent study also showed that people's ability to recognize faces varies widely. Face recognition systems are no exception as face recognition rate is high when a neutral face is used but significantly drops due to the variant of the facial expression. Other facial variations such as facial hair, positions, and scars are among other limitations that resulting in distorted or incomplete faces when capturing faces in different environments. It is thus significant to install a face reconstruction module in a face recognition system to improve recognition rate and identify faces. This benefits those trying to identify an individual based on limited data or for medical purposes. But, reconstructing the detailed geometric structure from a single face image is a challenging problem due to its contrarian nature and fine 3D structures to be recovered [Zeng *et al*., 2019)].

The choice of method varies depending on the purpose. The synthesis of facial expressions provides a series of reconstructed images of expressions a face may have. The synthetic expression is used in the facial analysis to achieve a better performance of the face recognition system identification and classification of face images. The most reliable approach in reconstructing facial expression is learning-based [Sharma & Kumar, 2022]. But it is complex to compute and interpret. While the most commonly used is statistical-based, specifically, the Active Shape Model (ASM) [Cootes *et al*., 1995], due to its flexibility to fit into any shapes and easy interpretations. Another challenge is neutralising facial expressions are more complex especially when it is required to retain the individual traits.

This study explores the potential of using a nonlinear approach called the modified kernel active shape model (mKASM) [Peter *et al*., 2020] for synthesising neutral facial expressions 3D geometric face models to improve the performance and recognition rates. The mKASM is a non-rigid template-based model that is used for the reconstruction of faces. This research elaborately exploit BU3DFE dataset to train and evaluate the reconstructed neutral faces. The performance of mKASM is evaluated qualitatively and quantitively. Qualitative evaluation is done by visualising each of the neutralised faces to compare with its

ground truth. Results indicates that the proposed mKASM can effectively reconstruct and retained each subject's identity even with an initially distorted face. One of the examples is as presented in Figure 1, a subject with a distorted face from surprised face dataset indicated in (a), after neutralised as shown in (b) looks almost similar to the ground truth (c).

Whereas face recognition is used to evaluate the reconstructed neutral faces whether it still preserving the traits of the person. Based on the generic framework of face recognition, there is a feature extractor and a matcher. The input data is the pre-processed 3D face data. The feature extracted by the

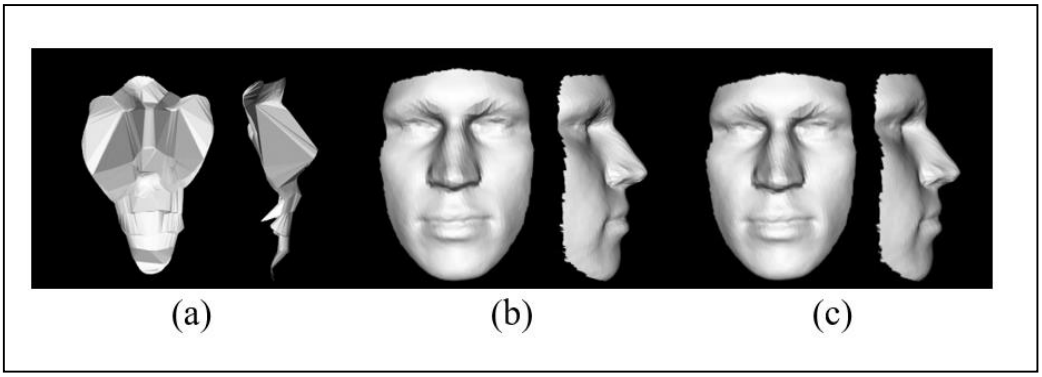

Figure 1: (a) Original surprised expression of a subject, (b) Reconstructed neutral face of the same subject, and (c) the ground truth neutral face of the same subject.

feature extractor, classify the faces using simple classifier, the K-Nearest Neighbour. The classified faces are fed up to the matcher as query for comparison against a trained face from the controlled database. Finally, the recognition rate is calculated. In conclusion, the qualitative results of reconstructed neutral face revealed the subject looks almost similar (if not) with the ground truth. Therefore, utilising the proposed modified kernel-based Active Shape Model can improve the synthesis of facial expressions, resulting in improved recognition rates.

References

Cootes, T., Taylor, C. J., Cooper, D. H., and Graham, J. (1995). Active shape models - their training and application. *Computer Vision and Image Understanding*. 61(1): 38–59.

Peter, M., Minoi, J. L., & Rahman, S. A. (2020). Neutral Expression synthesis using kernel active shape model. *Indonesian Journal of Electrical Engineering and Computer Science. 20*(1)*:* 150-157.

Sharma, S., & Kumar, V. (2022). 3D Face Reconstruction in Deep Learning Era: A Survey. Archives of Computational Methods in Engineering. *Archives of Computational Methods in Engineering.* 1-33.

Yin, L., Wei, X., Sun, Y., Wang, J., & Rosato, M. J. (2006). A 3D facial expression database for facial behavior research, paper presented in 7th International Conference on Automatic Face and Gesture Recognition, Southampton, UK.

Zeng, X., Peng, X., & Qiao, Y. (2019). Df2net: A dense-fine-finer network for detailed 3d face reconstruction. In Proceedings of the IEEE/CVF International Conference on Computer Vision (pp. 2315-2324).

PCR10042022 – 32: Phytomicrobiomes for the Sustenance of Agro-ecosystem

R. Z. Sayyed[a]

[a] Department of Microbiology, PSGVP Mandal's
Arts, Science & Commerce College, Shahada 425409, India

- Corresponding Author E-mail: SAYYEDRZ@GMAIL.COM

Keywords: Abiotic Stress; Biocontrol; Fungicide; PGPR; Plant Growth Promotion.

Extended Abstract

Abiotic stress (drought, salinity and heavy metal ions) are the major abiotic factor limiting crop production. Co-inoculating crops with nitrogen fixing bacteria and plant growth-promoting rhizobacteria (PGPR) improves plant growth and increases drought tolerance in arid or semiarid areas. The co-inoculation of salinity and drought-stressed plants with PGPR improves the root and the shoot growth, formation of nodules, nitrogen fixation capacity in soybean, and provide mineral nutrition to the plant. We report the usefulness single inoculation and co-inoculation of various PGPR strains in plant growth promotion; mitigation of salinity and drought and biocontrol of various fungal phytopathogens. PGPR cultures promoted plant growth, crop yield under salinity, drought and heavy metal ion stress conditions and helped in the mitigation of salt, water deficit and heavy metal contamination. Their application resulted in more root and shoot length, more chlorophyll content, and improved mineral nutrient uptake under these stress conditions. The results of the study showed that co-inoculation with *B. japonicum* USDA110 and *P. putida* NUU8 gave more benefits in nodulation and growth of plants compared to the single inoculation. Co-inoculation with *B. japonicum*, USDA 110 and *P. putida* NUU8 significantly enhanced plant and soil nutrients and soil enzymes compared to control under normal and drought stress and salinity stress conditions. The synergistic use of *B. japonicum* USDA110 and *P. putida* NUU8 improves plant growth and nodulation of soybean, and groundnut under drought and salinity stress conditions. These cultures also exhibited potent antifungal activities against fungal pathogens compared to the chemical fungicides such as Kitazine and tilt. The results suggested that these strains could be used to formulate a consortium of biofertilizers and biocontrol agents for sustainable production of soybean and groundnut under drought-stressed field conditions.

6th International Conference and
Postgraduate Colloquium for
Environmental Research 2022 (POCER
2022) 9 - 11 June 2022
Langkawi, Kedah, Malaysia

PCR18032022-33: Correlative modeling of algal biodiesel units using statistical algorithms and artificial neural networks

Abdullah Bin Mahfouz [a], Rizwan Nasir [a], Anas Ahmed [b] ,Mark Crocker [c] and Abulhassan Ali [a]

[a] Department of Chemical Engineering,
University of Jeddah, Jeddah, Saudi

[b] Department of Industrial and Systems Engineering,
University of Jeddah, Jeddah, Saudi

[c] Center for Applied Energy Research and Department of Chemistry, USA

Extended Abstract

Algal biodiesel is of growing interest in the quest to reduce carbon emissions in the atmosphere. The production of biodiesel is affected by many process parameters. Although several research works have been conducted, the contribution of each parameter for biodiesel production is not well understood when considered as a complete system. Therefore, the experimental data from various sources related to the effects of temperature, light intensity, carbon concentration, aeration rate, pH, and time on the biodiesel production rate of different algae were reviewed and introduced into a neural network inspired correlative (N2IC) model. The developed N2IC model was used to optimize biodiesel production based on the studied variables and produce a statistical algorithm. By using sensitivity measurements and error analysis, the results from the proposed N2IC model are shown to agree with the experimentally obtained values. The results indicate that the results determined with the proposed equation are of strong practical worth for researchers and experts in the biodiesel/biofuels industry.

PCR11042022 – 34: Micro Computerized Tomography: Potential Applications of Polychromatic and Monochromatic X-ray Source in Unconventional Gas Reservoirs

[a, *] Maqsood Ahmad, [b,c] Imtiaz Ali, [d] Asif Zamir

[a]Department of Petroleum Geosciences, Universiti Teknologi PETRONAS, 32610 Seri Iskandar, Perak, Malaysia.

[b]Department of Petroleum Engineering, Universiti Teknologi PETRONAS, 32610 Seri Iskandar, Perak, Malaysia.

[c]Department of Petroleum and Gas Engineering, Balochistan University of Information Technology, Engineering and Management Sciences (BUITEMS), Quetta, Pakistan

[d]Well Engineering department, International College of Engineering & Management. Muscat, Oman

- Corrensponsing Author E-mail: maqsood.ahmad@utp.edu.my

Keywords: micro-CT scan, Polychromatic and Monochromatic X-ray, Unconventional Gas Reservoirs, QEMSCAN analysis.

Extended Abstract

The microfocus X-ray computed tomography (μCT) techniques were applied to scan, image and build 3D model of Murtreee carbonaceous shale samples (Cooper Basin South Australia) in order to evaluate the potential of radiation technique for mineralogy, porosity distribution and fractures. Different shale samples of source rock were obtained from Murtree shale and prepared for imaging and analysis by micro-scale X-ray computed tomography (XCT). The objective of this work is to combine quantitative 2D mineralogical data obtained via QEMSCAN analysis with 3D XCT data for volumetric characterization of grain types (quartz, carbonates clays, etc.) within the samples. The obtained data could be utilized for numerical analysis of the surface area and volume of the different grains, as well as grain size and distribution. This study also determined the feasibility of petrophysical and mineralogical analysis using the XCT equipment. The characterization of mineral phases present in a rock sample by their characteristic X-ray attenuation should be possible, however this work has shown that it is not possible with the X-radia MicroXCT-400 without significant purposed modifications due to the nature of sample material used. The main limitation was the X-ray source. As the X-ray source was polychromatic, composed of many different X-rays with different wavelengths, the attenuated X-ray intensity measured at the detector results from a range of X-ray wavelengths, which cannot be used

for the identification of a standard mineral phase in the scanned sample. It was found that X-ray attenuation is proportional not only to the density and atomic number of a material, but also the wavelength of the applied radiation. As the X-ray source produced a range of wavelengths, then a band of X-ray attenuations was measured instead of a single characteristic grey value, which cannot be used for the identification of various phases in scanned samples. For this type of characterization, a monochromatic source was preferred ideally a synchrotron source. Also, the correlation of X-rays absorbance measured by Micro-X-ray with the mineral phase detected by the QEMSCAN analysis was found, not feasible (Figure 1).

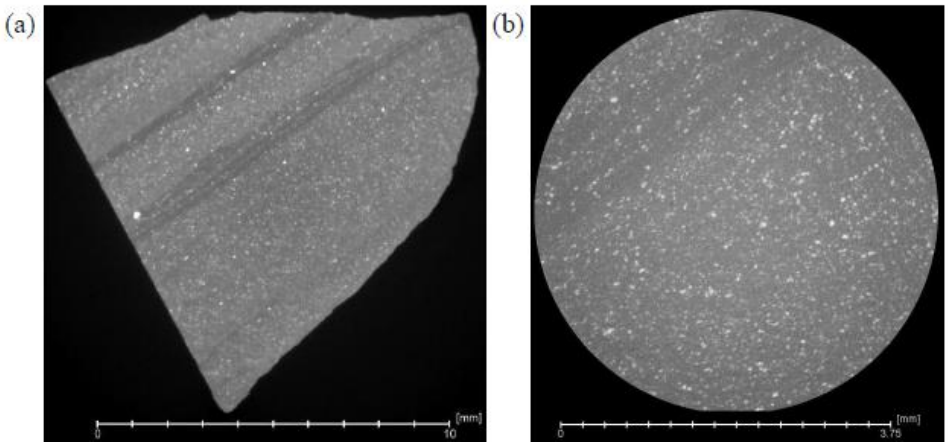

Figure 1: Slice of Murtree shale sample embedded in resin in X-Y plane imaged by Micro-XCT at (a) 1x magnification and (b) 4x magnification

Acknowledgements: The authors thank the Ministry of Higher Education (MOHE) Malaysia for providing the financial support under grant No. FRGS/1/2020/TK0/UTP/02/3.

References

1. Withers, P.J.; Bouman, C.; Carmignato, S.; Cnudde, V.; Grimaldi, D.; Hagen, C.K.; Maire, E.; Manley, M.; Du Plessis, A.; Stock, S.R. X-ray computed tomography. *Nature Reviews Methods Primers* **2021**, *1*, 1-21.

2. Hounsfield, G.N. Computerized transverse axial scanning (tomography): Part 1. Description of system. *The British journal of radiology* **1973**, *46*, 1016-1022.

3. Taina, I.; Heck, R.; Elliot, T. Application of X-ray computed tomography to soil science: A literature review. *Canadian Journal of Soil Science* **2008**, *88*, 1-19.

4. Yang, Y.; Tao, L.; Yang, H.; Iglauer, S.; Wang, X.; Askari, R.; Yao, J.; Zhang, K.; Zhang, L.; Sun, H. Stress sensitivity of fractured and vuggy carbonate: an X-Ray computed tomography analysis. *Journal of Geophysical Research: Solid Earth* **2020**, *125*, e2019JB018759.

6th International Conference and
Postgraduate Colloquium for
Environmental Research 2022 (POCER
2022) 9 - 11 June 2022
Langkawi, Kedah, Malaysia

PCR18032022-35: Simultaneous capture of H_2S and CO_2 from high sour Saudi natural gas using cryogenic packed bed

Abulhassan Ali[a], Aymn Abdulrahman[a], Mohd Mubashir[b], Mohamad Azmi Bustam[c]

[a] Department of Chemical Engineering, University of Jeddah, Jeddah, Saudi

[b] Department of Industrial and Systems Engineering, University of Jeddah, Jeddah, Saudi

Abstract

Saudi Arabia has huge natural gas reserves, but some are highly contaminated with CO_2 and H_2S. It is essential to remove these contaminations because it not only cause corrosion in the piping but also reduce the calorific value of natural gas. Cryogenic packed beds are a promising technology for the removal of CO_2 from natural gas but have not yet been tried for H2S. The proposed study will explore the simultaneous capture of CO_2 and H_2S from natural gas using cryogenic packed bed technology. The separation between CO_2 and H_2S from natural gas can be achieved based on differences in their freezing points. CO_2 and H_2S directly change the phase from gas to solid and capture inside the bed while clean natural gas can be obtained at the outlet. The effects of process parameters like temperature, gas composition, flow rate, and bed saturation times will be investigated in detail. In previous literature, the energy required for a cryogenic packed bed was 816 kJ/kg CO_2, while the cryogenic distillation process required 1472 kJ/kg CO_2, which shows that this technology holds promise.

6th International Conference and
Postgraduate Colloquium for
Environmental Research 2022 (POCER
2022) 9 - 11 June 2022
Langkawi, Kedah, Malaysia

PCR18032022-36: Multiobjective optimization, simulation, and modeling of biodiesel synthesis from used cooking using response surface methodology

Anas Ahmed [a]

[a] Department of Industrial and Systems Engineering, University of Jeddah, Jeddah, Saudi Arabia

Abstract

Biodiesel synthesis from used cocking oil is an attractive alternative energy source. Although used cooking oil is an attractive feedstock because it is a waste, but still, many challenges need to be addressed to make this technology economically viable. In this study, a process simulator was used to generate the biodiesel synthesis data for different temperatures and concentrations. The data were further used to find the optimum conditions where maximum yield was obtained. The paper is divided into two parts. The first part is involved in conducting a simulation study using a process simulator. The second part of the study involves model development using response surface methodology. A predictive model was developed, and it was found that the model's accuracy was good. The developed model was used to study the effect of process parameters such as temperature and concentration on biodiesel yield. Once the data was generated, it was further used to find the optimum condition of temperature and concentration to maximize biodiesel synthesis.

6th International Conference and Postgraduate Colloquium for Environmental Research 2022 (POCER 2022) 9 - 11 June 2022
Langkawi, Kedah, Malaysia

PCR18032022-37: Modeling and Optimization of Dynamic Viscosity of Titania Nanotubes Dispersions in Ethylene Glycol/Water-Based Nanofluids using Response Surface Methodology

Abdullah Bin Mahfouz [1], Abulhassan Ali [1*], Mustafa Alsaady[1] , Anas Ahmed[2] , Abdulkader S. Hanbazazah[2], , Pau Loke Show [3], *

[1] *Department of Chemical Engineering, University of Jeddah, Jeddah, Saudi Arabia*

[2] *Department of Industrial and Systems Engineering, University of Jeddah, Jeddah, Saudi*

[3] *Department of Chemical and Environmental Engineering, Faculty of Science and Engineering, University of Nottingham Malaysia, Jalan Broga, Semenyih 43500, Selangor*

- Corrensponsing Author E-mail: malsaady@uj.edu.sa

Extended Abstract

The growing use of nanofluids in heat transfer necessitates the investigation of viscous properties. For practical purposes, accurate physical properties must be known. The viscosity of nanofluids is an important property, and there are only a few studies on the modeling of effective viscosity designed to manage correct estimates. According to the current study, Titania (TiO2) nanotubes are synthesized through a traditional approach, and an investigational study is conducted on the viscosity performance of Titania (TiO_2) nanotubes dispersed in ethylene glycol/water-based nanofluid. The mass concentrations of nanotubes are varied from 0 to 1%. Initially, the nanofluid is stabilized, and then the viscosity is experimentally measured at a temperature range 25-65°C and a shear rate of 150-500 s-1. In addition, this study used response surface methodology (RSM) to conduct a detailed optimization study. The multivariate empirical model is constructed and used to optimize process constraints. The importance of process parameters was evaluated, and the results revealed that the most important parameter is nanofluid concentration, accompanied by shear rate and temperature. The optimum input parameters for the maximum viscosity were nanofluid concentration (1%), shear rate (499), and temperature 25 ^{0}C. The parameters for minimum viscosity were determined as nanofluid concentration (0%), shear rate (150) and temperature 65 ^{0}C.

6th International Conference and
Postgraduate Colloquium for
Environmental Research 2022 (POCER
2022) 9 - 11 June 2022
Langkawi, Kedah, Malaysia

PCR19032022 – 40: Optimization of natural gas dehydration using low-temperature techniques

Saeed Rubaiee [a,b]

[a] Department of Mechanical and Materials Engineering,
University of Jeddah, Jeddah, Saudi Arabia

[b] Department of Industrial and Systems Engineering,
University of Jeddah, Jeddah, Saudi Arabia

Extended Abstract

Natural gas is a clean fuel among many other fossil fuels. Saudi Arabia is focusing on increasing the utilization of natural gas as an energy source due to its less negative impact on the environment. Unlike the other fossil fuels, natural gas emits less CO2 and other harmful gases. Raw natural gas has many impurities such as water, CO2, N2, H2S, etc. All the mentioned impurities must be removed before using natural gas as fuel. This research focus is the removal of water from natural gas. The most common technology for natural gas dehydration is absorption using triethylene glycol (TEG) as a solvent. This drying equipment utilizes liquid triethylene glycol as its dehydrating agent to pull out water from a stream of natural gas flowing over it. The main disadvantage of this technology is the negative impact of TEG on the environment. The present study explores the use of the low-temperature packed bed for natural gas dehydration. A detailed simulation study was conducted to investigate the process parameter's effect on the separation. The simulation data was further used to find out the optimum temperature and pressure for maximum water capture.

6th International Conference and
Postgraduate Colloquium for
Environmental Research 2022 (POCER
2022) 9 - 11 June 2022
Langkawi, Kedah, Malaysia

PCR20032022 – 42: Adsorption of Methylene Blue Dye onto Graphene Composite

Wan Ting Tee[a], Nicholas Yung Li Loh[a, b], Billie Yan Zhang Hiew[c], and Lai Yee Lee[a*]

[a] Department of Chemical and Environmental Engineering, University of Nottingham Malaysia, Jalan Broga, 43500 Semenyih, Selangor Darul Ehsan, Malaysia.

[b] Department of Chemical and Environmental Engineering, University of Nottingham Ningbo China, Ningbo 315100, China.

[c] School of Engineering and Physical Sciences, Herriot-Watt University Malaysia, 62200 Putrajaya, Wilayah Persekutuan Putrajaya, Malaysia.

- Corrensponsing Author E-mail: LAI-YEE.LEE@NOTTINGHAM.EDU.MY

Keywords: Water pollution; Wastewater treatment; Three-dimensional graphene; Methylene Blue Dye; Adsorption mechanism.

Extended Abstract

The contamination of natural water resources by synthetic dyes is a major environmental issue worldwide. This research focussed on the synthesis of a new graphene oxide-chitosan composite (GO/CS) through cross-linking method with chitosan. Experimental studies were carried out to ascertain the adsorption performance of the as-synthesised GO/CS in the treatment of wastewater containing methylene blue dye. For this purpose, batch adsorption was implemented to investigate the effects of varying adsorbent mass, temperature, contact time and concentration on the adsorption of the dye. The experimental data were fitted with adsorption models such as the Langmuir, Freundlich, pseudo-first-order kinetic, pseudo-second-order kinetic and intraparticle diffusion models. The study on simultaneous effects of multiple parameters was performed by response surface methodology (RSM), with the selected parameters being adsorbent mass, time, concentration and temperature. The results showed that while multiple factors could influence the adsorption capacity of the GO/CS, the adsorbent mass showed the largest effect. The equilibrium adsorption of the dye onto GO/CS was best modelled by the Freundlich model, implying that the dye molecules were attached multilayerly onto GO/CS. On the other hand, the adsorption mechanism was well predicted by the pseudo-second-order model, thus suggesting chemisorption. The negative enthalphy change and Gibbs free energy change from thermodynamic study indicated that the adsorption process was exothermic, feasible and spontaneous. The RSM study revealed the adsorption parameters which were favourable for the dye removal. Overall, the results obtained supported the high potential application of the developed GO/CS adsorbent for the treatment of aquatic environment polluted by methylene blue dye.

Acknowledgements: The authors gratefully acknowledge the financial support provided by the Ministry of Higher Education (MOHE) Malaysia under the Fundamental Research Grant Scheme (FRGS/1/2020/STG05/UNIM/02/2).

6th International Conference and
Postgraduate Colloquium for
Environmental Research 2022 (POCER
2022) 9 - 11 June 2022
Langkawi, Kedah, Malaysia

PCR22032022 – 43: A Comprehensive Review on the Production Methods and Effect of Parameters for Glycerol-Free Biodiesel Production

Wan-Ying Wong[a], Steven Lim[a,b*] , and Yean-Ling Pang[a,b]

a Department of Chemical Engineering, Lee Kong Chain Faculty of Engineering and Science
Universiti of Tunku Abdul Rahman, 43000 Kajang, Selangor, Malaysia

b Centre for Photonics and Advanced Materials Research
Universiti Tunku Abdul Rahman, 43000 Kajang, Selangor, Malaysia

• Corresponding Author E-mail: stevenlim@utar.edu.my

Keywords: Biodiesel; Interesterification Technologies; Glycerol-free; Catalysis

Extended Abstract

The industrial revolution undeniably benefits people with an improved quality of life, but at the same time demands more energy access. There is indeed a significant necessity to look for alternative sustainable energy sources. Biodiesel is the most suitable candidate to replace petroleum diesel owing to its characteristics of environmental-benign, technical practicability, cost-effectiveness and widely accessible feedstocks. The concern of excessive low purity glycerol that is produced as byproduct in the conventional transesterification between triglycerides and methanol, usually in the presence of an alkali catalyst, makes the overall process to be unappealing. A promising reaction pathway, interesterification (Figure 1), which utilizes novel acyl acceptors such as methyl acetate, ethyl acetate and dimethyl carbonate instead of the typical alcohols to transform the oleaginous feedstock to biodiesel and triacetin or glycerol carbonate as well as eliminates the coproduction of glycerol, has been gaining a lot of attention from researches. The focus of this review is to appraise the recent research progress and the achievements of the interesterification technologies.

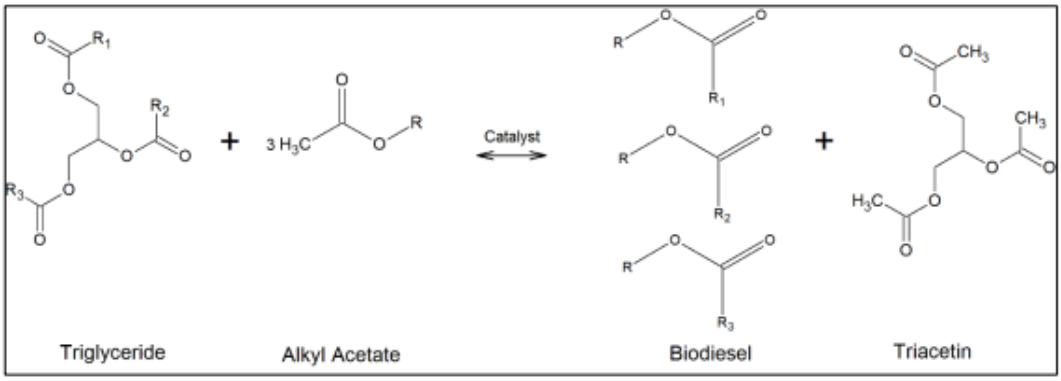

Figure 1: Catalytic Interesterification Reaction

Majority of the alkali-catalyzed interesterifications accomplished outstanding feedstock conversions or biodiesel yields regardless the types of acyl acceptors. Typical chemical catalysts such as alkali metal methoxides and hydroxides were widely employed with the former one acted heterogeneously in the reaction. This led to miscibility problem which the catalysts cannot perform effectively and the biodiesel yields were adversely affected. Researchers sought for alternatives by introducing alcohol back to the reaction systems via recrystallization or crystallization of the catalysts. Although alkaline interesterification can be conducted under mild conditions, only feedstocks with low free fatty acid (FFA) and water contents can be employed. Otherwise, an additional purification step is required which certainly increases the overall processing cost. Despite the fact that acid-catalyzed interesterification performs under the conditions of higher reactant loading and temperature as well as longer duration, it can take on any feedstocks, irrespective of water and FFA contents.

Alternative acyl acceptors do not exert any toxic effect on lipase activity in enzymatic interesterification. Nevertheless, enzymes tend to denature under high temperature condition and hence majority of enzymatic interesterifications were performed under 50 °C which led to lower reaction rate and longer reaction time. This can be alleviated by applying thermo-tolerant enzyme derived from mixed cultures which gave similar yield in a comparatively shorter duration. Although enzymatic interesterification is an emerging area of biodiesel production that provides advantages over conventional chemical synthesis, its relevant cost factor, tolerance towards impurities, long-term stability of enzyme under processing conditions and the impracticability of multiple reusability at industrial scale are the much needed criteria to be further studied.

On the other hand, supercritical interesterification reactions were originally conducted in the absence of catalyst but the extreme operating conditions were mitigated with the integration of catalysis into the process. The biodiesel yield of supercritical interesterification is not affected by the feedstock quality and hence this reaction pathway can adopt low-grade waste feedstocks. Despite the recorded high conversion and reaction rate with promising yield in a short period of time, the operating conditions of significantly high molar ratios of the reactants as well as extreme pressures (20-40 MPa) and temperatures (350-400 °C) as compared to chemical interesterification will consume large amount of energy for heating and cooling. This will render the biodiesel production to become economically unfavorable and restraining it from breaking through into larger industrial production. Economic consideration in terms of equipment and profit margin must be reviewed thoroughly to guarantee the profitability and sustainability of supercritical interesterification process in the industry.

In addition, the influence of reaction parameters such as reactant ratio, catalyst loading, reaction time, temperature, and addition of co-solvents were also discussed in depth. A preliminary kinetic test should be conducted to investigate the sufficient reaction time in advance for the reaction to reach the equilibrium before evaluating other variables. A detailed comparison of literature reveals that alkaline or acidic interesterification generally employs an acyl acceptor to oil molar ratio of lower than 40 while noncatalytic supercritical interesterification requires high reactant molar ratio of at least 42. In contrast, enzymatic interesterification demands lower acyl acceptor to oil molar ratio of 12. The effect of catalyst loading is more pronounced at short reaction time but this impact is diminished as the reaction time increases. Higher catalyst amount can promote the reaction kinetics to achieve the equilibrium point under shorter reaction time. The optimum catalyst loading is generally specific to a system and it is necessary to determine it in order to minimize the catalyst amount for practical usage from the economy standpoint.

The research works conducted were mainly at laboratory and mini-pilot scales. If the findings of previous research studies are being scaled up, it will lead to a very high degree of uncertainty. The viability of interesterification in commercial applications remains controversial. There are some imminent developments which can be performed in the future to fill up the knowledge gap. Detailed study regarding the process intensification technology to attain promising biodiesel yield under moderate reaction conditions should be done. The application of co-solvents or additives to mitigate the magnitude of operating conditions and reactants loading should be examined more closely, leading to lower process cost and greater process efficiency. In contrary to petroleum diesel, the cost of biodiesel product remains as one of the significant challenges for this industry. The non-edible renewable feedstock valorization for biodiesel production should also be encouraged not only in terms of costefficiency but also for a protected and sustainable environment based on an integrated bio-refinery and green concept. Reactor design and reactor volume should be included in the parameter studies as the literature information is still relatively insufficient. More in-depth studies are required to manage the by-products such as triacetin, acetic acid and glycerol carbonate. It would also be valuable to extend more studies on the existing information of interesterification in the process model, purification methods, energy consumption analysis, techno-economic feasibility and marketability of the byproducts in order to investigate the full potential of this reaction.

PCR22032022 – 44: Recovery of microalgae biodiesel using liquid biphasic flotation system

Nurul Syahirah Mat Aron[1] , Kit Wayne Chew[2,*], Wei Lun Ang[3] , Sakhon Ratchahat[4] , Jörg Rinklebe[5,6] , and Pau Loke Show[1,*]

1 Department of Chemical and Environmental Engineering, Faculty of Science and Engineering, University of Nottingham Malaysia, Jalan Broga, 43500 Semenyih, Selangor Darul Ehsan, Malaysia khby6nsm@nottingham.edu.my (N.S. Mat Aron); PauLoke.Show@nottingham.edu.my (P.L. Show)

2 School of Energy and Chemical Engineering, Xiamen University Malaysia, Jalan Sunsuria, Bandar Sunsuria, 43900 Sepang, Selangor Darul Ehsan, Malaysia. kitwayne.chew@xmu.edu.my (K.W. Chew)

3 Department of Chemical and Process Engineering, Faculty of Engineering and Built Environment, Universiti Kebangsaan Malaysia, 43600 Bangi, Selangor Darul Ehsan, Malaysia. wl_ang@ukm.edu.my (W.L. Ang)

4 Department of Chemical Engineering, Faculty of Engineering, Mahidol University, Nakhon Pathom, 73170, Thailand. sakhon.rat@mahidol.edu (S. Ratchahat)

5 School of Architecture and Civil Engineering, Laboratory of Soil- and Groundwater- Management, Institute of Foundation Engineering, Water- and Waste-Management, University of Wuppertal, Wuppertal, Germany. rinklebe@uni-wuppertal.de (J. Rinklebe)

6 Department of Environment, Energy and Geoinformatics, Sejong University, Seoul, Korea. rinklebe@uni-wuppertal.de (J. Rinklebe)

• *Correnspondsing Author E-mail: PauLoke.Show@nottingham.edu.my, showpauloke@gmail.com (P.L Show), kitwayne.chew@xmu.edu.my (K.W Chew)

Keywords: Bioprocessing, lipid extraction, Chlorella sorokiniana, aqueous two-phase flotation, microwave pretreatment

Extended Abstract

Exponential increase of greenhouse gases has raised a global concern. More than a quarter of the greenhouse gases (e.g. carbon dioxide) are released from the transportation sector driven by the burning of vehicle fuel. Biofuel was introduced to limit the emission of greenhouse gases due to its potential to cut the emissions by up to 86 %. Microalgae have shown to be a suitable biomass for the production of biofuel because they are

rich in biomolecules such as lipid. This study focuses on the extraction of natural lipid from Chlorella sorokiniana CY-1 for biodiesel production using liquid biphasic flotation (LBF) system. LBF system is a novel environmentally friendly method used for biomolecules extraction from microalgae. It is an integration of aqueous two-phase system with mass transfer mode of solvent sublation that eases the transfer of biomolecules from the bottom phase to the top phase. The study unveils the potential of the LBF system to recover up to 74.44 % lipid using 100 % (v/v) ethanol and ammonium sulphate in 20 min time. GC-FID confirmed the successful extraction of lipid from the microalgae. Three peaks of fatty acid methyl ester, mainly from the middle chains (C5:0) (C12:0) and (C20:0) were observed, expending new opportunity for microalgae biodiesel technology.

Figure:

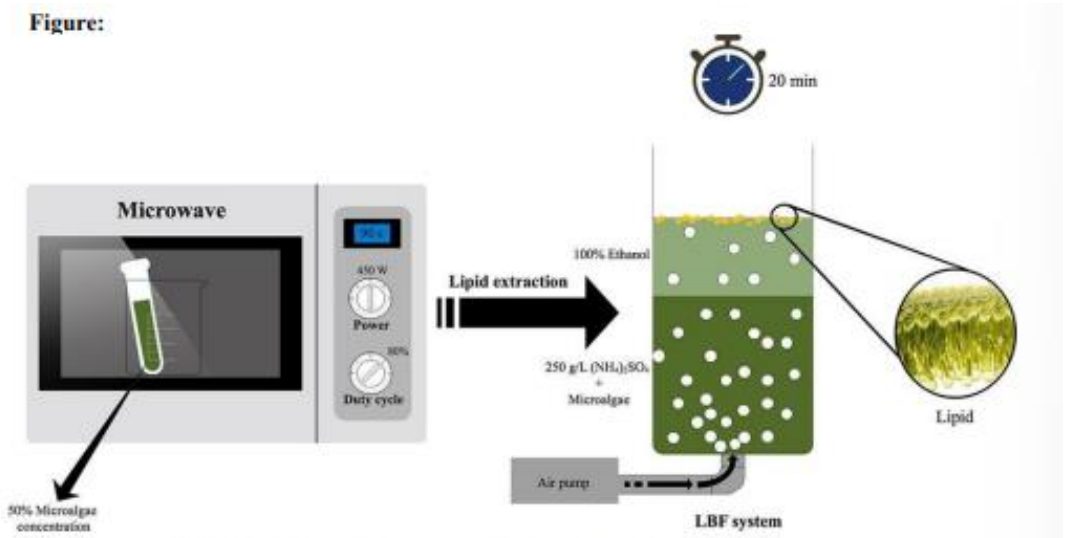

Figure 1: An overview of the conducted study (Mat Aron et al., 2022)

Acknowledgements: This work was supported by the Fundamental Research Grant Scheme, Malaysia [FRGS/1/2019/STG05/UNIM/02/2] and MyPAIR-PHC-Hibiscus Grant [MyPAIR/1/2020/STG05/UNIM/1]. The work is also financially supported by Xiamen University Malaysia (XMUM) under the XMUM Research Fund (Grant number: XMUMRF/2021- C7/IENG/0033).

References

Mat Aron, N. S., Chew, K. W., Ang, W. L., Ratchahat, S., Rinklebe, J., & Show, P. L. (2022). Recovery of microalgae biodiesel using liquid biphasic flotation system. Fuel, 317(June), 123368. https://doi.org/10.1016/j.fuel.2022.123368

6th International Conference and Postgraduate Colloquium for Environmental Research 2022 (POCER 2022) 9 - 11 June 2022
Langkawi, Kedah, Malaysia

PCR23032022 – 45: Purification of Phycocyanin by using Ionic Liquid Based Biphasic Flotation

Dingling Zhuang[a], Kit Wayne Chew[b], Pau Loke Show[c*], Tau Chuan Ling[a*]

[a] Institute of Biological Sciences, Faculty of Science, University of Malaya, 50603 Kuala Lumpur, Malaysia

[b] School of Energy and Chemical Engineering, Xiamen University Malaysia, Jalan Sunsuria, Bandar Sunsuria, 43900 Sepang, Selangor Darul Ehsan, Malaysia

[c] Department of Chemical and Environmental Engineering, Faculty of Science and Engineering, University of Nottingham Malaysia, Jalan Broga, 43500, Semenyih, Selangor, Malaysia

- Corrensponsing Author E-mail: PauLoke.Show@nottingham.edu.my, tcling@um.edu.my

Keywords: Microalgae; Recyclable extractant; Natural ingredients; Ionic liquid.

Extended Abstract

Phycocyanin is an intracellular protein abundantly present in Spirulina sp. which is widely used as a natural colorant in the cosmetics and food industries because of its non-toxic property. With the continuous upgrading of product uses, the market demand for high-purity and high-quality phycocyanin is increasing day by day. Since most of the existing phycocyanin extraction methods contain organic solvents which are harmful to the environment, the authors aim to reduce the environmental burden and obtain high-quality products by using more environmentally friendly extraction methods. The purification of spirulina by ionic liquid biphasic flotation can effectively extract high-purity phycocyanin and remove impurities. Moreover, the recyclable characteristics of ionic liquids will satisfy the pursuit of environmentally friendly extraction. Therefore, the use of an ionic liquid-based biphasic flotation system will help to achieve a more green and environmentally friendly biomass extraction in the future.

1. Introduction

As the negative impact of synthetic materials on health and the environment becomes more and more obvious, the green market trend of using and pursuing natural materials and additives is increasing (Mat Aron et al., 2020). Intracellular protein phycocyanin from Spirulina sp. is a nutritious protein with sufficient essential amino acids and can be used as protein supplement(Dingling Zhuang, 2021). The potential and applicability of phycocyanin in the treatment of human diseases, for example anti-cancer therapy such as breast cancer, colon cancer and lung cancer by inhibiting cancer cell proliferation and promoting apoptosis(Liangqian et al., 2017), has gradually been discovered. The development of cost-effective and efficient upstream and downstream processing of phycocyanin and its medical application to improve human health has always been the contemporary research directions.

The Liquid Biphasic System (LBS) is an innovative and non-conventional liquid-liquid extraction approach having extensive applications in the separation, recovery, purification and enrichment of many biotechnological and natural products (Leong et al., 2019). Researchers are still trying to improve phase-forming compositions and reactors to achieve better extraction effect. A liquid biphasic flotation (LBF) system was built by Chew et al. (2019) which is the combination of LBS (liquid biphasic system) and adsorptive bubble flotation system. The system effectively concentrates the product of interest to the top layer through the adsorption of the surface of the bubble, and then releases the product through the bubble collapse process to finally achieve the purpose of obtaining high-quality phycocyanin. Since the upper layer extractant (polymer) is expensive and the difficulty of recycling, also, its waste has a negative impact on the environment, our team hopes to replace the top phase by introducing a more environmentally friendly extractant. Optimized LBF system will be used to improve product recovery yield and separation efficiency in a fast and economy way.

2. Ionic Liquid Based Biphasic Flotation

In recent years, ionic liquid (IL) has been widely applied in various fields of chemistry as a green solvent. The introduction of ionic liquids as extractants into aqueous two-phase systems can achieve advantages such as negligible viscosity, little emulsion formation, without volatile organic solvent, quick phase separation, high extraction efficiency, and gentle biocompatible environment (Zhang et al., 2015). In this project, a certain amounts of $[B_{min}]Cl$ (1-Butyl-3-methylimidazolium chloride) and K_2HPO_4 were used as extractants to form the aqueous two phase. The interaction between ionic liquid cations and phycocyanin greatly facilitated protein purification and enriched the upper phase with phycocyanin. The crude extract obtained by ultrasonic assistance was added to the system and placed in a glassware with a sintered glass disk at the bottom for flotation. The presence of flotation helps to achieve a quick separation of the product from impurities. Finally, ionic liquids will be depressurized for recycling and evaluated for their recycling potential. Recycling of IL coluld effectively reduce the industrial cost of ionic liquids, allowing ionic liquid based biphasic flotation to be accepted by the industry as a more economical and green extraction technology in the future.

References

Chew, K.W., Chia, S.R., Krishnamoorthy, R., Yang, T., Show, P.L., 2019. Liquid biphasic flotation for the purification of C-phycocyanin from Spirulina platensis microalga. Bioresource Technology 288, 121519.

Dingling Zhuang, D.Y.Y.T., Kit Wayne Chew, Tau Chuan Ling, 2021. Phycocyanin: A Natural Antioxidant to Combat Free Radicals. Current Nutrition & Food Science, 1-7.

Leong, H.Y., Chang, C.-K., Lim, J.W., Show, P.L., Lin, D.-Q., Chang, J.-S., 2019. Liquid Biphasic Systems for Oil-Rich Algae Bioproducts Processing. Sustainability 11, 4682.

Mat Aron, N.S., Khoo, K.S., Chew, K.W., Show, P.L., Chen, W.H., Nguyen, T.H.P., 2020. Sustainability of the four generations of biofuels–A review. International Journal of Energy Research 44, 9266-9282.

Zhang, X., Zhang, F., Luo, G., Yang, S., Wang, D., 2015. Extraction and separation of phycocyanin from Spirulina using aqueous two-phase systems of ionic liquid and salt. Journal of Food and Nutrition Research 3, 15-19.

PCR13042022 – 46: An efficient method of heavy metal removal from wastewater using symbiosis of microalgae and bacterial consortium

Dehua Zhao[a] , Wai Yan Cheah[b] , Lai Sai Hin[a] , Pau-Loke Show[c] , Rosazlin Abdullah[d] , Tau Chuan Ling[d]

a Department of Civil Engineering, Faculty of Engineering, University of Malaya, 50603 Kuala Lumpur, Malaysia

b Centre for Research in Development, Social and Environment (SEEDS) Faculty of Social Sciences and Humanities, Universiti Kebangsaan Malaysia

c Department of Chemical and Environmental Engineering, Faculty of Engineering, University of Nottingham Malaysia Campus, Jalan Broga, 43500, Semenyih, Selangor Darul Ehsan, Malaysia

d Institute of Biological Sciences, Faculty of Science, University of Malaya, 50603 Kuala Lumpur, Malaysia

Corresponding Author E-mail: tcling@um.edu.my PauLoke.Show@nottingham.edu.my

Keywords: Microalgae-Bacterial Consortium; Heavy metals; Wastewater treatment; Adsorption; Bioremediation;

Extended Abstract

Heavy metals in industrial wastewater are harmful and not easy to be biodegraded, which may lead to serious environmental problems. The traditional physicochemical methods for the treatment of heavy metals exhibited disadvantages such as high cost and easy to cause secondary pollution. Biosorption is not only an efficient and low-cost method to treat heavy metal wastewater, but also an ideal method to treat large volume and low concentration heavy metals in wastewater. Bacteria and microalgae which are presently naturally in water play an important role in promoting the material circulation in the water environment and maintaining the ecological balance of the aquatic environment. The interaction between bacteria and algae is mutual as they may inhibit each other due to competition for nutrients, or they may use and promote each other, or even depend on each other to form a complex symbiotic system. Bacteria and microalgae that can form a symbiotic system are generally complementary in metabolic functions, mainly manifested in the release and utilization of oxygen, carbon dioxide and nutrients. Microalgae can absorb carbon dioxide and release oxygen through photosynthesis under light conditions, while microalgae and bacteria absorb oxygen and release carbon dioxide to complete respiration. In terms of nutrient metabolism, microalgae synthesize organic matter by absorbing inorganic nutrients such as nitrogen and phosphorus, and can release some organic matter to the surrounding. As an important decomposer, bacteria can decompose and utilize the organic matter secreted by algae and dead algal cells, and their decomposition products are absorbed and utilized by algae. Bacteria and microalgae secrete some extracellular products to the surrounding during their growth, and they interact with each other through these extracellular products. The effects of extracellular products can be divided into two kinds, which play a positive role in promoting growth and a negative role in inhibiting growth. Microorganisms (bacteria, microalgae, etc.) have attracted more and more attention as a biological adsorbent for the removal of heavy metals because of their high surface area volume ratio and rich functional groups on the surface. The cell walls of microalgae and bacteria are composed of polysaccharides and carbohydrates with negatively charged groups. Most metals bind to negatively charged ligand groups, which is the basis of metal removal in wastewater. In addition to being adsorbed on the cell

surface and extracellular polysaccharides, metals can also be absorbed into cells and precipitated on the cell surface or inside. Loutseti explored the effect of biofilter mixed with microalgae, cyanobacteria, diatoms and bacteria on the treatment of wastewater containing Cu and Cd. The results showed that after contact for 5 minutes, the removal rates of Cu and Cd reached 80% and 100%. In particular, the combination of microalgae and bacteria has great advantages as an adsorbent. In recent years, the application of algae bacteria synergistic symbiosis system in sewage treatment has been widely studied. In the bacteria algae symbiosis system, the interaction between microalgae cells and bacteria is beneficial to build a stable bacteria algae symbiosis system, so it can save the operation cost of aeration. Using bacteria algae symbiosis system to treat heavy metals is a green environmental protection process with small investment, low operation cost, no need to add other chemicals, efficient inorganic salt degradation and accumulation of microalgae biomass energy. In conclusion, the combined treatment of wastewater by bacteria and algae may be an attractive supplement to the existing biological treatment of wastewater.

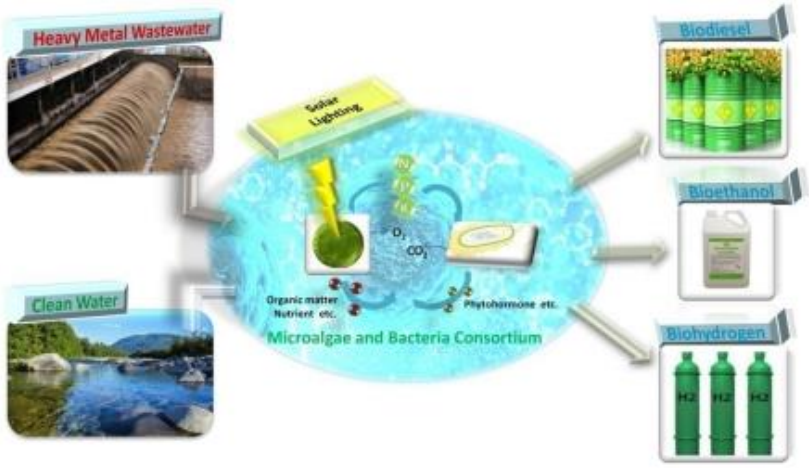

Figure 1: Image illustrating the mutually beneficial symbiotic and competitive relationship between microalgae and bacteria.

Acknowledgements: The authors thank the Fundamental Research Grant Scheme (FP109-2020) and IIRG004A-19IISS.

6th International Conference and
Postgraduate Colloquium for
Environmental Research 2022 (POCER
2022) 9 - 11 June 2022
Langkawi, Kedah, Malaysia

PCR24032022 – 47: Cloud-based residential façade analysis system: mobile application development using machine learning algorithms

Molood Seifi[a*], Huong-Yong Ting[b], Kie-Huf Ngu[b], and Saranya Balasubramaniam[b]

[a] Department of Architecture, School of Built Environment,
University of Technology Sarawak, Sarawak, Malaysia

[b]Drone Research and Application Centre,
University of Technology Sarawak, Sarawak, Malaysia

- Corresponding Author E-mail: seifi.molood@gmail.com

Keywords: Window-to-Wall Ratio; Artificial Intelligence; Machine Learning Algorithms; Building Performance; AEC Industry

Extended Abstract

Window-to-wall ratio (WWR) is the crucial determinant of environmental performance and energy saving in buildings. By studying the existing façade of the buildings through image processing, the window-to-wall ratio (WWR) can be detected and determined. The calculated WWRs then can be used to estimate the visual and thermal performance of the buildings either individually or at the city level. The majority of the past studies have focused on the accuracy of window detection rather than calculating window-to-wall-ratio (e.g: Neuhausen & Konig, 2018; Ali et al., 2007; Recky & Leberl, 2010; Li et al., 2020) except Szcześniak et al., (2021) who extracted the WWR of the commercial high-rise buildings. The shortcomings of the previous research are estimating WWR from google street-view and pre-processed façade aerial images which have issues related to distortion and pixel precision. Besides, a well-trained model to detect the components of the non-western residential facades is scarce. Hence, this study deploys the real-time images of the houses in the Malaysian context which provides better accuracy for the detection of windows and ultimately a better estimation of WWR.

In this study, the images of the façades of residential buildings in East and West Malaysia are captured and uploaded for image processing in Azure Custom Vision. A total of 464 images of 116 houses were used for the training of the image processing model out of which 54 images were used in the testing

phase of the system. The images uploaded are tagged as gate, door, window and the model is trained and its performance is checked. The iteration process to improve the model performance was repeated ten times. Furthermore, the prediction API algorithm developed by the Azure Custom Vision was exported and used in the development of the mobile application to enable the detection of the window to wall ratios effectively. The entire process of the methodology has been shown in figure 1.

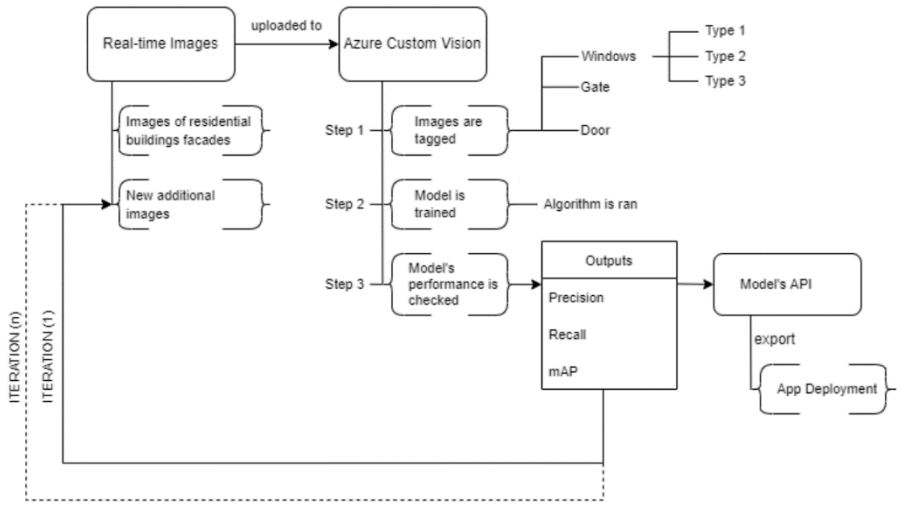

Figure 1: Application development methodology flowchart

The model has been trained to recognize all the components of the facades such as windows and doors. Figure 2 shows the overall model's performance with the precision of 60.5% and Table 1 shows the model's performance of each component given by Azure Custom Vision upon the completion of iteration ten. The precision of tags for the door and windows are respectively 66.7%, 54.5%. Since the precision rates are satisfactory, the mobile application can detect the windows correctly. The results indicate that the windows can be detected from the real-time images provided in the mobile phones and the window-to-wall ratio can be successfully estimated by the cloud-based residential façade analysis system. The outcome of this study is a well-trained and robust system with 70.5% precision that can detect the window-to-wall ratio of residential buildings in Malaysia. The proposed mobile application using machine learning algorithms can be used by AEC industry professionals who would want to estimate window to wall ratios in residential buildings in Malaysian or similar contexts which can be leveraged for environmental performance and energy assessments of buildings.

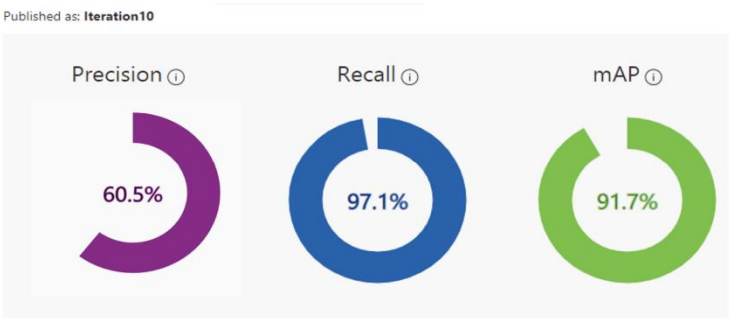

Figure 2: Model's Performance

Table 1: The Performance Per Tag of the Model

Tag	Precision	Recall	A.P.
Door	66.7%	100.0%	100.0%
Window	54.5%	100.0%	79.4%
Occlusions	60%	87.5%	87.5%

Acknowledgments: The authors would like to extend their appreciation to the Research Grant (URG), Ref: UTS/REASEARCH/<4/2020/01>(01) provided by University Technology Sarawak (UTS) for the financial support of this paper.

References

Ali, H., Seifert, C., Jindal, N., Paletta, L., & Paar, G. (2007, September). Window detection in facades. In *14th International Conference on Image Analysis and Processing (ICIAP 2007)* (pp. 837-842). IEEE.

Li, C. K., Zhang, H. X., Liu, J. X., Zhang, Y. Q., Zou, S. C., & Fang, Y. T. (2020). Window detection in facades using heatmap fusion. *Journal of Computer Science and Technology*, *35*(4), 900-912.

Neuhausen, M., & König, M. (2018). Automatic window detection in facade images. *Automation in Construction*, *96*, 527-539.

Recky, M., & Leberl, F. (2010, July). Window detection in complex facades. In *2010 2nd European Workshop on Visual Information Processing (EUVIP)* (pp. 220-225). IEEE.

Szcześniak, J. T., Ang, Y. Q., Letellier-Duchesne, S., & Reinhart, C. F. (2022). A method for using street view imagery to auto-extract window-to-wall ratios and its relevance for urban-level daylighting and energy simulations. *Building and Environment*, *207*, 108108.

6th International Conference and
Postgraduate Colloquium for
Environmental Research 2022 (POCER
2022) 9 - 11 June 2022
Langkawi, Kedah, Malaysia

PCR26032022 – 49: Structure characterisation for Hydroxypropyl Bispalmitamide MEA and Ceramide 3

Teng Jin Khoo [a] , Chien Hwa Chong [b]

[a] School of Pharmacy, Faculty of Science and Engineering,
University of Nottingham Malaysia, Jalan Broga, Semenyih 43500, Malaysia

[b] Department of Chemical and Environmental Engineering, Faculty of Science and Engineering,
University of Nottingham, Jalan Broga, Semenyih 43500, Malaysia

- Corrensponsing Author E-mail:

Keywords: Hydroxypropyl Bispalmitamide MEA; Ceramide 3; Physico chemical analysis; Sphingosine moiety

Extended Abstract

The objective of this study is to evaluate the structure characterisation of Hydroxypropyl Bispalmitamide MEA and Ceramide 3. Three different spectroscopy and physico chemical analysis conducted on the two samples reveal the structural formulae and chemical composition of Hydroxypropyl Bispalmitamide MEA to be different from Ceramide 3. Therefore, the two compounds cannot be considered to contain the same chemical structural make up, based on spectral analysis generated by instrumentation. The Hydroxypropyl Bispalmitamide MEA cannot be categorised as ceramide because it is lacking the sphingosine moiety.

6th International Conference and Postgraduate Colloquium for Environmental Research 2022 (POCER 2022) 9 - 11 June 2022
Langkawi, Kedah, Malaysia

PCR28032022 – 50: Critical Review of the Various Reaction Mechanisms For Glycerol Etherification

Prakas Palanychamy[a*], Steven Lim[a*], Yeow Hong Yap[a], and Loong Kong Leong[b]

[a] Department of Chemical Engineering, Lee Kong Chian Faculty of Engineering and Science University Tunku Abdul Rahman, Bandar Sungai Long, 43000 Kajang, Selangor, Malaysia

[b] Excelube Marketing Sdn. Bhd., IOI Boulevard, Jalan Kenari 5, Bandar Puchong Jaya 47170 Puchong, Selangor, Malaysia

- Correnspondsing Author E-mail: prakassp@utar.edu.my, stevenlim@utar.edu.my

Keywords: Glycerol Etherification; Mechanism; Alcohol Solvent; Olefin Solvent; Solvent Free

Extended Abstract

Commercial relevance of glycerol as a safe feedstock for various conversion processes has increased considerably owing to the fact that it is abundantly available at relatively low cost. Among the diverse reaction pathways for catalytic conversion of glycerol, etherification to yield polyglycerols is favoured to spearhead the research due to the wide applications of polyglycerols such as food industry, cosmetics, pharmaceutical, polymers and biomedicals. The lack of knowledge on each mechanism and pathways in the etherification process has hampered the selection on the best compromised mechanism in furthering the studies to enhance the selectivity and conversion of the glycerol. This review is steadfast in providing an understanding on the numerous mechanisms available for glycerol etherification process implying alcohol solvent, olefin solvent and solvent-free routes along with the products being formed at various stages of the reaction. Etherification of glycerol using tert-butyl alcohol (TBA), ethanol, *n*-butanol and benzyl alcohol were studied as the alcohol solvents. Utilising TBA in the etherification gives rise to three general ether products which are mono tert-butyl glycerol ether (MTBG), di tert-butyl glycerol ether (DTBG) and tri tert-butyl glycerol ether (TTBG) [García-Sancho et al., 2011]. Besides that, the dehydration of TBA to isobutene as an independent side reaction result in the undesired

consumption of glycerol, while the formation of isobutene triggers another side reaction which is the dimerization of isobutene which forms di-isobutene (DIB) [Cannilla et al., 2014; Estevez et al., 2017]. As for the glycerol etherification with ethanol, the products include two mono-ethyl glycerol ethers, two di-ethyl glycerol ethers as well as a tri-ethyl glycerol ether. The self-etherification of ethanol leading to the formation of diethyl ether (DEE) which can be attributed to the high ethanol to glycerol molar ratio as well as high reaction temperature are the main side reaction [Yadav, Maity and Shee, 2017; Lemos et al., 2018]. The reaction of glycerol etherification with *n*-butanol yields glycerol ether products bonded with the substituted butyl groups, including two mono-butyl glycerol ethers, two di-butyl glycerol ethers and a tri-butyl glyceryl ether with the loss of water molecule. The dehydration of butanol to butane, isomerization of butane to isobutene, dimerization of butanol to butyl ethers and oxidation of butanol to butanal are the potential side reactions involved in the reaction [Cannilla et al., 2015]. The prominently observed products when benzyl alcohol utilised as a solvent in the etherification reaction includes two mono-benzyl glycerol ether isomers, two di-benzyl glycerol ether isomers and tri-benzyl glycerol ether. The formation of dibenzyl ether (DBZ) from the dimerization of benzyl alcohol has reduced the yield of desired product as it competes in the utilization of benzyl alcohol in the glycerol etherification reaction [Gonzalez-Arellano et al., 2015]. The olefin solvent studied in the glycerol etherification process includes isobutene, 1-butene and isoamylene. The reaction of isobutene with glycerol proceeds via tert-butylation of glycerol yields similar glycerol ether products when TBA was used as a solvent in the etherification process [Cannilla et al., 2014] while the etherification of glycerol with 1-butene involves a set of consecutive equilibrium reactions to produce mono-ethers, di-ethers and tri-ether [Saengarun, Petsom and Tungasmita, 2017]. The undesired side reaction reported using both types of olefin solvents is the formation of a dimer (di-1-butene) from the dimerization of 1-butene, whereby the solvent is consumed in a large proportion which could affect the formation of the desired ethers [Liu, Yang and Yi, 2013; Saengarun, Petsom and Tungasmita, 2017] Five ether products are obtained from the glycerol etherification with isoamylene, which consist of two mono-ethers, two di-ethers and a tri-ether while undesired isomerization of isoamylene results in the formation of undesired isoamylene oligomers [Izquierdo et al., 2014]. Glycerol etherification without using solvent is known as oligomerization of glycerol which forms short chain oligomer of glycerol while long chain oligomers are known as polyglycerols. Two glycerol molecules join through the condensation reaction to form a diglycerol molecule with the elimination of one water molecule, whereby the formed diglycerol molecules can exist either in linear, branched, or cyclic structure. Further reaction with the diglycerol can yield polyglycerol where the length of the oligomers depends on the number of glycerol or diglycerol joined together [Lee et al., 2018]. Studies carried out using solvent-free glycerol etherification is gaining momentum as the by-product obtained is mainly water which can be removed from the reaction. In this respect, solvent-free etherification process could promise several advantages.

Using acid catalysts in solvent-free glycerol etherification process could lead to an undesired side reaction through the dehydration of glycerol, hence forming acrolein. Base catalysed solvent-free glycerol etherification showed promising catalytic results with no substantial acrolein formation [Gholami, Abdullah and Lee, 2014].

Acknowledgements: The authors would like to thank the financial support provided by Universiti Tunku Abdul Rahman for the UTARRF/2021-C1/P01 for this study.

References

Cannilla, C. *et al.* (2014) "Catalytic production of oxygenated additives by glycerol etherification," in *Central European Journal of Chemistry*. Versita, pp. 1248–1254. doi:10.2478/s11532-014-0546-y.

Cannilla, C. *et al.* (2015) "Batch reactor coupled with water permselective membrane: Study of glycerol etherification reaction with butanol," *Chemical Engineering Journal*, 282, pp. 187–193. doi:10.1016/j.cej.2015.03.013.

Estevez, R. *et al.* (2017) "Microwave-assisted etherification of glycerol with tert-butyl alcohol over amorphous organosilica-aluminum phosphates," *Applied Catalysis B: Environmental*, 213, pp. 42–52. doi:10.1016/j.apcatb.2017.05.007.

García-Sancho, C. *et al.* (2011) "Etherification of glycerol to polyglycerols over MgAl mixed oxides," in *Catalysis Today*, pp. 84–90. doi:10.1016/j.cattod.2010.11.062.

Gholami, Z., Abdullah, A.Z. and Lee, K.T. (2014) "Dealing with the surplus of glycerol production from biodiesel industry through catalytic upgrading to polyglycerols and other value-added products," *Renewable and Sustainable Energy Reviews*. Elsevier Ltd, pp. 327–341. doi:10.1016/j.rser.2014.07.092.

Gonzalez-Arellano, C. *et al.* (2015) "The role of mesoporosity and Si/Al ratio in the catalytic etherification of glycerol with benzyl alcohol using ZSM-5 zeolites," *Journal of Molecular Catalysis A: Chemical*, 406, pp. 40–45. doi:10.1016/j.molcata.2015.05.011.

Izquierdo, J.F. *et al.* (2014) "New biodiesel additives from glycerol and isoamylenes," *Biofuels, Bioproducts and Biorefining*, 8(5), pp. 658–669. doi:10.1002/bbb.1473.

Lee, J.H. *et al.* (2018) "Solventless Catalytic Etherification of Glycerol Using Acetate Salts as Efficient Catalysts," *Bulletin of the Korean Chemical Society*, 39(6), pp. 722–725. doi:10.1002/bkcs.11460.

Lemos, C.O.T. *et al.* (2018) "Study of glycerol etherification with ethanol in fixed bed reactor under high pressure," *Fuel Processing Technology*, 178, pp. 1–6. doi:10.1016/j.fuproc.2018.05.015.

Liu, J., Yang, B. and Yi, C. (2013) "Kinetic study of glycerol etherification with isobutene," *Industrial and Engineering Chemistry Research*, 52(10), pp. 3742–3751. doi:10.1021/ie400050v.

Saengarun, C., Petsom, A. and Tungasmita, D.N. (2017) "Etherification of glycerol with propylene or 1-butene for fuel additives," *Scientific World Journal*, 2017. doi:10.1155/2017/4089036.

Yadav, V.P., Maity, S.K. and Shee, D. (2017) "Etherification of Glycerol with Ethanol over Solid Acid Catalysts: Kinetic Study Using Cation Exchange Resin," *Indian Chemical Engineer*, 59(2), pp. 117–135. doi:10.1080/00194506.2016.1139472.

6th International Conference and
Postgraduate Colloquium for
Environmental Research 2022 (POCER
2022) 9 - 11 June 2022
Langkawi, Kedah, Malaysia

PCR28032022 – 51: Simultaneous Extraction of Low-gluten Flour and Gum from Durian Seed for Food Applications

Zhi Ling Chew[a] and Yin Leng Kua[b*]

[a] Department of Chemical Engineering, Xiamen University Malaysia, Sepang, Selangor, Malaysia
[b] Department of Chemical Engineering, Xiamen University Malaysia, Sepang, Selangor, Malaysia

*Corrensponding Author E-mail Address: yinleng.kua@xmu.edu.my

Abstract

A green and safe method was studied for simultaneous extraction of low-gluten flour and gum from durian seed for food applications. The effects of extraction temperature and water/seed (W/S) ratio on the extraction yield, colour, solubility, water absorption capacity (WAC) and oil absorption capacity (OAC) of whole durian seed flour (WDSF), demucilaged durian seed flour (DDSF) and durian seed gum (DSG) were investigated. Although higher extraction temperature would lead to darker colour products, it could maximize the yield of both flour and gum, as well as improve their solubilities and WAC. Higher W/S ratio produced higher gum yield but lower flour yield. Solubility generally increased in the order of DDSF, WDSF to DSG. Besides, the OAC of gum was slightly higher than the flour.

Keywords: Durian seed flour; Durian seed gum; Extraction; Biomass waste

Introduction

While the edible flesh is only 1/3, durians will generate about 60-75% of wastes where 20-25% are seeds and the remaining are husks (Villacis-Chiriboga et al., 2020). Durian seed is one of the abundant biomass wastes generated from the highly demanded durian, where approximately 60,000 MT of seeds were discarded per annum in Malaysia which can lead to environmental pollution. However, the seeds offer great potential applications in many food and non-food industries. Starch and polysaccharide (mucilage) are the major components of the durian seed, which could be further processed into value-added products like flour and gum to act as food ingredient and stabilizer (Baraheng and Karrila, 2019). Hence, this project is in line with Sustainable Development Goals (SDGs), National Agro-food Policy 2.0 (NAP 2.0) 2021-2030, 12th Malaysia Plan (2021-2025), and Shared Prosperity Vision (SPV) 2030

in efforts to achieve sustainability, enhance food security and nutrition, address waste disposal issues, and promote Malaysia's economic growth (TheSunDaily, 2019).

In fact, the chemical composition, yield and functional properties of flour and gum could be affected significantly by the seed processing and extraction conditions (Baraheng and Karrila, 2019). To date, aqueous and chemical extraction methods have been employed to extract either the gum or flour only from durian seed. In accordance with the 12 Principles of Green Chemistry, present research is a relatively greener and safer method for simultaneous extraction of durian seed flour and gum in comparison with others' works. The process efficiency and sustainability were maximized without the use of highly toxic and corrosive chemicals.

Methodology

Durian seeds were washed, dehulled, sliced, and blended with water. Aqueous gum extraction from the seed slurry was performed for 1 hour at different temperature and W/S ratio. It was then cooled down and filtered to separate the sticky filtrate from residue. The residue was washed thrice with water, followed by drying, milling and sieving to obtain DDSF. Meanwhile, the sticky filtrate was centrifuged for 10 min. The collected supernatant was precipitated with 95% ethanol and it was left at room temperature for 30 min. Filtration was then performed and the precipitated gum was washed thrice with ethanol. Similar to DDSF, the white precipitate was also dried, milled and sieved to produce DSG. Besides, WDSF was studied as the control.

Results and Discussions

This work revealed that higher extraction temperature was favoured for higher overall yield, better solubility and WAC of both flour and gum. This is because the molecular bonds could be broken easily at high temperature and the particles were cleaved into smaller sizes, resulting in more exposed hydroxyl groups to interact better with the polar water molecules (Amid and Mirhosseini, 2012). However, high extraction temperature would cause adverse effects on the darker colour products, which mainly due to the Maillard reaction took place upon heating (Malini et al., 2016). At lower temperature, lesser gum in the extract caused more releases of the starchy materials, leading to more product losses and lower yield (Baraheng and Karrila, 2019). Moreover, higher W/S ratio had greater driving force that facilitate the gum extraction.

Generally, the crude gum possessed abundant hydroxyl (-OH) and hydrophilic groups (carbonyl groups C=O and carboxyl groups -COOH) which contributed by the polysaccharides and polar amino acids

(Zainol et al., 2020). Hence, the gum was readily soluble and could bind more water than the flour. Meanwhile, the OAC of gum was also slightly higher than flour due to the presence of hydrophobic fractions like the fatty acids and nonpolar amino acids which having long carbon chains and bulky carbon rings. Conversely, DDSF that mainly composed of starch macromolecules was less soluble, but exhibited good swelling power and thickening ability after absorbing water due to the presence of amylose and amylopectin (Awuchi et al., 2019).

Conclusion

Higher extraction temperature could improve the overall yield, solubility and WAC of both flour and gum, but resulting in darker colour products. Higher W/S ratio produced higher gum yield but lower flour yield. DSG is a good emulsifier because the hydrocolloid had relatively high WAC, OAC and solubility, while DDSF had a good WAC and could thicken well. In conclusion, this study had simultaneously obtained both durian seed flour and gum from durian seeds via a green and simple aqueous extraction method.

Acknowledgements: The authors thank the Ministry of Higher Education Malaysia for the support to this research project through Fundamental Research Grant Scheme (FRGS), project number (FRGS/1/2021/TK0/XMU/02/2).

References

AMID, B. T. & MIRHOSSEINI, H. 2012. Optimisation of aqueous extraction of gum from durian (Durio zibethinus) seed: A potential, low cost source of hydrocolloid. *Food Chem,* 132**,** 1258-1268.

AWUCHI, C. G., IGWE, V. S. & ECHETA, C. K. 2019. The Functional Properties of Foods and Flours. *International Journal of Advanced Academic Research,* 5**,** 139-160.

BARAHENG, S. & KARRILA, T. 2019. Chemical and functional properties of durian (Durio zibethinus Murr.) seed flour and starch. *Food Bioscience,* 30**,** 1-8.

MALINI, D. R., ARIEF, I. I. & NURAINI, H. 2016. Utilization of Durian Seed Flour as Filler Ingredient of Meatball. *Media Peternakan,* 39**,** 161-167.

THESUNDAILY. 2019. *NAP 2.0 to be launched in 2021, will boost modernisation of agro-food business* [Online]. Available: https://www.thesundaily.my/local/nap-20-to-be-launched-in-2021-will-boost-modernisation-of-agro-food-business-MH1678187

VILLACIS-CHIRIBOGA, J., ELST, K., VAN CAMP, J., VERA, E. & RUALES, J. 2020. Valorization of byproducts from tropical fruits: Extraction methodologies, applications, environmental, and economic

assessment: A review (Part 1: General overview of the byproducts, traditional biorefinery practices, and possible applications). *Compr Rev Food Sci Food Saf,* 19**,** 405-447.

ZAINOL, N., SUBRAMANIAN, S., ADNAN, A. S., ZULKIFLI, N. H., ZAIN, A. A. M., KASSIM, N. R. W. & KAMARUDIN, A. A. 2020. The potential source for composite flours as food ingredient from local grown crops. *Food Research,* 4**,** 24-30.

6th International Conference and
Postgraduate Colloquium for
Environmental Research 2022 (POCER
2022) 9 - 11 June 2022
Langkawi, Kedah, Malaysia

PCR28032022 – 52: Biomass waste-based mesoporous silica

Abdul Rasheed Kadiri Kanakka Pillantakath[a,b], Amanuel Gidey Gebretatios[a], and Chin Kui Cheng[a,b*]

[a] Department of Chemical Engineering,
Khalifa University of Science & Technology, P.O.Box 127788, Abu Dhabi, UAE

[b] Center for Catalysis & Separation (CeCaS)
Khalifa University of Science & Technology, P.O.Box 127788, Abu Dhabi, UAE

- Corrensponsing Author E-mail: cheng.kui@ku.ac.ae

Keywords: Biomass waste; Mesoporous silica; Rice husk; SBA-15.

Extended Abstract

Porous material possesses larger specific surface area compared to its non-porous counterpart. Consequently, it is increasingly popular for various applications in chemical industries. In this work, mesoporous silica (SiO_2) was synthsized from biomass waste, specifically rice husk. From the literature, SiO_2 content in rice varies from 8.7 to 12.1%, averaging close to 10.6% [Ding *et al*., 2005]. However, SiO_2 present in rice husk is in a hydrated amorphous form [Asuncion *et al*., 2005].

In this work (cf. Figure 1), we have synthesized mesoporous silica of SBA-15 and MCM-41 morphologies from the rice husk. As a comparison, mesoporus silica SBA-15 was also synthesized from tetraethyl orthosilicate (TEOS), whereby TEOS acted as a silica source.

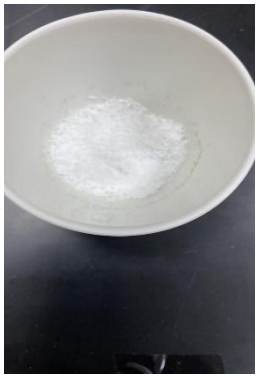

(a) (b)

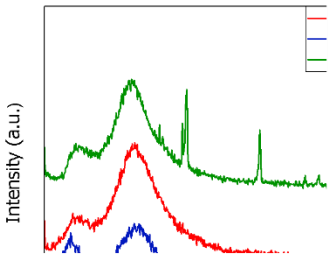

(c)

Figure 1: (a) Fresh rice husk; (b) as-synthesized mesoporus silica, and (c) XRD diffraction pattern of the as-synthesized mesoporus silica

Fresh rice husk was obtained from a local source (refer to Fig. 1(a)). The husk in its original condition has brownish colour. It was then subjected to high temperature treatment, followed by silica-extraction process, before finally templating into SBA-15 and MCM-41 using different chemical sources, for example CTAB. Fig. 1(b) shows the mesoporous silica in its final form. It comes in the form of white powder. The same preparation steps were repeated for templating TEOS into SBA-15 material. All these three materials were scanned using XRD technique (cf. Fig. 1(c)). The wide hump at circa 23^{o} denoted the amorphous silica (SiO_2) phase. Subsequently, further physicochemical characterization were carried out, i.e., N_2 physisorption, SEM, FTIR and XRF.

Acknowledgements: The authors would like to record their appreciation to Khalifa University of Science and Technology for FSU2021-003 with a project number of 8474000343.

References

Ding, T. P.; Ma, G. R.; Shui, M. X.; Wan, D. F.; Li, R. H., 2005. Silicon isotope study on rice plants from the Zhejiang province, China. *Chem. Geol*. 218: 41−50.

Asuncion, M. Z.; Hasegawa, I.; Kampf, J. W.; Laine, R. M., 2005. The selective dissolution of rice hull ash to form $[OSiO_{1.5}]_8[R_4N]_8$ (R =Me, CH_2CH_2OH) octasilicates. Basic nanobuilding blocks and possible models of intermediates formed during biosilicification processes. *J. Mater. Chem*. 15: 2114−2121.

6th International Conference and Postgraduate Colloquium for Environmental Research 2022 (POCER 2022) 9 - 11 June 2022
Langkawi, Kedah, Malaysia

PCR29032022 – 54: Stabilization of Protein-Fortified Pineapple Jam Using Natural Deep Eutectic Solvents (NADES)

Xue Yan, Sima and Yin Leng, Kua[a*]

[a] School of Energy and Chemical Engineering Xiamen University Malaysia, Selangor, Malaysia

• Corrensponsing Author E-mail: yinleng.kua@xmu.edu.my[a*]

Keywords: NADES, Pineapple Jam, Bromelain, Gelatin, Antimicrobial activity

Extended Abstract

This paper introduces natural deep eutectic solvents (NADES), the potential stabilisers that can use to prevent the breakdown of gelatin by bromelain enzyme in the pineapple jams. The fortification of gelatin in the pineapple jam improves the protein content, while the retention of bromelain protease brings health benefits to human being. Self-synthesised citric acid/fructose NADES and market-bought NADES were used in the research. Both NADES were highly compatible with the pineapple jam due to their hydrophylic properties. The greater the amount of citric acid/fructose NADES, the lower the syneresis degree which indicated the stabilisation of both bromelain and gelatin. High water addition will lead to a loosen hydrogen bond which might fail to stabilise bromelain and gelatin. At least 50 mL of citric acid/fructose NADES possessed antimicrobial ability in pineapple jam. In short, citric acid/fructose NADES with molar ratio 1:1 was able to stabilise bromelain and gelatin at the puree to NADES ratio from 1:1 to 5:1 and inhibited microbial growth at a relatively high dosage.

Introduction: Pineapple that is rich in bromelain enzyme could be processed into pineapple jam for a longer storage period and easier consumption. Pineapple jam can be fortified for value-adding purposes. Previous studies had investigated the fortification of protein in papaya jam. However, the existence of bromelain protease will result in the protein preservation difficulty in pineapple jams. It was suggested NADES could be a solution for incorporating higher protein content in fruit jams.

Methodology: In this study, the compatibility of NADES and pineapple jam, the effect of different combinations of NADES in stabilising bromelain and gelatin as well as the antimicrobial effect of NADES in pineapple jam were investigated. Pineapple jam was prepared with minimal heating to retain most of the bromelain and NADES served as the agent to harmonise bromelain and gelatin in pineapple jam. Self-synthesised citric acid/fructose NADES with the molar ratio of 1:1 which was prepared using heating and stirring method and market-bought honey NADES with approximately equimolar fructose and glucose were applied in this study [Daia et al., 2021].

Results and Discussions: NADES can be well mixed in pineapple jam without phase separation because NADES tended towards the formation of hydrogen bonds. The hydrogen bonding made NADES polar and allowed it to dissolve well in pineapple jam [Chen et al., 2019]. Citric acid/fructose NADES had greater carbonyl and hydroxyl groups than honey NADES, which resulted in greater hydrogen bond formation and

thus lowered the syneresis degree (free whey formation). When the puree to NADES ratio reduced from 10:1 to 5:1 to 1:1, the free whey formation decreased from 2.76 to 1.43 to 0.80 g/100 g, resulting in a lower syneresis. It was because the greater amount of NADES contributed to more carbonyl and hydroxyl groups which were able to restrict the bromelain and gelatin molecules within the network [de los Ángeles Fernández et al., 2018]. Furthermore, the greater amount of water added during NADES preparation might loosen the hydrogen bond network, resulting in weak interaction between the individual components in NADES [Olivares et al., 2018]. Evidently, jam sample with citric acid/fructose NADES made up of 50% water had slightly higher formation of free whey (2.85 g/100 g) than that of 20% water (2.76 g/100 g). Besides, a sufficiently high amount of citric acid/fructose NADES (at least 50 mL) possessed antimicrobial ability in jam sample with 50 g puree and total soluble solids (TSS) value ranged from 65 to 70%. 20% water in NADES synthesis and puree to NADES ratio from 1:1 to 5:1 yielded relatively firm, safe, and odour-pleasant protein-fortified pineapple jams using citric acid/fructose NADES as a stabiliser and gelatin as a source of protein in the jams. The prepared pineapple jams can last for at least one month without mould grown, alcoholic smell, and increased syneresis.

Conclusions: In conclusion, citric acid/fructose NADES and pineapple jam were highly compatible to each other and the formulated citric acid/fructose NADES was capable to stabilise both bromelain and gelatin in pineapple jam. However, a relatively high dosage of NADES was required to exert an antimicrobial effect in the jam and thus, further investigation is required in this area as a high dosage of NADES in foods may invoke adverse health effects.

Acknowledgements: This work is supported by the Xiamen University Malaysia Research Fund (XMUMRF), project number (XMUMRF/2019-C3/IENG/0010). Finally, a special thanks to the authors' family for their love and support.

References

Daia, Y., Choib, Y. H., Verpoorteb, R. 2021. Honey in traditional Chinese medicine: A guide to future applications of NADES to medicines. Eutectic Solvents and Stress in Plants. 97, 361.

Chen, J., Li, Y., Wang, X., Liu, W. 2019. Deep eutectic solvents for pretreatment, extraction, and catalysis of biomass and food waste. Molecules. 24, 4012.

de los Ángeles Fernández, M., Espino, M., Gomez, F. J., Silva, M. F. 2018. Novel approaches mediated by tailor-made green solvents for the extraction of phenolic compounds from agro-food industrial by-products. Food Chemistry. 239, 671-678.

Olivares, B., Martínez, F., Rivas, L., Calderón, C., Munita, J. M., Campodonico, P. R. 2018. A natural deep eutectic solvent formulated to stabilize β-lactam antibiotics. Scientific reports. 8, 1-12.

6th International Conference and Postgraduate Colloquium for Environmental Research 2022 (POCER 2022) 9 - 11 June 2022
Langkawi, Kedah, Malaysia

PCR29032022 – 55: Intensification of Biodiesel production by hydrodynamic cavitation: A critical review

Xun Sun[a,d*], Yang Tao[b], Sivakumar Manickam[c], and Dennis Y C Leung[d]

[a] School of Mechanical Engineering, Shandong University, Jinan, China

[b] College of Food Science and Technology, Nanjing Agricultural University, Nanjing, China

[c] Petroleum and Chemical Engineering, Faculty of Engineering, Universiti Teknologi Brunei, Bandar Seri Begawan, Brunei Darussalam

[d] Department of Mechanical Engineering, The University of Hong Kong, Hong Kong, China

- Corrensponsing Author E-mail: xunsun@sdu.edu.cn

Keywords: Biodiesel; Process intensification; Pretreatment; Hydrodynamic cavitation; Hydrodynamic cavitation reactor; Practicability

Extended Abstract

With rapid economic development and growing human populations, the greatly increasing demand for energy has been a major problem worldwide. Biodiesel, which chemically consists of alkyl (usually methyl) esters, has been widely considered as a promising alternative energy source to replace fossil fuel, because of its biodegradable, renewable, sustainable, and environmentally friendly features (Chuah et al., 2016). Moreover, by volumetrically blending with commercial fossil diesel in proper proportions (6–20%), biodiesel can be used in internal combustion engines without modifications (ASTM, 2018).

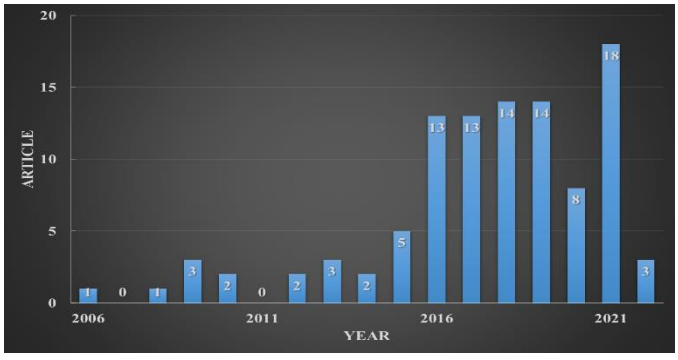

Figure 1: Articles about biodiesel production by HC from 2006 to 2022, based on Web of Science available on 10th April, 2022 (This figure will not be included in the full-length article).

Table 1: Intensification of biodiesel production by HC (partial content of the whole table).

Feedstock	HCR	Energy input	Capacity (L)	Temp. (°C)	Alcohol, molar ratio	Catalyst, concentration (wt.%)	Factor effect	Time (min)	Yield/Conversion (%)	Cavitational yield (mg/J)	Ref.
Castor oil	Nozzle	P_{in} = 2 bar	1.437 kg	60.3	CH_3OH, 9.82: 1	KOH, 1.06	CC, MR, T [a]	50.86	92.27 [b, c]	N/A	[1]
Hemp seed oil	Orifice	P_{in} = 3 bar	4 kg	60	CH_3OH, 6: 1	KOH, 1	CC, E, MR, T	20	97.5 [d]	1.1	[2]
Karanja oil	Orifice	P_{in} = 3 bar	4	N/A	CH_3OH, 5: 1	H_2SO_4, 2	CC, MR, T	60	70 [e]	N/A	[3]
Nagchampa oil	Orifice	P_{in} = 20 psi	10 [f]	<64.7	CH_3OH, 6: 1	KOH, 1	CC, MR	20	92.1 [d]	1.35	[4]
Palm oil, WCO	ARHCR	N = N/A, Q_{in}=390 L/h	7.5	55	CH_3OH, 0.23 vol%	NaOH, 3.67 g/L	N/A	15	99 [b]	0.030 kWh/L	[5]
Palm oil (crude)	ARHCR	N = 3000 rpm	25 L/h (continuous)	60	CH_3OH, 28.6 vol%	KOH, 6.2 g/L	CC, E, G, MR	N/A	99.163 [b, c]	0.049 kWh/L	[6]
Palm oil (crude)	ARHCR	N = 3000 rpm	25 L/h (continuous)	60	CH_3OH, 17.7 vol%	H_2SO_4, 2.9 vol%	CC, E, G, MR	N/A	91.27 [b, c]	0.0264 kWh/L	[7]
Palm oil	Homogenizer	N = N/A	1	60	CH_3OH, 6: 1	NaOH, 1	CC, V	60	90 [b]	0.169	[8]
Pig fat	Orifice	P_{in} = 17 bar	21.45 kg	60	CH_3OH, 6: 1	NaOH, 1	G	5	89.74 [b]	9.05	[9]
Rubber seed oil	Orifice	P_{in} = 3 bar	5 kg	55	CH_3OH, 6: 1	H_2SO_4, 8	CC, E, G, MR, T	30	96 [c, e]	0.218	[10]
Rubber seed oil	Orifice	P_{in} = 3 bar	50 [f]	50	MeOAC, 14: 1	CH_3KO, 0.75	CC, E, G, MR, T, t	20	88 [c, d]	0.0825	[11]
Rubber seed oil	Orifice	P_{in} = N/A	0.4 kg	N/A	C_2H_5OH, 6: 1	KOH, 4	CC, MR, t	40	92.5 [b]	4.13	[12]
Safflower oil	ARHCR	N = N/A	N/A	N/A	CH_3OH, 8.36: 1	KOH, 0.94	CC, G, MR, t	1.06	89.11 [b, c]	N/A	[13]
Soybean oil, WCO	Homogenizer	N = 12,000 rpm	0.15	50	CH_3OH, 10: 1	CaO, 3	CC, E, MR, T	30	84 [b]	N/A	[14]
Soybean oil	Orifice	P_{in} = 0.7 MPa	N/A	45	CH_3OH, 6: 1	KOH, 1	N/A	30	98.98 [b]	0.183 kWh/kg	[15]
Sunflower Oil	Venturi	P_{in} = 1013.2 kPa	0.3	25	CH_3OH, 3: 1 (tetrahydrofuran, 1.6: 1)	KOH, 1	CC, MR, T, t	0.083–1	94–99 [d]	56~528	[16, 17]
etc.											

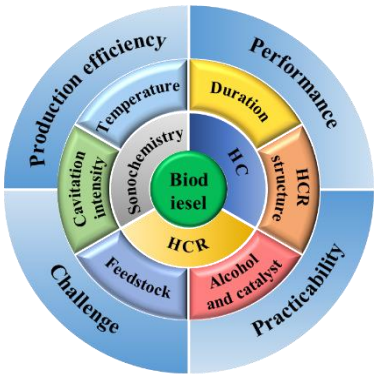

Figure 2 Intensification of biodiesel production by HC

Biodiesel can be produced from renewable feedstocks in nature, such as plant fat, animal fat, and microbial oils, by transesterification in the presence of catalysts (Verma and Sharma, 2016). To increase the mass transfer rate between oil and alcohol, various methodologies, such as mechanical stirring, microwave, AC, and hydrodynamic cavitation (HC) have been widely studied in previous studies. Among them, HC is considered a promising technology for industrial-scale biodiesel production, due to the advantages of high yield efficiency (Chuah et al., 2017), low equipment and operational costs, and ease of scaling up. Since Ji et al. (Ji et al., 2006), for the first time, enhanced the biodiesel production process by HC in 2006, HC technology has drawn increasing interest (Figure 1). Nowadays, HC is reported to be highly effective for intensifying biodiesel production from various feedstocks (e.g., edible, non-edible, and waste oils) under homogeneous (e.g., KOH, NaOH) and heterogeneous (e.g., CaO, TiO_2) catalyses, as shown in Table 1. Nevertheless, although HC has been studied for over ten

years, the amount of the relative research is relatively limited compared with other emerging technologies, indicating that this promising method has not attracted much attention of researchers yet. Moreover, the recent progress in this area is not clear and the corresponding mechanisms are still not well understood. For instance, few rotational hydrodynamic cavitation reactors appeared recently showed significantly high performance compared with conventional reactors, some of them can be operated in continuous mode, indicating great potential for commercial application. However, the research status is still not widely known, especially in the area of biodiesel production. Similar problems are also existing in the intensification mechanism and applicability (e.g., economical assessment and life cycle analysis) of HC technology. Therefore a critical and comprehensive review is an urgent need.

To this, the present review aims to highlight the effectiveness and practicability of HC-based intensification technology for biodiesel production (Figure 2). The principle of HC and the recent advances in the hydrodynamic cavitation reactors are explored. The effect of HC, including the representative applications, key operational factors, and relevant mechanisms, is summarized and discussed. Finally, several challenges and research directions that should be seriously considered are recommended after analyzing the applicability of HC.

Acknowledgements: This work was supported by the National Natural Science Foundation of China (Grant Nos. 51906125, 52111540266) and Hong Kong Scholars Program (Grant No. XJ2021030).

References

ASTM, 2018. ASTM D7467-18b, *Standard specification for diesel fuel oil, biodiesel blend (B6 to B20)*, West Conshohocken, PA.

Chuah, L.F., Yusup, S., Abd Aziz, A.R., Bokhari, A., Abdullah, M.Z., 2017. A review of cleaner intensification technologies in biodiesel production. *Journal of Cleaner Production*, 146: 181-193.

Chuah, L.F., Yusup, S., Abd Aziz, A.R., Bokhari, A., Abdullah, M.Z., 2016, Cleaner production of methyl ester using waste cooking oil derived from palm olein using a hydrodynamic cavitation reactor. *Journal of Cleaner Production*, 112: 4505-4514.4.

Ji, J., Wang, J., Li, Y., Yu, Y., Xu, Z., 2006. Preparation of biodiesel with the help of ultrasonic and hydrodynamic cavitation. *Ultrasonics*, 44: e411-e414.

Verma, P., Sharma, M.P., 2016. Review of process parameters for biodiesel production from different feedstocks. *Renewable and Sustainable Energy Reviews*, 62: 1063-1071.

6th International Conference and Postgraduate Colloquium for Environmental Research 2022 (POCER 2022) 9 - 11 June 2022
Langkawi, Kedah, Malaysia

PCR30032022 – 58: Some Physical Properties and Relationship Between Fractions of Dabai Fruit (*Canarium Odontophyllum Miq.*) Variety '*Ngemah*'

Rosnah Shamsudin*[a,b], Siti Hajar Ariffin[a], Wan Nor Zanariah Zainol @ Abdullah[c], Nazatul Shima Azmi[a], Arinah Adila Abdul Halim[a]

[a]Department of Process and Food Engineering, Faculty of Engineering, Universiti Putra Malaysia, 43400, Serdang, Selangor, Malaysia

[b]Laboratory of Halal Services, Halal Products Research Institute, Universiti Putra Malaysia, 43400, Serdang, Selangor, Malaysia

[c]Department of Basic Science and Engineering, Faculty of Agriculture and Food Sciences, Universiti Putra Malaysia Bintulu Sarawak Campus, Nyabau Road, 97008, Bintulu Sarawak, Malaysia

- Corresponding Author E-mail: rosnahs@upm.edu.my

Abstract

Some physical properties of different fractions part of Dabai fruit were determined for the useful application in appropriate mathematical model for the process optimization and designing processing equipment. The objective of this study is to determine and compare some physical properties of three different fractions (whole, kernel and nut) by taking the measurement of the Dabai fruit. Based on the result, the whole fruit reported the highest value in terms of length (L) (39.14 mm), thickness (T) (22.76 mm), geometric mean diameter (Dg) (26.86 mm), arimethic mean diameter (Da) (27.89mm), surface area (2269.80 mm2), mass (12.38 g), volume (11300 mm3), sphericity (68.67%), and aspect ratio (Ra) (55.69%). On the other hands, the true density, bulk density, and porosity, the nut fraction has the highest values with 2755.0 kg/m3,738.180 kg/m3, and 71.44% respectively. Based on principal component analysis (PCA), the first and second principal component showed related contributions to the physical properties.

Keywords: Dabai / physical properties / Pearson correlation/ principal component analysis

Equations

$$Dg = 3LTW \quad (1)$$

$$Da = (L+T+W)3 \quad (2)$$

$$Ø = (LWT)1/3L \quad (3)$$

Where, Dg = geometric mean diameter; Da = arithmetic mean diameter; Ø = sphericity; L= Length; T = thickness; W = width

$$SA = \Pi Dg2 \quad (4)$$

Where, SA= surface area; Dg = geometric mean diameter

$$pb = MpVc \quad (5)$$

Where, pb= bulk density; Mp= mass of the sample; Vc= volume of the container

$$T = mV \quad (6)$$

Where, = True density; m = mass of the sample; v = volume of the sample

$$\varepsilon = 1 - pbT \times 100 \quad (7)$$

Where, ε = porosity; pb= bulk density; T= true density

$$\theta = \tan -12HD \quad (8)$$

Where, = angle of repose; H= height of the pile; D = radius of the pile

$$Ra = WL \times 100 \quad (9)$$

Where, Ra= aspect ratio; W = width; L= Length

Table

Table 1. The physical properties of the fruit fractions of 'Ngemah' variety Dabai fruit

Properties	Fruit Fractions

	Whole Fruit	Nut	Kernel
Length (mm)	39.14±1.63a	34.48 ±1.47b	23.21±2.42b
Thickness (mm)	22.76±1.31a	17.38 ±1.20b	12.17±0.87c
Width (mm)	21.78±0.98a	16.59 ±0.94b	7.08±0.64c
Dg	26.86±1.06a	21.49±1.01b	12.72±0.69c
Da	27.89±1.05c	22.81±1.00a	14.02±7.00b
Surface area (mm2) (ellipsoid)	2269.80±181.1a	1454.40±139.70b	509.80±56.25c
Mass (g)	12.38±1.57a	5.19±0.75b	0.99±0.18c
Volume (mm3)	11300±2215a	2040±637.60b	1000±0.00c
Sphericity (%)	68.67±2.32a	62.35±2.12b	55.13±4.67c
True Density (kg/m3)	1112.00±119.40b	2755±804a	990.80±184.30b
Bulk Density (kg/m3)	717.60±26.80b	738.18 ±19.62a	640.28±11.83c
Porosity (%)	34.77±7.05b	71.44±6.50a	33.30 ±11.59b
Aspect ratio (%)	55.695±2.744a	48.135 ±2.362b	30.842±4.274c

Data is expressed as a mean with 50 samples of each fruit fractions. (±standard error). Different letters indicate significantly difference (P<0.05) by Tukey's HSD test within the same row.

Table 2. Pearson correlation coefficients for physical properties of fruit fractions of Dabai fruit 'Ngemah' variety

Variables	L	T	W	Mass	Volume	True Density	Bulk Density	Porosity	Sphericity	Ra	GMD
T	0.910										
W	0.961	0.960									

Mass	0.900	0.976	0.939								
Volume	0.751	0.893	0.804	0.950							
True Density	0.230	-0.007	0.178	-0.097*	-0.346						
Bulk Density	0.754	0.625	0.758	0.561	0.331	0.581					
Porosity	0.245	0.003	0.181	-0.112*	-0.386	0.913	0.552				
Sphericity	0.724	0.897	0.880	0.843	0.756	0.048*	0.617	0.050			
Ra	0.872	0.918	0.969	0.875	0.735	0.218	0.764	0.218	0.949		
Dg	0.972	0.973	0.996	0.953	0.824	0.150*	0.737	0.159	0.863	0.949	
Da	0.982	0.967	0.993	0.950	0.820	0.156	0.737	0.166	0.837	0.935	0.999

Table 3. Eigenanalysis of the Correlation Matrix

Eigenvalue	9.7533	2.5151	0.3504	0.2043	0.1059	0.0403	0.0215	0.0063	0.0020	0.0007	0.0002	0.0000	-0.0000

Proportion	0.750	0.193	0.027	0.016	0.008	0.003	0.002	0.000	0.000	0.000	0.000	0.000	-0.000
Cumulative	0.750	0.944	0.971	0.986	0.995	0.998	0.999	1.000	1.000	1.000	1.000	1.000	1.000

Table 4. Eigenvectors

Variable	PC1	PC2	PC3	PC4	PC5	PC6	PC7	PC8	PC9	PC10	PC11	PC12	PC13
L	0.305	-0.071	-0.459	0.002	-0.154	0.225	-0.083	-0.182	0.562	-0.149	-0.231	-0.252	-0.349
T	0.313	0.093	0.018	0.136	-0.041	-0.508	-0.524	-0.199	-0.376	0.313	0.032	-0.116	-0.216
W	0.319	-0.032	-0.016	0.021	-0.075	0.340	0.048	0.057	-0.236	0.139	0.758	-0.158	-0.309
Mass	0.307	0.159	-0.135	0.064	0.170	-0.208	0.251	0.780	0.081	-0.329	-0.003	0.014	-0.000
Volume	0.268	0.324	-0.124	0.064	0.406	-0.233	0.579	-0.486	-0.046	0.105	0.006	-0.006	0.000
True Density	0.043	-0.603	-0.028	0.181	0.746	0.089	-0.190	0.004	0.019	-0.008	0.004	0.001	-0.000
Bulk Density	0.237	-0.341	0.065	-0.873	0.023	0.225	0.096	-0.020	0.024	0.010	-0.004	0.001	0.000
Porosity	0.042	-0.605	-0.037	0.390	-0.443	-0.333	0.406	-0.031	-0.060	0.041	0.000	-0.003	0.000

Sphericity	0.286	0.046	0.738	0.132	0.002	-0.147	-0.074	-0.017	0.541	0.139	0.095	-0.067	0.000
Ra	0.308	-0.062	0.382	0.036	-0.063	0.522	0.209	-0.059	-0.363	-0.325	-0.437	-0.044	-0.000
GMD	0.319	-0.013	-0.106	0.049	-0.089	0.088	-0.125	-0.074	0.070	0.029	0.035	0.917	-0.000
AMD	0.318	-0.017	-0.188	0.043	-0.100	0.086	-0.148	-0.104	0.049	-0.089	0.171	-0.189	0.858
Surface Area	0.318	0.047	-0.107	0.057	-0.020	-0.006	-0.144	0.241	-0.203	0.778	-0.375	-0.122	0.000

Figure

Figure 1: From left the whole fruit; nut; and kernel of Dabai fruit

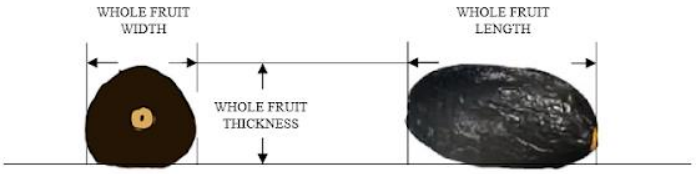

Figure 2. Dimensions of whole fruit of Dabai fruit 'Ngemah' variety

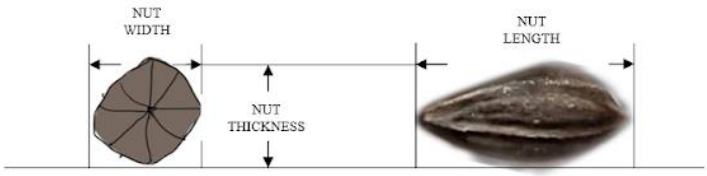

Figure 3. Dimensions of the nut of Dabai fruit 'Ngemah' variety

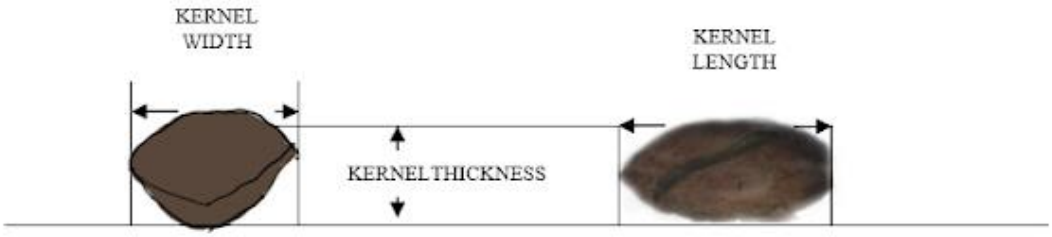

Figure 4. Dimensions of the kernel of Dabai fruit 'Ngemah' variety

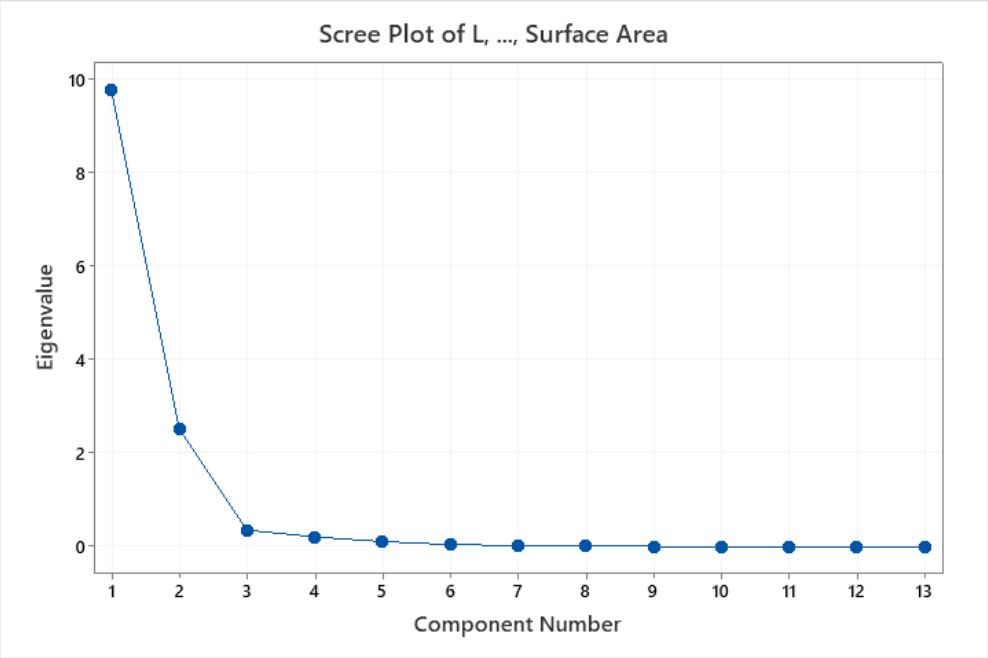

Figure 5: The scree plot of the physical properties of fruit fractions of Dabai fruit 'Ngemah' variety.

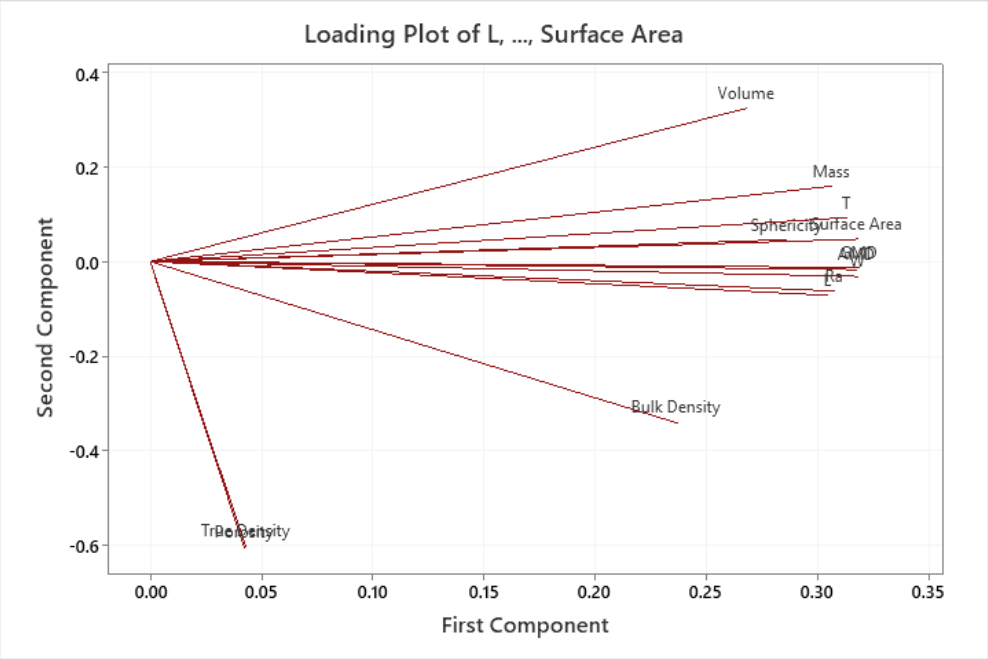

Figure 6: The loading plot of the physical properties of fruit fractions of Dabai fruit 'Ngemah' variety.

Acknowledgement: The authors would like to thank the Ministry of Higher Education of Malaysia, for providing financial support under the Fundamental Research Grants Scheme (FRGS) (Project Number: FRGS/1/2019/WAB01/UPM/02/30) and the Sarawak Biodiversity Centre for approved and issued the R&D permit.

6th International Conference and Postgraduate Colloquium for Environmental Research 2022 (POCER 2022) 9 - 11 June 2022
Langkawi, Kedah, Malaysia

PCR01042022 – 59: Substrate-enzyme mixing characteristics in a bio-inspired reactor for saccharification

Tong Zhu [a,b], Ao Xia [a,b], Yun Huang [a,b], Xianqing Zhu [a,b], Xun Zhu [a,b], Qiang Liao [a,b*]

[a] Key Laboratory of Low-grade Energy Utilization Technologies and Systems, Chongqing University, Ministry of Education, Chongqing 400044, China

[b] Institute of Engineering Thermophysics, School of Energy and Power Engineering, Chongqing University, Chongqing 400044, China

*Corrensponsing Author E-mail: lqzx@cqu.edu.cn

Keywords: Intestine bionics; Secondary flow; Mixing enhancement; Mass transfer; Shear strain rate; Numerical simulation.

Introduction

Biomass energy, specially lignocellulosic biomass, is expected to resolve the climate problems and rising global energy crisis. The bioconversion of lignocellulose into biofuels is considered as a promising energy utilization technology, with noteworthy energy and environmental benefits. Enzymatic saccharification, as an essential step in the bioconversion process, is usually performed in the continuous stirred-tank reactors (CSTRs). However, the CSTRs may suffer from poor performance in saccharification efficiency because the highly viscous lignocellulosic slurry impedes mixing and the excessive shear strain rates (above 1000 s^{-1}) deactivates the enzyme. Therefore, it is necessary to develop a new reactor for mixing viscous fluids to meet the needs of efficient bioconversion.

Inspired by the efficient mixing viscous chyme with the enzyme in the intestine, recent study designed and manufactured soft bionic reactors (Xiao et al., 2018). Although these reactors showed advantages in mixing highly viscous fluids in a relatively short time by exterior visualization and image analysis, the real-time information of interior flow and the mixing process were obscure, making it difficult to further analyze the mixing mechanism and measure the shear strain rate. To overcome the above limitations, numerical simulation has been devoted to mixing mechanisms in the intestine (Zha et al., 2021). The study found that the presence of vortex strongly affected the mixing performance.

Unfortunately, the quantitative parameters of vortex intensity during intestinal motility have not yet been reported. Meanwhile, the introduction of enzymes in current numerical models differed greatly from that in the real intestine. In this case, the mixing process is also different and the mixing enhancement mechanism induced by motility of the intestinal wall cannot be fully understood.

This study aims to investigate the mixing process in a numerical intestinal model, which combines an enzyme secretion boundary with wall motility. The secondary flow intensity in the lumen was quantified to explore the mechanism of mixing enhancement. Besides, the influences of segmental motion parameters and substrate viscosities on mixing performance were assessed. The shear strain rate was also calculated to valid this bionic reactor was suitable for saccharification.

Model and analysis methods

The static local intestine model can be simplified to a tube with a radius of r_0 (mm) and a length of L (mm) in this study. Since the intestine model is axial symmetric geometrically, a 2D axisymmetric model was developed. The laminar flow model, described by the continuity Eq. (1) and the Navier-Stokes Eq. (2), is employed in this work. The species transport Eq. (3) is adopted to calculate the mass fraction of each component.

$$\frac{\partial \rho}{\partial t} + \nabla \cdot (\rho \boldsymbol{u}) = S_m \tag{1}$$

$$\frac{\partial}{\partial t}(\rho \boldsymbol{u}) + \nabla \cdot (\rho \boldsymbol{u}\boldsymbol{u}) = -\nabla p + \nabla \cdot (\mu(\nabla \boldsymbol{u} + (\nabla \boldsymbol{u})^T) - \frac{2}{3}\mu(\nabla \cdot \boldsymbol{u})\boldsymbol{I}) \tag{2}$$

$$\frac{\partial \rho c_{i,m}}{\partial t} + \nabla \cdot (\boldsymbol{u}\rho c_{i,m}) = \nabla \cdot (\rho D \nabla c_{i,m}) + \mathrm{S}_m \tag{3}$$

The equation describing the displacement of the moving wall can be written as Eq. (4):

$$P(\mathrm{z}) = A\sin(\frac{\pi}{T} \cdot t) \cdot \sum_{i=1}^{n} e^{-\left(z-\frac{L}{n+1}\right)^2} \tag{4}$$

To quantitate the mixing level, the enzyme concentration field uniformity index is calculated as (Shao et al., 2020):

$$\gamma_c = 1 - \frac{\sum_{i=1}^{n}\left(\left|c_i - \overline{c}\right| a_i\right)}{2\overline{c}\sum_{i=1}^{n} a_i} \tag{5}$$

To identify and quantitate the secondary flow, the Liutex method is employed in this work. The explicit expression of its magnitude R is given as follow (Wang et al., 2019):

$$R = (\boldsymbol{\omega}\cdot\boldsymbol{r}) - \sqrt{(\boldsymbol{\omega}\cdot\boldsymbol{r})^2 - 4\lambda_{ci}^2} \quad (6)$$

Based on the Liutex method, dimensionless secondary flow intensity *Se* is defined as the ratio of inertial force induced by rotational linear velocity to viscous force:

$$Se = \frac{\rho \bar{R} d_e^2}{2\mu} \quad (7)$$

The above parameters (γ_c and *Se*) were averaged over time in the following research.

Results and discussion

The velocity field and streamlines with different time instants are shown in Fig. 1(a). the flow velocity at the center of the tube significantly augments and reaches the maximum value due to the huge reduction of the cross-section. After the first and second contraction peaks, two anticlockwise vortices occupying nearly half of the tube radius are formed. During the recovery stage from 3 s to 4 s, the contraction rate gradually decreases to zero, and the vortex disappears accordingly. In fig 1(b) at 2 s, there are two obvious colored blocks of Liutex whose sizes were almost in accordance with two anticlockwise vortices, with the local maximum up to 7.74 s^{-1} and 9.78 s^{-1}, respectively. A higher Liutex indicates a faster angular velocity of spinning motion or a stronger vortex in a local region of the lumen, implying a more drastic disturbance (Wang et al., 2019). Thus, it can be assumed that the mass transfer of enzyme and substrate is enhanced to achieve more uniform mixing

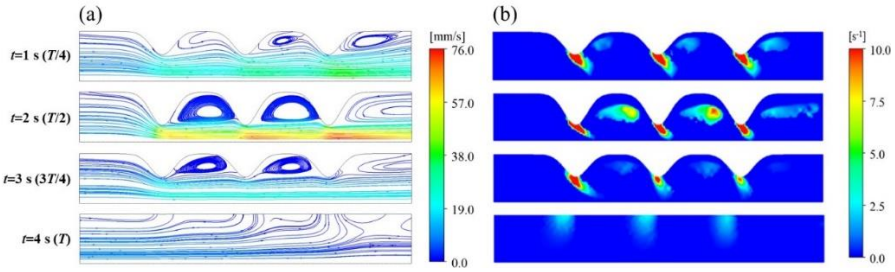

Fig. 1. Evolution of the velocity fields and Liutex fields in one segmentation cycle. (a) Streamline with arrows colored by velocity; (b) Liutex distribution in the lumen.

Fig. 3 (a) shows the evolution of enzyme concentration in the first cycle. The enzyme secreted by the intestinal wall is transferred to the center of the tube by these vortices and mixes with the substrate. (see Fig. 3(a) at 2 s). The vortices produced by wall motion facilitate the radial convection, which greatly strengthens the mixing of substrate and enzyme (Lim et al., 2015). the segmentation mainly promotes the radial mass transfer around the wall but has few contributions on the fluid at the central lumen region. the maximum SSR comes out at the maximum contraction moment on account of a greater

velocity gradient. The highest shear strain rate zones always exist around the contraction peak despite what the contraction rate is.

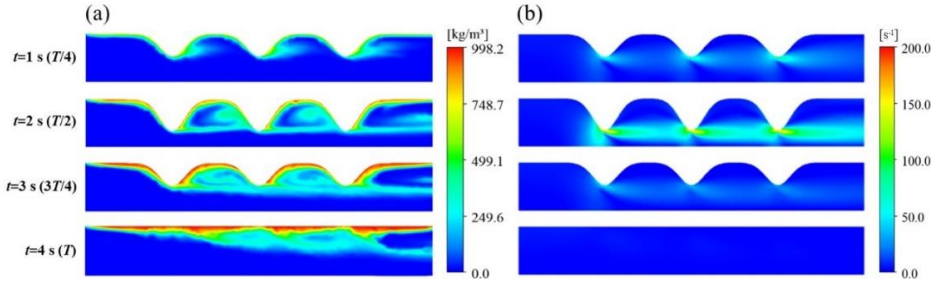

Fig. 2. Evolutions of the concentration fields and shear strain rates in one segmentation cycle. (a) Enzyme concentration expressed in mass concentration; (b) Shear strain rates in the lumen.

Conclusion

The mixing process of substrate and enzyme secreted by the wall has been investigated in a novel reactor. A dimensionless number *Se* is proposed to characterize the secondary flow intensity at different segmentation parameters and substrate viscosities. The results show that the time-averaged *Se* improved from 1.9 to 9.5 with the maximum contraction ratio from 16.6% to 66.7%.The time-averaged mixing level significantly increases by 106.9% compared with the static tube at a low viscous (1 mPa·s). Even at a very high substrate viscosity of 5 Pa·s, there is still a 76.0% mixing enhancement. According to the SSR distribution analysis, the maximum SSR is lower than 220.4 s^{-1} in all cases, indicating that the bio-inspired mixing enhancement is suitable for the enzymatic saccharification.

Acknowledgements: This work was supported by the National Natural Science Foundation of China (No. 51836001), the Innovative Research Group Project of National Natural Science Foundation of China (No.52021004), the National Natural Science Funds for Excellent Young Scholar (No. 52022015), and the Natural Science Foundation of Chongqing, China (Nos. cstc2021ycjh-bgzxm0342, cstc2021ycjh-bgzxm0200).

References

Lim, Y.F., de Loubens, C., Love, R.J., Lentle, R.G., Janssen, P.W.M., 2015. Flow and mixing by small intestine villi. Food & Function 6, 1787-1795.

Shao, Y., Agarwal, R.K., Wang, X., Jin, B., 2020. Numerical simulation of a 3D full loop iG-CLC system including a two-stage counter-flow moving bed air reactor. Chemical Engineering Science 217, 115502.

Wang, Y.Q., Gao, Y.S., Liu, J.M., Liu, C.Q., 2019. Explicit formula for the Liutex vector and physical meaning of vorticity based on the Liutex-Shear decomposition. Journal of Hydrodynamics 31, 464-474.

Xiao, J., Zou, C., Liu, M., Zhang, G., Delaplace, G., Jeantet, R., Chen, X.D., 2018. Mixing in a soft-elastic reactor (SER) characterized using an RGB based image analysis method. Chemical Engineering Science 181, 272-285.

Zha, J., Zou, S., Hao, J., Liu, X., Delaplace, G., 2021. The role of circular folds in mixing intensification in the small intestine: A numerical study. Chemical Engineering Science 229, 116079.

6th International Conference and
Postgraduate Colloquium for
Environmental Research 2022 (POCER
2022) 9 - 11 June 2022
Langkawi, Kedah, Malaysia

PCR01042022 – 60: Mixing Performance of Soft-elastic Bionic Reactor with Reciprocating Flow

Chenkun Zhao[a,b], Ao Xia[a,b], Kai Lin[a,b], Yun Huang[a,b], Xianqing Zhu[a,b], Xun Zhu[a,b], Qiang Liao[a,b*]

[a] Key Laboratory of Low-grade Energy Utilization Technologies and Systems
Chongqing University, Ministry of Education, Chongqing, China

[b] School of Energy and Power Engineering
Chongqing University, Chongqing, China

- *Corrensponsing Author E-mail: ao lqzx@cqu.edu.cn

1. Introduction

In the industrial production process, the mixing process in the reactors has an important influence on the efficiency and quality of products in the whole production process. However, at present, most reactors are made of rigid materials, and their walls do not participate in internal fluid mixing (Brunetti et al., 2007). The traditional mixing methods may lead to the mixing isolation zone, especially for high viscosity fluid mixing, which reduce the mixing efficiency of the reactors (Lamberto et al., 1996). The concept of bionics is widely used in various fields, and various soft-elastic reactor (SER) systems have been established by referring to the flexible wall models such as gastrointestinal system (Chen et al., 2013; Wright et al., 2016). It was found that the reactor systems with soft-elastic walls had better mixing performance than the ordinary rigid reactors for mixing high viscosity fluids (Liu et al., 2018; Deng et al., 2016). Currently, most SERs are driven by simple wall motions, and only can provide radial disturbances by extrusion, which is limited for the mixing. Therefore, a new type of soft-elastic bionic reactor with reciprocating flow was developed to enhance the axial mixing of fluid in the reactor while driving the radial deformation of the flexible wall. This can realize the interaction between the flexible wall and the internal fluid, which improving the mixing efficiency of the SER for high viscosity fluid.

2. Materials and methods

2.1 The design of the soft-elastic reactor

The SER is composed of rigid PVC pipe and natural latex pipe. The the transparent rigid pipe is connected to the transparent hard casing outside to limit the expansion of the hose fixed to the tail of the transparent rigid pipe, as shown in Figure 1(a). The inlet of the SER is fixed to the outlet of the piston cylinder, and the piston is connected to the crank-rod mechanism with a Cycloid pin gear

reduction motor to provide reciprocating flow in the SER, causing the expansion and contraction deformation of the latex hose. The sizes of the SER system are shown in Fig. 1, and the total length of the SER is 100 mm. In order to reduce the influence of inlet on the mixing performance test of SER, the inlet of SER is connected with 50 mm transparent rigid pipe. The total volume of the SER system is about 195 mL. The dye injection device was designed with concentric double pipes as shown in Figure 1(b). The opening of the outer tube is 180°, with an outer diameter of 5 mm and inner diameter of 3 mm. The opening of the inner tube is 90° with an outer diameter of 3 mm and inner diameter of 2 mm. The dye can be uniformly injected into the axis of the reactor by rotating the inner tube to reduce the influence of dye injection point on the mixing performance test of the reactor and study the radial mixing performance of the reactor.

2.2 The experimental method and data processing

Glycerol at 27.5 ℃ was selected as mixed medium with viscosity of 800 mPa · s. The variable parameters include motor frequency f, hose length and maximum deformation. 0.3 mL 1% methylene blue glycerol solution was uniformly injected on the axis of the reactor through the dye injection device, and the fluid mixing process in the reactor was recorded by a camera.

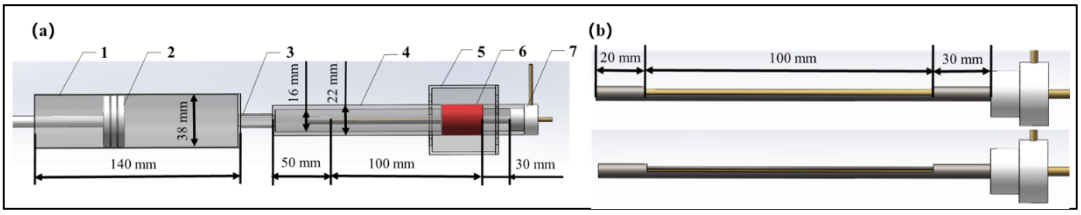

Figure 6: SER and dye injection device schematic: (a) SER schematic: 1-piston cylinder; 2-piston; 3-inlet of SER; 4-transparent rigid pipe section of SER; 5-transparent outer sleeve of SER; 6-hose section of SER; 7-dye injection device; (b) Dye injection device schematics.

The mixing time was deduced by analyzing the color change of the fluid in the image. The mixing time is defined as the time required from the dye injecting into reactors to the uniformity of color distribution reaching 99 %. The uniformity of color distribution is defined as

$$\xi(t)=\left(1-\frac{e(t)-e(\infty)}{e(\infty)}\right)\times 100\% \quad (1)$$

Where $e(t)$ is the uniformity of color distribution at time t.

$$e(t)=\sqrt{S_R^2(t)+S_G^2(t)+S_B^2(t)} \quad (2)$$

$S_R^2(t)$, $S_G^2(t)$ and $S_B^2(t)$ are square differences of R, G and B of each pixel in the screenshot area at time t. In order to ensure the accuracy of the calculation, it is necessary to determine that most of the fluid has been dyed at time t. Therefore, the average dyeing degree above 85 % is selected as the criterion. Average dyeing degree is defined as the proximity between the mean value of three primary colors of each pixel at time t and the ideal mixed state(Liu et al., 2018). Since the hose section in the SER is red latex with poor transparency, the screenshot area is the rigid PVC pipe with good transparency in the dye injection section of SER.

3. Results and discussion

Fig. 2(a) showed the influence of motor frequency on the mixing performance of SER when the hose length and maximum deformation are 3 cm and 46 mm, respectively. As the motor frequency increased from 2 Hz to 3 Hz, the mixing time decreased rapidly from 2319 s to 591 s, with a decrease of 75 %. When the motor frequency increased, the deformation period of the hose was shortened, and the radial transfer of the dye injection on the SER axis was enhanced. In the meantime, the velocity and velocity change rate of fluid reciprocating motion in the SER increased, which maked the radial mixing enhancement caused by the hose section transfer to the whole rapidly. As the motor frequency increased to 5 Hz, the mixing time decreased to 315 s and tended to be stable. In this condition, the velocity of fluid in the SER was large enough. Therefore, further increasing of the motor frequency is very limited to improve the fluid mixing performance in the flexible reactor.

Fig. 2(b) and Fig. 2(c) presented the influence of maximum deformation and hose length on the mixing performance of SER. As the maximum deformation increased from 41 mm to 46 mm, the mixing time decreased rapidly from 757 s to 315 s, with a decrease of 58 %. Likewise, when the hose length increased from 2.2 cm to 3 cm, the mixing time decreased rapidly from 676 s to 315 s, with a decrease of 53 %. This is due to the fact that the increase of maximum deformation could lead to the the enhancement of radial disturbance in the hose section. Similarly, the increase of hose length means the augment of the peristaltic segment which could also enhance the radial disturbance in the hose section. At the same time, the increase of the maximum deformation and hose length augmented the expansion volume, which could raise the velocity and velocity change rate of fluid reciprocating motion in the SER. Therefore, the radial mixing strengthening caused by the hose section could be quickly transferred to the whole, further enhancing the fluid mixing in the SER and shortening the mixing time. It was worth noting that because the latex hose was too thin, the latex hose would become uneven during expansion. The increase of the hose length would make the edge of the hose wrinkle during expansion, resulting in unstable mixing performance of the SER.

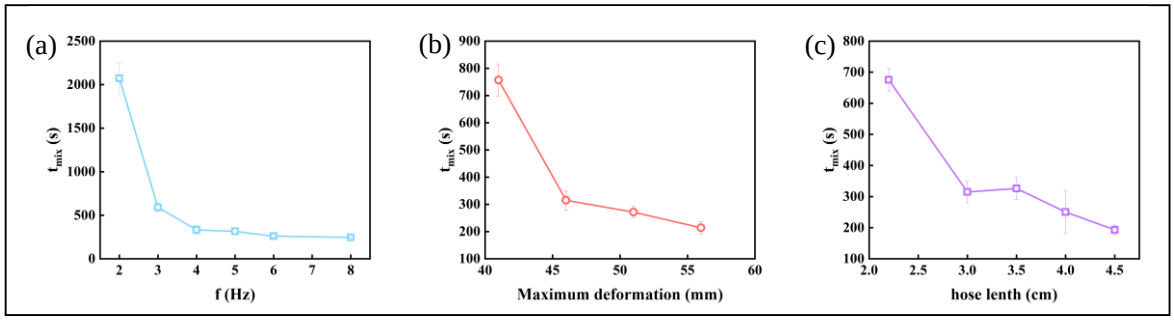

Figure 2: Influence of operating parameters on mixing performance of SER: (a) The influence of motor frequency on the mixing performance of SER when the hose length and maximum deformation are 3 cm and 46 mm; (b)The influence of maximum deformation on the mixing performance of SER when the motor frequency and hose length are 5 Hz and 3 cm; (c)The influence of hose length on the mixing performance of SER when the motor frequency and maximum deformation are 5 Hz and 46 mm.

4. Conclusion

Inspired by the intestinal peristalsis, a soft-elastic bionic reactor with reciprocating flow was designed to enhance the mixing of viscous fluids in the reactor. The reciprocating flow of fluid enhanced the axial mixing of the SER, and the periodic expansion and contraction of the hoes section could enhance the radial mixing in the SER. The mixing performance of SER could be adjusted by controlling motor frequency, hose length and maximum deformation. With the increase of motor frequency, maximum deformation and hose length, the mixing performance of SER enhanced quikly and then tended to be stable.

Acknowledgements: This work was supported by the National Natural Science Foundation of China (No. 51836001), the Innovative Research Group Project of National Natural Science Foundation of China (No.52021004), and the Natural Science Foundation of Chongqing, China (Nos. cstc2021ycjh-bgzxm0342, cstc2021ycjh-bgzxm0200).

References

Brunetti, A., Barbieri, G., Drioli, E., Sea, B., and Lee, D.W., 2007. WGS reaction in a membrane reactor using a porous stainless steel supported silica membrane. *Chemical Engineering and Processing Process Intensification*. 46(2): 119-126.

Chen, L., Wu, X., and Chen, X. D. (2013). Comparison between the digestive behaviors of a new in vitro rat soft stomach model with that of the in vivo experimentation on living rats – motility and morphological influences - sciencedirect. *Journal of Food Engineering*. 117(2), 183-192.

Deng, R., Selomulya, C., Wu, P., Woo, M. W., Wu, X., and Chen, X. D. (2016). A soft tubular model reactor based on the bionics of a small intestine – starch hydrolysis. *Chemical Engineering Research & Design*. 112: 146-154.

Lamberto, D. J., Muzzio, F. J., Swanson, P. D., and Tonkovich, A. L. (1996). Using time-dependent RPM to enhance mixing in stirred vessels. *Chemical Engineering Science*. 51(5): 733–741.

Liu, M. H., Zou, C., Xiao, J., and Chen, X. D. (2018). Soft-elastic bionic reactor. *Journal of Chemical Industry and Engineering(China)*. 69(01): 414-422.

Wright, N. D., Kong, F., Williams, B. S., and Fortner, L. (2016). A human duodenum model (hdm) to study transport and digestion of intestinal contents. *Journal of Food Engineering*. 171(FEB.): 129-136.

6th International Conference and
Postgraduate Colloquium for
Environmental Research 2022 (POCER
2022) 9 - 11 June 2022
Langkawi, Kedah, Malaysia

PCR01042022 – 61: Simultaneous mechanical and biological pretreatment of lignocellulose for enhancing the efficiency of enzymatic hydrolysis

Sheng Qiu[a, b], Ao Xia[a, b], Zhichao Deng[a, b], Yun Huang[a, b], Xianqing Zhu[a, b], Xun Zhu[a, b], and Qiang Liao[a, b*]

[a] Key Laboratory of Low-grade Energy Utilization Technologies and Systems
Chongqing University, Ministry of Education, Chongiqng, China

[b] School **of Energy and Power Engineering,** Chongqing University, Chongiqng, China

*Corrensponsing Author E-mail: lqzx@cqu.edu.cn

Keywords: Simultaneous Pretreatment; Lignocellulose; Mechanical; Biological; Enzymatic hydrolysis.

1. Introduction

As a potential source of green biofuel, lignocellulosic waste has received extensive attention. The main conversion process of using lignocellulose to produce biofuel includes three steps of pretreatment, hydrolysis and fermentation. As the first step in the biomass conversion process, the pretreatment process is considered a critical step, accounting for more than 40% of the total processing cost, having a great impact on the digestibility of cellulose and strongly affecting downstream costs [Sindhu *et al.*, 2016]. Biological pretreatment can effectively degrade or modify lignin by using microorganisms in nature or their secreted enzymes to achieve mild and environmentally friendly lignocellulose degradation, but it has lower conversion and longer reaction time. Therefore, it is necessary to develop a new biological pretreatment methods for efficient and green conversion of lignocellulose to monosaccharides for biofuel and chemical production.

In recent years, mechanical methods have become an effective green method for pretreatment of lignocellulosic biomass. Many studies combine it with chemical pretreatment [Shen *et al.*, 2020], but chemical pretreatment produces certain by-products that inhibit subsequent hydrolysis and fermentation processes. Inspired by the adsorption and catalytic degradation of enzymes in the chewing process of termites that efficiently degrade lignocellulose in nature [Ke *et al.*, 2012], this study develops a simultaneous mechanical and biological pretreatment method to combine the advantages of both

individual pretreatment to realizing a green and efficient pretreatment method to improve the efficiency of subsequent enzymatic hydrolysis.

2. Materials and methods

Wheat straw(WS) was obtained from Henan, China. Its main component was measured by National Renewable Energy Laboratory (NREL) method [Sluiter *et al.*, 2008] as 29.32% cellulose, 18.13% hemicellulose, 22.73% lignin and 10.33% ash with 1.25% moisture. The WS that passed through the 35-60 mesh screen was selected, dried in a vacuum drying oven at 105℃ for 24 h, and then placed in a desiccator for later use. Pretreatment, including laccase (LA) pretreatment for 12 h, ball milling (BM) pretreatment for 12 h, laccase first for12 h and then ball milling (LA-BM) pretreatment for 12 h, simultaneous ball milling and laccase (BM+LA) pretreatment for 12 h, and hydrolysis were carried out with 5% (w/w) biomass slurry, and the solution was sodium citrate buffer (0.1 M, pH=4.8), except deionized water for BM. Laccase (from Yunzhi, 0.9 U/mg) was loaded at 50 U/g biomass, and treated WS biomass in combination with 5% 1-Hydroxybenzotriazole hydrate (1-HBT) under O_2 atmosphere (2 bar). Cellulase (Cellic® CTec2, 200 FPU/mL) loading was 30 U/g biomass. The pretreatment was reacted in a planetary ball mill at 300 rpm and 40 °C, except for BM at room temperature. The hydrolysis was carried out in a shaker at 170°C and 50°C for 72 h. The hydrolyzed solution were sampled at 2, 4, 8, 12, 24, 48, and 72 h, respectively, and measured by high performance liquid chromatography (HPLC) after inactivation at 100°C for 10 min.

3. Results and discussion

The results of chemical composition of WS samples were illustrated in Table 1. As compared with untreated WS (23.02%), lignin content was reduced by 9.04% after LA pretreatment, which was due to laccase degrading part of the lignin, and the cellulose and hemicellulose content increased accordingly. The cellulose content of WS after BM pretreatment is increased compared with untreated, and the hemicellulose content is reduced by 1.01%, which was due to the fact that a small part of hemicellulose will be lost during the BM process, while the lignin content is almost unchanged. It indicated that only BM pretreatment could not degrade lignin. The lignin content of the LA-BM pretreatment was 1.65% lower than untreatd, which was higher than that of the only LA pretreatment. This might be due to the fact that the BM process will re-agglomerate the previously degraded and separated small particles into large particles, resulting in an increase in the lignin content. The content of the three components after BM+LA pretreatment is not much different from that of the LA-BM pretreatment, and the lignin content is reduced by 1.46%, indicating that the BM in the simultaneous pretreatment process can promote the mixing of the solution to promote the reaction of laccase. But compared with LA pretreatment, the

lignin content also increased, which was due to the inactivation of part of the laccase during the BA process, leading to reduced degradation of lignin.

Table 4: Component changes of differently pretreated dry WS samples

Samples	Cellulose (% TS)	Hemicellulose (% TS)	Lignin (% TS)
Untreated	30.64 ± 0.17	18.95 ± 0.22	23.02 ± 0.12
LA	33.18 ± 0.18	19.66 ± 0.13	20.94 ± 0.11
BM	35.42 ± 0.31	18.76 ± 0.26	23.11 ± 0.16
LA-BM	35.52 ± 0.07	20.07 ± 0.15	22.64 ± 0.05
BM-LA	34.99 ± 0.21	19.86 ± 0.18	22.31 ± 0.09

The sugers concentration and carbohydrates conversion after different pretreatment conditions were shown in Figure 1. All sugers concentration and carbohydrates conversion increased rapidly first and then tended to be stabilized with the increase of hydrolysis time. The glucose and xylose concentrations were 4.85 and 1.58 g/L for untreated WS at 72 h, corresponding to only 28.29% and 14.59% of cellulose and hemicellulose conversion, respectively. After LA pretreatment, the concentrations of glucose and xylose reached 8.85 and 2.39 g/L at 72 h, which were 82.47% and 51.27% higher than untreated, respectively; the corresponding conversion of cellulose and hemicellulose were 45.75% and 20.38%, which were increased by 61.72% and 39.68% compared with untreated, respectively. It was due to the fact that laccase degraded or modified the lignin of lignocellulose, reduced the unproductive adsorption of lignin to cellulase. As compared with untreated, the concentration of glucose and xylose after BM pretreatment reached 12.24 and 6.36 g/L at 72 h, which were increased by 1.52 and 3.03 times, with the conversion of cellulose and hemicellulose of 59.86% and 56.84%, which was incresed by 1.12 and 2.90 times, respectively. It was because BM reduced the particle size of wheat straw, increased the specific surface area, thus increased the accessibility of enzymes, and in addition, reduced the crystallinity of cellulose and made cellulose more easily degraded by cellulase. Due to combination of the advantages of LA and BM pretreatment, the glucose concentration after LA-BM pretreatmentv reached 17.85 g/L at 72 h, which was 2.68, 1.02 and 0.46 times higher than untreated, LA and BM pretreatment, with cellulose conversion of 87.38%, which was increased by 2.09, 0.91 and 0.46 times, respectively; the xylose concentration reached 8.28 g/L at 72 h, which was increased by 4.24, 2.46 and 0.30 times, with hemecillulose conversion of 70.12%, which were increased by 3.81, 2.44 and 0.23 times, respectively. Compared with the LA-BM pretreatment, the enzymatic hydrolysis efficiency of WS continued to improve after ball BM+LA pretreatment, and the glucose and xylose concentrations increased by 12.55%

and 6.76%, reaching 20.09 and 8.84 g/L at 72 h, corresponding to cellulose and hemicellulose conversion were 99.22% and 75.25%, which were increased by 13.55% and 7.32%, respectively.This indicating that the simultaneous pretreatment showed synergic effect of ball milling and laccase pretreatment methods. In the process of simultaneous pretreatment, BA could promote the mixing of slurry and improve the reaction probability between laccase and lignin, and laccase can reach the place where free diffusion cannot reach due to strong mechanical action of BM and then react with lignin.

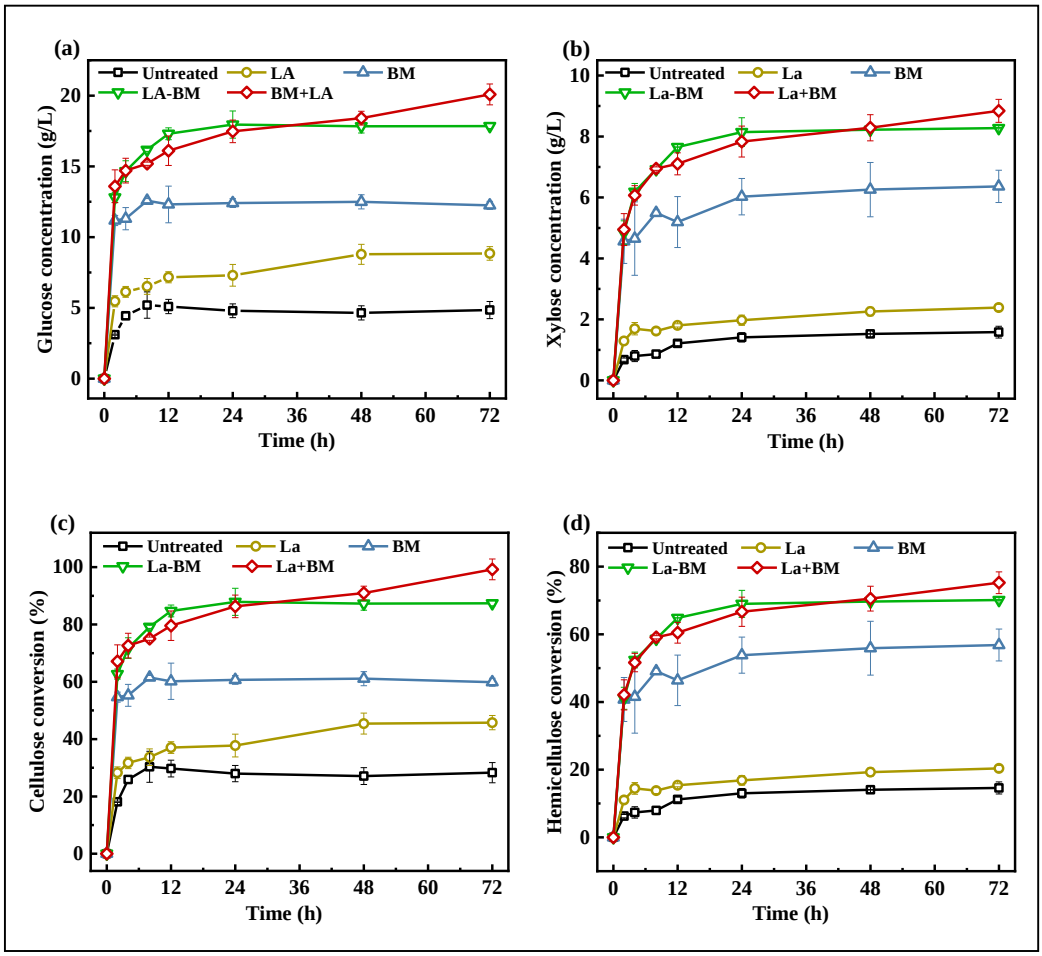

Figure 7: Comparison of different pretreatment conditions: (a) glucose concentration, (b) xylose concentration, (c) cellulose conversion, (d) hemicelllulose conversion.

4. Conclusions

Simultaneous BA+LA pretreatment showed synergic effect of BM and LA pretreatment methods and significantly improved the enzymatic hydrolysis efficiency of wheat straw. Glucose and xylose concentration of WS hydrolyzed for 72 h reached 20.09 and 8.84 g/L after BM+LA pretreatment, which was increasd by 3.14 and 4.59 times compared with untreated biomass,with cellulose and hemicellulose conversion of 99.22% and 75.25%, which was increasd by 2.51 and 4.16 times.

Acknowledgements: This work was supported by the National Natural Science Foundation of China (No. 51836001), the Innovative Research Group Project of National Natural Science Foundation of China (No.52021004), the National Natural Science Funds for Excellent Young Scholar (No. 52022015), and the Natural Science Foundation of Chongqing, China (Nos. cstc2021ycjh-bgzxm0342, cstc2021ycjh-bgzxm0200).

References

Sindhu, R., Binod, P. and Pandey, A. (2016). Biological pretreatment of lignocellulosic biomass–An overview. *Bioresource technology*, 199, 76-82.

Shen, F., Xiong, X., Fu, J., Yang, J., Qiu, M., Qi, X. and Tsang, D. C. (2020). Recent advances in mechanochemical production of chemicals and carbon materials from sustainable biomass resources. *Renewable and Sustainable Energy Reviews*, 130, 109944.

Ke, J., Laskar, D. D., Gao, D. and Chen, S. (2012). Advanced biorefinery in lower termite-effect of combined pretreatment during the chewing process. *Biotechnology for biofuels*, 5(1), 1-14.

Sluiter, A., Hames, B., Ruiz, R., Scarlata, C., Sluiter, J., Templeton, D. and Crocker, D. L. A. P. (2008). Determination of structural carbohydrates and lignin in biomass. *Laboratory analytical procedure*, 1617(1), 1-16.

6th International Conference and Postgraduate Colloquium for Environmental Research 2022 (POCER 2022) 9 - 11 June 2022
Langkawi, Kedah, Malaysia

PCR01042022 – 62: Continuous photoenzymatic decarboxylation of free fatty acids from waste oil for hydrocarbon fuels production in a microfluidic photobioreactor

Feng Li[a,b], Ao Xia[a,b*], Xiaobo Guo[a,b], Yun Huang[a,b], Xianqing Zhu[a,b], Xun Zhu[a,b] and Qiang Liao[a,b]

[a] Key Laboratory of Low-grade Energy Utilization Technologies and Systems, Chongqing University, Ministry of Education, Chongqing 400044, China

[b] Institute of Engineering Thermophysics, School of Energy and Power Engineering, Chongqing University, Chongqing 400044, China.

*Corrensponsing Author E-mail: aoxia@cqu.edu.cn.

Keywords: Hydrocarbon fuels; *Cv*FAP; Microfluidic photobioreactor; Waste oil.

Introduction

The conversion of waste oil, a widespread and abundant biomass resources, into high-quality hydrocarbon fuels can bring huge energy economic benefits as well as reduce food safety problems and environmental pollution, which has received significant attention from experts and scholars in various countries (Mawhood et al., 2016). Currently, hydrocarbon fuels are mainly produced from waste oil by hydrogenation. However, the harsh reaction conditions (200-500 °C, 2-15 MPa H_2) and high energy consumption in the hydrogenation process led to high production cost and difficult application (Natelson et al., 2015).

A novel blue light-driven enzyme, fatty acid photodecarboxylase sourced from *Chlorella variabilis* NC64A (*Cv*FAP), can convert fatty acids to corresponding (C1-shortened) alka(e)nes (Sorigué et al., 2017). This provides a promising approach for the production of hydrocarbon fuels at a mild condition. However, long reaction time (12-24 h) and low conversion rate (0.2-3.1 mM/h) were observed in conventional batch reactor for hydrocarbon fuels production by lipse and *Cv*FAP, which limits the potential application of *Cv*FAP (Ma et al., 2020). Microreactor has the advantages of high mass transfer efficiency and low light attenuation, and its application to photoenzymatic decarboxylation is expected to enhance the conversion of waste oil and the production of hydrocarbon fuels.

In this study, soybean oil, a model substrate for waste oil, was converted to free fatty acids by lipase hydrolysis, and then was uesed for photo-enzymatic decarboxylation in a microfluidic photobioreactor for hydrocarbon fuels production. The effects of lipase concentration, hydrolysis time, pH value, light intensity, *Cv*FAP concentration, flow rate and free fatty acids concentration on the production of hydrocarbon fuels were assessed in detail. A promising approach for hydrocarbon fuels

production by the continuous photoenzymatic decarboxylation of free fatty acids from waste oil is demonstrated in a microfluidic photobioreactor.

Methodology

All chemicals were analytical grade and obtained from Sigma–Aldrich, Sangon Biotech, and Sinopharm Chemical Reagent without further treatment prior to use. The crude enzyme containing *Cv*FAP was prepared according to a previous method with little modification.

As shown in Fig.1, The microchip was made of transparent polymethyl methacrylate (PMMA) and prepared by hot-press bonding. The channel size of chip is characted by 500 μm × 500 μm (length × width) and the total volume of channel is 500 μL. The free fatty acids solution from soybean oil hydrolysis and crude enzyme containing *Cv*FAP were syringed into microchennel by T-conjunction with syringe pumps. An LED array at 450 nm with 600 individual blue beads is placed below the microchip for the light irradiation.

Assays containing 50% (v/v) Tris-HCl buffer (pH 8.5, 100 mM), 50% (v/v) soybean oil was hydrolyzed into free fatty acids by lipase of 100 mg/mL at 30 °C and 500 rpm. Various hydrolysis time of 2, 4, 6 ,8, 12, 16 h was applied to assess the effects on free fatty acids content. The pH value of assay after hydrolysis for 16 h was measured.The pH value after oil hydrolysis was adjusted to 8.5 to match the optimum pH value of *Cv*FAP. Unless otherwise stated, the continuous decarboxylation for hydrocarbon fuels production was employed at 5 μL/min of free fatty acids (50 mM), 5 μL/min of crude enzyme containing *Cv*FAP(12 mg/mL), 30 °C and 500 μmol/(m^2 s) of light intensity. Various pH values of assay at 6.8, 8, 8.5, 9 were adopted to investigate the effect on hydrocarbon fuels production. The contents of various alka(e)nes and free fatty acids were derermined by gas chromatography (Agilent 7890B) equipped with an DB-FFAP column (30 m length × 250 μm inner diameter× 0.25 μm film thickness).

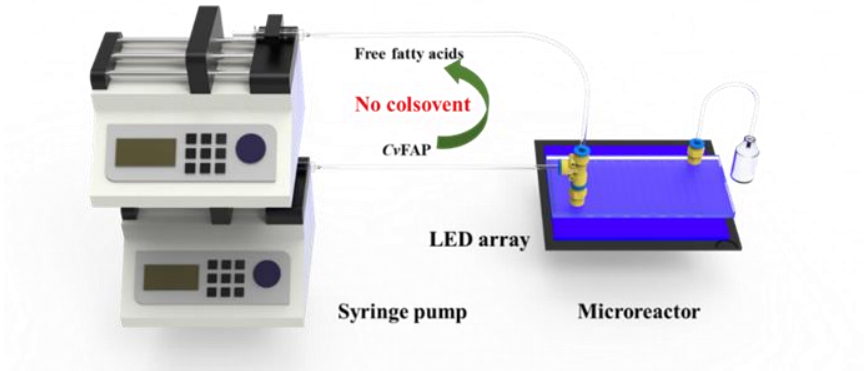

Fig.1. Schematic view of microchip reactor.

Results and discussion

As shown in Fig. 2a, the free fatty acid content was only 52.6% within the initial 2 h of soybean oil hydrolysis. As the hydrolysis time was gradually prolonged to 12 h, total free fatty acids content up to 92.3% was obtained. The free fatty acid content increased by 1.8% when the hydrolysis time was extended to 16 h, indicating that the hydrolysis of oil was completed in 12 h. The pH value decreased from 8.5 to 4.9 as an increase in the free fatty acids content. This will severely restrain the activity of *Cv*FAP and the decarboxylation of free fatty acids.

The horizontal coordinates in the Fig. 2b represent, from left to right, palmitic acid (C16), stearic acid (C18), oleic acid (C18:1), linoleic acid (C18:2), and linolenic acid (C18:3). The concentration of linoleic acid up to 791.3 mM was obtained after soybean oil hydrolysis, accounting for more than 50% of the total fatty acids. The concentration of oleic acid at 334.3 mM lower than linoleic acid was obtained. The content of palmitic acid, stearic acid and lionlenic acids in total free acids was 11.5%, 3.8% and 3.5%, respectively.

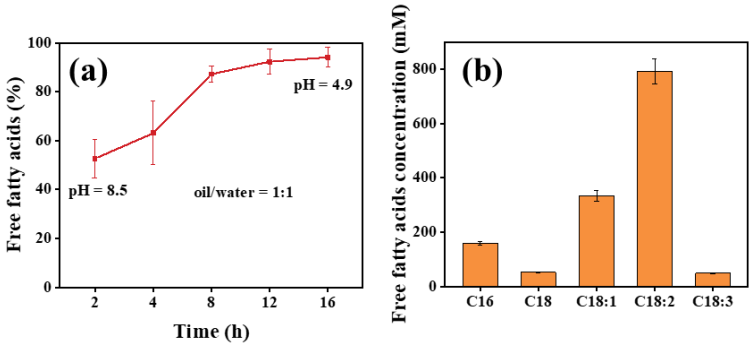

Fig. 2. (a) Time course of free fatty acids content; (b) Concentrations of various free fatty acids.

The pH value after soybean oil hydrolysis was adjusted to 8, 8.5, 9 to investigate the effect on photoenzymatic decarboxylation, as shown in Fig. 3a. The total concentration of alka(e)nes at 5.2 mM with a conversion of 20.8% was obtained, which indicates that the acidic environment restrains the activity of *Cv*FAP, thereby causing a poor performance of photoenzymatic decarboxylation. Elevating the pH value after oil hydrolysis to 8, alka(e)nes concentration was found to be significantly increased to 11.5 mM, which is 2.2 times higher than that at pH value of 6.8. This suggests that the increase in pH value effectively improve the activity of *Cv*FAP and the decarboxylation performance. The alka(e)nes concentration reached a maximum of 15.3 mM after the pH value was increased to 8.5. This is consistent with the literature who reported the highest activity of *Cv*FAP at pH 8.5 (Guo et al., 2022). Meanwhile, The conversion rate of soybean oil to hydrocarbon fuels up to 5.4 mM/h was increased by 74% compared to the previous literature (Ma et al., 2020). An decrease of alka(e)nes concentration to 11.8 mM when the pH value was increased to 9. This is ascribed to that free fatty acids, such as palmitic aicd, precipitated out of the solution, affecting their bingding with *Cv*FAP. Taken together, the pH value

after soybean oil at 8.5 was the optimum parameter for the photoenzymatic decarboxylation in microfluidic photobioreactor.

The horizontal coordinates in Fig. 3b, from left to right, represent pentadecane (C15), heptadecane (C17), 8-heptadecene (C17:1), 6,9-heptadecadiene (C17:2), 3,6,9-heptadecatriene (C17:3). High concentration of 8-heptadecene and 6,9-heptadecadiene at 3.6 mM and 9.1 mM, respectively, were obtained after photoenzymatic decarboxylation because of the high contents of oleic and linoleic acids in soybean oil. Meanwhile, the low concentration of pentadecane, heptadecane, and 3,6,9-heptadecatriene at 1.1 mM, 0.8 mM, and 0.7 mM, respectively, were obtained.

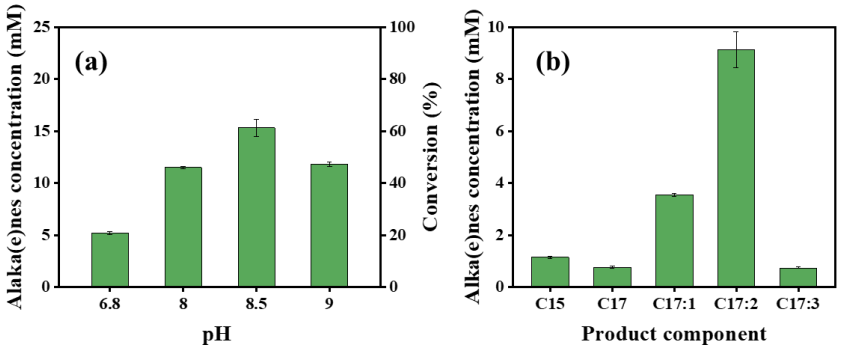

Fig. 3. (a) The effect of pH value on alka(e)nes concentration; (b) component and concentration of various alka(e)nes.

Conclusion

Microfluidic photobioreactor can effectively boost the decarboxylation of free fatty acids from waste oil for the hydrocarbon fuels production. Soybean oil was rapidly hydrolyzed in 2 h with a free fatty acid acid conversion rate of 92.3% at a lipase concentration of 100 mg/mL, a speed of 500 rpm and a temperature of 30 °C. The pH value after oil hydrolysis was adjusted from 6.8 to 8.5, which significantly increased the conversion of free fatty acids up to 61.2%. hydrocarbon fuels productivity up to 5.4 mM/h suggests that the continuous photoenzymatic decarboxylation of free fatty acids from waste oil is a promising approach for hydrocarbon fuels production.

Acknowledgements: This work was supported by the National Natural Science Foundation of China (Nos. 52022015, 51876016), the State Key Program of National Natural Science of China (No. 51836001), the Innovative Research Group Project of National Natural Science Foundation of China (52021004), and the Natural Science Foundation of Chongqing (cstc2021ycjh - bgzxm0160).

References

Guo, X., Xia, A., Li, F., Huang, Y., Zhu, X., Zhang, W., Zhu, X., Liao, Q., 2022. Photoenzymatic decarboxylation to produce renewable hydrocarbon fuels: A comparison between whole-cell and broken-cell biocatalysts. Energy Conversion and Management. 255, 115311.

Ma, Y., Zhang, X., Zhang, W., Li, P., Li, Y., Hollmann, F., Wang, Y., 2020. Photoenzymatic production of next generation biofuels from natural triglycerides combining a hydrolase and a photodecarboxylase. ChemPhotoChem. 4(1), 39-44.

Mawhood, R., Gazis, E., de Jong, S., Hoefnagels, R., Slade, R., 2016. Production pathways for renewable jet fuel: A review of commercialization status and future prospects. Biofuels, Bioproducts and Biorefining. 10(4), 462-484.

Natelson, R.H., Wang, W.C., Roberts, W.L., Zering, K.D., 2015. Technoeconomic analysis of jet fuel production from hydrolysis, decarboxylation, and reforming of camelina oil. Biomass and Bioenergy. 75, 23-34.

Sorigué, D., Légeret, B., Cuiné, S., Blangy, S., Moulin, S., Billon, E., Richaud, P., Brugière, S., Couté, Y., Nurizzo, D., Müller, P., Brettel, K., Pignol, D., Arnoux, P., Li-Beisson, Y., Peltier, G., Beisson, F., 2017. An algal photoenzyme converts fatty acids to hydrocarbons. Science. 357(6354), 903-907.

6th International Conference and Postgraduate Colloquium for Environmental Research 2022 (POCER 2022) 9 - 11 June 2022
Langkawi, Kedah, Malaysia

PCR10042022 – 63: ISOLATION AND SCREENING OF DETERGENT DEGRADING MICROBES FROM DETERGENT WASTEWATER

Wai Yan Cheah[a*] , Er A.C.[a]

aCentre of Research in Development, Social and Environment (SEEDS), Faculty of Social Sciences and Humanities, Universiti Kebangsaan Malaysia, 43600 Bangi, Selangor Darul Ehsan.

*E-mail: cheahwaiyan@ukm.edu.my

Keywords: Detergent; Microbes; Sodium dodecyl sulfate; Wastewater treatment

Extended Abstract

Sodium dodecyl sulfate, (SDS) is an anionic surfactant that is widely used all over the world. Its high foaming capabilities has caused water pollution, leading to toxic effects on organisms present in the ecosystem. Chemical antifoam could be applied to resolve river foaming issue. However, biological approach serves as an alternative for further enhance environmental sustainability. The objectives of the study are to investigate the detergent-degrading microorganisms and assess their potential in degrading the SDS present in the wastewater. The bacteria present in wastewater sample was initially enriched in Luria-bertani medium (LB) and further transferred to selective medium, which was the SDS-containing BSM medium. A strain of SDS – degrading bacterium was successfully isolated. The isolate was predicted to be a Pseudomonas sp. via 16S rRNA analysis. The isolated bacterium was subsequently grown in the SDS-containing wastewater to assess on its potential in SDS degradation. Methylene blue active substance assay was applied to quantitatively calculate residual SDS concentration remaining in the medium throughout the bacterial growth cycle at set intervals, so as to attain its biodegradation ability. The maximal concentration of SDS tolerated by the isolate was found to be 50 ppm. The results showed that the isolate was able to degrade more than 60%(v/v) of 50 ppm of SDS supplemented in LB medium, within 36 hours of incubation at 37ºC for 200 rpm. Furthermore, the isolate was able to degrade 20.82% and 34.14% of SDS in basal salt medium (BSM) and basal salt medium containing 0.2%(v/v) glucose, respectively.

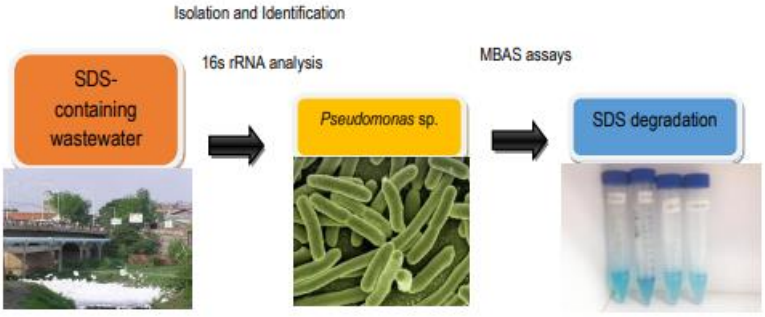

Figure 1: The conceptual framework

Acknowledgements: This work is supported financially by The authors would like to express their heartfelt gratitude to MPOB-UKM Endowed Chair Grant (EP-2020-024) under the leadership of Professor Dr. Er Ah Choy and Faculty of Social Sciences and Humanities for the funding of this research.

References

Adekanmbi, A.O. and Usinola, I.M., 2017. Biodegradation of Sodium Dodecyl Sulphate (SDS) by two Bacteria Isolated from Wastewater Generated by a Detergent-Manufacturing Plant in Nigeria. Jordan Journal of Biological Sciences, 10(4).

Shahbazi, R., Kasra-Kermanshahi, R., Gharavi, S., Moosavi-Nejad, Z. and Borzooee, F., 2013. Screening of SDS-degrading bacteria from car wash wastewater and study of the alkylsulfatase enzyme activity. Iranian journal of microbiology, 5(2), p.153.

Usharani, J., Rajasekar, T. and Deivasigamani, B., 2012. Isolation and characterization of SDS (sodium dodecyl sulfate) degrading organisms from SDS contaminated areas. Open Access Sci. Rep, 1(2), pp.1-4.

Othman, A.R., Yusof, M.T. and Shukor, M.Y., 2019. Biodegradation of Sodium Dodecyl Sulphate (SDS) by Serratia marcescens strain DRY6. Bioremediation Science and Technology Research, 7(2), pp.9-14.

Ojo, O.A. and Oso, B.A., 2009. Biodegradation of synthetic detergents in wastewater. African Journal of Biotechnology, 8(6).

Kogawa, A.C., Cernic, B.G., do Couto, L.G.D. and Salgado, H.R.N., 2017. Synthetic detergents: 100 years of history. Saudi pharmaceutical journal, 25(6), pp.934-938.

Oba, K., 1971. Studies on biodegradation of synthetic detergents by microorganisms. Nippon Eiseigaku Zasshi (Japanese Journal of Hygiene), 25(6), pp.494-511.

6th International Conference and Postgraduate Colloquium for Environmental Research 2022 (POCER 2022) 9 - 11 June 2022
Langkawi, Kedah, Malaysia

PCR01042022 – 64: Is it necessary to adopt a two-step catalytic transesterification for producing black soldier fly larvae biodiesel?

Chin Seng Liew[a], Ratchaprapa Raksasat[a], Jun Wei Lim[a*], Hemamalini Rawindran[a], Yeek Chia Ho[b], Mardawani Mohamad[c], Man Kee Lam[d], Syukriyah Ishak[d], Seteno Karabo Obed Ntwampe[e], Woei Yenn Tong[f] and Pau Loke Show[g]

[a] Department of Fundamental and Applied Sciences, HICoE-Center for Biofuel and Biochemical Research, Institute of Self-Sustainable Building, Universiti Teknologi PETRONAS, 32610 Seri Iskandar, Perak Darul Ridzuan, Malaysia

[b] Department of Civil & Environmental Engineering, Center for Urban Resource Sustainability, Institute of Self-Sustainable Building, Universiti Teknologi PETRONAS, 32610 Seri Iskandar, Perak Darul Ridzuan, Malaysia

[c] Faculty of Bioengineering and Technology, Universiti Malaysia Kelantan, Jeli Campus, 17600 Jeli, Kelantan, Malaysia

[d] Department of Chemical Engineering, HICoE-Center for Biofuel and Biochemical Research, Institute of Self-Sustainable Building, Universiti Teknologi PETRONAS, 32610 Seri Iskandar, Perak Darul Ridzuan, Malaysia

[e] Centre of Excellence for Carbon-Based Fuels, School of Chemical and Minerals Engineering, North-West University Private Bag X1290, Potchefstroom 2520, South Africa

[f] Drug Discovery and Delivery Research Laboratory, Malaysian Institute of Chemical and Bioengineering Technology, Universiti Kuala Lumpur, Alor Gajah, Melaka 78000, Malaysia

[g] Department of Chemical and Environmental Engineering, Faculty of Science and Engineering, University of Nottingham Malaysia, Semenyih 43500, Selangor, Malaysia

- Corrensponsing Author E-mail: junwei.lim@utp.edu.my

Extended Abstract

BSFL biodiesel is normally produced from a 2-step transesterification process. The first-stage acid-catalysed transesterification reduces the free fatty acid (FFA) content in the lipid by converting them into fatty acid methyl esters (FAME). Meanwhile, the second-stage base-catalysed transesterification convert the remaining triglyceride into FAME. While this is the most guaranteed way in converting all

lipid content (FFA and triglyceride) into FAME, this might not be the most sustainable approach. This is because transesterification of triglyceride also happened in parallel during the first-stage acid-catalysed transesterification.

Therefore, this work aimed to elucidate the necessity of a 2-step transesterification after an optimized first stage acid-catalysed transesterification, to see whether the additional procedures, chemicals, costs and environmental damages are justifiable or simply redundant. In this work, only one variable will be optimized for the first stage acid-catalysed transesterification, more specifically, the acid catalyst amount. Other transesterification conditions were adopted from the optimum conditions reported by Lam et al. (Lam & Lee, 2013). The FFA content would be referred as the performance indicator for the first stage transesterification. Subsequently, the second stage of base-catalysed transesterifications would be executed and their performances would be measured by two main indicators, namely, the change in biodiesel yield and the change in FAME yield.

During the 1-step acid-catalysed transesterification, Figure 1 and Figure 2 shown that 20 µL is the optimum amount of acid catalyst to be used as it produces among the highest biodiesel yield (84.55%) while leaving the lowest FFA content (0.29%).

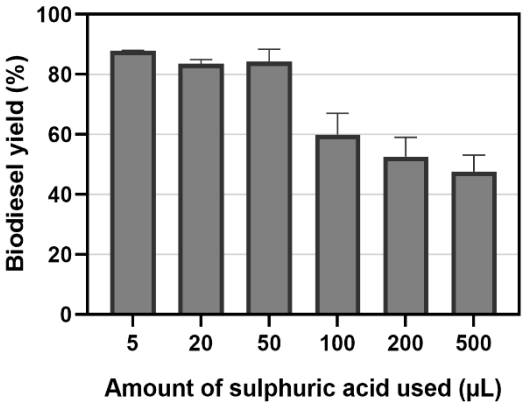

Figure 8: Biodiesel yields derived from the use of different amounts of concentrated sulphuric acid catalyst.

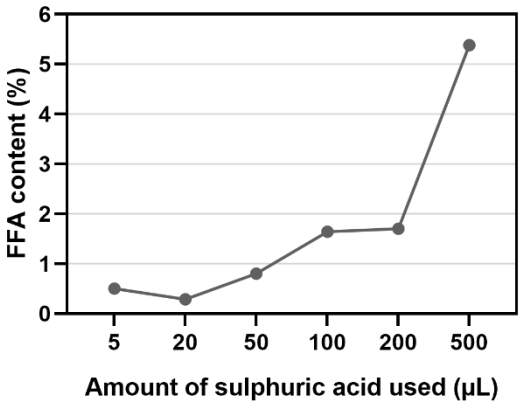

Figure 9: FFA contents after the transesterification process using different amounts of concentrated sulphuric acid catalyst.

Meanwhile, it was observed that subsequent 2-step transesterification did not improve the biodiesel yield and FAME yield of samples as displayed in Figure 3 and Figure 4. Therefore, the necessity of a 2-step

transesterification was unjustified. The optimum transesterification condition concluded was to perform a 1-step acid-catalysed transesterification, with 20 µL of acid catalyst to generate the highest FAME yield of 81.31%.

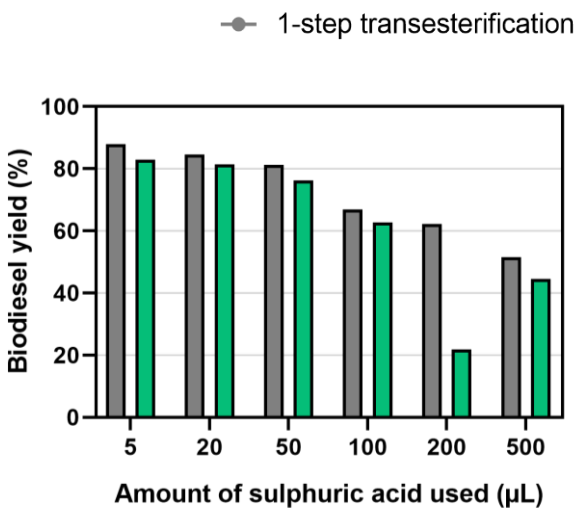

Figure 3: Comparison of biodiesel yields after 1-step and 2-step transesterification processes.

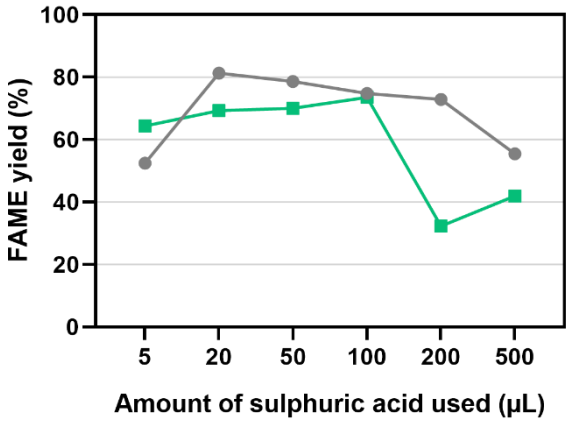

Figure 4: Comparison of FAME yields after 1-step and 2-step transesterification processes.

Keywords: Black Soldier Fly Larvae, Waste Valorization, Biodiesel, Waste-To-Energy, Transesterification, Free Fatty Acid

Acknowledgements: The financial support received from the Ministry of Higher Education Malaysia via HICoE-Center for Biofuel and Biochemical Research with the cost center of 015MA0-052 and Yayasan Universiti Teknologi PETRONAS (YUTP) with the cost center 015LC0-341 are gratefully acknowledged.

References

Lam, M. K., & Lee, K. T. (2013). Catalytic transesterification of high viscosity crude microalgae lipid to biodiesel: Effect of co-solvent. *Fuel Processing Technology*, *110*, 242–248. https://doi.org/10.1016/j.fuproc.2012.12.021

PCR01042022 – 65: Characterization of Lignocellulosic Biomass and Synthesis of Low Transition Temperature Mixture (LTTM) as Green Delignification Approach

Vienoth Segar [a*] ,Chai Yee Ho[a] and Mohd Hizami Mohd Yusoff[b]

a Chemical Engineering Department, HiCoE, Centre for Biofuel and Biochemical Research (CBBR), Universiti Teknologi PETRONAS, Seri Iskandar, Perak 32610, Malaysia

Corrensponsing Author E-mail: yeeho.chai@utp.edu.my

Keywords: LTTM, Green Solvent, Kenaf Fiber, Kenaf Bast, EFB

Extended Abstract

Conventional biomass delignification technologies and organic solvents pre-treatment techniques pose major drawbacks such as energy-intensive, prolonged reaction time, low efficiency, and utilization of costly and hazardous materials. Low-transition-temperature-mixtures (LTTMs) are proven to be most prominent green solvents due to their environmental-friendliness and high effectiveness in the extraction of lignin extraction from biomass. It is believed that the hydrogen bonding of in the LTTM mixtures disrupts the three-dimensional structure of lignin hence able to remove lignin from biomass to produce a good quality of paper pulp. In this study, the characterization of lignoellulosic biomass such as empty fruit bunch and kenaf fiber is studied based on proximate and thermogravimetric analysis (TGA). Higher volatile matter is obtained for kenaf (84.64%) followed by EFB (74.99%). The moisture content among three biomasses do not vary much as the range is between 8.42%-8.92%. The synthesis of LTTM is studied by the formulation of different starting materials such as malic acid, lactic acid, sucrose and choline chloride in a molar ratio of 2:4:2 (w/w/w) respectively.

Introduction: The consumption for pulp and paper products is rising proportionally with the population growth in the world. (Kok, (2018)). Pulp and paper industry utilizes both hardwood and softwood for the manufacturing of paper and pulp products such as printing papers, cardboards, diapers, etc.. In this sense, about 15.8 million tonnes of empty fruit bunch (EFB) which accounts for 20% of fresh fruit weight are produced every year (Shamsuddin, 2021) . Oil palm EFB consists of 20.6–33.5% of hemicellulose, 23.7–65.0% of cellulose and 14.1–30.5% of lignin (Kurniawan, 2022) Due to its high content of cellulose and hemicellulose, EFB emerges as a major potential source in pulp and paper industry.The objectives of this part of research is to characterize the selected lignocelulosic biomass in terms of proximate analysis and thermogravimetric analysis and to formulate the low transition temperature mixture (LTTM) according to given molar ratio by conventional method.

Methodology.

Preparation of Feedstock and Starting Material. The starting materials (HBA and HBD) used in the preparation of LTTMs such as sucrose, choline chloride as hydrogen bond acceptor (HBA) and L-malic acid and Lactic acid as hydrogen bond donor (HBD).The chemicals obtained had purity ≥ 95% and were obtained from Sigma Aldrich.Empty fruit bunch were obtained from palm mill, Kilang Sawit FELCRA Berhad Nasaruddin. The EFB, were washed with distilled water and dried in oven at 100ºC until a consistent weight is obtained. The dried EFB were chopped and cut before ground using PULVERISTE cutting mill and sieved to a particle size below 500µm.

Synthesis of LTTM. The LTTMs were synthesized from the mixture of L-malic acid–sucrose–water (MSW) with a molar ratio of 2:4:2 (w/w/w) in a beaker placed in an oil bath at 80°C. The mixtures were stirred with magnetic stirring and heated up slowly in an oil bath until the formation of transparent liquid mixtures without any solid particles. The other batches of mixture consisting of Lactic acid-Choline chloride, were synthesized.

Proximate Analysis. Proximate analysis is the determination by prescribed methods of moisture, volatile matter, fixed carbon, and ash. The volatile matter, moisture content, ash content is obtained according to ASTMD3175, ASTM D3173 and ASTM E1755-01 respectively. Meanwhile the fixed carbon was obtained by difference(%) from volatile matter, moisture content and ash content.

Thermogavimetric Analysis. The TGA pyrolysis of the biomass sample was carried out under a nitrogen,N2 atmosphere at 50 ml/min and a heating rate of 20°C min-1 . A biomass sample of 6.00 mg was pyrolyzed to a maximum temperature of 700 °C.

Results and Discussion

Synthesis of LTTM. After constant stirring and heating of the LTTM in an oil bath, the solution turns colourless at the respected synthesis time as tabulated in Table 1. The same physical observation were noticed for different LTTM formulations.This is due to the strong hydrogen bonding between both components formed during the LTTM preparation.The formulation which contains lactic acid as the HBD showed a shorter synthesis time most likely due better intermolecular interaction that present in the mixture compared to formulation containing malic acid as hydrogen bond donar (HBD) (Guimarães, 2022).

Table 1 : Synthesis time and ratio of LTTM formulation

No	LTTM	Synthesis Time (min)	Ratio(w:w:w)
1	Malic Acid: Sucrose: Water	120	2:4:2
2	Malic Acid: Choline Chloride: Water	120	2:4:2
3	Lactic Acid : Sucrose: Water	65	2:4:2
4	Lactic Acid :Choline Chloride: Water	65	2:4:2

Proximate Analysis. Proximate and ultimate analysis were performed to study the properties of each biomass feedstock. The moisture contents of the three biomasses did not show much variation as the range of moisture content is between 8.42% to 8.92%., probably due to the lower surface area to volume ratio

resulting in a lower evaporation rate. Therefore, these materials have a higher water storage capacity. Kenaf Bast recorded the highest volatile matter which is 84.64% followed by empty fruit bunch which is about 74.99%. The high volatile matter content usually reduces the solid yield in the carbonization stage while a low inorganic content is vital due to their abilities to produce a low ash and high fixed carbon.

TGA. Thermogravimetric analysis of empty fruit bunch (EFB) and kenaf bast (KW). Generally, biomass pyrolysis can be divided into three main stages: drying and evaporation of light particles (stage I), volatilization of hemicellulose and cellulose (stage II) and decomposition of lignin (stage III).During stage I the drying of evaporation of light components occur which reduce the moisture hence resulting in weight loss. Stage II denotes the volatilization of hemicellulose and cellulose which observed a significant drop of weight in the temperature range of 210°C - 460°C. At stage III, which deduced the degradation of lignin compound with a slow and stable mass loss accompanied with other strong chemical bond compounds over long and high temperature.

Table 2: Thermogravimetric Analysis of Empty Fruit Bunch and Kenaf

Lignocellulosic Biomass	Stage	Temperature Range (°C)	Residual mass at 700°C (g)
Empty Fruit Bunch	I	40-170	0.1560
	II	220-460	
	III	470-700	
Kenaf Bast	I	40-170	0.0054
	II	210-410	
	III	420-700	

Acknowledgments: The authors would like to acknowledge HICoE-CBBR, for funding of this project (015MA0-104) under the Graduate Research Assistantship Scheme (GRA) and Universiti Teknologi PETRONAS.

References

Guimarães, T. G. (2022). Mixture design and physicochemical characterization of amino acid-based DEEP eutectic solvents (AADES) for sample preparation prior to elemental analysi. Journal of Molecular Liquids, 345.

Kok, M. T. (2018). Pathways for agriculture and forestry to contribute to terrestrial biodiversity conservation: a global scenario-study. Biological Conservation, 137-150.

Kurniawan, E. M. (2022). . Synthesis of Cellulose Stearate Ester as Wet Strength Agent for Synthesis of Bio-polybag from Oil Palm Empty Fruit Bunch. International Journal of Engineering, Science and Information Technology, 1-7.

Shamsuddin, R. S. (2021). Palm oil industry—Processes, by-product treatment and value addition. Sustainable Bioconversion of Waste to Value Added Products, 121-143.

6th International Conference and
Postgraduate Colloquium for
Environmental Research 2022 (POCER
2022) 9 - 11 June 2022
Langkawi, Kedah, Malaysia

PCR01042022 – 66: Effect of Different Iron Percentage in Sulphonated Activated Carbon Catalyst for Microwave-Assisted Acetylation of Glycerol

Nadzirah Azmi[a] , Mohd Hizami Mohd Yusoff[a*] and Chai Yee Ho[a,b]

a Chemical Engineering Department, Universiti Teknologi PETRONAS, Perak Malaysia

b HiCOE-Centre for Biofuel and Biochemical Research (CBBR), Institute of Self-Sustainable Building, Chemical Engineering Department, Universiti Teknologi PETRONAS, Perak, Malaysia

• Corresponding Author E-mail: hizami.yusoff@utp.edu.my

Keywords: Glycerol; Activated Carbon; Acetylation; Triacetin.

Extended Abstract

High demand for biodiesel leads to the surplus production of glycerol as a by-product. The valorisation of glycerol is one of the ways to reduce the overproduction of glycerol while at the same time increasing the economic value of the biodiesel industry. There are many methods to valorise glycerol into valueadded chemicals. Among them, acetylation is one of the promising techniques. For this particular process, existing homogenous and heterogeneous catalysts that are commercially available in the market have several drawbacks that require further improvement. Therefore, the present study focused on the utilization of sulphonated iron catalysts with activated carbon support (FeS/AC) in the conversion of glycerol to triacetin via acetylation. Based on the analysis, $Fe_{(10)}S$/AC has the highest selectivity of triacetin compared to other formulations which is 1.25%. While wet impregnation without filtration is the best method of preparing the catalyst by referring to the percentage of triacetin selectivity.

Introduction. In order to reduce reliance on fossil fuels and stabilize the palm oil industry, Malaysia's government released a policy called National Biofuel Policy in 2006 that led to the production of biodiesel. Although the usage of biodiesel gives many good impacts, especially on the environment, the increasing demand for biodiesel has led to the overproduction of the by-product which is glycerol. Interestingly, glycerol can be converted into value-added chemicals such as acetin which finds importance in some applications including cosmetics and pharmaceuticals industries. Generally, acetin can be synthesized via esterification or acetylation of glycerol in the presence of acetic acid and undergoes three consecutive equilibrium reactions to produce monoacetin (MAG), diacetin (DAG), and triacetin (TAG), while water is generated as a by-product in each reaction because of dehydration (Mufrodi et al., 2014). Among the product formed, TAG is preferred because the addition of TAG into biodiesel can improve its viscosity, decreases the cloud point, and pour point of biodiesel (Costa et al., 2017). The acetylation of glycerol is generally

carried out over an efficient catalyst such as montmorillonite and sulphuric acid to enhance the glycerol conversion and the production of MAG, DAG, and TAG (Rane et al., 2016). Two types of catalysts can be used for the process which are homogenous and heterogeneous acid catalysts. But, there are several drawbacks to the usage of homogenous catalysts which are highly corroded to the equipment, high toxicity, complicated for water disposal, and difficult to separate from the homogenous catalyst and the product (Trifoi et al., 2016). Therefore, the heterogeneous catalyst is used as an alternative to fulfil all the limitations of homogeneous catalysts. For example zeolite and amberlyt. Still, these catalysts have shown low thermal stability, poor textural properties, poor selectivity towards DAG and TAG, and loss of catalytic activity due to leaching. Towards sustainable development, the usage of a heterogeneous catalyst from activated carbon has gained interest due to its green properties, user-friendly, low-cost material, and high surface area (Abdulkareem-Alsultan et al., 2016). The objective of this paper is to synthesize and screen the best formulation of sulphonated iron catalysts with activated carbon support (FES/AC) for the acetylation of glycerol by evaluating the selectivity of triacetin.

Methodology. The preparation of sulphonated iron catalyst with activated carbon support (FeS/AC) at four weight percentages, x of 2, 5, 10, and15 wt% of Fe precursors were conducted via incipient wetness impregnation method and direct sulphonation with sulphuric acid. Next the Fe(x)S/AC catalysts were subjected to a screening process with the assistance of microwave irradiation. The generated product was analysed using GC-FID to quantify the concentration of produced triacetin.

Results and Discussion. By referring to the analysis result in Table 1, there is no triacetin produced in the blank, activated carbon (AC), and sulphonated AC. Besides, the prepared catalysts using the wet impregnation method without filtration have a higher selectivity of triacetin compared to the catalysts that have been synthesised with filtration. The $Fe_{(10)}S/AC$ catalyst has the highest selectivity of triacetin which is 1.25% while the Fe(2)S/AC catalyst has the lowest selectivity which is 0.75%. This showed that the amount of catalyst loading is also one of the factors that influence the percentage of triacetin selectivity. The characterization of the catalysts will give more explanation about the different selectivity of triacetin among the catalysts.

Table 1: Screening Results for Acetylation of Glycerol

Type of Catalayts	Selectivity of Triacetin (%)	Type of Catalayts	Selectivity of Triacetin (%)
Blank	0.00	$Fe_{(15)}S/AC$	1.16
With AC	0.00	$Fe_{(2)}S/AC$ filter	0.06
Sulphonated AC	0.00	$Fe_{(5)}S/AC$ filter	0.06
$Fe_{(2)}S/AC$	0.75	$Fe_{(10)}S/AC$ filter	0.06
$Fe_{(5)}S/AC$	1.07	$Fe_{(15)}S/AC$ filter	0.06
$Fe_{(10)}S/AC$	1.25		

Conclusion. The presences of catalysts have a significant impact on generating the triacetin from glycerol. The result showed that the $Fe_{(10)}S/AC$ catalyst has the highest selectivity compared to the other catalyst.

Upon that, future studies for enhancing the production of triacetin using $Fe_{(10)}S$/AC catalyst will be done to get a better outcome.

Acknowledgments: The author would like to acknowledge the Malaysian Ministry of Higher Education through the Higher Institution Centre of Excellence Program (HICoE) at CBBR, for funding this project (grant no. 015MA0-104). Monetary support via FRGS (015MA0-121) is also acknowledged.

References

Abdulkareem-Alsultan, G., Asikin-Mijan, N., Lee, H. V., & Taufiq-Yap, Y. H. (2016). A new route for the synthesis of La-Ca oxide supported on nano-activated carbon via vacuum impregnation method for one-pot esterification-transesterification reaction. Chemical Engineering Journal, 304, 61–71. Costa, B. O. D.,

Decolatti, H. P., Legnoverde, M. S., & Querini, C. A. (2017). Influence of acidic properties of different solid acid catalysts for glycerol acetylation. Catalysis Today, 289, 222– 230.

Ibrahim, N. A., Rashid, U., Taufiq-Yap, Y. H., Yaw, T. C. S., & Ismail, I. (2019). Synthesis of carbonaceous solid acid magnetic catalyst from empty fruit bunch for esterification of palm fatty acid distillate (PFAD). Energy Conversion and Management, 195, 480–491.

Mufrodi, Z., Rochmadi, S., & Budiman, A. (2014). Synthesis Acetylation of Glycerol Using Batch Reactor and Continuous Reactive Distillation Column. Engineering Journal, 18(2), 29–40.

Rane, S. A., Pudi, S. M., & Biswas, P. (2016). Esterification of Glycerol with Acetic Acid over Highly Active and Stable Alumina-based Catalysts: A Reaction Kinetics Study. Chemical and Biochemical Engineering Quarterly, 30(1), 33–45.

Trifoi, A. R., Agachi, P. Ş., & Pap, T. (2016). Glycerol acetals and ketals as possible diesel additives. A review of their synthesis protocols. Renewable and Sustainable Energy Reviews, 62, 804–814.

PCR01042022 – 67: Co-pyrolysis of plastics and food waste mixture under flue gas condition for bio-oil production

Huei Yeong Lim[a], Shu Hui Tang[a], Yee Ho Chai[a*], Suzana Yusup[b], and Mook Tzeng Lim[c]

[a] Biomass Processing Lab, HICOE-Centre for Biofuel and Biochemical Research (CBBR), Institute of Sustainable Building, University Teknologi PETRONAS, Perak, Malaysia

[b] Generation Unit, Fuel and Combustion Section, TNB Research Sdn. Bhd., Selangor, Malaysia

[c] Biomass & Plasma Technologies, Renewable Energy & Green Technology, TNB Research Sdn. Bhd., Selangor, Malaysia

- Corrensponsing Author E-mail: yeeho.chai@utp.edu.my

Keywords: co-pyrolysis; bio-oil; plastics waste; food waste;

Extended Abstract

Over the years, the global energy consumption has surged due to rapid urbanization and development, in which majority of the energy supplies come from non-renewable fossil fuels. Despite increasing demands and public attentions, the renewable energy sources such as solar, wind, and biomass only contributed to a small portion in the energy nexus. In retrospect with rising human population around the globe, generation of municipal solid waste (MSW) had steadily rising, which possess challenges in MSW disposal whilte maintaining the environment. Most of the MSW collected were commonly disposed via open dumping and landfills, while only about 19% were properly recycled or composted in 2016 (Kaza *et al*., 2018). This presented a huge potential for untapped renewable energy sourced from MSW via several technologies. In Malaysia, almost 8 million tonnes of MSW were generated annually in Malaysia, out of which about 45 % was food waste and 13 % was plastic waste (National Solid Waste Management Department, 2013). Both organic and plastics wastes are potential carbon-based feedstocks for the production of biofuels through technologies such as pyrolysis. The pyrolysis process utilized heat energy to thermally break down the feedstocks to produced biochar, bio-oil or pyrolysis oil, and non-condensable gases (Ong *et al*., 2019). Pyrolysis of food and plastics waste were

previously studied by many, however less attention was garnered by food wastes with low carbohydrates and lipid content such as animal bones. It is understandable that bones were not extensively studied for pyrolysis due to its high ash content of 39%, nonetheless alkali metal such as calcium that present in the bones exert catalytic properties to pyrolysis (Jia *et al*., 2021). For example, co-pyrolysis of pig meat with the bones had found to reduce water yield and increase gas yield in the products (Zhang *et al*., 2018). This provided an opportunity to utilize co-pyrolysis of MSW containing food and plastics waste to produce bio-oil, while providing a solution to the disposal of the ever increasing generation of MSW.

This study investigated the co-pyrolysis of food wastes namely, fish bone (FB), chicken bone (CB), and rice (R), together with plastics wastes as municipal solid wastes components in a downdraft fixed-bed pyrolyzer. Plastics wastes were comprised of a mixture of polypropylene (PP), polyethylene (PE), and high-density popyethylene (HDPE) with a constant ratio. The materials were dried and grinded to particle size of below 1 mm, and were mixed together to form three homogenous feedstock mixtures: FB + plastics, CB + plastics, and R + plastics. Three reaction temperatures were studied: 300, 350, and 400 °C, and the yield and quality of the bio-oil were determined for each of the feedstock mixture. Synthetic flue gas consituted of a mixture of nitrogen, carbon dioxide, and small amount of oxygen, was used as the sweeping gas in the pyrolyzer at a flowrate of 2 mL/min. Condensors system with three different condensing temperature namely, 25 °C, 0 °C, and -10 °C, was set up using tap water, iced water, and portable chiller with ethylene glycol-water coolant, respectively.

Table 5: Bio-oil yields of feedstocks at different reaction temperatures.

Feedstocks	Bio-oil yield (wt%)		
	300 °C	350 °C	400 °C
FB + plastics	7.5	13.4	15.8
CB + plastics	7.2	18.6	20.3
R + plastics	18.8	20.1	29.0

Table 1 showed the results for bio-oil yields from the experiment. It was found that higher reaction temperatures resulted in higher bio-oil yield for all three feedstocks due to the increasing thermal degradation of the feedstocks. However, reaction temperature beyond 400 °C promoted excessive amount of tar to form and clog the system, forming the limitation of this study. Nonetheless, among the three feedstocks, pyrolysis of rice + plastics provided with the highest bio-oil yield due to the high carbohydrate content, in which it can be converted into glucose and other simpler compounds. Furthermore, ash content of rice is also significantly lower than the bones at only about 0.48% (Rahman

et al., 2020). On the other hand, GC-MS results indicated slgiht differences in chemical compounds of bio-oil from pyrolysis of the three feedstock mixtures. Acidic compounds such as hexadecanoic acid and octadecadienoic acid were found in bio-oil from all three feedstocks, with high peak area% of 22.39-37.17% and 6.68-9.77%, respectively. Fatty acid methyl ester (FAME) such as methyl stearate was also detected in all feedstocks at 2.29-4.22% peak area. For CB and FB, nitrile compounds was detected, which may be due to the catalytic effect of the bones in the co-pyrolysis (Jia *et al*., 2021). Moreover, furfural was determined in rice + plastics, which may be sourced from the degradation of carbohydrate (Bayu *et al*., 2019). Other than that, CHNS and bomb calorimetry analyses had shown that among the feedstock mixtures and reaction temperatures, FB + plastics at 350 °C had provided with the best results with O/C ratio of 2.19, H/C ratio of 1.66, and calorific value of 32.339 MJ/kg, in which the H/C ratio was approaching to that of diesel and gasoline at 1.83 and 1.98, respectively. However, high nitrogen and sulphur content of 7.70% and 0.17% showing that the bio-oil would requires treatments such as denitrogenation and desulphurization to be used as biofuel.

Acknowledgements: The authors would like to acknowledge funding from Tenaga Nasional Berhad (TNBR/SF367/2020) for this work. Furthermore, the authors would like to acknowledge the HICoE funding support from Ministry of Higher Education Malaysia.

References

Bayu, A., Abudula, A., Guan, G., 2019. Reaction pathways and selectivity in chemo-catalytic conversion of biomass-derived carbohydrates to high-value chemicals: A review. Fuel Process. Technol. 196, 106162.

Jia, T., Zhou, F., Ma, H., Zhang, Y., 2021. A highly stable waste animal bone-based catalyst for selective nitriles production from biomass via catalytic fast pyrolysis in NH3. J. Anal. Appl. Pyrolysis 157, 105217.

Kaza, S., Yao, L.C., Bhada-Tata, P., Van Woerden, F., 2018. What a Waste 2.0 : A Global Snapshot of Solid Waste Management to 2050. Urban Development. World Bank, Washington, DC.

National Solid Waste Management Department, 2013. Survey on Solid Waste Composition, Characteristics & Existing Practice of Solid Waste Recycling in Malaysia. Putrajaya.

Ong, H.C., Chen, W.-H., Farooq, A., Gan, Y.Y., Lee, K.T., Ashokkumar, V., 2019. Catalytic thermochemical conversion of biomass for biofuel production: A comprehensive review. Renew. Sustain. Energy Rev. 113, 109266.

Rahman, A., Genisa, J., Zainal, 2020. Maltodextrin quality prepared from spoiled and leftover rice. IOP Conf. Ser. Earth Environ. Sci. 575.

Zhang, Y., Ma, Z., Yan, J., 2018. Influence of pork and bone on product characteristics during the fast pyrolysis of pig carcasses. Waste Manag. 75, 352–360.

6th International Conference and
Postgraduate Colloquium for
Environmental Research 2022 (POCER
2022) 9 - 11 June 2022
Langkawi, Kedah, Malaysia

PCR01042022 – 68: Role of Supercritical Fluid Extraction in Biorefinery Application: A Perspective from Malaysia

Siti Nur Syaza Abdul Rahman[a,b], Yee Ho Chai[a,b*], Tan Kiin Yiin[a,c], Lam Man Kee [b], and Quek Ven Chian[c]

[a] Department of Chemical Engineering, Faculty of Engineering,
Universiti Teknologi PETRONAS, Perak, Malaysia

[b] HICOE Center for Biofuel and Biochemical Research, Institute of Sustainable Building Engineering Department, Universiti Teknologi PETRONAS, Perak, Malaysia

[c] Group Research & Technology, PETRONAS, Kuala Lumpur, Malaysia

- Corresponding Author E-mail: yeeho.chai@utp.edu.my

Keywords: Supercritical Extraction; Biorefinery; Application; Biomass; Renewable Energy; Green Extraction Technology

Abstract

Supercritical fluid extraction has a huge potential in processing industries. Green extraction technologies especially supercritical fluid extraction are explored to increase sustainable manufacturing with greater yield and value-added products. Apart from its distinctive qualities including nonflammability, nontoxicity, environmental friendliness, and high solubility properties, supercritical fluid extraction plays an pivotal role in biorefinery industry. The applications of supercritical fluid extraction can also be expanded to food, pharmaceutical, cosmetic, and health care sectors due to the aforementioned advantages in extraction. This article explains the role of supercritical fluid extraction in biorefineries especially with a niche focus on Malaysia. The report highlights Malaysian researchers' commitment to exploiting and exploring supercritical extraction for biorefinery applications using local bioresources. Therefore, this paper discusses on the mechanism, application, challenges, and mitigation in implementing supercritical fluid extraction, especially in Malaysia for biorefinery applications.

1.0 Introduction

Supercritical fluid extraction, also known as green extraction, is the most efficient method of extracting specific biocompouds due to its innately high solvation power, which is tunable by pressure, temperature, and extraction time modifications (Chai et al., 2021). In comparison to the usual method of extraction, the approach demonstrates high extraction selectivity for end products (Geow et al., 2021). Daud et al. (2022) stated that conventional extraction is mostly dependent on the polarity of the solvent for the targetted compounds. This contradicts with supercritical fluid extraction that is able to tune the extraction parameters to cater to the targetted compounds. Despite the distinct qualities of supercritical fluid extraction, industrial scale deployment are uncommon, especially in Malaysia, that covers supercritical extractions for biorefinery applications. Significant developments in conventional extraction are done to increase yield with the green technology approach and solventless supercritical fluid extraction has shown a great potential.

2.0 Supercritical extraction mechanism and application

Supercritical fluid extraction works by heating the extractive solvent to a specific temperature and followed by diffusion into the material (Chai et al., 2020). The extraction fluid attains a supercritical phase in specific conditions critically in temperature and pressure to achieve the desired form. The supercritical state allows the extraction fluid to act and perform like a liquid, but at a molecular level, it behaves more like a gas. According to Daud et al. (2022) in-depth study, supercritical extraction was divided into three mechanisms which are constant extraction rate (CER), falling extraction rate (FER), and diffusion extraction rate (DER). This mechanism has its specific functionalities based on the extraction rate curve and the equilibrium solubility of the fluid.

One of the common applications used for supercritical extraction technology is the extraction of bioactive compounds such as phytochemicals (Arumugham et al., 2021) and carotenoids (Hwang et al., 2021). Furthermore, Khoo et al. (2020) and Syimir Fizal et al. (2021) also consider the exploration of supercritical fluid extraction due to the advantages of the technology in manipulating biomass as feedstock for biofuel production.

3.0 Challenges and mitigation

It is known that the conventional extraction method has improved over the decades in enhancing the extracted yield and/or high quality of final products by the changes in the type of equipment and/or solvent used for the extraction process (Geow et al., 2021). This improvement of the traditional extraction method does highlight the challenge faced by supercritical fluid extraction which requires higher pressure during the extraction process that leads to higher operating and capital costs compared

to other extraction methods. Besides, supercritical fluid extraction limits its ability in extracting highly polar compounds alterable by adding a suitable polar modifier during the extraction process. Based on Hwang et al. (2021) findings, the interaction between nonpolar solvent and polar solvent might result in the co-extraction of undesired polar biomolecules. Thus, the type and ratio of nonpolar and polar solvents must be determined to ensure that the crude extract profile is suitable for high-quality production. Most of the challenges faced by this green technology had their possible ways to accommodate the issue faced.

Conclusion: The role of supercritical fluid extraction in biorefinery applications was discussed in this paper. To date, there is limited literature on supercritical fluid extraction in biorefinery applications in Malaysia, despite its potential for extraction of biomass and its byproducts. The authors believe that supercritical fluid extraction has a promising future in biorefinery applications due to its distinct properties and greener technology.

Acknowledgments: The authors would like to acknowledge the Ministry of Higher Education Malaysia for awarding the Higher Institution Centre of Excellence award to the Centre for Biofuel and Biochemical Research (HICoE-CBBR), Universiti Teknologi PETRONAS (Grant no. 015MA0-052, no. 015MA0-104 and no. 15MA0-136). This work was supported by Universiti Teknologi PETRONAS for the infrastructure and the Center for Biofuel and Biochemical Research (CBBR) for the assistance in conducting the review that enabled the progression of the research work.

References

Arumugham, T., K, R., Hasan, S. W., Show, P. L., Rinklebe, J., & Banat, F. (2021). Supercritical carbon dioxide extraction of plant phytochemicals for biological and environmental applications - A review. *Chemosphere, 271*, 129525. doi:10.1016/j.chemosphere.2020.129525

Chai, Y. H., Yusup, S., Ruslan, M. S. H., & Chin, B. L. F. (2020). Supercritical fluid extraction and solubilization of Carica papaya linn. leaves in ternary system with CO2 + ethanol solvents. *Chemical Engineering Research and Design, 156*, 31-42. doi:https://doi.org/10.1016/j.cherd.2020.01.025

Chai, Y. H., Yusup, S., Seer, Q. H., Ruslan, M. S. H., & Chin, B. L. F. (2021). Influence of supercritical CO2 flowrate in one-pot supercritical fluid extraction of Carica papaya linn. leaves: A broken-intact-cell approach. *E3S Web of Conferences, 287*. doi:10.1051/e3sconf/202128702012

Daud, N. M., Putra, N. R., Jamaludin, R., Md Norodin, N. S., Sarkawi, N. S., Hamzah, M. H. S., . . . Md Salleh, L. (2022). Valorisation of plant seed as natural bioactive compounds by various

extraction methods: A review. *Trends in Food Science & Technology, 119*, 201-214. doi:10.1016/j.tifs.2021.12.010

Geow, C. H., Tan, M. C., Yeap, S. P., & Chin, N. L. (2021). A Review on Extraction Techniques and Its Future Applications in Industry. *European Journal of Lipid Science and Technology*, *123*(4). doi:10.1002/ejlt.202000302

Hwang, T. Y., Kin, C. M., & Shing, W. L. (2021). Extraction solvents in microalgal lipid extraction for biofuel production: A review. *Malaysian Journal of Analytical Sciences*, *25*(5), 728-739.

Khoo, K. S., Chew, K. W., Yew, G. Y., Leong, W. H., Chai, Y. H., Show, P. L., & Chen, W.-H. (2020). Recent advances in downstream processing of microalgae lipid recovery for biofuel production. *Bioresource Technology*, *304*, 122996. doi:https://doi.org/10.1016/j.biortech.2020.122996

Syimir Fizal, A. N., Hossain, M. S., Zulkifli, M., Khalil, N. A., Abd Hamid, H., & Ahmad Yahaya, A. N. (2021). Implementation of the supercritical CO2 technology for the extraction of candlenut oil as a promising feedstock for biodiesel production: potential and limitations. *International Journal of Green Energy*, *19*(1), 72-83. doi:10.1080/15435075.2021.1930007

Zougagh, M., Valcárcel, M., & Ríos, Á. J. T. i. A. C. (2004). Supercritical fluid extraction: a critical review of its analytical usefulness. *23*, 399-405.

6th International Conference and
Postgraduate Colloquium for
Environmental Research 2022 (POCER
2022) 9 - 11 June 2022
Langkawi, Kedah, Malaysia

PCR01042022 – 69: Parametric Study and Energy Analysis of the Progressive Freeze Concentration of Cucumber Juice

Wan Nur Aisyah Wan Osman[a], Nirosha Thambyraja[a], Wan Nur Athirah Mazli[a], Shafirah Samsuri[a,b*], Nurul Aini Amran[a,b], Mazura Jusoh[c], Farah Hanim Ab Hamid[d], and Nor Zanariah Safiei[e]

[a] Chemical Engineering Department,
University Teknologi PETRONAS, 32610 Seri Iskandar, Perak, Malaysia

[b] HICoE-Centre for Biofuel and Biochemical Research (CBBR), Institute of Sustainable Buiding,
University Teknologi PETRONAS, 32610 Seri Iskandar, Perak, Malaysia

[c] Chemical Engineering Department, Faculty of Chemical Engineering,
Universiti Teknologi Malaysia, 81310 UTM Skudai, Johor, Malaysia.

[d] Faculty of Chemical Engineering,
Universiti Teknologi MARA, 40450 Shah Alam, Selangor, Malaysia.

[e] Faculty of Chemical Engineering,
UniKL MICET, 78000 Alor Gajah, Melaka, Malaysia.

- Corrensponsing Author E-mail: shafirah.samsuri@utp.edu.my

Keywords: Antioxidant Activity; Anti-Elastase Activity; Cucumber Juice, Phenolic Content; Progressive Freeze Concentration

Extended Abstract

The concentration of fruits and vegetables have become popular in the food and cosmetic industries. Cucumber has been widely used in these industries, and it has a high content of water. According to (Kausar et al., 2012; Majumdar et al., 2010), many cucumbers are spoiled due to the excess production during harvesting season. This issue does not only cause loss to farmers, which affects the economy. It also contributes to the amount of waste. It is easier and more convenient to store and consume cucumber

juice compared to the fruit itself. Besides, it is costly to deal with many liquids due to its high cost for packaging, storing and shipping.

Several methods had been carried out for the separation process of water content from the cucumber. Progressive freeze concentration (PFC) is identified as one of the prominent methods to extract cucumber concentrate from cucumber juice. This method is being experimented to separate water content and concentrated juice for different types of vegetables and fruits (Ahmad et al., 2020; Miyawaki et al., 2016; Safiei et al., 2017). PFC able to remove water from the solution by freezing out the water into ice crystals (Samsuri et al., 2019). This method had been used since 1786 to concentrate the solution (Englezos, 1993). This method uses crystallization, where the water content freeze and is detached from the concentrated solution in the form of ice crystal. This method is easier to use as it offers a simpler step for separation where it forms a single block of ice crystal in the crystallizer when it introduces to the cooler surface (Mazli et al., 2020).

According to (Englezos, 1993), high purity of p-xylene was obtained through the freeze concentration process. Thus, more research and studies related to the PFC are continuously being carried out to improve the whole process. PFC has been applied to orange juice (Sánchez et al., 2010), pineapple juice (Petzold et al., 2015), blueberry juice (Orellana-Palma et al., 2017), sugarcane juice (Rane & Uphade, 2016) and apple juice (Ding et al., 2019; Qin et al., 2021). This project applied PFC to concentrate cucumber juice under different operating conditions to obtain a high-quality concentrate with high antioxidant, phenolic content and anti-elastase activity. Besides, this paper also presents the energy analysis of PFC for cucumber juice.

Several factors was investigated to measure the effect of operating conditions (coolant temperature, concentration time and stirring speed) towards the process of PFC. The cucumber concentrate for each experiment set had been tested for antioxidant activity (see Eq. 1) using DPPH scavenging and total phenolic content (see Eq. 2) using Folin-Ciocalteu reagent. Afterwards, anti-elastase activity (see Eq.3) analysis was also carried out to measure which operating conditions would gave the highest anti-elastase activity.

$$DPPH\ radical\ scavenging\ (\%) = \frac{A_{control} - A_{sample}}{A_{control}} \times 100\% \quad (1)$$

Where $A_{control}$ is the absorbance of the control, and A_{sample} is the absorbance of a sample.

$$TPC = cV/m \quad (2)$$

Where c is the sample concentrate that obtained from the calibration curve (mg/ml), V is the volume of cucumber juice used for extraction (ml) and m is the mass of fruit used (Ahmad et al., 2020).

$$Anti - elastase\ activity\ (\%) = \frac{\left(OD_{control} - \left(OD_{sample} - OD_{blank}\right)\right)}{OD_{control}} \times 100\% \quad (3)$$

Where $OD_{control}$ is the absorbance of the control, OD_{sample} is the absorbance of a sample and OD_{blank} of a blank solution.

The best parameter to obtain cucumber concentrate with highest antioxidant activity (93.17%) is at -2℃ of coolant temperature, 20 minutes of concentration time and 70 rpm stirring speed. Meanwhile, to obtain cucumber concentrate with highest total phenolic content (0.93 mg GAE/g), the best parameters are at -8 ℃ of coolant temperature, 15 minutes of concentration time, and 70 rpm stirring speed. In addition, to obtain cucumber concentrate with highest anti-elastase activity (206.06%), the best parameters are at -10 ℃ of coolant temperature, 15 minutes of concentration time, and 210 rpm stirring speed. The energy consumption of the process reached up to 1071.88 kWh/m^3 for highest antioxidant activity, 753.67 kWh/m^3 for highest total phenolic content and 779.87 kWh/m^3 for highest anti-elastase activity.

Acknowledgements: The authors would like to acknowledge the financial assistance from Universiti Teknologi PETRONAS via UTP-UTM JRP (Cost Centre: 015MD0-045) and facilities support from HICoE – Centre for Biofuel and Biochemical Research (CBBR) and Chemical Engineering Department. Support from the Ministry of Education Malaysia through the HICoE award to CBBR is duly acknowledged.

References

Ahmad, M. A., Ghazali, N. S. M., Samsuri, S., & Ruslan, M. S. H. (2020). Comparative study of total phenolic content and total flavonoid content extraction from guava juices by progressive freeze concentration and evaporation. *IOP Conference Series: Materials Science and Engineering*, *778*. https://doi.org/10.1088/1757-899X/778/1/012170

Ding, Z., Qin, F. G. F., Yuan, J., Huang, S., Jiang, R., & Shao, Y. (2019). Concentration of apple juice with an intelligent freeze concentrator. *Journal of Food Engineering*, *256*(March), 61–72. https://doi.org/10.1016/j.jfoodeng.2019.03.018

Englezos, P. (1993). The Freeze Concentration Process and its Applications. *The Freeze Concentration Process and Its Applications*.

Kausar, H., Saeed, S., Ahmad, M. M., & Salam, A. (2012). Studies on the Development and Storage Stability of Cucumber-Melon Functional Drink. *Journal Agricultural Research*, *50*(2).

Majumdar, T., Wadikar, D., & Bawa, A. (2010). Development, stability and sensory acceptibility of cucumber-basil juice blend. *African Journal of Food Agriculture Nutrition and Development*, *10*(9), 4093–4108.

Mazli, W. N. A., Samsuri, S., & Amran, N. A. (2020). Study of progressive freeze concentration and eutectic freeze crystallization technique for salt recovery. *IOP Conference Series: Materials Science and Engineering*. https://doi.org/10.1088/1757-899X/778/1/012167

Miyawaki, O., Gunathilake, M., Omote, C., Koyanagi, T., Sasaki, T., Take, H., Matsuda, A., Ishisaki, K., Miwa, S., & Kitano, S. (2016). Progressive freeze-concentration of apple juice and its application to produce a new type apple wine. *Journal of Food Engineering*, *171*, 153–158. https://doi.org/10.1016/j.jfoodeng.2015.10.022

Orellana-Palma, P., Petzold, G., Pierre, L., & Pensaben, J. M. (2017). Protection of polyphenols in blueberry juice by vacuum-assisted block freeze concentration. *Food and Chemical Toxicology*, *109*, 1093–1102. https://doi.org/10.1016/j.fct.2017.03.038

Petzold, G., Moreno, J., Lastra, P., Rojas, K., & Orellana, P. (2015). Block freeze concentration assisted by centrifugation applied to blueberry and pineapple juices. *Innovative Food Science and Emerging Technologies*, *30*, 192–197. https://doi.org/10.1016/j.ifset.2015.03.007

Qin, F. G. F., Ding, Z., Peng, K., Yuan, J., Huang, S., Jiang, R., & Shao, Y. (2021). Freeze concentration of apple juice followed by centrifugation of ice packed bed. *Journal of Food Engineering*, *291*(February 2020), 110270. https://doi.org/10.1016/j.jfoodeng.2020.110270

Rane, M. V., & Uphade, D. B. (2016). Energy efficient jaggery making using freeze pre-concentration of sugarcane juice. *Energy Procedia*, *90*(December 2015), 370–381. https://doi.org/10.1016/j.egypro.2016.11.204

Safiei, N. Z., Ngadi, N., Johari, A., Zakaria, Z. Y., & Jusoh, M. (2017). Grape juice concentration by progressive freeze concentrator sequence system. *Journal of Food Processing and Preservation*, 1–11. https://doi.org/10.1111/jfpp.12910

Samsuri, S., Nor Rizan, N. A., Hung, S. H., Amran, N. A., & Sambudi, N. S. (2019). Progressive Freeze Concentration for Volume Reduction of Produced Water and Biodiesel Wastewater. *Chemical Engineering Technology*, *42*(9), 1764–1770. https://doi.org/10.1002/ceat.201800505

Sánchez, J., Ruiz, Y., Raventós, M., Auleda, J. M., & Hernández, E. (2010). Progressive freeze concentration of orange juice in a pilot plant falling film. *Innovative Food Science and Emerging Technologies*, *11*(4), 644–651. https://doi.org/10.1016/j.ifset.2010.06.006

6th International Conference and Postgraduate Colloquium for Environmental Research 2022 (POCER 2022) 9 - 11 June 2022
Langkawi, Kedah, Malaysia

PCR04042022 – 70: Comparison Study on Sunway BRT's Terminus Stations' Visual Assessments

Hamsareka Thevadass[a], Goh Boon Hoe[a*], Wong Kok Cheong[a], Teo Fang Yenn[a], Christina Chin May May [a], Yuen Choon Wah [b], and Yap Eng Hwa [c]

[a] Faculty of Science and Engineering, University of Nottingham Malaysia, Jalan Broga, 43500 Semenyih, Selangor, Malaysia

[b] Centre for Transportation Research, University of Malaya, 50603 Kuala Lumpur, Malaysia

[c] Faculty of Transdisciplinary Innovation, University of Technology Sydney, Broadway, NSM 2007, Australia.

- Corrensponsing Author E-mail: Boon-Hoe.Goh@nottingham.edu.my

Keywords: Bus Rapid Transit; Sunway BRT Line; Walkability; Visual Assessment; First-Last Mile; Physical Infrastructures; Active Transportation

Extended Abstract

In Malaysia, no physical infrastructure evaluation tool for Bus Rapid Transit (BRT) has been published to measure the performance of local BRT and the walkability index associated with any BRTs operating locally. In addition, the number of modified motor vehicles utilised to obtain unrestricted mobility has rapidly expanded, resulting in increased congestion, disruptions, pollution, and deaths. The most challenging problem of all is establishing a set of measures necessary to develop a more successful transit system, which includes efficiency in quality transport, stimulation of non-motorized traffic, and integration of land use with transit systems. As a result, it is critical to evaluate the first and last mile journeys of all BRT passengers in order to fully comprehend the accessibility and interconnectedness of present and future BRT stops. This is because, while the length of the transit corridor is frequently analysed, the accessibility to stations and pedestrian catchments are frequently overlooked.

Hence, a Visual Assessment Form was developed to assess the physical infrastructure along the walkways radiating from the BRT Sunway Line stations. BRT Scoring Tools and Walkability

Evaluation Tools (ITDP, 2016), ((India), 2012) and (Stutsman, 2002) were investigated in order to understand the primary performance measurements and indicators associated with BRT and walkability in general. Following the identification of the unique observations and limits of all papers, a complete and pedestrian-passenger-based grading mechanism was built in accordance with the Malaysian environment and Malaysians' expectations on transit services. This tool consists of a set of grading factors concentrating on the physical infrastructures that help walkability; it is used to assess each BRT station and the 800-meter-long pathways radiating from the station. This paper compares the derived Visual Assessment results for the terminus stations of Sunway BRT, which is the Sunway Setia Jaya Station (SB 1) and USJ 7 Station (SB 7). SB 1 is the first station of the line and interconnected with KTM Port Klang Line, meanwhile SB 7 is the last station of the Sunway BRT line and interconnected to LRT Kelana Jaya Line. the Visual Assessment comprises the Station, Walkway and Junction Assessment. Table 1 below shows the Visual Assessment result for both stations and the number of walkways as well.

Table 6: Total Visual Assessment for SB 1 & SB 7

Station	Visual Assessment	Number of walkways radiating from the Station
Standard	226	1
SB 1 Sunway Setia Jaya	353/226	5
SB 7 USJ 7	191/226	2

Although both stations are terminus stations, there are prominent differeneces between the stations' walkways, in terms of number of walkways radiating from the station and the condition of the physical infrastructures which was derived from the Visual Assessment. The standard points for perfect station is 226 considering as for 1 walkway.

As can be seen here, the SB 1 scores higher than the SB 7 station, yet, the higher number of walkways for SB 1, added more value to the assessment points. The same observation also depicts the higher accessibility and connectivity to the station, making more possible paths to reach the station. In contrast, SB 7 only has 2 walkways, hence scoring lesser than the SB 1. On the other hand, it also scored lesser than the Standard score, which makes it more argumental. Hence, the scores of each walkways were presented in the Table 2, to further understand and study the comparisons of the assessment.

Table 2: Total Visual Assessment for SB 1 & SB 7 by Walkways

Station	Walkways (as W1-W5)				
	W1	W2	W3	W4	W5
SB 1 Sunway Setia Jaya	71 /226	70 /226	74 /226	71 /226	67 /226
SB 7 USJ 7	75.5 /226	115 /226			

Here, it can be observed that walkways in SB 7 has performed better indidually as compared to the SB 1's walkways. The walkways in the SB 1 has scored higher in terms of number of walkways connected, meanwhile, SB 7 scored higher than SB 1 in terms of facilities in the Station, parkings provided, and for having mixed land use within the walkability catchment area (also known as pedestrian generating areas). On the other hand, in terms of walkways Visual Assessment, walkways of SB 1 scored 20% of the total 78 points, and SB 7 walkways scored 35% of the total points. Still, as the terminus stations, both stations need more enhancement in terms of physical infrastructures in the Station, Walkways and Junctions. Visual Assessment developed for this purpose of the study can be used as the guide to rectify the low scored physical infrastructures.

This study focuses on terminus BRT stations because it is connected to the other type of public transportation which makes the terminus of BRT as the node of public transportation. Hence it is vital for the station and its catchment areas to be sufficient in terms of physical infrastructures aiding more practices of active transportation in the first-last mile travels.

Acknowledgements: Special appreciation to the co-authors and colleagues who provided guidance and experience that greatly aided the study and would like to thank the Ministry of Higher Education for granting me the Fundamental Research Grant Scheme for fully sponsoring the research.

References

(India), I. of U. T. (2012). *Bus Rapid Transit System (BRTS) Evaluation and Design (BEAD) Tool*. *3304*(January), 1–148.

ITDP. (2016). *The BRT Standard*. 81. https://www.itdp.org/wp-content/uploads/2014/07/BRT2016-REV7.75.pdf

Stutsman, J. (2002). Bus Rapid Transit or Light Rail Transit. *Transportation Research Record*, *1793*(1), 55–61. https://doi.org/10.3141/1793-08

6th International Conference and
Postgraduate Colloquium for
Environmental Research 2022 (POCER
2022) 9 - 11 June 2022
Langkawi, Kedah, Malaysia

PCR01042022 – 71: Reduction of Anaerobic Pretreated Sewage Sludge via Assimilation by Black Soldier Fly Larvae for Growth

Ratchaprapa Raksasat[a], Jun Wei Lim[a*], Chin Seng Liew[a], Hemamalini Rawindran[a], Mardawani Mohamad[b] and Boredi Silas Chidi[c]

[a] Department of Fundamental and Applied Sciences, HICoE-Center for Biofuel and Biochemical Research, Institute of Self-Sustainable Building, Universiti Teknologi PETRONAS, 32610 Seri Iskandar, Perak Darul Ridzuan, Malaysia

[b] Faculty of Bioengineering and Technology, Universiti Malaysia Kelantan, Jeli Campus, 17600 Jeli, Kelantan, Malaysia

[c] Bioresource Engineering Research Group (BioERG), Cape Peninsula University of Technology, P.O. Box 652, Cape Town 8000, South Africa

* Corrensponsing Author E-mail: junwei.lim@utp.edu.my

Extended Abstract

The incipient utilization of biomass from larvae is being investigated extensively in recent time due to low cost and environmentally friendly traits. This study had selected black soldier fly larvae (BSFL) since it has the ability to consume myriad types of organic wastes, inclusive of valorizing sewage sludge. Waste from sewage sludge is constantly generated to date and the utilization of BSFL as a potent recycler is an economical method to manage the hazardous components in sewage sludge. While sewage sludge contains nutrition for the nourishment of larvae, the complex substances in sludge pose challenge to the degradation and may retard the larval growth. This setback motivated the anaerobic pre-treatment employment in this study to break the complex matters in sewage sludge prior to feeding the BSFL, improving larvae to digest sewage sludge. Therefore, the improvement of larval growth with pre-treated sewage sludge at different conditions was determined in terms of larval growth rate in this study. The pre-treated condition of sewage sludge was studied at acidic, neutral, and alkali condition at pH3, pH7, and pH11, respectively. Thereafter, the best pH condition for larval growth was continually studied by varying the durations of anaerobic pre-treatment at 8, 16, and 32 days.

The total organic carbon (TOC) was highest at 48.7% in un-treated sewage sludge as opposed to the anaerobically pre-treated sewage sludge as presented in Figure 1 due to the organic substances were

being metabolized by microorganisms during anaerobic pre-treatment. However, black soldier fly larvae fed with un-treated sewage sludge was found to obtain the lowest larval growth rate at 0.068 mg/larva/day as shown in Figure 2 as the dominant composition in un-treated sewage sludge was organic compounds made up of complex matters; thereby, leading to the difficulty to be assimilated (Hermansson, 2012). The recovery of larval growth rate once being administered with anaerobic digested sewage sludge was observed had proven that the pre-treatment could breakdown the presence of complex organic compounds into simpler fragments to facilitate larval digestion (Hermansson, 2012).

Sewage sludge pre-treated at acidic condition (pH3) was found to obtain the highest TOC level at 46.6%. Likewise, for the larval growth rate, larvae fed with pre-treated sewage sludge at pH 3 showed the highest larval growth rate (0.253 mg/larva/day) in comparison with the ones fed by pre-treated sewage sludge at pH 7 and pH 11. The further increase of pre-treatment time to 32 days had caused a significant drop in TOC level and larval growth rate. This might be attributed by the inadequate nutrition to nourish the larvae. The decline of TOC could be justified by the depletion of nutrition for larval growth such as carbohydrates or protein due to the nutrients being scavenged by competitive microorganisms (Wong *et al*., 2019).

In addition, the dominant elements such as carbon and nitrogen contents extracted from larval biomass explicated that larva fed with pre-treated sewage sludge obtained higher carbon content than larvae fed with un-treated sewage sludge by 7% while the nitrogen content showed no significant effect in relation to larval feeds.

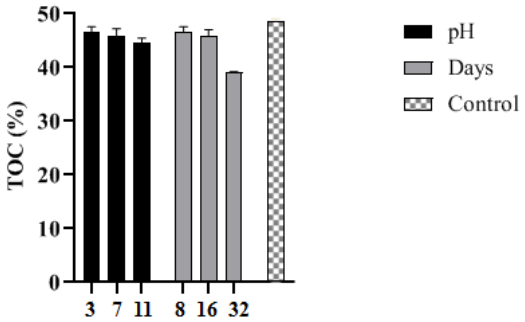

Figure 1: Total organic carbon (TOC) in sewage sludge upon pre-treatment at pH; 3, 7, 11 for 8 days: TOC at different days; 8, 16, 32 at pH 3 in comparison with un-treated sewage sludge)Control(

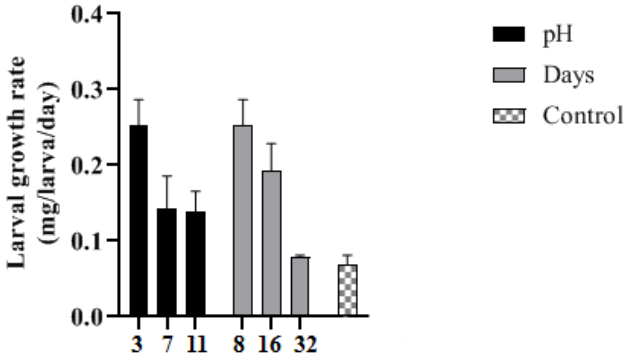

Figure 2: Larval growth rate)mg/larva/day(upon feeding with pre-treated sewage sludge at different pH; 3, 7, 11 for 8 days: Larval growth rate different days; 8, 16, 32 at pH3 in comparison with un-treated sewage sludge)Control(

Keywords: Black soldier fly larvae; Sewage sludge; Anaerobic; Pre-treatment; pH

Acknowledgements: The financial supports received from the Ministry of Higher Education Malaysia via HICoE-Center for Biofuel and Biochemical Research with the cost center of 015MA0-052 and Yayasan Universiti Teknologi PETRONAS (YUTP) with the cost center 015LC0-341 are gratefully acknowledged.

References

Hermansson, M., 2012. Evaluation of anaerobic digestion after pretreatment of wastwaters from pulp and paper industry.

Wong, C.Y., Rosli, S.S., Uemura, Y., Ho, Y.C., Leejeerajumnean, A., Kiatkittipong, W., Cheng, C.K., Lam, M.K., Lim, J.W., 2019. Potential protein and biodiesel sources from black soldier fly larvae: insights of larval harvesting instar and fermented feeding medium. *Energies.* 12, 1570.

6th International Conference and Postgraduate Colloquium for Environmental Research 2022 (POCER 2022) 9 - 11 June 2022
Langkawi, Kedah, Malaysia

PCR01042022 – 72: Utilization of Lignocellulosic Solid Waste for Attached Microalgal Growth and its Lipid Accumulation in Relation to pH of Cultivation Medium

Hemamalini Rawindran[a], Jun Wei Lim[a*], Ratchaprapa Raksasat[a] Chin Seng Liew[a], Mardawani Mohamad[b] and Boredi Silas Chidi[c]

[a] Department of Fundamental and Applied Sciences, HICoE-Center for Biofuel and Biochemical Research, Institute of Self-Sustainable Building, Universiti Teknologi PETRONAS, 32610 Seri Iskandar, Perak Darul Ridzuan, Malaysia

[b] Faculty of Bioengineering and Technology, Universiti Malaysia Kelantan, Jeli Campus, 17600 Jeli, Kelantan, Malaysia

[c] Bioresource Engineering Research Group (BioERG), Cape Peninsula University of Technology, P.O. Box 652, Cape Town 8000, South Africa

* Corresponding Author E-mail: junwei.lim@utp.edu.my

Extended Abstract

The attached growth of microalgae encompassing the generation of algal biofilm could plausibly render a promising approach in curbing the economical infeasibility issue faced by the conventional microalgal growth system. Hence, commercialization of the biofilm technology for algal biomass requires an inexpensive and easily sourced materials as biofilm carriers to render high biomass and lipid indexes. The research gap in the cultivation system of microalgae thus far had motivated a niche approach focusing on the attachment of *Chlorella Vulgaris* microalgae by cultivating them onto organic lignocellulosic solid support, palm kernel expeller. This study was conducted in relation to pH of cultivation medium.

Positive correlation was observed between cultivation medium pH towards the attached growth of *Chlorella vulgaris* onto PKE. An increase in microalgal densities was detected from pH 3 to pH 5, sustaining its growth until pH 9 and declined subsequently as exhibited by pH 11 (Figure 1). Similar trend was observed in heterotrophic metabolism which emphasizes on the activity of microalgae in metabolizing the PKE. The microalgal density and heterotrophic metabolism for all pH were evaluated statistically and deemed fit (one-way ANOVA: $p > 0.05$) with highest activity at 10.94 ± 0.83 g/g-PKE in pH 5 medium, followed by 10.28 ± 0.31 g/ g-PKE for pH 7 and 10.01 ± 0.36 g/ g-PKE for pH 9 medium. An interruption in growth at pH 11 could be due to the extreme alkaliphilic medium which had caused diminution of nutrients leading to ineffective nourishment for microalgal growth

(Vadlamani et al., 2017). Microalgae require carbon dioxide for growth while the presence of pH may alter its availability. As a small concentration of carbon dioxide dissolves into cultivation medium through the continuous aeration, it may exist as one of the three different species according to pH. Carbon dioxide (CO_2) is found at low pH, bi-carbonate (HCO_3-) at neutral pH, and carbonate (CO_3^{2-}) at high pH. Presence of carbonate ions at high pH impedes microalgal growth justifying its abrupt decrease at pH 11 (Qiu et al., 2017). However, the coupling effect of organic carbon from PKE and inorganic carbon from the dissociation of carbon dioxide in the cultivation medium resulted in the significant increase from pH 3 to pH 9.

On another note, the lipid contents obtained from attached microalgal biomasses had demonstrated a significant correlation with the surge in pH mediums ($p < 0.05$). The maximum attached microalgal lipid content was documented at 372 ± 0.07 mg/g in the cultivation medium of pH 11. From Figure 2, the disparities of lipid productions between the upper and lower limit ranges for the respective pH 3 and 11 values vindicated a significant growth by about two-fold. In this perspective, the microalgal cells yielding smaller lipid content at lower pH is highly likely due to the mechanism of intracellular pH regulations. Similar observation was reported by literatures which validated the lower accretion of lipid at acidic pH as compared with alkaline pH conditions, displaying superior lipid accumulations within pH 7 - pH 8.5 (D'Mello & Chemburkar, 2018; Peng et al., 2020). The increase in lipid contents progressed in the sequence of pH 11 > pH 9 > pH 7 > pH 5 > pH 3. In general, the increase in lipid content in relation to the increase in pH is due to the trigger which has switched the use of carbon metabolism from reproduction to energy storage (Shah et al., 2014). Similar phenomenon in cultivation medium of pH 11 had caused the termination of cell proteins development due to enzyme denaturation at extreme pH; thus, invigorating higher lipid production (Vadlamani et al., 2017). While the lipid contents from pH 5 and pH7 mediums were significantly lower than pH 11, their high microalgal densities had narrowed the gap of lipid contents as seen by the gradual increase in lipid productivities along with increasing pH mediums.

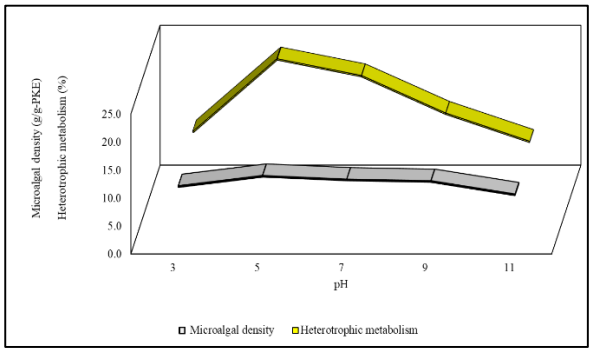

Figure 1: Attached microalgal densities and heterotrophic metabolisms of *Chlorella Vulgaris* in relation to cultivation medium pH

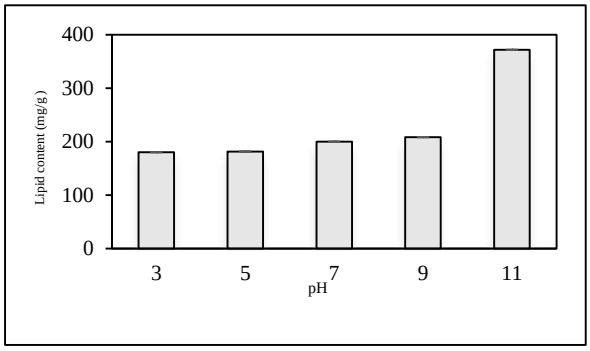

Figure 2: Attached microalgal lipid content of *Chlorella Vulgaris* in relation to cultivation medium pH

Keywords: Attached microalgae; Microalgal density; pH; Lignocellulosic; Palm kernel expeller; Lipid

Acknowledgements: The financial supports received from the Ministry of Higher Education Malaysia via HICoE-Center for Biofuel and Biochemical Research with the cost center of 015MA0-052 and Yayasan Universiti Teknologi PETRONAS (YUTP) with the cost center 015LC0-341 are gratefully acknowledged.

References

D'Mello, B., Chemburkar, M. (2018). Effect of temperature and pH variation on biomass and lipid production of Auxenochlorella pyrenoidosa. *Res J Life Sci Bioinform Pharm Chem Sci, 4*, 378-387.

Peng, X., Meng, F., Wang, Y., Yi, X., & Cui, H. (2020). Effect of pH, temperature, and CO2 concentration on growth and lipid accumulation of Nannochloropsis sp. MASCC 11. *Journal of Ocean University of China, 19*(5), 1183-1192.

Qiu, R., Gao, S., Lopez, P. A., & Ogden, K. L. (2017). Effects of pH on cell growth, lipid production and CO2 addition of microalgae Chlorella sorokiniana. *Algal Research, 28*, 192-199.

Shah, S. M. U., Che Radziah, C., Ibrahim, S., Latiff, F., Othman, M. F., & Abdullah, M. A. (2014). Effects of photoperiod, salinity and pH on cell growth and lipid content of Pavlova lutheri. *Annals of microbiology, 64*(1), 157-164.

Vadlamani, A., Viamajala, S., Pendyala, B., & Varanasi, S. (2017). Cultivation of microalgae at extreme alkaline pH conditions: a novel approach for biofuel production. *ACS Sustainable Chemistry & Engineering*, *5*(8), 7284-7294.

6th International Conference and
Postgraduate Colloquium for
Environmental Research 2022 (POCER
2022) 9 - 11 June 2022
Langkawi, Kedah, Malaysia

PCR01042022 – 73: The Effect of Temperature on Anaerobic Co-Digestion of Chicken Manure and Empty Fruit Bunch at Optimized C/N Ratio.

M.Devendran Manogaran, M Rashid Shamsuddin*, Mohd Harith Nizam Basheer Ahmad, Mohd Hakimi Rosli, Ahmer Ali Siyal and Yeow Khai Zhi

HICoE-Centre for Biofuel and Biochemical Research, Institute for Self-Sustainable Living Chemical Engineering Department
Universiti Teknologi PETRONAS, 32610, Seri Iskandar, Perak, Malaysia

• Corrensponsing Author E-mail: mrashids@utp.edu.my

Keywords: Anaerobic Digestion; Chicken Manure; Empty Fruit Bunch; Psychrophilic; Mesophilic; Thermophilic

Extended Abstract

The demand for chicken meat in Malaysia has grown in the few past years which has resulted in chicken manure (CM) production in abundance. Untreated CM is often used as organic fertilizer, leading to several environmental concerns. Anaerobic digestion (AD) is one of the potential treatment methods for CM that is able to produce circular economy outputs in the form of biogas and digestate. However, AD of CM alone exhibits poor yield of biogas and methane (CH4) due to its low carbon-to-nitogen (C/N) ratio which calls for a co-substrate (Hakimi et al., 2021). Empty fruit bunch (EFB) is a carbon rich biomass waste produced in large quantities by the palm oil industry as Malaysia is the second largest palm oil producer globally (Shamsuddin et al., 2021). Incorporation of EFB as a carbon adjuster for anaerobic co-digestion has been proven favourable to enhance biogas and CH4 generation (Cahyono et al., 2021). Another key parameter for AD is the operating temperature however, the effect of different temperature conditions on co-digestion of CM and EFB has yet to be evaluated. Hence, this study aims to observe the effect of psychrophilic (25℃), mesophilic (35℃) and thermophilic (45℃) temperature conditions on biogas and CH4 production at optimized C/N ratio for co-digestion of CM and EFB.

In this study, cow dung was used as the innoculum. The C/N ratio was fixed at 25:1 as it is deemed the most optimum as reviewed by Shamsuddin et al. (2021). The 25:1 C/N ratio feedstock was obtained by mixing CM, EFB and cow dung at a ratio of 3:2:5. Solid-to-liquid ratio was fixed at 1:3. The pH was then tested and adjusted to pH 7.0. The AD process was conducted in 1.5 L plastic bottles simulating the function of a digester body. The setup is as shown in Figure 1. These makeshift digesters were made airtight with the aid of a compressor pump to create an anaerobic condition and were painted black as microbes are sensitive to light. Bubble leak test (ASTM F2096) was conducted for the setups to ensure there was no leakage throughout the tubes, fittings and connectors. The setups for mesophilic (35℃) and thermophilic (45℃)

temperature conditions were placed in water baths. Biogas volume was measured every 5 days using the water displacement method with sodium chloride solution as solvent to prevent the absorption of biogas into the water (Walker et al., 2009). Biogas was also collected every 5 days to be analysed for CH4 content using gas chromatography with thermal conductivity detector.

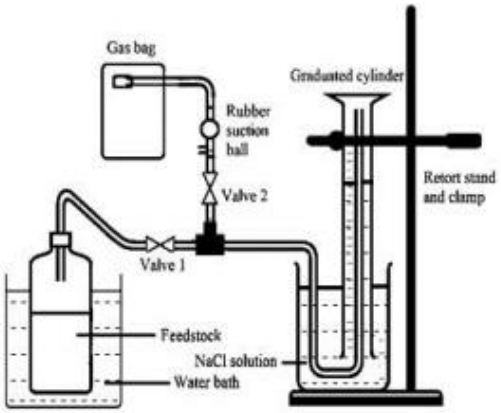

Figure 1: Experimental setup.

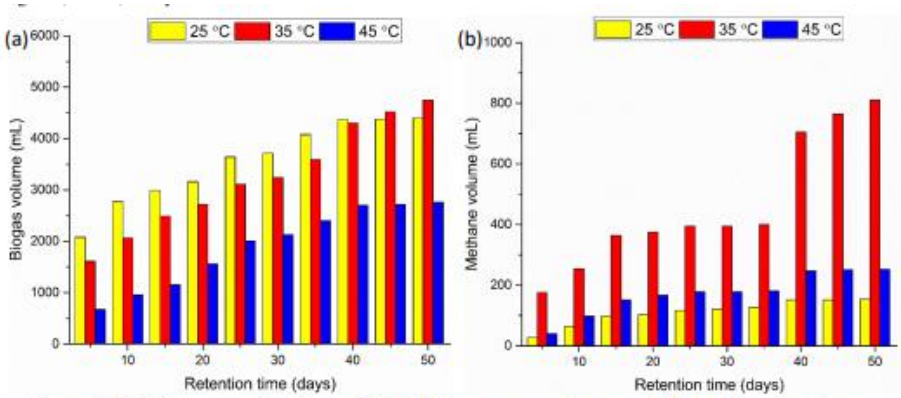

Figure 2: (a) Biogas production and (b) Methane generation over 50-day retention time.

Figure 2a shows that the biogas generation under all three temperature conditions increased consistently for the first 40 days. However, for the remaining 10 days biogas generation at 25℃ and 45℃ plateaued, peaking at 3900 ml and 2760 ml respectively unlike the trend observed at 35℃ whereby the biogas volume continued to increase up to 4750 ml at the end of the 50 day retention time. Although biogas generation at 25℃ was abundant during the first 40 days, significantly less CH_4 was produced compared to the setups at 35℃ and 45℃ throughout the 50 day period as exhibited in Figure 2b. The setup at 35℃ generated the most CH_4, 811 ml cumulatively, although the trend seemed to plataeu from day 15 up to day 35 before it continued to show constant increament until day 50. The CH_4 concentration at 25℃ and 45℃ exhibited little to no significant increament from day 15 up to day 35 and from day 40 up to day 50 with the cumulative CH_4 generation at 153.7 ml and 251.8 ml respectively.

The CH_4 generation at 25°C is significantly low due to the nature of psychrophlic anaerobic digestion (PAD) that has been deemed unstable (Akindolire et al., 2022). The incorporation of EFB to enhance the C/N ratio also poses a hurdle for PAD as EFB is rich in cellulose, hemicellulose and lignin, which are naturally recalcitrant to microbial degradation (Ona et al., 2019). Fundamentally, AD comprises of four steps which are hydrolysis, acidogenesis, acetogenesis and methanogenesis. With respect to PAD, the hydrolysis phase is regarded as the rate-limiting step which explains the trend for CH_4, depicting no significant increament from day 15 onwards. Accordingly, Rajagopal et al. (2017) suggested that the solid retention time for PAD be extended to enhance CH_4 yield. CH_4 generation under mesophilic anaerobic digestion (MAD) and thermophilic anaerobic digestion (TAD) on the other hand have been discussed extensively. Bayrakdar et al. (2017) claims that TAD is more accomodating to the hydrolysis phase hence the threat posed by the hydrolysis rate limit can ideally be overcomed. However, Yin et al. (2018) debunked that theory by obversing that the rate limits for all four stages of AD of CM were higher under TAD compared to MAD. Bi et al. (2019) also supported this theory by observing that MAD is more favourable compared to TAD. This is because CM is a nitrogen rich biomass waste and under TAD, it promotes high presence of total ammonium nitrogen (Niu et al., 2015). Free ammonia nitogen content, which forms a pivitol fraction of total ammonium nitrogen increases as the temperature rises thus effectively, TAD is more easily susceptible to ammonia inhibition compared to MAD (Yang et al., 2018). With respect to EFB solely for AD, Lee et al. (2020) observed that although TAD produced CH4 at a faster rate due to the shorter lag phase, the yield was lower in comparison to MAD. The current study on the other hand is an anaerobic co-digestion setup hence both CM and EFB are accountable for the rate of CH4 generation. Accordingly, it can be deduced that ammonia inhibition is greater a challenge to overcome under TAD which resulted in a prolonged lag phase from day 15 onwards in comparison to MAD which plateaued from day 15 up to day 35, afterwhich the CH_4 generation flourished.

Acknowledgements: The authors acknowledge UTP Prototype Fund (015PBA-031) for funding the research. The authors also thank HiCOE-Centre for Biofuel and Biochemical Research, Universiti Teknologi PETRONAS for the facilities provided for the research conduct.

References

Akindolire, M. A., Rama, H., Roopnarain, A., 2022. Psychrophilic anaerobic digestion: A critical evaluation of microorganisms and enzymes to drive the process. *Renewable and Sustainable Energy Reviews.* 161, 112394.

Bayrakdar, A., Molaey, R., Sürmeli, R. Ö., Sahinkaya, E., Çalli, B., 2017. Biogas production from chicken manure: Co-digestion with spent poppy straw. *International Biodeterioration & Biodegradation.* 119, 205-210.

Bi, S., Qiao, W., Xiong, L., Ricci, M., Adani, F., Dong, R., 2019. Effects of organic loading rate on anaerobic digestion of chicken manure under mesophilic and thermophilic conditions. *Renewable Energy.* 139, 242-250.

Cahyono, N. A. D., Shamsuddin, M. R., Ayoub, M., Mansor, N., Isa, N. H. M., Gunny, A. A. N., 2021. Anaerobic co-digestion of chicken manure with energy crop residues for biogas production. *IOP Conference Series. Earth and Environmental Science.* 765 (1).

Hakimi, M., Shamsuddin, R., Pendyala, R., Siyal, A. A., AlMohamadi, H., 2021. Co-anaerobic digestion of chicken manure with the addition of Cymbopogan citratus, Mentha piperita and Citrus sinensis as fly deterrent agents: Biogas production and Kinetic study. *Bioresource Technology Reports.* 15, 100748.

Lee, J. T. E., Khan, M. U., Tian, H., Ee, A. W. L., Lim, E. Y., Dai, Y., Tong, Y. W., Ahring, B. K., 2020. Improving methane yield of oil palm empty fruit bunches by wet oxidation pretreatment: Mesophilic and thermophilic anaerobic digestion conditions and the associated global warming potential effects. *Energy Conversion and Management.* 225, 113438.

Niu, Q., Takemura, Y., Kubota, K., Li, Y. Y., 2015. Comparing mesophilic and thermophilic anaerobic digestion of chicken manure: Microbial community dynamics and process resilience. *Waste Management.* 43, 114-122.

Ona, J. I., Halling, P. J., Ballesteros, M., 2019. Enzyme hydrolysis of cassava peels: treatment by amylolytic and cellulolytic enzymes. *Biocatalysis and Biotransformation.* 37 (2), 77-85.

Rajagopal, R., Bellavance, D., Rahaman, M. S., 2017. Psychrophilic anaerobic digestion of semi-dry mixed municipal food waste: For North American context. *Process Safety and Environmental Protection.* 105, 101-108.

Shamsuddin, R., Singh, G., Kok, H. Y., Hakimi Rosli, M., Dawi Cahyono, N. A., Lam, M. K., Lim, J. W., Low, A. (2021). Palm Oil Industry—Processes, By-Product Treatment and Value Addition. In Inamuddin and A. Khan (Eds.), *Sustainable Bioconversion of Waste to Value Added Products* (pp. 121-143). Cham: Springer International Publishing.

Walker, M., Zhang, Y., Heaven, S., Banks, C., 2009. Potential errors in the quantitative evaluation of biogas production in anaerobic digestion processes. *Bioresource Technology*. 100 (24): 6339-6346.

Yang, Z., Wang, W., He, Y., Zhang, R., Liu, G., 2018. Effect of ammonia on methane production, methanogenesis pathway, microbial community and reactor performance under mesophilic and thermophilic conditions. *Renewable Energy.* 125, 915-925.

Yin, D. M., Westerholm, M., Qiao, W., Bi, S. J., Wandera, S. M., Fan, R., Jiang, M. M., Dong, R. J., 2018. An explanation of the methanogenic pathway for methane production in anaerobic digestion of nitrogen-rich materials under mesophilic and thermophilic conditions. *Bioresource Technology*. 264, 42-50.

6th International Conference and
Postgraduate Colloquium for
Environmental Research 2022 (POCER
2022) 9 - 11 June 2022
Langkawi, Kedah, Malaysia

PCR01042022 – 74: Overview on Potential of Biogas Generation: A Case Study of Poultry Industry in The Manjung Region

Yeow Khai Zhi, M Rashid Shamsuddin*, M.Devendran Manogaran and Ahmer Ali Siyal

HICoE-Centre for Biofuel and Biochemical Research, Institute for Self-Sustainable Living,
Chemical Engineering Department
Universiti Teknologi PETRONAS, 32610, Seri Iskandar, Perak, Malaysia

- Corrensponsing Author E-mail: mrashids@utp.edu.my

Keywords: Biogas; Chicken Manure; Renewable Energy; Electric Power Generation; Biomass

Extended Abstract

Poultry farming in the Manjung region, Perak, Malaysia has been constantly growing throughout the past few years to meet the requirement of protein intake in Malaysia. The field of poultry farming has been known for its high consumption of energy and poor waste management. In the current study, green energy in the form of biogas production is introduced to poultry houses as an alternative energy source for energy generation while reducing carbon emissions to the environment in comparison to the conventional means of energy acquisition. The waste from the poultry houses can potentially undergo anaerobic digestion (AD) process to produce green energy in the form of biogas. Ideally, the biogas will be used to offset the heating requirement of the poultry houses and in the case of surplus, it can be converted into electricity for the main supply grid. This treatment approach also can reduce the greenhouse gases (GHGs) release from this industry, primarily in the form of carbon dioxide and methane.

As for the methodology of the project, firstly all the data required for the modelling were collected from sources such as journals articles, news articles, interviews and theses. Then, poultry-related data such as the chicken population, locality, rearing process, electricity usage and manure generation were obtained via case study at Dindings Poultry Development Centre (DPDC) Sdn Bhd. The data collected was analyzed to determine the correlation of the independent variables such as time, energy generation and amount of waste in the broiler house for potential biogas production.

According to Catarino (2009), the biogas potential for poultry litter is 0.1576 m^3/kg, with a calorific value of 6.21 kWh/m^3 and with biogas to power/electricity conversion efficiency of 25 %, the real calorific value of biogas is 1.55 kWh/m^3. The bedding material (rice husk or sawdust) used for manure collection was also taken into consideration. Application of such carbon additives is advantegeous to the AD system as it can improve the biogas generation (Hakimi,2021. Using these information, the estimated potential power generation of chicken manure feedstock (including bedding material) for one cycle of chicken farming was calculated.

In one cycle, the total amount of chicken manure obtained in the Manjung region is about 112,379.4 kg and through Equation 1 (Oliveira et al., 2012), the total amount of biogas produced is 17,710.99 m^3.

$$B = m * P_b \quad (1)$$

where B is total biogas volume(m^3), m is the total mass of chicken manure (kg), and P_b is the potential of biogas (m^3/kg).
Then, the electricity generated over 60 days was estimated using Equation (2) (Oliveira et al., 2012) by mutiplying the total amount of biogas produced (17,710.99 m^3) with the energy potential value of biogas (1.55 kWh/m^3)

$$E = B * P_{cr} \quad (2)$$

where E is the electricity energy (kWh), B is the total biogas volume (m^3) and P_{cr} is the energy potential value of biogas (kWh/m^3)

The calculated electricity generated with Equation (2) is 27,452.04 kWh. On average, the amount of electricity used for each cycle was about 11,930 kWh. This shows that the electricity used by the broiler house can be covered for each cycle witha surplus of 15,522.04 kWh electricity produced as well. The total amount of poultry litter produced in Manjung for one year is estimated to be 124,740,000 kg. With this average calorifc value, the gross energy potential of the Manjung region is estimated to be 44.5 MJ/s, or 44.5 MW. The following Equation (3) was used to calculate this value while Equation (4) is used to calculate the technical energy potential of poultry litter (Oliveira et al., 2012).

$$PB = \frac{m * P_c}{k} \quad (3)$$

where PB is the gross energy potential (MW), m is the biomass amount in one year, P_c is the average calorific value of poultry litter (MJ/kg) and k is the seconds in one year= 31,536,000 s

$$PT = PB * n \quad (4)$$

where PT is the technical energy potential (MW), PB is the gross energy potential (MW) and N is the efficiency of conversion system.

Poultry litter can be used as a primary source of energy in steam motors with a turbine. Assuming a 30 % average efficiency, the technical energy potential of poultry litter in past studies is approximately 13.35 MW. Table 1 represents a summary of the technical energy potential to Manjung Region.

Table 1 Theoretical Energy Potential to Manjung Region

Element	Units	Value
Number of Broiler House	Number	185
Number of Chickens	Number	5.5 million
Amount of chicken litter in one year	kg	124,740,000
Average calorific value	MJ/kg	11.25
Gross Energy Potential	MJ/year	1,403,325,000
	MW	44.5
Efficiency of conversion system	%	30
Technical Energy Potential	MW	13.35

Acknowledgements: The authors acknowledge Research Grant 015LC0-198 from Yayasan Universiti Teknologi PETRONAS for the support.

References

Catarino, R. P., González, A. P. N., & Oliveira, L. R. P. (2009). Optimization of methane production from chicken manure bed. In I International Symposium on Animal Waste Management.

Hakimi, M., Shamsuddin, R., Pendyala, R., Siyal, A. A., & AlMohamadi, H. (2021). Co-anaerobic digestion of chicken manure with the addition of Cymbopogan citratus, Mentha piperita and Citrus sinensis as fly deterrent agents: Biogas production and Kinetic study. Bioresource Technology Reports, 15, 100748.

de Lucas Jr, J., & Santos, T. M. (2000). Aproveitamento de resíduos da indústria avícola para produção de biogás. Simpósio Sobre Resíduos da Produto Avícola, 27-43.

Oliveira, M. O., Somariva, R., Junior, O. A., Neto, J. M., Bretas, A. S., Perrone, O. E., & Reversat, J. H. (2012, March). Biomass electricity generation using industry poultry waste. In International Conference on Renewable Energies and Power Quality, Santiago de Compostela, Spain, 28th to 30th March.

Uddin, W., Khan, B., Shaukat, N., Majid, M., Mujtaba, G., Mehmood, A., ... & Almeshal, A. M. (2016). Biogas potential for electric power generation in Pakistan: A survey. Renewable and Sustainable Energy Reviews, 54, 25-33.

6th International Conference and
Postgraduate Colloquium for
Environmental Research 2022 (POCER
2022) 9 - 11 June 2022
Langkawi, Kedah, Malaysia

PCR 10032022 – 75: Characterization of Lithium Doped Calcium Oxide from Organic Waste for Biodiesel Production

Siti Aminah Mohd Johari [a] and Muhammad Ayouba*

[a] Center for Biofuel and Biochemical Research (CBBR) Department of Chemical Engineering University of PETRONAS, Perak, Malaysia

• Corrensponsing Author E-mail: muhammad.ayoub@utp.edu.my

Keywords: Biodiesel; calcium oxide; eggshell; lithium; organic waste; transesterification

Extended Abstract

Biodiesel is one of the renewable fuels that has vast potential to reduce the usage of petroleum. Biodiesel is made from 100% renewable resources such as animal waste, dairy waste as well as food waste via catalytic transesterification (Ayoub and Abdullah, 2012). For catalyst, there are three types which are Heterogenous base catalyst such as calcium oxide (CaO) (Kavitha, Geetha, and Jacqueline 2019), alumina supported salts (Xie and Li, 2006) and zeolites (Xie, Peng, and Chen, 2006) are suitable for biodiesel yield as it can be separated easily from the product compare with homogenous catalyst. Not only the CaO catalyst can be obtained from the chemicals but also can be synthesized from biomass wastes such as eggshell and bones. The previous reseaarchers (Kavitha, Geetha, and Jacqueline, 2019) have combusted eggshell waste in a furnace at 800℃ for 3 h to synthesize nano CaO which used to yield biodiesel from dairy waste scum. They produced 96% of biodiesel with methanol to oil molar ratio of 6:1, 2.4 wt.% catalyst at 65℃ in 3 h operating condition. Metal doped base catalyst is generally synthesized via wet impregnation and co-precipitation and then calcined at high temperature by using furnace to form active site (Dhawane et al. 2017; Khatibi, Khorasheh, and Larimi, 2021) A number of studies have been carried out in synthesis the modified catalyst via conventional method for biodiesel production including Baskar, Selvakumari and Aiswarya where they prepared Ni doped ZnO nanocatalyst via co-precipitation method in biodiesel yield from castor oil (Baskar, Selvakumari, and Aiswarya, 2018). However, study in applying Li as metal support with organic waste for biodiesel production is still limited. In the present study, the analysis of Li based with CaO from eggshell are observed and discussed as well as comparing the catalyst with CaO from eggshell alone.

For methodology, the eggshell was subsequently soaked in hot water for 2 h to remove their white membrane. The eggshells were rinsed with distilled water and subsequently dry in oven at 100℃ for 24 h. The dehydrated eggshells were grinded into a powder with particle size of 100µm. Calcination of the resulting powder was carried out in a furnace at the temperatures of 800℃ for 3 h to decompose $CaCO_3$ into CaO. The metal selected for doping with CaO synthesized from eggshell is Lithium. The Li/CaO catalysts with 1 wt.% of Li was synthesized by the wet impregnation method. An appropriate amount of LiNO3 precursors was dissolved in deionized water and then added to CaO powder. The resulting mixture was then be stirred for 2 h at 60℃ under constant stirring until a paste is formed. The resulting paste was then be dried in an oven for 16 h at 90℃ and subsequently calcined at 600℃ for 5 h in a furnace. High calcination temperature favoured stronger interaction between the support and the active component to form more active sites (Khatibi, Khorasheh, and Larimi, 2021). Then, the Li/CaO catalyst was aanalysed by using X-ray diffraction (XRD), Fourier transform infrared spectroscopy (FTIR), Field emission scanning electron microscopy (FESEM) and Brunauer–Emmett–Teller (BET).

The Figure 1 presented the functional groups of Li/CaO (eggshell). A narrow infrared band at 3645 cm-1 are observed represented hydroxyl groups with stretching mode of OH groups in Ca(OH)2 samples (Kavitha, Geetha, and Jacqueline, 2019). The catalyst also showed presence of CaO correlated with carbonates bands at 1427 and 875 cm-1 (Alba-Rubio et al., 2010). Another absorption bands 1089 cm-1 presented the existence of carbonyl group of primary alcohol. Based on these functional groups, Li/CaO and CaO have similar bands (FTIR for CaO is not shown) with only difference in the intensity of the bands. Lithium cannot be detected in the FTIR most probably due to very low concentration of the metal.

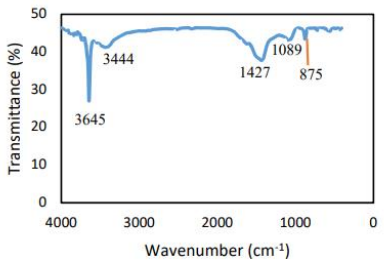

Figure 1: FTIR pattern of Li/CaO

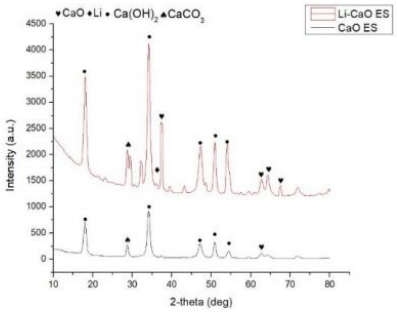

Figure 2: XRD pattern of Li/CaO

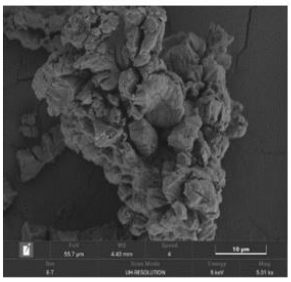

Figure 3: FESEM pattern of Li/CaO

Based on Figure 2, the XRD analysis is shown for Li/CaO and CaO alone. The Li/CaO showed three different type of peaks which indicated Ca(OH)2, CaO and CaCO3. The XRD pattern showed medium sharp diffraction peaks of crystallized cubic CaO at the Bragg's angle 2Θ = 37.39º, 64. 28º, 64.28º and 67.49º which is similar to the previous study (Krishnamurthy, Sridhara, and Ananda Kumar, 2020). There is small diffraction peak located at 36.00º which shows the small amount of Li presence

as only 1% concentration was added to the CaO catalyst. There are intense sharp peaks at 2Θ of 18.06º, 34.19º, 47.32º, 50.92º and 54.09º which corresponds to crystalline phase for $Ca(OH)_2$ which is comparable to diffraction peaks in earlier studies (Kavitha, Geetha, and Jacqueline 2019; Suryaputra et al., 2013a). While for eggshell derived CaO, the CaO peak is very low intense at 2Θ angle of 62.65º but obvious diffraction peaks were observed at 2Θ of 18.01º, 34.16 º, 47.13 º, 50.88 º and 54.43 º indicated the crystalline phase of Ca(OH)2 (Kavitha, Geetha, and Jacqueline, 2019; Suryaputra et al., 2013b) which is most probably due to exposure of air and water from the environment that combined with the CaO. Both catalysts (CaO and Li/CaO) showed presence of unreacted CaCO3 at 2Θ of 28.75º and 28.74º respectively but only in small intensity. The surface morphology of Li/CaO at 1000x magnification is presented in Figure 3. The Li/CaO showed the agglomerates of particles and irregular shape which most probably combination of lithium and CaO on its surface. From the Figure 3, the structure patterns have suggested that the Li2O has dispersed on the CaO surface and merging with the CaO to forms the agglomerated particle which was in line with previous study by Khatibi et al. (Khatibi, Khorasheh, and Larimi, 2021). The elemental compositions were detected by energy dispersive X-ray that has been coupled with FESEM analysis. Li/CaO showed sharp and high intensity of O (45.2 wt.%) followed by Ca (36.7 wt.%) which indicated that CaO compound is presence in the catalyst. The content of Ca was clearly higher and maximum than O composition which is similar with previous study done by Kibukaran and Arul (Kirubakaran and V, 2018). The presence of these elements showed that the calcination was successfully converted to CaO catalyst. However, the lithium element is not appeared most likely due to very low concentration (1 wt. %) used. Other composition like Mg, C and P are presence in low amount.

Table 1: Summary of Physical Properties of Li/CaO and CaO

Samples	Brunauer – Emmett – Teller properties		
	Surface area (m^2/g)	Pore volume (cm^3/g)	Pore size (nm)
Li/CaO	5.83	0.043	24.16
CaO	5.58	0.027	15.33

Table 1 shows the surface area, pore volume and pore size of both catalysts obtained from BET analysis. This BET surface area is important in heterogenous catalyst utilization as large surface area of catalyst can aids the access of ingression of reactant molecules to basic site of the catalyst (Zhao, Qiu, and Stagg-Williams, 2013). The surface area of Li/CaO was higher than CaO which was 5.83 m2 /g. This trend was the same for pore volume and obviously for pore size. These results indicated that the presence of lithium metal as the metal support could enlarge the surface area and pore size (24.16 nm) which can enhance the catalytic activity by higher adsorption capacity for large molecules of oil

on the surface of the catalyst which will increase the biodiesel yield. This results can be supported by other study where their catalyst (K-CaO) increase in their surface area most probably due to creation of new $CaSO_4$ crystal which in this study was the formation of $Ca(NO_3)_2$ crystal (Khatibi, Khorasheh, and Larimi, 2021). This new formation of crystal might have triggered new formation of pores on the CaO surface catalyst (Aziz, Triwahyono, and Jalil, 2016; Khatibi, Khorasheh, and Larimi, 2021). In conclusion, this study set out to determine the properties of dairy scum oil to know the suitability for biodiesel feedstock and synthesize and characterize the eggshell catalyst with and without metal support to show the differences in their properties. The findings of this study suggest that DWSO is suitable to be used as the biodiesel feedstock due to adequate presence of FFA (7.55%). This work contributes to existing knowledge of CaO from calcined eggshell by providing data when the CaO is supported with lithium to increase the catalytic activity in transesterification process. The Li/CaO shows better surface area and pore volume compared with eggshell derived CaO which could enhance the adsorbent of reactant to catalyst site. In future, the CaO can be derived from other waste such as fish bone to increase the concentration of CaO.

Acknowledgements: We thank and appreciate the support from Higher Institution Centre of Excellence (HiCoE) grant (015MA0-104), Malaysia for funding the research on biodiesel production from dairy waste scum.

6th International Conference and
Postgraduate Colloquium for
Environmental Research 2022 (POCER
2022) 9 - 11 June 2022
Langkawi, Kedah, Malaysia

PCR01042022 – 76: A Short Review on the Enhancement of Biogas Production from Anerobic Digestion of Animal Manure

Ahmer Ali Siyal[a], Rashid M Shamsuddin[a*], Masaharu Komiyaama[a], M. Devendern Manogaran[a], and Yeow Khai Zhi[a]

[a] HICoE Center for Biofuel and Biochemical Research (CBBR)
Institute of Self-sustainable Building, Department of Chemical Engineering
Universiti Teknologi PETRONAS, 32610 Bandar Seri Iskandar, Perak Darul Ridzuan, Malaysia

- Corresponding Author E-mail: MRASHIDS@UTP.EDU.MY

Keywords: Anaerobic Digestion; Animal Manure; Biogas; Methane; Additives; Optimization.

Extended Abstract

The renewable energy presents an alternative to current reliance of the world on fossil fuel based energy which has many environmental problems. The problems of release of chemical compounds like sulphur and nitrogen oxides from the burning of fossil fuels and global warming which cause melting of ice caps, heat wasves and draughts, rising sea levels, and changing global ecosystem are associated with the use of fossil fuel based energy sources. Most of developed countries are moving towards adopting biofuels such as biogas in place of natural gas, biodiesel in place of diesel, and biochar in place of coal (Judit, Péter et al. 2017, Bhatnagar, Ryan et al. 2022). Animal manures are produced in large quantities worldwide and their disposal or reuse is essential to avoid the emission of green house gases (GHGs). Animal manures contain nitrogen, proteins and phosphorous. The composition of different animal manures is given in Table 1. They are commonly used as natural fertilizers but their direct use can cause various problems such as GHGs emissions, eutrophication, patheogen contamination, and air polution due to the excess quantity of nutrients supplied to the crops. Animal manure can be an ideal feedstock material for anaerobic digestion (AD) process. The production of biogas through AD is the most preferred alternative option for the use of animal manure due to cheap biogas production and digestate as a byproduct which can be used as a fertilizer (Yangin-Gomec and Ozturk 2013).

AD is a four step process which consists of hydrolysis, acidogensis, acetogenesis, and methanogenesis. Typical biomass materials for biogas production are food waste, agricultural waste, municipal solid waste, municipal sewage and industrial organic waste, domestic animal manure, and forest waste. AD

converts organic matter into biogas and digestate. Biogas mainly consists of methane (CH_4) and carbon dioxide (CO_2) and small portions of hydrogen sulphide (H_2S) and carbon monoxide (CO). Besides biogas AD also produces digestate which contains low pathogens and has less odour as compared to untreated manure. Digestate contains nitrates, phosphates and other organic compounds which can be used as a fertilizer to promote plant growth (Auer, Vande Burgt et al. 2017). AD is a slow process with an average hydralic retention time of 30-50 days in conventional biogas plants (Yadvika, Santosh et al. 2004). Furthermore, the biogas production reduces in winter season which may limit its global acceptability. The co-digestion of animal manure with other substrates (Meneses-Reyes, Hernández-Eugenio et al. 2017, Scarlat, Dallemand et al. 2018), optimization of operational parameters, and use of nanomaterials (Yadvika, Santosh et al. 2004) are used to improve the efficiency of AD of animal manure. This paper describes a comprehensive overview on the enhancement of biogas production using above strategies. The challenges in the enhancement of biogas production are also discussed.

Co-digestion of animal manure with corn stover (CS), wheat straw (WS), spent poppy straw (SPS), apple pulp (AP), microbial mass, lignocellulosic residues, maize stover (MS), food waste (FW), and palm oil mill effluent (POME) has been conducted to enhance the biogas production. The operational parameters of pH, temperature, hydraulic retention time (HRT), and particle size of substrate through pretreatment have been used optimzed increase the biogas production. Various types of additive nanomaterials such as iron (Fe), nickel (Ni), cobalt (Co), ferrous oxide (Fe_2O_3), nano copper oxide (CuO), nano zinc oxide (ZnO), nano zero valent iron nanoparticles (nZVO), titanium dioxide (TiO_2) and carbon nanomaterials (CNMs) with varying concentrations and particle sizes have been used for the enhancement in biogas production from AD of animal manure.

Table 7: Composition of Animal Manures

Type of manure	TS	VS	C	N	H	S	pH	C/N	Ref.
	(%)								
Cattle	90.40	95.74	-	-	-	-	-	22.9	(Gaballah, Abomohra et al. 2020)
Chicken	-	-	21.12	5.52	-	-	6.10	3.83	(Singh, Shamsuddin et al. 2018)
Cow	19.8	85.7	-	-	-	-	8.57	-	(Chiumenti, da Borso et al. 2018)
Pig	31.97	20.16	35.59	1.72	4.84	0.44	8.58	20.70	(Zhang, Zeng et al. 2021)

Elephant	25.46	18.78	39.52	1.49	5.34	<0.5	-	-	(Zhang, Chen et al. 2022)

Acknowledgements: The authors thank HICoE Center for Biofuel and Biochemical Research (CBBR) for supporting this work under HICoE grant (015 MAO-104).

References

Auer, A., N. H. Vande Burgt, F. Abram, G. Barry, O. Fenton, B. K. Markey, S. Nolan, K. Richards, D. Bolton, T. De Waal, S. V. Gordon, V. O'Flaherty, P. Whyte and A. Zintl (2017). "Agricultural anaerobic digestion power plants in Ireland and Germany: policy and practice." Journal of the Science of Food and Agriculture 97(3): 719-723.

Bhatnagar, N., D. Ryan, R. Murphy and A. M. Enright (2022). "A comprehensive review of green policy, anaerobic digestion of animal manure and chicken litter feedstock potential – Global and Irish perspective." Renewable and Sustainable Energy Reviews 154: 111884.

Chiumenti, A., F. da Borso and S. Limina (2018). "Dry anaerobic digestion of cow manure and agricultural products in a full-scale plant: Efficiency and comparison with wet fermentation." Waste Management 71: 704-710.

Gaballah, E. S., A. E.-F. Abomohra, C. Xu, M. Elsayed, T. K. Abdelkader, J. Lin and Q. Yuan (2020). "Enhancement of biogas production from rape straw using different co-pretreatment techniques and anaerobic co-digestion with cattle manure." Bioresource Technology 309: 123311.

Judit, O., L. Péter, B. Péter, H.-R. Mónika and P. József (2017). "The role of biofuels in food commodity prices volatility and land use." Journal of competitiveness 9(4): 81-93.

Meneses-Reyes, J. C., G. Hernández-Eugenio, D. H. Huber, N. Balagurusamy and T. Espinosa-Solares (2017). "Biochemical methane potential of oil-extracted microalgae and glycerol in co-digestion with chicken litter." Bioresource Technology 224: 373-379.

Scarlat, N., J.-F. Dallemand and F. Fahl (2018). "Biogas: Developments and perspectives in Europe." Renewable Energy 129: 457-472.

Singh, G., M. R. Shamsuddin, Aqsha and S. W. Lim (2018). "Characterization of Chicken Manure from Manjung Region." IOP Conference Series: Materials Science and Engineering 458: 012084.

Yadvika, Santosh, T. R. Sreekrishnan, S. Kohli and V. Rana (2004). "Enhancement of biogas production from solid substrates using different techniques—a review." Bioresource Technology 95(1): 1-10.

Yangin-Gomec, C. and I. Ozturk (2013). "Effect of maize silage addition on biomethane recovery from mesophilic co-digestion of chicken and cattle manure to suppress ammonia inhibition." Energy Conversion and Management 71: 92-100.

Zhang, J., J. Chen, R. Ma, V. Kumar, Y. Wah Tong, Y. He and F. Mao (2022). "Mesophilic and thermophilic anaerobic digestion of animal manure: Integrated insights from biogas productivity, microbial viability and enzymatic activity." Fuel 320: 123990.

Zhang, Q., L. Zeng, X. Fu, F. Pan, X. Shi and T. Wang (2021). "Comparison of anaerobic co-digestion of pig manure and sludge at different mixing ratios at thermophilic and mesophilic temperatures." Bioresource Technology 337: 125425.

6th International Conference and
Postgraduate Colloquium for
Environmental Research 2022 (POCER
2022) 9 - 11 June 2022
Langkawi, Kedah, Malaysia

PCR04042022 – 77: Development of Ridership Forecasting Model for Sunway BRT's Riderships

Hamsareka Thevadass[a], Goh Boon Hoe[a*], Wong Kok Cheong[a], Teo Fang Yenn[a], Christina Chin May May [a], Yuen Choon Wah [b], and Yap Eng Hwa [c]

[a] Faculty of Science and Engineering, University of Nottingham Malaysia, Jalan Broga, 43500 Semenyih, Selangor, Malaysia

[b] Centre for Transportation Research, University of Malaya, 50603 Kuala Lumpur, Malaysia

[c] Faculty of Transdisciplinary Innovation, University of Technology Sydney, Broadway, NSM 2007, Australia.

- Corrensponsing Author E-mail: Boon-Hoe.Goh@nottingham.edu.my

Keywords: Ridership Forecast Model; Bus Rapid Transit; Sunway BRT Line; Regression; Gross Floor Area (GFA); Walkability Index, Walkability; Active Transportation

Extended Abstract

Looking specifically at Malaysia's Bus Rapid Transit (BRT) Sunway Line, despite the fact that the BRT stations are strategically positioned in one of the important nodes in Bandar Sunway, where diverse land-use activities can be found, and functions as a magnet for Bandar Subang, BRT ridership has declined since 2015 (Ming, 2017). This might be owing to the BRT Sunway Line's inadequate integration with the rest of the catchment regions, which may have prospective BRT users. The connection and accessibility of BRT stations influence people's willingness to walk or cycle to surrounding stations to travel through BRT. Improving the pedestrian environment is one of the most important factors in encouraging BRT users to walk to the stops. Hence, ridership predicting variables were identified and studied in order to develop Ridership Forecasting Modelling for BRT in Sunway, which utilised ridership data of BRT Sunway Line in the year 2019, and with other possible riders generating variables.

Regression modelling was utilised to build anticipated ridership data for the Sunway BRT Line stations in order to create a function that may be used in the future to estimate ridership if the independent variable is included. Linear regression is a regression model that uses a straight line to quantify the connection between an independent variable and a dependent variable. Each parameter is expected to have a numerical value. The forecasting modelling equation that will be produced at the end of this research is shown below.

$\hat{y} = bo + b1x$ (1)

$\hat{y}$, the forecasted Sunway BRT Line Ridership by station;

bo, Intercept or Constant;

b1, slope or coefficient;

x, independent variable(s)

After calculating the walkability index with and without weightage, the indexes were connected with BRT Sunway Line ridership data to produce a ridership forecasting modelling tool. In the year 2019, linear regression was performed between the index with and without weightage and ridership. Regression modelling was performed, and the best fit line was created to establish the relationship between the independent variables and the ridership data; based on this, further corrective actions can be offered for each walkway based on the index score for each element. In addition to the indexes as independent variables, other factors were taken into account in the regression computations. Table 1 shows the other factors include the Sunway BRT stations' Gross Floor Area (GFA) and the number of walkways connecting the stations, which were also incorporated in the index calculation for each station. This is an effort to explore the range of variables that might have an impact on ridership, whether adversely or positively.

Table 8: Regression Modelling Variables for BRT Ridership Forecast Modelling

Independent variable (x)		Dependent variable (y)
x_{wo1}	Index without Weightage	y, Ridership in 2019
x_{w1}	Index with Weightage	
x_2	Gross Floor Area of the station	
x_3	Number of walkways connecting the station	

Another alternate methodology was also investigated in the research for circumstances when there is no linearity between the independent factors and the dependent variable. As a result, data transformation was used and explored in this study to attain the linearity of the relationships. Few considerable functions were finalised in the function's discussion from the sets of regression analysis

that were completed. Only two functions acquired a P-value of less than 0.05 and an acceptable R-squared value out of 56 regressions from both portions of the Walkability Index without and with weightage.

$$\hat{y} = 1{,}107{,}535.52x + 219{,}082.80 \quad (2)$$

x_2, the Gross Floor Area (GFA) of the Sunway BRT Stations in acres; y, (y hat) Forecasted Ridership of Sunway BRT stations; P-value = 0.03; R-Squared = 66.61%

$$\hat{y} = 213{,}461{,}621.43x + 49{,}964.18 \quad (3)$$

x_{wo1}, the Inverse of Walkability Index without Weightage; y, (y hat) Forecasted Ridership of Sunway BRT stations; P-value = 0.04; R-Squared = 59.40%

Based on the preceding regression functions and graphs, the modelling function (2) was selected as the best function for estimating BRT passenger ridership in Sunway Line. This function was chosen because it has a better R-squared value than the other functions for ridership versus the GFA of the BRT Sunway Line. To the best of our knowledge, from a subject matter standpoint, mentioning the fact that the station's bigger Gross Floor Area can improve traffic might still be up for additional investigation and dispute. This might be a first step in investigating the Floor Area of the station in terms of anticipating ridership.

Aside from modelling function (2), the modelling function (3) has a lower R-squared value that falls below the moderate level. Although this may be an adequate function for predicting ridership statistically, the results may not reflect the right forecast due to the high coefficient value for the independent variable, the Walkability Index without Weightage. From the standpoint of the subject matter, this could be the most viable function for forecasting ridership because the index and the parameters could be used to improve the index, which would then increase the ridership. This can eventually lead to a shift in the mode of transportation of choice.

Acknowledgements: Special appreciation to the co-authors and colleagues who provided guidance and experience that greatly aided the study and would like to thank the Ministry of Higher Education for granting me the Fundamental Research Grant Scheme for fully sponsoring the research.

References

Ming, O. K. (2017, October 5). Public transport ridership falling, despite the billions spent. *Malaysia Kini*. https://www.malaysiakini.com/news/397308

6th International Conference and
Postgraduate Colloquium for
Environmental Research 2022 (POCER
2022) 9 - 11 June 2022
Langkawi, Kedah, Malaysia

PCR04042022 – 78: Optimization of Deep Eutectic Solvent Pretreatment for Bioethanol Production from Napier Grass

Elizabeth Jayex Panakkal[a], Marttin P. Gundupalli[a], Santi Chuetor[b], Atittaya Tandhanskul[c], Kraipat Cheenkachorn[b] and Malinee Sriariyanun [a*]

[a] Biorefinery and Process Automation Engineering Center, Department of Chemical and Process Engineering, TGGS, King Mongkut's University of Technology North Bangkok, Bangkok, Thailand

[b] Department of Chemical Engineering, Faculty of Engineering,
King Mongkut's University of Technology North Bangkok, Bangkok, Thailand

[c] Department of Food Technology, Faculty of Biotechnology, Assumption University, Bangkok, Thailand

*Corresponding Author E-mail: macintous@gmail.com

Keywords: Deep eutectic solvent; Enzymatic hydrolysis; Fermentation; Pretreatment; Biorefinery

Extended Abstract

The growing demands of fossil fuel consumption led to the depletion of fossil fuels, and global warming problem. Sustainable development has thus become a necessity in the current scenario. Lignocellulose with its rich carbon source is considered as an alternative for fossil fuels to produce biofuels and several platform chemicals. Napier grass has been identified as an important energy crop due to its high growth rate, and carbohydrate content (Nantasaksiri et al., 2021). This study aimed to enhance conversion of Napier grass to bioethanol by pretreatment with acidic deep eutectic solvent (DES) , choline chloride: lactic acid (ChCl/LA).

The physical properties of the synthesized ChCl/LA were also determined in this study (pH of 0.15, density of 1.04 g/ml, and viscosity of 125 mPa). The pH for ChCl, varying in composition from 1:1 to 1:9 was reported within the range of 1.50 to 0.47 (Kumar et al., 2018). The change in pH is due to the difference in the molar ratio of components along with temperature (Fanali et al., 2021). In addition to

this, the change in viscosity for increasing temperature was also determined. This trend could be due to the altered nature of DES by the thermal expansion of the structure (Fanali et al., 2021).

Even though several studies are carried out using different types of DESs, until now these studies could not confirm the best DES type or any optimized process conditions (Xu et al., 2020). However, optimized pretreatment conditions are necessary to maximize sugar yield from biomass. Therefore, the pretreatment conditions for choline chloride: lactic acid (1:4) were optimized using Box Behnken Design (BBD) of Response Surface Methodology (RSM). The optimization study has considered three factors namely, biomass loading (1:5 to 1:20, w/w), pretreatment temperature (80 to 130 ℃) and pretreatment time (0.5 to 5 h) and sugar concentration (mg/mL) after enzymatic hydrolysis was considered as the response. The model could predict the optimal pretreatment condition as biomass loading of 15.30% (w/w), pretreated at 80 ℃ for 5 h. Pretreatment at optimal conditions was predicted to provide a sugar yield of 4.140 mg/mL. Also, the BBD model could reveal the factors and their interaction effect on pretreatment. The study obtained maximum sugar yield at either lower temperature and longer pretreatment time or higher temperature and shorter pretreatment time suggesting that pretreatment temperature and time as influential factors in pretreatment (Figure 1). Under optimized pretreatment conditions, there were significant changes in the biomass composition, which confirms the positive effect of pretreatment (Table 2). The pretreatment with DES has contributed to the removal of lignin and enhancing cellulose content after pretreatment.

Further studies conducted to analyze the inhibitor formation in the pretreatment hydrolysate after pretreatment under optimized conditions. However, only acetic acid could be detected in the hydrolysate, which could be formed from the acetyl group of the hemicellulose. Fermentation studies were also conducted to evaluate the bioethanol production from the biomass. The pretreated Napier grass could produce 96.3% of the theoretical ethanol yield. Overall, this study provides optimized pretreatment conditions for choline chloride: lactic acid (1:4) for pretreating Napier grass and demonstrates the potential of Napier grass for producing bioethanol.

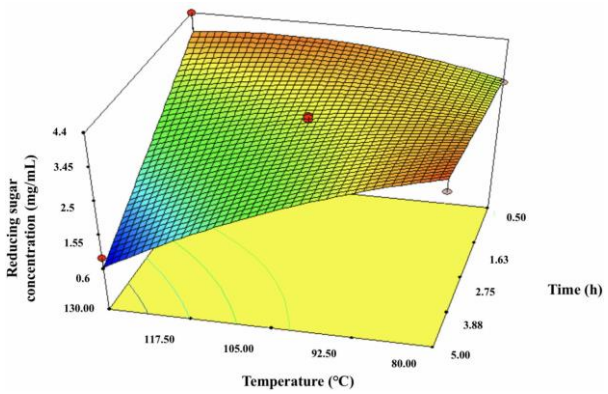

Figure 10: Effect of pretreatment temperature and time on reducing sugar concentration

Table 2: Biomass composition of Napier Grass

Biomass	Biomass Composition (%)		
	Glucan	Xylan	Lignin
Untreated Napier Grass	22.315 ± 0.07	7.754 ± 0.18	19.309 ± 0.43
Pretreated Napier Grass	31.635 ± 0.02	12.550 ± 0.28	10.986 ± 2.43

Acknowledgments: The authors would like to thank King Mongkut's University of Technology North Bangkok for providing all facilities and financial support (Grant Contract no: KMUTNB-FF-65-37, KMUTNB-PHD-64-02) for conducting the research.

References

Fanali, C., Gallo, V., Posta, S. Della, Dugo, L., Mazzeo, L., Cocchi, M., Piemonte, V., & De Gara, L. (2021). Choline chloride–lactic acid-based NADES as an extraction medium in a response surface methodology-optimized method for the extraction of phenolic compounds from hazelnut skin. *Molecules*, *26*(9). https://doi.org/10.3390/molecules26092652

Kumar, A. K., Shah, E., Patel, A., Sharma, S., & Dixit, G. (2018). Physico-chemical characterization and evaluation of neat and aqueous mixtures of choline chloride +lactic acid for lignocellulosic biomass fractionation, enzymatic hydrolysis and fermentation. *Journal of Molecular Liquids*, *271*, 540–549. https://doi.org/10.1016/j.molliq.2018.09.032

Nantasaksiri, K., Charoen-Amornkitt, P., & Machimura, T. (2021). Land potential assessment of napier grass plantation for power generation in thailand using swat model. Model validation and parameter calibration. *Energies*, *14*(5). https://doi.org/10.3390/en14051326

Xu, H., Peng, J., Kong, Y., Liu, Y., Su, Z., Li, B., Song, X., Liu, S., & Tian, W. (2020). Key process parameters for deep eutectic solvents pretreatment of lignocellulosic biomass materials: A review. *Bioresource Technology*, *310*. https://doi.org/10.1016/J.BIORTECH.2020.123416

PCR04042022 – 79: Physiochemical Properties of Choline Chloride Based Green Solvents in Water

Kok Liang Yap[a], Chung Loong Yiin[a*], Bridgid Lai Fui Chin[b], Serene Sow Mun Lock[c]

[a] Department of Chemical Engineering & Energy Sustainability,
Universiti Malaysia Sarawak (UNIMAS), Sarawak, Malaysia
[b] Department of Chemical Engineering,
Curtin University Malaysia, Sarawak, Malaysia
[c] Department of Chemical Engineering,
Universiti Teknologi PETRONAS, Perak, Malaysia

- Corresponding Author E-mail: clyiin@unimas.my

Keywords: Green Solvents; Choline Chloride; Hydrogen Bonding; Biomass Pretreatment; Stabilizing Capacity.

Extended Abstract

Green technology and sustainable development goals acquired unprecedented global attention over the past decades. The intensive use of conventional solvents in the industries raises environmental concern, therefore urges for green alternatives to substitute these conventional solvents. Advances in lignocellulosic biomass pretreatment techniques are continuously developed and improvised to improve the yield of certain substrates in the lignocellulosic biomass. Considering the recent emphasis on green chemistry, there will be a large room for advancements in green solvents for the pretreatment of lignocellulosic biomass considering the near-infinite possible combinations of deep eutectic solvents (DESs)/Low-transition-temperature mixtures (LTTMs) with different pairs of hydrogen bond acceptor (HBA) and hydrogen bond donor (HBD) (Yiin et al., 2021). The wide liquid range and befitting physicochemical properties evinced the key qualities of DESs/LTTMs suitable to be used as solvents. The strong hydrogen bond interactions are accredited for the similar benefits exhibited by DESs/LTTMs as compared to ionic liquids (ILs) while at the same time overcome the limitations of conventional ILs. Although both DESs/LTTMs and ILs present highly similar core characteristics, DESs/LTTMs are deemed a more complete representation of the green chemistry benchmarks, rendering DESs/LTTMs a compelling interest as the more favourable alternative compared to their analogue ILs (Silva et al.,

2019). Nonetheless, the application of DESs/LTTMs, comprehensive studies and characterisation of the physicochemical properties of DESs/LTTMs are still scarce. A gap exists in fully understanding DESs/LTTMs, which can be attributed to the ambiguity in the building principles, incomprehensive knowledge on the mechanisms of formation, as well as the intermolecular interactions within the solvent. After all, the pivotal key to explore deeper into DESs/LTTMs lies upon its fundamental, where its physicochemical properties play a significant role in modulating the species reactivity and behaviour of the DESs/LTTMs (Savi et al., 2019). As discussed herein, this research project aims to investigate the effects of water on the physicochemical properties of Choline chloride/Malic acid (CCMA) and Choline Chloride/Lactic acid (CCLA) DESs/LTTMs since the solvents are often much likely to be exposed to water during its application, either by purpose or otherwise. A total of 12 compatible DESs/LTTMs with different water content were synthesized and characterized. The addition of water modulated the density and conductivity of the green solvents by decreasing density and increasing conductivity with higher water content. FTIR characterization found the broadened OH stretching within the range 3700 cm^{-1} to 2500 cm^{-1}, the diminished choline chloride characteristic peak associated with its OH group at 3221 cm^{-1}, and the bathochromic shift of the C=O stretch associated with carboxylic acids within 1680 cm^{-1} to 1725 cm^{-1} which evidenced the hydrogen bond formation between the hydrogen bond acceptor and hydrogen bond donor, as the prerequisite for DESs/LTTMs formation. Water addition also demonstrated significant effect on biopolymer solubility despite the retention of original DESs/LTTMs structure when subjected to water addition. CCLA demonstrated highest lignin solubility at 6.32 wt% and further hydration results in weakened DESs/LTTMs structure causing degradation in dissolution performance. CCMA reported slight improvement on lignin selectivity and solubility with water addition at which the maximum solubility was recorded at 3.67 wt% with 40 wt% water content. The different effects of water addition on the ChCl/Malic acid and ChCl Lactic acid were due to the two different mechanisms of lignin solubilization (i.e. hydrotropy and co-solvency) as shown in Figure 1 (Soares et al., 2019). In this scenario, the ChCl/Malic acid DESs/LTTMs demonstrated hydrotropy behavior involving cooperative intermolecular reactions while the ChCl/Lactic acid DESs/LTTMs is an instance of co-solvency solubilization behavior in water. The self-degradation of ChCl and carboxylic acids **DESs/LTTMs** due to esterification reaction was also prevented with the addition of water which further enchanced their stabilizing capacity. Thus, both CCMA and CCLA green solvents demonstrated potential to be used in biomass valorisation and addition of water to DESs/LTTMs to modulate the physicochemical properties were proven feasible.

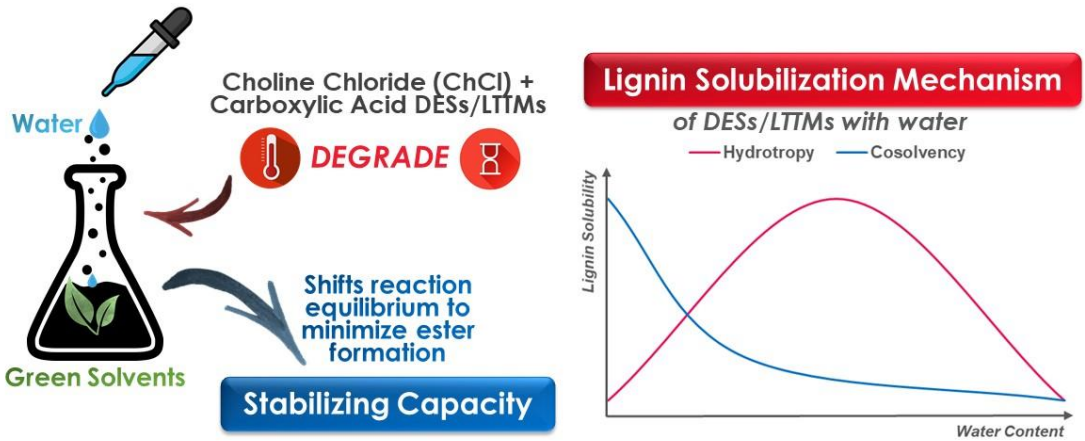

Figure 11: The effects of water in stabilizing capacity and lignin solubilization mechanism of DESs/LTTMs

Acknowledgements: The authors would like to acknowledge the funding supports from Ministry of Higher Education Malaysia, Fundamental Research Grant Scheme, FRGS/1/2020/TK0/UNIMAS/03/2.

References

Savi, L. K., Dias, M. C. G. C., Carpine, D., Waszczynskyj, N., Ribani, R. H., Haminiuk, C. W. I., 2019. Natural deep eutectic solvents (NADES) based on citric acid and sucrose as a potential green technology: a comprehensive study of water inclusion and its effect on thermal, physical and rheological properties. *International Journal of Food Science and Technology*, *54*(3): 898-907.

Silva, J. M., Pereira, C. V., Mano, F., Silva, E., Castro, V. I. B., Sá-Nogueira, I., Reis, R. L., Paiva, A., Matias, A. A., Duarte, A. R. C., 2019. Therapeutic Role of Deep Eutectic Solvents Based on Menthol and Saturated Fatty Acids on Wound Healing. *ACS Applied Bio Materials*. *2*(10): 4346-4355.

Soares, B., Silvestre, A. J. D., Rodrigues Pinto, P. C., Freire, C. S. R., Coutinho, J. A. P., 2019. Hydrotropy and Cosolvency in Lignin Solubilization with Deep Eutectic Solvents. *ACS Sustainable Chemistry and Engineering*. *7*(14): 12485-12493.

Yiin, C. L., Yap, K. L., Ku, A. Z. E., Chin, B. L. F., Lock, S. S. M., Cheah, K. W., Loy, A.C.M., Chan, Y. H., 2021. Recent advances in green solvents for lignocellulosic biomass pretreatment: Potential of choline chloride (ChCl) based solvents. *Bioresource Technology*. 125195.

PCR04042022 – 80: Improvement of Enzymatic Saccharification and Ethanol production from Organic Acid-Pretreated Coffee Shells

Nichaphat Kitiborwornkul[a], Prapakorn Tantayotai[b], Suvaluk Asavasanti[c], Siripan Pochailert[d], Patchanee Yasurin[d] and Malinee Sriariyanun[a*]

[a] Biorefinery and Process Automation Engineering Center, Department of Chemical and Process Engineering, TGGS, King Mongkut's University of Technology North Bangkok, Bangkok, Thailand

[b] Department of Microbiology, Faculty of Science, Srinakharinwirot University, Bangkok, Thailand

[c] Food Technology & Engineering Laboratory, Pilot Plant Development & Training Institute, King Mongkut's University of Technology Thonburi, Bangkok 10140, Thailand

[d] Department of Food Technology, Faculty of Biotechnology, Assumption University, Bangkok, Thailand

*Corresponding Author E-mail: macintous@gmail.com

Keywords: Enzymatic hydrolysis; Fermentation; Pretreatment; Bioethanol; Coffee husk; Optimization

Extended Abstract

Coffee is consumed as favorite beverage worldwide, and it is the second largest commodity in the world market. It is reported that the global coffee production in 2019 was 10.2 million tons [Lopes et al., 2022]. Coffee beans have been produced in large quantity leading to over production of coffee waste, such as spent coffee grounds and coffee husks. Coffee husks are obtained during a process to prepare coffee beans from coffee fruits, however they are not yet utilize in any use and discard as trash. So, it is important to convert coffee husks to value added product and chemical such as biofuel.

To produce a value-added products and chemicals, a coffee husk have to goes through a multistep process of biorefinery including pretreatment, hydrolysis, and fermentation. In this biorefinery process, the bottlenecks that limit the efficiency of the process are pretreatment and

hydrolysis because lignocellulose in coffee husk is inaccessible by cellulase enzyme to hydrolyze to sugars. In this research, pretreatment by using organic and inorganic acids were selected to enhance the efficiency of cellulase enzyme. Acid pretreatment helps to remove the lignin and hemicellulose in lignocellulose, so cellulase can access and hydrolyze cellulose with higher efficiency [Kumar and Sharma., 2017]. Previously, it has been demonstrated that inorganic acid is corrosive chemicals to instrument, and it also leads to production of inhibitor during pretreatment that interfere enzymatic hydrolysis reaction. Here, inorganic acid (hydrochloric and sulfuric acids) and organic acids (oxalic, citric and acetic acids) were applied and optimized in coffee husk pretreatment based on Response Surface Methodology (RSM) with Box-Behnken design (BBD).

A total of 17 RSM pretreatment experiments were conducted based on the BBD by varying three pretreatment parameters, including Temparature (50-140 °C), Time (30-240 min), and Acid concentration (5-12 %). The RSM mathamatical model obtained from experiment data showed that the 2FI model was suggested with R^2 at 0.7428 and model p-value at 0.0146, advocating the reliablility of the predicted model (Figure 1). Thus, the optimal condition of organic acid pretreatment was predicted to be at 137.36 °C, 240 min, and 11.7% acid concentration. Based on the pretreatment and enzymatic saccharification, the amounts of reducing sugars from pretreatment liquor ranged between 13.80-33.25 mg and from hydrolysates ranged between 4.33-6.78 mg/ml (Table 1). The reducing sugar obtained in pretreatment liquor of oxalic acid was the highest yield at 33.25 mg/ml, which was increased for 2.40, 2.20, and 2.41 time compared to untreated, hydrochloric acid-pretreated, and sulfuric acid-pretreated samples, respectively (Table 1). After pretreatment and hydrolysis, pretreatment liquor and biomass hydrolysate were subjected to ethanol fermentation by *Saccharomyces cerevisiae* and the ethanol yields were measured [Sriariyanun et al., 2019]. The highest ethanol yield at 2.29 and 1.12 % were obtained from citric acid-pretreatment liquor and from citric acid-hydrolysate (Table 1).

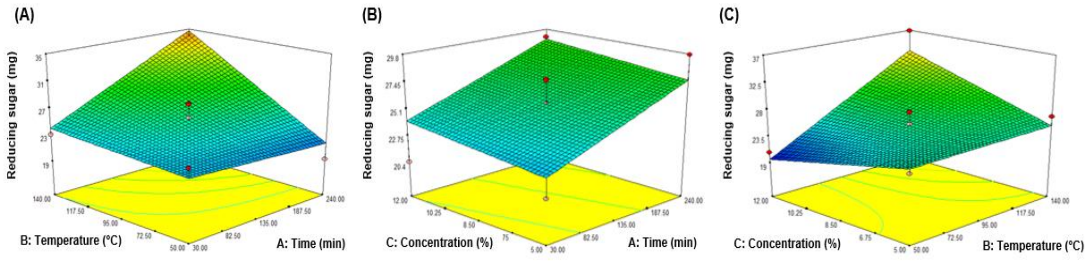

Figure 12: Response surface plots representing influence of the pretreatment parameters on sugar yields. (A) effect of temp x time, (B) effect of conc x time, and (C) effect of conc x temp

Table 9: Production of reducing sugar and ethanol yield from pretreatment liquor and biomass hydrolysate.

Sample	Pretreatment liquor		Biomass hydrolysate	
	Reducind sugar (mg/ml)	Ethanol yield (%)	Reducind sugar (mg/ml)	Ethanol yield (%)
Untreated	13.83 ± 0.68	1.12 ± 0.03	4.20 ± 0.12	0.22 ± 0.04
Oxalic acid	33.25 ± 1.86	1.17 ± 0.06	6.32 ± 0.04	0.35 ± 0.04
Citric acid	23.07 ± 0.22	2.29 ± 0.12	6.79 ± 0.02	1.12 ± 0.07
Acetic acid	21.73 ± 0.13	0.56 ± 0.06	6.39 ± 0.03	0.34 ± 0.06
Hydrochloric acid	15.09 ± 0.10	0.73 ± 0.04	5.86 ± 0.05	0.77 ± 0.06
Sulphuric acid	13.80 ± 0.03	1.73 ± 0.10	6.78 ± 0.13	0.36 ± 0.08

Acknowledgements: The authors would like to thank King Mongkut's University of Technology North Bangkok for providing all facilities and financial support (Grant Contract no: KMUTNB-FF-65-37) for conducting the research.

References

Lopes, A.C.A., Andrade, R.P., Casagrande, M.D.R., Santiago, W.D., de Resende, M.L.V., Cardoso, M.D.G., Vilanova, M., Duarte, W.F., 2022. Production and characterization of a new distilled beverage from green coffee seed residue, *Food Chemistry*, Volume 377, 2022, 131960

Kumar, A.K., Sharma, S. Recent updates on different methods of pretreatment of lignocellulosic feedstocks: a review. Bioresour. Bioprocess. 4, 7 (2017).

Sriariyanun M, Mutrakulcharoen P, Tepaamorndech S, Cheenkachorn K, Rattanaporn K. 2019. A rapid spectrophotometric method for quantitative determination of ethanol in fermentation products. Oriental Journal of Chemistry. 35(2) 744-750

6th International Conference and
Postgraduate Colloquium for
Environmental Research 2022 (POCER
2022) 9 - 11 June 2022
Langkawi, Kedah, Malaysia

PCR04042022 – 81: Bioethanol and Biogas Production From Organic and Mineral Acid Pretreated Sugarcane Bagasse: Comparative and Optimization Studies

Marttin Paulraj Gundupalli[a], Babu Dharmalingam[a], Roungdao Klinjapo[b], Prapakorn Tantayotai[c], and Malinee Sriariyanun[a*]

[a] Department of Chemical and Process Engineering, TGGS, King Mongkut's University of Technology North Bangkok, Bangkok, Thailand

[b] Department of Food Technology, Faculty of Biotechnology, Assumption University, Bangkok, Thailand

[c] Department of Microbiology, Faculty of Science, Srinakharinwirot University, Bangkok, Thailand

Corresponding Author E-mail: macintous@gmail.com

Keywords: anaerobic digestion, biorefinery, fermentation, mineral acid, optimization, organic acid, saccharification

Extended Abstract

Biofuels have proven to be a promising strategy to overcome the energy crisis, global warming caused by the excessive use of fossil fuels (Talukder et al., 2019). Lignocellulose is a rich source of sugar substrates (cellulose and hemicellulose) and lignin. The lignin layer hinders the process efficiency and thereby requires pretreatment step to break the hydrogen bonds between lignin and polysaccharides (Amnuaycheewa et al., 2016). Pretreatment improves cellulose digestibility during saccharification due to increased cellulase accessibility and surface area. The effect of the pretreatment on the dissolution of hemicellulose and lignin depends on a variety of factors including biomass type, pretreatment method, biomass loading, reaction time, reaction temperature, catalyst concentration (Amarasekara, 2013). In present study, sugarcane bagasse (SB) was processed for the bioenergy production by pretreatment, saccharifiucation, fermentation and anaerobic digestion (Figure 1). Acid pretreatment using organic acid (acetic acid (AA), oxalic acid (OA), and citric acid (CA)) were selected to convert the SB biomass to ethanol and biogas. The organic acid pretreatment performance was compared to the results of mineral acid (hydrochloric acid (HA)) pretreatment. The pretreatment operational parameters such as reaction time, temperature, and acid concentration was optmized using response surface methodology (RSM) by considering the Box-Behnken Design (BBD) matrix. The independent variable such as time (X_1, min), temeprature (X_2, ^oC), organic acid contcentration (X_3, %w/v), and mineral acid concentration

(X_3, % v/v) was varied as 30 – 90, 100-140, 2-12, and 0.5-2, respectively. The reducing sugar (Y, mg/mL) obtained after saccharification of pretreated solids obtained after indiviudal runs was considered as dependent variable. The change in the fucntional groups related to cellulose, hemicellulose and lignin were analyzed through FTIR analysis of the treated biomass. In this study, the acid pretreatment was evaluated for achieving maximum ethanol and biogas from SB biomass.

The reducing sugar after saccharification for AA, OA, CA, and HA pretreated solids varied as 0.9-8.07, 3.2-5.9, 1.96-7.73, and 2.73-5.13 mg/mL, respectively. The optimum condition for the acid pretreatment were detemined after multiple regression analysis of the second order model generated based on the experimental results. The hydrolysate obtained for biomass pretreated at optimum conditions were subjected to fermentation for ethanol production using *Saccharomyces cerevisiae* (TISTR 5596 and TISTR 5339). In another process, the pretreated solids were subjected to the anaeorobic digestion (AD) for biogas production. During fermentation, the ethanol yield was higher for hydrolysate related to CA followed by OA and HA pretreatment. Maximum ethanol yield was obtained for *S. cerevisiae* 5596 compared to *S. cerevisiae* 5339. The ethanol yield increased 1.14 fold for CA pretreatment compared to OA and HA pretreatment, respectively. On the other hand, maximum biogas yield for a 30 day period was observed for OA pretreated biomass compared to other biomass pretreated using different acids. The biogas yield increased 2.01 fold compared to the untreated biomass. The biogas yield for OA pretreated biomass increased 1.76, 1.66, and 2.03 fold compared to AA, CA, and HA pretreated biomass, respectively. The increase in ethanol and biogas yield for organic acid pretreated biomass shows that organic acid have advantage over mineral acids. The lower ethanol and biogas yield for mineral acid pretreatment is attributed to the degradation of hemicellulose and cellulose to furfural and 5-hydroxymethylfurfural that are referred to as the inhibitory compounds. The loss of sugar during pretreatment is reflected during the fermentation and AD process. Furthermore, the production of ethanol and biogas from SB biomass is dependent upon the selection of organic acid and pretreatment conditions. Pretreatment of lignocellulosic biomass using organic acid benefits the biorefineries during commercilization.

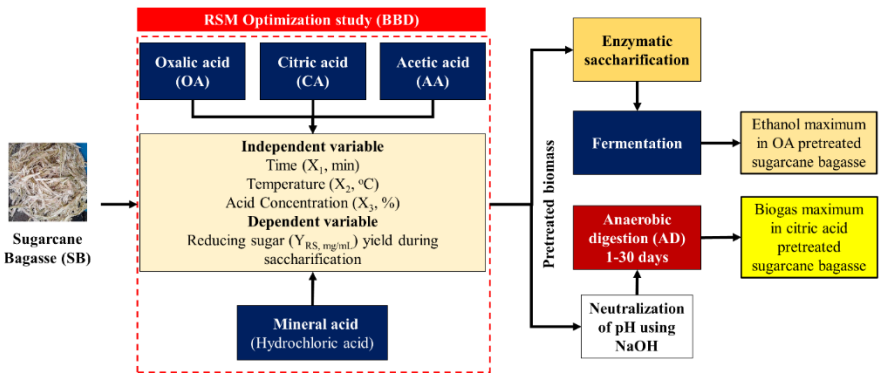

Figure 1. The process to study the effects of organic acid pretreatment of SB on ethanol and biogas production

Acknowledgments: The authors would like to thank KMUTNB for providing all facilities and financial support (Grant Contract no: KMUTNB-PHD-65-05, KMUTNB-FF-65-37) for conducting the research.

References

Amarasekara, A.S., 2013. Pretreatment of Lignocellulosic Biomass, in: *Handbook of Cellulosic Ethanol*. John Wiley & Sons, Inc., Hoboken, NJ, USA, pp. 147–217. https://doi.org/10.1002/9781118878750.ch5

Amnuaycheewa, P., Hengaroonprasan, R., Rattanaporn, K., Kirdponpattara, S., Cheenkachorn, K., Sriariyanun, M., 2016. Enhancing enzymatic hydrolysis and biogas production from rice straw by pretreatment with organic acids. *Ind. Crops Prod*. 87, 247–254. https://doi.org/10.1016/j.indcrop.2016.04.069

Talukder, A.A., Adnan, N., Siddiqa, A., Miah, R., Tuli, J.F., Khan, S.T., Dey, S.K., Lertwattanasakul, N., Yamada, M., 2019. Fuel ethanol production using xylose assimilating and high ethanol producing thermosensitive Saccharomyces cerevisiae isolated from date palm juice in Bangladesh. *Biocatal. Agric. Biotechnol*. 18, 101029. https://doi.org/10.1016/j.bcab.2019.101029

6th International Conference and
Postgraduate Colloquium for
Environmental Research 2022 (POCER
2022) 9 - 11 June 2022
Langkawi, Kedah, Malaysia

PCR04042022 – 82: Towards the Enhancement of Microalgae Cultivation as Biofertilizer for Sustainable Agriculture

Zahidah Ab Razak[a,b], Rosazlin Abdullah[a, b], Ling Tau Chuan[a], Pau Loke Show[c], Aaronn Avit Ajeng[a], Jamilah Syafawati Yaacob[a,b] and Salmah Ismail[a]

[a] Institute of Biological Sciences, Faculty of Science, Universiti Malaya,
50603 Kuala Lumpur, Malaysia
[b] Centre for Research in Biotechnology for Agriculture (CEBAR), Institute of Biological Sciences, Faculty of Science, Universiti Malaya, 50603 Kuala Lumpur, Malaysia
[c] Department of Chemical and Environmental Engineering, Faculty of Science and Engineering, University of Nottingham Malaysia, 43500 Semenyih, Malaysia

*Corrensponding Author E-mail: rosazlin@um.edu.my

Keywords: *Sustainable; Biofertilizers; Biochar; Phytohormones; Soil Fertility; Crop Productivity*

Extended Abstract

To address the present trend of pesticide and fertilizer reduction, modern agriculture requires appropriate solutions. One of the possible levers to promote this transformation is the usage of bioproducts that are less harmful to human health and more environmentally friendly. Biofertilizers are gaining attention in sustainable agriculture as a technique of increasing crop output while lowering the polluting impacts of synthetic fertilizers in an environmentally friendly and economically viable way (Renuka et al., 2018; Nosheen et al., 2021). Among the numerous forms of biofertilizers, formulations based on photosynthetic organisms, such as eukaryotic microalgae and cyanobacteria, are gaining popularity due to their important benefits, notably to soil fertility management and crop production enhancement (Guo et al., 2020). Microalgae are the most distinctive organisms on the earth, with potential applications such as agricultural applications as biofertilizers and soil conditioning agents for improving soil fertility and plant productivity (Chapman, 2013, Duarteet al., 2018). Besides, microalgae also can produce plant growth hormones, polysaccharides, antibacterial compounds, and other metabolites (Ronga et al. 2019). Co-culture of algae with other microorganisms (such as bacteria or fungi) has been proposed to improve the efficacy of microalgae as biofertilizers (Leng et al., 2021, Prosenc et al., 2021). To elevate the formulation, biochar can be added to the system to promote microbe

immobilisation as shown in Figure 1. Biochar is a carbonaceous material created by the thermo-chemical conversion of biomass under low oxygen conditions (Wang et al., 2021). Biochar has a high porosity and biocompatibility, which can provide a growth matrix for microorganisms and improve their biodegradability (Ouyang et al., 2021). Based on its unique features, biochar can be utilized as a microalgae immobiliser via simple ionic interactions or by attracting algal cells to micronutrient domains on the charcoal surface. Because the biochar particle size is substantially larger than the algal cell particle size, the biochar anchored algal cells may be easily removed from the growing media by filtration. Algae will enrich the biochar carrier with useful organic volatiles such as lipids, improving the combustion parameters of the algae-biochar slurry fuel. However, to our knowledge, little research on the combination application of microorganisms and biochar with microalgae as biofertilizers has been published. Aside from that, a thorough understanding of microalgae-biochar-microbe interactions is an essential component of biological research, which may be analyzed using phytohormones production analysis. From a systematic perspective, this review not only presents an effective and proper environmentally friendly bio-based fertiliser from microlagae for pollution-free agricultural applications to boost soil fertility and crop productivity, but also dicover the mechanisms of phytohormones production that are related to plant growth.

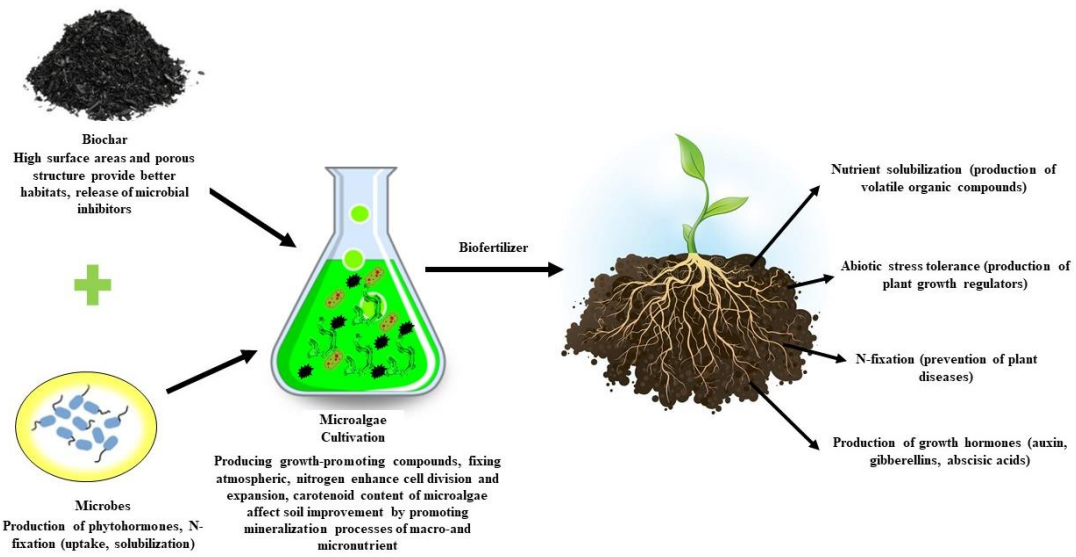

Figure 1: Schematic illustrations for microalgae cultivated with biochar and microbes and their benefits.

Acknowledgements: The authors would like to thank the Institute of Biological Sciences, Faculty of Science, University of Malaya for providing research facilities.

References

Renuka, N., Guldhe, A., Prasanna, R., Singh, P., and Bux, F., 2018. Microalgae as Multi-Functional Options in Modern Agriculture: Current Trends, Prospects and Challenges. *Biotechnology Advances*. 36: 1255–1273.

Nosheen, S., Ajmal, I., and Song, Y., 2021. Microbes as Biofertilizers, a Potential Approach for Sustainable Crop Production. *Sustainability*. 13: 1-20.

Gou, J.Y., Suo, S.Z., and Shao, K.Z., 2020. Biofertilizers with Beneficial Rhizobacteria Improved Plant Growth and Yield in Chili (*Capsicum annuum* L.). *World Journal of Microbiology and Biotechnology*. 36(86).

Wang, J., Shi, L., Zhai, L., Zhang, H., Wang, S., Zou, J., Shen, Z., Lian, C., and Chen, Y., 2021. **Analysis of the Long-Term Effectiveness of Biochar Immobilization Remediation on Heavy Metal Contaminated Soil and The Potential Environmental Factors Weakening the Remediation Effect: A Review.** *Ecotoxicology and Environmental Safety*. 207: 111261.

Ouyang, X., Yin, H., Yu, X., Guo, Z., Zhu, M., Lu, G., and Dang, Z., 2021. Enhanced Bioremediation of 2,3′,4,4′,5-Pentachlorodiphenyl by Consortium GYB1 Immobilized on Sodium Alginate-Biochar. *Science of the Total Environment*. 788: 147774.

Leng, L., Li, W., Jie Chen, S., Leng, J., Chen, L., Wei, H., Peng, J., Li, W., Zhou, H., 2021. **Co-Culture of Fungi-Microalgae Consortium for Wastewater Treatment: A Review.** *Bioresource Technology*. 330: 125008.

Prosenc, F., Piechocka, J., Škufca, D., Heath, E.,Griessler Bulc, T., Istenič, D., Buttiglieri, G., 2021. **Microalgae-based Removal Of Contaminants of Emerging Concern: Mechanisms in *Chlorella Vulgaris* and Mixed Algal-Bacterial Cultures.** *Journal of Hazardous Materials*. 418: 126284.

Chapman, R.L., 2013. **Algae: The World's Most Important "Plants"- An Introduction**. *Mitigation and Adaptation Strategies for Global Change.* 18: 5-12.

Duarte, I., Hernández, S., Ibañez, A., and Canto, A., 2018. **Macroalgae as Soil Conditioners or Growth Promoters of *Pisum sativum (L).*** *Annual Research & Review Biology*. 27: 1-8.

Ronga, D., Biazzi, E., Parati, K., Carminati, D., Carminati, E., and Tava, A., 2019. Microalgal Biostimulants and Biofertilisers in Crop Productions. *Agronomy.* 9:192.

6th International Conference and
Postgraduate Colloquium for
Environmental Research 2022 (POCER
2022) 9 - 11 June 2022
Langkawi, Kedah, Malaysia

PCR05042022 – 83: Investigation of nondamaging mud filtration properties in high-pressure, high-temperature conditions

Imtiaz Ali[a,b], Maqsood Ahmad[c]

[a] Department of Petroleum Engineering, Universiti Teknologi PETRONAS, 32610, Seri Iskandar, Perak, Malaysia

[b]Department of Petroleum and Gas Engineering, BUITEMS, Pakistan.

[c]Department of Geosciences, Universiti Teknologi PETRONAS, 32610, Seri Iskandar, Perak, Malaysia

- Corrensponsing Author E-mail: imtiaz_17003333@utp.edu.my

Keywords: Nondamaging mud, modified starch, filtration characterisitics, filter cake.

Extended Abstract

In overbalanced drilling conditions, the mud filtrate and tiny solid particles invade the porous and permeable strata during drilling. This fluid intrusion develops solids on the borehole wall called filter cake. The filtrate amount and filter cake thickness are the two key parameters that must be minimized during drilling a wellbore. The increase in the wellbore depth also increases the wellbore temperature and pressure, further boosting this process. Various natural and synthetic materials have been tested to reduce filtrate loss and filter cake thickness in high-pressure, high-temperature conditions. The critical challenge for the biopolymers is their low thermal stability, which initiates further problems. Since the environmental agencies have great concern about the disposal of substantial chemical quantities which demand the drilling industry to use degradable and eco-friendly additives.

Various agro and waste materials have been tested in water-based mud formulations to control fluid loss with superior performance. These materials include but are not limited to rice husk, date seeds, powdered grass, grass ash, soybean peel powder, coconut shells, potato peel powder, mandarin peels powder, detarium microcarpum, and brachystegia Eurycoma, hydrated basil seed (Agwu et al., 2019; Al-Hameedi et al., 2020a; Al-Hameedi et al., 2020b; Gao et al., 2021; Nwabueze and Ighalo, 2020; Okon et al., 2020).

Similarly, starch has also been used as a filtrate loss control agent and rheology modifier in the petroleum industry. It is considered the second most biopolymer after cellulose which has almost zero

impact on the environment. Numerous researchers have examined its performance at API and HPHT conditions for filtrate loss control. Various starches, including corn, cassava, banana, and potato have been tested in mud formulations under different applied conditions (Dankwa et al., 2018; Ghazali et al., 2015; Jimoh et al., 2020). Starch can significantly control the fluid loss volume when added to the bentonite mud blends. Owing to its least thermal stability and bacterial attach susceptibility, the efficiency declines, particularly in high-temperature conditions. Furthermore, the environmental agencies have concerns about the disposal of ample chemical quantities, which require the drilling industry to use eco-friendly alternatives.

In this work, the performance of modified starch has been evaluated by formulating a nondamaging water-based mud. The modified starch was added in a dosage of 0-7g. In addition, the API filtration characteristics were determined using an API filter press. Moreover, the samples were aged for 16 hours in a hot roll oven at 250 °F. The filtrate volume and filter cake thinness were measured after 30 minutes of static filtration.

The experimental findings revealed that modified starch with 6.5 g reduced the filtrate volume by producing 13.7 mL filtrate volume after 16 hours of hot rolling. Similarly, the filter cake thickness was also reduced with the increase in modified starch concentration. This work shows that the current formulation can replace bentonite with soluble materials, which can reduce the formation damage and other consequences associated with the excess filtrate loss. Figure 13 shows the filtration results. The filtrate volume after 16 hours of aging is still acceptable. Likewise, the filter cake thickness of the sample containing 6.5 grams of modified starch showed the least cake thickness.

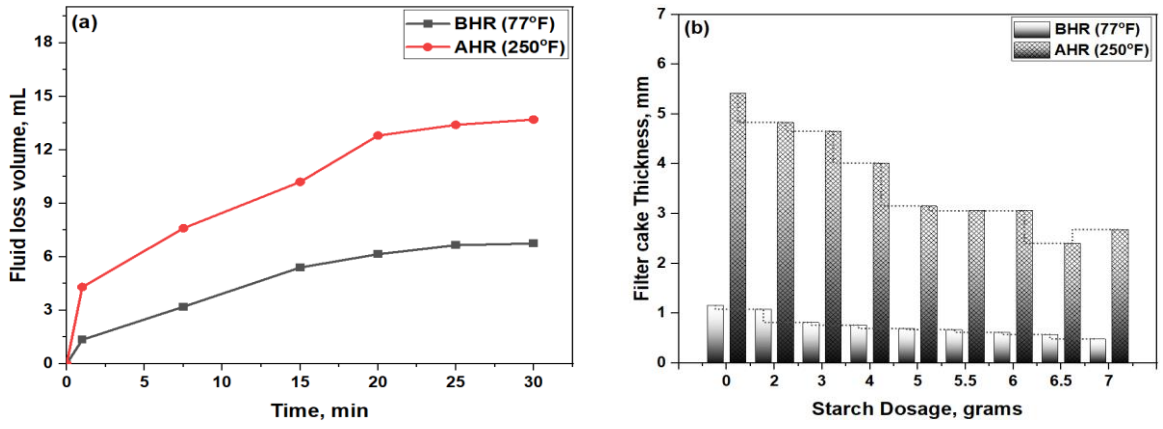

Figure 13: (a) Mud filtrate loss volume and (b) filter cake thickness

Acknowledgements: The authors thank the Ministry of Higher Education (MOHE) Malaysia for providing the financial support under grant No. FRGS/1/2020/TK0/UTP/02/3 and Universiti Teknologi PETRONAS for providing the required facilities.

References

Agwu, O.E., Akpabio, J.U. and Archibong, G.W., 2019. Rice husk and saw dust as filter loss control agents for water-based muds. Heliyon, 5(7): e02059.

Al-Hameedi, A.T. et al., 2020a. Proposing a new biodegradable thinner and fluid loss control agent for water-based drilling fluid applications. International Journal of Environmental Science and Technology, 17(8): 3621-3632.

Al-Hameedi, A.T.T. et al., 2020b. Experimental investigation of environmentally friendly drilling fluid additives (mandarin peels powder) to substitute the conventional chemicals used in water-based drilling fluid. Journal of Petroleum Exploration and Production Technology, 10(2): 407-417.

Dankwa, O., Appau, P.O. and Tampuri, M., 2018. Performance evaluation of local cassava starch flour as a secondary viscosifier and fluid loss agent in water based drilling mud. Ghana Mining Journal, 18(2): 68-76.

Gao, X. et al., 2021. Application of sustainable basil seed as an eco-friendly multifunctional additive for water-based drilling fluids. Petroleum Science.

Ghazali, N.A., Alias, N.H., Mohd, T., Adeib, S. and Noorsuhana, M., 2015. Potential of corn starch as fluid loss control agent in drilling mud, Applied Mechanics and Materials. Trans Tech Publ, pp. 682-687.

Jimoh, M.O., Salawudeen, T.O., Arinkoola, A.O. and Daramola, M.O., 2020. Rheological study of a new water-based drilling fluid using Ubakala clay in the presence of natural polymers. Chemical Engineering Communications.

Nwabueze, Q.A. and Ighalo, J.O., 2020. Utilisation of Sweet Potato (Ipomoe batatas) and Rice Husk (Oryza sativa) Starch Blend as a Secondary Viscosifier and Fluid Loss Control Agent in Water-based Drilling Mud. Petroleum & Coal, 62(4).

Okon, A.N., Akpabio, J.U. and Tugwell, K.W., 2020. Evaluating the locally sourced materials as fluid loss control additives in water-based drilling fluid. Heliyon, 6(5): e04091.

PCR06042022 – 84: Adhesion of Bacillus consortium on Sago Starch-Oil Palm Kernel Shell Biochar as Soil Organic Amendment: Optimization and Kinetic Analysis

Aaronn Avit Ajeng[a*] , Rosazlin Abdullah[a,b], and Ling Tau Chuan[a]

a Institute of Biological Sciences, Faculty of Science,
University of Malaya. 50603 Kuala Lumpur, Malaysia.

b Centre for Research in Biotechnology for Agriculture (CEBAR),
Institute if Biological Sciences, Faculty of Science, University of Malaya. 50603 Kuala Lumpur, Malaysia.

• Corrensponding Author E-mail: aaronnavit@um.edu.my

Keywords: Optimization, Bacillus,Adhesion, Modelling, Organic Amendment, Biopolymer

Extended Abstract

Biochar is a carbonaceous and porous material derived from the thermal decomposition processes of biomass under limited to no oxygen (Lehman and Joseph, 2015). In a number of biotechnological fields, biochar is employed as a microbe carrier. Researchers are intrigued by the physicochemical properties of this carbonaceous material, as well as its microenvironment, which may potentially house microorganisms (Ajeng et al., 2020, Ajeng et al., 2021). The formation of bacterial biofilm on biomaterials is not desirable in most of application particularly in the medical and food industries due to the prevalence of antimicrobial resistance (Thallinger et al., 2013). However, in the production of organic amendments and biofertilizers for crop application, bacterial biofilm formation provides a revolutionary technique since it promotes the survival of plant probiotics such as Plant Growth Promoting *Rhizobacteria* (PGPR) (Backer et al., 2018). Because of the widespread interest in the use of biochar as a microbe carrier, this work sets out to develop an organic amendment based on the use of oil palm kernel shell biochar (OPKSB) as a carrier for effective PGPR consortia consisting of *Bacillus salmalaya* 139SI, *Bacillus amyloliquefaciens D203 and Bacillus cereus ATCC 14579*. The influence of operating parameters (temperature, pH, agitation speed, and sago starch as co-carbon source concentration) on *Bacillus* consortium survival on oil palm kernel shell biochar (OPKSB) was investigated using response surface methodology (RSM) analysis. After the optimization, in a batch experiment, the adhesion behaviour of the consortium on optimized organic formulation was investigated using different adhesion kinetic models and isotherms. The Bacillus consortium's adhesion to the sago starch – OPKSB (SOPKSB) was accurately explained by the pseudo-second-order kinetics model ($R2 > 0.99$). After 80 minutes, the bacteria consortium attained adhesion equilibrium on SOPKSB biochar with a cell concentration of 108 CFU/g. The result fits within the Langmuir isotherm

suggesting that cells could be reversibly adhered during the initial adhesion process to the heterogeneous surface of SOPKSB. Because effective probiotics may be able to promote crop development with low fertiliser inputs, the developed organic amendment will set out to be a sustainable solution in greening the agricultural sector.

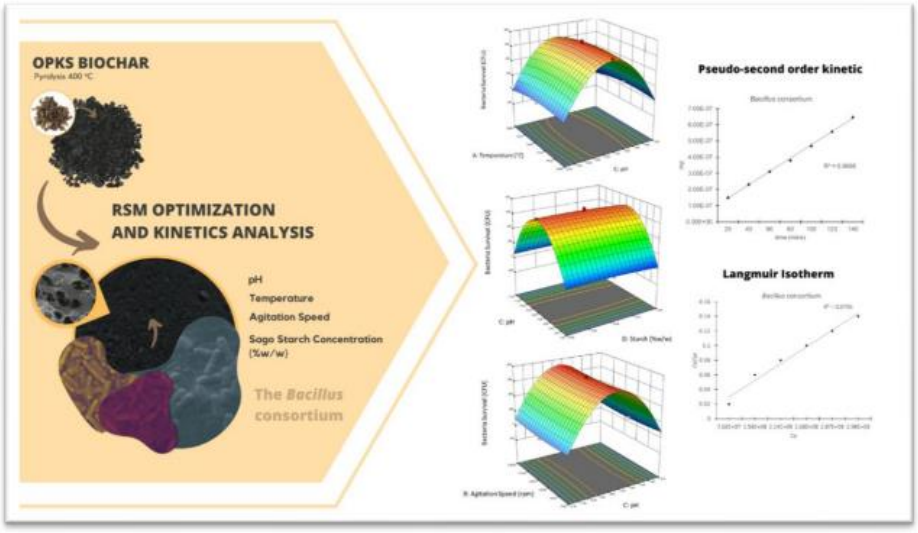

Figure 1: A Graphical abstract.

Acknowledgements: The authors would like to acknowledge the technical and financial support from Universiti Malaya Impact-Oriented Interdisciplinary Research Grant (IIRG) (grant number IIRG004-19IISS).

References

Ajeng, A. A., Abdullah, R., Ling, T. C., Ismail, S., Lau, B. F., Ong, H. C., ... & Chang, J. S. (2020). Bioformulation of biochar as a potential inoculant carrier for sustainable agriculture. Environmental Technology & Innovation, 20, 101168.

Ajeng, A. A., Abdullah, R., Ling, T. C., & Ismail, S. (2022). Adhesion of Bacillus salmalaya and Bacillus amyloliquefaciens on oil palm kernel shell biochar: A physicochemical approach. Journal of Environmental Chemical Engineering, 10(1), 107115.

Backer, R., Rokem, J. S., Ilangumaran, G., Lamont, J., Praslickova, D., Ricci, E., ... & Smith, D. L. (2018). Plant growth-promoting rhizobacteria: context, mechanisms of action, and roadmap to commercialization of biostimulants for sustainable agriculture. Frontiers in plant science, 1473.

Thallinger, B., Prasetyo, E. N., Nyanhongo, G. S., & Guebitz, G. M. (2013). Antimicrobial enzymes: an emerging strategy to fight microbes and microbial biofilms. Biotechnology journal, 8(1), 97- 109.

Lehmann, J., & Joseph, S. (Eds.). (2015). Biochar for environmental management: science, technology and implementation. Routledge.

PCR06042022 – 85: The Influence of Biochar on Plant-Soil Metabolites in Shaping the Rhizosphere

Rosazlin Abdullah[a,b*], Aaronn Avit Ajeng[a], and Ling Tau Chuan[a]

[a] Institute of Biological Sciences, Faculty of Science, University of Malaya. 50603 Kuala Lumpur, Malaysia.

[b] Centre for Research in Biotechnology for Agriculture (CEBAR), Institute if Biological Sciences, Faculty of Science, University of Malaya. 50603 Kuala Lumpur, Malaysia.

- Corrensponding Author E-mail: rosazlin@um.edu.my

Keywords: Biochar, Metabolomics, Plant-Soil Interaction, Microbiome

Extended Abstract

Microorganisms in the soil play an important role in nutrient cycling, carbon sequestration, fertility management, and crop health and productivity (Dai et al., 2021). Microorganism reactions to biochar addition, such as the microbial activity, diversity, community structure, and nutrient cycle mechanisms, have been widely described to date. However, there is no summary of the links between soil microbial groups particularly the rhizobacteria and biochar amendment especially on the metabolites production by the plants and microbial communities that help shaping the rhizosphere. Biochar influences soil microbial growth, diversity, and community compositions by directly supplying growth boosters for soil biota or indirectly affecting soil basic characteristics, according to the findings of this review. The porous structure, labile C, high pH, and electrochemical properties of biochar all play a role in determining soil microbial abundance and communities, as well as their mediated N and P cycling processes (Thomas et al., 2015, Yin et al., 2021). Soil amendment using biochar is one of the eco-friendly solutions for controlling and managing a variety of pests and harmful diseases in crops. Biochar not only improves soil fertility and health, but it also promotes systemic resistance to foliar and soil-borne plant diseases. Plant protein processing in the endoplasmic reticulum, plant-pathogen interaction, metabolic pathways, hormone signal transduction, phenylpropanoid/flavonoid biosynthesis, and photosynthesis were all activated by biochar application are among the metabolites that can be quickly absorbed by biochar (Zhu et al., 2021). However, when compared to activated carbon, biochar adsorbs

fewer of these metabolic precursors quantitatively. Biochar treatment is less disruptive than activated carbon throughout metabolism, according to an analysis of important chemicals in the tricarboxylic acid cycle and glycolysis (Hill et al. 2019). Hill et al., (2019) 's research demonstrates that biochar may be used as a beneficial soil additive while reducing bacterial viability. In addition, the investigations indicate how biochar might affect certain bacterial metabolic pathways and provide a basis for biochar's efficiency in soil conditioning. Certain polycyclic aromatic hydrocarbon (PAH) degraders are also enhanced by biochar amendment and the rhizosphere, and their combination encouraged PAH degrader cooperation (Li et al., 2020). Simultaneously, the functional genes involved in upstream PAH degradation were dramatically increased by the combined impacts of biochar and the rhizosphere. Second, there were significant co-occurrences between members of the soil microbial community and metabolites, with several PAH degraders and metabolites, such as PAH degradation products or shared carbon supplies, being emphasised in the networks. It demonstrates that the combined impacts of biochar and plant roots significantly increased the total downstream carbon metabolism of PAH breakdown, indicating good soil microbiome survival and contributing to PAH biodegradation. The combined effects of biochar and plant roots are anticipated to modify both soil carbon metabolism and direct pollutant biodegradation, benefiting PAH breakdown via soil microbiota.

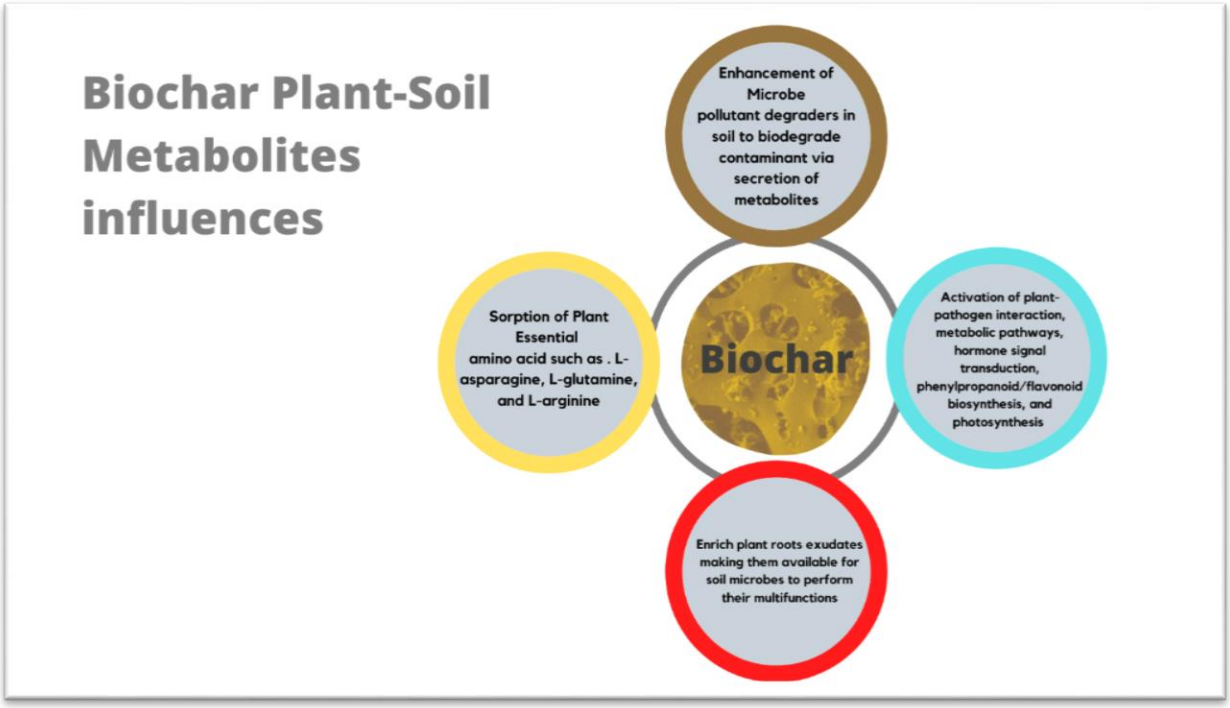

Figure 14: The plant-soil metabolites influences following biochar amendment.

Acknowledgements: The authors would like to acknowledge the technical and financial support from Universiti Malaya Impact-Oriented Interdisciplinary Research Grant (IIRG) (grant number IIRG004-19IISS).

References

Dai, Z., Xiong, X., Zhu, H., Xu, H., Leng, P., Li, J., ... & Xu, J. (2021). Association of biochar properties with changes in soil bacterial, fungal and fauna communities and nutrient cycling processes. *Biochar*, 3(3), 239-254.

Hill, R. A., Hunt, J., Sanders, E., Tran, M., Burk, G. A., Mlsna, T. E., & Fitzkee, N. C. (2019). Effect of biochar on microbial growth: a metabolomics and bacteriological investigation in E. coli. *Environmental science & technology*, *53*(5), 2635-2646.

Joseph, S., Husson, O., Graber, E. R., Van Zwieten, L., Taherymoosavi, S., Thomas, T., ... & Donne, S. (2015). The electrochemical properties of biochars and how they affect soil redox properties and processes. *Agronomy*, *5*(3), 322-340.

Li, X., Song, Y., Bian, Y., Gu, C., Yang, X., Wang, F., & Jiang, X. (2020). Insights into the mechanisms underlying efficient Rhizodegradation of PAHs in biochar-amended soil: from microbial communities to soil metabolomics. *Environment International*, *144*, 105995.

Yin, D., Li, H., Wang, H., Guo, X., Wang, Z., Lv, Y., ... & Lan, Y. (2021). Impact of different biochars on microbial community structure in the rhizospheric soil of rice grown in albic soil. *Molecules*, *26*(16), 4783.

Zhu, Q., Chen, L., Chen, T., Xu, Q., He, T., Wang, Y., ... & Jin, A. (2021). Integrated transcriptome and metabolome analyses of biochar-induced pathways in response to Fusarium wilt infestation in pepper. *Genomics*, *113*(4), 2085-2095.

6th International Conference and
Postgraduate Colloquium for
Environmental Research 2022 (POCER
2022) 9 - 11 June 2022
Langkawi, Kedah, Malaysia

PCR06042022 – 86: A Review on the Life Cycle Assessment of Different Advanced Wastewater Treatment Systems

Najwa Alia A'adil Bohara[a], Zainura Zainon Noor[a,b*], and Azmi Aris[b,c]

[a] School of Chemical and Energy Engineering, Faculty of Engineering,
Universiti Teknologi Malaysia, Skudai, Johor

[b] **Centre for Environmental Sustainability and Water Security (IPASA),**
Universiti Teknologi Malaysia, Skudai, Johor

[c] School of Civil Engineering, Faculty of Engineering,
Universiti Teknologi Malaysia, Skudai, Johor

- Corrensponsing Author E-mail: najwaalia0205@gmail.com

Keywords: Life Cycle Assessment, Advanced Treatment, Wastewater Treatment, Ozonation, Granular Activated Carbon, Photo-Fenton

Extended Abstract

Due to recent environmental and health concerns about the amount of wastewaters and effluents, as well as its downsides, new and advanced treatment technologies have been developed. It is indeed necessary for environmental and economic stability, but it is also influenced by social, political, and environmental factors. Advanced wastewater treatment (AWT) systems are currently being studied as a way to target urban micropollutants (MPs) before they are discharged into receiving water bodies and to meet specified reuse criteria. Nonetheless, the negative contributions of these technologies must be minimised so that the solution to the initial problem does not lead to additional environmental impacts, and a tool suitable for this interpretation is the life cycle assessment (LCA), which takes into account the entire life cycle of these processes. Using the Life Cycle Assessment framework, this study assesses net environmental efficiencies for three AWTs (i) ozonation systems (air-fed and pure oxygen-fed), (ii) photo-fenton, and (iii) granular activated carbon. This review was also conducted to provide information about the above well-established advanced wastewater treatment systems.

1. Introduction

Urban wastewater treatment plants (UWWTPs) enable the reuse or return of water to ecosystems, making it significant contributors in wastewater management sustainability. The goal of UWWTPs is to improve the quality of effluents that are generally discharged to water bodies, hence lowering their environmental impact (J. Pesqueira, Marugan, Pereira, & Silva, 2022). Nonetheless, according to the 2018 European Waters Assessment, atmospheric deposition and effluent discharge from UWWTPs are the primary causes of poor chemical quality in surface waters. UWWTPs are still a major source of water pollution since various chemicals from industrial or domestic usage will unavoidably enter the sewage system and be directed to UWWTPs, where they will be discharged to surface waters if the treatment does not eliminate them (J. F. J. R. Pesqueira, Pereira, & Silva, 2020).

A proven way to address this issue is by incorporating advanced wastewater treatment such as (i) ozonation systems, (ii) photo-fenton, and (iii) granular activated carbon is a proven technique to handle this issue. Technology selection takes into account not only efficiency, but also environmental, social, and economic factors. To avoid problem shifting, when the goal is to lessen an impact from an environmental aspect, attention must be taken to ensure that the solution contributes the least to other environmental issues (J. Pesqueira, Pereira, & Silva, 2021). Environmental sustainability is important because the goal of these technologies is to reduce environmental impact; therefore, it is necessary to ensure that we are contributing minimally to other impacts and avoiding issue shifting. The life cycle assessment (LCA) tool can be used to examine potential environmental impacts, considering all phases from resource extraction to manufacture, usage, end of life, recycling, and final deposition (J. Pesqueira et al., 2022).

2. Life Cycle Assessment Methodology

The goal of LCA, which determines the possible environmental impacts of these systems on individuals and resources, as well as the resulting emissions throughout time starting from all phases since resource extraction, production, use, end of life, recycling and final deposition). Its "cradle-to-grave" method prevents environmental problems from being transferred from one stage of the life cycle to the next.

As a result, it can be used to help decision-makers establish objectives and reformulate projects and policies, as well as improve environmental performance. The goal of this study was to evaluate and compare the environmental impacts of three promising AWT systems that targeted wastewater over their entire life cycle by identifying their primary environmental hotspots (Risch, Jaumaux, Maeseele, & Choubert, 2022).

3. LCA on Advanced Wastewater Treatment Systems

According to (Risch et al., 2022), on the ecosystem's quality objective, air-fed ozone and GAC are superior AWT alternatives than oxygen-fed ozone under the specific operating conditions in this study (using a French electricity mix). Air-fed ozone is by far the greatest AWT option for human health, followed by GAC and finally pure oxygen-fed ozone. However, these findings must be carefully evaluated and combined with information of local water quality issues to create an understanding of regionally distributed life cycle implications.

A review from (Foteinis, Monteagudo, Durán, & Chatzisymeon, 2018) and (Ioannou-Ttofa, Foteinis, Chatzisymeon, Michael-Kordatou, & Fatta-Kassinos, 2017) stated that, the impact of energy use for the ozonation process accounts for 28% of the overall impact, while it accounts for only 8% for the photo Fenton. The energy required to mix the system in the photo-Fenton process (CPC) is three times less than that required to produce O3 from O2. Given the area's strong solar irradiation, the environmental implications of energy demand could be reduced if the energy supply was switched from the current grid to a photovoltaic source (Arzate, Pfister, Oberschelp, & Sanchez-Perez, 2019).

Rahman et al. (2018) compared reverse osmosis, ozonation, and granular activated carbon and discovered that the latter had low toxicity and one of the lowest impacts on the global warming potential (GWP), ozone depletion potential (ODP), and acidification potential (AP) categories due to its low energy consumption (Rahman, Eckelman, Onnis-Hayden, & Gu, 2018). In contrast, when granular activated carbon was compared to ozonation and reverse osmosis, Li et al. (2019) discovered that granular activated carbon performed the worst in the categories of ecotoxicity and human toxicity cancer, due to its low percentage removal of micro pollutants (Li et al., 2019)

4. Conclusions

Finally, it can be stated that energy and chemical production were the primary stages responsible for the majority of environmental impacts. As a result, it is critical to find alternatives to the used reagents or their production methods, as well as to invest in cleaner energy sources. This fact also emphasises the importance of keeping in mind that results are heavily influenced by local conditions, such as the energy mix. It should also be noted that LCA is a powerful decision-making tool that provides a complete overview of the environmental impacts. Decisions, however, must be based on a balance of environmental sustainability, cost, time, available resources, social impacts, and other influential factors.

References

Arzate, S., Pfister, S., Oberschelp, C., & Sanchez-Perez, J. A. (2019). Environmental impacts of an advanced oxidation process as tertiary treatment in a wastewater treatment plant. *Sci Total Environ, 694*, 133572. doi:10.1016/j.scitotenv.2019.07.378

Foteinis, S., Monteagudo, J. M., Durán, A., & Chatzisymeon, E. (2018). Environmental sustainability of the solar photo-Fenton process for wastewater treatment and pharmaceuticals mineralization at semi-industrial scale. *Science of The Total Environment, 612*, 605-612. doi:https://doi.org/10.1016/j.scitotenv.2017.08.277

Ioannou-Ttofa, L., Foteinis, S., Chatzisymeon, E., Michael-Kordatou, I., & Fatta-Kassinos, D. (2017). Life cycle assessment of solar-driven oxidation as a polishing step of secondary-treated urban effluents. *Journal of Chemical Technology & Biotechnology, 92*(6), 1315-1327. doi:https://doi.org/10.1002/jctb.5126

Li, Y., Zhang, S., Zhang, W., Xiong, W., Ye, Q., Hou, X., . . . Wang, P. (2019). Life cycle assessment of advanced wastewater treatment processes: Involving 126 pharmaceuticals and personal care products in life cycle inventory. *Journal of Environmental Management, 238*, 442-450. doi:https://doi.org/10.1016/j.jenvman.2019.01.118

Pesqueira, J., Marugan, J., Pereira, M. F. R., & Silva, A. M. T. (2022). Selecting the most environmentally friendly oxidant for UVC degradation of micropollutants in urban wastewater by assessing life cycle impacts: Hydrogen peroxide, peroxymonosulfate or persulfate? *Sci Total Environ, 808*, 152050. doi:10.1016/j.scitotenv.2021.152050

Pesqueira, J., Pereira, M. F. R., & Silva, A. M. T. (2021). A life cycle assessment of solar-based treatments (H2O2, TiO2 photocatalysis, circumneutral photo-Fenton) for the removal of organic micropollutants. *Sci Total Environ, 761*, 143258. doi:10.1016/j.scitotenv.2020.143258

Pesqueira, J. F. J. R., Pereira, M. F. R., & Silva, A. M. T. (2020). Environmental impact assessment of advanced urban wastewater treatment technologies for the removal of priority substances and contaminants of emerging concern: A review. *Journal of Cleaner Production, 261*, 121078. doi:10.1016/j.jclepro.2020.121078

Rahman, S. M., Eckelman, M. J., Onnis-Hayden, A., & Gu, A. Z. (2018). Comparative Life Cycle Assessment of Advanced Wastewater Treatment Processes for Removal of Chemicals of Emerging Concern. *Environmental Science & Technology, 52*(19), 11346-11358. doi:10.1021/acs.est.8b00036

Risch, E., Jaumaux, L., Maeseele, C., & Choubert, J. M. (2022). Comparative Life Cycle Assessment of two advanced treatment steps for wastewater micropollutants: How to determine whole-system environmental benefits? *Sci Total Environ, 805*, 150300. doi:10.1016/j.scitotenv.2021.150300

6th International Conference and Postgraduate Colloquium for Environmental Research 2022 (POCER 2022) 9 - 11 June 2022
Langkawi, Kedah, Malaysia

PCR06042022 – 87: Activated carbon monoliths, from eucalyptus and patula pine biomass and their mixtures with residual tires and polystyrene, for CO_2 capture

Siby I. Garces Polo[a*], Gabriel de Jesús Camargo Vargas[b], Rafael Nikolay Agudelo Valencia[b], Liliana Giraldo Gutiérrez[c] and Juan Carlos Moreno Piraján[d], Jenny Paola Rodríguez[d]

[a] Faculty of Engineering
Universidad Libre, Barranquilla, Colombia

[b] Faculty of Engineering
Universidad Libre, Bogotá, Colombia

[c] Department of Chemistry
Universidad Nacional de Colombia, Bogotá, Colombia

[d] Department of Chemistry
Universidad de los Andes, Bogotá, Colombia

- Corresponding Author E-mail: siby.garces@unilibre.edu.co

Keywords: CO_2 adsorption; Activated Carbon; monoliths adsorbent. biomass

Extended Abstract

The increasing emissions of gaseous pollutants of anthropogenic origin, such as carbon dioxide (CO_2), which causes global warming, have promoted a great interest in developing and improving processes that allow their elimination. The Intergovernmental Panel on Climate Change (IPCC) has considered the capture and storage of CO_2 as an option within mitigation strategies for stabilizing the concentration of greenhouse gases in the atmosphere (IPCC, 2005). In this sense, CO_2 adsorption is the initial stage of this capture process, and the development of porous solid materials with high adsorption capacity has been the focus of the study.

This work explored the obtaining of monoliths of activated carbons prepared by chemical activation of biochar derived from lignocellulosic residues of patula pine and eucalyptus seeds. The preparation of carbonaceous materials from used tires, crushed and oxidized with nitric acid was also studied. The

preparation of carbonaceous materials from used tires oxidized with nitric acid was also studied. Thermogravimetric analysis characterized the starting solids and activated carbons by nitrogen adsorption-desorption isotherms, FTIR spectroscopy, Raman spectroscopy, and potentiometric titration. Subsequently, they were used as powders to obtain monoliths by the technique of uniaxial compaction and different binding agents such as starch, carboxymethylcellulose, polyvinyl alcohol, and montmorillonite.

In the monolith preparation tests, better results were found in terms of mechanical properties obtained through the use of montmorillonite as a binding material. From the physical-chemical characterization analyses in the proximate analysis, it was found that the percentage of volatile matter for the prepared samples ranges between 7,766 and 12.48 and the percentage of fixed carbon between 76.55 and 91.04, evidencing the effect on the pre-degradation of the biopolymers containing the lignocellulosic residues in the impregnation stage. Regarding the textural characteristics of the activated carbons, Figure 1 presents the N_2 adsorption isotherms obtained, which are type I(b), for the solids, PP-P50-450 and ES-P50-450 from the lignocellulosic residues patula pine and eucalyptus seed, respectively.

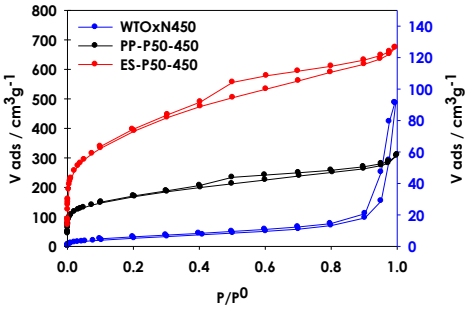

Figure 1. N2 Isotherm

Table 1 shows a summary of the textural characteristics of the three materials

Table 1. Textural characteristics of activated carbons

Sample	BET		DA ($P/P^0 < 0.1$)				QSDFT (P/P^0 10^{-5}-1)	
	S_{BET} [m^2/g]	C	Vmic [cm^3/g]	Eo [kJ/mol]	n	Ancho de Poro [nm]	V_P [cm^3/g]	Average Pore Width [nm]
ES-P50-450	1398	143	0,466	5,516	2,10	1,580	0,950	0,926
PP-P50-450	602	234	0,229	5,823	1,70	1,540	0,413	1,701
WTOxN450	20.1	52.2	0,005	4,606	2,00	1,680	0,072	27,04

The differences in textural characteristics found between activated carbons show the effect of the precursor material on the final properties of the solid. As for the solid obtained from tires, WTOxN450, no values of the high textural parameters are observed, evidencing the low attack of both chemical and thermal treatment. On the other hand, for the activated carbons ES-P50-450 and PP-P50-450 a contribution of porosity with structure with dimensions between 0.7 to 2.0 nm and a small contribution of pores of greater dimension between 2 and 8 nm, which allows evidence of the presence of mesoporous structures in the porous network of the prepared solids. About the WTOxN450 sample, a Pore Size Distribution (PSD) is observed with a small contribution of microporous structure with diameters close to 2 nm, and wide distribution of porous structures between 4 and 30 nm, ratifying the non-activation of the inner surface of the solid.

The results of IR spectroscopy show the presence of characteristic peaks for carbonaceous solids, associated with functional groups such as alcohols and carboxylic acids. The presence of different low-intensity bands around 2950-2800 cm-1 in the spectra of solids ES-P50-450 and PP-P50-450 suggests the existence of $-CH_3$ or $-CH_2-$ structures of aliphatic species. At 2908 cm^{-1} there is a band associated with carboxylic acid groups, carbonyls, and chemisorbed water, these bands are not observed for the solid WTOxN450. The band between 1300-1000 cm^{-1} is assigned to structures such as ethers, epoxides, and phenols, also only present in solids from lignocellulosic residues. Raman spectra showed scattering for the prepared activated carbons. As the solids are of lignocellulosic origin, after chemical and thermal treatment the presence of graphene structures was observed. Activated carbons from patula pine and eucalyptus seeds show great potential to be applied as adsorbents, so in this work, these materials were used in the adsorption of CO_2 at high pressures (up to 4.5 MPa) and low temperatures (<50 °C) where it was shown that adsorption capacity is favored, which suggests the potential use of these materials in CO_2 capture technologies such as pre-combustion processes (Garcés, 2016).

Acknowledgments: The authors thank la Universidad Libre and Universidad de Los Andes for the support of experimental research

References

Garcés (2016). Elimination and recovery of CO_2 present in gaseous effluents through adsorption and dry reforming of methane. Doctoral thesis, Universidad Pública de Navarra, España.

IPCC (2005). In B. Metz, O. Davidson. H. C. De Coninck, M. Loos & L. A. Meyer (Eds.). *IPCC Special Report on carbon dioxide capture storage*. Working Group III of the Intergovernmental Panel of Climate Change**.** Cambridge, the U.K., and New York, NT, USA.

6th International Conference and
Postgraduate Colloquium for
Environmental Research 2022 (POCER
2022) 9 - 11 June 2022
Langkawi, Kedah, Malaysia

PCR06042022 – 88: Evaluation of pyrolysis in CO_2 atmosphere for obtaining liquid fuel through the waste compact disc (CDs)

Sergio A. Medina Gaspar[a], Gabriel de Jesús Camargo Vargas[a], Siby I. Garces Polo[b*], Rafael Nikolay Agudelo Valencia[a], Liliana Giraldo Gutiérrez[c] and Juan Carlos Moreno Piraján[d]

[a] Faculty of Engineering
Universidad Libre, Bogotá, Colombia

[b] Faculty of Engineering
Universidad Libre, Barranquilla, Colombia

[c] Department of Chemistry
Universidad Nacional de Colombia, Bogotá, Colombia

[d] Department of Chemistry
Universidad de los Andes, Bogotá, Colombia

- Corresponding Author E-mail: siby.garces@unilibre.edu.co

Keywords: pyrolysis CO_2, pyrolysis, alternatives fuel, calorific power polycarbonate

Extended Abstract

The inappropriate use of plastic is still an incalculable challenge that over the years has increased exponentially, reaching millions of tons per day (Fonseca et. al., 2017) According to the environmental Non-Governmental Organization (NGO), Greenpeace in Colombia "56% is single-use plastic such as straws, cutlery, soft drink caps or juice containers. In fact, it has been established that the country generates about 12 million tons of solid waste per year and only 17% is recycled". Bogotá, being the city with the largest population in the country, is generating around 7,500 tons per day, of which 15% is recycled and approximately 56% of plastic waste single-use, discarded CDs contribute an estimated 10 tons per month, just in the Colombian capital without counting that most of this waste reaches

landfills, contributing even more to the environmental problem currently experienced and, in addition, that of the country which, according to the Ministry of Environment and Sustainable Development, the 321 landfills in the country will fulfill their useful life in the coming years

This work was carried out to determine the possibility of generating liquid fuels through waste generated by used CDs due to pyrolysis in a CO_2 atmosphere. For this project, a 2k factorial design was used, with two response variables: final pyrolysis temperature of 400 and 600°C and heating rate of 5°C/min and 10°C/min were found with the help of thermogravimetric analysis (Syamsiro S, et al., 2017). The characterization of the raw material and the compounds obtained is carried out qualitatively and quantitatively, through close analysis, ultimate analysis, higher calorific value, solubility in different, as well as identification of functional chemical groups using FTIR, and the calorific power of the products and starting material. The solid and liquid that showed the best physicochemical properties was the one that was subjected to a temperature of 600 °C, obtaining a heating value of 35809.74 and 35969.61KJ/kg respectively, 39.438% of fixed carbon and high solubility in the ether in the obtained liquids, with this it is concluded that the process is mainly affected by the reaction temperature, allowing better results. Tables 1 and 2 show higher heating values (HHV for liquid and solid products).

Table 1. Higher heating value (HHV) for Liquid products

EXPERIMENTAL CONDITIONS	CALORIFIC POWER (kJ/kg)
RAW MATERIAL (CD)	26054,5
TEST 1: 400 C, 5 °C/min	26674, 6
TEST 2: 400 C, 10 °C/min	29471,7
TEST 3: 600 C. 5 °C/min	35636,5
TEST 4: 600 C, 10 °C/min	35969,6
TEST 5: 600 C, 10 °C/min	35672,1

Table 2: Higher heating value (HHV) for solid products

EXPERIMENTAL CONDITIONS	CALORIFIC POWER (kJ/kg)
RAW MATERIAL (CD)	26054,5
TEST 1: 400 C, 5 °C/min	29320,2

TEST 2: 400 C, 10 °C/min	30941,2
TEST 3: 600 C. 5 °C/min	35905,4
TEST 4: 600 C, 10 °C/min	35809,7
TEST 5: 600 C, 10 °C/min	35173,9

It was possible to obtain both solid and liquid fuels from residual CD, through the process of thermochemical decomposition of pyrolysis. Liquid products have a calorific power that is approximately 17% lower than that of commercial gasoline, being an encouraging factor because ultimately this product could be used as an alternative fuel. On the other hand, the obtained solid also has interesting characteristics since it contains a calorific value close to 36 MJ/kg, making it attractive for its use in iron manufacturing industries as alternative coal. It was possible to obtain both solid and liquid fuel compounds from residual CD, through the process of thermochemical decomposition of pyrolysis. Liquid products have a calorific power that is approximately 17% lower than that of commercial gasoline, being an encouraging factor because ultimately this product could be used as an alternative fuel.

The Solid obtained was activated and tested in CO_2 adsorption at atmospheric pressure and low temperature to prove that this material is a potential adsorbent to the CO_2 storage and capture process.

Acknowledgments: The authors thank la Universidad Libre for the support of experimental research

References

Fonseca S, Rodriguez H, Camargo G. (2017) Characterization of corn waste of the municipality of ventaquemada, colombia. Av. cien. ing.: 8(2), 29-36 (Abril/Junio, 2017).

Syamsiro M, Mathias D.Y., Saptoadi, H., Sawitri, D.R., Nizami A-S., Reham, M. (2018). Pyrolysis of Compact Disc (CD) Case Wastes to Produce Liquid Fuel as a Renewable Source of Electricity Generation. Energy Procedia, Volume 145, July 2018, Pages 484-489. https://doi.org/10.1016/j.egypro.2018.04.096

6th International Conference and
Postgraduate Colloquium for
Environmental Research 2022 (POCER
2022) 9 - 11 June 2022
Langkawi, Kedah, Malaysia

PCR07042022 – 89: Impacts of different sparger designs for micro-sized bubbles generation on mixing performances in flat panel photobioreactors to improve microalgae growth and carbon capture

Yi An Lim[a] , I.M.S.K. Ilankoon [a*] , Meng Nan Chong [a] , and Su Chern Foo[b]

aSchool of Engineering, Chemical Engineering Discipline,
Monash University Malaysia, Jalan Lagoon Selatan, Bandar Sunway, Selangor Darul Ehsan 47500, Malaysia

b School of Science,
Monash University Malaysia, Jalan Lagoon Selatan, Bandar Sunway, Selangor Darul Ehsan 47500, Malaysia

Keywords: Carbon capture; Mass transfer; Micro-sized bubbles; Microalgae; Photobioreactor

Extended Abstract

Anthropogenic activities have caused significant generations of greenhouse gases (GHGs), where carbon dioxide (CO_2) emissions were reportedly the highest contents among them. This necessitated the needs for immediate remedial actions in the mitigations of excessive CO_2 concentrations, so as to ease the impacts of climate change. Mass carbon capture and storage (CCS) via microalgae cultivations have been proven prominent for its high CO_2 capturing abilities, as well as its prospects of converting CO_2 into rich contents in commercially valuable bioproducts (e.g. proteins, lipids). This fulfills the aspects of green industrial revolution, where microalgae cultivations can be used to address both environmental and economic aspects. However, current microalgae cultivation systems have yet to achieve the rates required for large-scale mass CCS. In order to improve microalgae growth, CO_2 gas bubbles are often fed to sustain microalgae cultures in photobioreactors (PBRs). Studies have shown significant increases in microalgae growth and CO_2 capturing rates with the reduction of gas bubble sizes to micro-size. Therefore, this paper compared the various methods in micro-sized bubble generations via 3 different gas spargers, where their mixing performances were evaluated.

Introduction. Due to anthropogenic activites that involve fossil fuel burning, significant volumes of greenhouse gases (GHGs) released atmosphere lead to adverse environmental effects, known as climate change. Studies reported that GHGs generally contain more than 50% of carbon dioxide (CO_2) [Pachauri et al., 2014]. The cultivation of microalgae has been identied as a promising mass carbon capture and storage (CCS) solution. This is mainly contributed by the high microalgae photosynthetic abilitles and CO_2 capturing rates, with every tonne of microalgae being able to fixate approximately 1.83 tonnes of CO2 [Chisti, 2004]. The cultivation of microalgae is commonly performed in closed system photobioreactors (PBRs), as PBRs are able to provide better control conditions of cultivation parameters, in comparasion to open systems (e.g. raceway ponds). These cultivation parameters include pH, temperature, dissolved oxygen concentrations,

mixing mechanisms and more. It should be highlighted that mixing is one of the crucial methods to enhance microalgae growth. Maintaining well mixed microalgae cultures is required to evenly distribute nutrients and prevent cell sedimentations. Typically, gas bubbles are applied as part of mixing mechanisms in PBRs, as well as CO_2 feeding methods. Studies have shown that the reduction of gas bubble diameters to micro-size (i.e. less than 1000µm) would greatly enhance the dissolution rates of CO_2 gas bubbles due to higher surface to volume ratio, hence accelerating microalgae CO_2 uptake [Zimmerman et al., 2011; Pires et al., 2017]. This acceleration would lead to higher photosynthetic rates, improved biomass productivity and CO_2 fixation rates. Therefore, this paper discusses and compares the generation of micro-sized bubbles via 3 different gas spargers designs, namely pipe spargers, commercial spargers and customised spargers (Table 1). This paper also highlights the key challenges of micro-sized bubble generations on the aspects of techincalilty, where micro-sized sparger cavities do not always produce micro-sized bubbles, as well as economics, where the cost of micro-sized bubble spargers will also be discussed. Hence, the outcomes from this paper has the prospects to provide engineering pragmatic recommendations for micro-sized bubbles generation for other microalgae cultivation applications, in hopes to further improve microalgae biomass productivity for mass carbon capture and climate change mitigations.

Materials & Methods. The pipe spargers (PVC pipe spargers), commercial spargers (Zhongle, China) and customised spargers (Shinkai filter Co.ltd, China) were tested out in a 10L flat panel PBR (Figure 1), where the mixing performances were evaluated at air flow rates ranging 0.05 to 0.5 vvm (volumetric flow rate of gas aeration per unit volume of culture medium per minute), in terms of mixing time, bubble sizes and CO2 mass transfer rates.

Results & Discussion. It was found that only the pipe spargers were not able to generate gas bubbles less than 1000µm. Even though pipe spargers attained CO_2 mass transfer coefficients of 13% to 38% higher than the commercial and customised spargers, these coefficients were achieved at higher air flow. In other words, high CO_2 mass transfer coefficients were also attainable with both the commercial and customised spargers at 70% to 90% lower air flow rates, as compared to the pipe spargers. This signified that the application of commercial and customised spargers with comprable CO_2 mass transfer coefficients at a much lower air flow requirement could translate into cost effectiveness in microalgae cultivations in flat panel PBRs. In addition, the electricity requirements during the cultivation could also be reduced by lowering the air flow and energy consumptions required for micro-sized bubble generations.

Table 1: Spargers employed in this work and their specifications.

Sparger	Pore size	Material	Length
Pipe spargers	0.3-0.5 mm	Polyvinyl chloride (PVC)	40 cm
Commercial spargers	NA	NA	30cm
Customised spargers	5-10 µm	Stainless steel membrane	20cm

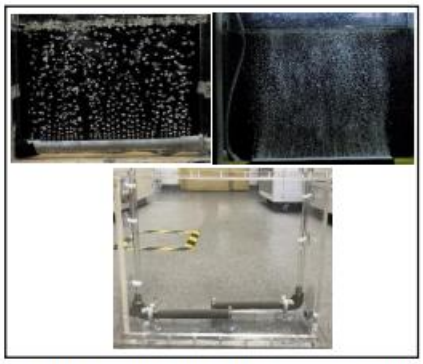

Figure 1: (a) pipe sparger, (b) commercialized sparger, (c) customized sparger in 10L flat panel photobioreactor

Acknowledgements: This study is supported by the Monash University Malaysia Sustainable Community Grant Scheme (SDG-2018-04-SCI).

References

Chisti, Y 2007, 'Biodiesel from microalgae', Biotechnology advances, vol. 25, no. 3, pp. 294-306.

Pachauri, RK, Allen, MR, Barros, VR, Broome, J, Cramer, W, Christ, R, Church, JA, Clarke, L, Dahe, Q & Dasgupta, P 2014, Climate change 2014: synthesis report. Contribution of Working Groups I, II and III to the fifth assessment report of the Intergovernmental Panel on Climate Change, Ipcc.

Pires, JC, Alvim-Ferraz, MC & Martins, FG 2017, 'Photobioreactor design for microalgae production through computational fluid dynamics: a review', Renewable and Sustainable Energy Reviews, vol. 79, pp. 248-54.

Zimmerman, WB, Zandi, M, Bandulasena, HH, Tesař, V, Gilmour, DJ & Ying, K 2011, 'Design of an airlift loop bioreactor and pilot scales studies with fluidic oscillator induced microbubbles for growth of a microalgae Dunaliella salina', Applied energy, vol. 88, no. 10, pp. 3357-69.

PCR07042022 – 90: E-waste recycling using dimethylacetamide: Organic swelling mechanisms of coarse waste printed circuit boards

Kai Dean Kang[a], I.M.S.K. Ilankoon[a*], Meng Nan Chong[a], Ta Yeong Wu[a]

[a] Discipline of Chemical Engineering, School of Engineering, Monash University Malaysia, Jalan Lagoon Selatan, Bandar Sunway, Selangor Darul Ehsan 47500, Malaysia

- [*]Corrensponding Author E-mail: saman.ilankoon@monash.edu, +60 3 5515 9640

Keywords: E-waste or electronic waste; Recycling; Printed circuit boards; Coarse particles; Swelling; Delamination

Extended Abstract: Being integral parts of electrical and electronic equipment (EEE), printed circuit boards (PCBs) remain as crucial e-waste streams and coarse PCB particles based value recovery operations could alleviate operational costs compared to the conventional hydrometallurgical route that employs fine PCB particles. Organic swelling mechanisms are proven effective in liberating the sandwiched structure of PCBs, but the underlying mechanisms are not understood in detail. Current work investigates organic swelling mechanisms of PCBs using dimethylacetamide (DMAc). The study shows the variation of swollen and delaminated PCBs fractions at different time intervals due to the organic swelling reaction. The swelling degree of PCBs at different time intervals is captured using a microscope, and noticeable cracks are observed at different sites within the multi-layered structure of PCBs. At the same time, the formation and distribution of delaminated PCBs components (i.e. halved PCBs, compound unit, copper-glass fibre cloth laminate, copper foil and glass fibre cloth) across the organic swelling timeline elucidates the delamination extent varies with time. The possible swelling mechanisms are proposed, which align with the experimental results. Hindrances that occur during delamination were identified, including the presence of the through-hole pins on PCBs, and those potentially reduce the effectiveness of organic swelling. Due to the loss of structural integrity of PCBs after undergoing organic swelling, it is suggested that a less energy intensive mechanical can be employed to separate valuable copper foils from glass fibre cloth fractions. (234 words)

Introduction

Typically, PCBs are heterogeneous in composition, comprising 40% metals, 30% ceramics and 30% plastics. Depending on the type and application of EEE, the metal content of waste PCBs vary, with

copper being the main metallic component. On the other hand, the non-conducting substrate is a composite material made up of thermosetting epoxy resin reinforced with woven glass fibre cloth (GFC). Brominated epoxy resin (BER) forms by adding brominated flame retardants to the epoxy resin and this adhesive binds metal layers and GFC together, forming the sandwiched-structure of PCBs.

Various organic solvents such as dimethyl sulfoxide (DMSO), dimethylformamide (DMF) (Verma et al., 2016; Tatariants et al., 2017) and dimethylacetamide (DMAc) (Verma et al., 2017; Han et al., 2019) are explored due to the reagent regeneration ability and the successful removal of hazardous components (BER) from waste PCBs is reported. The high organic reagent regeneration ability is also examined such that the capability to dissolve BER with the regenerated DMF is almost equivalent to that of pure DMF (Verma et al., 2016). Recovery of the metallic fraction and the entire GFC after organic swelling elucidates the high recyclability rate of this method (98.5%), which also minimises dust generation (Yousef et al., 2020).

Most of the aforementioned studies primarily emphasised on the dissolution of BER from the PCBs and its detection using a plethora of characterisation techniques and the re-employment of regenerated organic reagent after the treatment (Verma et al., 2017; Tatariants et al., 2017). The change in the properties of PCBs after organic swelling pre-treatment and the effect of variability in BER concentration on separation time due to different waste PCB streams is rarely discussed (Kang et al., 2021). This work thus aims to study organic swelling mechanisms of waste PCBs and the potential development of a different organic swelling mechanism route due to the identified hindrances.

Materials and methods

Organic swelling experiments were carried out in a beaker filled with DMAc and it was heated to 160°C. Waste PCBs were cut into 1 cm by 1 cm pieces and these are known as coarse PCBs particles. The particles were then charged into the beaker when the setpoint (160°C) was reached and the experiments were performed with varied time intervals (i.e. 15 minutes, 30 minutes, 45 minutes, 60 minutes and 75 minutes). The solid-to-liquid ratio was fixed at 1:10. The reaction mixture was stirred continuously at 150 rpm using a magnetic stirrer. Once the experiment was completed, the treated PCBs were separated by filtration and rinsed twice with tap water. The washed PCBs were dried at 60°C for 2 hours. The images of treated PCBs were captured and thickness values were measured using a Vernier calliper.

Results and discussion

When PCBs are subjected to organic swelling treatment, swollen and delaminated PCBs are produced. An expected trend of declination of swollen PCBs fraction is observed with time, which means that the

swelling of PCBs will eventually leads to the delamination of PCBs. The swelling degree of PCBs in different time intervals is observed, evidently shown by the increased PCBs thickness. The difference in the coefficient of thermal expansion (CTE) of PCBs material composition (i.e. BER: 83.27 μm/T; copper: 18.50 μm/T) causes the expansion rate of BER to be higher than copper (Han et al., 2019). This exerts internal expansion force on copper, and gaps are generated during the expansion. DMAc penetrates through the internal structure of the PCBs and occupies the formed pores spaces, causing the swelling of PCBs (Han et al., 2019). As time progresses, swelling of PCBs reaches saturation (Zhu et al., 2013), which accelerates the delamination. Moreover, heating beyond the glass transition temperature (T_g) of BER (i.e. 135°C) ultimately causes the structural deformation of PCBs.
It is worth noting that delaminated PCBs are produced at all the time intervals (15 to 75 minutes). The distribution of different types of delaminated PCBs components further elucidate that the delamination extent varies with time.

Conclusion: In summary, the swelling and delamination degree of PCBs in the organic swelling reaction is analysed, which can be observed through the noticeable cracks under the microscope and the formation of different delaminated PCBs components, respectively. These findings are useful for the design of suitable coarse PCBs particles based metal and non-metal separation process to obtain copper foils and GFC streams, which is beneficial to the downstream treatment of e-waste streams.

Acknowledgements: The authors thank the Fundamental Research Grant Scheme, Ministry of Education Malaysia for funding this project *(FRGS/1/2018/TK02/MUSM/03/1)*.

References

Han, J., Duan, C., Lu, Q., Jiang, H., Fan, X., Wen, P., Ju, Y., 2019. Improvement of the crushing effect of waste printed circuit boards by co-heating swelling with organic solvent. *Journal of Cleaner Production.* 214, 70-78.

Kang, K.D., Ilankoon, I.M.S.K, Dushyantha, N. and Chong, M.N., 2021. Assessment of Pre-Treatment Techniques for Coarse Printed Circuit Boards (PCBs) Recycling. *Minerals.* 11(10): 1134.

Tatariants, M., Yousef, S., Sidaraviciute, R., Denafas, G., Bendikiene, R., 2017. Characterization of waste printed circuit boards recycled using a dissolution approach and ultrasonic treatment at low temperatures. *RSC advances.* 7(60): 37729-37738.

Verma, H.R., Singh, K.K., Mankhand, T.R., 2016. Dissolution and separation of brominated epoxy resin of waste printed circuit boards by using di-methyl formamide. *Journal of Cleaner Production*. 139, 586-596.

Verma, H.R., Singh, K.K., Mankhand, T.R., 2017. Delamination mechanism study of large size waste printed circuit boards by using dimethylacetamide. *Waste Management.* 65, 139-146.

Yousef, S., Tatariants, M., Bendikiene, R., Kriūkienė, R., Denafas, G., 2020. A new industrial technology for closing the loop of full-size waste motherboards using chemical-ultrasonic-mechanical treatment. *Process Safety and Environmental Protection*. 140, 367-379.

6th International Conference and
Postgraduate Colloquium for
Environmental Research 2022 (POCER
2022) 9 - 11 June 2022
Langkawi, Kedah, Malaysia

PCR07042022 – 91: Microalgal Extract as Bio-coating to Enhance Biofilm Growth of Marine Microalgae on Microporous Membranes

C.Y. Tong[a], and C.J.C Derek[a]

a School of Chemical Engineering, Engineering Campus,
Universiti Sains Malaysia, 14300 Nibong Tebal, Penang, Malaysia

● Corrensponsing Author E-mail: chderekchan@usm.my

Keywords: Biocoating, Biofilm, Cell adhesion, Extracellular polymeric substances, Microalgae

Extended Abstract

Microalgal biofilm is a popular platform for algal production, nutrient removal and carbon capture; however, it was always suffering from significant biofilm exfoliation under shear force exposure. Hence, a biologically-safe coating made up of algal extracellular polymeric substances (EPS) was utilized to secure the biofilm cell retention and cell loading on commercial microporous membrane (polyvinylidene fluoride). Results demonstrated that initial cell adhesion of three marine microalgae (Amphora coffeaeformis, Cylindrotheca fusiformis and Navicula incerta) was accelerated and enhanced by at least 1.3 times higher than that of pristine control within only seven days. Bounded extracellular polysaccharide gathered was approximately 23% higher on EPS-coated membranes to improve the biofilm's hydraulic resistance, whereas bounded extracellular protein would only be substantially elevated after the attached cells re-accommodate themselves onto the EPS pre-coating of themselves. In accounting the rises of hydrophobic protein content, biofilm was believed to be more stabilized, presumably via hydrophobic interactions. EPS biocoating would generate a groundswell of interest for biotechnology applications though there are lots of inherent challenges to be further investigated in future.

Acknowledgements: Acknowledgement to "Ministry of Higher Education Malaysia for Fundamental Research Grant Scheme with Project Code: FRGS/1/2018/TK02/USM/02/1.

6th International Conference and
Postgraduate Colloquium for
Environmental Research 2022 (POCER
2022) 9 - 11 June 2022
Langkawi, Kedah, Malaysia

PCR07042022 – 92: Real-time biomonitoring of Spirodela polyrhiza for the detection of heavy metals via image analysis approach

Win Hung Tan, and C.J.C Derek

School of Chemical Engineering, Engineering Campus
University Sains Malaysia, 14300 Nibong Tebal, Malaysia

- Corrensponsing Author E-mail: chderekchan@usm.my

Keywords: Duckweeds; Image analysis; Heavy metals; Biomonitoring.

Extended Abstract

Water pollution has been regarded as a global issue which not only is threatening aquatic communities but also distrupting the ecological balance. The critical occurence of pollution leads to the development of protocols for detection of water contaminants and monitoring in attempt to preserve quality of water. Several developed water monitoring techniques included the usage of instruments such as chromatography, mass spectrometry and different type of water quality sensors or biosensors could archive the purposes [Zulkifli *et al*., 2018]. However, the limited efficiency of these laboratory-based analytical tool in real-time water monitoring, and high cost of multiple sensors installation at monitoring site has inspired the employment of aquatic plants to detect water contaminants. Plants were known to uptake and accumulate metals from the living environment. While essential heavy metals are contributing in plants metabolism, excess amount of essential metals and trace amount of non-essential metals could negatively influence the cellular organelles and homeostasis in plants [Subpiramaniyam, 2021]. The morphological, physiological and behaviour changes of plants after exposure to heavy metals were expected to reflect the possible type of heavy metals uptaked. Thus, this study intended to explore the possibility of detecting type and concentration of heavy metals presence in water through image analysis technique. *Spirodela.polyrhiza* used in the experiment were aseptically subcultured in sterilized Hoagland's medium. To evaluate the respond of plant to heavy metal, the medium was spiked with 10 ppm, 5 ppm and 1 ppm of cadmium and nickel. *S.polyrhiza* were then transferred into the petri dish which contained the prepared medium. Images of the *S.polyrhiza* in the petri dish were captured every 8 hrs, consequently for 72 hrs and the obtained images were processed using ImageJ software. The image processing, analysis procedures and calculation models were adopted from [Tan *et al*.,2021] and figure 1 showed the simple schematic of the image analysis conducted to analyze the changes of

mass, chlorophyll and anthocyanin contents of *S.polyrhiza*. From the observation, *S.polyrhiza* exposed to 10 ppm of cadmium has negative changes of anthocyanins at first 24 hours compared to exposure at 1 and 5 ppm. A slight reduction of anthocyanin changes was observed at 16 to 24 hours when the plant exposed to 5 ppm cadmium. The overall anthocyanin changes percentage of *S.polyrhiza* at 72 hours decreased with increased concentration of cadmium. However, the changes of anthocyanin in *S.polyrhiza* at 72 hours was found to be higher with greater exposure to nickel. *S.polyrhiza* exhibited a minor decrement of anthocyanin changes at different period depending on the amount of nickel it was exposed to. 10 ppm of nickel caused the decrement of anthocyanin changes at 24 to 32 hours while 5 ppm of nickel reduced the anthocyanin changes at 8 to 16 hours. 1 ppm of nickel leads to increment of anthocyanin gradually throughout the experimented period. The chlorophyll content also an important indicator of the plants health.Chlorophyll contents was found to decrease at initial 16 hours and the 64th hours when treated with 5 ppm and 1 ppm of cadmium while 10 ppm cadmium results in decrement of chlorophyll at 32th and 64th hours. A fluctuation of chlorophyll content was observed in the 10 ppm nickel treatment for the first 40 hours. 1 and 5 ppm of nickel eventually induce reduction in chlorophyll at the initial stage. .In general, cadmium would stimulate the mass changes at different rate depending on the concentration of cadmium. The greater amount of cadmium caused a lower rate of biomass increment and vice versa. While 10 ppm of nickel lowered the mass of *S.polyrhiza* at initial 24 hours, 1 and 5 ppm nickel showed insignificant effect on the mass at the beginning of 24 hours . Nickel and cadmium were found to interfere with the synthesis of chlorophyll and induce the production of reactive oxygen species which oxidise chlorophylls [Chen *et al*., 2020]. The effect of heavy metals on plants could manifest as stresses that could be observed from their appearance. Anthocyanins, chlorophylls and mass changes become significant and inituitive measure of plant responses towards the metal stresses. Thus, image analysis would be the potential technique to capture these information.Related study has presented the possibility of using *S.polyrhiza* to monitor nickel with high sensitivity, by assessing the chlorophyll content and frond number which reflected the phytotoxic responses of plants [Appenroth *et al*., 2010]. Duckweed as one of the most profound metals hyperaccumulator, known be outstanding, eco-friendly candidate to utilized as agent for water management, either in phytoremediation or water quality monitoring. The study was expected to extend the usage of *S.polyrhiza* in water management, not limited to remediate and monitor the water quality, but to provide accurate detection on the type and concentration of pollutants invading the water reservoir.

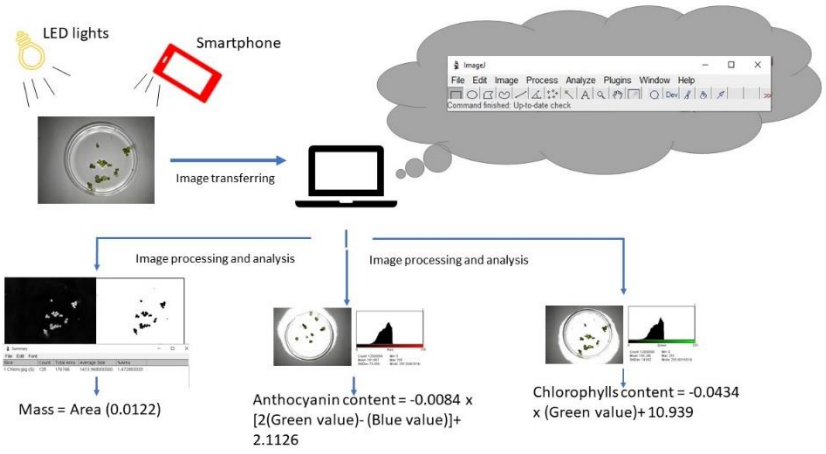

Figure 1: Simple schematic of the image analysis conducted to analyze the changes of mass, chlorophyll and anthocyanin contents of *S.polyrhiza*

Acknowledgements: The authors wish to thank Ministry of Higher Education Malaysia for the financial support of Long-Term Research Grant Scheme (LRGS/1/ 2018/USM/01/1/2) (UTAR/ 4411-S01) (USM 6770007).

.

References

Appenroth, K.-J., Krech, K., Keresztes, Á., Fischer, W., & Koloczek, H. (2010). Effects of nickel on the chloroplasts of the duckweeds Spirodela polyrhiza and Lemna minor and their possible use in biomonitoring and phytoremediation. *Chemosphere*, *78*(3), 216–223. https://doi.org/https://doi.org/10.1016/j.chemosphere.2009.11.007

Chen, D., Zhang, H., Wang, Q., Shao, M., Li, X., Chen, D., … Song, Y. (2020). Intraspecific variations in cadmium tolerance and phytoaccumulation in giant duckweed (Spirodela polyrhiza). *Journal of Hazardous Materials*, *395*, 122672. https://doi.org/https://doi.org/10.1016/j.jhazmat.2020.122672

Subpiramaniyam, S. (2021). Portulaca oleracea L. for phytoremediation and biomonitoring in metal-contaminated environments. *Chemosphere*, *280*, 130784. https://doi.org/https://doi.org/10.1016/j.chemosphere.2021.130784

Tan, W. H., Ibrahim, H., & Chan, D. J. C. (2021). Estimation of mass, chlorophylls, and anthocyanins of Spirodela polyrhiza with smartphone acquired images. *Computers and Electronics in Agriculture*, *190*, 106449. https://doi.org/https://doi.org/10.1016/j.compag.2021.106449

Zulkifli, S. N., Rahim, H. A., & Lau, W.-J. (2018). Detection of contaminants in water supply: A review on state-of-the-art monitoring technologies and their applications. *Sensors and Actuators B: Chemical*, *255*, 2657–2689. https://doi.org/https://doi.org/10.1016/j.snb.2017.09.078

6th International Conference and
Postgraduate Colloquium for
Environmental Research 2022 (POCER
2022) 9 - 11 June 2022
Langkawi, Kedah, Malaysia

PCR07042022 – 93: A Novel Cultivation of Giant Duckweed via Application of Superhydrophobic Coatings

Mei Xia Chua[a], Gayathri Saravanan[a], and Derek Juinn Chieh Chan[a*]

[a] School of Chemical Engineering,
University Sains Malaysia, Penang, Malaysia

- Corrensponsing Author E-mail: chderekchan@usm.my

Keywords: Duckweed; Superhydrophobic; Wax; Biomass Production.

Extended Abstract

Conventional establishment of laboratory cultures of giant duckweed *Spirodela polyrhiza* has always been prepared in beakers, Erlenmeyer flasks or Scott bottles [Guo *et al.,* 2020; Sun *et al.,* 2020]. However, layering of fronds are observed in these conventional cultivation methods due to the limitation of surface area available which affect the efficiency of the giant duckweed in sunlight capturing [Ziegler *et al.,* 2015]. Here, acrylic sheets were spray-coated with a superhydrophobic (SHP) wax suspension which comprised of beeswax and ethanol, where the spray-coated acrylic sheets were used as novel cultivation platform for *S. polyrhiza*. *S. polyrhiza* grown for 7 days in conventional glass jar which acted as the control and were compared to SHP suspension coated acrylic sheet (SHPA) and SHP suspension coated acrylic sheet with aluminium mesh centerly placed (SHPAM) at similar duration and cultivation conditions. The effect of cultivation methods on growth rate and biochemical compositions of *S. polyrhiza* were monitored. The biomass growth in SHPAM showed the highest growth with a mass gain of about 98% compared with 44% in the control. The total chlorophyll content of *S. polyrhiza* grown on SHPA and SHPAM were 1.0237 ± 0.002 mg total chlorophyll/ g fresh weight biomass and 1.0587 ± 0.039 mg total chlorophyll/ g fresh weight biomass, which were 1.18 times and 1.23 times higher than the control. Hence, this study proved that the proposed method that applied superhydrophobic properties in cultivation of *S. polyrhiza* provided a larger surface area for *S. polyrhiza* to grow, which then resulted in a greater biomass production while at the same time maintaining the quality of the biochemical compositions of giant duckweeds.

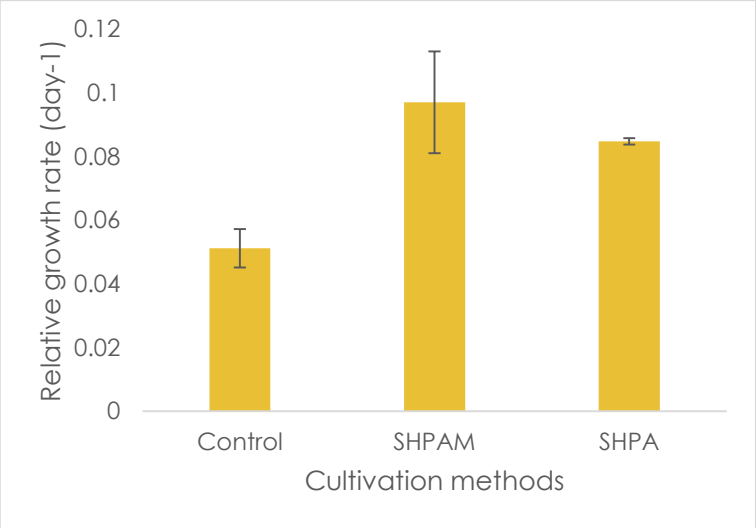

Figure 15: Relative Growth Rate of *Spirodela polyrhiza* on Different Cultivation Methods

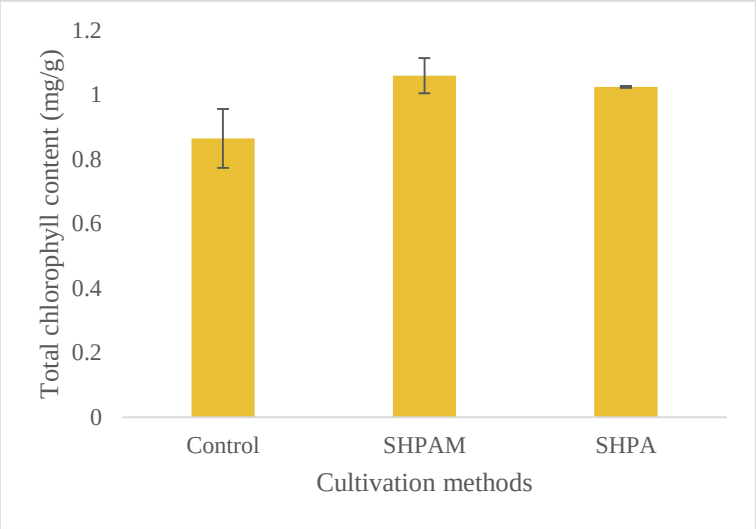

Figure 2: Total chlorophyll content of *Spirodela polyrhiza* on Different Cultivation Methods

Acknowledgements: The authors wish to thank Ministry of Higher Education Malaysia for the financial support of LongTerm Research Grant Scheme (LRGS/1/2018/USM/01/1/12) (UTAR/4411-S01) (USM 6770007).

References

Guo, L., Jin, Y., Xiao, Y., Tan, L., Tian, X., Ding, Y., He, K., Du, A., Li, J., Yi, Z., Wang, S., Fang, Y., & Zhao, H. (2020). Energy-efficient and environmentally friendly production of starch-rich duckweed biomass using nitrogen-limited cultivation. *Journal of Cleaner Production*, *251*.

Sun, Z., Guo, W., Yang, J., Zhao, X., Chen, Y., Yao, L., & Hou, H. (2020). Enhanced biomass production and pollutant removal by duckweed in mixotrophic conditions. *Bioresource Technology*, *317*.

Ziegler, P., Sree, K. S., & Appenroth, K. J. (2016). Duckweeds for water remediation and toxicity testing. *Toxicological and Environmental Chemistry*, *98*(10), 1127–1154.

6th International Conference and
Postgraduate Colloquium for
Environmental Research 2022 (POCER
2022) 9 - 11 June 2022
Langkawi, Kedah, Malaysia

PCR08042022 – 94: Antioxidant potential of herbal extracts from sea buckthorn seeds oil

Sang Mun Jeong[a], Sumin Pyo[b], Parveen Akhter[c], Taseer Yasrab Bhatti[c], Iqrash Shafiq[d], Rabia Nazar[e], Muhammad Shahid Nazir[f], Murid Hussain[d], Young-Kwon Park[b*]

[a] Department of Chemical Engineering
Chungbuk National University, Cheongju, Korea

[b] School of Environmental Engineering
University of Seoul, Seoul, Korea

[c] Department of Chemistry
The University of Lahore, Lahore, Pakistan

[d] Department of Chemical Engineering
COMSATS University Islamabad, Lahore Campus, Lahore, Pakistan

[e] Department of Polymer and Process Engineering
University of Engineering and Technology, Lahore, Pakistan

[f] Department of Chemistry
COMSATS University Islamabad, Lahore Campus, Lahore, Pakistan

- Corrensponsing Author E-mail: catalica@uos.ac.kr

Keywords: Sea buckthorn seeds; Solvents; FRAP assay; Antioxidant activity

Extended Abstract

Herbal extracts of sea buckthorn (SBT) seeds oil were prepared in n-hexane, isopropyl alcohol, ethyl acetate, ethanol, and methanol. The herbal extracts of SBT seed oil are being used in various fields of life, including health, medicine, pharmaceutics, bakeries, beverages, and cosmetics. Moreover, SBT seed oil has different minerals and nutrients, such as vitamin C, vitamin E, flavonoids, carotenes, flavanones, and phytosterols. The presence of phenolics in the SBT seeds and their herbal extracts are

used as an antioxidant. On the other hand, the antioxidant activity of such extracts was checked using the ferric chloride ($FeCl_3$) method based on the ferric reducing ability of plasma (FRAP) assay using UV–Vis spectroscopy. In addition, the herbal extract of SBT seed oil is being used as an anti-aging agent in herbal cosmetics, medicines, and the food industries.

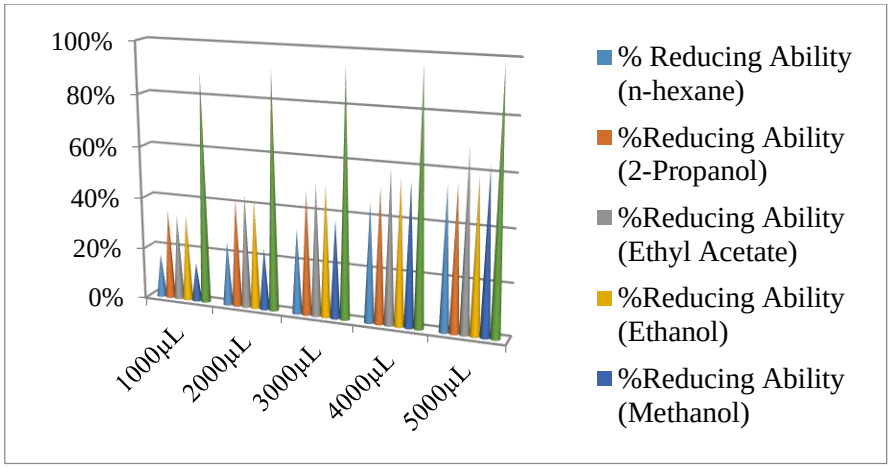

Figure 16: Comparison of percent ferric reducing ability of ferric ions to ferrous ions for the concentration of 1000–5000 µL

As shown in Figure 1, the antioxidant activity was observed using a ferric reducing ability of plasma (FRAP) assay, and the absorbance at 510 nm was assessed by ultraviolet–visible spectroscopy. The ethyl acetate and methanol extracts showed the maximum (68%) and minimum (62%) scavenging FRAP, respectively.

Acknowledgements: This work was partially supported by National Research Foundation of Korea (NRF-2021R1A2C3011274).

6th International Conference and
Postgraduate Colloquium for
Environmental Research 2022 (POCER
2022) 9 - 11 June 2022
Langkawi, Kedah, Malaysia

PCR08042022 – 95: Research on the Intelligent System Construction of Street Landscape for Smart City

Xiao Han[a], Zhe Li[a*], YinYin Cao[a] and ZeYi Sun[a]

[a] School of Architecture
Southeast University, Jiangsu, China

- Corrensponsing Author E-mail: lizheseu@seu.edu.cn

Keywords: Smart City; Complex Network; Street Landscape; Intelligent System; Means of Realization.

"Intelligent" development has become the new engine in modern society due to the advancement of information technology represented by the Internet of Things (IoT). Meanwhile, as an essential part of smart city construction, the urban landscape is also facing the opportunities and challenges brought about by the intelligent process. Smart landscapes changing the construction, operation, and management modes of traditional gardens can effectively improve the efficiency in landscape industry, realizing the digitization, networking, and intelligence of urban landscape renewal [De-Francesco and Angelini, 2014]. The urban street landscape is a vital component of the cityscape as it weighs heavily in shaping the urban image. Thus, systematic research on the construction and implementation methods of its intelligent system has become a significant starting point and foundation for the design and construction of an intelligent urban landscape [Caprotti and Cowley, 2019].

As a key supporter of the realization of smart landscapes, the construction of a landscape intelligence system needs to be based on the theory of systems science and take the landscape information interaction mechanism as the core to form a closed loop information system of "objective environment-sensing layer-information processing layer-reaction layer-objective environment". Meanwhile, combined with the needs of the street environment itself (things) and the needs of users (people), an intelligent horizontal system of urban street landscapes, including intelligent infrastructure, intelligent services, intelligent protection and maintenance, intelligent management and evaluation system can be built. Through the cooperative supply of the energy system and other related systems, a complete operation network of the intelligent system can be established(Figure 1).

In addition, the realization of the urban street landscape intelligent system depends on the effective application of intelligent technology, mainly including IoT technology, spatial information integration technology, virtual reality and visualization technology, etc. All stages of urban street landscape construction (Figure 2), from scheme design to engineering construction and maintenance management, shall integrate these intelligent technologies to achieve the intensive building of street space, thereby assisting in the provision of travel assistance, convenience service, security assurance and other functions on the premise of basic road operation. Meanwhile, it would ensure accurate and comprehensive urban street landscape design and management.

Therefore, by combining smart landscape theory and urban street practice achievements and constructing the basic framework of urban street landscape intelligent system, a sophisticated intelligent mechanism based on big data and the Internet of Things shall be formed, ranging from real-time perception, data acquisition and analysis to response decision-making and feedback formation. At the same time, the interconnection and collaborative sharing of information resources enable dynamic monitoring and rapid response of the landscape environment, as well as precise positioning and interactive feedback to users, and provides efficient and flexible tools for refined street construction, governance and operation regarding decision-making and action-taking, all of which contribute to comprehensively improving the management level of urban streets and promoting the construction of a smart city.

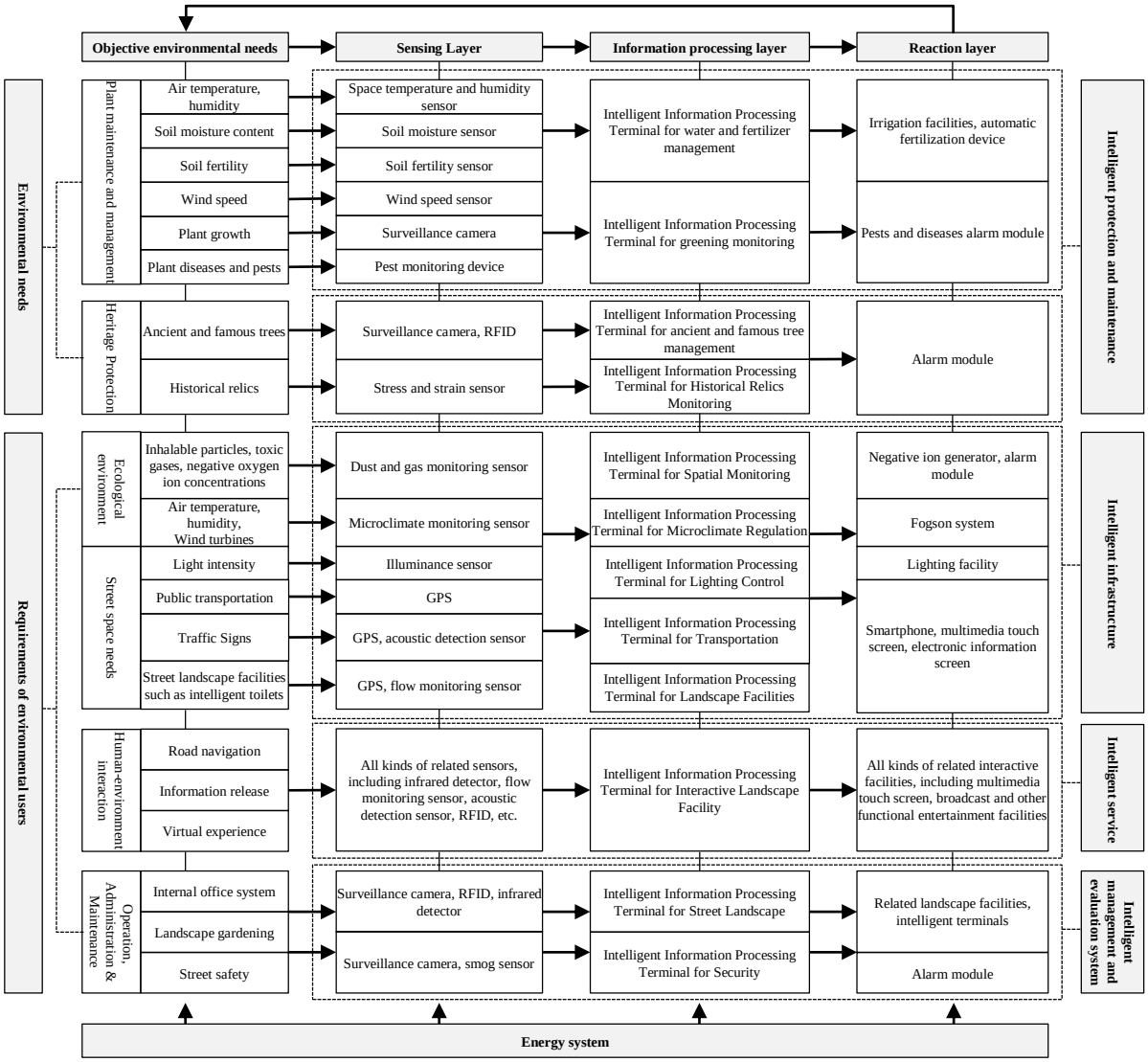

Figure 17: Operating mechanism of urban street landscape intelligent system

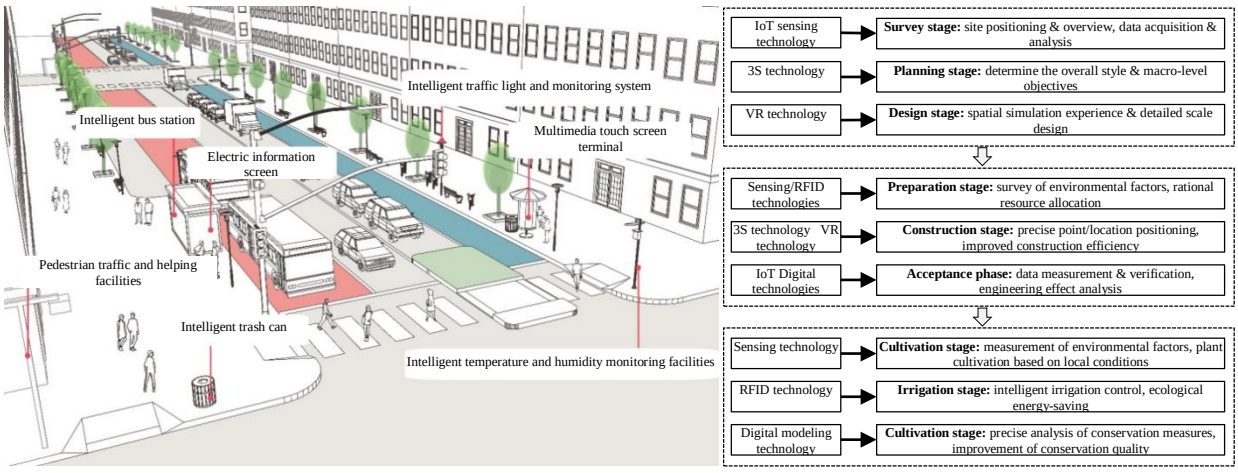

Figure 2: Basic street services and application of intelligent technologies at different stage

References

Caprotti, F., & Cowley, R. 2019. Varieties of smart urbanism in the UK: Discursive logics, the state and local urban context. *Transactions of the Institute of British Geographers*. 44 (3): 587-601.

De Francesco, G., Angelini, R. 2014. Creative autoregulation Towards an interactive urban landscape. *INTERNATIONAL CONFERENCE ON INTELLIGENT ENVIRONMENTS*. 388-391.

6th International Conference and
Postgraduate Colloquium for
Environmental Research 2022 (POCER
2022) 9 - 11 June 2022
Langkawi, Kedah, Malaysia

PCR08042022 – 96: Research on Carbon System Measurement Model of Rural Landscape Based on Emission Factor Method: A Case Study of Paifang Village

Futian Yuan [a], Zhe Li[a*], Zheng Zhou[a] and Yifan Li[a]

[a] School of Architecture
Southeast University, Jiangsu, China

- Corrensponsing Author E-mail: lizheseu@seu.edu.cn

Keywords: Carbon Emission; Emission Factor Method; Measurement Model; Carbon System; Rural Landscape.

1. Introduction

With the high-quality development and low-carbon construction of contemporary landscape architecture, the carbon system measurement and algorithm of rural landscape has become one of the most concerning problems in rural low-carbon quantitative research. The low-carbon village idea is used to structure the Carbon System Measurement Model. The Paifang Village is instanced by starting from the production space, living space, and ecological space, to construct the carbon system measurement model in the emission factor method and to quantitatively analyze the carbon system characteristics of the rural landscape. This helps to offer a scientific basis to rebuild rural landscape, how to design them, how to manage them, and how to promote high-quality rural landscape development while working toward a low-carbon goal.

2. Methods and Formulas

The carbon system of rural landscape is screened in conjunction with the carbon emission measurement method, and the carbon system measurement model is built using the emission factor method. The emission factor method[Holmberg et al., 2021], as a greenhouse gas emission calculation methodology, focuses on "energy consumption type" and may be utilized well in the rural landscape setting[Srinivasarao et al., 2016].

Taking Paifang Village as an example, the measurement object and scope are immediately evident. The scope of production space, living space, and ecological space in rural landscape are then recognized in order to analyze their landscape resources.The list of carbon sources and sinks in the rural landscape is

derived from the IPCC's list of emission sources[Paustian et al., 2006]. The list's specific contents include 3 types of space systems, carbon source and sink objectives, 8 types of rural landscape, 21 types of carbon source and sink factors, and 29 activity level data. In the end, the basic formula(1) and integration formula(2.3.4) are applied for carbon system measurement based on the contents of the list. The data comes from CAD and remote sensing data, relevant energy statistics websites, statistical data from the rural administrative department, and field surveys.

Carbon emission: $C = \sum E_a \cdot k_a$ (1)

Carbon emission in production space: $C_p = \sum S_a \cdot \alpha_a + \sum E_b \cdot \alpha_b - \sum Q_k \cdot \alpha_k / H_k$ (2)

Carbon emission in living space: $C_l = \sum E_c \cdot \alpha_c + \sum \left(V_i \cdot M_i \cdot Y_i\right) \cdot \alpha_i - S_g \cdot \alpha_g$ (3)

Carbon uptake in ecological space: $C_e = \sum S_j \cdot \alpha_j$ (4)

3. Results and Discussions

The model measurement results are used to create a histogram(Figure 1) concerning carbon emissions in rural landscape, and GIS software is used to create a three-dimensional spatial carbon emission map(Figure 2). The findings of the study represent the peculiarities of Paifang Village's carbon system. When it comes to carbon emissions, the emphasis is on energy consumption in the service industry and residential buildings, with buildings taking up the most space and traffic taking up the least. In terms of carbon sink, it is low overall, with the tea plantations serving as the primary carrier of the carbon sink. The overall performance is of the “high-source low-sink type”, in which the carbon source is concentrated in the living area, with little land but a high carbon source coefficient. Although there is a lot of carbon sink space, the carbon sink coefficient is low since tea plantations make up the majority of it.

The carbon emissions of rural landscape are calculated using categorization, and the net carbon emission measurement findings represent the carbon system features of the target village. Meantime, it's important to note that the accuracy of basic data has a big impact on the results of the analysis due to the complexity of rural landscape. Carbon emission activities are also affected by changes in population, industrial development, and land change, and the resulting conclusion is often volatile because low carbon is procedural, complex, and dynamic.

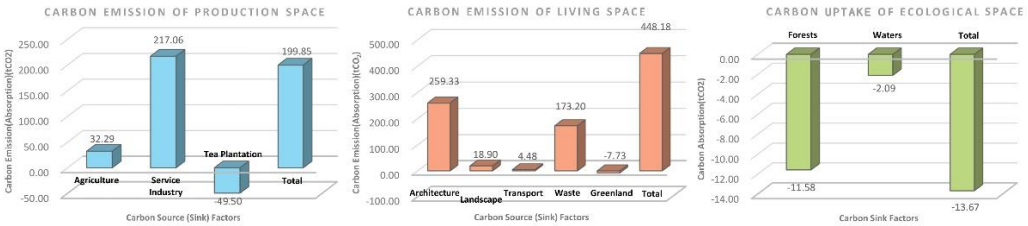

Figure 1: The Histogram of Carbon Emission(Uptake)

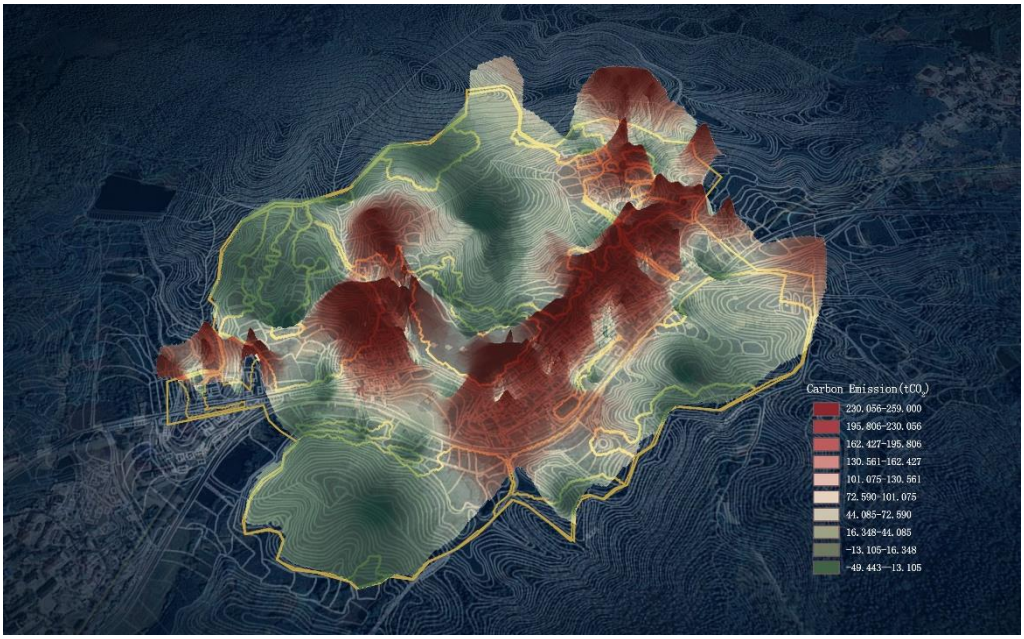

Figure 2: The 3D Spatial Carbon Emission Map

Acknowledgements: We thank Xiao Han, Liya Wang ,Tongyi Zhu and Xiyi Lu for their indispensable help with this research, and the Digital Landscape Laboratory of Southeast University for the RS and GIS data support. Our research is supported by the National Key R&D Program of China (No. 2019YFD1100405).

References

Holmberg, M., Akujrvi, A., Anttila, S., Autio, I. and Forsius, M., 2021. Sources and sinks of greenhouse gases in the landscape: approach for spatially explicit estimates. *Science of the Total Environment*.146668.

Paustian K, Ravindranath N H, Amstel A V., 2006. *2006 IPCC Guidelines for National Greenhouse Gas Inventories*. International Panel on Climate Change.

Srinivasarao C， Rani Y S, et al., 2016. Assessing village-level carbon balance due to greenhouse gas mitigation interventions using EX-ACT model. *International Journal of Environmental Science & Technology*. 13(1):97-112.

6th International Conference and
Postgraduate Colloquium for
Environmental Research 2022 (POCER
2022) 9 - 11 June 2022
Langkawi, Kedah, Malaysia

PCR11042022 – 98: Bio Conversion of Biomasses for Enhancing Food Security in Changing Climatic Scenario

Noshin Ilyas[a*], Fatima Bibi[a], Qudsia Bano[a]

[a] Department of Botany, PMAS Arid Agriculture University Rawalpindi Pakistan

- Corrensponsing Author E-mail: noshinilyas@yahoo.com

Keywords: Agricultural pollution; Crops; Soil fertility: Waste ttreatment

Extended Abstract

Pakistan is the 7th most vulnerable country to climate change. There is a dire need to manage the risks to sustainable agriculture in an environment threatened by climate change. Soil is a limited resource, and stresses such as drought, salinity, and heavy metal decrease agricultural productivity day by day. Agricultural chemicals are causing physicochemical and biological soil deterioration and disrupting agro-ecosystems all over the world. Concerns about soil and environmental health are prompting interest in alternative eco-friendly techniques. Different biomasses are bio-converted into value-added bio-fertilizers using beneficial microorganisms for direct application in fields. We aimed to check the potential of Plant Growth Promoting Rhizobacteria and various modified biomasses as effective soil amendment techniques for improving plant growth under predicted climatic change's abiotic stresses. Experiments were conducted to isolate and characterize stress-tolerant Rhizobacteria and check their mitigation potential. Modified biomasses like compost, biochar, and bio-organic fertilizer were used as soil amendments techniques. Various morphological, physiological, biochemical, growth and productivity parameters were studied. Microbial strains were isolated from the stressed region. The identification of isolated microbial strains was carried out by physiochemical and 16s rDNA sequencing, whole genome sequences, and phylogenetic analysis. Stress tolerance and different plant growth-promoting traits of isolated strains were evaluated under normal and stressed conditions. Inoculation of seeds with PGPR, compost, biochar, and bio-organic fertilizer improved all growth and productivity parameters, increased nutrient status, and improved osmolyte production and hence helped survival and growth under stress conditions. Building our understanding of the interdependence of micro-organism communities, soil nutrient status, and plant health will be necessary for understanding climatic effects on soil health and plant growth.

Acknowledgements: The authors thank the Punjab Higher Education Commission for providing the travel grant.

References

Bibi, F., Ilyas, N., Arshad, M., Khalid, A., Saeed, M., Ansar, S., & Batley, J. (2022). Formulation and efficacy testing of bio-organic fertilizer produced through solid-state fermentation of agro-waste by Burkholderia cenocepacia. *Chemosphere*, *291*, 132762. https://doi.org/10.1016/J.CHEMOSPHERE.2021.132762

6th International Conference and
Postgraduate Colloquium for
Environmental Research 2022 (POCER
2022) 9 - 11 June 2022
Langkawi, Kedah, Malaysia

PCR11042022 – 99: Technical and environmental analysis of a product produced by additive manufacturing from recycled PET

Beatriz A. S. Teles[a], Sandro D. Mancini[b], and Luiz Kulay[a*]

[a] Chemical Engineering Department, Polytechnic School, University of São Paulo (USP), Brazil

[b] Institute of Science and Technology, São Paulo State University (UNESP), Brazil

- Corresponding Author E-mail: beatrizarioliteles@usp.br

Keywords: LCA; Plastic pollution; Recycling; additive manufacturing; Circular Economy.

In recent decades, polymers have become essential to modern society. On the other hand, the inadequate treatment of these materials in the post-consumption stage makes them important precursors of environmental impact. In this way, the reintegration of polymers in the various production chains has become necessary to reduce the consumption of resources (mainly of fossil origin), generate emissions, and leverage circularity. Polyethylene terephthalate (PET) is a polymer regularly applied for processing one-way consumption goods, and so it's usually discarded in expressive amounts into the environment. Integrating this practice with modern technologies, such as additive manufacturing (AM), could result in an effective strategy in the search for sustainable development if, in fact, this arrangement showed satisfactory results in terms of technical and environmental performances. The challenge in technical terms would be to manufacture products derived from PET with mechanical resistance as high as those obtained from Acrylonitrile Butadiene Styrene (ABS), a polymer for which AM achieves better results. In addition, the scheme would be considered environmentally satisfactory if it achieved a lower level of environmental impacts than a production cycle established from crude oil.

This study explored the perspective by proposing a sequence of processes for producing a cell phone holder via additive manufacturing and using PET resin recycled from beverage bottles. The technical performance of the process was verified from the properties of the product obtained, which were characterized by the techniques of Differential Scanning Calorimetry (DSC) and Thermogravimetric Analysis (TGA), Rheology (IV: Intrinsic Viscosity), and Mechanical Strength. The environmental performance was measured by the Life Cycle Assessment (LCA). As the production chain includes the recycling stage, the LCA technique was applied according to an open-loop recycling (OLR) approach.

Backgrounds: Open-looping recycling (OLR)

A system is classified as OLR if a product that is no longer able to perform its original function can be treated by recycling practices to replace virgin raw materials in the manufacture of another consumption good, whose function is (necessarily) different from that performed by the predecessor. Modeling an OLR system involves dealing with multifunctional situations; this means deciding how to distribute all the environmental burdens among their functions. The literature describes six procedures for treating multifunctionalities in OLR systems; nevertheless, the *Cut-off* practice used to be the most adopted alternative. According to this approach, the environmental burdens associated with fulfilling the first function will exclusively be attributed to it. On the other hand, consumption and emissions generated from the collection of material to be recycled until the second product's final disposal are integrally attributed to the next function. The *Cut-off* practice was also selected to treat the multifunctional situation in the present case study. Thus, the environmental performance associated with the cell phone support started to be measured from the collection of used PET bottles used in its manufacture.

Life Cycle Modeling

LCA was applied under the attributional approach for an OLR-type system and following the normative guidelines of ISO 14044. The Reference Flow (RF) was established as the manufacture of a cell phone support (30.12g). In addition, obtaining resins from recycled PET, filament production, and additive manufacturing were described by primary data. The product system is described in Figure 1 (system 2), and the impact assessment considered the Global Warming Potential (GWP) and Primary Energy Demand (PED) categories.

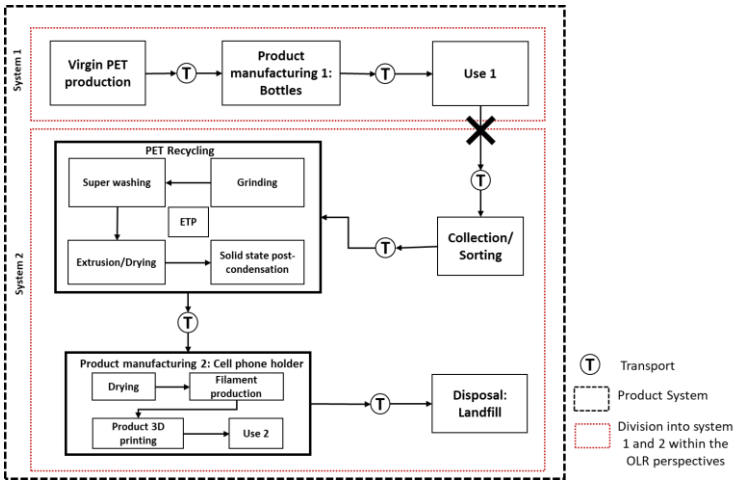

Figure 18: Schematic representation of the product system

Results and Discussion

The technical performance of the resin obtained from recycled PET, the extruded filaments, and the cell phone support are shown in Table 1. The results were equivalent to those registered in the literature for

virgin and recycled polymers (mainly ABS) for commercial use. This finding confirms the compatibility of recycled PET with the intended application of the product.

Table 1: Technical performance of prototype obtained by AM from recycled PET resin

Analysis	Thermal							Rheology	Mechanical		
	TGA			DSC				IV	Tensile Test		
Sample	T_{onset} (°C)	Residual mass (%)	T_{max} (°C)	T_g (°C)	T_m (°C)	ΔH_f (J/g)	X_c (%)	η $\left(dL/g\right)$	Tensile strength (MPa)	Modules elasticity (MPa)	Failure strain (%)
Pellet	391	21.2	481	86.0	246	55.4	39.6	0.803	-	-	-
Filament	398	20.1	493	87.1	248	48.2	34.5	0.667	-	-	-
Prototype	395	18.8	491	87.7	248	50.1	35.8	0.622	37.7 ± 5.60	771 ± 29.4	7.64 ± 1.50

Table 2 compares the environmental performance of obtaining the prototype by the conventional route (from virgin input) with that achieved by recycled PET resin in terms of GWP and PED. The results showed the supremacy of the OLR arrangement over its congener mainly due to the low impacts of pellet production compared to the synthesis of virgin PET from crude oil. However, the high energy demands associated with extrusion and additive manufacturing are limitations that need to be addressed to practice the process on a commercial scale.

Table 2: Environmental performance analysis of the OLR process

Scenario	Impacts (/ RF)	
	GWP ($gCO_{2\ eq}$)	PED (MJ)
Conventional (from crude oil)	488	50.4
OLR (Cut-off)	351	13.8

Acknowledgements: The authors thank the National Council for Scientific and Technological Development (CNPq: process 130548/2021-9) and the Coordination for the Improvement of Higher Education Personnel – Brazil (CAPES: Code 001) for the support granted to carry out this study.

References

Garcia, FL et al. 2021. Comparative LCA of conventional manufacturing vs. additive manufacturing: the case of injection molding for recycled polymers. Int. J. Sustain. Eng., 14 (6), 1604-1622.

Nicholson, AL. et al. 2009. End-of-life LCA allocation methods: open loop recycling impacts on robustness of material selection decisions. In: IEEE Symposium, 1-6.

6th International Conference and
Postgraduate Colloquium for
Environmental Research 2022 (POCER
2022) 9 - 11 June 2022
Langkawi, Kedah, Malaysia

PCR11042022 – 100: Verifying the effect of alternative NH_3 and CO_2 production routes on the environmental performance of urea synthesis

Luise P. Martins[a], Luiz Kulay[a]

[a] Chemical Engineering Department, Polytechnic School, University of São Paulo (USP), Brazil

- Corresponding Author E-mail: luise.martins@usp.br

Keywords: Life Cycle Assessment; Environmental performance; Carbon Capture Usage; Process Integration; Industrial Ecology.

Urea ($CO(NH_2)_2$) is the most produced N-fertilizer worldwide, reaching 181 Mt in 2020, after growing by more than 17% in a decade. This evolution is justified by its high capacity to supply nitrogen to different crops, regardless of cultivation conditions and soil type, and the fact that it is used as input to produce complex NPK. Therefore, urea has become one of the central pillars of support for global agribusiness from an economic point of view. On the other hand, its typical synthesis route largely depends on non-renewable resources to produce raw materials and inputs and generate thermal and electrical energy. In addition, Greenhouse Gases (GHG) are emitted into the air due to these operations. This situation motivates the search for arrangements for obtaining urea that reduce the incompatibilities between the economic and environmental perspectives. An alternative being explored in this field is the production of ammonia (NH_3) via biomass gasification. In theory, this approach reduces the influence exerted by natural gas on the original process and emits CO_2 biogenic, i.e. neutral. The use of sugarcane bagasse as a source of biomass for this process opens up an optimistic perspective for Brazil since the country is the world's leading producer of that agricultural commodity. Another possibility is to use less energy-intensive technologies to generate CO_2 in conditions to be used as an input in the production of $CO(NH_2)_2$. This study follows this path by verifying the effect of alternative NH_3 and CO_2 production routes on the global environmental performance of urea synthesis. Because of the holistic nature of the analysis, we decided to apply the Life Cycle Assessment technique to carry out the estimates.

Synthesis of Urea

The typical route of urea synthesis consists of the Bosch–Meiser process, a mechanism established from two equilibrium reactions that occur in series. In the first one (fast step), NH_3 reacts with CO_2 under extreme conditions (160°C and 110 atm) to form ammonium carbamate:

$$NH_{3(l)} + CO_{2(g)} \rightleftharpoons NH_4CO_2NH_2 + 117\frac{KJ}{mol}$$

In the next (slow) step, the dehydration of the carbamate occurs when it is subjected to high temperatures (160 – 180°C), giving rise to urea

$$NH_4CO_2NH_2 \; + \; 15.5\frac{KJ}{mol} \; \rightleftharpoons \; CO(NH_2)_2 \; + \; H_2O$$

Description of scenarios

This analysis was performed for three possible scenarios (S1 – S3) for obtaining the raw materials used by the Bosch–Meiser process to manufacture urea (Table 1). In S1, ammonia is produced from the reaction between N_2 in the air and H_2 from steam reforming of natural gas (Haber–Bosch process). The CO_2 consumed during urea manufacturing arises as a by-product during the production of NH_3.

For S2 and S3, the NH_3 is the product of the reaction between syngas and methanol (CH_3OH). Syngas is provided by sugarcane bagasse gasification in an entrained flow reactor (EFG) using air as a gasifying fluid, and CH_3OH is obtained from the interaction between CO and H_2, also processed from natural gas. The CO_2 used in S2 is contained in the waste gas from various processes and must be concentrated and compressed before feeding the reactor where the $(NH_2)_2CO$ is obtained (looping urea). This treatment comprises two stages: (i) CO_2 extraction from the gas stream by contact with monoethanolamine (MEA: 15 – 20%$_{w/w}$) and (ii) contaminant removal (including MEA) until the final product reaches 99%$_{v/v}$ CO_2. The CO_2-rich gas is liquefied by compression (675°C and 150 bar) before entering the urea synthesis plant. Carbon dioxide consumed in S3 is also recovered from the gas released from the urea loop reactor.

Table 1: Sources of NH_3 and CO_2 consumed in urea synthesis via the Bosch-Meiser process

Scenario	Source of NH_3	Source of CO_2
S1	Haber-Bosh process (H_2: steam reforming)	Bosch-Meiser process (extraction with MEA)
S2	Syngas (Gasification of sugarcane bagasse)	Waste gas (extraction with MEA)
S3	Syngas (Gasification of sugarcane bagasse)	Bosch-Meiser process (extraction with PSA)

The stream, originally containing 66%$_{v/v}$ of CO_2, circulates through a pressure swing adsorption (PSA) unit, until the concentration of carbon dioxide exceeds 95%$_{v/v}$. As occurs in S2, the CO_2 stream is also compressed before its reinjection into the reactor.

Life Cycle Modeling

The application of the LCA technique followed methodological guidelines described in the ISO 14044 standard for the attributional modality. The analysis occurred for a scope from cradle to gate and

considered a Reference Flow (RF) of '1.0 kg urea, fertilizer grade'. The use of process simulation to specify each scheme made the environmental modeling based only on secondary data. Furthermore, the multifunctional situations identified in each arrangement were treated by allocation based on physical criteria. Only Global Warming Potential (GWP) and Primary Energy Demand (PED) impact categories were evaluated in this study. Such effects were chosen because they corroborate the expectations of the research, to reduce the consumption of fossil assets and the emissions of GHG.

Results and Discussion

Table 2 presents the environmental performances of GWP and PED for the synthesis of urea from the arrangements depicted in scenarios S1 – S3. These results indicate that for PED, the fossil route is more suitable than the alternative processes. The impacts of S1 originate from the consumption of crude oil (13.2 MJ/RF) for heavy oil production, an input of NH_3 synthesis via steam reforming of natural gas. In addition, 8.1 MJ/RF is caused by natural gas burning (also) to generate the heat that keeps the Bosch-Meiser process at 160°C. S2 and S3 were surpassed by S1 due to the consumption of natural gas in the CH_3OH plant, as this is both a process input and a source of utility (0.43 m^3 and 16.4 MJ/ kg CH_3OH).

Table 2: GWP and PED impacts from urea synthesis from different sources of NH_3 and CO_2

Impact Category	Unit (/RF)	Scenarios		
		S1	S2	S3
GWP	kg CO_{2eq}	2.48	1.85	1.51
PED	MJ	24.8	50.9	51.9

The study also shows that using NH_3 derived from sugarcane bagasse gasification and CO_2 recovered from the process reactor via PSA brings gains for GWP. The common contributions of S3 and S2 to the category are due to CO_2 emissions in the urea loop reactor and the synthesis of ammonia (382 and 154 $gCO_{2\,eq}$/FR), and the releases of GHG for heat supply from CH_3OH and $(NH_2)_2CO$ (412 and 374 g $CO_{2\,eq}$/RF). However, their performances differ because the energy demand of PSA is almost three times less impactful for GWP than the thermal demand required by the MEA system. Finally, the performance of S1 in GWP is deeply affected by carbon dioxide emissions from steam reforming (1.46 kg $CO_{2\,eq}$/kg NH_3) and, once again, by the thermal demand of the Bosch-Meiser process.

Acknowledgements: The authors are grateful to the Coordination of Improvement of Higher Education Personnel (CAPES: Financial Code 001) for the financial support to carry out this project.

References:

Baena-Moreno, F. M. et al., 2019. Carbon capture and utilization technologies: a literature review and recent advances. Energy Sources, Part A, *41,12*, 1403–1433.

Cardoso, H. F., 2019. Desempenho ambiental e energético da gaseificação de biomassa de cana-de-açúcar como rota alternativa de produção de amônia, São Paulo.

6th International Conference and Postgraduate Colloquium for Environmental Research 2022 (POCER 2022) 9 - 11 June 2022
Langkawi, Kedah, Malaysia

PCR11042022 – 101: Heavy Metal effect on seed of *C. comosum*: morphological and molecular study

Modhi O. Alotaibi[1]

[1] Department of Biology, College of Science, Princess Nourah Bint Abdulrahman University, Postal Code 84428, Riyadh, Saudi Arabia.

Keywords: Wild plant; phytoremediation; lead; cadmium; germination; protein

Extended Abstract

Background: Increased concern about environmental contamination by heavy metals that affect human health via food chain have led to necessity for developing new strategies to overcome such problem. Therefore, it is essential to identify the exact mechanism of heavy metals from the soil on seeds characteristics. Current investigation aimed to study the effect of lead (Pb) and cadmium (Cd) on the germination of *Calligonum comosum* seeds under laboratory conditions via physiological and molecular parameters. To address our goal, treatments were performed by germinating *C. comosum* seeds in Petri dishes and irrigating them separately with solutions of lead and cadmium at concentrations of 25, 50, 75 and 100 μM/L for a period of three weeks. Consequently, germination percentage and speed were calculated as well as protein profiles of seeds treated with heavy metals were examined by SDS-PAGE. Further influence of heavy metals on antioxidant enzymes catalase (CAT) and Beta subunit of ATP (AtpB) activities was assessed. The germination percentage and speed of *C. comosum* seeds were affected by both treatments and reduced in dose dependent style. SDS-PAGE analysis indicated that, exposure to both metal types led to the disappearance and degradation of some protein compared to untreated controls. Furthermore, western blot analysis indicated that the activity of catalase and beta subunit of ATP in the seeds were induced under Cd and Pb stress conditions. Treatments of *C. comosum* by Cd and Pb enhanced protein degradation and denaturation beside oxidation stress leading to reduction in seeds viability and therefore, seed germination and speed were reduced. It was also approved that oxidoreduction proteins and those involved in ATP synthesis were enhanced in *C. comosum* as response to Cd and Pb stress which might be a mechanism for seeds to tolerate heavy metal stress.

6th International Conference and
Postgraduate Colloquium for
Environmental Research 2022 (POCER
2022) 9 - 11 June 2022
Langkawi, Kedah, Malaysia

PCR11042022 – 102: Estimating ammonium changes in pilot and full - scale constructed wetlands using kinetic model, linear regression and machine learning

X C. Nguyen[1,2], JaeHoon Jeung [2], SW. Chang[2], Wjin Chung[2], BX Thanh[2], D. Duc Nguyen3,*

[1]Faculty of Environmental Chemical Engineering, Duy Tan University, Da Nang, 550000, Vietnam

[2]Faculty of Environment and Natural Resources, Ho Chi Minh City University of Technology, Ho Chi Minh City, Viet Nam

[3]Department of Environmental Energy Engineering, Kyonggi University, Republic of Korea

* **Corresponding author email address**: nguyensyduc@gmail.com (DDN)

Keywords: Ammonium, full scale constructed wetland, kinetics, linear regression, machine learning, pilot.

Abstract

As an attractively nature-based wastewater treatment method and has been popularly applied for a wide range of effluents, but not mesocosm-scale constructed wetlands (CWs), pilot or full-scale CW with a large surface area and long operation time are more meaningful in real applications. This work compared kinetics, linear regression (LR), and machine learning (ML) models to forecast effluent ammonium ($NH4_{ef}$) in pilot or full-scale CWs. From screening 1476 papers, 24 pilot and full-scale CW studies were selected to extract data - contains 15 features and 975 data points. Nine models fitted such data, and the results disclosed that linear models were not capturing CW's effluent well compared to non-linear ML algorithms. For training data, Monod kinetic model predicted the worst with RMSE of 41.84 mg/L and R^2 of 0.34, followed by simple LR (RMSE 24.29 mg/L and R^2 0.77) and multiple LR (RMSE 22.63 mg/L and R^2 0.80). Meanwhile, Cubist and Random forest (RF) achieved high performances with 12.01±5.38 in RMSE & 0.93±0.07 in R^2, and RMSE of 15.94±10.69 and R^2 of 0.91±0.08, respectively. For new data, trained RF performed the best in predicting $NH4_{ef}$, with R^2 of 0.93, RMSE of 13.48 mg/L and mean absolute percentage error of 0.38%. Thus, RF is recommended for forecasting effluent ammonium concentration in CW.

Graphical abstract

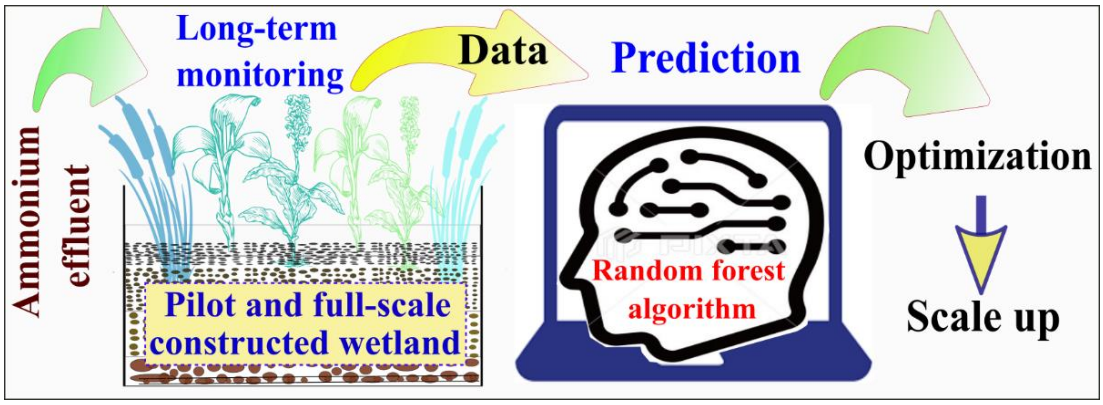

Acknowledgements: The authors thank the National Research Foundation of Korea (Grant No. 2020R1A2C1101849).

6th International Conference and
Postgraduate Colloquium for
Environmental Research 2022 (POCER
2022) 9 - 11 June 2022
Langkawi, Kedah, Malaysia

PCR12042022 – 103: Utilization of Biomass Wastes as Sustainable Electrocatalyst Precursors in Metal-Air Batteries: A Review

Brenda-Ai-Lian Lim[a], Steven Lim[a,b*], Yean-Ling Pang[a,b], and Siew-Hoong Shuit[a,b]

[a] Department of Chemical Engineering, Lee Kong Chian Faculty of Engineering and Science, Universiti Tunku Abdul Rahman, Sungai Long Campus, Jalan Sungai Long 43000 Kajang, Selangor, Malaysia

[b] Centre for Photonics and Advanced Materials Research, Universiti Tunku Abdul Rahamn, Malaysia

- Corrensponsing Author E-mail: stevenlim@utar.edu.my

Keywords: Biomass waste; Metal-air battery; Electrocatalyst.

Extended Abstract

The progress of research done on biomass waste-derived carbon materials for air electrodes used in metal-air batteries were reviewed in this report. This report also aims to provide greater understanding as well as to identify the strength and challenges of metal-air batteries (MAB), biomass wastes as precursor and the synthesis steps of carbon materials from biomass wastes as well as to propose several research routes for the shortcomings of carbon material synthesis from biomass wastes. MAB is a promising energy storage technology due to its favorable features compared to the conventional lithium-ion batteries (LiB) such as high theoretical energy density, lower cost and safer characteristics (Chen et al. 2020). However, MAB is rarely applied commercially due to the sluggish reaction kinetics and mass transfer of the discharge products at the air cathode. The performance of a rechargeable metal air battery is mainly influenced by the Oxygen Reduction Reaction (ORR) as well as the Oxygen Evolution Reaction (OER) at the air cathode during the discharge and charge process, respectively (Lee et al. 2016). Figure 1 illustrates the transfer of ions and charges during charge and discharge.

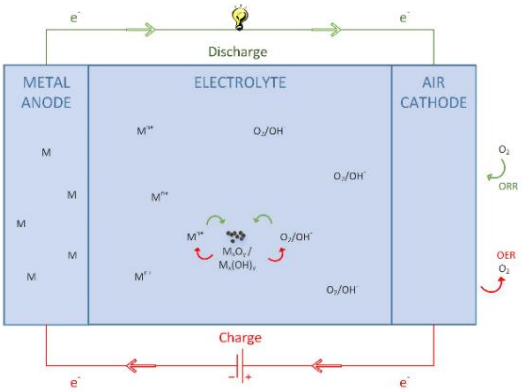

Figure 19 Movements of ions and charges during MAB mechanism

The practical use of MAB was hindered due to the absence of a stable and active bifunctional electrocatalyst. To date, the most commercially implemented catalysts for ORR and OER are the Pt-based catalysts, RuO_2 and IrO_2, respectively. These materials are costly, limited and have inferior stability which hindered MAB from being used commercially (Zeng et al. 2020). Carbon materials were found to be able to perform as an electrode material with its porous structure while acting as a catalyst towards the charge-discharge reactions (Zhu & Xu 2020). Carbon nanotube (CNT) has advantageous propeties as an electro-catalyst material for air cathode but it is not commercially implemented due to its high cost. Hence, it is desired to find a cheaper and comparably efficient alternative electro-catalyst material as an air electrode for MAB. Due to its abundance and renewability, biomass wastes have great potential as low-cost and sustainable precursors to synthesize carbon materials while achieving waste reduction. Biomass wastes are generally composed of carbohydrates and polysaccharides in which they can offer several elements such as carbon, phosphorus, nitrogen and sulfur at the same time which enables the synthesis of carbon materials and heteroatom doping simultaneously. The synthesis of carbon electrocatalyst from biomass waste usually include but not limited to pretreatments, carbonization, activation and doping. Table 1 summarizes the purposes and additional information of each synthesis steps (Zhang et al. 2020).

Table 10 Purpose and Method of Individual Synthesis Steps

Steps	Purpose	Method
Pretreatment	Remove impurities and moisture as well as size reduction.	Washing with water, drying in oven or under sunlight, grinding or milling.
Carbonization	Decompose precursor into heteroatoms. Affects physical	Pyrolysis - inert condition at temperature above 450°C

	and chemical properties of the carbon including pore size, structure and elemental content	Hydrothermal - in liquid medium within a high-pressure vessel at 150 to 250 °C and 30 minutes to 30 hours - sometimes implemented as a pretreatment step before pyrolysis
Activation	Increased surface area as well as adjustable pore size and distribution	Physical Activation - steam or CO_2 purging at high temperature Chemical Activation - KOH, H_3PO_4, $ZnCl_2$ impregnation
Heteroatom and metal doping (N, P, S, Si, etc)	Improve the catalytic activity by modification in charge distribution and defect formation.	Commonly carried out through pyrolysis of carbon material with compound containing the desired elements.

Acknowledgements: The authors thank the Ministry of Education (MOE) Malaysia for the Fundamental Research Grant Scheme (FRGS/1/2018/TK10/UTAR/02/1) as well as Universiti Tunku Abdul Rahman Research Grant (IPSR/RMC/UTARRF/2020-C2/W01) for the financial support and Universiti Tunku Abdul Rahman Research Publication Scheme (6251/S06) for the scholarship to Ms. Brenda Lim Ai-Lian.

References

Chen, X., Memon, I., Song, L., Song, P., Zhang, Y., Maria, S., Saadat, N., Yang, W., Dhakal, H., Li, H., Sain, M. & Ramakrishna, S., 2020, "A review on recent advancement of nano-structured-fiber-based metal-air batteries and future perspective," *Renewable and Sustainable Energy Reviews*, 134.

Lee, D.U., Xu, P., Cano, Z.P., Kashkooli, A.G., Park, M.G. & Chen, Z., 2016, "Recent progress and perspectives on bi-functional oxygen electrocatalysts for advanced rechargeable metal-air batteries," *Journal of Materials Chemistry A*, 4(19), 7107–7134.

Zeng, K., Zheng, X., Li, C., Yan, J., Tian, J.H., Jin, C., Strasser, P. & Yang, R., 2020, "Recent Advances in Non-Noble Bifunctional Oxygen Electrocatalysts toward Large-Scale Production," *Advanced Functional Materials*, 30(27), 1–23.

Zhang, G., Yao, Y., Zhao, T., Wang, M. & Chen, R., 2020, "From Black Liquor to Green Energy Resource: Positive Electrode Materials for Li-O2 Battery with High Capacity and Long Cycle Life," *ACS Applied Materials and Interfaces*, 12(14), 16521–16530.

Zhu, Z. & Xu, Z., 2020, "The rational design of biomass-derived carbon materials towards next-generation energy storage: A review," *Renewable and Sustainable Energy Reviews*, 134, 110308.

6th International Conference and
Postgraduate Colloquium for
Environmental Research 2022 (POCER
2022) 9 - 11 June 2022
Langkawi, Kedah, Malaysia

PCR12042022 – 104: Comparative growth inhibitory activities of resin cyanoacrylate nanoparticles

Fean Davisunjaya Sarian[a, *], Kazuki Ando[a] , Shorta Tsurumi[a] , Ayaka Shimizono[a] , Sara Yoshimura[a] , and Takeshi Ohama[a]

a School of Environmental Science and Engineering, Kochi University of Technology, Kochi, Japan

*Corrensponding Author E-mail: fean.d.sarian@kochi-tech.ac.jp

Keywords: cyanoacrylate nanoparticles, oxidative stress, reactive oxygen species

Extended Abstract

Despite the exponential growth in the development and application potential of engineered nanomaterials, there are safety concerns surrounding their wide exploitation. In recent years, numerous scientific investigations have been performed to evaluate various kinds of nanoparticles impact on organisms and cells. However, information on the toxicity of nano-sized resin cyanoacrylate particles (PACA-NPs) is still limited. It is well-known that PACA-NPs are instable and decompose easily to produce cyanoacetate and formaldehyde. Recent study showed that ethyl cyanoacrylate nanoparticles (ECA-NPs), one of PACA-NPs studied, induced significant mortality in wide range of organisms, bacteria, yeast, and microalgae. The growth inhibitory effect of PACA-NPs on microorganisms was distinguished by monitoring microbial growth in the presence and absence of nanoparticles. Effect of ECA-NPs have been analyzed on agar plate in liquid medium against Gram-positive bacteria (*Bacillus subtilis, Brevibacillus agri, Microbacterium aurum, Propionibacterium acnes, Staphylococcus aureus*), Gram-negative bacteria (*Escherichia coli, Klebsiella pneumoniae, Pseudomonas aeruginosa, Salmonella typhimurium, Serratia marcescens*), yeasts (*Saccharomyces cerevisiae, Schizosaccharomyces japonicas, Schizosaccharomyces pombe*), and a microalga *(Chlamydomonas reinhardtii*). We found some microorganisms are more susceptible to ECA-NPs than others. Among the tested microorganisms, Gram-positive bacteria (*Bacillus subtilis, Microbacterium aurum, Staphylococcus aureus*), Gram-negative bacteria (*Escherichia coli, Salmonella typhimurium*), yeast (*Schizosaccharomyces japonicas*) were the most susceptible to ECA-NPs. Addition of N-acetyl Lcysteine, a reactive oxygen species (ROS) scavenger, significantly reduced the effect of the nanoparticles, regardless of the exposed organisms or species of the nanoparticles. This fact suggests that PACA-NPs induce cell death or tentative cell growth inhibition by inducing the generation of excessive amounts of ROS in the cells. The results of this study could help to develop environmental standards and regulations for PACA-NPs applications.

Acknowledgements: The authors thank the Japan Science, Sports and Culture, Grant-in Aid for Scientific Research ©

6th International Conference and
Postgraduate Colloquium for
Environmental Research 2022 (POCER
2022) 9 - 11 June 2022
Langkawi, Kedah, Malaysia

PCR12042022 – 105: Screening and Benchmarking of Commercial Corrosion Inhibitors for Organic Acid Corrosion Mitigations

Almila Hassan[a], Khairulazhar Jumbri[a*], Zulkifli Merican Aljunid Merican[a], Kee Kok Eng[b], Noorazlenawati Borhan[c], Nik M Radi Nik M Daud[c], Azmi M Nor A[c], Firdaus Suhor[c], and Roswanira Abdul Wahab[d]

[a] Department of Fundamental and Applied Sciences, Universiti Teknologi PETRONAS, 32610 Seri Iskandar, Perak, Malaysia

[b] Department of Mechanical Engineering, Universiti Teknologi PETRONAS, 32610 Seri Iskandar, Perak, Malaysia

[c] PETRONAS Research Sdn Bhd, 43000 Bandar Baru Bangi, Selangor, Malaysia.

[d] Department of Chemistry, Faculty of Science, Universiti Teknologi Malaysia, 81310 UTM Johor Bahru, Johor, Malaysia.

- Correnspoonsing Author E-mail: khairulazhar.jumbri@utp.edu.my

Keywords: Corrosion inhibitors; metal steel; carbon dioxide; organic acid; inhibition efficiency.

Extended Abstract

More aggressive reservoir conditions, such as the higher concentrations of CO_2 corrosive gases, have a massive effect on corrosion. Moreover, the presence of additional aqueous species such as organic acids has complicated the conditions and enhanced corrosion to the maximum rate. This study investigates and screens three commercial corrosion inhibitors on their performance in mitigating corrosion in high CO_2 conditions with the presence of organic acids. These investigations were conducted via chemical elucidations to study the functional groups present in the compounds that affect the inhibition performance and the electrochemical measurements to evaluate the inhibition activities and efficiency of these commercial inhibitors under the extreme conditions of high CO_2 and organic acids. The results indicated that only two of these three inhibitors gave a high inhibition efficiency of 90% in the absence and presence of organic acid, while the other gave the worst inhibition performance under these

conditions. The elucidation of these inhibitors also found that specific functional groups such as hydroxy, carboxylic acid, alkyl and alkene presence in the structure were believed to affect the inhibition performance of these commercial inhibitors in mitigating corrosion. These could be used as a future reference for the new development of corrosion inhibitors in similar conditions.

6th International Conference and
Postgraduate Colloquium for
Environmental Research 2022 (POCER
2022) 9 - 11 June 2022
Langkawi, Kedah, Malaysia

PCR12042022 – 106: Theoretical Studies of Quaternary Ammonium Surfactant Corrosion Inhibitors on FE (110) in Acetic Acid Media via DFT Calculation and MD Simulation

Mohd Sofi Numin[a], Almila Hassan[a], Khairulazhar Jumbri[a*], M Faisal Taha[a], Kee Kok Eng[b], Noorazlenawati Borhan[c], Nik M Radi Nik M Daud[c], Azmi M Nor A[c], Firdaus Suhor[c], Roswanira Abdul Wahab[d]

[a]Department of Fundamental and Applied Sciences
Universiti Teknologi PETRONAS, 32610 Seri Iskandar, Perak, Malaysia

[b]Department of Mechanical Engineering
Universiti Teknologi PETRONAS, 32610 Seri Iskandar, Perak, Malaysia

[c]PETRONAS Research Sdn Bhd
43000 Bandar Baru Bangi, Selangor, Malaysia

[d]Department of Chemistry, Faculty of Science
Universiti Teknologi Malaysia, 81310 UTM Johor Bahru, Johor, Malaysia

- Corrensponsing Author E-mail: khairulazhar.jumbri@utp.edu.my

Keywords: Corrosion inhibitor; Quaternary ammonium; MD simulation; DFT calculation; Adsorption.

Extended Abstract

Corrosion can cause a major failure to the pipelines and destroy the transportation systems in the oil & gas industry. The addition of corrosion inhibitors (CI) was the most promising method in reducing the corrosion rate of the metal surface in the pipelines. The development of a new CI molecule becomes the primary problem between researchers due to the lack of an in-depth investigation on the CI molecule's mechanism as a corrosion inhibitor. Hence, in this study, density functional theory (DFT) calculation and molecular dynamics (MD) simulation was used to do an in-depth study on the inhibition mechanism of quaternary ammonium surfactant CI molecules with a different chain length (C6, C8, C10, C12, C14, C16, and C18) in the presence of 1 m HCl and 500 ppm acetic acid on the Fe (110)

metal surface. Results from DFT calculation showed that all surfactant CI molecules have good inhibition properties where the ammonium groups (N^+) act as a reactive centre to donate electrons to the metal surface with low band-gap energy (1.26 eV). In the MD simulation, C12 showed the most promising CI molecules with high adsorption energy and binding energy value, low diffusion coefficient towards the corrosion particles and randomly scattered at low concentration that give better adsorption towards the Fe (110) metal surface. The inhibition efficiency of all CI molecules based on computer modelling data and the success of an in-depth study on the theoretical understanding of quaternary ammonium surfactant CI molecules in the acidic medium corrosion system towards metal surface could be used as the future development of new surfactant CI molecules with ammonium-based functional groups.

6th International Conference and
Postgraduate Colloquium for
Environmental Research 2022 (POCER
2022) 9 - 11 June 2022
Langkawi, Kedah, Malaysia

PCR13042022 – 108: Quantification of Leachate Using Material Flow Analysis and Transport of Leachate Using Water Quality Modelling

Tengku Nilam Baizura Tengku Ibrahim[a*] , Noor Zalina Mahmood[b] , and Faridah Othman[c]

a Department of Environmental Health, Faculty of Health Science, Universiti Teknologi MARA, Pulau Pinang Branch, Bertam Campus, Pulau Pinang, Malaysia

b Institute of Biological Sciences, Faculty of Science, University of Malaya, Kuala Lumpur, Malaysia

c Department of Civil Engineering, Faculty of Engineering, University of Malaya, Kuala Lumpur, Malaysia

• Corrensponsing Author E-mail: tengkunilam@uitm.edu.my

Keywords: Solid waste, Leachate, Water quality, Material Flow Analysis, Water Quality Index, QUAL2K.

Extended Abstract

Leachate from landfills is known to be one of the major environmental impacts, particularly those constructed near rivers. Therefore, this study is conducted to assess the impact of discharged leachate, using SL Landfill and Sembilang River as the case study. Solid waste generated served as input data on volume and composition of the solid waste that was sent to SL Landfill. A material flow analysis (MFA) is employed to trace the fate of solid waste that has been disposed and leachate that is produced at SL Landfill using STAN software. Six parameters in Water Quality Index (WQI), viz. DO, pH, BOD, COD, NH3N, TSS were used to define the quality of the river water. A total of 80 water samples were collected monthly for 1 year from 10 sampling stations. In order to predict and assess the pollutant transport in Sembilang River basin, QUAL2K was used as a simulation model. Water quality parameters (DO, BOD and NH3-N) were chosen to model the impact from the SL landfill effluent towards Sembilang River. The findings showed that the highest composition of waste that was present at the landfill can be categorized as food waste with 32% of the total waste input. Results from the MFA model showed that the amount of leachate generated from SL landfill was 123,386 m3 /year. The finding had also successfully identified the input and output flow of SL Landfill, with an overall input values of 948,505 ton per year and the output at 393,292 ton per year. From 3 different possible scenarios that were chosen, results from the MFA showed that composting was the most effective method in terms of reducing leachate production in SL Landfill which expected to reduce leachate production by up to 92%. The Sembilang River water quality results show that it falls in Class III of the WQI, which ranges from

43.46 to 68.03 mg/L. Different water quality model scenarios were simulated in order to assess the pollutant transport on the Sembilang River water quality and it was found that the effects of different scenarios for water quality parameters were particularly noticeable for DO and BOD. However, for the NH3N parameters there were no significant change and had remained in Class IV and V. This was due to the high NH3N concentration from a few points along the river. These findings showed that the MFA, water quality assessment and modeling were found to be the best methods to predict and analyzed the composition of waste to the leachate production and the effect to the river water pollution.

6th International Conference and Postgraduate Colloquium for Environmental Research 2022 (POCER 2022) 9 - 11 June 2022
Langkawi, Kedah, Malaysia

PCR13042022 – 110: A Short Review on Recent $NiCo_2O_4$-based Composite Materials for Fuel Cell Applications

Nor Fatina Raduwan[a] , Norazuwana Shaari[a*]

a Fuel Cell Institute Universiti Kebangsaan Malaysia, Selangor, Malaysia

• Corrensponsing Author E-mail: norazuwanashaari@ukm.edu.my

Keywords: $NiCo_2O_4$; composite; synthesis; electrochemical; morphology; fuel cell.

Extended Abstract

Recent studies demonstrate outstanding electrochemical activity and better electrical conductivity of binary metal nickel cobaltite ($NiCo_2O_4$). $NiCo_2O_4$ exhibits good material stability and higher electronic conductivity, at least two orders of magnitude higher than its single-component metal oxides NiO and Co_3O_4. These metal oxides also show impressive potential as composited based materials for fuel cell application and can be synthesized through various methods.

Introduction: With the rapid depletion of fossil fuels due to colossal energy demand and environmental pollution, there is a critical effort to develop green and sustainable electrochemical energy conversion devices. Among the various energy conversion system, a fuel cell has gained significant interest as it produces low-to-zero emissions, high efficiency coupled with high energy density (Fang et al. 2020). However, the major obstacle that hinders its commercialization comes from the high material cost for its components. Hence, the exploration of low cost and high-performance materials has been actively carried out in recent days by utilizing non-noble materials with high catalytic activity such as low-cost binary transition metals like $NiCo_2O_4$. Various synthesis methods like electrodeposition, precipitation and hydrothermal were reported to prepare different morphological nanostructures $NiCo_2O_4$. Assembled from several levels of structure, 3D nanostructures possess outstanding properties compared with 1D and 2D nanostructures in terms of material stability and electrochemical performance due to larger specific surface area (Li et al. 2019).

Table 1: Different morphologies of $NiCo_2O_4$ for various fuel cell application

$NiCo_2O_4$ structures	Method of synthesis	Application	References
Nanorods	Hydrothermal	Electrocatalyst for MOR	(Narayanan & Bernaurdshaw 2020)
3D ordered porous structures	Salt precipitation	Electrocatalyst for ORR	(Fang et al. 2020)
Needle-like	Hydrothermal	Electrode for MOR	(Hamdedein et al. 2021)
Flower-like	Hydrothermal	Dual functional supercapacitors and methanol electro-oxidation	(Gopalakrishnan & Badhulika 2021)

$NiCo_2O_4$-based composites materials As single $NiCo_2O_4$ suffers from poor redox reaction and stability issues that lead to low performance, combining it with other materials like carbon, metal and conducting polymers seems to overcome the disadvantages of individual components. For example, Narayanan and Bernaurdshaw had developed highly active hybrid materials of reduced graphene oxide (rGO) supported $NiCo_2O_4$ ($NiCo_2O_4$/rGO) nano-rods as electrocatalyst for methanol oxidation reaction (MOR). The morphologies and microstructure of $NiCo_2O_4$/rGO were elucidated by SEM, as shown in Figure 1(a). This composite showed 3.11 folds (78 mA/cm2) and was nearly 50 times higher in electrocatalytic activity and stability, respectively, compared to commercial catalysts (Narayanan & Bernaurdshaw 2020).

The resulting functional hierarchical nanostructures contribute to a more high level of electrochemical performance, as reported by Gopalakrishnan and Badhulika. They had synthesized unique hierarchical dahlia flower-like $NiCo_2O_4$ nanograss/$NiCoSe_2$ nanosheets on Ni foam (NCO/NCS/NF) as bifunctional binder-free electrodes for high energy density hybrid supercapacitors and methanol electro-oxidation applications. The as-synthesized nanoflowers $NiCo_2O_4$ and $NiCoSe_2$ nanosheets are uniformly grown on a substrate by electrodeposition technique. The nanoflowers $NiCo_2O_4$ and $NiCoSe_2$ nanosheets are very thin, which can be observed in the magnified images of Figure 1(b). Impressively, the electrochemical test reveals that the obtained hybrid exhibited good specific capacitance and stability as supercapacitor electrode and high tolerance toward methanol oxidation and current density as fuel cell electrocatalyst (Gopalakrishnan & Badhulika 2021).

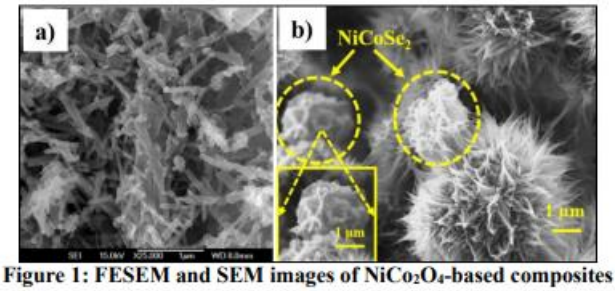

Figure 1: FESEM and SEM images of $NiCo_2O_4$-based composites

Conclusion: Notably, $NiCo_2O_4$-based materials are widely used on energy storage applications like supercapacitors based on a higher number of past publications. However, very few studies on this material in fuel cell applications are limited to electrocatalyst and electrode synthesis. $NiCo_2O_4$-based composite materials can be extensively used on other fuel cell components such as PEM due to their potential and performance in electrocatalysts and electrodes. Different morphologies can be synthesized to yield the best performance based on different applications in fuel cell. Besides that, the approach of fabricating hybrid materials composites by combining different materials has been proved to be a promising strategy to boost the electrochemical performance of $NiCo_2O_4$.

Acknowledgements: This work was supported by Universiti Kebangsaan Malaysia (UKM) via research sponsorship DIP-2020-015.

6th International Conference and
Postgraduate Colloquium for
Environmental Research 2022 (POCER
2022) 9 - 11 June 2022
Langkawi, Kedah, Malaysia

PCR13042022 – 111: Effect of Cellulose Passivator on Enhancing Power Conversion Efficiency of Perovskite Solar Cell in High Humidity Condition

Muhammad Athir Anuar[a], Danial Hakim Hisyam[a], Lim Mook Tzeng[a*], Mohamad Firdaus Mohamad Noh[b], Mohd Asri Mat Teridi[b]

[a] Renewable Energy Green Technology Department,
TNB Research, 43000 Kajang, Selangor, Malaysia

[b] Solar Energy Research Institute,
Universiti Kebangsaan Malaysia, 43600 Bangi, Selangor, Malaysia

- Correnspondding Author E-mail: mook.tzeng@tnb.com.my

Keywords: Perovskite Solar Cells; Ethyl Cellulose; Power Conversion Efficiency, Current Density-Voltage; Fill Factor

Extended Abstract

Perovskite solar cell (PSC) is a type of solar cell that converts sunlight to electricity, which is called the third generation solar cell. It uses a perovskite structured material such as methylammonium lead iodide ($CH_3NH_3PbI_3$) as the light harvested layer (Khalid et al., 2022; Kumary, 2022). Figure 1 shows the example of a complete cell of a PSC. According to (Wu et al. 2021), PSC appeared to be the fastest progressing solar cells in terms of power conversion efficiency (PCE) since their first development in 2009 from 3.1% to 25.7%. PSC has the potential to be commercialized in large scale in the future since it requires low material cost, easier to manufacture and the flexible device compared to silicon based PV cells (Kukkikatte Ramamurthy Rao et al., 2021; Seri et al., 2021).

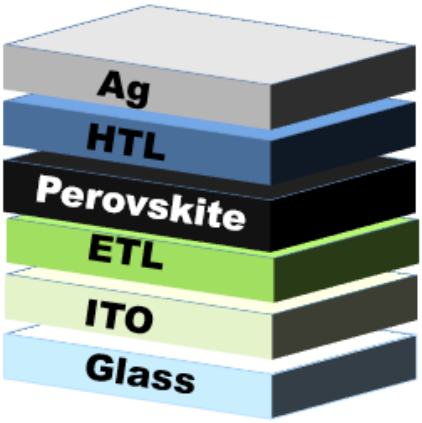

Figure 1: The Example of Complete Cell of a Perovskite Solar Cell (Krückemeier et al., 2021).

For a PSC device, the properties to compare performance and effciencies involves open- circuit voltage (V_{OC}), short-circuit current (I_{SC}) and fill factor (FF) (see Eq.1).

$$PCE = \frac{I_{SC} V_{OC} FF}{P_{in}}$$

Where P_{in} is 1000W/m^2 from sunlight.

The barrier between the layers's interface and the presence of grains remain the dominant factors that affect passage of the charge currents in a PSC device (Hu et al., 2020). The defects in the interface between layers caused the tranfer of electrons become inefficient. Therefore, addition of biomaterial based passivation such as cellulose is required to increase the device's efficiency (Gao et al., 2018; Yang et al., 2019). This study compares the PCE of PSC using three different perovskite layers. The PSC layers investigated were standard (no passivation), ethyl cellulose (EC) passivated and poly (methyl methacrylate) passivated perovskite layers (see Figure 2).

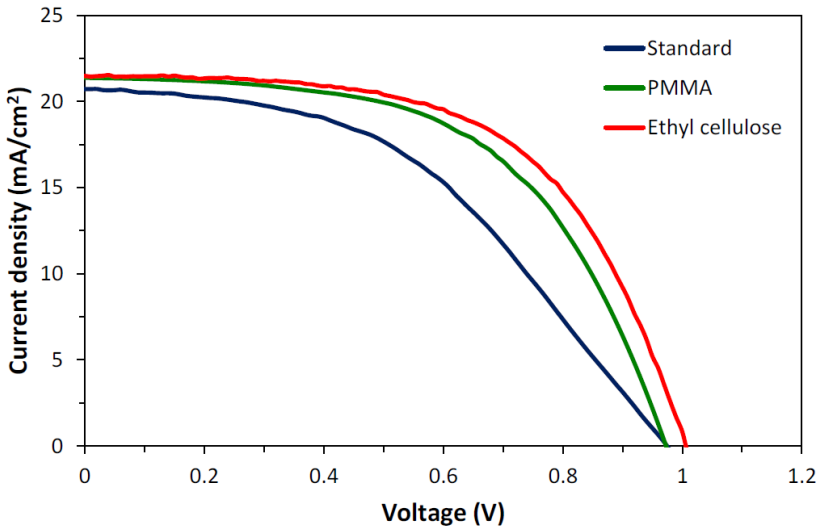

Figure 2: The Current Density Plotted with Respect to The Voltage for Non-passivated PSC (Blue), PMMA Passivated PSC (Green) and Ethyl Cellulose Passivated PSC (Red).

From the solar simulator and photovoltaic analyzer, EC passivated PSC showed highest efficiency of 12.5%, followed by PMMA passivated PSC of 11.8% and standard, non passivated PSC at 9.2%. The optimum PCE by using EC passivation had a short circuit current density (J_{SC}), open circuit voltage (V_{OC}), and fill factor (FF) of 21.5 mA/cm2, 1.006 V, and 57.95%, respectively. This demonstrates that biomaterials such as cellulose are able to passivate the defect and improve the performance of PSC.

Acknowledgements: The authors would like to acknowledge the financial assistance from Tenaga Nasional Berhad (TNBR/SF392/2021) and those who have contributed directly or indirectly to this work..

References

Gao, C., Yuan, S., Cui, K., Qiu, Z., Ge, S., Cao, B., & Yu, J. (2018). Flexible and Biocompatibility Power Source for Electronics: A Cellulose Paper Based Hole-Transport-Materials-Free Perovskite Solar Cell. *Solar RRL*, *2*(11), 1800175. https://doi.org/10.1002/solr.201800175

Hu, Q., Chen, W., Yang, W., Li, Y., Zhou, Y., Larson, B. W., Johnson, J. C., Lu, Y.-H., Zhong, W., Xu, J., Klivansky, L., Wang, C., Salmeron, M., Djurišić, A. B., Liu, F., He, Z., Zhu, R., & Russell, T. P. (2020). Improving Efficiency and Stability of Perovskite Solar Cells Enabled by A Near-Infrared-Absorbing Moisture Barrier. *Joule*, *4*(7), 1575–1593. https://doi.org/10.1016/j.joule.2020.06.007

Khalid, M., Roy, A., Bhandari, S., Selvaraj, P., Sundaram, S., & Mallick, T. K. (2022). Opportunities of copper addition in CH3NH3PbI3 perovskite and their photovoltaic performance evaluation. *Journal of Alloys and Compounds*, *895*, 162626. https://doi.org/10.1016/j.jallcom.2021.162626

Krückemeier, L., Krogmeier, B., Liu, Z., Rau, U., & Kirchartz, T. (2021). Understanding Transient Photoluminescence in Halide Perovskite Layer Stacks and Solar Cells. *Advanced Energy Materials*, *11*(19), 2003489. https://doi.org/10.1002/aenm.202003489

Kukkikatte Ramamurthy Rao, H., Gemechu, E., Thakur, U., Shankar, K., & Kumar, A. (2021). Techno-economic assessment of titanium dioxide nanorod-based perovskite solar cells: From lab-scale to large-scale manufacturing. *Applied Energy*, *298*, 117251. https://doi.org/10.1016/j.apenergy.2021.117251

Kumary, K. L. U. (2022). *Effect of Copper Phthalocyanine Interfacial Layer on the Performance of Mixed Halide Perovskite Solar Cells*. 80–88. https://doi.org/10.21741/9781644901878-11

Seri, M., Mercuri, F., Ruani, G., Feng, Y., Li, M., Xu, Z.-X., & Muccini, M. (2021). Toward Real Setting Applications of Organic and Perovskite Solar Cells: A Comparative Review. *Energy Technology*, *9*(5), 2000901. https://doi.org/10.1002/ente.202000901

Wu, Z., Li, W., Ye, Y., Li, X., & Lin, H. (2021). Recent progress in meniscus coating for large-area perovskite solar cells and solar modules. *Sustainable Energy & Fuels*, *5*(7), 1926–1951. https://doi.org/10.1039/D0SE01774D

Yang, J., Xiong, S., Qu, T., Zhang, Y., He, X., Guo, X., Zhao, Q., Braun, S., Chen, J., Xu, J., Li, Y., Liu, X., Duan, C., Tang, J., Fahlman, M., & Bao, Q. (2019). Extremely Low-Cost and Green Cellulose Passivating Perovskites for Stable and High-Performance Solar Cells. *ACS Applied Materials & Interfaces*, *11*(14), 13491–13498. https://doi.org/10.1021/acsami.9b01740

6th International Conference and
Postgraduate Colloquium for
Environmental Research 2022 (POCER
2022) 9 - 11 June 2022
Langkawi, Kedah, Malaysia

PCR13042022 – 112: Degradation of Polyethylene Microplastic by Plasma in Liquid Process

Sang-Chul Jung[a] and Heon Lee[a*]

[a] Department of Environmental Engineering
Sunchon National University, Suncheon, Republic of Korea

*Corresponding Author E-mail: honylee@hanmail.net

Keywords: Microplastics; Polyethylene; Plasma in liquid process; Degradation; Hydroxyl radical.

Extended Abstract

It is known that microplastics, which have a size of 5 mm or less, can cause ecosystem disruption through bioaccumulation and behave as toxic substances harmful to human health. Most of the microplastics are organic polymers and are released by personal care products and detergents [Xu *et al.*, 2021]. Microplastics are being detected in effluent and stream water because it is difficult to completely remove them with conventional wastewater treatment, which is a biological treatment [Uheida *et al.*, 2021]. Several studies are being conducted on the removal of microplastic using various processes including photocatalysis, biodegradation, and electro-Fenton oxidation [Du *et al.*, 2021]. Recently, the plasma in liquid process has been attracted to the process for the generation of nanomaterials or removal of pollutants. Plasma in liquid process provides the plasma fields having high energy and generated chemically active species such as hydroxyl radical and excited atoms in an aqueous solution. In this work, we have attempted plasma in liquid process to degrade microplastics in an aqueous solution. Polyethylene (PE) was selected as a target material and the decomposition behavior was considered.

The plasma in liquid process had consisted of a reactor, power supply, and refrigerator. The details of plasma in liquid process were described in our previous literature [Chung *et al.*, 2019]. The initial concentration of PE microplastic was 50 ppm. The degradation rate of PE microplastics was determined by weight loss.

The plasma phenomena in an aqueous solution could generate various chemically active species. Figure 1 shows the optical emission spectra of plasma reactions in deionized water. The five peaks were observed and attributed to hydroxyl radical, hydrogen radical, and oxygen radical. Among chemically active species, hydroxyl radicals have strong oxidizing power and can decompose organic substances in an aqueous solution exactly. The plasma reaction in an aqueous solution is affected by various

parameter as electric operation parameter, conductivity, pH of the solution, etc. The peak intensity of the optical emission spectrum is proportional to the amount of chemically active species. As results of peak intensity were compared by varying the applied voltage of the power supply, the amount of hydroxyl radical and oxygen radical was increased as increasing of applied voltage.

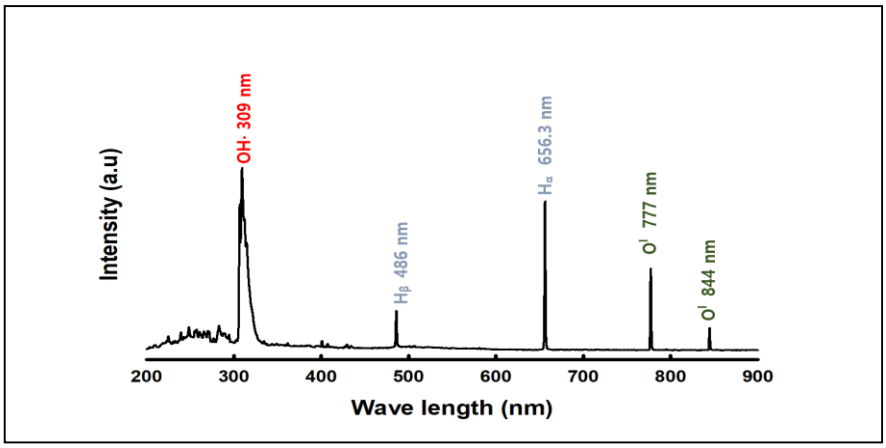

Figure 20: The optical emission spectra of plasma in liquid process with deionized water.

Figure 2 shows the correlation between the applied voltage of power supply and the degradation efficiency of PE microplastics in an aqueous reactant. The degradation efficiency of PE microplastics is actively performed with the increase of the applied voltage. In particular, it can be seen that the degradation efficiency of PE microplastics at 250 V for applied voltage was significantly increased compared to that at 225 V. The hydroxyl radical generated by plasma reaction in an aqueous solution attacks the main polymeric chain of PE microplastics, thereby causing the degradation reaction of PE microplastics [Kamalian *et al.*, 2020]. The degradation of PE microplastics is dependent on the amount of hydroxyl radical. When the applied voltage increased, the amount of hydroxyl radical and oxygen radical was increased so that the degradation efficiency of PE microplastics was increased. Also, the effect of pH of solution on PE microplastics degradation rate was evaluated. As the pH of the aqueous solution was increased, the degradation reaction of PE microplastic was improved. This is because the hydroxyl radical was more generated in the solution with higher pH. In an acidic solution, the hydroxyl radical could be consumed by hydrogen ions in an aqueous solution [Wang *et al.*, 2021].

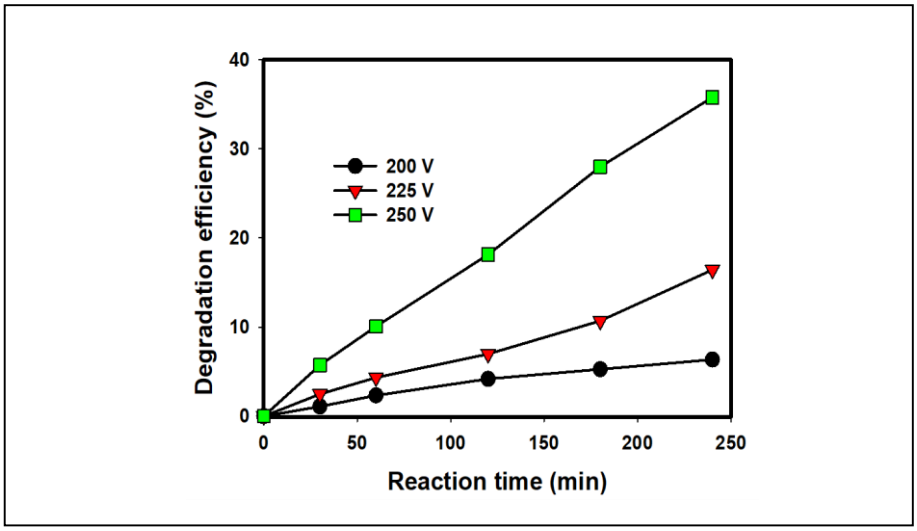

Figure 2: The effect of applied voltages on PE microplastic degradation.

Acknowledgments: This research was supported by Basic Science Research Program through the National Research Foundation of Korea (NRF) funded by the Ministry of Education(NRF-2020R1I1A3073397).

References

Chung, K., Park, I., Bang, H., Park, Y., Kim, S., Kim, B., Jung, S., 2019. Heterogeneous photocatalytic degradation and hydrogen evolution from ethanolamine nuclear wastewater by a liquid phase plasma process. *Sci. Total Environ.*. 676:190-196.

Du, H., Xie, Y., Wang, J., 2021. Microplastic degradation methods and corresponding degradation mechanism: Research status and future perspectives. *J. Hazard. Mater.*. 418:126377.

Kamalian, P., Khorasani, S. N., Abdolmaleki, A., Karevan, M., Khalili, S., Shirani, M., Neisiany, R. E., 2020. Toward the development of polyethylene photocatalytic degradation. *J. Polym. Eng.*. 40:181-191.

Venkataramana, C., Botsa, S. M., Shyamala, P., Muralikrishna, R., 2021. Photocatalytic degradation of polyethylene plastics by $NiAl_2O_4$ spinels-synthesis and characterization. *Chemosphere*. 265: 129021.

Wang, S., Zhou, Z., Zhou, R., Fang, Z., Cullen, P. J., 2021. Effect of solution pH on the characteristics of pulsed gas-liquid discharges and aqueous reactive species in atmospheric air. *J. Appl. Phys.*. 130:103302.

Xu, Q., Huang, Q. S., Luo, T. Y., Wu, R. L., Wei, W., Ni, B. J., 2021. Coagulation removal and photocatalytic degradation of microplastics in urban waters. *Chem. Eng. J.*. 416:129123.

PCR13042022 – 113: Solar-mediated phase-changing materials: Design and innovations on solar energy conversion and storage

Arni M. Pornea and Hern Kim*

Department of Energy Science and Technology
Myongji University, Yongin, Republic of Korea

*Corresponding Author E-mail: hernkim@mju.ac.kr

Keywords: Solar thermal energy storage, Phase changing materials (PCM), Thermal energy storage (TES), Enhanced broadband absorption, Light-thermal-electric conversion

Extended Abstract

Abundant energy sources are readily accessible, and the conversion and storage of these energies are critical in amending the current immense global energy demand, solar energy is recognized as one of the most renewable and sustainable energy sources due to its abundance and comprehensive harvesting techniques. With equal importance, energy conversion, and storage of these techniques are needed to attain optimal solar energy harvesting. Among these solar energy harvesting techniques is phase-changing material. With the ability to seamlessly convert and store an immense amount of solar-thermal energy during phase change transition without any harmful emission, encapsulated PCM (EPCM) provides a benevolent route for solar energy harvesting. However, considering the limited solar absorption and conversion ability of PCM and its traditional support and encapsulating material, which is dominated by conductivity modifications through heterogeneous incorporation of conductive additives towards the EPCM shell. In the premise of effective solar thermal harvesting materials, both spectral solar absorption and light-to-heat conversion efficiency are essential aspects of photo energy cultivation. Approaches for the enhancement of light to heat conversion had been explored such as the following: (i) tuning the broadband absorption capability to cover the full spectral range (UV-Vis-NIR), (ii) tuning the band structure characteristic to facilitate effective light to heat conversion efficiency, and (iii) structural engineering modification to enable better thermal distribution. Inspired by these techniques construction of enhanced encapsulating materials is facilitated, these advanced solar-thermal conversion PCM can effectively facilitate the transformation of light energy into thermal energy, thereby insinuating a significant contribution to sustainable energy application. Light absorbance over

a broad range of the solar spectrum is the first step toward effective solar harvesting. The next step is ensuring the efficient conversion of the absorbed light photons, these were facilitated through bandgap tuning granting non-radiative recombination of the absorbed phonons. Moreover, structure and engineering articulation posed an accretion towards the heat dissipation of the absorbed heat, surpraparticle arrangement is enforced as a compounded encapsulating shell. The distribution of smaller and more photoactive particles onto the interface of the EPCM channels the absorbed energy. Herein a comprehensive strategy and advancement were conferred particularly on the design and engineering of the encapsulating material attributed to effective solar absorption and light to thermal energy conversion. We aim to present a thorough understanding of the light to thermal conversion mechanism. Thereby providing insightful techniques and mechanisms for the fabrication of improved PCM energy harvesting and storage. Moreover, PCM's present struggles and future direction were also conferred.

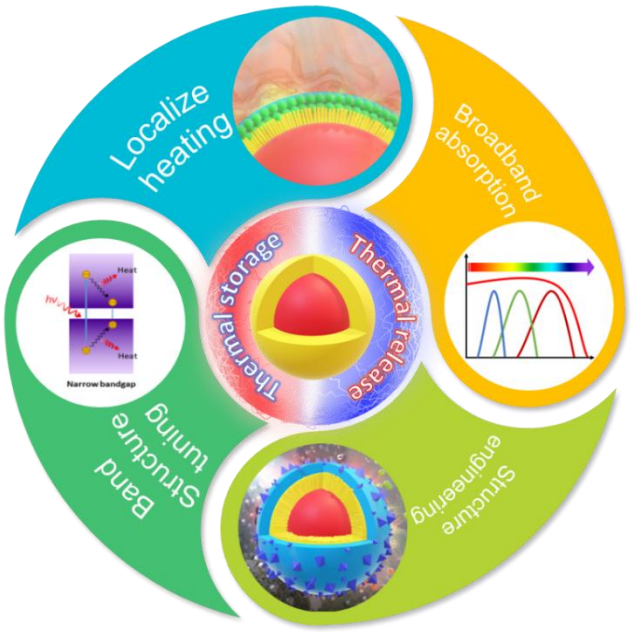

Figure 1: Photothermal advancement of solar-mediated encapsulated phase-changing material.

Acknowledgements: This work was supported by the National Research Foundation (NRF) grant funded by the Ministry of Education (2020R1A6A1A03038817) and by the Ministry of Science and ICT (MSIT) (2020R1A2C2101759), Republic of Korea.

References

Pornea, A. M., Kim, H., 2021. Design and Synthesis of SiO2/TiO2/PDA Functionalized Phase Change Microcapsules for Efficient Solar- Driven Energy Storage. *Energy Conversion and Management*. 232: 113801.

Zheng Z, Chang Z, Xu G-K, McBride F, Ho A, Zhuola Z, et al., 2017. Microencapsulated Phase Change Materials in Solar-Thermal Conversion Systems: Understanding Geometry-Dependent Heating Efficiency and System Reliability. *ACS Nano.* 11: 721–729.

PCR13042022 – 115: Ecotoxicology of moxifloxacin on freshwater microalgae: growth, photosynthesis and antioxidant responses

Zhuo Li[a*]

[a] Wuhan University

- Corresponding Author E-mail: zhuoli2000@whu.edu.cn

Extended Abstract

As one of the fourth-generation fluoroquinolone antibiotics, moxifloxacin (MOX) has been frequently released to aquatic environment, threatening local organisms. However, researches on its ecotoxicity to aquatic organisms are still limited. In the present study, we investigated the effects of MOX on the growth, photosynthesis and oxidative stress of two common types of microalgae, *Chlorella sorokiniana* and *Scenedesmus dimorphus*. The results of the 96 h-EC_{50} values of MOX for *C. sorokiniana* and *S. dimorphus* were 28.42 and 26.37 mg/L, respectively. Although the variations of specific indicators of photosynthetic fluorescence intensity were different, they all suggested that the photosystems of two types of microalgae were irreversibly damaged. The malondialdehyde content and superoxide dismutase of *C. sorokiniana* and *S. dimorphus* significantly increased, indicating that exposure of MOX caused serious oxidative stress. Chlorophyll a, b and carotenoids contents of *C. sorokiniana* increased, being probably related to resistance to oxidative stress, whereas they were inhibited as for *S. dimorphus* due to oxidation damage. Our results demonstrate that MOX has a considerable risk to aquatic environment, especially in the context of its increasing use in practice.

6th International Conference and
Postgraduate Colloquium for
Environmental Research 2022 (POCER
2022) 9 - 11 June 2022
Langkawi, Kedah, Malaysia

PCR13042022 – 116: Simulation of acid gas removal unit using ternary amine mixture of MDEA, sulfolane, and AMP

Abid S Farooqi[1,2*], Raihan M Ramli[1,2*] and Serene S M Lock[1,3]

1 Department of Chemical Engineering, Universiti Teknologi PETRONAS, Bandar Seri Iskandar, 32610 Seri Iskandar, Perak, Malaysia

2 Centre of Innovative Nanostructures & Nanodevices, Universiti Teknologi PETRONAS, Bandar Seri Iskandar, 32610 Seri Iskandar, Perak, Malaysia

3 CO2 Research Center (CO2RES), Department of Chemical Engineering, Universiti Teknologi PETRONAS, 32610 Seri Iskandar, Malaysia

Corrensponsing Author E-mail: abid_20001276@utp.edu.my; raihan.ramli@utp.edu.my

Keywords: Absorption; Aspen HYSYS; Simulation; Amines; Seperation; Distillation.

Extended Abstract

One of the most seek fossil fuel now a days is natural gas (NG) because it is efficient, convenient and relatively clean energy source as compared to coal and oil. NG consist mainly of methane (CH_4), some hydrocarbons and impurities of acid gases such as carbon dioxide (CO_2) and hydrogen sulfide (H_2S). The presence of acid gases in NG is undesirable since it lowered the heating value of the gas and possibly can corrode the equipment used for the transportation upon contact with water [1]. In Malaysia, most of the NG reserves are found to be sour gas fields where sour gas refers to natural gas that consists of high amount of CO_2 and H_2S. Typically, the NG reserves in Malaysia are high in CO_2 composition which ranges between 28 and 87% but with a relatively low H2S content [2]. Therefore, this shows that the removal of high CO_2 composition from the raw natural gas has always been a major challenge to the oil and gas operators in Malaysia in order to meet the sales gas specifications. Various separation techniques have been established to purify the natural gas by removing and reducing CO_2 and H_2S from the NG which include absorption, adsorption, cryogenic distillation and membrane separation [3]. More than 95% of the natural gas processing plants are operated through the acid gas removal unit (AGRU) using aqueous amine solvent in removing sour gas components from the hydrocarbon gas due to the availability of amine solvent at low cost [4].

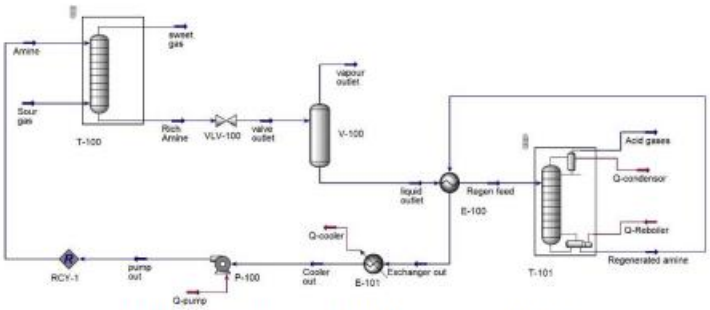

Figure 1: Simulation of AGRU on Aspen HYSYS

However, the major drawback of this process is the high operating cost in providing sufficient thermal energy at the reboiler for solvent regeneration. Meanwhile, the reboiler duty requirement generally increases with the requirement of CO_2 removal efficiency as higher energy consumption is required to strip off a larger amount of CO_2 from the rich solvent [5]. The present study addresses the performance of mixture of physical and chemical solvent for the absorption of CO_2 and H_2S. The main goal of this study is to reduce the reboiler heat duty which consume most of the energy for the solvent regeneration by using hybrid solvent with the optimum mixing ratio. Methyldiethanolamine (MDEA) and sulfolane was used as a fixed solvent with the addition of other solvent which act as an activator. Primary and secondary amines are usually used as an activator, 2-amino-2-methy-1-propanol (AMP) was used as an activator. AGRU model was simulated using Aspen HYSYS software. The activator amine concentration was varied at 3, 5, 10, 15 and 20 wt% while keeping the total amine concentration fixed at 50 wt%. Effect of temperature, pressure and amine circulation rate on the reboiler duty for the solvent regeneration were studied in this case.

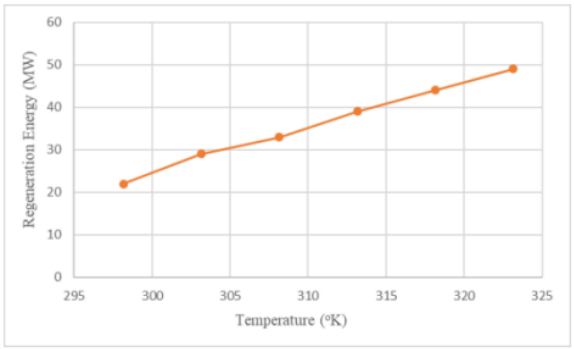

Figure 2: Effect of temperature on reboiler duty

The results revealed that as the pressure increased, lesser reboiler duty was required. While increasing temperature shows an increas in reboiler duty requirement for solvent regeneration as shown in Figure 2. Similarly, regeneration energy requirement is propotionally related to the amine circulation rate. As the solvent circulation rate increased, higher energy is required for the solvent regeneration.

Acknowledgements: The authors gratefully acknowledge financial support from Universiti Teknologi PETRONAS, Malaysia, under the Yayasan Universiti Teknologi PETRONAS (YUTP) grant number 015LC0-293.

References

[1] B. Shimekit and H. Mukhtar, "Natural Gas Purification Technologies - Major Advances for CO_2 Separation and Future Directions," Adv. Nat. Gas Technol., Apr. 2012, doi: 10.5772/38656.

[2] L. S. Tan, K. K. Lau, M. A. Bustam, and A. M. Shariff, "Removal of high concentration CO_2 from natural gas at elevated pressure via absorption process in packed column," J. Nat. Gas Chem., vol. 21, no. 1, pp. 7–10, Jan. 2012, doi: 10.1016/S1003-9953(11)60325-3.

[3] J. Park, S. Yoon, S. Y. Oh, Y. Kim, and J. K. Kim, "Improving energy efficiency for a lowtemperature CO_2 separation process in natural gas processing," Energy, vol. 214, p. 118844, Jan. 2021, doi: 10.1016/J.ENERGY.2020.118844.

[4] M. Torabi Angaji, H. Ghanbarabadi, and F. Karimi Zad Gohari, "Optimizations of Sulfolane concentration in propose Sulfinol-M solvent instead of MDEA solvent in the refineries of Sarakhs," J. Nat. Gas Sci. Eng., vol. 15, pp. 22–26, Nov. 2013, doi: 10.1016/J.JNGSE.2013.08.003.

[5] R. Sakwattanapong, A. Aroonwilas, and A. Veawab, "Behavior of Reboiler Heat Duty for CO_2 Capture Plants Using Regenerable Single and Blended Alkanolamines," Ind. Eng. Chem. Res., vol. 44, no. 12, pp. 4465–4473, Jun. 2005, doi: 10.1021/IE050063W

PCR14042022 – 117: Technical and environmental evaluation of a Biogas Power Plant operating in Amazon

Denis da Silva Miranda[1], Luiz Kulay

Chemical Engineering Department,
Polytechnic School, University of São Paulo (USP), São Paulo, Brazil

- [1]Corrensponsing Author E-mail: denismiranda@usp.br

Keywords: Biogas, Life cycle assessment, Amazon, Energy production

Extended Abstract

In recent decades, the socio-economic development experienced in Brazil has generated great demand pressures on the goods market and, consequently, increased the production of waste associated with them. This is the case of the demand for beef. To supply the domestic and foreign markets, the livestock advances into forested areas such as the Amazon, the region with the country's worst social indices and serious obstacles to development. In addition, the expansion causes land-use changes and waste generation, as manure and other emissions associated with cattle raising and slaughtering. Economic maturation also increases the domestic demand for electricity, which averaged 4.4% per year in the last decade. Therefore, the search for energy sources with low environmental impact becomes increasingly timely and urgent for Brazilian development. This study seeks to contribute to the management of both situations, evaluating environmental and technical aspects of installing a biogas production plant (BGPP) from manure and agricultural waste to supply the energy demand of a municipality isolated from the Amazon Interconnected System. National (NIS). In the current context, the electrical needs of these locations are supplied by plants operated with diesel oil (DOPP).

General aspects of the study

The technical analysis started with constructing a BGPP plant model based on data available in the literature. Bovine manure and corn stover tailings collected from farms in the region served as substrates

for biogas production (Figure 1). The biogas obtained from anaerobic digestion is dehumidified before going to the electric generation unit (combined gas cycle), with a generating capacity of 500 kW.

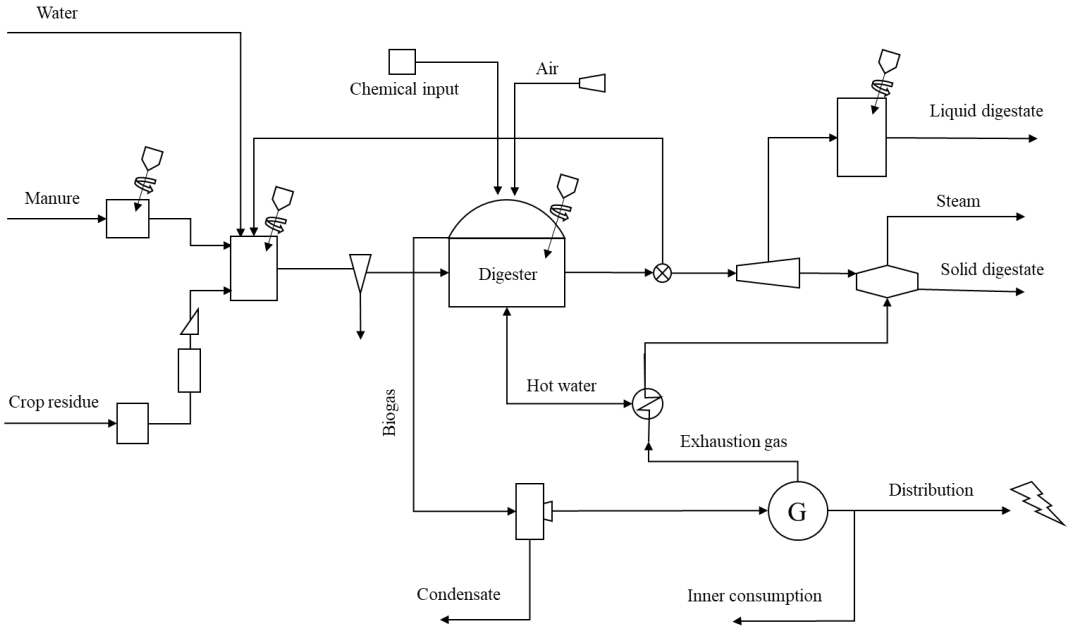

Figure 21. Scheme of a biogas plant

In addition to fuel, the arrangement also produces digestate, a fluid that could complement macro and micronutrients in agricultural soils due to its contents of N-P-K, Ca, Mg, and metals. However, the absence of an adequate operational structure for the collection and spraying of this flow makes it to be discarded as water effluent. The environmental performance of the BGPP was determined using the Life Cycle Assessment (LCA) technique. The results were compared to those of a DOPP and the electricity generation in a typical grid for the Amazon region based on hydro (86%) and thermopower: oil (9.0%) and natural gas (5.0%). This condition simulates a hypothetical inclusion of the municipality in the NIS.

Life Cycle Modeling

The LCA-based study followed the methodological guidelines of ISO 14044 for the attributional modality. The analysis took place for a cradle-to-gate scope and considered a Reference Flow (RF) of 1.0 kWh injected into the local network of a municipality in the Brazilian Amazon. Secondary data were used for environmental modeling of all electricity production alternatives. Multifunctionality situations were addressed by allocation using physical criteria. Finally, the impact assessment was

carried out for the effects of Global Warming Potential (GWP), Freshwater Ecotoxicity (FWET), and Primary Energy Demand (PED).

Results and discussion

According to the results depicted in Table 1, it is possible to observe that the BGPP has about 25 times less impact in terms of GWP and PED than the DOPP system. In both categories, the energy produced by biogas also performs environmentally better than a hypothetic supply from the northern Brazilian grid. The supremacy of BGPP can be justified due to the system using manure and corn stover, which are waste in their original processes, as substrates. On the other hand, the electricity provided by diesel and from the regional grid strongly depends on fossil fuels with high GWP and PED impacts associated. Table 1 also shows significant impacts of BGPP for FWET compared to those obtained by DOPP and the regional Grid. The disparity is associated with the release of digestate into the environment without any prior treatment. This finding only reinforces the need to systematically and carefully observe the environmental interactions between human endeavors and their surroundings.

Table 11. Environmental impacts of the energy supply from DOPP, Regional Grid and BGPP

Impact	Unit	Scenarios		
Category	**(/RF)**	**DOPP**	**Grid**	**BGPP**
GWP	g $CO_{2\ eq}$	692	165	27.7
FWET	g 1,4-DB	0.19	0.03	19.5
PED	MJ	10.0	4.70	0.42

Conclusions

Even with the logistical difficulties and peculiarities of the Amazon, a BGPP fed by wastes from cattle raising and agriculture proved to be a good alternative to energy supply for the region in environmental terms compared to the possibilities currently available. However, engineering design choices that consider the proper disposal of effluents are essential for the mitigation of impacts in a broader way.

Acknowledgements: The authors thank the National Council for Scientific and Technological Development (CNPq: process 130548/2021-9) and the Coordination for the Improvement of Higher Education Personnel – Brazil (CAPES: Code 001) for the support granted to carry out this study.

References

Akbulut, A., Arslan, O., Arat, H. and Erbas, O., 2021.Important aspects for the planning of biogas energy plants: Malatya case study. Case Studies in Thermal Engineering, v. 26.

Spyridonidis, A; Vasiliadou, I. A.; Akratos, C. S. and Stamatelatou, K., 2020. Performance of a Full-Scale Biogas Plant Operation in Greece and Its Impact on the Circular Economy. Water, 12, 3074.

6th International Conference and
Postgraduate Colloquium for
Environmental Research 2022 (POCER
2022) 9 - 11 June 2022
Langkawi, Kedah, Malaysia

PCR14042022 – 118: Tunable nanochannels of NiAl-LDH/SiO_2 for power generation performance by natural water evaporation

Jingjing Tu[a], Nanyu Lin[a], Ziyi Zhang[a], Jiangying Qu[a*], Feng Gao[a], Yunhao Zang[a]

[a] School of Environment and Civil Engineering,
Dongguan University of Technology, Dongguan 523808, P. R. China

- Corresponding Author E-mail: qujianggaofeng@163.com; fenggao2003@163.com

Extended Abstract

Natural water evaporation generation (NWE) is a green method to explore the electric energy. However, the relation between nanochannels constructed by generation materials and output electrical performance is unclear. In this paper, NiAl layered double hydroxide/SiO_2 (NiAl-LDH/SiO_2) as the power generation material with the tunable nanochannels has been prepared by using NiAl-LDH as the template and SiO_2 as the coated layer. The nanochannel size can be tunable by the coated thickness of SiO_2 on the surface of NiAl-LDH. When the coated thickness of SiO_2 increases from 0 to 14 nm, the surface charge will change due to the increases in negative charged SiO_2. Meanwhile, the nanochannel size build by NiAl-LDH/SiO_2 material decreases from 3.524 to 2.397 nm and then increases to 3.674 nm. The output electricity performances have been tested by the natural water evaporation generators (NWEGs). Although the zeta potential value of NiAl-LDH/SiO_2-9nm is smaller than pure SiO_2 and pristine NiAl-LDH, the open-circuit voltage (V_{oc}) of the NiAl-LDH/SiO_2-9nm NWEG is the largest owing to its smallest pore size. By experimental verification, the V_{oc} of the NWEGs shows an opposite trend with the nanochannel sizes of generation materials. The V_{oc} value increases from 0.4 to 1.4 V and then decreases to 0.25 V. When the nanochannel of 2.397 nm constructed by NiAl-LDH/SiO_2-9 nm, the NWEG obtains a maximum V_{oc} of 1.4 V and a maximum short-circuit current (I_{sc}) of 240 nA. This work reveals that the output electrical performance of NWEG is relative to surface charge and has a quantitively relative with pore size.

6th International Conference and
Postgraduate Colloquium for
Environmental Research 2022 (POCER
2022) 9 - 11 June 2022
Langkawi, Kedah, Malaysia

PCR14042022 – 119: In-situ synthesised hydroxyapatite coated on wood powder for efficient copper(II) removal from wastewater

Yunyi Liang[a], Changlei Xia[a*]

[a] College of Materials Science and Engineering
Nanjing Forestry University, Jiangsu, China

- Corrensponsing Author E-mail: changlei.xia@njfu.edu.cn

Keywords: Poplar Wood; Copper Adsorption; Hydroxyapatite; Environmental Purification.

Copper (Cu) is an essential micronutrient that is vital to wildlife. Excessive copper can cause a series of hazards to health, i.e., neurotoxicity, jaundice, and liver toxicity [Taylor et al, 2020]. Therefore, finding highly efficient remediation of heavy metal-contaminated water materials is highly desirable. can be used as an environmentally friendly adsorbent of heavy metal ions. Hydroxyapatite (HAp) as a unique inorganic compounad which can be used as an environmentally-friendly adsorbent for divalent heavy metals ions. The agglomeration and precipitation of HAp will result in the loss of adsorption capacity to heavy metal ions [Shrestha et al., 2020]. In this study, the wood powder surface decorated with hydroxyapatite (HAp@wood) was used as a green adsorbent for efficient Cu(II) ions removal from wastewater. Physical and chemical characteristics of the HAp@wood were characterized by Fourier transform infrared spectroscopy (FT-IR), X-ray diffraction technique (XRD), BET surface area, and Thermogravimetric analysis (TGA) (Fig. 1). The thermal stability of the wood increased with the loading of HAp particles from TGA and DTG curves. The residual weights of wood and HAp@wood were 13.82% and 57.40%, respectively. Thus, the HAp@wood nanocomposites were composed of at least 53.5% HAp. Based on N_2 adsorption–desorption isotherms investigation, the pore size, surface area and pore volume of HAp@wood were 21.46 nm, 61.72 m^2/g and 0.31 cm^3/g. The maximum adsorption capacity of HAp@wood for Cu(II) ions was found to be 98.95mg/g-HAp (Fig. 2). Adsorption kinetics indicated the adsorption equilibrium of HAp@wood was within 720 min and the adsorption process was well described by the pseudo-second-order kinetic model. The Langmuir and Freundlich isotherm models could fit the experimental data well. All the results revealed that this method as a low-cost and ecofriendly alternative modification treatment to increase the adsorption efficiency of agricultural waste and avoid the agglomeration of HAp.

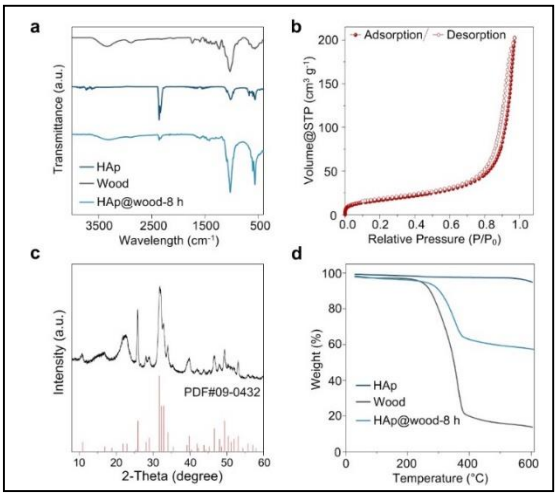

Figure 1: (a) FTIR spectra of HAp, Wood, and HAp@wood. (b) Nitrogen absorption/desorption isotherm curves of HAp@wood. (c) XRD patterns of HAp@wood. (d) TGA curves for HAp, wood, and HAp@wood.

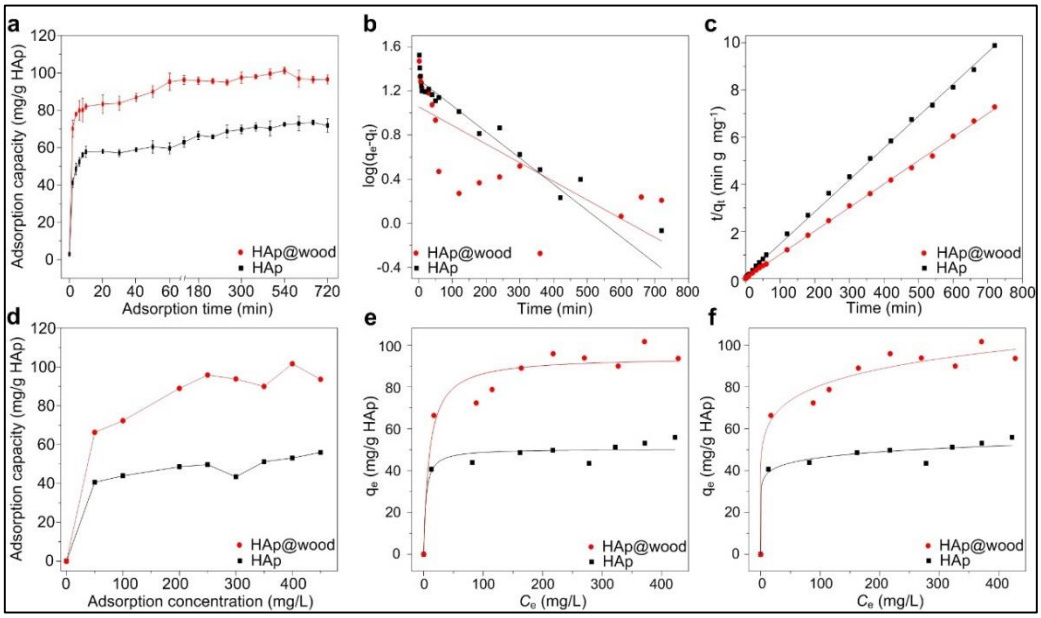

Figure 2: (a) Effect of time on the adsorption capacity of Cu(II) ions by HAp and HAp@wood. (b) Pseudo-first-order model. (c) Pseudo-second-order model. (d)Effect of initial concentration on the adsorption capacity of Cu(II) ions by HAp and HAp@wood. (e) Langmuir isotherm model. (f) Freundlich isotherm model.

Acknowledgements: The authors thank for Jiangsu Specially-Appointed Professor funding.

References

Taylor, A.A., Tsuji, J.S., Garry, M.R., McArdle, M.E., Goodfellow, W.L., Adams, W.J., Menzie, C.A.J.E.m., 2020. Critical review of exposure and effects: Implications for setting regulatory health criteria for ingested copper. *Environmental Management.* 65, 131-159

Shrestha, S., Wang, B., Dutta, P., 2020. Nanoparticle processing: Understanding and controlling aggregation. *Advances in Colloid and Interface Science.* 279, 102162

PCR14042022 – 120: Bionanocomposite of chitosan and ZnO and its functionality in the preservation of strawberries.

Dulce Jeanette Garcia-Garcia [a] , Francisco Gerardo Pérez-Sancheza , Heriberto Hernández-Cocoletzi[b,*] , Carolina Morán-Raya [a] , Maria Lorena Luna-Guevara[b] , Madai Gizeh Sanchez-Arzubide[b] ,Eva ÁguilaAlmanzab and, Nicolás Morales-López[a]

aBenemérita Universidad Autónoma de Puebla, Centro de Investigación en Fisicoquímica de Materiales, ICUAP, Ecocampus Valsequillo, Edificio Val-3, San Pedro Zacachimalpa, Puebla, 72960, México.
bBenemérita Universidad Autónoma de Puebla, Facultad de Ingeniería Química, Avenida San Claudio y 18 Sur, S/N edificio FIQ7 CU San Manuel C.P. 72570, Puebla, México.

• *Correnspondig Author E-mail: heriberto.hernandez@correo.buap.mx

Keywords: Strawberry, Chitosan, edible coating, food spoilage, nanobiopolymer, shelf life, nonthermal technologies.

Extended Abstract

The consumption of fresh fruits and vegetables has been associated with many health benefits due to the nutritional importance in human diet. However, their short shelf-life, associated with deterioration rate, is one of the most important issues that should be enhanced [Halonen, et. al., 2020; Ochoa-Velasco et. al., 2014]. Particularly, strawberry is one of the fruits with a very short shelf-life, mainly, because of fungal contamination and due its delicate tissue. Therefore, diminishing the rate of deterioration is one of the most important challenges to guarantee flavour, colour, and nutritional value. In this context, recently has been studied edible coatings to extend the shel-life and quality of fruits and vegetables. Some edible coatings like chitosan possess antimicrobial characteristics [Treviño-Garza, et. al., 2015; Ziv, et. al., 2021]. The aim of this work was to evaluate the effect of chitosan-ZnO based bionanocomposite edible coating on the physicochemical, antioxidant, microbiological and sensorial hproperties of fresh strawberries. Strawberries were submerged into a chitosan-ZnO solution (dissolved in acetic acid) for 4 and 8 seconds. To evaluate the efficacy of the coating, the colour and humidity in coated and uncoauted samples were measured, using only chitosan. Main results are reported in Table 1; where L* indicates the bright red, a* (chromatid) indicates the intensity in the red colour, and b* (chroma) indicates the colour intensity. As can be see from Table 1, L* values are higher for coated strawberries. The humidity at day 1 increased as the immersion time increased; after 10 days of applied the coating, this parameter decreased to 88.1% for 4 and 8 s of immersion. The uncoated strawberry diminished the humidity to 83.5% in the same time; it may be concluded that the coating helps to maintain the fruit freshness, which can be attractive to the consumer. Concerning the

appearence, the samples coated with the chitosan solution look less damage at day 10, compared to those that were not coated (Figure 1); it is evident the damage of the uncoated samples, in which fungus has appeared. Experiments where the incorporation of 5% ZnO nanopartices into the chitosan solution are now conducted; results will be presented during the congress. It is expected that parameters like taste, colour and smell will not be affected.

Table 1. Colour evolution of coated and uncoated strawberries for 1o days.

	day 1			day 10		
Immertion time (s)	0	4	8	0	4	8
L	31.8±2.09	33.1±2.18	33.0±3.05	31.8±2.09	34.1±3.45	33.4±3.49
*a**	35.2±3.01	32.5±4.03	33.9±4.75	35.2±3.01	24.9±1.95	26.3±3.60
*b**	8.3±3.44	10.5±2.19	10.0±1.69	8.3±3.44	9.3±2.45	8.8±1.60

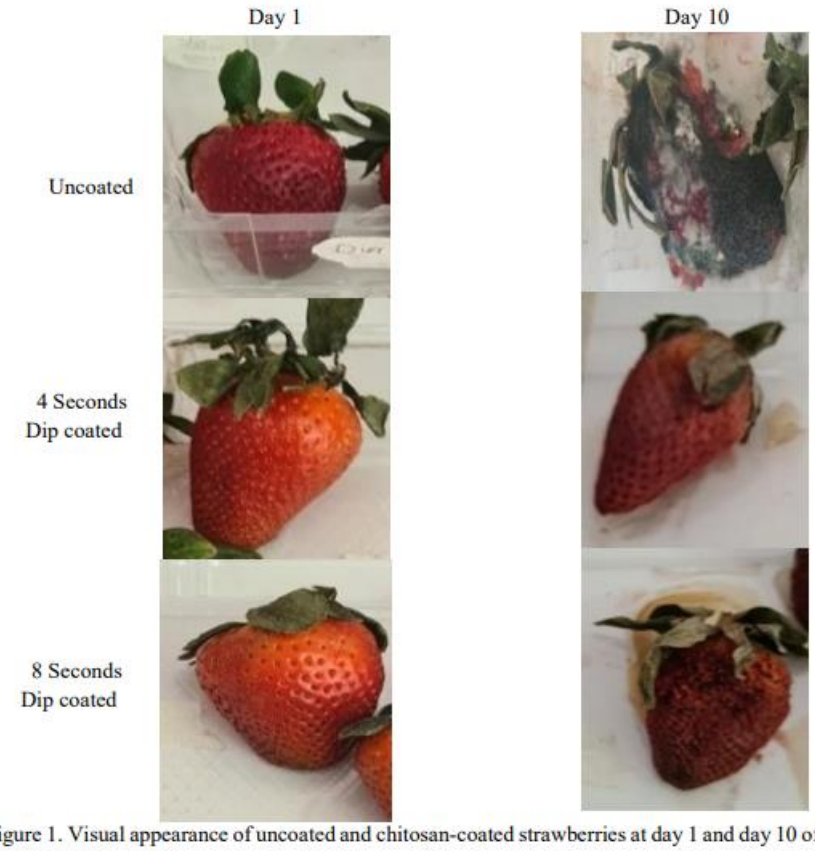

Figure 1. Visual appearance of uncoated and chitosan-coated strawberries at day 1 and day 10 of storage at room temperature.

Acknowledgement: This work was partially supported by VIEP-BUAP, Puebla México.

6th International Conference and
Postgraduate Colloquium for
Environmental Research 2022 (POCER
2022) 9 - 11 June 2022
Langkawi, Kedah, Malaysia

PCR14042022 – 121: Conductivity and Crystallinity Correlation Study Of MnO2/3D-G Nanocatalyst for MAFC Application

Khalimatul Saadiah Ahmad[a] , Sahriah Basri[a] , and Siti Kartom Kamarudin[a,b]

a Fuel Cell Institute
Universiti Kebangsaan Malaysia, Selangor, Malaysia
b Faculty of Engineering & Build Environment
Universiti Kebangsaan Malaysia, Selangor, Malaysia

• Corrensponsing Author E-mail: sahriah@ukm.edu.my

Keywords: Three-Dimensional Graphene; DFT Calculations; Magnesium Air Fuel Cell

Extended Abstract

Magnesium air fuel cells (MAFC) are considered as a promising source of alternative energy. However, MAFC performance is not optimal due to low ORR conductivity and kinetics. Recent studies show that MnO_2 is often used to overcome the problem (Zhang et al., 2017, Zhang et al., 2019). Thus, this article will examine the conductivity and crystalline correlation of 3D-G-supported MnO_2 nanocatalysts. MnO_2/3D-G. Conductivity studies will be performed using Density Functional Theory (DFT) via Material Studio software by Accelrys. Then, MnO_2/3D-G will be synthesized using the template method before its crystallinity is analyzed using X-ray diffraction (XRD).

Figure 1 shows the three optimal molecules that have been developed. While, figure 2 shows the band structure achieve after some times of calculations for 3D-G and MnO_2 is 0.728 eV and 0.433 which indicate that 3D-G is a direct band gap semiconductor. Upon the interactions, the resulting in an opening band gap about 360meV for the 3D-G between the bonding and antibonding states for both spin up and spin down.

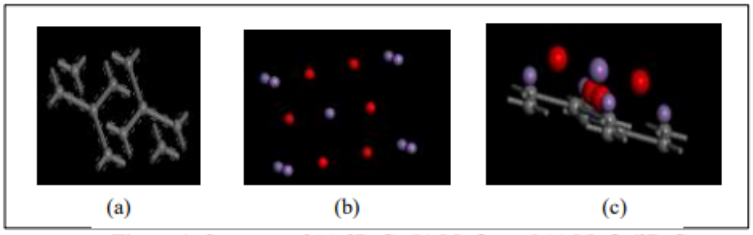

Figure 1: Stucture of (a) 3D-G, (b) MnO_2 and (c) MnO_2/3D-G

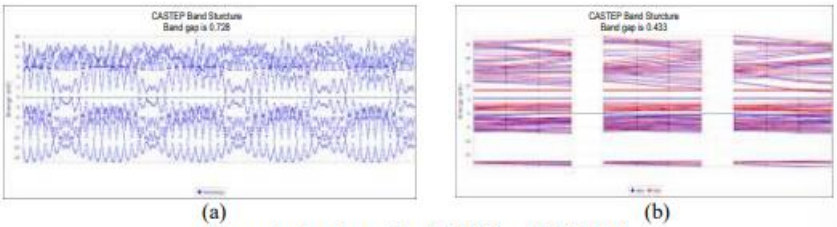

(a) (b)

Figure 2: Band gap for (a) 3DG and (b) MnO_2

Experimentally, the 3D-G as support for MnO_2 nanocatalyst showed (002) graphene and a peak at approximately 2θ = 43° corresponding to the (100) in-plane hexagonal atom arrangement overlapped with MnO_2 the (111) peak, resulted in a broad diffraction peak at approximately 25° (figure 3a). The peaks and values were indexed to for the MnO_2/3D-G (figure 3b), the major diffraction peaks were at 2θ= 12.7, 18.1, 28.9, 37.4, 41.9, 49.8 and 56.1°, which correspond to the (110), (200), (310), (211), (301), (411) and (600) planes of MnO_2/3D-G, respectively. Upon interaction between 3D-G and MnO_2 (111) substrate, a forbidden gap of about 350 meV was opened between its bonding and antibonding π bands. A forbidden gap and the local magnetic moments in bilayer graphene can be controlled by changing the oxygen nonstoichiometry or by oxygen adsorption. Hence, 3D-G structure will potentially increase the catalytic activity.

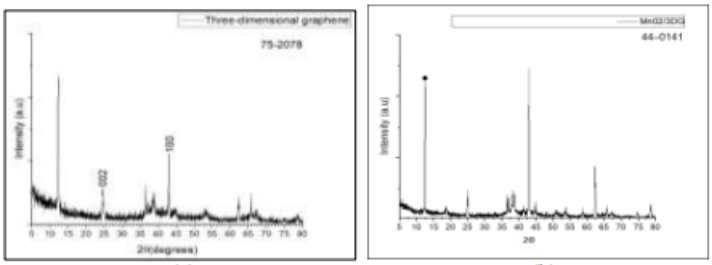

(a) (b)

Figure 3: XRD result on (a) 3D-G and (b) MnO_2/3DG

From the resutls, it can conclude that

1. The band structure indicates that 3DG is semiconducting. It is indicate of potential various electronic applications which may hold to the high conductivity escpecially after doped with MnO_2 nanocatalyst.

2. The study of crystalline structure is 3D-D showed a broad peak at approximately 2θ = 25°corresponding to the (002) graphene and a peak at approximately 2θ = 43° corresponding to the (100) in-plane hexagonal atom arrangement were observed. This result is comparable as reported by Zhang et al., 2019.

3. A forbidden gap of about 350 meV was opened between its bonding and antibonding π bands

4. The particle size of template can control the pore size of 3D-G and the number of graphene layers is adjusted by controlling mass ratio of carbon precursor and template

Acknowledgements: The authors thank to Kementerian Pengajian Tinggi Malaysia under research grant FRGS/1/2020/STG04/UKM/03/1. We also appreciate the fruitful cooperation by Persatuan Nelayan Sepang.

6th International Conference and
Postgraduate Colloquium for
Environmental Research 2022 (POCER
2022) 9 - 11 June 2022
Langkawi, Kedah, Malaysia

PCR14042022 – 122: Synthesis of Novel Adsorbents on Commercial Activated Carbon for H_2S Adsorption Capability Using the Core Shell Technique

Nurul Noramelya Binti Zulkefli1[a], Lee Jun Xiong[b], Nazatul Aziqah Ramli[b], Usshana Saengchoad Peradit[b], Muhammad Na'im Najmi Mohammad Salji[b], Shahbudin Masdar[a,b,c], Wan Nor Roslam Wan Isahak[a,b], Nabilah Mohd Sofian[c]

[a] Research Centre for Sustainable Process Technology (CESPRO)
Universiti Kebangsaan Malaysia, Selangor, Malaysia

[b] Chemical Engineering Programme, Faculty of Engineering & Built Environment
Universiti Kebangsaan Malaysia, Selangor, Malaysia

[c] Fuel Cell Institute
Universiti Kebangsaan Malaysia, Selangor, Malaysia

- Corrensponsing Author E-mail: shahbud@ukm.edu.my

Keywords: Hydrogen Sulfide; Core Shell Technique; Adsorption-desorption, Adsorbents Performance.

Extended Abstract

Biogas purification is a key step in enhancing biogas quality by capturing and eliminating pollutants including hydrogen sulphide (H_2S) and carbon dioxide (CO_2). The presence of H_2S gas causes ineffective biogas production, corrosion of mechanical equipment, and harmful gas emissions into the environment. Adsorption technology is one of the viable approaches for purifying biogas, particularly for removing H_2S gas. The fundamental issue of this technology, however, is the selection of adsorbents that require a high adsorption capacity of H_2S gas as well as improved stability and shelf-life. As a result, the focus of this research is on the development of adsorbent materials for enhancing H_2S adsorption capacity and stability in the adsorption-desorption cycle. Surface modifications were made to commercial coconut-type activated carbon (CAC) through core shell (CS/CAC) technique. By adjusting the solvent concentration, time, and temperature of CAC immersion, the CS technique were implemented. The adsorbent was next characterised by analysing the surface morphology and element

presence (SEM-EDX), functional group (Fourier Transform Infrared), stability and degradation (Thermal Gravimetric Analyzer), and surface characteristics (Brunauer–Emmett–Teller). The CS/CAC adsorbents prepared with 0.2 M for solvent concentration, immersion time, and temperature at 50 min and 95°C, respectively. Furthermore, the adsorption capacity of H_2S gas and the adsorption-desorption cycle were used to evaluate the performance of these adsorbents. The effects of operational parameters on adsorbent performance were investigated by varying the desorption process temperature (50-150°C) in a real adsorption-desorption process with a supplied concentration of 5000 ppm of H_2S gas at 5.5 L/min. Based on the morphological characterization, the chemical was impregnated and uniformly covered the surface of CAC. In general, the adsorbent and the operating settings have an impact on adsorption-desorption performance. Based on this research, the CS/CAC has the maximum stability based on the rate of degradation in H2S adsorption capacity across multiple cycles compared to single impregnation [Zulkefli et al. 2019] and dual-chemical mixture-CAC (DCM/CAC) [Zulkefli et al. 2020]. As a result, this study is essential work which could improve the selectivity and stability of adsorbents to H_2S gas, and hence has a potential in improving the removal of H_2S in biogas purification technology.

Acknowledgements: The authors thank the Ministry of Higher Education, Malaysia under research code FRGS/1/2020/TK0/UKM/02/4 and Universiti Kebangsaan Malaysia under research code DPK-2020-009 & PP-SELFUEL-2021..

References

Zulkefli, N.N.; Masdar, M.S.; Isahak, W.N.R.W.; Jahim, J.M.; Rejab, S.A.M.; Lye, C.C. Removal of hydrogen sulfide from a biogas mimic by using impregnated activated carbon adsorbent. PLoS ONE 2019, 14, e0211713.

Zulkefli N.N., Khaia T.Z., Nadaraja S., Venugopal N.R., Yusri N.A.M., Sofian N.M., Masdar M.S. Capabilities dual chemical mixture (DCM) adsorbents through metal anchoring in H2S captured. Solid State Technol. 2020;63:181–191.

6th International Conference and
Postgraduate Colloquium for
Environmental Research 2022 (POCER
2022) 9 - 11 June 2022
Langkawi, Kedah, Malaysia

PCR14042022 – 123: Hydrogen Production via Electrolysis Unit: Mathematical Modelling and Simulation on Parametric Towards PEM Electrolysis Performance

Adam Mohd Izhan Bin Noor Azam[a], Mohd Shahbudin Mastar @ Masdar[a*]

[a] Fuel Cell Institution,
Universiti Kebangsaan Malaysia, 43600 UKM Bangi, Selangor

- Corresponding Author E-mail: shahbud@ukm.edu.my

Keywords: Hydrogen production, clean energy, PEM electrolysis, mathematical model, simulation..

Extended Abstract

Huge quantities of apple orchard waste generated which regarded as a promising alternative energy source for biofuel and biomaterial production. Biorefinery emerged as a sustainable approach and recognized promising transformation platforms for products, to achieve circular bioeconomy which focuses on the biomass efficient and sustainable valorization, promotes resource regeneration and restorative. The emerged biowaste biorefinery has proved as sustainable approach for integrated bioproducts further applied in industrial, commercial, agricultural and energy sectors. Based on carbon neutral sustainable development, this review comprehensive explained the apple orchard waste as renewable resource generation and resource utilization technologies from the perspective of energy, nutrient and material recovery in the concept of biorefinery. Integrate biorefinery concepts into apple orchard waste management is promise for conversion into value-added materials and contribute as driving force to cope with resource scarcity, climate changes and huge material demand in circular bioeconomy.

6th International Conference and
Postgraduate Colloquium for
Environmental Research 2022 (POCER
2022) 9 - 11 June 2022
Langkawi, Kedah, Malaysia

PCR14042022 – 124: Polymer-Encapsulated Crystalline Zirconium Phosphates as NH_4^+ and K^+ Ion Exchangers for Application in Sorbent Dialysis Cartridges

Ismail Samsudin[a], Leon Goh Zhi Wei[a], Stephan Jaenicke[a], and Gaik-Khuan Chuah[a*]

[a] Department of Chemistry
National University of Singapore, Singapore

*E-mail: Chmcgk@nus.edu.sg

Abstract

The ion exchange properties of crystalline α- and γ-zirconium phosphates in the sodium and hydrogen forms were investigated. The zirconium phosphates were synthesized by a mechanochemistry-assisted protocol. Amongst the compounds, α-Na_2-zirconium phosphate and γ-H_2-zirconium phosphate were found to be excellent ion exchangers for NH_4^+ and K^+ ions, two key cations in renal sorbent dialysis systems. The maximum NH_4^+ uptake by α-Na_2-zirconium phosphate was 5.5 mmol/g, close to the theoretical limit of exchangeable sites. In multi-ion solutions, γ-H_2-zirconium phosphate was a selective exchanger for K^+ with total uptake capacity of 2.9 mmol/g. The as-synthesized microcrystalline zirconium phosphates were encapsulated by polyacrylonitrile to form spherical porous beads of tailorable sizes. Owing to the porosity, access to the ion exchange sites of the embedded zirconium phosphates particles was unaffected, enabling fast kinetics in the uptake of NH_4^+ and K^+. In this form, the PAN/ZrP beads can be easily handled in sorbent cartridges. The activity of the PAN/ZrP beads could be fully restored by simple regeneration with the appropriate electrolyte.

Keywords: Ion Exchanger; Layered Materials; Mechanochemistry; Water Treatment; Dialysis.

1. Introduction

The kidney has important functions in the body such as removing extra fluids, maintaining the acid-base and electrolyte balance and eliminating metabolic waste products. In Chronic Kidney Disease (CKD) patients, the ability of the kidney to remove waste substances and acid load from the body declines [Schwartz et al., 1959]. Such patients require dialysis where the function of the kidney to remove ions such as ammonium , sodium, potassium and magnesium from the blood, is taken over by an external device. In sorbent dialysis, the spent dialysate is continuously regenerated, providing an uninterrupted supply of fresh dialysate. The sorbent cartridge contains a number of layers to remove

solutes transferred from the blood into the dialysates, one of which is a layer with zirconium phosphate to exchange NH_4^+, K^+, and other cations with Na^+ and H^+ [Roberts, 1998].

Amorphous zirconium phosphate (ZrP) is used as the cation exchanger in current sorbent systems. However, the lack of long-range order poses difficulties in characterization so that batch to batch variations are difficult to be detected. Moreover, due to irregular positioning of the phosphate groups in the amorphous crystal lattice, the cavities in gel vary in their dimensions [Clearfield, 2000]. In contrast, the crystalline form possesses uniform cavities which are essential for reproducible performance in its applications, especially as a medical device. However, the synthesis of crystalline zirconium phosphates requires excess phosphates and is energy intensive and time consuming, requiring reflux or hydrothermal treatment for days to weeks to achieve the desired crystallinity.

Recently, our lab has successfully developed a convenient protocol to prepare crystalline zirconium phosphates of different phases [Cheng et al., 2018]. Using this mechanochemistry-assisted protocol, bulk quantities of highly crystalline zirconium phosphates can be readily formed without involving solvents or additional reagents other than the reactants. In addition, to address practical considerations, we investigated their encapsulation in polyacrylonitrile (PAN). The spherical beads formed should overcome operational problems such as pressure build-up and clogging in the dialyzer.

2. Methodology

Crystalline zirconium phosphates were first synthesised using a mechanochemistry-assisted protocol. They were then encapsulated with PAN to form spherical porous beads of tailorable sizes. Their ion-exchange properties were evaluated for application in sorbent dialysis cartridges.

3. Results and Discussion

Crystalline sodium and hydrogen zirconium phosphates with α- and γ-structures were synthesised via a liquid-assisted mechanochemistry based route. They were then subjected to encapsulation with PAN. Among them, PAN/α-Na_2ZrP demonstrated remarkable ion exchange properties. The total uptake of NH_4^+ was 5.5 mmol/g, which is very close to its theoretical exchange capacity while the total uptake of K^+ was 1.5 mmol/g (Figure 1a). α-Na_2ZrP was a good ion exchanger as compared to α-H_2ZrP because the latter has a very small interlayer spacing of 7.55 Å (Figure 1b). Substituting the H^+ with Na^+ greatly increased its interlayer spacing to 8.60 Å which reduced diffusion constraints.

Beads with tailorable sizes can be synthesized depending on the needle internal diameter used during drop formation (Figure 1c). The strength of the beads increased with weight fraction of PAN used and the optimum composition to balance high sorption and mechanical stability was found to be at 33 wt. %. The polymer formed a highly porous network (Figure 1d) with mesopores of 5 to > 30

nm, resulting in 3 – 4 fold increase in the pore volumes for the PAN/ZrP composites. The ion-exchange properties of the zirconium phosphates were unaffected by the polymer encapsulation.

The PAN/γ-H_2ZrP beads show preferential uptake of K^+ while PAN/α-Na_2ZrP was ~ fourfold more selective for NH_4^+ than K^+. The PAN/ZrP beads have high rates of sorption and retained their ion-exchange properties even after multiple cycles.

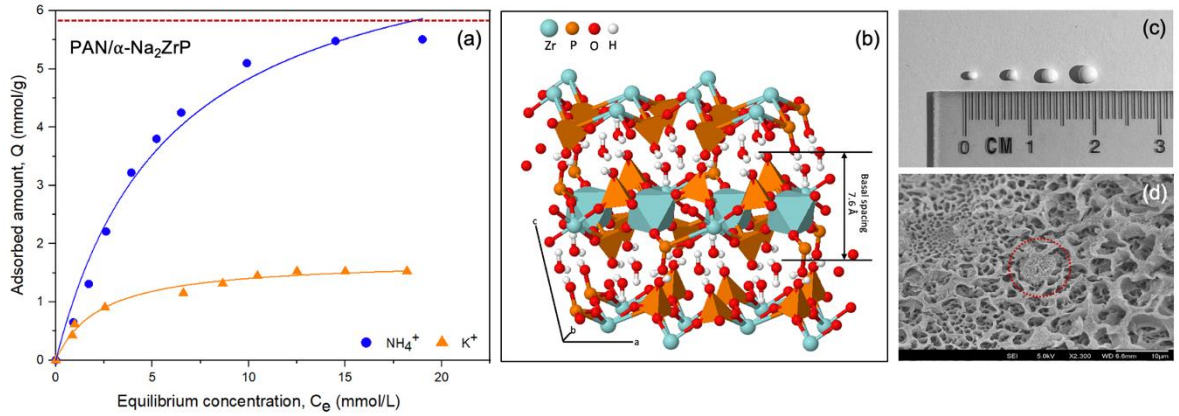

Figure 22: (a) Adsorption isotherms of (●) NH_4^+ and (▲) K^+ on PAN/α-Na_2ZrP beads from aqueous solutions of NH_4NO_3 and KCl respectively where the horizontal dashed line indicates the theoretical ion-exchange capacity, (b) crystal structure of α-$Zr(HPO_4)_2{\cdot}H_2O$, (c) spherical beads of tailorable sizes and (d) cross section showing encapsulation of α-Na_2ZrP in a highly porous PAN network.

4. Conclusion

Crystalline zirconium phosphates were successfully encapsulated with PAN to form spherical porous beads of tailorable sizes. These beads were found to be excellent ion exchangers for NH_4^+ and K^+, with high rates of sorption and recyclability potential. Together with its ability to alleviate pressure build-up and clogging in the dialyzer as compared to powdered samples, these PAN/ZrP beads are promising materials for sorbent dialysis cartridges.

Acknowledgements: Financial support from the Ministry of Education AcRF Tier 1, R-143-000-B07-114 is gratefully acknowledged.

References

Cheng, Y., Dong Wang, X., Jaenicke, S., Chuah, G.-K., 2018. Mechanochemistry-based synthesis of highly crystalline γ-zirconium phosphate for selective ion exchange. *Inorganic Chemistry*. 57 (1): 4370-4378.

Clearfield, A., 2000. Inorganic Ion Exchangers, Past, Present, and Future. *Solvent Extraction and Ion Exchange*. 18 (1): 655-678.

Roberts, M., 1998. The regenerative dialysis (REDY) sorbent system. *Nephrology*. 4 (1): 275-278.

Schwartz, W.B., Hall, P.W., Hays, R.M., Relman, A.S., 1959. On the mechanism of acidosis in chronic renal disease. *Journal of Clinical Investigation.* 38 (3): 39-52.

6th International Conference and
Postgraduate Colloquium for
Environmental Research 2022 (POCER
2022) 9 - 11 June 2022
Langkawi, Kedah, Malaysia

PCR14042022 – 125: Pretreatment of secondary sludge with bacteriophage T4, T7 or λ lysozyme to increase hydrolysis efficiency and biogas production

Sangmin Kim[a], Sujin Choi[a], and Seokhwan Hwang [a*]

[a] Division of Environmental Science and Engineering
Pohang University of Science and Technology (POSTECH), 77 Cheongam-Ro, Nam-Gu, Pohang, Gyeongbuk, Republic of Korea

- Corrensponsing Author E-mail: shwang@postech.ac.kr

Keywords: Lysozyme; Secondary sludge; Pretreatment; BMP test

Extended Abstract

The current concern in the activated sludge processes is its hydrolysis in an anaerobic digester. Because the secondary sludge mainly consists of the aerobic biomass cells, it induces the hydrolysis rate-limiting step in the anaerobic digestion (AD) [Kor-Bicakci and Eskicioglu, 2019]. Each microorganism in the digesters can secrete the hydrolytic enzymes degrading the organic wastes. However, the AD processes can reduce only 30 ~ 50 percent of volatile solids in secondary sludge [Gonzalez *et al*., 2018]. Of the hydrolytic enzymes, the lysozyme can break up the β-1,4 glycosidic bonds in the cell wall, so it is the proper enzyme for enzymatic pre-treatment [Wu *et al*., 2019].

In this study, our group aimed to improve a solubilization rate and methane conversion efficiency of the secondary sludge treating the recombinant lysozyme. The sludge sample was taken from the secondary sedimentation tank of Pohang wastewater treatment plant in South Korea. Physicochemical properties were analyzed by 'Standard methods' [APHA, 2005]. The activities of recombinant bacteriophage lysozyme (BL) from bacteriophage T4, T7, and λ (KRIBB, Daejeon, South Korea) were about 662, 95, and 294 U/mg. The following equation (1) was used for estimation of a biogas production rate coefficient.

$$Y_t = A\,(1 - \exp^{-k \cdot t}) \quad (1)$$

where, Y_t is the cumulative biogas production (NmL/g VS_{in}) at time t; A is the maximal biogas production (NmL/g VS_{in}); k is the rate coefficient of biogas production (d^{-1}); and t is the reaction time (d).

Energy conversion rate (mL CH4/g VS_{in}) and sludge reduction rate (Δg VS/g VS_{in} x 100) was calculated. T4 lysozyme (T4L), T7 lysozyme (T7L) and λ lysozyme (λL) responded optimally with secondary sludge under the conditions: T4L (pH 7.2, 47°C), T7L (pH 7.1, 37.1°C), λL (pH 7.0, 38.4°C). After lysozyme treated with secondary sludge under the optimal condition, a biochemical methane potential (BMP) test was performed to investigate the change of methane conversion efficiency by treating the different lysozyme. Volatile suspended solid (VSS) reduction shows the range of 23.6 ± 4.8% (Pohang secondary sludge) to 50.1 ± 2.3% (Busan cultivated sludge) by three different lysozymes. T4L, T7L and LaL also improved the biogas production and coefficients of first order models. These values more related with the type of BLs than the type of substrate sludge. *Simplicispira* (10.3 ± 12.5%), *Flavobacterium* (5.8 ± 4.1%), and *Dokdonella* (4.9 ± 3.7%) were dominant bacterial genera in secondary sludges without BL treatment, and the relative abundance of these genera was decreased in all samples treating BLs. On the other hand, the major groups in cultivated sludge were changed before and after BL treatment: *Klebsiella* (3.7 ± 3.3% → 23.0 ± 8.5%), *Kosakonia* (1.8 ± 1.5% → 19.0 ± 5.3%) and *Dysgonomonas* (0.0 ± 0.0 → 15.3 ± 3.3%). This research demonstrated the effect of lysozyme on activated sludge. These results can be referred to increase the efficiency of methane gas generation through the enzymatic pre-treatment of sludge by recombining the enzyme.

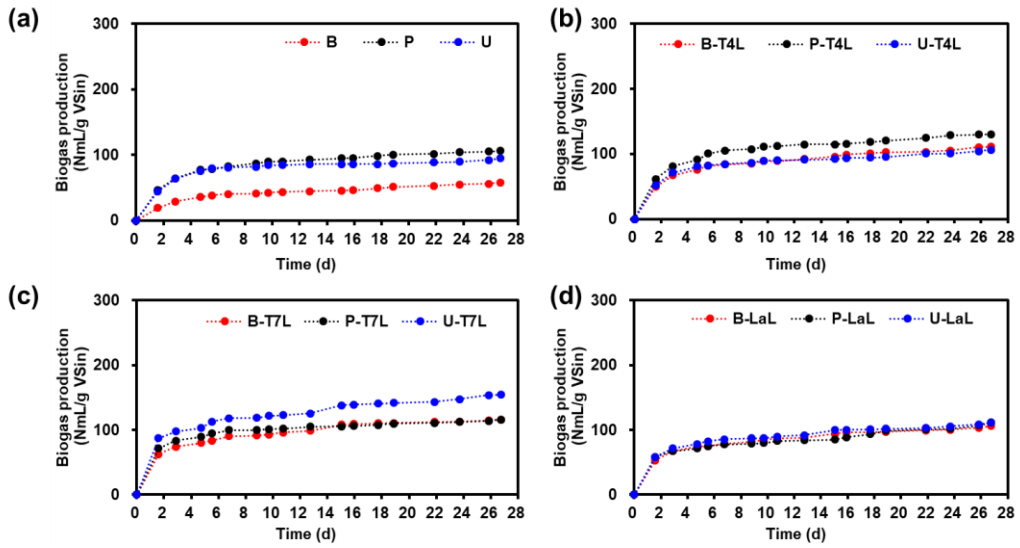

Figure 23. Acculmulated biogas production using (a) raw secondary sludge and cultivated sludge, (b) sludges treated with T4L, (c) sludges treated with T7L, and (d) sludges treated with LaL

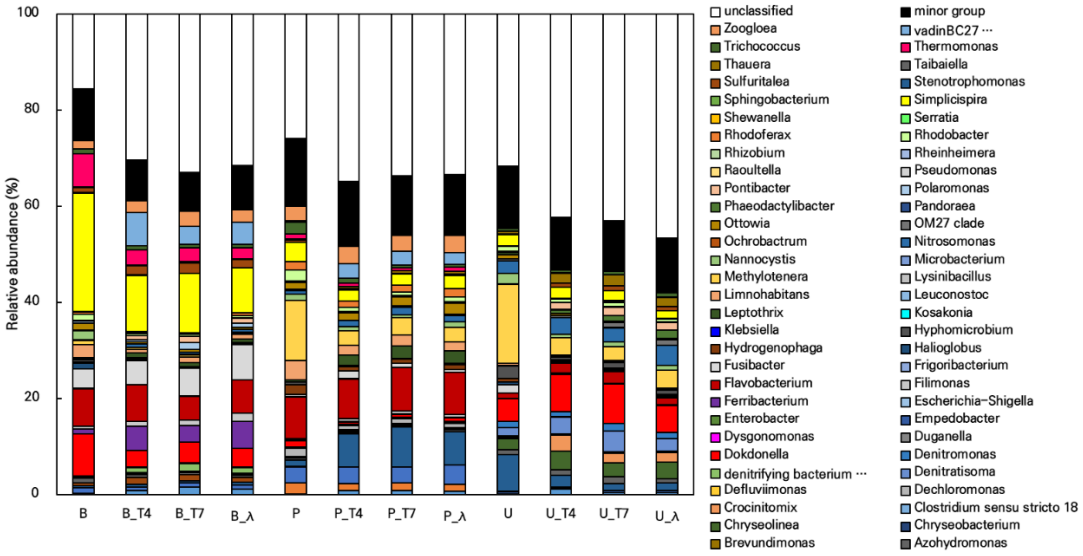

Figure 24. Relative abundance (RA, %) of bacterial genera in the secondary sludge and cultivated sludge from WWTPs in Busan, Pohang, and Ulsan (RA ≥ 1% in at least one sample)

Acknowledgements: This research was financially supported by the Korea Ministry of Environment as Waste to Energy-Recycling Human Resource Development Project (No. YL-WE-21-002).

References

American Public Health Association. 2005. *APHA standard methods for the examination of water and wastewater: Standard methods for the examination of water & wastewater*. Washington, DC: American Public Health Association.

Kor-Bicakci, G., Eskicioglu, C., 2019. Recent developments on thermal municipal sludge pretreatment technologies for enhanced anaerobic digestion. *Renewable and Sustainable Energy Reviews*. 110: 423-443

Gonzalez, A., Hendriks, A. T. W. M., Van Lier, J. B., De Kreuk, M., 2018. Pre-treatments to enhance the biodegradability of waste activated sludge: elucidating the rate limiting step. *Biotechnology Advances*. 36 (5): 1434-1469.

Wu, T., Jiang, Q., Wu, D., Hu, Y., Chen, S., Ding, T., Chen, J., 2019. What is new in lysozyme research and its application in food industry? A review. *Food Chemistry*. 274: 698-709.

6th International Conference and
Postgraduate Colloquium for
Environmental Research 2022 (POCER
2022) 9 - 11 June 2022
Langkawi, Kedah, Malaysia

PCR14042022 – 126: Mechanochemical Synthesis of Highly Crystalline Magneisum Zirconium Phosphate for Fast Sorption of Scandium

Leon Goh Zhi Wei[a] , Chuah Gaik Khuan[a*]

a Department of Chemistry University of Singapore, Singapore

• Corresponding Author E-mail: chmcgk@nus.edu.sg

Keywords: Mechanochemical; Scandium; Wastewater treatment.

Extended Abstract

Scandium is currently seen as a valuable rare-earth element and with little mining sites available, recovery and recycling of scandium should be focused on. With bauxite residues containing a high amount of scandium ions, it presents as a opportunity for us to explore recovery of scandium from these rich sources. However, recovery of scandium in bauxite residues are often done in acidic conditions. Crystalline magesium zirconium phosphate was synthesied via a mechanchemical protocol and its ion exchange capacity was explored on scandium. This material displays a fast uptake on scandium with a ion exchange capacity of 24 mg g^{-1} under acidic conditions. It is also selective to scandium when exposed to other ions commonly found in bauxite residues, which presents magesium zirconium phosphate as a fast and selective material for scnadium ions.

Introduction. Scandium is classified as a rare-earth element (REE) and has been recognised as a valuable commodity for various advanced applications. One such example will be in the maufacturing of solidoxide fuel cells (SOFC) (Binnemans et al., 2018). There are not many mining sites for scandium and with the strong industrial development of fuel cells, recovery and recycling of scandium are a pressing issue to be addressed. Bauxite residues (BR) or red mud contains a high amount of scandium ranging from 50 to 110 mg kg^{-1} (Vind et al., 2018, Borra et al., 2015). The extraction of scandium from BR is often under acidic conditions, as the scandium ions are first leached from the wastes. Thus, employing an ion exchanger which can withstand the acidic conditions yet uptake scandium will be advantageous. In this work, we synthesised highly crystalline magnesium zirconium phosphate (MgZrP) for the adsorption of scandium under acidic conditions.

Methodology. MgZrP was first synthesised using a mechanochemical protocol and the ion exchange performance was tested with scandium ions done via batch uptake. The selecvitvity and kinetics was determined as well.

Results and Discussion. Previous synthesis methods of MgZrP resolves around ion exchange or hydrothermal synthesis. These processes either requires the formation of α-zirconium phosphate first, which followed by an ionexchange or a direct hydrothermal synthesis, where both requires additional time and

energy for its synthesis. However, our lab proposed a mechanochemical approach, which the precurors of MgZrP are ground together and the resultant gel is heated in an oven for 24 hours.

The crystalline MgZrP was synthesised via a minimal liquid assisted mechanochemical approach and its structure was confirmed with x-ray diffraction and inductively coupled plasma atomic emission specstrocopy. Scanning electron microscopy revealed the morphology of MgZrP (Figure 1a), which has a hexagoal shape and sizes of approximately 100 – 300 nm.

The adsorption of Sc^{3+} ions was done via a batch uptake and the ion exchange capacity of MgZrP for Sc^{3+} under acidic conditions was determined to be 24.7 mg g^{-1} (Figure 1b). Selectivty of Sc3+ among other ions was compared with common ions found in BR such was Al^{3+}, Cu^{2+} , Fe^{3+}, and Zn^{2+} . MgZrP was found to be very selective to Sc^{3+} when equimolar of the ions mentioned earlier (Figure 1c) are in the same system. This is advantageous since Fe^{3+} and Sc^{3+} have similar chemical properties and MgZrP is able to selectively adsorp Sc^{3+} over Fe^{3+} .

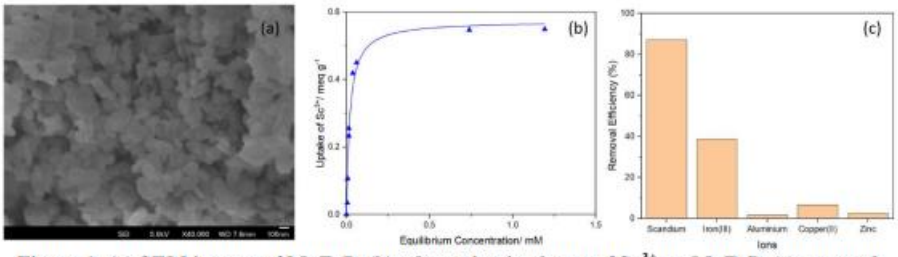

Figure 1: (a) SEM images of MgZrP, (b) adsorption isotherm of Sc^{3+} on MgZrP, (c) removal efficiency of Sc^{3+} in an equimolar multiplie ion solution.

Conclusion. In conclusion, crystalline magnesium zirconium phosphate was successfully synthesied via the mechanochemical approach. This method allows the material to be formed in 24 hours which is much shorter to conventional synthesis strategies. This material was found to have both fast and selective adsorption of scandium over other ions such as iron and copper, which are commonly found in bauxite residues.

References

C.R. Borra, Y. Pontikes, K., T. Van Gerven, Leaching of rare earths from bauxite residue (red mud) Min. Eng. 76 (2015) 20–27.

Binnemans, K., Jones, P.T., Müller, T. et al. Rare Earths and the Balance Problem: How to Deal with Changing Markets?. J. Sustain. Metall. 4, 126–146 (2018).

Binnemans Vind J, Malfliet A, Blanpain B, Tsakiridis PE, Tkaczyk AH, Vassiliadou V, Panias D. Rare Earth Element Phases in Bauxite Residue. Minerals. 2018; 8(2):77.

6th International Conference and
Postgraduate Colloquium for
Environmental Research 2022 (POCER
2022) 9 - 11 June 2022
Langkawi, Kedah, Malaysia

PCR14042022 – 127: EFFECT OF MAGNETIC FIELD ON THE PREPARATION OF Fe-COATED CELULLOSE/PLA NANOCOMPOSITE

Siti Hajar Omar, Rosli Mohd Yunus and Md. Maksudur Rahman Khan
Department of Chemical Engineering, College of Engineering, University of Malaysia Pahang

- E-mail: sitihajaromar1998@gmail.com

Keywords: Packaging; Polylactic acid(PLA) ; Cellulose nanocrystal(CNC); Iron particle (FeNp) ; Magnetic field ; Modified nanocellulose.

Extended Abstract

In recent years, the recognition of waste disposal problems and their impacts on the environment has risen the demand for packaging manufactured from renewable materials such as biopolymer. However, there are some limitations of using biopolymers such as brittleness and low mechanical properties for packaging applications. These issues may be addressed by incorporating biopolymers and nanomaterials. Cellulose nanocrystals (CNC) has shown a potential to be implemented as filler to reinforce synthetic polymer for packaging applications, equating its unique attributes of biodegradability to high surface area but their alignment and dispersion is a major limitation.Hence, this research was proposed to study an effect of magnetic field on modified nanocellulose with iron particles (FeNp) as a filler of PLA composites matrix. The procedure was based on 2 steps ; firstly preparation of nanocellulose modified with metal NP and next combination with PLA by solvent casting method. The influence of iron cellulose/PLA nanocomposites on morphology, hydrophilic and wettability of obtained nanocomposites was evaluated.

Introduction

Nowadays, plastic is the most widely used material. A large amount of petroleum based plastic waste is created each year around the world. Despite the growing number of appliances that are reused or recycled, a large amount of plastic is still accumulating in landfills. This final disposal option is causing major problems in the environment. As a result, researchers began to pay attention to biodegradable materials in order to lessen the environmental impact of residential plastics, as biodegradable plastics can be readily degraded by microbial action and be converted into biomass. These days, biodegradable plastic such as polylactic acid (PLA) made from renewable biomass like plant starch (usually corn). However, PLA is brittle and poses inferior mechanical properties. Therefore, certain modifications are needed to improve the properties of PLA.One common method is to blend PLA to form a composite with a reinforcing filler material [Nuthong et al.,213] which can be either synthetic or natural fibre. For this study, nanocellulose

form oil palm fruit bunches are selected as the filler reinforcement for PLA due to the abundance of this biomass in Malaysia. Reinforcing fibres can be employed as a reinforcement, however their dispersion and alignment is a major limitation. The mechanical properties of composite largely depend on fibre volume fraction and fibre direction/alignment.

To improve the dispersion and alignment, magnetic fields can be applied but NCC is not magnetically responsive. To incorporate magnetic properties into the NCC, it can be coated by metal particles [Mutiah et al. 2013]. The amount of metal nanoparticle loading and the magnetic field strength is a critical factor on the degree of the dispersion, which eventually controls the properties. So, it is necessary to study the interaction of the magnetic field strength, NP and NCC loading to achieve the best mechanical properties. Hence, the cellulose coated with iron particle was used in this study to generate nanocellulose with improved dispersibility (magnetic field) which was then used during the preparation of PLA films to elucidate on the mechanical properties and their characterization.

Materials and Method

Preparation of Iron Cellulose/Polylactic Acid (PLA) Films. For the preparation of the films, we used the procedure reported by Hossain et al. (2012) with some modifications. Pure PLA films,PLA/CNC and PLA/FE/CNC nanocomposite films were prepared using a solvent cast method. 5g of PLA was dissolved in 100 ml of chloroform under continuous stirring until the PLA completely dissolved. The desired amount of CNC (1%, 3%,5%) and iron cellulose (1%,3%,5%) was suspended in 10 ml of distilled water and then added to the PLA solution. After that, the two solutions were mixed for 45 minutes and then homogenized for 15 minutes. Afterwards, the homogenized solution was poured into stainless steel dishes and allowed to evaporate at room temperature for 24 h.

Examine Morphology of Iron Cellulose/PLA films. In order to analyze prepared films morphology, scanning electron microscope (SEM) and energy dispersive xray analysis (EDX) was utilized using Hitachi/TM3030 Plus. Next, characterization of the morphology of decorated CNCs were performed on JEOL-1400, 120 kV transmission electron microscopy (TEM).

Contact Angle Test. The contact angles of 5 μL water droplets on the film's surface attached to microscopic slides by doublesided tape were measured. The Rame Hart 200Std goniometer (Rame Hart Instrument co., Succasunna, NJ, USA) was used. The measurements were performed for 10 min with 1-s time intervals. A longer measurement did not give any reliable results, and it was decided to be completed after 10 min. Each contact angle value corresponded to the mean value of the left and right contact angle at a given point in time.

Result and Discussion

Morphology Analysis. The characterization of iron nanoparticles,SEM-EDX to prove the presence of iron nanoparticles.SEM images showed that the surface of nanocomposite films changed when the concentration of iron cellulose increased. The energy dispersive X-ray analysis (EDX) spectrum of $Fe(NO_3)_3.9H_2O$ nanoparticles is shown in Figure 1.0. The EDX spectrum indicates that the iron nitrate structures are composed of Ferum, Oxygen and Carbon. However, a small percentage of gold is present due to the need to coat the sample with a thin layer of gold in order to prevent charging of the surface and to provide a homogeneous surface for analysis and imaging. The morphology of the CNCs decorated with iron nanoparticles (IONPs) has been characterized by TEM and is shown in figure 2. The result showed that the surface of CNC is perfectly coated with IONPs so can proceed to produce PLA film by solvent casting method.

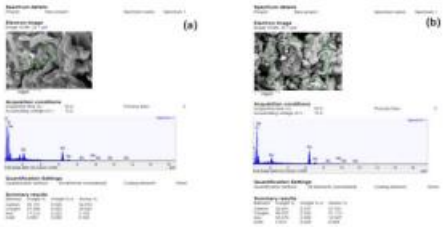

Figure 1.0: SEM-EDX images for iron nanocellulose (a) 2.5 % iron concentration (b) 5% iron concentration

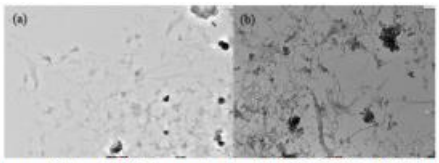

Figure 2.0: The morphology of the CNC decorated with IONPs (a) TEM of CNC with 2.5% IONPs (b) TEM of CNC decorated with 5% IONPs

Contact Angle. Water contact angles were measured for films and are presented in Table 1.0.The hydrophobic/hydrophilic properties are important features of packaging materials, influencing their resistance to humidity. Previously, it has been shown that the addition of cellulose nanocrystals to the PLA matrix causes a decrease of contact angle (from 80º to 70º) [Arieta et al.,2015]. The values of water contact angle above 65º are considered as acceptable.

Samples	Contact Angle,θ
Pure PLA	72.33
PLA/CNC 1 wt%	56.47
PLA/CNC 3 wt%	61.16
PLA/CNC 5 wt%	64.30
PLA/FE/CNC 1 wt%	51.59
PLA/FE/CNC 3 wt%	66.95
PLA/FE/CNC 5 wt%	63.73

Table 1.0: Water contact angle for each samples

Conclusion

PLA/ CNC nanocomposite films were successfully prepared through the solvent casting method with various internal mixers at CNC content 1,3,5 wt%. The impact of CNC on barrier, optical, and mechanical properties were investigated in this work as well as the morphology of the prepared films. The physical characterization of SEM-EDX and TEM proved the morphology changing and element contents present indicates the success of iron nanocomposites.

In addition, analysis on tensile strength of prepared film will be investigated to compare the ultimate strength point of the film and anti-microbial also will be analyzed to ensure packaged quality and safety.Lastly, further analysis on magnetic alignment will be designed to measure the effect of magnetic field on the preparation Fe-coated cellulose / pla nanocomposite.

Acknowledgement: This work supported by FRGS/1/2018/TK05/UMP/01/2

References

Arrieta, M.P.; Fortunati, E.; Dominici, F.; López, J.; Kenny, J.M. Bionanocomposite films based on plasticizedPLA–PHB/cellulose nanocrystal blends. Carbohyd. Polym. 2015, 121, 265–275.

Hossain, K. M. Z., Ahmed, I., Parsons, A. J., Scotchford, C. A., Walker, G. S.,Thielemans, W., & Rudd, C. D. (2012). Physico-chemical and mechanical properties of nanocomposites prepared using cellulose nanowhiskers and poly(lactic acid). Journal of Materials Science, 47(6), 2675-2686.

Nuthong, W., Uawongsuwan, P., Pivsa-Art, W., & Hamada, H. (2013). Impact property of flexible epoxy treated natural fiber reinforced PLA composites. Energy Procedia, 34, 839-847.

6th International Conference and Postgraduate Colloquium for Environmental Research 2022 (POCER 2022) 9 - 11 June 2022
Langkawi, Kedah, Malaysia

PCR15042022 – 128: Peptides purified from jellyfish wastewater with antimicrobial activity against *Propiobacterium acnes*

Benjamaporn Wonganu [a*], Suvimol Surassmo[b], Nichakorn Ocha[a], Sawanya Charoenlappanit[c], Benjawan Thumthanaruk[d], and Sittiruk Roytrakul[c]

[a] Department of Biotecnology, Faculty of Applied Science, King Mongkut's University of Technology North Bangkok, Bangkok 10800, Thailand

[b]Nanotechnology Center (NANOTEC), National Science and Technology Development Agency (NSTDA), 113 Paholyothin Road, Klong 1, Klong Luang, Pathumthani 12120, Thailand

[c] Functional Ingredients and Food Innovation Research Group, National Center for Genetic Engineering and Biotechnology, National Science and Technology Development Agency (NSTDA), 113 Paholyothin Road, Klong 1, Klong Luang, Pathumthani 12120, Thailand

[d]Department of Agro-Industrial, Food and Environmental Technology, Faculty of Applied Science, King Mongkut's University of Technology North Bangkok, Bangkok 10800, Thailand

*Corrensponsing Author E-mail: Benjamaporn.w@sci.kmutnb.ac.th

Keywords: Jellyfish; *Propiobacterium acnes*; Wastewater; antibacterial peptides; hydrophobic peptides; Added-value peptides

Extended Abstract

In jellyfish processing, processing wastewater due to the autolysis of jellyfish after harvesting is found as a vast source of protein. A nature jellyfish hydrolysate may be a relevant by-product of this process producing many short bioactive peptides used as ingredients in several products such as cosmetics, foods, and drugs. Recently, many pieces of research revealed that peptides found in marine organisms can inhibit *P.acne* and could promote a cell immune system [Marcinkiewicz and Majewski, 2016; Han *et.al*., 2018]. Therefore, those peptides are applied as anti-aging compounds in a moisturizer cream or as a cosmetic ingredient to deter dermatological pathogens.

The research focuses on the significance of wastewater from jellyfish processing, which might be a crucial unknown protein source, especially wastewater from white jellyfish processing. In the study, bioactive peptides in antimicrobial activity against pathogen bacteria, especially, *Propionibacterium acnes* (*P. acnes*), will be identified and analyzed because it is involved in the pathogenesis of acne, which is one of the most critical skin inflammatory. This research can resolve

environmental problems in waste disposal issues. Still, it also helps reuse waste for high-added values products that could be developed to be bioactive ingredients in cosmeceuticals.

5.45 kG of the processing wastewater was freeze-dried to concentrate proteins from nature jellyfish hydrolysate. 1.8 g of wastewater powder was washed with 70% ethanol and redissolved in 0.5%(w/v) Sodium Dodecyl Sulfate in 10 mM Acetate Buffer pH 4.0 before using PD-10 desalting column to remove salt excess in the sample. Most Antimicrobial peptides were revealed as positive charged and hydrophobic peptides [Stone *et.al.*,2019]. Therefore, A cation exchange column and a reversed-phase column were used for peptide purifications. Using the Broth dilution method, the purified sample determined an inhibitory activity against P. acnes. The results revealed that the purified sample contained an antibacterial activity against *P. acnes*.

To identify anti-*P. acnes* peptide sequences from the purified samples, Nano/Capillary LC (Ultimate3000 LC System, ThermoScientific, UK) with Hybrid quadrupole Q-Tof impact II™ (Bruker Daltonics) and Nano-captive spray ion source, peptide sequences present in the purified samples were used. Next, by applying the results to Bruker compass data analysis 4.4 software (Bruker Daltonics), the peptide sequences were analyzed. The appropriate antibacterial peptides were identified by DeCyder MS differential analysis 2.0 software (DeCyderMS, GE Healthcare) and Mascot (Matrix Science). Six peptide sequence candidates were chemically synthesized (GenScript Biotech, USA) depending on their helical symmetry, hydrophobicity or charge. Although all six chemically synthesized peptide sequences did not have antibacterial activity against *P.acnes*, they still contained inhibitory activity against *Klebsiella pneumoniae* and *Vibrio parahaemolyticus*, other human pathogen. The experiments still are in the process with other candidate synthesized peptides. Peptide sequences derived from wastewater samples with similar sequence structures or properties to Defensins or Cathelicidine would be screened for inhibitory against *P.acnes*. Many cysteines in the peptide sequence could induce a mechanism of action of bacterial cell-wall destruction. [Marcinkiewicz and Majewski, 2016; Wang, 2014; Wang *et.al.*,2015]

Table 1: Inhibitory activity against pathogenic bacterias of the synthesized peptides

Peptide sequences	*Propionibacterium acnes*	*Escherichia coli*	*Staphylococcus aureus*	*Klebsiella pneumoniae*	*Vibrio parahaemolyticus*	*Salmonella enterica*
	Inhibition (%)	Inhibition (%)	Inhibition (%)	Inhibition (%)	Inhibition (%)	Inhibition (%)
CVICRSIYDRNEIG	0.00	0.00	0.00	5.17	18.66	0.00
NLVDLAEKAQLLHE	0.00	0.00	0.00	2.98	18.37	0.00
ARIKFNSKLKPMLYIM	0.00	2.05	0.00	9.01	21.24	0.00
KNIQYKVVKKK	0.00	0.00	0.00	11.93	36.19	0.00
KEKNPPYLRFLTVL	0.00	0.00	0.00	10.05	22.22	0.00
RYRLRKKFPFPPT	0.00	0.00	0.76	12.46	21.36	0.00

Acknowledgments: The research was funded by the National Science and Technology Development Agency, Thailand. Contract no. JRA-CO-2564-15262-TH.

References

Marcinkiewicz, M., and Majewski, S. 2016. The role of antimicrobial peptides in chronic inflammatory skin diseases, Advances in Dermatology and Allergology. 33, 6-12.

Han, R., Blencke, H.-M., Cheng, H., and Li, C. 2018. The antimicrobial effect of CEN1HC-Br against *Propionibacterium acnes* and its therapeutic and anti-inflammatory effects on acne vulgaris, Peptides. 99, 36-43.

Stone, T.A., Cole, G.B., Ravamehr-Lake, D., Nguyen, H.Q., Khan, F., Sharpe, S., Deber, C.M. 2019. Positive Charge Patterning and Hydrophobicity of Membrane-Active Antimicrobial Peptides as Determinants of Activity, Toxicity, and Pharmacokinetic Stability. Journal of Medicinal Chemistry. 62(13), 6276-6286.

Wang, G. 2014. Human Antimicrobial Peptides and Proteins, Pharmaceuticals. 7, 545-594.

Wang, G., Mishra, B., Lau, K., Lushnikova, T., Golla, R., and Wang, X. 2015. Antimicrobial peptides in 2014, Pharmaceuticals. 8, 123-150.

6th International Conference and
Postgraduate Colloquium for
Environmental Research 2022 (POCER
2022) 9 - 11 June 2022
Langkawi, Kedah, Malaysia

PCR15042022 – 129: The ammonium based ionic liquids for gas hydrate mitigation

Ihtisham Ul Haq [1,2], Bhajan Lal [1,2], Muhammad Saad Khan [2], Dzulkarnain B Zaini[1]

[1] Chemical Engineering Department, Universiti Teknologi PETRONAS, Bandar Seri Iskandar, 32610 Perak, Malaysia b

[2] CO2 Research Centre (CO2RES), Universiti Teknologi PETRONAS, Bandar Seri Iskandar, 32610 Perak, Malaysia

Keywords: AILs; CO2 hydrates; Flow Assurance; HLVE; THI.

Extended Abstract

The thermodynamic hydrate inhibition (THI) behaviour of two ammonium-based ionic liquids (AILs), namely tetramethyl ammonium tetrafluoroborate ($TMABF_4$), tetraethylammonium tetrafluoroborate ($TEABF_4$), and their mixtures with the mixture of glycols for CO_2 hydrates are investigated in the present work. The T-cycle method is used to calculate the Hydrate liquid-vapour Equilibrium (HLVE) values for CO_2 hydrates at pressures ranging from 2.0 to 4.0 MPa for 5 wt% and 10% wt concentrations. The inhibition effect (average suppression temperature (Ŧ)) and dissociation enthalpies (Hdiss) are also determined. The mixture of $TMABF_4$ + glycols demonstrated a higher THI effect than the mixture of $TEABF_4$ + glycols owing to its shorter alkyl chain length. Therefore, using these AILs with CO_2 or natural gas pipelines may lead to their potential application in flow assurance strategies.

PCR15042022 – 130: Synthesis and characterization of MIL-101(Cr) and ZnO@MIL-101(Cr) nanocomposites for photocatalytic degradation of phenanthrene

Usman Abubakar Adamu and Noor Hana Hanif Abu Bakar*

Nanoscience Research Laboratory, School of Chemical Sciences, Universiti Sains Malaysia, 11800 Penang, Malaysia

- Corresponding Author E-mail: hana_hanif@usm.my

Keywords: MOFs; ZnO; Photocatalysts; Wastewater; PAHs; Phenanthrene

Extended Abstract

A series of crystalline and porous MIL-101(Cr) metal-organic frameworks and its ZnO@MIL-101(Cr) nanocomposites were synthesized using the hydrothermal technique at 160 and 220 ºC, while the ZnO nanoparticles were synthesized using banana peel (BP) extract as capping and reducing agents at room temperature. The idea is to incorporate the green synthesized ZnO into MOFs to enhance the photodegradation of phenanthrene. The as-synthesized MIL-101(Cr) and its ZnO nanocomposites were characterized using powdered X-ray diffraction (XRD), Scanning electron Microscopy (SEM), Fourier Transform Infrared (FT-IR) spectroscopy, Nitrogen adsorption-desorption analyses, ultraviolet-visible (UV-vis) diffuse reflectance (DRS) spectroscopy and photoluminescence (PL) spectroscopy. Fig. 1(a) shows the FTIR spectrum of the green synthesized ZnO nanoparticles. The main bands are observed at the 400-600 cm^{-1} region. The broadband at 505 cm^{-1} is attributed to the Zn-O vibration. The O-H stretching vibrations of hydroxyl groups from the phenolic compounds of BP extract appeared at ~3400 cm^{-1} (Abdullah et al., 2021). Similarly, Fig.1(b-e) shows the FTIR spectra of MIL-101(Cr) and ZnO@MIL-101 nanocomposites. The main peaks observed at 1404, 1630, 1680, and 933 cm^{-1} are attributed to the presence of aromatic O-C-O, C=C, C=O, and O-H out of plane stretching vibrations modes from the terephthalate ligand (Tang et al., 2020). In the case of ZnO@MIL-101@160 and ZnO@MIL-101@220, Fig. 1(d and e), another important peak at 505 is attributed to the Zn-O vibration. The XRD patterns of the green synthesized ZnO in Fig. 2 shows characteristic peaks at 2θ = 31.6º, 34.4º, 36.3º, 47.6º, 56.6º, 62.8º, 67.9º and 69.2º, which match well with the (100), (002), (101), (102), (110), (103), (112) and (201) crystalline planes of the hexagonal wurtzite structure of ZnO as reported by (Abdullah et al., 2021). High intensity of diffraction peaks and the absence of impure reflections confirmed the high crystallinity and purity of the prepared ZnO. Furthermore, in Fig. 2 (B), it can be observed that the 2θ values of 2.7° 3.3°, 5.12°, 5.83°, 8.5°, 9.1°, and 10.4° corresponded to the diffraction peaks of the calculated (220), (311), (511), (822), (753), (1022 and (880) planes of the MIL-101 and ZnO@MIL-101 nanocomposites respectively. The characterizations indicate that the

preparation of MIL-101(Cr), is successful (Tang et al., 2020). Interestingly, the above characteristic peaks observed, indicate that the crystalline structure of ZnO@MIL-101 is not destroyed after the addition of the ZnO. In addition, compared to MIL-101(Cr), these peak intensities of ZnO@MIL-101(Cr), are significantly weakened, which indicates that the crystallinity of the ZnO nanocomposite decreases and the crystalline structure becomes more disordered than that of pure MIL-101(Cr) (Tang et al., 2020 Hassan et al., 2017). Furthermore, large pore structures are generated in the composites which are due to uniform morphology, high surface area, and pore volume. The nitrogen adsorption-desorption analysis revealed a high BET surface area for the ZnO@MIL-101(Cr) composites (>1000 m^2/g) irrespective of synthesis temperature compared to MIL101(Cr). The UV-visible spectra of the ZnO@MIL-101(Cr) composites showed a strong absorption peak at 443 and 598 nm with a low bandgap of 3.10-3.30 eV while MIL101(Cr) has a bandgap of 3.5 eV. Finally, the MIL-101(Cr) and their ZnO@MIL-101(Cr) composites have been applied for the photocatalytic degradation of Phenanthrene.

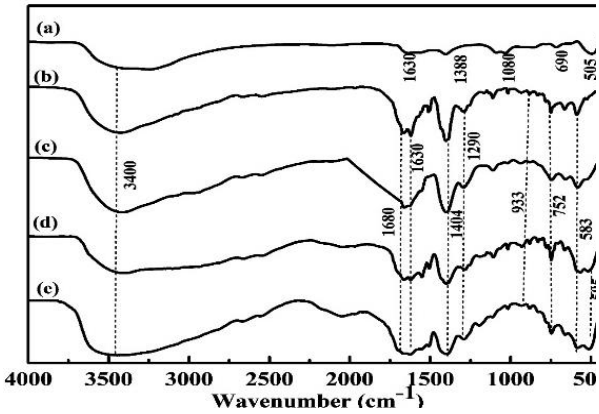

Fig. 1: FTIR spectrum of (a) ZnO (b) MIL-101@160, (c) MIL-101@220, ZnO@MIL-101@160 and (d) ZnO@MIL-101@220.

Table 1: Properties of ZnO, MIL-101, and their nanocomposites.

Catalyst	BET (m^2/g)	V_{BJH}(cm^3/g)	D_{BJH}(Å)
ZnO	15.05	0.096	280.46
MIL-101@160	862.7	0.1792	24.390
MIL-101@220	760.69	0.1528	23.56
ZnO@MIL-101@160	1811.99	0.427	25.11
ZnO@MIL-101@220	1181.07	0.382	2397

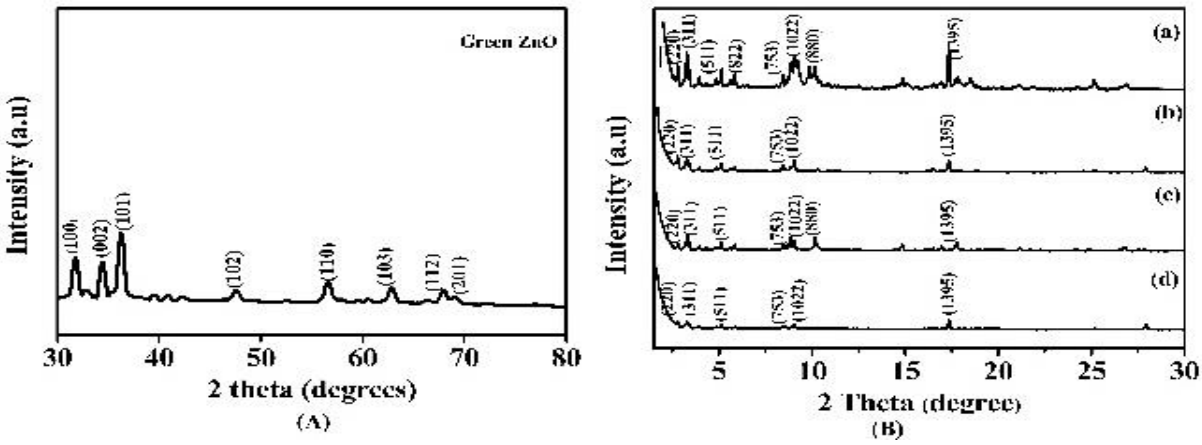

Fig. 2: XRD of (A) green synthesized ZnO; (B) MIL-101(Cr) and ZnO/MIL-101 nanocomposites.

Acknowledgment: The authors thank Universiti Sains Malaysia for the grant 1001/PKIMIA/8011071

References

Abdullah, F. H., Abu Bakar, N. H. H., & Abu Bakar, M. (2021). Comparative study of chemically synthesized and low temperature bio-inspired Musa acuminata peel extract mediated zinc oxide nanoparticles for enhanced visible-photocatalytic degradation of organic contaminants in wastewater treatment. *Journal of Hazardous Materials*, *406*(August 2020), 124779. https://doi.org/10.1016/j.jhazmat.2020.124779

Hassan, H. M. A., Betiha, M. A., Mohamed, S. K., El-Sharkawy, E. A., & Ahmed, E. A. (2017). Stable and recyclable MIL-101(Cr)–Ionic liquid based hybrid nanomaterials as heterogeneous catalyst. *Journal of Molecular Liquids*, *236*(May), 385–394. https://doi.org/10.1016/j.molliq.2017.04.034

Tang, Y., Yin, X., Mu, M., Jiang, Y., Li, X., Zhang, H., & Ouyang, T. (2020). Anatase TiO2@MIL-101(Cr) nanocomposite for photocatalytic degradation of bisphenol A. *Colloids and Surfaces A: Physicochemical and Engineering Aspects*, *596*(March), 124745. https://doi.org/10.1016/j.colsurfa.2020.124745

6th International Conference and Postgraduate Colloquium for Environmental Research 2022 (POCER 2022) 9 - 11 June 2022
Langkawi, Kedah, Malaysia

PCR15042022 – 131: Acceleration the recalcitrant synthetic dyes biodegradation processing by modification culture conditions: A case study by *Fusarium oxysporum*

Nguyen Duc Huy[a], Le Thi Kim Thoa[b], Trinh Thi Phuong Thao[b], Nguyen Thi My Le[b], Nguyen Duc Chung[c], Kuan Shiong Khoo[d], Ooi Chien Wei[e], Pau Loke Show[f], Seung-Moon Park[b]

[a] Insitute of Biotechnology, Hue University, Hue, 49000, Vietnam.

[b] Jeonbuk National University, Jeonju-si, Jeollabuk-do, 54896, Republic of Korea.

[c] University of Agriculture and Forestry, Hue University, Hue, 49000, Vietnam.

[d] Faculty of Applied Sciences, UCSI University. No. 1, Jalan Menara Gading, UCSI Heights, 56000, Cheras Kuala Lumpur, Malaysia.

[e] Chemical Engineering Discipline and Advanced Engineering Platform, School of engineering, Monash University Malaysia, Jalan Lagoon Selatan, Bandar Sunway 47500, Selangor Darul Ehsan, Malaysia.

[f] Department of Chemical and Environmental Engineering, Faculty of Science and Engineering, University of Nottingham Malaysia, Jalan Broga, 43500 Semenyih, Selangor Darul Ehsan, Malaysia.

- Corrensponsing Author E-mail:

Keywords: bioremediation, waste water treatment, remazol brilliant blue R, optimization.

Extended Abstract

Synthetic dyes are widely using in many industries areas. Most of synthetic dyes can be degraded by microorganism. However, some of dyes strongly resist against biodegradation processing. Thus, these recalcitrant dyes caused numerous problems for the treatment processing that need to overcome. In this study, the biological degradations of recalcitrant dyes including aniline blue, reactive black 5, orange II, and crystal violet were assessed and evaluated through modification the culture conditions of *Fusarium oxysporum* HUIB02. The results indicated biodegradation efficiency significantly enhanced after modifying the cells biomass, nutrient conditions, and mediators. Supplementation glucose

concentration at 1% improved aniline blue, reactive black, orange II, and crystal violet by 2.24, 1.51, 4.46, and 2.1 folds, respectively. Meanwhile, mediators significantly increased biodegradation aniline blue, reactive black, orange II, and crystal violet, reaching 86.07%, 68.29%, 76.35%, and 95.3% total color removal, respectively. Interestingly, pre-culture the fungal with 1% remazol brilliant blue R (RBBR) boost the biodegradation up to 97.06%, 89.86%, 91.38%, and 86.67% for aniline blue, reactive black, orange II, and crystal violet, respectively. Under optimal culture conditions, the fungal could degrade these synthetic dyes concentration up to 1%. The present study demonstrated recalcitrant dyes can be efficiently degraded by *F. oxysporum*.

6th International Conference and Postgraduate Colloquium for Environmental Research 2022 (POCER 2022) 9 - 11 June 2022
Langkawi, Kedah, Malaysia

PCR15042022 – 132: Identification and analysis of short peptides derived from wastewater in pre-salted jellyfish (*Lobonema smithii*) processing

Nichakorn Ocha[a], Sawanya Charoenlappanit[b], Malinee Sriariyanun[d], Benjawan Thumthanaruk[c], Sittiruk Roytrakul[b], and Benjamaporn Wonganu[a*]

[a] Department of Biotechnology, Faculty of Applied Science, King Mongkut's University of Technology North Bangkok, Bangkok 10800, Thailand

[b] Functional Ingredients and Food Innovation Research Group, National Center for Genetic Engineering and Biotechnology, National Science and Technology Development Agency, 113 Paholyothin Road, Klong 1, Klong Luang, Pathumthani 12120, Thailand

[c]Department of Agro-Industrial, Food and Environmental Technology, Faculty of Applied Science, King Mongkut's University of Technology North Bangkok, Bangkok 10800, Thailand

[d]Department of Mechanical and Process Engineering, The Sirindhorn International Thai-German Graduate School of Engineering (TGGS), King Mongkut's University of Technology North Bangkok (KMUTNB), Bangkok 10800, Thailand

*Corrensponsing Author E-mail: Benjamaporn.w@sci.kmutnb.ac.th

Keywords: Jellyfish; *Lobonema smithii*; Wastewater; Short peptides; Antioxidant; Added-value peptides

Extended Abstract

Wastewater from Jellyfish (*Lobonema smithii*) harvesting and processing impacts people living in close contact with the sea because of water pollution. However, the wastewater in pre-salted jellyfish contains many short peptides produced by proteolysis-induced mucus secretion of the jellyfish after removing them from seawater [Liu et al., 2018]. The vast source of small peptides in that waste, as mentioned above, the researcher was interested in analyzing short peptides derived from wastewater in pre-salted jellyfish.

This research aimed to study the purification process and analyze antioxidant short-chain peptides derived from wastewater in pre-salted jellyfish (*Lobonema smithii*) processing using different chromatography techniques. In addition, the crude peptides are sequenced by using Liquid Chromatography-Tandem Mass Spectrometry (LC-MS/MS) for antioxidant peptides determination. Consequently, the active peptides would be studied for their stability.

There are six steps in the research. First, wastewater in pre-salted jellyfish (*Lobonema smithii*) processing was collected and freeze-dried. Second, the peptides were extracted from the wastewater with 0.5% Sodium dodecyl sulfate (SDS) [Kaweewong et al., 2013]. Third, the peptides were purified using various chromatography techniques (such as gel filtration, ion-exchange, and reversed-phase chromatography). Then, the isolated peptides were determined by DPPH (2,2-diphenyl-1-picrylhydrazyl radical) assay [Xiao et al., 2020] to observe the highest antioxidant activity. The activity's results were calculated from the following equation (1) and shown as DPPH radical scavenging activity (%) per milligram of protein.

$$\text{DPPH radical scavenging activity (\%)} = (A1-A2) \times 100/A1 \quad (1)$$

where A1 is the absorbance of the control and A2 is the absorbance of the testing sample solution.

After that, the antioxidant peptides were sequenced by LC-MS/MS and were analyzed using DeCyder MS differential analysis 2.0 software (DeCyderMS, GE Healthcare) and Mascot software (Matrix Science). The peptides were matched to the published sequence of the relative protein data in the Scombridae database (NCBInr databank). The candidate peptides were chemically synthesized by GenScript Biotech (NJ, USA) as above 85% purity and were determined again for antioxidant activity test. The stability of the antioxidant peptides with the highest antioxidant activity would be further studied to develop these peptides for the food and pharmaceutical industries.

The results showed that 3.41 % was the freeze-dried yield of five kilograms of wastewater. The fifteen gram of wastewater freeze-dried was dissolved for an antioxidant activity test and protein purification. The results revealed that the peptides purified using gel filtration, reversed-phase, and cation exchange chromatography contained 166.9, 126.8, and 161.5 DPPH (%) / mg of protein. However, the peptides purified from anion exchange chromatography had no antioxidant activity against the DPPH assay (Figure 1). Therefore, the various sodium chloride (NaCl) concentrations of 50-1000 mM were used for elution cation exchange chromatography. Then, 5 to 100% Acetonitrile (ACN) concentration was varied in the reversed-phase column to determine peptides with high antioxidant activity. The results showed that the fractions were first eluted with 150 mM and 900 mM NaCl in cation exchange chromatography and then purified and eluted with 10%, 35%, and 95% ACN in the reverse-phase column, respectively, obtained high antioxidant activity. The crude peptides from these fractions were sequenced using LC/MS/MS, and candidate peptides were sent to chemically synthesized by GenScript Biotech. The obtained peptides with antioxidant activity from wastewater of pre-sated jellyfish processing could be one solution to decrease waste from the production process and change it to value-added peptides.

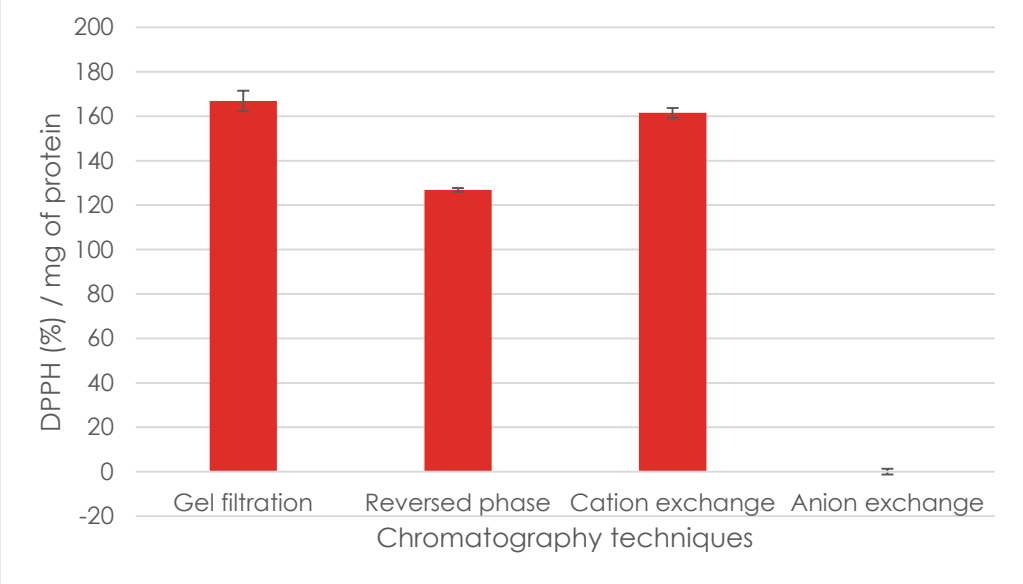

Figure 1: Antioxidant activity of the peptides purified using various chromatography techniques.

Acknowledgements: The research was funded by King Mongkut's University of Technology North Bangkok and National Science and Technology Development Agency, Thailand. Contract no. B.002 /2563

References

Kaweewong, K., Garnjanagoonchorn, W., Jirapakkul, W., and Roytrakul, S. (2013). Solubilization and identification of hen eggshell membrane proteins during different times of chicken embryo development using the proteomic approach. *Protein J*, 32(4), 297-308.

Liu W., Mo F., Jiang G., Liang H., Ma C., Li T., Zhang L., Xiong L., Mariottini GL., Zhang J., Xiao L. (2018). Stress-Induced Mucus Secretion and Its Composition by a Combination of Proteomics and Metabolomics of the Jellyfish Aurelia coerulea. *Mar Drugs*, 16(9).

Xiao, F., Xu, T., Lu, B., and Liu, R. (2020). Guidelines for antioxidant assays for food components. *Food Frontiers*, 1(1), 60-69.

6th International Conference and
Postgraduate Colloquium for
Environmental Research 2022 (POCER
2022) 9 - 11 June 2022
Langkawi, Kedah, Malaysia

PCR15042022 – 133: The Reliance on Zirconate for the Production of Proton-conducting Solid Oxide Fuel Cell Electrolyte: A Short Review

Nur Wardah Norman[a], Mahendra Rao Somalu[a*], Andanastuti Muchtar[a, b], Nurul Akidah Baharuddin[a], and Muhammed Ali S.A. [a]

[a] Fuel Cell Institute, Universiti Kebangsaan Malaysia, 43600 UKM Bangi, Selangor, Malaysia

[b] Department of Mechanical and Manufacturing Engineering, Faculty of Engineering and Built Environment, Universiti Kebangsaan Malaysia, 43600 UKM Bangi, Selangor, Malaysia

- Corrensponsing Author E-mail: mahen@ukm.edu.my

Keywords: Proton-conducting electrolyte; Solid oxide fuel cell; Zirconate material.

Extended Abstract

Solid oxide fuel cells (SOFCs) have gained a huge attention due to their fuel diversity, high efficiency, improved performance, better heat utilisation in both heat and power systems, improved life span and low production of noise and pollutants. This short review will be focusing on the importance of zirconate material in the production of proton-conducting solid oxide fuel cell electrolyte.

Introduction

In proton-conducting SOFCs (H^+-SOFCs) as shown in Figure 1, by-products are obtained at the cathode thus eliminating fuel dilution problem and eliminating the need for fuel reforming. Proton-conducting electrolytes must have high ionic conductivity, be dense enough to inhibit gas diffusion and be chemically and thermally stable in relation to other components. Perovskite type-oxide ABO_3, such as those based on cerates or zirconates or cerate-zirconates, is widely regarded as a promising electrolyte material for H^+-SOFCs. Solid electrolytes that are based on cerate–zirconates have been studied extensively because of their acceptable proton conductivity and chemical stability in hydrogen and/or water vapour atmospheres. These perovskite oxides are usually doped with low valence cation at the A- and B-site to create oxygen ion vacancy which is essential for proton conduction. The most common proton-conducting electrolytes studied till now are Ba-based A-site due to their high conductivity [Radenahmad et al., 2020].

The basis for using zirconate as an electrolyte material

Despite being a promising electrolyte with the highest proton conductivity, doped-cerate material has a tendency to react with acidic gases (CO_2, SO_2) and water vapour (H_2O). The low chemical stability leads to the formation of carbonate, sulphate or hydroxide phases, thus resulting in total or partial surface deterioration. Zirconates have strong chemical stability in CO_2, but they have lower electrical or proton conductivity whenever grain boundaries are prominent. Thus, cerate-based perovskites and zirconate-based perovskites have mutually opposing drawbacks and benefits in terms of stability and conductivity. Satisfactory H^+-SOFCs performances were also broadly documented in which dopant-optimised electrolytes such as $Ba(Ze_{0.1}Ce_{0.7}Y_{0.2})O_{3-\delta}$, displayed the highest ionic conductivity along with encouraging stability in both CO_2 and H_2O atmosphere [Zhang et al., 2021].

Several studies focus on combining $BaZrO_3$ and $BaCeO_3$ to create chemically stable and highly conductive electrolytes. Since they are mutually stable, manipulating a fraction of Zr in $BaZrO_3$ with Ce can result in a chemically stable electrolyte with desired proton conductivity. Throughout most cases, increasing the Ce content in $BaZrO_3$ improved overall conductivity, sinterability, and decreased instability in ambient atmospheres. $BaCe_{0.9-x}Zr_xY_{0.1}O_{3-\delta}$ electrolyte for example was discovered to be stable under the condition of 40 mol% of Zr through this approach [Kim et al., 2019]. The yttria composition of 20 mol % in $BaZr_{0.8}Y_{0.2}O_{3-\delta}$ electrolyte is considered most suitable due to appropriate microstructure for high conductivity. They exhibit unique properties due to similar electron density of O^{-2} to Y^{+3} and Zr^{+4} cations. [Irshad et al., 2019]. Based on the findings, the researchers concentrated their efforts on improving the cerate-zirconate materials by varying the dopants for the formation of oxygen vacancies which in return enhances proton transport.

Despite its high-temperature findings on conductivity, the stability of the electrolyte materials in ambient settings is crucial, as it affects SOFC systems. Higher Zr doping ratio slowed down the aging degradation of BZCY and can be reversible by re-calcining the material to become pure BZCY perovskite [Yan et al., 2015]. However, compositions with a high Zr content (> 40 mol%), have a high grain boundary resistance and require a high sintering temperature (> 1600 °C). On the other hand, a composition with a low Zr content is unsuitable for long-term operation in a reducing environment. The moderate incorporation of Zr (10–30%) is a reasonable and practically the most realistic method for obtaining excellent thermal stability and high protonic conductivity [Sonu et al., 2021].

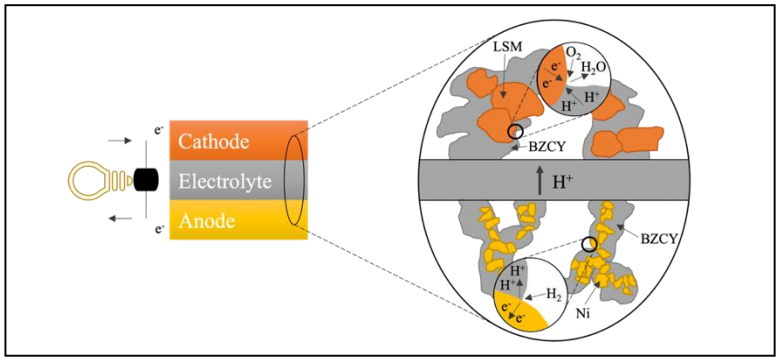

Figure 25: A typical proton-conducting solid oxide fuel cell (H^+-SOFC)

Conclusions

To alleviate the deficiency in perovskite materials, more developments have been focused on doping the cerate-zirconate materials. Enhancing the ionic conductivity of zirconate-based perovskite seems to be more crucial than that of cerate-based perovkite.

Acknowledgements: The authors would like to thank the Universiti Kebangsaan Malaysia for the funding support through the research sponsorship of GUP-2021-076.

References

Irshad, M., Ain, Q., Siraj, K., Raza, R., Tabish, A. N., Rafique, M., Idrees, R., Khan, F., Majeed, S., & Ahsan, M.,. 2019. Evaluation of BaZr0.8X0.2 (X= Y, Gd, Sm) proton conducting electrolytes sintered at low temperature for IT-SOFC synthesized by cost effective combustion method. *Journal of Alloys and Compounds*, *815*, 152389.

Kim, J., Sengodan, S., Kim, S., Kwon, O., Bu, Y., & Kim, G.,. 2019. Proton conducting oxides: A review of materials and applications for renewable energy conversion and storage. *Renewable and Sustainable Energy Reviews*, *109*, 606–618.

Radenahmad, N., Afroze, S., Abedin, A., Azad, A., Shin, J.-S., Park, J., Haji Zaini, J., & Azad, A.,. 2020. High conductivity and high density SrCe0.5Zr0.35Y0.1A0.05O3-δ (A = Gd, Sm) proton-conducting electrolytes for IT-SOFCs. *Ionics*, *26*, 1–9.

Sonu, B. K., & Sinha, E.,. 2021. Structural, thermal stability and electrical conductivity of zirconium substituted barium cerate ceramics. *Journal of Alloys and Compounds*, *860*, 158471.

Yan, N., Zeng, Y., Shalchi Amirkhiz, B., Wang, W., Gao, T., Rothenberg, G., & Luo, J.-L.,. 2015. Discovery and Understanding of the Ambient-Condition Degradation of Doped Barium Cerate Proton-Conducting Perovskite Oxide in Solid Oxide Fuel Cells. *Journal of The Electrochemical Society*, *162*, F1408–F1414.

Zhang, W., & Hu, Y. H.,. 2021. Progress in proton-conducting oxides as electrolytes for low-temperature solid oxide fuel cells: From materials to devices. *Energy Science & Engineering*, *9*(7), 984–1011.

6th International Conference and
Postgraduate Colloquium for
Environmental Research 2022 (POCER
2022) 9 - 11 June 2022
Langkawi, Kedah, Malaysia

PCR15042022 – 134: Optimum hole-depth of porous anodes for electrically active microorganisms at specific apertures

Pinpin Yang [a], Yujie Feng [a] , Weihua He [a*],

[a] School of Environmental Science and Engineering, Academy of Ecology and Environment, Tianjin University,No 92 Weijin Road, Nankai District Tianjin 300072. Tianjin, China

- Corrensponsing Author E-mail: weihua.he@tju.edu.cn

Keywords: Electroactive biofilm; Microbial fuel cells; Porous anode; Pore size; Colonisation depth

Extended Abstract

Porous anodes can improve electrode performance by increasing microbial attach-ment through increased specific surface area, but the optimal pore size and effective depth are not known. In order to explore the relationship between the electrochemical performance of three-dimensional porous biological anodes and their pore size and hole depth, we customized a multilayer, removable "bacterial apartment" to provide a "standard room" with an aperture size of 0.5-4 mm for electroactive microorganisms. This "layered" structure is helpful to study the penetration depth and layer by layer bioelectrochemical performance of electroactive microorganisms. By using CV, confocal microscopy, high-throughput sequencing and other techniques, we obtained the penetration depth, biofilm thickness, living and dead state, species composition and electricity generation intensity of electroactive microorganisms in micropores. The effective hole depths of 0.5 mm, 1 mm, 2 mm, 3 mm and 4 mm are 2 mm, 2 mm, 4 mm, 7-8 mm and more than 10 mm respectively. At the same depth, the larger the hole diameter is, the higher the current density is. As can be seen from the data of the second layer, the current density of D4 is 0.23 A m^{-2}, while the current density of D0.5-3 is 0.17, 0.13, 0.073 and 0.069 A m^{-2}, respectively. In all pores, *Geobacter* is the main type of biofilm acclimated by sodium acetate, and the abundance can reach more than 70%. In addition, the thickness and current density of biofilm increase with the increase of pore size, but decrease with the increase of hole depth. In this paper, the laws of electricity generation and penetration of electroactive microorganisms in different pore sizes were obtained successfully, which provided theoretical basis for the design and application of porous bio-anodes.

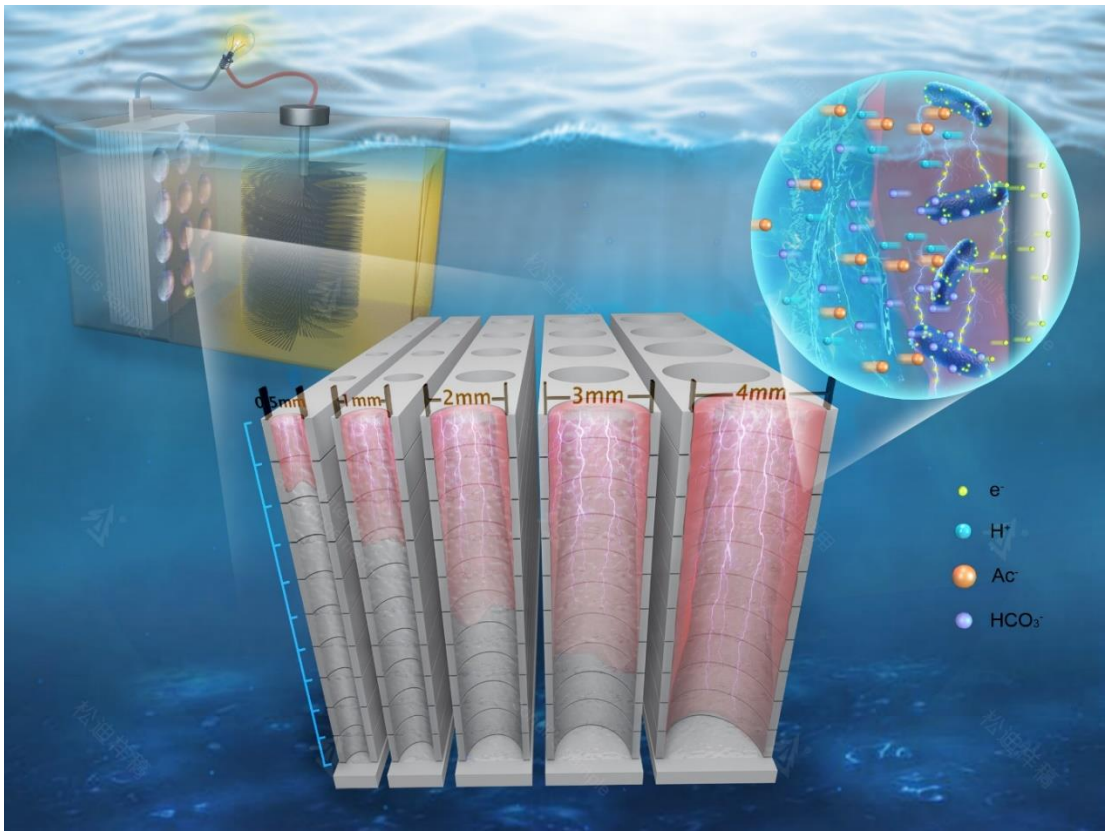

Figure 26: Graphical Abstract

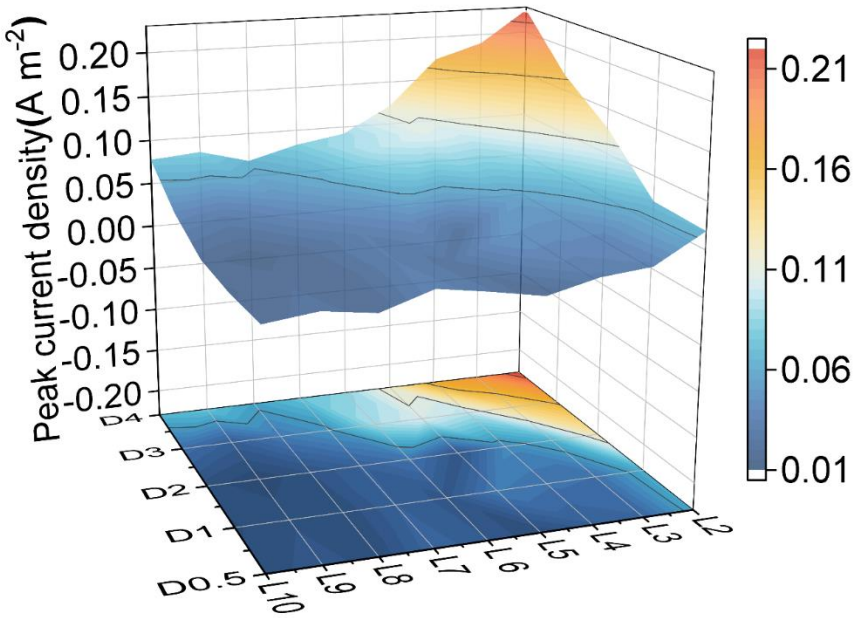

Figure 2: The CV peak current intensity changes with the increase of depth in different pore sizes.

6th International Conference and
Postgraduate Colloquium for
Environmental Research 2022 (POCER
2022) 9 - 11 June 2022
Langkawi, Kedah, Malaysia

PCR15042022 – 137: Modelling of Oxygen Diffusion Mechanism at SOFC Cathode using AdlerLane-Steele Mathematical Method: Applied to 5% wt $SrFe_{0.9}Ti_{0.1}O_{3-\delta}$ and 5% wt SDC

Azreen Junaida Abd Aziz[a] , Nurul Akidah Baharuddin[a*], Mahendra Rao Somalu and Andanastuti Muchtar[b]

a Institut Sel Fuel, Universiti Kebangsaan Malaysia, Bangi, Selangor, Malaysia
b Department of Mechanical Engineering Universiti Kebangsaan Malaysia, Bangi, Selangor, Malaysia

• Corresponding Author E-mail: akidah@ukm.edu.my

Keywords: Solid Oxide Fuel Cell; Cathode; Adler-Lane-Steele model; oxygen diffusion

Extended Abstract

Solid oxide fuel cells are of interest technologically because they provide high-efficiency energy conversion through an electrochemical reaction within the cells. Understanding the fundamental characteristics of oxygen self-diffusion in solid-state ionic systems is critical for developing next-generation electrolyte and cathode material compositions and microstructures that enable SOFCs to operate more effectively, durably, and inexpensively at lower temperatures (Abd Aziz et al. 2020). Due to the slower oxygen reduction kinetics at a lower temperature, the electrochemical performance of SOFC is highly dependent on the catalytic activity of the cathode materials engaged in the oxygen reduction reaction. Modelling approaches have been utilised to understand the reaction mechanism, oxygen diffusion coefficient and kinetics of electrode reactions in SOFC, including the mixed ionic electronic conductor (MIEC)-based cathode. Recently, various models were developed to represent the reaction mechanisms of SOFCs, particularly at the cathode electrode (Flura et al. 2016).

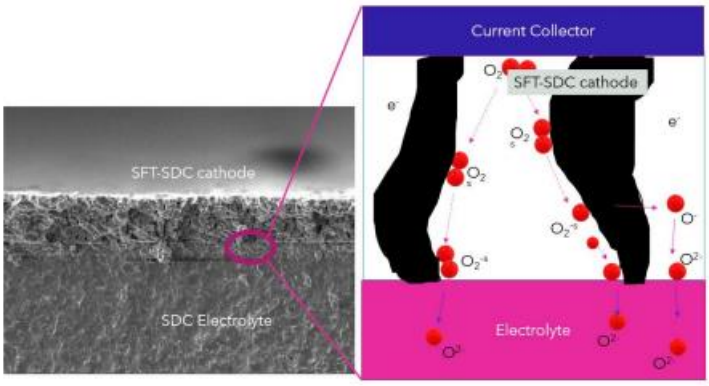

Figure 1: Oxygen Diffusion Pathway

For the cathode, Adler-Lane-Steele's (ASL) mathematical theory is suitable for predicting the oxygen gas diffusion through the pores for the MIEC-based materials (Adler 2004) (Adler, Lane, and Steele 1996).

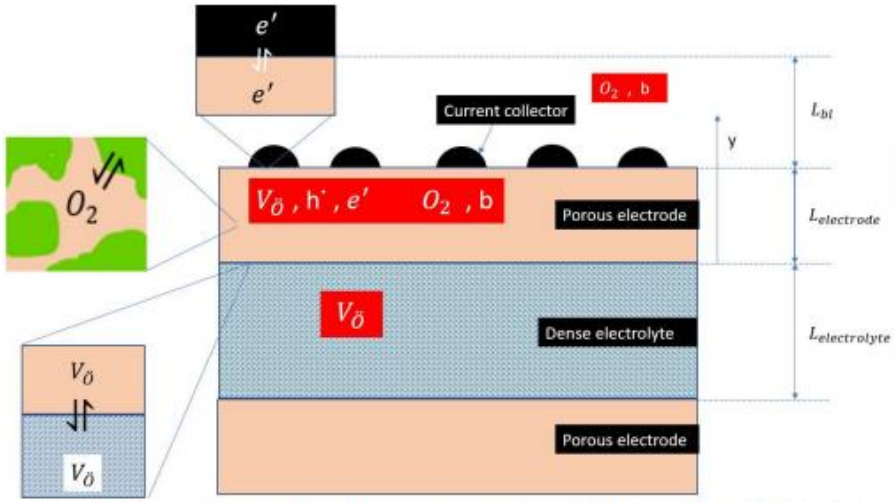

Figure 2: Schematic of the reaction mechanism considers by ALS model

This review attempted to summarise cathode's modelling works via the ASL mathematical theory. This article will help the researchers anticipate and validate the cathode performance regarding the oxygen gas diffusion mechanism

Acknowledgements: The authors thank the Research Grant GUP-2020-080

References

Abd Aziz, Azreen Junaida, Nurul Akidah Baharuddin, Mahendra Rao Somalu, and Andanastuti Muchtar. 2020. "Review of Composite Cathodes for Intermediate-Temperature Solid Oxide Fuel Cell Applications." Ceramics International 46(15):23314–25.

Adler, S. B., J. A. Lane, and B. C. H. Steele. 1996. "Electrode Kinetics of Porous Mixed-Conducting Oxygen Electrodes." Journal of The Electrochemical Society 143(11):3554–64.

Adler, Stuart B. 2004. "Factors Governing Oxygen Reduction in Solid Oxide Fuel Cell Cathodes." Chemical Reviews 104(10):4791–4843.

Flura, A., C. Nicollet, V. Vibhu, B. Zeimetz, A. Rougier, J. M. Bassat, and J. C. Grenier. 2016. " Application of the Adler-Lane-Steele Model to Porous La 2 NiO 4+ δ SOFC Cathode: Influence of Interfaces with Gadolinia Doped Ceria ." Journal of The Electrochemical Society 163(6):F523–32.

6th International Conference and
Postgraduate Colloquium for
Environmental Research 2022 (POCER
2022) 9 - 11 June 2022
Langkawi, Kedah, Malaysia

PCR15042022 – 138: Bibliometric Analysis of Research Trends in Plant Ageing Management and Application of Industry 4.0 Technologies

Tengku Nor Azira Tengku Mohamed Salim[a], Masli Irwan Rosli[a*], and Mohd Sobri Takriff[b]

[a] Department of Chemical and Processes Engineering
National University of Malaysia, Selangor, Malaysia

[b] Department of Chemical and Processes Engineering
National University of Malaysia, Selangor, Malaysia

- Corrensponsing Author E-mail: tengkunorazira@gmail.com

Keywords: Equipment ageing; Industry 4.0; bibliometric analysis; research trends; VOSviewer

Extended Abstract

Ageing of equipment is garnering global attention due to several major industrial accidents. Other ageing factors besides equipment age include damage, failure, degradation mechanism, unscheduled shutdown, and near-miss accidents that may cause unrecognized ageing of newly used equipment that has not yet surpassed the intended lifespan limit (Milazzo et al. 2018).

Two systematic bibliometric analyses of the extensive research development of equipment ageing and the application of Industry 4.0 technologies in asset management have been performed. The first bibliometric study is analyze the equipment ageing publications in the Scopus database from 2000 to 2021. According to the growth pattern of publications on equipment ageing from 2000 to 2021, the increased cumulative number of publications in the last decade (2011 to 2021) has resulted in a 3.5-fold rise in total publications from 40 to 143 papers, as shown in Figure 1. Chemical Engineering Transactions (4 publications), United States (36 publications), and Millazo M.F. is the top journal, country, and author in equipment ageing research publications (6 publications). Analysis of keywords was conducted using VOSviewer highlighted five main clusters of equipment ageing management in various industries, and the suitable sub-categorizations are as follows. The respective industries are Cluster 1: chemical and petroleum industries (red), Cluster 2: nuclear and process industries (green),

Cluster 3: oil and gas industry (blue), Cluster 4: upstream petroleum industry (yellow), and Cluster 5: electric industry (purple).

The following bibliometric analysis focused on applying Industry 4.0 technologies in asset management. According to the growing trend of publications in this study, the total cumulative number of publications has expanded exponentially from 1 to 69 papers in 6 years (2016 to 2021). IFAC Papersonline (5 publications), Germany (8 publications), and Guillén, A. (5 publications) is the top journal, country, and author for this bibliometric analysis. Six primary clusters of keyword analysis were emphasized by the VOSviewer software, as illustrated in Figure 2. The appropriate subfield categorizations consist of the types of Industry 4.0 technologies implementation for asset management are as follows. Cluster 1: information technology solution in operation and maintenance (red), Cluster 2: big data in equipment information management (green), Cluster 3: Artificial Intelligence in condition monitoring and decision making (blue), Cluster 4: Internet of Things in predictive maintenance and process control (yellow), and Cluster 5: economic aspect in digital twin (purple), and Cluster 6: Industrial Internet of Things and digital transformation (cyan).

In conjunction with reducing the risk of industrial accidents due to ageing equipment, the future research prospects that have the potential to be exploited are the implementation of 6 out of 9 Industry 4.0 technologies in asset management. The possible emerging technologies are the Internet of Things (IoT), big data, simulations, cloud computing, cybersecurity, and Augmented Reality (AR).

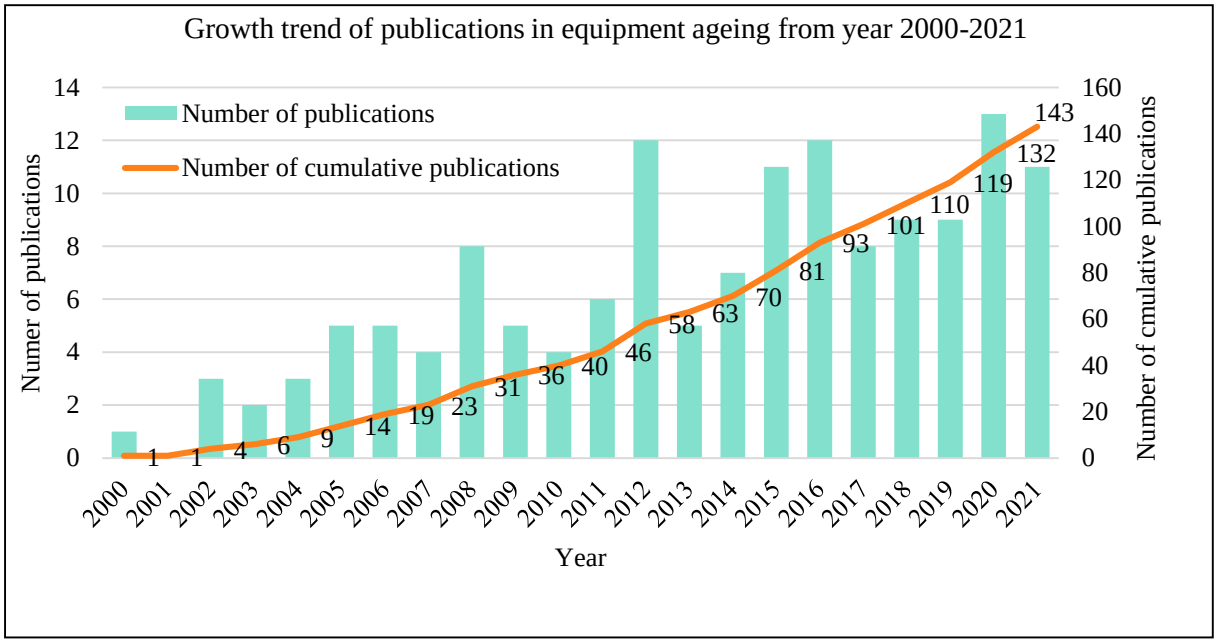

Figure 27: Growth Trend of Publications in Equipment Ageing from Year 2000 to 2021

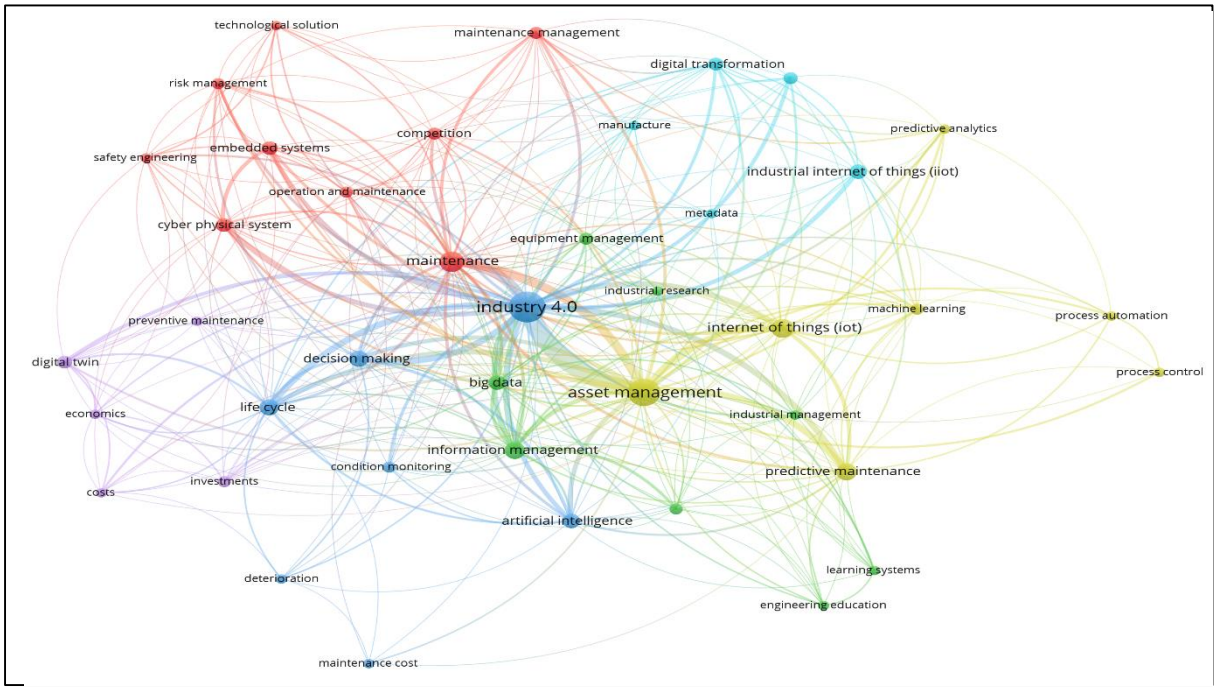

Figure 2: Keyword Network Visualization of Asset Management and Industry 4.0 Technologies in VOSviewer

Acknowledgements: The authors thank the UKM-YSD Sustainability Chair for funding this project.

References

Milazzo, M.F., Bragatto, P., Ancione, G. & Scionti, G. 2018. Ageing assessment and management at major-hazard industries. *Chemical Engineering Transactions* 67: 73–78.

6th International Conference and
Postgraduate Colloquium for
Environmental Research 2022 (POCER
2022) 9 - 11 June 2022
Langkawi, Kedah, Malaysia

PCR15042022 – 139: Effects of the current collector on the microstructural and electrochemical performance of modified lithiated nickel based electrode

Wan Nor Anasuhah Wan Yusoff[a], Nurul Akidah Baharuddin[a*], Mahendra Rao Somalu[a], Nigel P. Brandon[b], Nor Anisa Ariffin[a]

[a] Fuel Cell Institute
Universiti Kebangsaan Malaysia, 43600 UKM Bangi, Selangor, Malaysia

[b] Department of Earth Science and Engineering
Imperial College London, South Kensington Campus, London SW 2 AZ, UK

- Corrensponsing Author E-mail: akidah@ukm.edu.my

Keywords: Electrode; Lithium; Microstructural; Electrochemical Performance; Symmetrical Solid Oxide Fuel Cell

Extended Abstract

Solid oxide fuel cell is a renowed device in energy field which are able to generate energy via electrochemical process. Despite of the device high efficiency as well as the fuel flexibilty advantages, SOFC oftenly met issues whenever operated at operating temperature (Meng et al. 2021). Not to mention the multiple fabrication process for both electrode in obtaining a single cell. Thus, a new configuration by utilizing the same electrode materials in order to reduce the fabrication thermal treatment and minimising the thermal expansion coefficient of the dissimilar electrode materials (Zhao et al. 2021). In this work, modified lithiated nickel oxide electrode were reported as a potential electrode for symmetrical solid oxide fuel cell. Two different types of current collector were employed onto the $LiNi_{0.5}Ru_{0.5}O_2$ electrode screen printed film and compared in different operating atmosphere (Ma et al. 2020). A total of three symmetrical cell were fabricated where the S1 as the control without any current collector, S2 with the gold sputtered coat and S3 with the hand painted silver paste. All the symmetrical cells have an electrode with active area of $1cm^2$ with the configurations of $LiNi_{0.5}Ru_{0.5}O_2$/SDC/$LiNi_{0.5}Ru_{0.5}O_2$. Electrochemical impedance spectroscopy analysis was done in both oxidized and reduced environment. The ASR values obtained as showed in Nyquist plot in Figure 1 for S1 is 5.92 Ωcm^{-2} in air (cathode) and 0.26 Ωcm^{-2} in H_2:N_2 gas mixture (anode) environment measured

at 800 °C. S2 exhibit ASR value of 2.20 Ωcm^{-2} and 1.96 Ωcm^{-2} at 800 °C in air and gas mixture respectively. As for S3 with silver paste as current collector, the ASR value is much lower which are at 0.70 Ωcm^{-2} and 0.02 Ωcm^{-2} measured at the 800 °C with the same environment sequence. In particularly, FESEM micrographs were analyzed on the cross-section area for a better understanding regarding the interface of the printed electrode and the substrate (SDC electrolyte). To generalised, sample S3 offered an outstanding performance which related to the coverage area of particular current collector. In this case, sample S3 with maximise contact area with the current collector of the set up system exhibit the lowest resistance. Based on Figure 2 micrograph, the surface of the electrode active area showed a homogen particle size with almost spherical particle shape. Homogen particles size ensure constant porosity in active area film for ions transfer. Meanwhile the cross section micrograph, the electrode film was well adhered to the electrolyte substrate which reducing the polarization resistance resorted by the gap in between the film layer. A detailed version of discussion on this study will cover the relation of morphologycal characteristic and electrochemical performance of the symmterical cell. The results indicated that the modified lithiated nickel oxide electrode with silver paste as current collector displayed a great potential as an electrode for the symmetrical solid oxide fuel cell application which is not only an alternative to improve the SOFC performance with minimal optimization for the configuration.

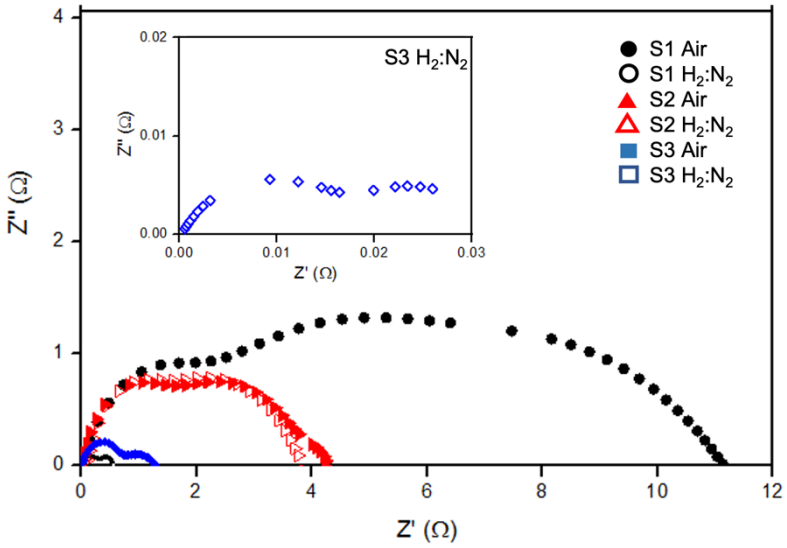

FIGURE 28 Nyquist plot for S1, S2 and S3 in both working environment (air and H2:H2 gas mixture)

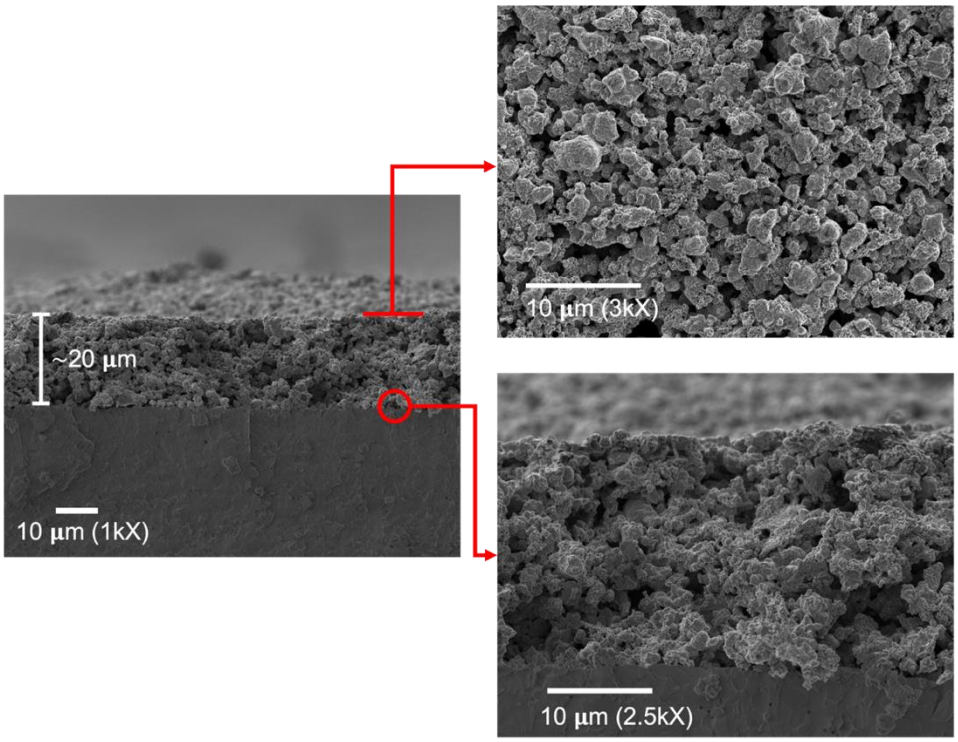

Figure 29: Surface and cross section morphology of screen printed LNR5 electrode film, S1 (without current collector).

Acknowledgements: The authors would like to express their gratitude to the Ministry of Higher Education, Malaysia for the funding support via the research sponsorship under Fundamental Research Grant Scheme grant number FRGS/1/2019/TK07/UKM/02/1 and Universiti Kebangsaan Malaysia for providing insights and expertise that greatly assisted this research.

References

Ma, L., Liu, Z., Chen, T., Liu, Y. & Fang, G. 2020. Aluminum doped nickel-molybdenum oxide for both hydrogen and oxygen evolution reactions. *Electrochimica Acta* 355: 136777.

Meng, Y., Zhang, W., He, Z., Liu, C., Gao, J., Akbar, M., Guo, R., et al. 2021. Partially reduced $Ni_{0.8}Co_{0.15}Al_{0.05}LiO_{2-\delta}$ for low-temperature SOFC cathode. *International Journal of Hydrogen Energy* 46(15): 9874–9881.

6th International Conference and
Postgraduate Colloquium for
Environmental Research 2022 (POCER
2022) 9 - 11 June 2022
Langkawi, Kedah, Malaysia

PCR15042022 – 140: A Review on Glass Fiber Reinforced Polymer Composites in Marine Water Applications

Yuan Jingfan[a,b], Teo Fang Yenn[a*], Selavarajoo Anurita[a], Lau Teck Leong[a], Zheng Yu[b], Qin Renyuan[b]

a. Department of Civil Engineering
University of Nottingham Malaysia, Selangor, Malaysia

b. School of Environmental and Civil Engineering
Dongguan University of Technology, Dongguan, China

- Corresponding Author E-mail: FangYenn.Teo@nottingham.edu.my

Keywords: Glass Fiber Reinforced Polymer Composites; Marine Water; Environmental Conditions; Application.

Extended Abstract

Concrete is widely used for infrastructures due to its low initial cost, but with the increasing awareness of its full life cycle and money-saving in the long run, fiber-reinforced polymer (FRP) composites are becoming more prevalent compared with the concrete types, especially with the glass fiber reinforced polymer (GFRP) composites because of their relatively cheaper price from different FRPs, light-weight, high strength-weight ratio, and good anti-corrosion performance(Morampudi et al., 2021, Sathishkumar et al., 2014). Another cause for the limited application of GFRP is the seawater effect such as the creep effect and time-dependent impacts on the material, which holds a larger effect than some traditional composites (Xian et al., 2022). This paper provides a comprehensive review of how the GFRP composites function in the marine water environment, and how the GFRP composites would change under different loading conditions with one or more parameters. Another thing is that the review was conducted by using the ScienceDirect® and Web of Science® databases (Chong et al., 2021) to search the short-term and long-term performance under sustained loading or environmental conditions of GFRP and its composites, especially when the GFRP composites have the degradation effect on the interface between the matrix and fiber, or the micro damages of fiber under the environmental conditions and subjected loading conditions(Wang et al., 2018, Sá et al., 2011). To fully understand the reasons for the damage formation, characteristics

tools such as Scanning Electron Microscope (SEM), and Fourier-transform infrared spectroscopy (FTIR), would be required for quality control and supervision and further studies (Alabtah et al., 2021). The review mainly stresses the significance of further research in GFRP composites by comparing different countries' criteria, since the durability study needs to be conducted especially when it comes to a certain amount of altitude in marine water and conservative parameters values. Few studies have considered the GFRP composites for long-term applications and studies even, though it has been applied in serval fields (e.g. bridges of GFRP composites(Yingxiang, 2018), external pipes of GFRP composites).

Acknowledgments: Authors sincerely thank the Chinese National Science Funding Commission (NSFC) and its counterpart in Malaysia. Plus, writers sincerely thank the reviewers and other peers for comments and suggestions.

References

ALABTAH, F. G., MAHDI, E. & KHRAISHEH, M. 2021. External Corrosion Behavior of Steel/GFRP Composite Pipes in Harsh Conditions. *Materials (Basel, Switzerland),* 14**,** 6501.

CHONG, X. Y., VERICAT, D., BATALLA, R. J., TEO, F. Y., LEE, K. S. P. & GIBBINS, C. N. 2021. A review of the impacts of dams on the hydromorphology of tropical rivers. *Science of The Total Environment,* 794**,** 148686.

MORAMPUDI, P., NAMALA, K. K., GAJJELA, Y. K., BARATH, M. & PRUDHVI, G. 2021. Review on glass fiber reinforced polymer composites. *Materials Today: Proceedings,* 43**,** 314-319.

Sá, M. F., GOMES, A. M., CORREIA, J. R. & SILVESTRE, N. 2011. Creep behavior of pultruded GFRP elements – Part 1: Literature review and experimental study. *Composite Structures,* 93**,** 2450-2459.

SATHISHKUMAR, T. P., SATHEESHKUMAR, S. & NAVEEN, J. 2014. Glass fiber-reinforced polymer composites – a review. *Journal of Reinforced Plastics and Composites,* 33**,** 1258-1275.

WANG, Z., ZHAO, X.-L., XIAN, G., WU, G., RAMAN, R. K. S. & AL-SAADI, S. 2018. Effect of sustained load and seawater and sea sand concrete environment on the durability of basalt- and glass-fibre reinforced polymer (B/GFRP) bars. *Corrosion Science,* 138**,** 200-218.

XIAN, G., GUO, R. & LI, C. 2022. Combined effects of sustained bending loading, water immersion and fiber hybrid mode on the mechanical properties of carbon/glass fiber reinforced polymer composite. *Composite Structures,* 281**,** 115060.

YINGXIANG, L. 2018. *Composites for Hydraulic Structures: a Review.* Master Science Problem/Project Report, West Virginia University.

PCR15042022 – 141: Effects of rice straw and gabage enzyme (GE) addition on soil and rice plant growth at early vegetative stage

Nguyen-Sy Toan*,Nguyen Anh Tai, Do Hong Hanh, and Nguyen Thi Yen Anh

Department of Chemical Technology and Environmental Engineering
University of Technology and Eduation- The University of Danang, Danang, Vietnam

- Corrensponsing Author E-mail: nstoan@ute.udn.vn

Keywords: Extracted carbohydrate; gabage enzyme; rice plant; rice straw; soil nutrient.

Extended Abstract

This study aims at investigate the effect of rice straw and gabage enzyme to rice plant growth and soil carbohydrate, ammonium content. The results show that no significant difference for plant height and biomass among treatments. The extracted carbohydrate was enhanced by rice straw addition, while ammonium production was enhanced by gabage enzyme addition. Further research with longer observation on the impact of rice straw and gabage addtion is recommended.

1. Introduction

Rice straw application plays an important role to improve soil organic matter in long-term paddy field (Nguyen-Sy et al., 2019; Tang et al., 2016). However, one of the limitation of applying rice straw is long time decompose of matterial. Gabage enzymes (GE) are solutions obtained by fermenting fruit or vegetable skins, molasses and water, which have multiple functions to degrade, modify and speed up the reaction (Arun & Sivashanmugam, 2015; Polprasert & Koottatep, 2017). However, studies on application of waste enzymes have not been studied in post-harvest treatment of rice straw. Therefore, this study aims to find a solution to apply waste enzymes in rice straw treatment in an environmentally friendly way, and increase nitrogen fixation capacity for rice soil.

2. Methodology

Fifteen rice seeds per bottle were planted in five treatments are design as following: soil and water only (Control), soil and rice straw addition (RS), soil and gabage enzyme addtion (GE), and soil and rice straw combine gabage enzyme (Combine). After 1 month growth, plants were harvested to measure biomass and height, while soil was extracted by distilled water to measure extracted carbohydrate (ECH), ammonium (NH_4^+) and nitrate. For stastistical annalysis to determine the effects of rice straw and gabage enzyme based on SPSS ver 20 software.

3. Result and dicussion

Fresh weight and dry weight of all treatments ranged from 1.60-1.83 and 0.27-0.32 mg, but no significance ($p>0.05$) was observed (Figure 1). Interestingly, root length ranged from 4.7-7.7 cm with the highest with Control and lowest with Combine treatment, meanwhile, shoot height ranged from 17.8-20.3 cm and longest in RS treatment and shortest in Control treatment ($P<0.05$) (Table 1, Figure 2). We suppose that in the initial stage of rice growth, rice mostly comsume energy from its seeds, therefore, the effect of soil nutrient is less effective.

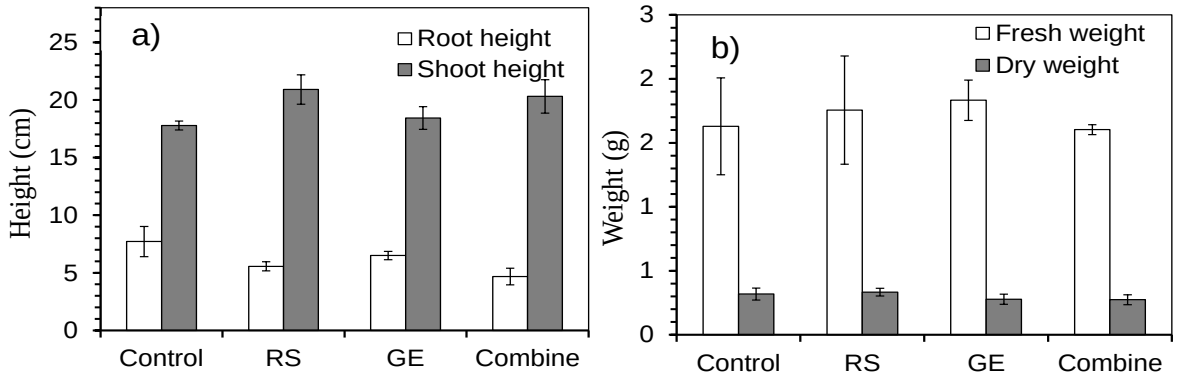

Figure 30: The Plant height (a) and biomass (b) after 1 month growth

Extracted carbohydrate (ECH) ranged from 61-207 mg kg^{-1} and classified into two groups, once with Control and GE (60.0 and 60.3 mg kg^{-1}), and the other once with higher values with RS and Combine (185.9 and 206.5 mg kg^{-1}). The application of rice straw enhanced ECH production, while gabage enzyme did not effect on this. The previous report by Nguyen-Sy et al. (2021) also confirmed that adding rice straw at 0.2% soil would enhance mineralize carbohydrate in anaerobic incubation. In this current research, with exist of rice plants have the similar result.

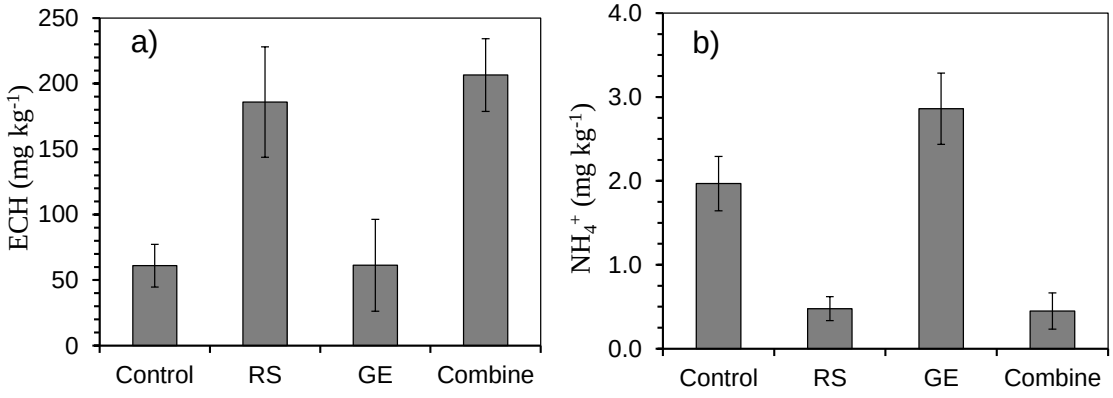

Figure 31: Soil extracted carbohydrate (a) and ammonium extraction (b) after 1 month growth

Extracted inorganic nitrogen was measured with ammonium and nitrate, however, nitrate was not detected. The ammount of ammonium ranged from 0.45-2.86 mg kg-1, and also made of two groups, once with Control and GE (1.97-2.86 mg kg^{-1}), and other with RS and Combined treatment (0.45-0.48 mg kg^{-1}) (Figure 2). It seems gabage enzyme enhance slightly the ammonium production, while rice

straw against this process. Despite that gabage enzyme did not affect on cellulose degradability (presented through ECH productivity), it enhanced soil nitrogen mineralization. However, the production of ammonium is not high (less than 5mg/kg^{-1}).

4. Conclusion

Rice straw and gabage enzyme has been applied into paddy soil aimed to enhance plant growth and soil labile carbon and nitrogen. Plant biomass and plant height was not regulated at the initial stage. Soil carbohydrate was enhanced by rice straw additionand, meanwhile, ammonium extracted was enhanced by gabage enzyme. Combination of rice straw and gabage enzyme was not significant for ECH and NH_4^+ improvement.

Acknowledgements: This research is funded by University of Technology and Education - The University of Danang.

References

Arun, C., & Sivashanmugam, P. (2015). Investigation of biocatalytic potential of garbage enzyme and its influence on stabilization of industrial waste activated sludge. *Process Safety and Environmental Protection, 94*, 471-478. doi:10.1016/j.psep.2014.10.008

Nguyen-Sy, T., Cheng, W., Kimani, S. M., Shiono, H., Sugawara, R., Tawaraya, K., . . . Kumagai, K. (2019). Stable carbon isotope ratios of water-extractable organic carbon affected by application of rice straw and rice straw compost during a long-term rice experiment in Yamagata, Japan. *Soil Science and Plant Nutrition, 66*(1), 125-132. doi:10.1080/00380768.2019.1708209

Nguyen-Sy, T., Nguyen Thi Dong, P., Tran Thi Ngoc, T., Duong Thi, L., Pham Duy, D., Nguyen Thanh, G., . . . Show, P. L. (2021). Soil mineralization as effects of plant growth promoting bacteria isolated from microalgae in wastewater and rice straw application in a long-term paddy rice in Central Viet Nam. *Environmental Technology & Innovation*, 101982. doi:10.1016/j.eti.2021.101982

Polprasert, C., & Koottatep, T. (2017). Organic Waste Recycling: Technology, Management and Sustainability - 4th Edition. *Water Intelligence Online, 16*, 9781780408217. doi:10.2166/9781780408217

Tang, S. R., Cheng, W. G., Hu, R. G., Guigue, J., Kimani, S. M., Tawaraya, K., & Xu, X. (2016). Simulating the effects of soil temperature and moisture in the off-rice season on rice straw decomposition and subsequent CH4 production during the growth season in a paddy soil. *Biology and Fertility of Soils, 52*(5), 739-748. doi:10.1007/s00374-016-1114-8

6th International Conference and Postgraduate Colloquium for Environmental Research 2022 (POCER 2022) 9 - 11 June 2022
Langkawi, Kedah, Malaysia

PCR15042022 – 142: Potential of Nata de Coco as Pectinase Immobilization Support for Guava Juice Clarification and Techno-Economic Analysis of Its Process Design

Nurul Azira Zahari[a], Mohd Noriznan Mokhtar[a,b*]

[a] Department of Process and Food Enginering, Faculty of Engineering, Universiti Putra Malaysia, Serdang, Selangor, Malaysia

[b] Laboratory of Processing and Product Development, Institute of Plantation Studies, Universiti Putra Malaysia, Serdang, Selangor, Malaysia

*Corrensponsing Author E-mail: noriznan@upm.edu.my

Keywords: Guava Juice; Juice Clarification; Pectinase; Enzyme Immobilization; Reaction Kinetics; Techno-economic Analysis.

Extended Abstract

Guava (*Psidium guajava L.*) is being recognized as "super food" and it is getting attention in the agro-food business due to the attractive characteristics of the fruit, such as health-promoting bioactive components and functional elements [Verma et. al., 2013]. The extraction of fruit juice always encountered undesirable turbidity due to the suspension of polysaccharide particulates, mainly pectin arising from the primary and inner cell wall [Deng et al., 2019]. In most cases, pectin makes the juice clarification difficult, as it is generally associated with plant polymers and cell debris having fiber-like molecular structure, thereby creating fouling during membrane filtration. Enzymatic clarification is a method in which pectinase breaks down pectin molecules into smaller oligalacturonans causing pectin-protein complexes to flocculate, so the resultant juice is much lower pectin and viscosity. The resulting enzymatically treated can therefore be easily clarified through centrifugation or filtration [Ninga et al., 2021]. In spite of high catalytic properties of pectinase, free enzyme always presents some drawbacks such as poor stability under operational conditions, impossibility of multiple reuses in an industrial process, and the presence of compounds arising from enzyme preparation in the final food product. Nata de coco is a bacterial cellulose produced from coconut water by fermentation of *Acetobacter xylinum*, and it has high potential as a support for pectinase immobilization. For reaction kinetics study, non-elementary kinetics model was used in which *n*-reaction order and reaction rate constant (*k*) were estimated by using graphical differentiation (Figure 1) as equation below:

$$\ln\left(-\frac{dC_T}{dt}\right) = lnk + nlnC_T \quad (1)$$

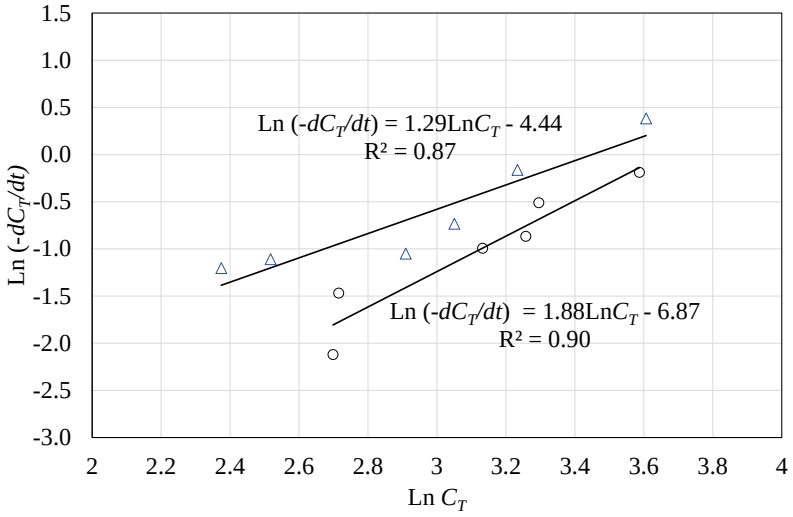

Figure 1: Kinetic parameters estimation by linearization method (Δ free pectinase, O **immobilized pectinase)**

In conjunction with this, applying simulation (SuperPro Designer v12) for process design of juice clarification using immobilized peactinase with techno-economic analysis is very important in evaluating optimistic scenario of investigated project at an industrial scale as shown in Figure 2. As a results, a more interesting project can be proposed based on high profitability, and the most important is its sustainability.

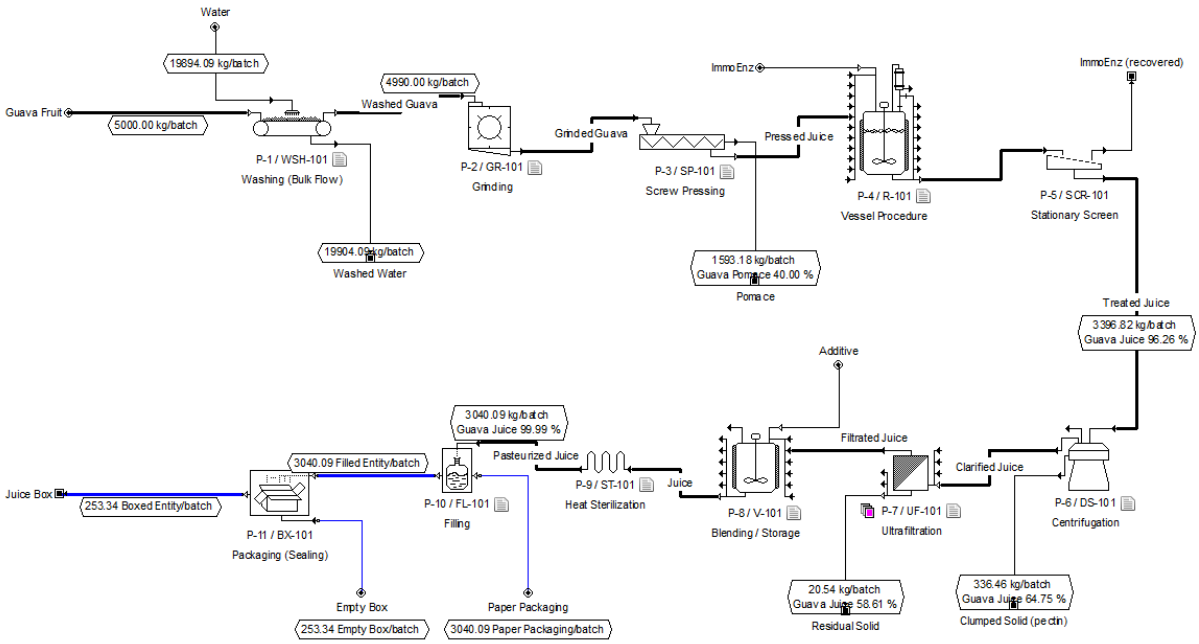

Figure 2: Guava juice extraction plant developed by SuperPro Designer v12.

References

Deng, Z., Wang, F., Zhou, B., Li, J., Li, B., & Liang, H. (2019). Immobilization of pectinases into calcium alginate microspheres for fruit juice application. *Food Hydrocolloids, 89*, 691 - 699.

Ninga, K. A., Carly Desobgo, Z. S., De, S., & Nso, E. J. (2021). Pectinase hydrolysis of guava pulp: effect on the physicochemical characteristics of its juice. *Heliyon, 7*(10), e08141.

Verma, A. K., Rajkumar, V., Banerjee, R., Biswas, S., & Das, A. K. (2013). Guava (Psidium guajava L.) Powder as an Antioxidant Dietary Fibre in Sheep Meat Nuggets. *Asian-Australas J Anim Sci, 26*(6), 886-895. doi:10.5713/ajas.2012.12671

6th International Conference and
Postgraduate Colloquium for
Environmental Research 2022 (POCER
2022) 9 - 11 June 2022
Langkawi, Kedah, Malaysia

PCR15042022 – 143: Rice Husks as Carrier for Lipase Immobilization and Its Application in Continuous Monoacylglycerol Production Using a Packed Bed Bioreactor

Ng Lin Cieh[a], Mohd Noriznan Mokhtar[a,b]*, Azhari Samsu Baharuddin[a] and Mohd Afandi P. Mohammed[a]

[a] Department of Process and Food Enginering, Faculty of Engineering, Universiti Putra Malaysia, Serdang, Selangor, Malaysia

[b] Laboratory of Processing and Product Development, Institute of Plantation Studies, Universiti Putra Malaysia, Serdang, Selangor, Malaysia

*Corrensponding Author E-mail: noriznan@upm.edu.my

Keywords: Rice Husks; Enzyme; Immobilized Lipase; Monoacylglycerol; Glycerolysis; Packed Bed Bioreactor.

Extended Abstract

Rice husks is one of the major by-products produced in the form of wastes by rice milling industries. In Malaysia, it was reported that approximately 0.48 million tonnes of rice husks is generated each year [Shafie *et al.*, 2017]. The current practice adopted to manage the disposed rice husks is through open burning or leaving the rice husks to rot slowly in the field [Rozainee *et al.*, 2009; Shafie, 2016]. Consequently, this results in negative environmental impacts snce open burning can generate various pollutants (such as smoke and acid gases) while the slow-rotting process can lead to the emission of methane, which is a greenhouse gas causing global warming [Rozainee *et al.*, 2009]. Recently, it was revealed that rice husks showed good potential to be utilized as support matrix for enzyme immobilization. Due to its high silica body content with nanoporous structure, effective enzyme immobilization with excellent loading rate is achievable [Corici *et al.*, 2016; Le *et al.*, 2017]. Therefore, the present research aims to utilize rice husks as carrier for lipase immobilization and applies the prepared immobilized biocatalyst in packed bed bioreactor for continuous production of monoacylglycerol (MAG), which is a valuable lipid product often used as food emulsifiers. In the present study, lipase from Thermomyces lanuginosus was immobilized on oxidized rice husks functionalized with different combination of spacer arms (hexamethylenediamnine, HMDA or ethylenediamine, EDA) and ligands (glutaraldehyde, GA or o-phthalaldehyde, OPA). The results show

that the highest enzyme loading was achieved by lipase immobilized with HMDA and OPA as can be seen in Table 1. Besides, the FTIR analysis, as shown in Figure 1, have also confirmed the presence of lipase on rice husks. The immobilized lipase with the best properties will then be applied in packed bed bioreactor system for continuous glycerolysis reaction. This will be followed by the evaluation on the performance of the bioreactor system such as MAG productivity and operational stability. It is believed that the outcome of the present study will effectively mitigate the environmental impacts brought by rice husk disposal while simultaneously achieve the target of transforming waste into wealth.

Table 1: Percentage of Protein Loading on Rice Huks upon Immobilization

Immobilized lipase	Protein added (mg/g support)	Protein load (mg)	Percentage of proten loading (%)
HMDA-GA-lipase	10	4.35	43.50±1.27
	20	8.28	41.40±2.47
	30	10.93	36.42±1.01
	40	10.30	25.74±0.90
HMDA-OPA-lipase	10	6.34	63.40±3.82
	20	12.25	61.25±1.56
	30	16.42	54.72±1.63
	40	16.70	41.75±0.85
EDA-GA-lipase	10	4.63	46.30±3.55
	20	8.44	42.20±1.63
	30	10.39	34.63±2.88
	40	9.85	24.63±1.94
EDA-OPA-lipase	10	5.67	56.70±0.14
	20	10.71	53.55±0.21
	30	14.19	47.28±1.72
	40	14.97	37.43±1.66

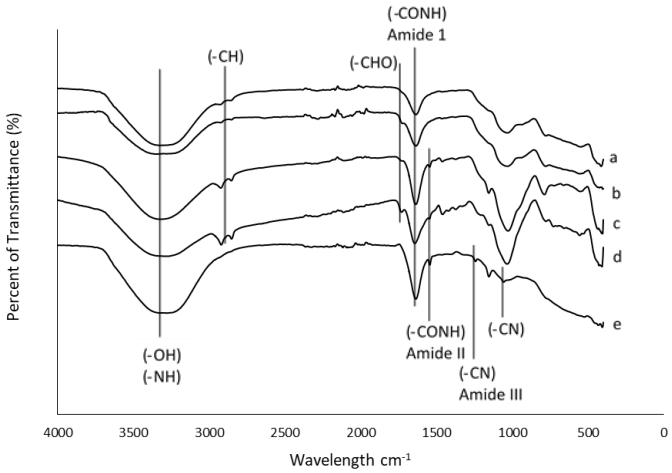

Figure 1: FTIRSpectra of a) Rice husks, b) Oxidized rice husks, c) Oxidized rice husks with HMDA, d) Oxidized rice husks with HMDA and GA, e) Oxidized rice husks with HMDA, GA and immobilized lipase

References

Corici, L., Ferrario, V., Pellis, A., Ebert, C., Lotteria, S., Canton, S., Voinovich, D., Gardossi, L., 2016. Large scale applications of immobilized enzymes call for sustainable and inexpensive solutions: Rice husk as renewable alternative to fossil-based organic resins. *RSC Advances*. 6: 63256-63270.

Le T.B., Han, C.S., Cho, K., Han, O., 2017. Covalent immobilization of oxylipin biosynthetic enzymes on nanoporous rice husk silica for production of cis(+)-12-oxophytodienoic acid. *Artificial Cells, Nanomedicine, and Biotechnology*. 46(8): 1523-1529.

Rozainee, M., Ngo, S.P., Johari, A., Salema, A.A., Tan, K.G., 2010. Utilisation Of Rice Husk Waste And Its Ash (Part 1). *The Ingenieur*. 41: 46-50.

Shafie, S.M., 2016. A review on paddy residue based power generation: Energy, environment and economic perspective. *Renewable and Sustainable Energy Reviews*. 59: 1089-1100.

Shafie, S.M., Othman, Z., Hami, N., 2017. Critical Process in Paddy Residue-Based Power Generation in Malaysia: Economic and Environmental Perspective. *Advanced Science Letters*. 23(9): 8149-8153.

6th International Conference and
Postgraduate Colloquium for
Environmental Research 2022 (POCER
2022) 9 - 11 June 2022
Langkawi, Kedah, Malaysia

PCR15042022 – 144: Techo-Economic Analysis of Palm Oil Mill After Addition of Unit Procedures for 3-Monochloropropane-1,2-diol (3-MCPD) Mitigation

Siti Naderah Sulin[a], Afandi P. Mohamad[a], Azhari Samsu Baharuddin[a] and Mohd Noriznan Mokhtar[a*]

[a] Department of Process and Food Enginering, Faculty of Engineering, Universiti Putra Malaysia, Serdang, Selangor, Malaysia

[b] Laboratory of Processing and Product Development, Institute of Plantation Studies, Universiti Putra Malaysia, Serdang, Selangor, Malaysia

*Corrensponsing Author E-mail: noriznan@upm.edu.my

Keywords: Palm Oil Mill; 3-MCPD; Process Modelling; CPO Washing; Hot Water Sterilization.

Extended Abstract

3-monochloropropane-1,2-diol (3-MCPD) is a contaminants forms when the edible oil heated at very high temperature during refinery process. It is important to address this issue because the 3-MCPD giving risk to human health such as kidney failure. The mitigation strategies of 3-MCPD can be done prior to refinery process as early as in the field and during milling process according to Sulin et al., 2020. In order to mitigate the formation of 3-monochloropropane-1,2-diol (3-MCPD), some additional process added to the mill to remove its precursors. Widely known that, the precursors of 3-MCPD is glyceride, chlorin and some paramters such as temperature and pH as mentioned by Destaillats et al.,2012. Removing the chloride for instance can reduce the formation of 3-MCPD. However, the addition of more unit procedures could impact plant capital costs, operating costs and utility rates. Energy saving is one of the main interest in palm oil mill and more researchers aim to asses the mill utilization of steam and electricity. Based on the literature review, two case scenarios were made for chlorine removal constructed and compared with the baseline case scenarios. Base case scenario is a conventional method of crude palm oil (CPO) processing shown in Figure 1. The case 1 involves a process to wash the final product (CPO).The quality of washed and unwashed CPO is shown in table 1 which is 74% chloride difference according to Lakshmanan et al., 2021. Case 2 involves integrated process to remove the chloride before it go further in the milling process by washing the fresh fruit bunch (FFB) and chloride removal during raw water treatment sections using membrane separation technology. For this study, Superpro Designer 12.0 Software used to facilitate modelling and evaluation of integrated process palm oil mill. The results will help millers and researchers to gain an understanding

of the actual future scenario as early and as detailed as possible. Decision can be make based on sound estimates of costs and potential of a process to reduce the 3-MCPD precursor.

Table 12: Different quality value of unwash and washed CPO (Lakshmanan et al., 2021)

Quality	Unwash CPO	Washed CPO	Different (%)
FFA (%)	4.2 ± 0.3	4.1 ± 0.3	-2
DOBI	2.3 ± 0.1	2.4 ± 0.1	+4
Impurities (%)	0.045 ± 0.004	0.010 ± 0.004	-78
Peroxide Value (meq kg^{-1})	2.1 ± 0.7	2.1 ± 0.7	-5
Chloride (mg kg^{-1})	7.6 ± 0.9	2.0 ± 0.2	-74

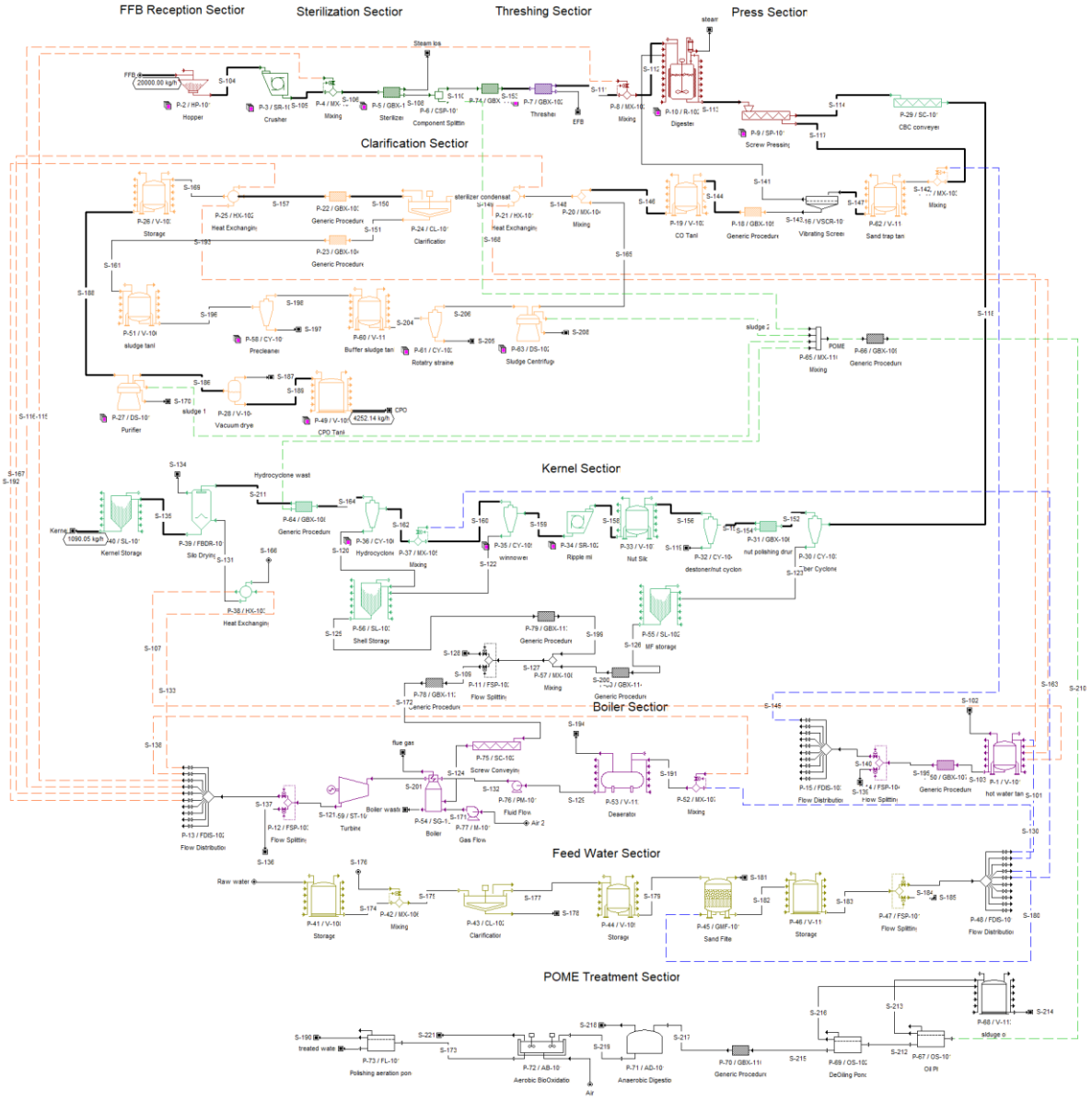

Figure 32: Base case scenario of conventional Palm oil mill model in Superpro Designer software.

References

Destaillats, F., Craft, B.D., Sandoz, L. and Nagy, K., 2012. Formation mechanisms of monochloropropanediol (MCPD) fatty acid diesters in refined palm (Elaeis guineensis) oil and related fractions. *Food Additives and Contaminants Part A Chemical Analysis control Expo Risk Assessment*, 29 (1): 29–37.

Lakshmanan, S and Yung, Y. L., 2021. Chloride reduction by water washing of crude palm oil to assist in 3-monochloropropane-1, 2 diol ester (3-MCPDE) mitigation. *Food Additives and Contaminants*. 38(3): 371–387

Sulin, S. N., Mokhtar, M. N., Mohammed, M. A. P., and Baharuddin, A. S., 2020. Review on palm oil contaminants related to 3-monochloropropane-1,2-diol (3-MCPD) and glycidyl esters (GE). *Food Research.* 4 (6):11-18.

PCR15042022 – 147: A biorefinery approach of two different Marine macroalgae *Sargassum polycystum* and *Rosenvingea intricata*: extraction and characterization of fucoxanthin, fucoidan and bioethanol

Nagamalai Sakthi Vignesh[1], Murugan Kiruthika[1], Sathaiah Gunaseelan[1], Muniyasamy Shanmugam[3], Balasubramaniem Ashokkumar[2], Perumal varalakshmi[1*]

1. Department of Molecular microbiology, School of Biotechnology, Madurai Kamaraj University, Tamil Nadu, India.

2. Department of Genetic Engineering, School of Biotechnology, Madurai Kamaraj University, Tamil Nadu, India.

3. AquAgri private limited, Manamadurai, Tamil Nadu, India.

1* - Corresponding author.

Keywords: *Sargassum polycystum*, *Rosenvingea intricata*, Fucoxanthin, Fucoidan, bioethanol

Extended Abstract

The progress of various approaches in developing the commercialized drugs versus energy from the renewable sources such as lignocellulosic biomass, marine macroalgal sources and other common feedstocks. Marine seaweeds are well known for its specific features in nutraceutical and bioactive compounds related to cancer, obesity, diabetics etc., and it prolongs the life span (Ragumaran *et al.*, 2018). Meanwhile, the leftover seaweed biomass after bioactives extraction used for energy applications specifically liquid fuels like bioethanol and biodiesel and so on. Commercially, the bioenergy production requires the minimal cost of feedstock that should not exceed the production rate, feedstock availablity, and improving the yield percentage. Thus, this study majorly focused on two marine seaweeds used for different end-products from several machinery using two different brown seaweeds. The bioactive compounds from seaweeds is due to the substantial availablity of carotenoids, polyphenols and polysaccharides that shows significant activity in anti-cancer, anti-diabetic, anti-inflammatory and anti-obesity etc. (Gupta and Abu-Ghannam, 2011). In this study, a known quantity of seaweed was taken for fucoxanthin extraction using different solvents (ethanol and acetone) by Ultrasound assisted method (UAE) method. The UAE is a modern methodology used for extracting the compounds by producing acoustic cavitation on feedstock that improving the yield by increasing the shearing force on biomass, further the UAE is a cost and time consuming process (Ragumaran et al., 2018). The fucoxanthin is an eccentric carotenoid that have an allenic bond having more anti-oxidant properties. Earlier, the conventional methods were used for extracting fucoxanthin production was lower due to its extended timings, solid-liquid ratio. On the otherhand, the solvent (ethanol and acetone)

used in this study is also taken in consideration. According to the previous reports, the ethanol is the major food grade solvent which helps in efficient carotenoids, and acetone also favors the same, but the drawback in methanol is its toxicity. In this report, the extraction of fucoxanthin using two different solvents employed in two seaweeds showed a fold increase in acetone extracted fucoxanthin compared to ethanol fraction. Further, the crude sample was purified by

using silica gel packed column and further confirmed by using High performance liquid chromatography (HPLC). Aftermath, the extracted crude and pure fucoxanthin will be carried out to check for its potential in anti-oxidant activity by DPPH assay (lim *et al.,* 2018). Further, the leftover seaweed from the fucoxanthin extraction was used for extracting sulphated polysaccharide called fucoidan. So far, the fucoidan was extracted from various seaweeds using conventional methods are well reported but using modern extraction techniques for fucoidan was scarce. Hence, this report focused on extracting the sulphated polysaccharide using UAE and microwave assisted extraction (MAE) (Yuan et al., 2015). From the experimental result, it clearly depicted that the extraction efficiency is equally significant in both UAE and MAE process. Further, the fucoidan was purified using column chromatography and subjected to several characterization techniques such as FT-IR, XRD and NMR for structural conformation. Then, the partially purified fucoidan was employed in Zebrafish models to know the activity of anti-obesity. The Zebrafish were purchased and maintained under the laboratory conditions. Ten fishes per group was selected and allowed to grow in separate tanks. To which the formulated feed was fed for 15 days continuosly three times per day. After the feeding period, the fucoidan was also given along with normal feed for thrice a day upto 15 to 20 days. Further, the gene expression related to anti-obesity biomarkers were performed. Owing to this, the residual seaweeds biomass (approx 10.5 g) was used for ethanol production. The seaweed biomass was subjected into pretreatment using sulphuric acid for an hour, followed that neutralization, overliming process were also carried out (Sakthivignesh *et al*., 2020). Then, the aqueous extract was allowed for fermentation process using *Sacharomyces cerviseae* for 5-7 days. Finally, the ethanol yield was quantified through headspace GC-MS analysis. The resultant peak showed that presence of ethanol than the control. Thus, this is the first report dealt with the ethanol production from leftover biomass of seaweeds with simultaneous fucoxanthin and fucoidan extraction. Further, the leftover seaweed biomass was used for composting as fertilizer for plants. This study highlighted that the significant way for extracting two different end-products (Fucoxanthin and Fucoidan) and the other bioenergy product of ethanol was produced from leftover seaweed biomass and remaining seaweed used as fertilizer for efficient plant growth in biorefinery approach.

Acknowledgements:

Authors thankfully acknowledge AquAgri for funding the project, RUSA funding facility and Central Instrumentation facility of Madurai Kamaraj University, Madurai for the instrumentation facilities.

References

1. Gupta, S., & Abu-Ghannam, N. (2011). Bioactive potential and possible health effects of edible brown seaweeds. *Trends in Food Science & Technology*, *22*(6), 315-326.

2. Raguraman, V., MubarakAli, D., Narendrakumar, G., Thirugnanasambandam, R., Kirubagaran, R., & Thajuddin,

3. N. (2018). Unraveling rapid extraction of fucoxanthin from Padina tetrastromatica: Purification, characterization and biomedical application. *Process Biochemistry*, *73*, 211-219.

4. Lim, M. W. S., Tan, K. M., Chew, L. Y., Kong, K. W., & Yan, S. W. (2018). Application of two-level full factorial design for the extraction of fucoxanthin and antioxidant activities from Sargassum siliquosum and Sargassum polycystum. *Journal of aquatic food product technology*, *27*(4), 446-463.

5. Láinez M, Ruiz HA, Castro-Luna AA, Martínez-Hernández S. Release of simple sugars from lignocellulosic biomass of Agave salmiana leaves subject to sequential pretreatment and enzymatic saccharification.BiomassBioenergy2018;118:133–40.

6. Fakhrudin J, Setyaningsih D, Rahayuningsih M. Bioethanol production from seaweed eucheuma cottonii by neutralization and detoxification of acidic catalyzed hydrolysate. Int J Environ Sci Dev 2014;5:455–8. https://doi.org/10.7763/ijesd. 2014.v5.526.

PCR15042022 – 149: Gastrointestinal digestion stability and zinc absorption mechanism of casein peptide-zinc chelate

Keywords: Casein peptied; Peptides-zinc chelate; Structural characterization; Simulated gastrointestinal digestion; Caco-2 cells

Introduction

Nowadays, zinc deficiency is a common problem in many countries and regions, especially developing countries[1]. The absorption site of zinc in the human body is mainly the small intestine, and its absorption is mainly through the ZnT zinc transporter or the Zip transporter, and it is transported to and from the membrane through transmembrane transport. However, dietary zinc is generally poorly absorbed in the human body, and certain food matrix components, such as phytic acid, polyphenols, saponins, and cellulose, combine with zinc to form insoluble complexes in the gastrointestinal tract, hindering zinc absorption and use [2]. On the other hand, other minerals in food, such as iron, calcium, and copper ions, also compete with valence metal ion transporters and carrier proteins, thereby inhibiting the absorption of zinc.

The peptide-zinc chelate was prepared and entered into cells and blood circulation in whole form [3]. In this process, zinc ions can avoid the formation of precipitates with phytic acid, etc., and share the peptide transport pathway, thereby improving the bioavailability of zinc.

In the study, a novel kind of peptides-zinc chelate was obtained using the casein peptide as raw material,the reaction was carried out with the mass ratio of the casein peptide to $ZnSO_4 \cdot 7H_2O$ of 1:1 ; based on gastric juice-intestinal juice-Caco-2 cell model, the gastrointestinal digestion of casein peptide-zinc chelate was investigated. Stability and absorption in small intestinal epithelial cells; on this basis, the changes in the transmembrane transport flux of chelates were analyzed by means of pathway inhibitors, and the mechanism of chelates promoting zinc absorption was clarified.

Methods

In the study, we intends to prepare a nutrient delivery system peptide-zinc chelate with casein peptide and inorganic zinc salt as raw materials; Digestive stability and absorption in small intestinal epithelial cells; on this basis, the changes in the transmembrane transport flux of chelates were analyzed by means of pathway inhibitors, and the mechanism of chelates promoting zinc absorption was clarified. Specific research contents include:

(1) Preparation of casein polypeptide and polypeptide-zinc chelate

Preparation of zinc chelated peptides by fermentation of lactic acid bacteria. Polypeptide-zinc chelates were prepared, and the ability of casein polypeptides to chelate zinc ions and the binding sites of zinc ions were detected by techniques such as infrared spectroscopy, atomic absorption spectroscopy and mass spectrometry.

(2) Correlation study on gastrointestinal digestive stability of polypeptide-zinc chelate

Gastrointestinal digestion of polypeptide-zinc chelates was simulated by an in vitro gastric-intestinal digestion model. Monitor the changes of the chelation state of the chelate during the digestion process, and use infrared spectroscopy, atomic absorption spectroscopy and mass spectrometry to detect the changes in the ability of polypeptides to chelate zinc, the dissociation degree of zinc ions and the dissociation rate and other indicators.

(3) The role of polypeptide charge properties in the mechanism of polypeptide-zinc chelate transmembrane transport

The Caco-2 cell model was used to simulate the absorption of different properties of peptide-zinc chelate in small intestinal epithelial cells. The transmembrane absorption of chelates was intervened by different means, and the content changes of polypeptide-zinc chelates and free zinc ions during the whole transmembrane transport process were monitored.

(4) Verification experiment

Polypeptides were synthesized by solid-phase synthesis and the peptide-zinc chelate was prepared. Then, the digestion and absorption of chelates were simulated by the three-stage digestion and absorption model of gastric juice-intestinal fluid-Caco-2 cells; the dissociation degree of zinc ions in the digestion process, the apparent permeability coefficient of chelates and other indicators were detected, and the The changes of chelate transmembrane transport pathway were observed to verify the above research conclusions.

On the basis of exploring the pathways through which peptide-zinc chelates can pass through shared peptides, the link between the structural properties of the peptide itself and the transmembrane transport mechanism of chelates was investigated, and the final bioavailability of zinc via different pathways was investigated.

Conclusions and Discussion

The zinc chelates of the products under different conditions are shown in Figure 1. The zinc chelation rate of LP1 was the highest, which was 23.08±2.61%, and the zinc chelation rate of LP2 was 17.49±1.33%. After mixed fermentation, the zinc chelation rate became lower, which may be due to the increase in the degree of hydrolysis of the product, resulting in a part of zinc chelation sites point is destroyed.

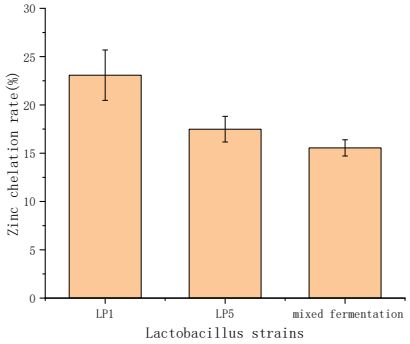

Figure 33: The Drawing Canvas

References

[1] Gerbino E , Mobili P , Tymczyszyn E , et al. FTIR spectroscopy structural analysis of the interaction between Lactobacillus kefir S-layers and metal ions[J]. Journal of Molecular Structure, 2011, 987(s 1–3):186-192.

[2] Fredlund，K.，Isaksson，M.，Rossander-Hulthén，L.，Almgren，A.，&Sandberg，A.-S.(2006).Absorption of zinc and retention of calcium: dose-dependent inhibition by phytate，20，49–57.

[3] Wang, B., & Li, B. (2017). Effect of molecular weight on the transepithelial transport and peptidase degradation of casein-derived peptides by using Caco-2 cell model. Food Chemistry, 218, 1-8.

6th International Conference and
Postgraduate Colloquium for
Environmental Research 2022 (POCER
2022) 9 - 11 June 2022
Langkawi, Kedah, Malaysia

PCR15042022 – 150: Lichen as the Biological Indicator for Environment Tobacco Smoke (ETS) Detection in Malaysia

Azlan Abas[a*], Kadaruddin Aiyub[a], Azmi Aziz[a] and Azahan Awang[a]

[a] Centre for Research in Development, Social and Environment (SEEDS)
Faculty of Social Sciences and Humanities
Universiti Kebangsaan Malaysia, Selangor, Malaysia

- Corrensponsing Author E-mail: azlanabas@ukm.edu.my

Keywords: Biomonitoring; Indoor Air Quality; Indoor built; Lichens; Nicotine; Trace elements

Extended Abstract

Many studies have investigated indoor air quality (IAQ) in relation to cigarette smoke. It is not easy to assess Environment Tobacco Smoke (ETS) exposure and IAQ owing to the variability of concentrations, exposure profiles and other factors. Air nicotine and heavy metals are among the most used ETS indicators and their indoor levels have been found to be related to the number of smoked cigarettes. The interaction of lichen thalli with chemical compounds (e.g., heavy metals) has been extensively and critically investigated (Paoli et al., 2019). Biomonitoring with lichens allows to detect variations in environmental levels of trace elements and provides useful evidence of the biological effects of atmospheric pollutants. So far, lichens have been widely used as biomonitors of outdoor air quality, but only rarely for the assessment of indoor air quality, such as in the case of schools (Protano et al., 2017). Therefore, this study aims to investigate the indoor air pollution from the nicotine and other heavy metals in the office building using transplanted lichen *Usnea Misaminensis*. This study underlined two hypotheses; a) that the transplant lichen can accumulate relevant amounts of nicotine and heavy metals from cigarette smoke, and b) that such exposure effects their vitality.

This study was conducted in an office building at the Universiti Kebangsaan Malaysia, Selangor, Malaysia. Five office rooms were selected as the sampling location which 2 out of 5 are the office rooms of a smoker (Table 1). The average time spending by the occupant of the selected office rooms is between 8 hours per day during working day. Lichen samples were collected from Bukit Larut, a pristine forest area and distant from any pollutant (Abas et al. 2021). Bukit Larut, Perak are known as the wettest area in Malaysia and it has the best climate for lichen to grow abundantly. The lichen samples were

exposed in all 5 selected office rooms (3 samples for each room) for 3 months, and one lichen sample were exposed in the lab under ambient condition as a control sample. After th 3 months exposure, all lichen samples were brought into the lab and lichen samples were immediately stored at−18 °C in paper bags to prevent nicotine degradation. Heavy metals concentration (Al, As, Cd, Cr, Cu, Fe, Ni, Pb, Sb and V)were analyzed using ICP-MS, nicotine content were analyzed by using HPLC and the lichen's vitality rate (F_V/F_M) were measured using Plant Efficiency Analyzer (Abas 2021). The bioaccumulation of heavy metals and nicotine, as well as the loss in vitality were assessed in terms of the ratio between exposed to control samples (EC ratios). According to Frati et al. (2005), EC ratios>1.25 and<0.75 indicate values significantly different from the control.

Table 13: Sampling locations' description

Sampling Location	Description
Control	Lab, under ambient condition, no exposure to nicotine
1	Smoker's room
2	Smoker's room
3	Non-smoker's room, connected with the smokers' room
4	Non-smoker's room, connected with the smokers' room
5	Non-smoker's room, disconnected from the smokers' room

Based on table 2, the concentration of nicotine and heavy metals are higher in both of the smoker's room, and lower in all of the non-smokers' room. The EC ratio of the smoker's rooms shows there is significant uptake of the heavy metals and nicotine by the transplanted lichen. In term of the vitality of lichen, room no 1 shows very high impact compare to the room no 2 eventhough both are occupied by smoker.

Table 2: EC ratio for each sampling station

	Room 1	Room 2	Room 3	Room 4	Room 5
Al	1.31 ± 0.05	1.27 ± 0.11	1.03 ± 0.06	0.99 ± 0.12	1.03 ± 0.01
As	1.43 ± 0.01	1.17 ± 0.20	0.99 ± 0.04	1.02 ± 0.03	0.84 ± 0.07
Cd	1.48 ± 0.15	1.33 ± 0.04	0.82 ± 0.19	1.14 ± 0.10	0.77 ± 0.13
Cr	1.37 ± 0.04	1.28 ± 0.09	1.07 ± 0.14	0.93 ± 0.04	1.05 ± 0.19
Cu	2.21 ± 0.12	1.62 ± 0.03	0.88 ± 0.05	1.30 ± 0.07	1.07 ± 0.22
Fe	1.72 ± 0.03	1.69 ± 0.02	0.78 ± 0.03	1.26 ± 0.02	1.19 ± 0.02

Ni	1.95 ± 0.08	1.31 ± 0.01	1.10 ± 0.02	1.21 ± 0.01	0.97 ± 0.05
Pb	1.39 ± 0.02	1.44 ± 0.02	1.32 ± 0.03	1.29 ± 0.05	1.14 ± 0.08
Sb	1.18 ± 0.11	1.21 ± 0.06	1.17 ± 0.01	0.87 ± 0.01	1.21 ± 0.05
Sr	1.09 ± 0.01	1.17 ± 0.11	1.09 ± 0.01	0.90 ± 0.02	1.08 ± 0.01
V	1.46 ± 0.03	1.51 ± 0.21	0.71 ± 0.05	1.01 ± 0.07	0.99 ± 0.02
Nicotine	1.99 ± 0.05	1.30 ± 0.02	1.00 ± 0.01	1.00 ± 0.09	1.00 ± 0.01
F_V/F_M	1.43 ± 0.02	0.98 ± 0.03	0.81 ± 0.02	0.89 ± 0.11	0.74 ± 0.04

This study has found that nicotine and heavy metals can be detected by using lichen as the biological indicator. This study also confirms that the increase of nicotine and heavy metals will decrease the vitality rate of living things. Nicotine and heavy metals does not travel very well through the building's ventilation system due to its heavy molecular weight and also being filtered by the ventilator. Hence, this study suggests for better ventilation system in the public office building to secure the health well being of the occupants.

Acknowledgements: The authors thank the Universiti Kebangsaan Malaysia for the financial support for this research through research grant (SK-2021-025).

References

Abas, A., Awang, A., & Aiyub, K. 2020. Analysis of heavy metal concentration using transplanted lichen *Usnea misaminensis* at Kota Kinabalu, Sabah (Malaysia). *Applied Ecology and Environmental Research*, *18*(1), 1175–1182. doi: 10.15666/aeer/1801_11751182

Abas, A. (2021). A systematic review on biomonitoring using lichen as the biological indicator: A decade of practices, progress and challenges. *Ecological Indicators*, *121*. https://doi.org/10.1016/j.ecolind.2020.107197

Abas, A., Mazlan, S. M., Latif, M. T., Aiyub, K., Muhammad, N., & Nadzir, M. S. M. (2021). Lichens reveal the quality of indoor air in Selangor, Malaysia. *Ecological Processes*, *10*(1). https://doi.org/10.1186/s13717-020-00274-1

Frati, L., Brunialti, G. & Loppi, S. 2005. Problems related to lichen transplants to monitor trace element deposition in repeated surveys: A case study from central Italy. *J. Atmos. Chem.* 52: 221–230.

Paoli, L., Maccelli, C., Guarnieri, M., Vannini, A. & Loppi, S. 2019. Lichens "travelling" in smokers' cars are suitable biomonitors of indoor air quality. *Ecol. Indic*. 103: 576–580.

Protano, C., Owczarek, M., Antonucci, A., Guidotti, M. & Vitali, M. 2017. Assessing indoor air quality of school environments: Transplanted lichen *Pseudevernia furfuracea* as a new tool for biomonitoring and bioaccumulation. *Environ. Monit. Assess.* 189: 358.

PCR15042022 – 151: Advanced Fabrication of Ultra-lightweight Cotton Waste-derived Aerogels for Rapid Oil-spill Cleaning Up

Nga Hoang Nguyen Do[a,b], Tuan Quang Pham[a,b], Duyen Khac Le[c], Huy Vo Tuan Nguyen[c], Kien Anh Le[d], and Phung Kim Le[a,b*]

a Refinery and Petrochemical Technology Research Centre Ho Chi Minh City University of Technology (HCMUT), 268 Ly Thuong Kiet Street, District 10, Ho Chi Minh City, Vietnam

b Vietnam National University Ho Chi Minh City Linh Trung Ward, Thu Duc District, Ho Chi Minh City, Vietnam

c DPN Aerogels Joint Stock Company 57/29 Pham Thai Buong Street, Tan Phong Ward, District 7, Ho Chi Minh City, Vietnam

d Institute for Tropicalization and Environment 57A Truong Quoc Dung Street, Phu Nhuan District, Ho Chi Minh City, Vietnam

• Corresponding Author E-mail: phungle@hcmut.edu.vn

Keywords: Cotton Waste; Cellulose Aerogel; Characterization; Heat Insulation; Oil Absorption.

Extended Abstract

During the production of cotton-woven fabrics in textile factories, a huge amount of unsatisfactory cotton yarn is discarded. So far, this waste has been used as filler material in downcycling products such as teddy bears and decorative products, landfilled on-site, or burned in an incinerator. With a large amount of cellulose content (above 80 wt%), cotton waste is a potential cellulose-based ingredient for the synthesis of high-value engineering aerogels. In this study, the cotton waste fibers (CFs) are successfully converted into cellulose aerogels by using polyvinyl alcohol (PVA) as a cross-linker and freeze-drying method. The prepared aerogels are extremely lightweight with a low density in a range of 18.52-32.18 mg/cm3 and high porosity of 97.81-98.73%. After being modified with methyltrimethoxysilane, the coated-aerogels exhibit enhanced hydrophobicity with water contact angles of 92-122°. They also express their ability to deal with oil pollution with a maximum oil absorption capacity of 30.61-47.19 g oil/g aerogel within only 20 sec, which is 2 times higher than that of commercial oil-absorbents made of non-renewable polypropylene and polyurethane. This work

provides a sustainable procedure to recycle the solid products of the apparel industry by creating valuable products from cotton waste fibers for water treatment.

Table 1: Density, porosity and maximum oil adsorption capacity of CF aerogels.

CF content (wt%)	PVA content (wt%)	Density (mg/cm^3)	Porosity (%)	Maximum oil adsorption capacity (g/g)
1.0	0.2	18.52 ± 0.67	98.73 ± 0.046	47.19 ± 2.08
1.5	0.2	24.23 ± 0.95	98.35 ± 0.065	38.69 ± 0.58
2.0	0.2	29.97 ± 1.33	97.98 ± 0.090	32.81 ± 0.89
2.0	0.1	28.79 ± 0.90	98.08 ± 0.060	33.70 ± 1.76
2.0	0.3	32.18 ± 1.04	97.81 ± 0.071	30.61 ± 0.56

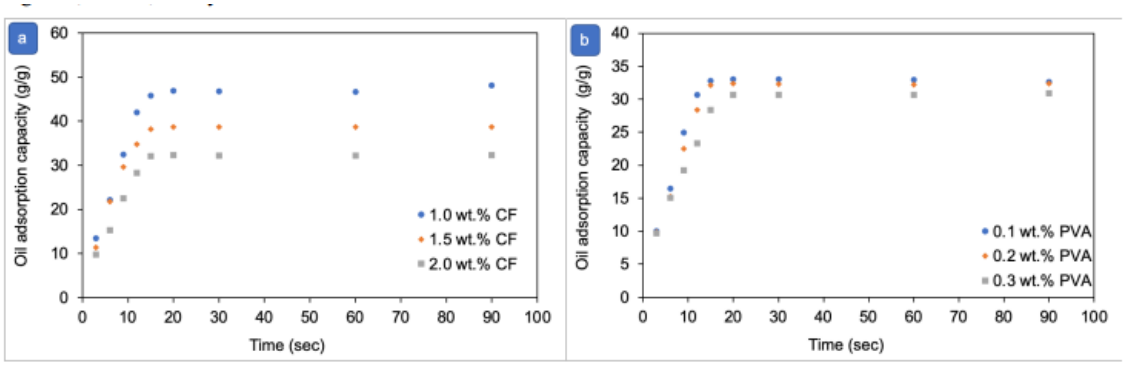

Figure 1: Oil absorption kinetics of PF aerogels with increasing CF (a) and PVA (b) content.

Acknowledgements: This work was funded by the Vietnam Ministry of Science & Technology (MOST) under project code DAĐL.CN-04/21. We also acknowledge the support of time and facilities from Ho Chi Minh City University of Technology (HCMUT), VNU−HCM for this study.

References

Do, N.H.N., Luu, T.P., Thai, Q.B., Le, D.K., Chau, N.D.Q., Nguyen, S.T., Le, P.K., Phan-Thien, N., Duong, H.M., 2020. Advanced fabrication and application of pineapple aerogels from agricultural waste. Materials Technology. 35 (11-12): 807-814.

Do, N.H.N., Luu, T.P., Thai, Q.B., Le, D.K., Chau, N.D.Q., Nguyen, S.T., Le, P.K., Phan-Thien, N., Duong, H.M., 2020. Heat and sound insulation applications of pineapple aerogels from pineapple waste. Materials Chemistry and Physics. 242: 122267.

Do, N.H.N., Tran, V.T., Tran, Q.B.M., Le, K.A., Thai, Q.B., Nguyen, P.T.T., Duong, H.M., Le, P.K., 2021. Recycling of pineapple leaf and cotton waste fibers into heat-insulating and flexible cellulose aerogel composites. Journal of Polymers and the Environment. 29: 1112-1121.

Fauziyah, M.A., Widiyastuti, W., Balgis, R., Setyawan, H., 2019. Production of cellulose aerogels from coir fibers via an alkali–urea method for sorption applications. Cellulose. 26: 9583-9598.

Mathangadeera, R.W., Hequet, E.F., Kelly, B., Dever, J.K., Kelly, C.M., 2020. Importance of cotton fiber elongation in fiber processing. Industrial Crops and Products. 147: 112217.

Rahman, S.S., Siddiqua, S., Cherian, C., 2022. Sustainable applications of textile waste fiber in the construction and geotechnical industries: A retrospect. Cleaner Engineering and Technology. 6: 100420.

Salmeia, K.A., Jovic, M., Ragaisiene, A., Rukuiziene, Z., Milasius, R., Mikucioniene, D., Gaan, S., 2016. Flammability of cellulose-based fibers and the effect of structure of phosphorus compounds on their flame retardancy. Polymers, 8 (8): 293.

Thai, Q.B., Nguyen, S.T., Ho, D.K., Tran, T.D., Huynh, D.M., Do, N.H.N., Luu, T.P., Le, P.K., Le, D.K., Phan-Thien, N., Duong, H.M., 2020. Cellulose-based aerogels from sugarcane bagasse for oil spill-cleaning and heat insulation applications. Carbohydrate Polymers. 228: 115365.

Tran, D.T., Nguyen, S.T., Do, N.D., Thai, N.N.T., Thai, Q.B., Huynh, H.K.P., Nguyen, V.T.T., Phan, A.N., 2020. Green aerogels from rice straw for thermal, acoustic insulation and oil spill cleaning applications. Materials Chemistry and Physics. 253: 123363.

Vehmas, K., Raudaskoski, A., Heikkilä, P., Harlin, A., Mensonen, A., 2018. Consumer attitudes and communication in circular fashion. Journal of Fashion Marketing and Management. 22 (3): 286-300.

Vu, P.V., Doan, T.D., Tu, G.C., Do, N.H.N., Le, K.A., Le, P.K., 2022. A novel application of cellulose aerogel composites from pineapple leaf fibers and cotton waste: Removal of dyes and oil in wastewater. Journal of Porous Materials.

Zakerzadeh, M., Abtahi, S.M., Allafchian, A., Chamani, M.R., 2018. Examining the effect of different super hydrophobic nanomaterials on asphalt pavements. Construction and Building Materials. 180: 285-290.

6th International Conference and
Postgraduate Colloquium for
Environmental Research 2022 (POCER
2022) 9 - 11 June 2022
Langkawi, Kedah, Malaysia

PCR15042022 – 152: Novel Heat Insulating and Flame Retardant Aerogel Composites from Recycled Plastic Fibers and Rice Husk Ash-derived Silica Aerogels

Nga Hoang Nguyen Do[a,b], Oanh Thi Hong Cao[a,b], Nguyen Nguyen Thao Can[a,b], Phong Thanh Mai[a,b], and Phung Kim Le[a,b*]

a Refinery and Petrochemical Technology Research Centre Ho Chi Minh City University of Technology (HCMUT), 268 Ly Thuong Kiet Street, District 10, Ho Chi Minh City, Vietnam
b Vietnam National University Ho Chi Minh City Linh Trung Ward, Thu Duc District, Ho Chi Minh City, Vietnam

• Corresponding Author E-mail: phungle@hcmut.edu.vn

Keywords: Aerogel Composite; Polyethylene Terephthalate Fibers; Silica; Ambient Drying; Flame Retardant; Heat Insulation.Faculty of Social Sciences and Humanities

Extended Abstract

To handle serious environmental pollution caused by municipal solid wastes, the general trend of the world today is to develop a cost-effective procedure for recycling waste into high-value engineering products. In this study, rice husk ash, which is one of the abundant by-products of industrial incinerators, is firstly treated with sodium hydroxide for silica recovery. The obtained sodium silicate is then gelated on a matrix of recycled polyethylene terephthalate (rPET) fibers, followed by low-cost ambient drying to generate heat-insulating and flame retardant silica aerogel composites. The developed method is economical and user-friendly due to no consumption of expensive and toxic organosiloxane as being commonly used in the previous studies. The composites remain lightweight properties with a low density of 0.126-0.176 g/cm3 and high porosity above 90%. The strong adhesion of silica aerogels to the aerogel composite not only reduces heat transfer through it with the low thermal conductivity of 0,040-0,056 W/(m·K) but also enhances its flame retardancy effectively with a flame propagation speed is approximately 0.27 mm/s. With a structure of 4 layers of rPET fibers stacked on top of each other and alternating layers of silica aerogels, the prepared aerogel composite has a high Young's modulus of 84.099 kPa and can withstand 695 times its weight. The novel silica aerogel composites are also considered an alternative to brittle silica aerogels.

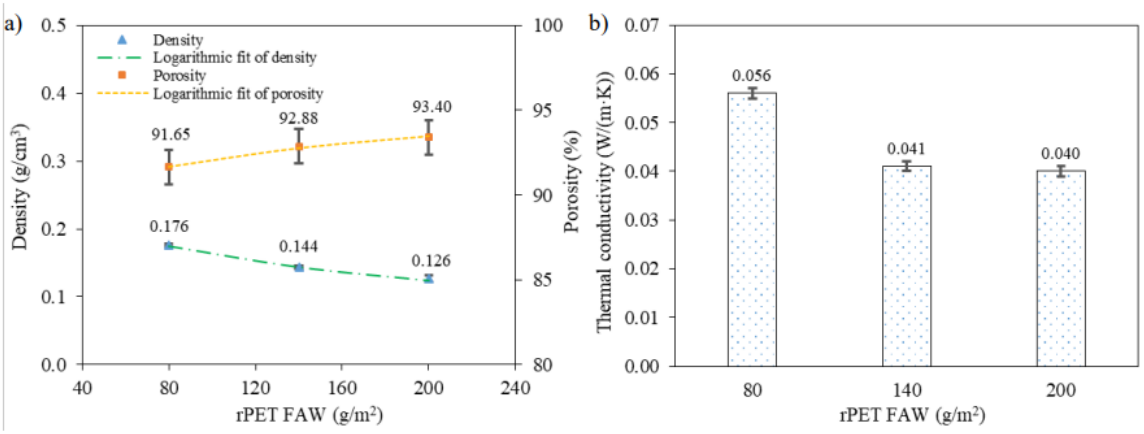

Figure 1: Physical properties (a), and thermal conductivity (b) of silica aerogel composites with increasing fiber areal weights (FAW).

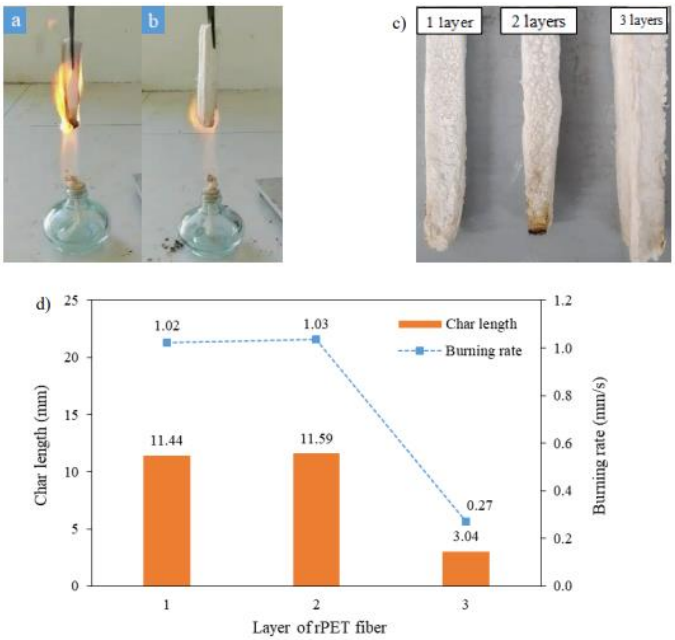

Figure 2: Flame exposure of uncoated rPET non-woven sample (a) and silica aerogel composite (b); photograph of burnt silica aerogel composites (c); flame retardancy of silica aerogel composites with increasing layers of rPET fabric (d).

Acknowledgements: This work was funded by Vingroup Joint Stock Company and supported by Vingroup Innovation Foundation (VINIF) under project code VINIF.2020.NCUD.DA112. We also acknowledge the support of time and facilities from Ho Chi Minh City University of Technology (HCMUT), VNU-HCM for this study.

References

Chen, H., Zhang, Y., Zhong, T., Wu, Z., Zhan, X., Ye, J., 2020. Thermal insulation and hydrophobization of wood impregnated with silica aerogel powder. Journal of Wood Science. 66: 81.

Do, N.H.N., Le, T.M., Tran, H.Q., Pham, N.Q., Le, K.A., Nguyen, P.T.T., Duong, H.M., Le, T.A., Le, P.K., 2021. Green recycling of fly ash into heat and sound insulation composite aerogels reinforced by recycled polyethylene terephthalate fibers. Journal of Cleaner Production. 322: 129-138.

Ghica, M.E., Almeida, C.M.R., Fonseca, M., Portugal, A., Durães, L., 2020. Optimization of polyamide pulp-reinforced silica aerogel composites for thermal protection systems. Polymers. 12 (6): 1278.

Lee, K.-J., Choe, Y.-J., Kim, Y.H., Lee, J.K., Hwang, H.-J., 2018. Fabrication of silica aerogel composite blankets from an aqueous silica aerogel slurry. Ceramics International. 44 (2): 2204- 2208.

Liu, K.-S., Zheng, X.-F., Hsieh, C.-H., Lee, S.-K., 2021. The application of silica-based aerogel board on the fire resistance and thermal insulation performance enhancement of existing external wall system retrofit. Energies. 14 (15): 4518.

Parale, V.G., Han, W., Jung, H.-N.-R., Lee, K.-Y., Park, H.-H., 2018. Ambient pressure dried tetrapropoxysilane-based silica aerogels with high specific surface area. Solid State Sciences. 75: 63-70.

Qin, L., Gao, X., Chen, T., 2018. Recycling of raw rice husk to manufacture magnesium oxysulfate cement based lightweight building materials. Journal of Cleaner Production. 191: 220-232.

Quispe, I., Navia, R., Kahhat, R., 2019. Life cycle assessment of rice husk as an energy source: A Peruvian case study. Journal of Cleaner Production. 209: 1235-1244.

Salomo, S., Nguyen, T.X., Le, D.K., Zhang, X., Phan-Thien, N., Duong, H.M., 2018. Advanced fabrication and properties of hybrid polyethylene tetraphalate fiber–silica aerogels from plastic bottle waste. Colloids and Surfaces A: Physicochemical and Engineering Aspects. 556: 37-42.

PCR15042022 – 153: Indoor Pollutants and Its Impact on Respiratory Health Symptoms and Lung Functions among School Children Exposed to Bauxite Mining

Nur Azalina Suzianti Feisal[a*], Juliana Jalaludin[b], Zailina Hashim[b], Vivien How[b], Wan Nurul Farah Wan Azmi[c] and Rafiza Shaharudin

[a] Department of Environmental Health, Faculty of Health Sciences,
MAHSA University, Selangor, Malaysia

[b]Department of Environmental and Occupational Health, Faculty of Medicine and Health Sciences, Universiti Putra Malaysia, Serdang, Selangor, Malaysia.

[c]Environmental Health Research Centre, National Institute of Health, Malaysia

- Corrensponsing Author E-mail: nurazalinasuzianti@mahsa.edu.my

Keywords: Indoor Pollutants; Respiratory Health; School Children; Bauxite Mining; Lung Functions

Extended Abstract

Exposure to indoor dust pollution is one of the public health concerns especially in children, who are one of the most susceptible groups of the population in our world. Children are more vulnerable in terms of exposure by virtue of their susceptibility and the doses of the receiving. The uncontrolled mining activities in Pahang has created a dusty environment that leads to health impacts especially respiratory health among children. A comparative cross-sectional study was conducted on 270 students randomly selected from the Primary 4 and 5 clusters. Questionnaires were used to collect the information on their background and their respiratory health symptoms. Lung function test was performed for each student using a spirometer according to the American Thoracic Society standards. Environmental sampling for particulate matter (PM_{10}) and indoor air and indoor dust of heavy metals pollutants dust samples from each of the eight classes (four classes from Primary 4 and another four classes from Primary 5) were collected using a Gillian Personal High-Volume Air Sampler and 400W vacuum cleaner that consists of a special filter. The heavy metals concentrations in indoor air and indoor dust samples were analysed using Inductively Coupled Plasma-Mass Spectrometry (ICP-MS). Results showed the concentration of particulate matter (PM_{10}) and heavy metals (As, Cd, Ni and Pb) in indoor air and dust and soil was significantly higher in the studied area compared to comparative area ($p<0.001$). Highest reported symptoms among students in the studied area was cough with flu (48.0%) followed by nasal congestion

(45.9%) and runny nose (42.6%) and headache (41.2%). While in comparative group was cough with flu (35.9%) and cough only (35.2%) for the past 3 months. Symptoms such as diagnosed asthma ($p=0.033$), runny nose ($p<0.001$), nasal congestion ($p<0.001$), sore throat ($p<0.001$), dry throat ($p<0.001$) and chest tightness after outdoor activities ($p<0.001$) showed significant differences between two groups. This study also showed students in studied area have significantly lower ($p<0.01$) of FEV1, FVC, and FEV1/FVC ratio compared to the comparative group. Students from studied area have 68.2% of FEV1 abnormalities followed by 50% of FEV1/FVC abnormalities and 38.5% of FVC abnormalities. Higher pollutants concentration of PM_{10} and heavy metals concentration in indoor air, window dust and corridor dust were significantly associated with all reported health symptoms except for cough and chest tightness at night. PM_{10} and heavy metals exposure in school environments especially air, window dust and corridor dust were significantly associated with reduction of lung functions ($p<0.05$). Lower values of FEV1, FVC and FEV1/FVC were found to be significantly associated with runny nose, nasal congestion, dry throat, chest tightness, chest tightness at night and chest tightness after outdoor activities. The study revealed that concentration of PM_{10} and heavy metals in indoor air and indoor dust were higher in the studied school compared to comparative school. The elevated or increasing concentrations of these pollutants in the school investigated should be one of our cause for concern especially for stakeholders in the education sector. Therefore, all appropriate measures needs to be taken safely and urgently for any safeguard the health of the concerned children. Logistic analysis showed that increasing exposure to heavy metals in indoor air and dust will lead to reported health symptoms and lung function abnormalities.

References

Abdollah, G., Javad, S., Behzad, F. D., Leila, I. G., Gholamheidar, T. B., Abdoljalil, T., and Mohse, A. (2018). Lung Function and Respiratory Symptoms among Mine Workers in The Eastern Part of Iran, Hygiene and Environmental Health, 7(3). doi: https://doi.org/10.15275/rusomj.2018.0306

Abdullah, M. Z., and Alias, N. A. (2018). Variation of PM_{10} and Heavy Metals Concentration of Sub-Urban Area Caused by Haze Episode. *Malaysian Journal of Analytical Sciences*, 22 (3), 508-513. doi: https://doi.org/10/17576/mjas-2018-2203-19

Asrul, S., and Juliana, J. (2017). Indoor Aiq Quality and Its Association with Respiratory Health among Preschool Children in Urban and Suburban Area. *Malaysian Journal of Public Health Medicine 2017,* Special Volume (1), 78 – 88.

Ayuni, N., and Jalaludin, J. (2014). Exposure to PM_{10} and NO_2 and Association with Respiratory Health among Primary School Children Living Near Petrochemical Industry Area at Kertih, Terengganu. *Journal of Medical and Bioengineering*, 3 (4). doi: https://doi.org/10.12720/jomb.3.4.282-287

Bergstra, A. D., Brunekreef, B., and Burdorf, A. (2018). The Effect of Industry-Related Air Pollution on Lung Function and Respiratory Symptoms in School Children. *Environmental Health: A Global Access Science Source*, 17(1), 30. doi: https://doi.org/10/1186/s12940-018-0373-2

6th International Conference and Postgraduate Colloquium for Environmental Research 2022 (POCER 2022) 9 - 11 June 2022
Langkawi, Kedah, Malaysia

PCR15042022 – 154: Two-stage Ultrafiltration for the Separation of α-Amylase from Red Pitaya Peel

Nurelyzurina Sukri[a], Mohd Zuhair Mohd Nor[a,b*], Mohd Noriznan Mokhtar[a], Khairul Faezah Md. Yunos[a], Rosnah Shamsudin[a,b], and Pau Loke Show[c]

[a]Department of Process and Food Engineering, Faculty of Engineering, Universiti Putra Malaysia, 43400 UPM Serdang, Selangor, Malaysia

[b]Laboratory of Halal Science Research, Halal Products Research Institute, Universiti Putra Malaysia, Putra Infoport, 43400 UPM Serdang, Selangor, Malaysia

[c]Department of Chemical and Environmental Engineering, Faculty of Science and Engineering, University of Nottingham Malaysia, Jalan Broga, 43500 Semenyih, Selangor, Malaysia

- Correnspoonsing Author E-mail: zuhair@upm.edu.my

Keywords: α-Amylase; Enzyme; Membrane Filtration; Pitaya; Separation.

Extended Abstract

Red pitaya fruits (*Hylocereus polyrhizus*) also known as dragon fruit, is one of the popular tropical fruits and belongs to the cactus family, *Cactaceae*. The fruit has an exotic look and flavor, and offers numerous nutrients, including vitamin B and C, phosphorus, protein, calcium, fiber, and antioxidants. While the flesh part is high in demand, the peel of pitaya usually will be discarded as waste. Without proper waste management, the discarded peel may contribute to a major ecological problem. Hence, efforts have been done to retrieve valuable bioactive compounds from the pitaya peel including dietary fiber, natural colorant, and many enzymes such as pectinase and amylase (Jiang et al., 2021). Among all, amylase separation, particularly from pitaya peel is one of a few attractive options considering this enzyme is dominating the biotechnology industry. Separation of this enzyme from pitaya peel may require the advancements in the extraction technology which may involve the membrane filtration process. Multistage membrane filtration process was reported to successfully separate proteins and enzymes such as bromelain from pineapple waste (Nor et al., 2018). Hence, this work focused on the separation of α-amylase from red pitaya peel by employing a two-stage ultrafiltration (UF) scheme.

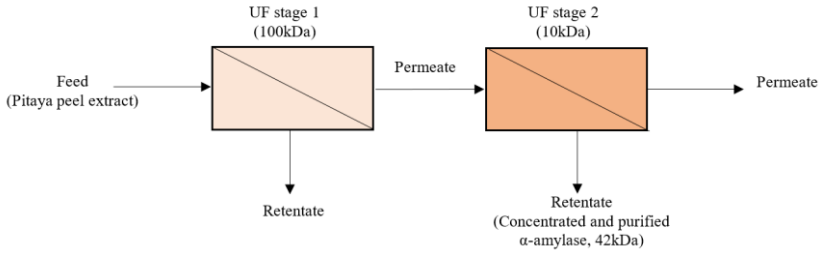

Figure 1: Schematic diagram of the two-stage UF for α-amylase separation

All pitaya samples were first pre-treated with pectinase to hydrolyze the pectic substances prior to the UF process. The pitaya peel extract was then purified by using a two-stage UF system which consisted of polyethersulphone membranes with molecular weight cut-off (MWCO) bigger in the ultrafiltration stage 1 (100kDa) and smaller in the ultrafiltration stage 2 (10kDa) than the α-amylase molecular weight of 42 kDa as shown in Figure 1. The UF stage 1 is considered the pre-filtered stage since it was aimed to separate the targeted enzyme in the permeate from the high molecular weight molecules including polysaccharides. The permeate from UF stage 1 will be taken back to be further filtered in the UF stage 2 to obtain concentrated α-amylase solution as the retentate. The process was performed up to the permeate recovery (PR) of 80% in UF stage 1, and volume reduction factor (VRF) of 10 in UF stage 2.

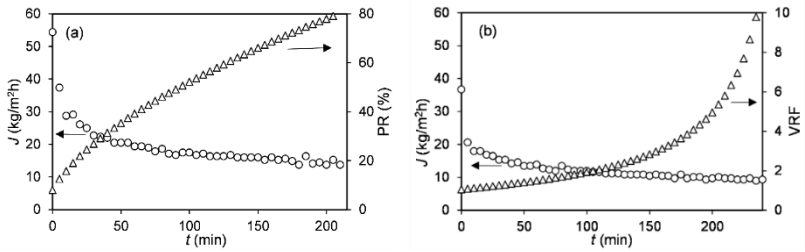

Figure 2: Flux profiles of (a) UF stage 1; and (b) UF stage 2

The findings indicate that both UF stages produced declining flux profiles with three obvious phases; (1) drastic declination, (2) minor declination, and (3) steady-state flux as shown in Figure 2. The declination of the flux is influenced by the fouling phenomenon taking place on the surface membrane during the filtration process (Omar et. al, 2020). The rapid decline observed at the beginning of both UF processes is probably due to the blocking of the membrane pores. It was then followed by the gel polarization phenomenon when the suspended solids were rejected by the membrane.

Table 1: Properties of red pitaya peel extract in two-stage ultrafiltration

Properties	UF stage 1 (100 kDa)			UF stage 2 (10 kDa)		
	Feed	Permeate	Retentate	Feed	Permeate	Retentate
Volume (ml)	300	240	60	240	216	24
Protein content (mg/ml)	0.82± 0.02[a]	0.83 ± 0.03[a]	0.65 ± 0.01[b]	0.82 ± 02[a]	0.74 ± 0.04[c]	1.2 ± 0.02[d]
Enzyme activity (U/ml)	7.58 ± 0.22[a]	7.4 ± 0.15[a]	4.82 ± 0.11[b]	7.38 ± 16[a]	4.60 ± 0.06[b]	25.74 ± 0.31[c]
Specific activity (U/mg protein)	9.24 ± 0.04[a]	8.92 ± 0.17[a]	7.47 ± 0.49[b]	8.97 ± 32[a]	6.19 ± 0.18[c]	21.41 ± 0.63[d]
Enzyme recovery (%) after UF stage 1		97.80 ± 4.83				
Purification fold in UF stage 2						2.39 ± 0.08

*Different letters in the same row indicate the significant differences ($p < 0.05$)

The properties of the sample in each UF stage in Table 1 also displayed promishing results. In UF stage 1, there was no significant change in protein content and enzyme activity of the permeate compared to the feed after the process was concluded at the 80% PR. This signifies the high recovery of the enzyme after passing the membrane in UF stage 1 with 97.8% recovery. For UF stage 2, the protein and enzyme activity was significantly high in the retentate indicating high rejection of the compounds by the membrane. Hence, an increment of enzyme specific activity by 2.39-fold in the retentate was observed after the total volume of the feed was reduced by 10 times. The purity fold obtained in this study exceeds the targeted purification requirement since the extract needs to be purified to 2 to 4 folds necessary for commercialization purposes as reported by Nor et al. (2018). With the high enzyme recovery in UF stage 1, and acceptable enzyme purity fold in UF stage 2, this study indicates the successfulness of this technology for the separation of α-amylase from the pitaya extract.

Acknowledgements: The authors would like to thank the Ministry of Higher Education Malaysia for sponsoring this work under UPM Putra Grant: GP/2018/9656000.

References

Jiang, H., Zhang, W., Li, X., Shu, C., Jiang, W., & Cao, J., 2021. Nutrition, phytochemical profile, bioactivities and applications in food industry of pitaya (*Hylocereus spp.)* peels: a comprehensive review. *Trends in Food Science & Technology*, 116, 199-217

Nor, M. Z. M., Ramchandran, L., Duke, M., Vasiljevic, T., 2018. Performance of a two-stage membrane system for bromelain separation from pineapple waste mixture as impacted by enzymatic pretreatment and diafiltration. *Food Technology and Biotechnology*, 56 (2): 218-227

Omar, J. M., Nor, M. Z. M., Basri, M. S. M., Che Pa, N. F., 2020. Clarification of guava juice by an ultrafiltration process: analysis on the operating pressure, membrane fouling and juice qualities. *Food Research*, 4 (S1), 85-92.

6th International Conference and
Postgraduate Colloquium for
Environmental Research 2022 (POCER
2022) 9 - 11 June 2022
Langkawi, Kedah, Malaysia

PCR15042022 – 155: Utilisation of palm kernel shell biochar for supplementary cementitious replacement

Aan Mohammad Nusrat Aman[a] and Anurita Selvarajoo[a*]

[a] Department of Civil Engineering
University of Nottingham Malaysia, Selangor, Malaysia

- Corresponding Author E-mail: Anurita.Selvarajoo@nottingham.edu.my

Keywords: Palm Kernel Shell; Pyrolysis; Biochar; Supplementary Cementitious Material.

Extended Abstract

Concrete is one of the most widely used material in the construction industry resulting in high demand of its raw materials. One of the raw materials in concrete is cement. The cement industry has generally known to have negative impact on the environment, living things and climate change (Mohamad et al., 2021). Due to this, research has expanded to utilize different materials to replace cement in the concrete mix that would be environmentally and economically beneficial. Recently, there has been an increase in studies using biochar in concrete mix as a supplementary cementitious material (Wang et al., 2020). Use of biochar as cement replacements is found to be very beneficial (Gupta et al., 2018). This would eventually motivate the construction industry to adapt biochar usage and will lead to a decrease in the cement demand which can the production. Malaysia is one of the largest producers of palm oil in the world as reported by the Malaysian Palm Oil Council. Large amount of palm kernel shells are available as wastes after the palm oil extraction process.

Pyrolysis is a thermochemical conversion process that is conducted under the absence of oxygen to convert biomass into biochar, syngas and bio-oil. The target product of this of study is biochar, slow pyrolysis has been adopted as it has confirmed that in order to obtain a higher yield of biochar slow pyrolysis would be preferred in comparison to fast pyrolysis (Al Arni, 2018). Palm kernel shells used in this study was collected locally from Seri Putra Oil Palm Mill, Banting, Selangor. The palm kernel shells were washed to remove impurities, dried in an oven, milled and then sieved to 1.18 -2 mm. Slow pyrolysis was conducted in a tubular reactor at different temperatures ranging from 200-800 ℃. Nitrogen flow of 30 ml/min, heating rate 10 ℃/min and residence time of 70 min were adopted for all pyrolysis runs. The weight of sample remaining after the pyrolysis process was weighed to obtain the

biochar yield. The biochar yield (y_{mass}) in equation (1) has been adopted from Weber et al., (2018), $m_{feedstock}$ representing the mass of the raw palm kernel shells and m_{char} representing the mass of biochar.

$$y_{mass\ (\%)} = \frac{m_{char}}{m_{feedstock}} \times 100 \quad (1)$$

As illustrated in Table 1, the palm kernel shell biochar yield is inversely proportional to the temperature. Highest biochar yield of 98.7 % was obtained at pyrolysis temperature of 200 ℃ and the yield decreased to around 29.5 % at temperature of 800 ℃. These results are in agreement with the study conducted with different types of feedstock biomass (wheat straw, corn straw, rape straw and rice straw) at different ranges of pyrolysis temperatures 300 ºC to 600 ºC and show a gradual decrease of yield with temperature (Zhang et al., 2020). It shows that temperature has significant effect on the biochar yield. The loss of mass during pyrolysis as the temperature increases is due to the decomposition of the volatile matter and the appearance of larger pores that were generated with the release of volatile compounds (Liu et al., 2018).

Table 14: Biochar yield results through slow pyrolysis

Temperature (℃)	Biochar Yield (%)
200	96.7
300	64.2
400	41.3
500	35.1
600	32.3
700	32.2
800	29.5

There is a potential of producing biochar from palm kernel shell which could be used as cement replacement. These results would then motivate further studies that can be experimented on the different amount of biochar as cement replacements and conduct mechanical tests on the resultant concrete mix to study the concrete strength.

References

Al Arni, S., 2018. Comparison of slow and fast pyrolysis for converting biomass into fuel. Renew. Energy 124, 197–201.

Gupta, S., Kua, H.W., Koh, H.J., 2018. Application of biochar from food and wood waste as green

admixture for cement mortar. Sci. Total Environ. 619–620, 419–435.

Liu, Z., Niu, W., Chu, H., Zhou, T., Niu, Z., 2018. Effect of the Carbonization Temperature on the Properties of Biochar Produced from the Pyrolysis of Crop Residues. BioResources 13, 3429–3446.

Malaysian Palm Oil Council. 2022. Malaysian Palm Oil Industry. [online] Available at: <https://mpoc.org.my/malaysian-palm-oil-industry/>

Mohamad, N., Muthusamy, K., Embong, R., Kusbiantoro, A., Hashim, M.H., 2021. Environmental impact of cement production and Solutions: A review. Mater. Today Proc.

Wang, L., Chen, L., Tsang, D.C.W., Guo, B., Yang, J., Shen, Z., Hou, D., Ok, Y.S., Poon, C.S., 2020. Biochar as green additives in cement-based composites with carbon dioxide curing. J. Clean. Prod. 258.

Weber, K., Heuer, S., Quicker, P., Li, T., Løvås, T., Scherer, V., 2018. An Alternative Approach for the Estimation of Biochar Yields. Energy & Fuels 32, 9506–9512.

Zhang, X., Zhang, P., Yuan, X., Li, Y., Han, L., 2020. Effect of pyrolysis temperature and correlation analysis on the yield and physicochemical properties of crop residue biochar. Bioresour. Technol. 296, 122318.

6th International Conference and
Postgraduate Colloquium for
Environmental Research 2022 (POCER
2022) 9 - 11 June 2022
Langkawi, Kedah, Malaysia

PCR15042022 – 157: From strain improvement to lutein extraction: Attempts to CO_2 Capture And Utilization by Microalgae

Quanyu Zhao[a*]

[a] School of Pharmaceutical Science,
Nanjing Tech University, Jiangsu, China

- Corrensponsing Author E-mail: zhaoqy@njtech.edu.cn

Keywords: CO_2 capture; Lutein ; Microalgae ; Flue gas ; Metabolic regulation; Nanoemulsion.

Extended Abstract

It is widely recognized that the large-scale emission of greenhouse gases, such as carbon dioxide, leads to global climate anomalies and frequent natural disasters, which is not conducive to the long-term survival and development of mankind. In order to achieve the carbon neutrality target, microalgae - based approaches are potential ones for carbon capture and utilization. Reducing CO_2 emmision is not enough and the development of high value-added products will improve the technical economy of microalgae - based approaches.

Microalgae have high photosynthesis efficiency but environmental stresses lead to negative effects on growth of microalgae. It is essential to enhance the tolerances to these environmental stresses, for exampel, high concentration of CO_2, flue gas and phenol during environmental remediation process (Zhao and Huang, 2021).

There are some studies improving the metabolic phenotype and tolerance by adaptive laboratory evolution (ALE). Firstly, the growth phenotype of *Chlamydomonas reinhardtii* gene deficient strains was enhanced by adaptive laboratory evolution. The results showed that the oil yield was significantly increased by more than 40% (Yu et al., 2013). This is a successful application to enhance microalgae growth and lipid synthesis in microalgae. It should be mentioned that it was not performed under stress contions. In addition, 10% and 20% CO_2 (Li et al., 2015), simulated flue gas (10% CO_2, 200 ppm NOx and 100 ppm SOx) (Cheng et al., 2019), and 30 g/L salt (Li et al., 2018) were selected as environmental stresses for *Chlorella vulgaris*. Then, the tolerances to high concentration of CO_2, simulated flue gas, and salt through shown in Fig. 1. The starting algal strain is *Chlorella* sp. L3, and the evolved algal strains are AE10, CV, L5 and S30, respectively. It should be noted that S30 can maintain high carbon

fixation capacity and salt tolerance at the same time. It is possible to make CO_2 capture in seawater or high salinity wastewater.

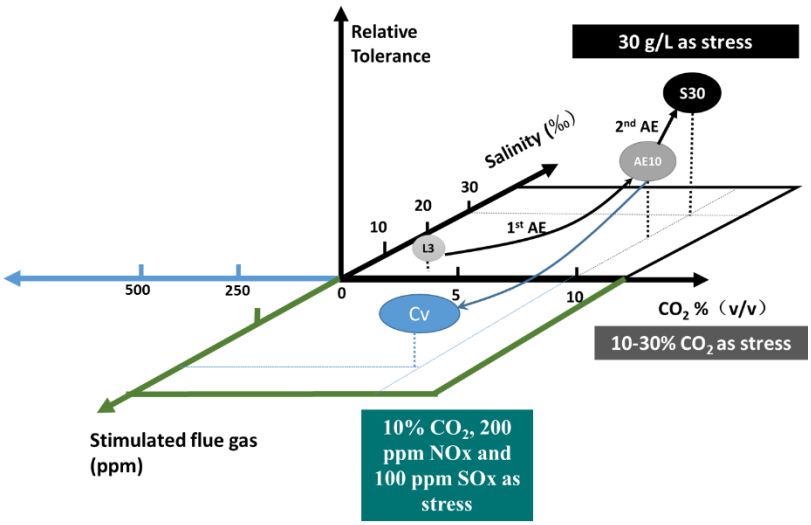

Figure 1: ALE of microalgae for CO_2 capture

Full utilization of microalgae is helpful to realize carbon neutrality based on the concenpt biorefinary (Li et al., 2019). There are carbohytrates, proteins, lipids and pigments in microalgae. An approch based on ionic liquid was developed to help pretreatment of cell wall of microalgae and lutein extraction from *Chlorella* sp. (Zhu et al., 2021). Nano-emulsion of lutein has been prepared and the bioactivities were determined. It was shown that the nano-emulsion was stable under 25 ºC.

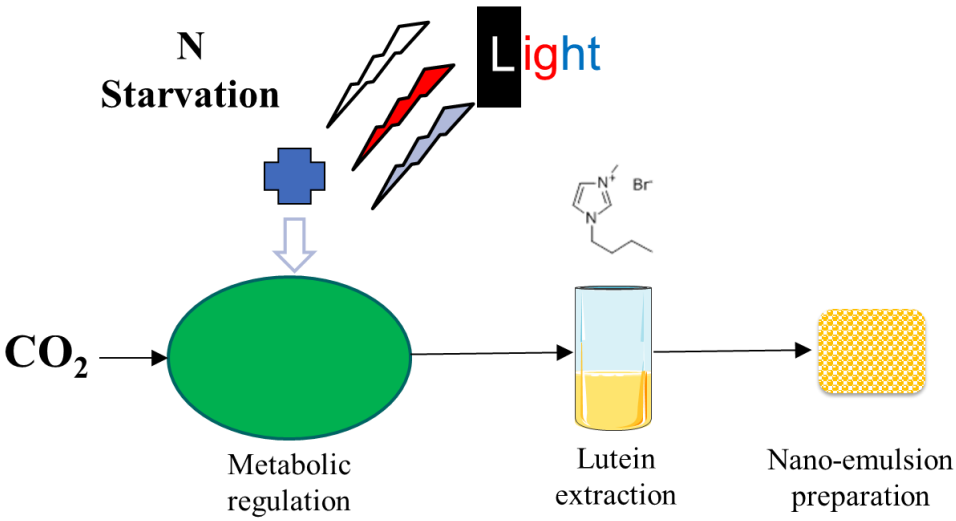

Figure 2: From biorefinary of microalgae, lutein extraction and nano-emulsion preparation

Strain improvement is the first step in microalgae biotechnology. Extractions of pigment and other products are downstream process. Both of them are important for CO_2 capture and utilization.

Acknowledgements: The authors acknowledge the supports received from National Natural Science Foundation of China (21576278).

References

Cheng, D.J., Li, X.Y., Yuan, Y.Z., Yang, C.Y., Tang, T., Zhao, Q.Y., Sun, Y.H., 2019. Adaptive Evolution and Carbon Dioxide Fixation of *Chloroella* Sp. in Simulated Flue Gas. *Science of the Total Environment* 650: 2931-2938.

Li, D., Wang, L., Zhao, Q., Wei, W., Sun, Y., 2015. Improving High Carbon Dioxide Tolerance and Carbon Dioxide Fixation Capability of *Chlorella* sp. by Adaptive Laboratory Evolution. *Bioresource Technology*. 185: 269-275.

Li, D., Yuan, Y., Cheng, D., Zhao, Q., 2019. Effect of Light Quality on Growth Rate, Carbohydrate Accumulation, Fatty Acid Profile and Lutein Biosynthesis of *Chlorella* sp. AE10. *Bioresource Technology*. 291: 121783.

Li, X., Yuan, Y., Cheng, D., Gao, J., Kong, L., Zhao, Q., Wei, W., Sun, Y., 2018. Exploring Stress Tolerance Mechanism of Evolved Freshwater Strain *Chlorella* sp. S30 under 30 g/L Salt. *Bioresource Technology*. 250: 495-504.

Yu, S., Zhao, Q., Miao, X., Shi, J. 2013. Enhancement of Lipid Production in Low-Starch Mutants *Chlamydomonas reinhardtii* by Adaptive Laboratory Evolution. Bioresource Technology, 147: 499-507.

Zhao, Q., Huang, H., 2021. Adaptive Evolution Improves Algal Strains for Environmental Remediation. Trends in Biotechnology. 39(2): 112-115.

Zhu, Y., Li, X., Wang, Y., Ren, L., Zhao, Q., 2021. Lutein Extraction by Imidazolium-Based Ionic Liquid-Water Mixture from Dried and Fresh *Chlorella* sp. *Algal Research*, 60: 102528.

6th International Conference and Postgraduate Colloquium for Environmental Research 2022 (POCER 2022) 9 - 11 June 2022
Langkawi, Kedah, Malaysia

PCR15042022 – 158: Clogging detection in anaerobic co-digestion continuous system using machine learning approach

Sujin Choi[a], Md Abu Hanifa Jannat[a], Wonseob Lee[a] and Seokhwan Hwang[a,b*]

[a] Division of Environmental Science and Engineering, Pohang University of Science and Technology, 77 Cheongam-Ro, Nam-Gu, Pohang, Gyeongbuk, South Korea

[b] Yonsei University Institute for Convergence Research and Education in Advanced Technology (I-CREATE), 85, Songdogwahak-ro, Yeonsu-gu, Incheon 21983, Republic of Korea

- Corrensponsing Author E-mail: shwang@postech.ac.kr

Keywords: Anaerobic co-digestion; clogging; FOG deposits; machine learning

Extended Abstract

Vessel clogging often occurs in both lab-scale and full-scale anaerobic digestion system especially when fed with substrate containing high suspended solids or lipid [Cirne, 2007; Spanjers, 2006]. The clogging from lipid-rich substrate is usually induced by fat, oil and grease (FOG) deposits created by the saponification of free fatty acids and Ca^{2+} [He, 2017]. This can cause substrate transfer problem which will eventually deteriorate reactor performanc. However, clogging is difficult to be noticed in advance until the following outcome happens. In this study, early detection of clogging in substrate tube had been performed with machine learning using substrate and effluent characteristics. Two laboratory-scale anaerobic CSTR reactors were operated for 120 days and fed continuously with a mixture of foodwaste and waste activated sludge from wastewater treatment plant through peristaltic pump and tygon tube. The mixture created sufficient amount of FOG deposits to hinder the inlet tube and showed reducing flow after several days. The influent amount was recorded to indicate the degree of clogging and some of the potential features to predict the clogging was analyzed from the substrate and effluent. The data is a multidimensional data which is the combination of a cross-sectional (substrate characteristics) and a time-series data (effluent characteristics). Therefore, the algorithm to use this type of data has been selected from several types of candidate models including deep neural network, recurrent neural network with and without attention mechanism based on R^2 evaluation metric. Moreover, in order to clarify the cause and effect of the attributes, time scale of the target attribute (influent amount) had been moved forward to assure it as an effect. The data from one of the reactors

was used as train dataset and the other reactor was used as test dataset. The feautre importance analysis had been performed as well to select which kind of attributes contribute the most to detect clogging. The result from this study demonstrates the possibility of predicting tube clogging through machine learning algorithm and determines the important factors that affect clogging in anaerobic digestion system.

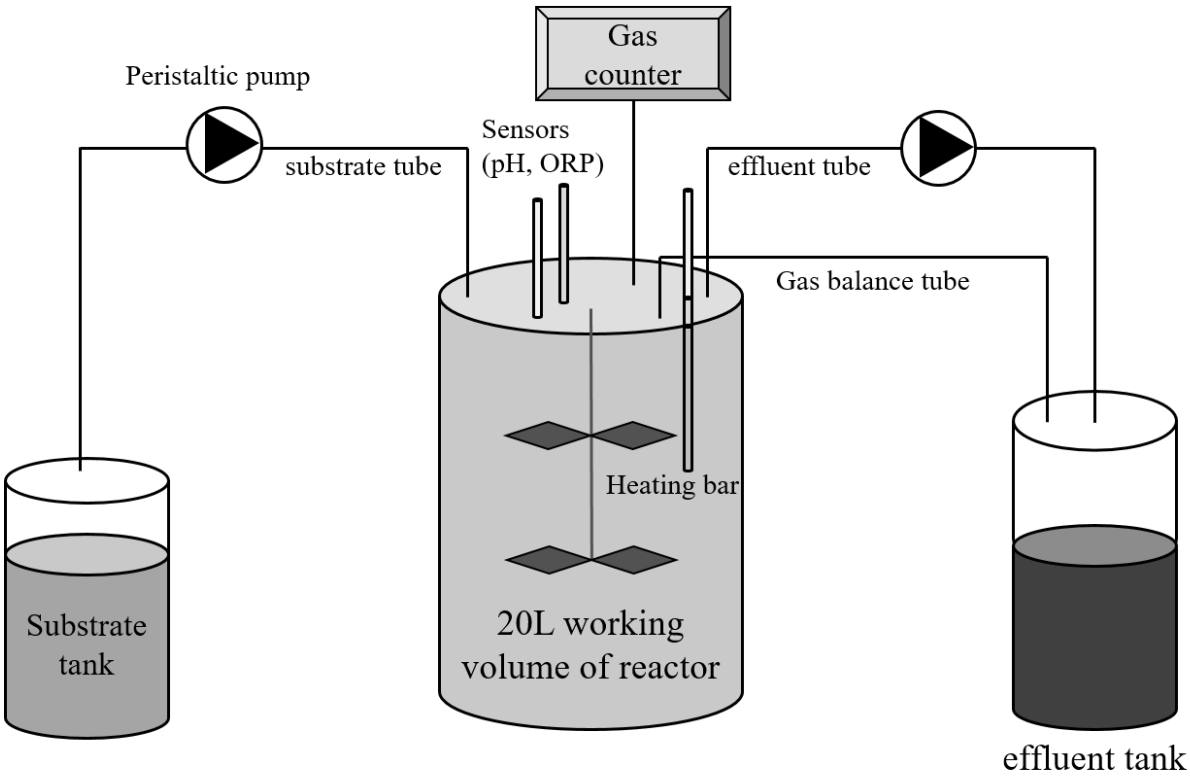

Figure 34 : Schematic experimental diagram anaerobic CSTR system

Acknowledgements: This research was financially supported by the Korea Ministry of Environment as Waste to Energy-Recycling Human Resource Development Project (No. YL-WE-21-002).

References

Cirne, D. G., Paloumet, X., Björnsson, L., Alves, M. M., & Mattiasson, B. (2007). Anaerobic digestion of lipid-rich waste—Effects of lipid concentration. Renewable Energy, 32(6), 965-975.

He, X., de los Reyes, F. L., & Ducoste, J. J. (2017). A critical review of fat, oil, and grease (FOG) in sewer collection systems: Challenges and control. Critical Reviews in Environmental Science and Technology, 47(13), 1191-1217.

Spanjers, H.; Bouvier, J. C.; Steenweg, P.; Bisschops, I.; van Gils, W.; Versprille, B. (2006). Implementation of in-line infrared monitor in full-scale anaerobic digestion process. Water Science and Technology, 53(4-5), 55–61.

6th International Conference and
Postgraduate Colloquium for
Environmental Research 2022 (POCER
2022) 9 - 11 June 2022
Langkawi, Kedah, Malaysia

PCR15042022 – 159: Reduction of polycyclic compounds and biphenyls generated by pyrolysis of polyethylene terephthalate by using supported metal catalysts

Chanyeong Park[a], Jechan Lee[ab*]

[a] Department of Energy Systems Research

Ajou University, Suwon 16499, Republic of Korea

[b] **Department of Environmental and Safety Engineering**

Ajou University, Suwon 16499, Republic of Korea

- Corrensponsing Author E-mail: jlee83@ajou.ac.kr

Keywords: ; Municipal solid waste; Plastic waste; Waste treatment; Air pollution control; Catalytic process; Thermochemical process

Extended Abstract

Plastic waste in the environment is a global growing concern. Polyethylene terephthalate (PET) is a common plastic used in industry and human life. Thermochemical process is a preferred method to dispose plastic waste mainly because it can reduce volume of the waste; however, the thermochemical disposal of plastic waste can emit harmful chemical species such as benzene derivatives and polycyclic hydrocarbons. Therefore, it is critical to prevent the generation of polycyclic aromatic compounds during pyrolysis of PET waste to make it more environmentally benign and more sustainable for the disposal of PET. As an effort to overcome this challenge, supported metal catalysts (carbon-supported Pd and Pt catalysts) were used to inhibit the formation of polycyclic compounds and biphenyl derivatives by pyrolysis of PET. Less polycyclic compounds and biphenyl derivatives were generated during the Pd or Pt-catalyzed PET pyrolysis than non-catalytic PET pyrolysis. The concentrations of polycyclic compounds and biphenyl derivatives were 107 % and 56 % lower for the Pt-catalyzed pyrolysis at 700 °C than non-catalytic pyrolysis, respectively. The Pt catalyst was more effective to suppress the generation of polycyclic compounds and biphenyl derivatives during the PET pyrolysis than the Pd catalyst at temperatures from 400 to 800 °C. This was likely because the Pt sites catalyzes decyclization reaction and/or free radical mechanism that is dominant in thermal cracking of carbonaceous substances such as PET. The results of this study would help develop environmentally friendly plastic waste treatment methods via thermochemical processes.

Acknowledgements: The authors thank the National Research Foundation of Korea (NRF) grant funded by the Korean Government (MSIT) (No. NRF-2020R1C1C1003225).

6th International Conference and
Postgraduate Colloquium for
Environmental Research 2022 (POCER
2022) 9 - 11 June 2022
Langkawi, Kedah, Malaysia

PCR15042022 – 160: Valorization of waste tea bags via CO_2-assisted pyrolysis

Nahyeon Lee[a], Soosan Kim[b], and Jechan Lee[a,b*]

[a] Department of Energy Systems Research,
University of Ajou, Suwon, 16499, Republic of Korea

[b] Department of Environmemtal Engineering,
University of Ajou**, Suwon, 16499, Republic of Korea**

- Corrensponsing Author E-mail: jlee83@ajou.ac.kr

Keywords: CO2 utilization; Tea waste; Thermochemical process; Waste-to-energy; Waste treatment; Waste valorization

Extended Abstract

Pyrolysis is an effective method for both waste valorization and treatment. Herein, carbon dioxide-assisted pyrolysis was conducted for the valorization and treatment of everyday waste, namely used tea bags. The effects of pyrolysis temperature and medium (N_2 and CO_2) on the composition and yield of the pyrolytic products were explored. The changes in the pyrolysis temperature and pyrolysis medium affected the compositions and yields of pyrolytic products. More non-condensable gases and less char were produced as the temperature increased. CO_2 increased the yield of pyrolytic gases, particularly hydrogen and also prevented the formation of environmental pollutants such as phenolic compounds, benzene derivatives, and polycyclic aromatic hydrocarbons. The char produced from waste tea bags via CO_2-assisted pyrolysis had a higher heating value (26.8 MJ kg^{-1}) comparable to that of coal. This study demonstrates the effectiveness of CO_2 utilization in pyrolysis for valorization of everyday waste.

Acknowledgements: This work was supported by the National Research Foundation of Korea (NRF) grant funded by the Korean Government (Ministry of Science and ICT) (No. NRF-2020R1C1C1003225).

6th International Conference and
Postgraduate Colloquium for
Environmental Research 2022 (POCER
2022) 9 - 11 June 2022
Langkawi, Kedah, Malaysia

PCR15042022 – 161: Thermochemical conversion of mulching film waste via pyrolysis with the addition of cattle excreta

Junghee Joo[a*], Nahyeon Lee[a], and Jechan Lee[a,b,*]

[a] Department of Energy Systems Research
University of Ajou, Suwon 16499, Republic of Korea
[b] **Department of Environmental and Safety Engineering**
University of Ajou, Suwon 16499, Republic of Korea

- Corrensponsing Author E-mail: jlee83@ajou.ac.kr

Keywords: Plastic waste; Agricultural waste; Livestock manure; Thermochemical process; Waste-to-energy

Extended Abstract

The pyrolysis of mulching film waste (an agricultural plastic waste) with cattle excreta (livestock organic waste) was investigated as the efficient simultaneous treatment of plastic and organic wastes. For pyrolysis of mulching film waste or cattle excreta, an increase in temperature increased the yield of non-condensables and decreased the yield of condensables or solid residue. The mulching film waste-derived pyrolytic product was composed largely of a wide range of hydrocarbons (C_1–C_{44}), while the cattle excreta-derived pyrolytic product was composed of a variety of chemical groups such as oxygenates, polycyclic aromatic compounds, N-, S-, and B-containing compounds, and halogenated compounds. Pyrolysis temperature had no significant effect on the selectivity toward each chemical groups found in the condensables derived from either the mulching film waste or cattle excreta. The addition of the cattle excreta to the pyrolysis of the mulching film waste increased the yield of non-condensables and enhanced selectivity toward H_2 between 500 ℃ and 900 ℃, compared to the pyrolysis of the mulching film waste only. The pyrolysis of the mulching film waste/cattle excreta mixture led to the condensables with lower contents of N, S, B, and halogens than the pyrolysis of a single feedstock. This study is to propose thermochemical conversion pathway of agricultural plastic waste along with livestock organic waste as an effective strategy for waste-to-resources.

Acknowledgements: This work was supported by the National Research Foundation of Korea (NRF) grant funded by the Government of Republic of Korea (Ministry of Science and ICT) (No. 2020R1C1C1003225). This work was also supported by the National Research Foundation of Korea (NRF) grant funded by the Government of Republic of Korea (Ministry of Science and ICT) (No. 2021R1A4A1031357).

6th International Conference and Postgraduate Colloquium for Environmental Research 2022 (POCER 2022) 9 - 11 June 2022
Langkawi, Kedah, Malaysia

PCR15042022 – 162: Quarry Respirable Dust Pollutant Impact on Fractional Exhaled Nitric Oxide (FENO) and Interleukin-8 (IL-8) Concentration

Noor Haziqah Kamaludin[a], Juliana Jalaludin[b,c*]

[a]Center of Environmental Health & Safety, Faculty of Health Sciences, Universiti Teknologi MARA, Puncak Alam 42300, Selangor, Malaysia

[b]Department of Environmental and Occupational Health, Faculty of Medicine and Health Science, 43400 Universiti Putra Malaysia (UPM), Serdang, Selangor, Malaysia

[c]Department of Occupational Health and Safety, Faculty of Public Health, Universitas Airlangga, 60115 Surabaya, East Java, Indonesia

- Corrensponding Author E-mail: juliana@upm.edu.my

Keywords: Quarry respirable dust; Fractional Exhaled Nitric Oxide (FENO); lung function; Interleukin-8.

Extended Abstract

INTRODUCTION: The respirable dust from quarry sites may contain harmful minerals that can penetrate deep into the lungs. Mineral dust contains a variety of carcinogenic and non-carcinogenic substances. **AIMS:** This study was to investigate the impact of exposure to quarry respirable dust on respiratory health performance by interpreting Fractional Exhaled Nitric Oxide (FENO) and Interleukin-8 (IL-8) concentrations. **METHODS:** A cross-sectional study was carried out among 173 school staff who have been exposed within a 10km radius of the quarry sites. An air sampling pump was used to collect personal exposure to quarry respirable dust. A human ELISA kit was used to analyze IL-8 concentrations, whereas NIOX MINO and Chestgraph H1-105 spirometers were used to measure FENO levels and lung function. **RESULT:** The mean and standard deviation of quarry respirable dust was 1.18±0.78 mg/m³. The FVC% predicted and FEV_1% predicted had normal lung function levels of 91.83±12.37 and 96.21±11.40. The geometric mean (GM) concentration of IL-8 was 87.34±2.38 pg/mL. The geometric mean (GM) concentration of FENO was 21.08 ± 7.98 ppb. FENO concentrations among

study respondents were significantly influenced by the exposure to quarry respirable dust (R2=0.051, p=0.001).

CONCLUSION: The public is at high risk of lung impairment by developing respiratory health symptoms, reducing lung function levels and increasing high levels of FENO cause of their exposure to quarry respirable dust.

Acknowledgements: The authors would like to express their gratitude to the Faculty of Medicine and Health Sciences, Universiti Putra Malaysia, and all of the school participate in this study for their cooperation and valuable assistance in completing this research. This project was funded by Universiti Putra Malaysia grant (Project Code: GP-IPS/2017/9527800).

References

Ahn, Y. S. and Jeong, K. S. (2014). Epidemiologic Characteristics of Compensated Occupational Lung Cancers among Korean Workers. *Journal of Korean Medical Science*, 29:1473-1481.

Amran, S., Latif, M. T., Khan, M.F., Goh, E., Leman, A. M., and Jaafar, S. A. (2017). Underestimation of Respirable Crystalline Silica (RCS) compliance status among the granite crusher operators in Malaysian quarries *Air Quality Atmosphere Health*, 10:371-379.

Kamaludin, N. H., Jalaludin, J., Mohd Tamrin, S. B., and Md Akim, A. (2018b). Biomarker of occupational airways inflammation for exposure to inorganic dust. *Asian Journal of Agriculture and Biology*, Special Issue:23-28.

Kim, H. J., Choi, M. G., Park, M. K., and Seo, Y. R. (2017). Predictive and prognostic biomarkers of respiratory disease due to particulate matter exposure. *Journal of Cancer Prevention*, 22(1):6-15.

Othman, M., Latif, M. T., and Mohamed, A. F. (2016). The PM10 compositions, sources and health risks assessment in mechanically ventilated office buildings in an urban environment. *Air Quality Atmosphere Health*, 9:597-612

Oyinloye, M. A. (2015). Environmental Pollution and health risks of residents living near Ewekoro cement factory, Ewekoro, Nigeria. *International Journal of Environmental, Chemical, Ecological, Geological and Geophysical Engineering*, 9(2):108-114.

Zerguine, H., Jalaludin, J., and Mohd Tamrin, S. B. (2016). Behaviour-based safety approach and factors affecting unsafe behavior in construction sectors: A review. *Asia Pacific Environmental and Occupational Health Journal*, 2(2):1-12.

6th International Conference and
Postgraduate Colloquium for
Environmental Research 2022 (POCER
2022) 9 - 11 June 2022
Langkawi, Kedah, Malaysia

PCR15042022 – 164: Single-Use Disposable Waste Upcycling via Thermochemical Conversion Pathway

Heeyoung Choi[a], Jechan Lee[a,b*], Junghee Joo[a] and Seonho Lee[a]

[a] Department of Energy Systems Research
University of Ajou, Suwon, 16499, Republic of Korea
[b] Department of Environmental and Safety Engineering
Ajou University, Suwon, 16499, Republic of Korea

- Corrensponsing Author E-mail: chk6788@ajou.ac.kr

Keywords: municipal solid waste; plastic waste; recycling; thermochemical process; waste-to-energy.

Extended Abstract

Herein, the pyrolysis of two types of single-use disposable waste (single-use food containers and corrugated fiberboard) was investigated as an approach to cleanly dispose of municipal solid waste, including plastic waste. For the pyrolysis of single-use food containers or corrugated fiberboard, an increase in temperature tended to increase the yield of pyrolytic gas (i.e., non-condensable gases) and decrease the yield of pyrolytic liquid (i.e., a mixture of condensable compounds) and solid residue. The single-use food container-derived pyrolytic product was largely composed of hydrocarbons with a wide range of carbon numbers from C1 to C32, while the corrugated fiberboard-derived pyrolytic product was composed of a variety of chemical groups such as phenolic compounds, polycyclic aromatic compounds, and oxygenates involving alcohols, acids, aldehydes, ketones, acetates, and esters. Changes in the pyrolysis temperature from 500 ◦C to 900 ◦C had no significant effect on the selectivity toward each chemical group found in the pyrolytic liquid derived from either the single-use food containers or corrugated fiberboard. The co-pyrolysis of the single-use food containers and corrugated fiberboard led to 6 times higher hydrogen (H2) selectivity than the pyrolysis of the single-use food containers only. Furthermore, the co-pyrolysis did not form phenolic compounds or polycyclic aromatic compounds that are hazardous environmental pollutants (0% selectivity), indicating that the co-pyrolysis process is an eco-friendly method to treat single-use disposable waste.

Acknowledgements: This work was supported by the National Research Foundation of Korea (NRF) grant funded by the Korea government (MSIT) (No. 2021R1A4A1031357)..

6th International Conference and
Postgraduate Colloquium for
Environmental Research 2022 (POCER
2022) 9 - 11 June 2022
Langkawi, Kedah, Malaysia

PCR15042022 – 165: The assessment of the ability of urban parks to self-sustain the GHG emissions in densely populated cities through carbon sequestration

Phahmee Ahanaf Khalid[1], Saleh Shadman[1], Inzamamul Islam[4], Marlia Mohd. Hanafiah[2,3]

[1]EcoThinkers, House 59, Road 1, Block i, Banani, 1213, Dhaka, Bangladesh
[2]Centre for Tropical Climate Change System, Institute of Climate Change, Universiti Kebangsaan Malaysia, Bangi, Selangor, 43600, Malaysia
[3]Department of Earth Sciences and Environment, Faculty of Science and Technology, Universiti Kebangsaan Malaysia, Bangi 43600, Selangor, Malaysia
[4] Department of Electrical and Computer Engineering, Morgan State University, Baltimore, USA.

- Correnspondsing Author E-mail: khairulazhar.jumbri@utp.edu.my

Extended Abstract

Green spaces and urban parks are in limited supply in densely populated cities across the world caused by rapid population growth, urbanisation, and increased land-use demands. Globally, rising energy demand and consumption, particularly of fossil fuels in the residential and industrial sectors, is the major driver of increased GHG emissions. However, urban parks with plantations and vegetations have the potential to capture carbon and other GHG's naturally. Carbon emission from the urban parks and the total carbon sequestration for Baishakhi park in Banani, Dhaka has been assessed for this particular study. The motivation behind this research is to understand whether urban parks as such in densely populated cities can self-sustain in terms of their GHG emissions and provide cleaner air for the neighbourhood surrounding them. This study has been done as a case study for the park in Dhaka city to draw baseline conclusions on how similar parks around the city within similar neighbourhood can contribute in reducing GHG from the atmosphere. The methods used for this study includes GHG protocol to develop the GHG inventory and calculate the total GHG emissions in tonnes of carbon dioxide equivalent (tCO2e) and their sources. A total of 2 scopes are considered for the GHG emission; scope 1 (direct emission) from stationary and mobile combustion and scope 2 (indirect emissions) from purchased electricity. The data collection sheet provided by the research group is the instrument of data collection for this method. Secondly, the carbon sequestration is done using a above and below ground biomass calculation and their ability to capture GHG's. A total station was used to measure the dimensions of the plantations around the park and the total dimension of the park. The identification of

plantations and they type of vegetation were done to identify the species and their dominance within the park to understand which species has higher sequestration potential for future afforestation or reforestation projects. The total carbon emissions and the total sequestration of GHG's will give us an insight into the park's ability to sustain the emissions from day to day activities. The net emission within the park will be calculated to determine whether the parks is an emitter of more GHG's than an absorber. Mitigation strategies, a framework and plan will be implemented at the end of the project to reduce the emissions from multiple sources within scope 1 and 2 and ways to increase the sequestration potential. The aim is to ensure that urban parks in these localities can provide not just place for people to socialise and rejuvenate but also to allow them to breathe cleaner air, provide shade and reduce the impact of climate change around them.

6th International Conference and Postgraduate Colloquium for Environmental Research 2022 (POCER 2022) 9 - 11 June 2022
Langkawi, Kedah, Malaysia

PCR15042022 – 166: Dehydration of apple slices and black chokeberries by sequential drying pretreatments and ultrasound-assisted air drying: Study on mass transfer, profiles of phenolics and PPO activity

Rui Zhu[a,b], Dandan Li[a,b], Chung Lim Law[c], Yongbin Han[a,b], Yang Tao[a,b,*]

[a] College of Food Science and Technology, Nanjing Agricultural University, Nanjing 210095, Jiangsu, China

[b] Whole Grain Food Engineering Research Center, Nanjing Agricultural University, Nanjing 210095, Jiangsu, China

[c] Department of Chemical and Environmental Engineering, Faculty of Science and Engineering, University of Nottingham Malaysia, Jalan Broga, 43500 Semenyih, Selangor Darul Ehsan, Malaysia

- Corrensponsing Author E-mail: yang.tao@njau.edu.cn (Yang Tao)

Keywords: ultrasound drying; diffusional modeling; phenolics; PPO activity;

Extended Abstract

Drying is one of the most widely applied methods for reducing the moisture content of materials so as to facilitate transportation, storage and preservation (Kahraman et al., 2021). However, drying are considered to be the most energy-intensive units, and some quality deterioration could happen during long-time dehydration process. Therefore, to improve the drying process, more efforts are needed in the aspects of novel drying technology development and process optimization.

Hybrid or rapid drying technology is more efficient than the individual drying technology in food drying, while that the pretreatments can also preserve food quality, speed up drying. Pretreatments and airborne or contact ultrasound, microwave drying were selected for our research. Square apple slices and spherical black chokeberries were used as experimental materials. In the study of apple slices, pretreatments of either water blanching or NaCl immersion and airborne ultrasound-assisted air drying were combined to dehydrate materials. For the drying of black chokeberries, the fast remove of water can lead to the severe deformation problem. Therefore, calcium immersion was performed as a pretreatment and combined with ultrasonic or microwave drying to carry out the drying process of black chokeberries.

Food drying involves heat and mass transfer mechanism, as well as the knowledge referring to food chemistry. Mathematical simulation is an important tool to explore the physical phenomenon underneath drying (Gamboa-Santos et al., 2014; Magalhães et al., 2017). However, the shrinkage law, porosity and temperature change would all affect the mass transfer process (Tao et al., 2021). To improve the applicability of the mass transfer model, the model in the drying of apple slices incorporated the temperature-dependent diffusivity in an Arrhenius pattern into the partial differential equations, and this model well depicted the moisture decline (Zhu et al., 2022). While in the drying of black chokeberries, the factors about temperature rising, deformation and porosity were considered together in the model. In the drying study of these two materials, the drying time was found to be greatly reduced when the ultrasonic and microwave drying was applied, and they lowered the activation energy required for the enhancement of moisture diffusive ability. In terms of quality attributes, both water blanching and NaCl immersion significantly increased the amounts of procyanidin B2 in dehydrated apple slices, while procyanidin B2 in black chokeberries were also well preserved when ultrasonic drying was applied. However, sonication promoted the loss of procyanidin B2 in apple slices and black chokeberries with pretreatments during air drying, and the samples dried by microwave suffered the sever loss of procyanidin B2. In addidtion, sonication had no obvious influences on PPO activity and individual organic acids throughout drying, but POD was significantly inactivated in all drying methods. Overall, the sequential NaCl immersion pretreatment (or water blanching pretreatment) and drying with airborne sonication are effective to improve the quality of dried apple slices, but only the calcium immersion pretreatment combined with contact ultrasonic drying is suitable for the drying of black chokeberries.

Acknowledgements： This work was supported by the National Natural Science Foundation of China (No.32072351) and the Priority Academic Program Development of Jiangsu Higher Education Institutions (PAPD).

References

Gamboa-Santos, J., Montilla, A., Cárcel, J.A., Villamiel, M., & Garcia-Perez, J.V. (2014). Air-borne ultrasound application in the convective drying of strawberry. *Journal of Food Engineering*, 128, 132-139.

Kahraman, O., Malvandi, A., Vargas, L., & Feng, H. (2021). Drying characteristics and quality attributes of apple slices dried by a non-thermal ultrasonic contact drying method. *Ultrasonics Sonochemistry*, 73, 105510.

Magalhães, M.L., Cartaxo, S.J.M., Gallão, M.I., García-Pérez, J.V., Cárcel, J.A., Rodrigues, S., & Fernandes, F.A.N. (2017). Drying intensification combining ultrasound pre-treatment and ultrasound-assisted air drying. *Journal of Food Engineering*, 215, 72-77.

Miao, X., Tao, Y., Shi, Y., Law, C.L., Han, Y., Li, D., Xie, G., & Xu, Y. (2020). Effects of freezing and thermal pretreatments on drying of Vaccinium bracteatum Thunb leaves: Drying mechanism, physicochemical properties and ability to dye glutinous rices. *Food and Bioproducts Processing*, 122, 1-12.

Tao, Y., Li, D., Chai, W., Show, P.-L., Yang, X., Manickam, S., Xie, G., & Han, Y. (2021). Comparison between airborne ultrasound and contact ultrasound to intensify air drying of blackberry: Heat and mass transfer simulation, energy consumption and quality evaluation. *Ultrasonics Sonochemistry*, 72, 105410.

Zhu, R., Jiang, S., Li, D., Law, C., Han, Y., Tao,Y., Kianid, H., & Liu, D. (2022). Dehydration of apple slices by sequential drying pretreatments and airborne ultrasound-assisted air drying: Study on mass transfer, profiles of phenolics and organic acids and PPO activity. *Innovative Food Science and Emerging Technologies*, 75, 102871.

6th International Conference and Postgraduate Colloquium for Environmental Research 2022 (POCER 2022) 9 - 11 June 2022
Langkawi, Kedah, Malaysia

PCR15042022 – 167: Hydrodynamic Modelling of an Idealised Coastal Reservoir with Consideration of Algal Bloom Occurrence

Wong Hui Ling[a*], Teo Fang Yenn[a]

[a] Faculty of Sciene and Engineering, University of Nottingham, Selangor, Malaysia

- Corrensponsing Author E-mail: evyhw2@nottingham.edu.my

Keywords: Algal Bloom; Coastal Reservoir; Hydrodynamic Modelling; Water Quality; Eutrophication; Water Resources

Extended Abstract

Relevance and Background

Coastal Reservoir has been given prominence and attention due to its potential to becoming the next major freshwater storage option. One of the successful operating examples of coastal reservoir would be Qingcaosha, constructed in Shanghai China since year 2010 and it has been a major freshwater intake for Shanghai City, China. In many of the published research and books on Coastal Reservoir, eutrophication has been a great concern to coastal reservoir due to its low flow velocity. Thus, there is a great need to water researchers to take in consideration of the algal blooming and pinpoint the areas that are prone to algal bloom occurrence for further prevention and mitigation. A hydrodynamic modelling has therefore done on Qingcaosha Coastal Reservoir to locate the areas that are prone to algal bloom based on the flow velocity in the reservoir.

Methodology

MIKE 21 Modelling was used to model the Qingcaosha based on idealised condition. To simulate the critical flow velocity in the reservoir, only the tidal and river discharge were considered in the simulation based on the tidal gauge data near the project boundary determined. Hence the locations of the area prone to algal blooming are solely due to the depth, existing geometry and flow velocity of Qingcaosha Reservoir without taking the effect of nutrients, salinity, carbon dioxide and other factors that are affecting the growth of algal bloom. The critical velocity for the growth of algae and chlorella are 0.05 m/s and for filamentous algae is 0.01 m/s according to (Jiao, 2017). Therefore, in the modelling, areas with velocity lesser than 0.05 m/s will be marked as area with potential occurrence of algae and

chlorella, whereas area with velocity lesser than 0.01 m/s for filamentous algae mapping. The tidal height utilised for the upper boundary was -0.33m and -0.15 m for the lower boundary to simulate the flow in the esturary on the 25th of February 2002, 10 a.m. obtained from (Antolinez *et.al.*, 2015). With that result, it reflects the effectiveness of the current geometry and depth of Qingcaosha to minimise algal blooming.

Results and discussion

Table 1 shows the percentage of areas in the idealised Qingcaosha Reservoir that are prone to algae, chlorella and filamentous algae blooming based on the flow velocity in the reservoir, affected by the geometry and the depth. The locations that prone to the occurrence of algae bloom and chlorella are mostly shallow, otherwise located at the bends or corners that are of challenge for water to flow easily. With these mapping, mitigation such as dredging or changing the existing shape with lesser corners can be done to reduce the areas prone to algal blooming in the reservoir.

Velocity Interval <0.05 m/s (m/s)	Midpoint of the Velocity Interval (m/s)	Percentage of Area with the Respective Velocity (%)	Percentage of Occurrence for Algae and Chlorella (%)	Percentage of Occurrence for Filamentous Algae (%)	Total Percentage of Area with Algal and Chlorella Occurrence (%)	Total Percentage of Area with Filamentous Algae Occurrence (%)
0.04-0.05	0.045	11.75	10.00	0.00	52.49	10.38
0.03-0.04	0.035	12.47	30.00			
0.02-0.03	0.025	6.94	50.00			
0.01-0.02	0.015	10.95	70.00			
0.00-0.01	0.005	10.38	90.00	50.00		

Table 1 Result Summary Showing the Percentage of Area in the reservoir with velocity lesser than 0.05 m/s and 0.01 m/s and its respective percentage of algae, chlorella and filamentous algae bloom occurrence

Conclusions

Based on the modelling result on idealised condition, 52.49% of the areas in Qingcaosha Coastal Reservoir are prone to Algae and Chlorella Occurrence whereas 10.38% of the area are prone to filamentous algae blooming based on the flow velocity. These are the areas in the coastal reservoir that should be given attention to prevent the growth of algal blooming. Mitigation such as dredging or optimising the shape based on the water flow within the coastal reservoir should be done to reduce the algal bloom occurrence and improve the water quality of the freshwater stored.

Acknowledgement

I would like to thank DHI Malaysia for sponsoring MIKE 21/3 software suites to support the research work. Other than that, I would like to thank the staffs in Angkasa Consulting Services for the basic guidance on MIKE 21 usage

References

Antolinez, *et.al*. (2015) 'Journal of Geophysical Research : Oceans', *Journal of Geophysical Research: Oceans*, pp. 775–791. doi: 10.1002/2015JC011107.

Jiao, S.J. (2007) 'The Effects of Velocity of Glow to the Growth of Algae in Low Current Area of the Three Gorges.' *Master's Thesis, Southwest University, Chongqing, China*

Li, M. *et al.* (2017) 'Estimating urban water demand under conditions of rapid growth : the case of Shanghai', *Regional Environmental Change*. doi: 10.1007/s10113-016-1100-6.

6th International Conference and
Postgraduate Colloquium for
Environmental Research 2022 (POCER
2022) 9 - 11 June 2022
Langkawi, Kedah, Malaysia

PCR15042022 – 168: Effects of Palm Oil Ash on Hydration, Development, and Strength of Cement

Giam Li Ann, Anurita Selvarajoo, Teo Fang Yenn

[a] Faculty of Science and Engineering, University of Nottingham Malaysia, Selangor, Malaysia

- Corrensponsing Author E-mail: kefey6gla@nottingham.edu.my

Keywords: Ordinary Portland Cement (OPC); Biochar; Palm Oil Ash and response surface methodology (RSM).

Extended Abstract

Ordinary Portland Cement (OPC) concrete is considered not environmentally friendly due to the large amount of carbon dioxide gas generated during its manufacturing process. Recent studies have proven that by incorporating palm oil ash (POA) into cement as a supplementary cementing material can reduce waste and benefit the environment. This research will provide an overview of POA's physical and chemical properties, and its effect as a partial cement substitute. Figure 1 shows flow chart of analytical test. OPC was replaced by 0%, 10% and 20% of POA by cement weight. Dry mixing and pre-soaked POA (wet mixing) were used during this experiment. The mortar properties like workability, compressive strength, flexural strength, and microstructural analysis were investigated. The substitution of 10% (dry and wet) of POA in mortar per unit weight of cement gave 1% and 8% increased of compressive strength compared to control sample at 7 days whereas 20% (dry and wet) produce 9% and 11% increment, respectively at 28 days. Additionally, the optimization of the POA dosage, the curing period and the mixing method of mortar was investigated using the response surface methodology (RSM). Modelling and statistical analysis were carried out using historical data design model, which was based on experimental data. Polynomial regression equation was found to be the best fit with a coefficient of regression (R^2) of 0.89. The analysis of variance implies that the model for compressive strength was significant. The outcome achieved suggest 20% of POA (dry method) and 28 days of curing period are the optimum operating parameters to obtain maximum strength.

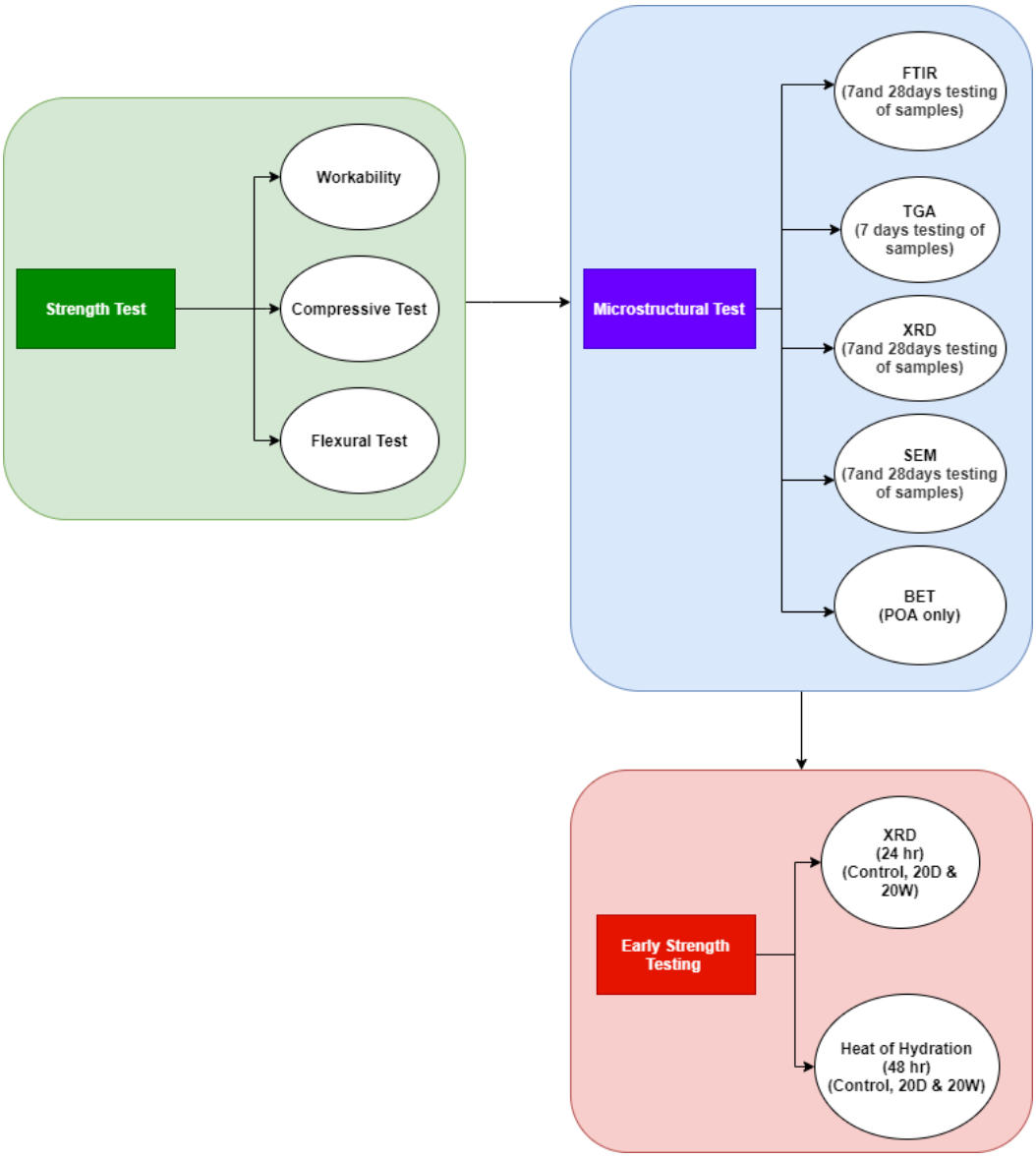

Figure 1: Flow chart of analytical test

Acknowledgements: The authors thank Taimur Mazhar Sheikh.

References

Gupta, S., Kua, H. W. and Low, C. Y. (2018) 'Use of biochar as carbon sequestering additive in cement mortar', Cement and Concrete Composites, 87, pp. 110–129. doi: 10.1016/j.cemconcomp.2017.12.009.

Suarez-Riera, D., Restuccia, L. and Ferro, G. A. (2020) 'The use of Biochar to reduce the carbon footprint of cement-based', Procedia Structural Integrity, 26(2019), pp. 199–210. doi: 10.1016/j.prostr.2020.06.023.

6th International Conference and
Postgraduate Colloquium for
Environmental Research 2022 (POCER
2022) 9 - 11 June 2022
Langkawi, Kedah, Malaysia

PCR15042022 – 169: A Study on the Current Status and Issues of Integrated River Basin Management in Malaysia

Lim Chow Hock[a*], Wong Hui Ling[a], Teo Fang Yenn[a]

[a] Department of Civil Engineering, University of Nottingham, Selangor, Malaysia

Corrensponsing Author E-mail: evxcl6@nottingham.edu.my

Keywords: Integrated River Basin Management, Integrated Water Resources Management, Water Governance

Extended abstract

Relevance background

Despite of having an average annual rainfall of about 3,000mm, Malaysia still experiences numerous incidences of water supply disruptions and rationing. From the 672 rivers monitored, 9 % are polluted while another 36% are moderately polluted (Jabatan Alam Sekitar, 2020). On top of that, flooding is also another water hazard, in which a total of 10% of Malaysia are categorised as flood-prone area, affecting 21% of the total population (DID, 2021). On the other hand, there is also the issue of mild to moderate hydrological drought which may occur once in every 5 to 7 years, causing water stress in some developed states. All these three major issues can be minimised or mitigated through good water governance which must in turn be based on the principles of Integrated Water Resources Management (IWRM). Application of the principles of IWRM can best be achieved if carried out at basin level, and such process may also be referred to as Integrated River Basin Management (IRBM).

The Global Water Partnership (GWP) has defined IRBM as a process of coordinating conservation, management and development of water, land, and related resource across sectors within a given river basin, in order to maximise the economic and social benefits derived from water resource in an equitable manner (GWP, 2009). All form of land uses in a river basin, such as land development for residential, commercial, and industrial purposes, agricultural and plantation activities, logging, mining, and other forestry activities, can have profound impacts on the water resources in the basin.

A basin-level perspective allows water managers to address effectively the interactions between water resources management and the management of land and other related natural resources.

Methodology

A desktop and systematic study was done to identify the current status and issues on IRBM in Malaysia. The thirteen (13) thematic areas focused for the study include policy, legislation, institution, finance, water assessment and allocation, pollution control, flood management, drought management, river basin and land use planning, information system, R&D, river basin monitoring and stakeholder participation.

Results and discussion

Three (3) out of the thirteen (13) thematic areas from this study are listed in Table 1.0, together with their status and issues identified.

Thematic Focus Areas	**Status**	**Issues**
Policy	A roadmap of IWRM status was developed, showing the evolution of IWRM approach in Malaysia over the past 20 years. Some of them include the organisation of the awareness programme in year 1993, formation of National Water Resources Council in year 1998, implementation of IWRM BMP in year 2009 and finally the formulation of the National Water Resource Policy in year 2012.	Some key policy issues identified are still in its implementation stage at the state-level, and development of state-level collaboration for its implementation is slow.
Water Assessment and Allocation	The Federal Constitution grant the states with the right to access to water resources and thus there is a need to identify the water resources available in each basin for water allocation priorities. Currently, water extractions for portable water supply and irrigated paddy crops were given priorities. All the operators for the water supply will have to apply for license from state to extract water from the river.	Inconsistent and no standard in state legislation for water allocation governance. Other than that, the water allocation is not guided by an IRBM plan or IWRM principles.
River Basin and Land Use Planning	The land use planning was carried out by Town and Country Planning Department with the basis on the 3-stage urban planning system. The country's level is governed by the National Physical Plan, State Structure Plan for states and Local Plan for the local authority level. In year 2001, DID had done a study on the development of a Register of Rivers in Malaysia. A list of River Basin Management Units	Insufficient legislative support for land use control in river basin that is IRBM-compliant. Moreover, land use control at the local level is not based on the river basin plan. Besides that, there is also

	(RBMU) was also recommended. In year 2003, IRBM plans for all the RBMU were initiated and 25 have been completed by year 2021.	insufficient technical capacity to monitor IRBM implementation master plans.

Table 1.0 Three (3) out of the thirteen (13) thematic areas focused from this research with its respective status and issues

Conclusion

The implementation of IRBM is the key for sustainable water resources management in Malaysia. As part of the good water governance, there is an urgent need for the formation of River Basin Authority with the necessary legal mandate. This is to ensure that all the principles, policy and strategies can be effectively implemented. In addition to that, the IRBM plan should be the basis for all the land use planning and approval in Malaysia.

Reference

Department of Irrigation and Drainage (DID), Malaysia (2021). Available at: https://www.water.gov.my/.

Global Water Partnership (GWP) and International Network for River Basin Organisations (INBO) (2009) Handbook for IWRM in Basins, GWP.

Jabatan Alam Sekitar (2020) *Environmental Quality Report 2020, Portal Rasmi Jabatan Alam Sekitar*. Available at: https://www.doe.gov.my/portalv1/wp-content/uploads/formidable/5/Kualiti-Air- Sungai.pdf.

6th International Conference and
Postgraduate Colloquium for
Environmental Research 2022 (POCER
2022) 9 - 11 June 2022
Langkawi, Kedah, Malaysia

PCR15042022 – 170: Hydro-Environmental Modelling of Putrajaya Lake

Lim Sin Poh[a], Teo Fang Yenn[a*]

[a]Faculty of Science and Engineering, Nottingham University of Malaysia

- Corrensponsing Author E-mail: fangyenn.teo@nottingham.edu.my

Keywords: Putrajaya Lake; Modelling; Hydro-Environmental; current; flow.

Extended Abstract

Putrajaya lake was created by construction of a dam across Chuau River as shown in Figure 1. The dam was constructed in 1999, together with the 24 wetland cells. The constructed wetland is 200 ha and comprises 5 arms, namely Upper West (UW), Upper North (UN), Upper East (UE), (Lower East) LE & Upper Bisa (UB). The lake is a 400-ha surface area with a 38 km shoreline and an estimated 26.5 mil m^3 of water.

The lake and wetland system plays an important role in purification the water by natural processes of trapping of sediment, uptake of nutrients and pollutants by wetland plants before flowing into the Putrajaya main lake. Figure 1 shows the overall configuration of the Putrajaya Wetlands and Lake. \

This study aims to investigate the hydrodynamic behaviours in Putrajaya Lake under various weather conditions. Water quality modelling was also conducted for key parameter such as Temperature, Disolve Oxygen, Nitrate and Phosporite.

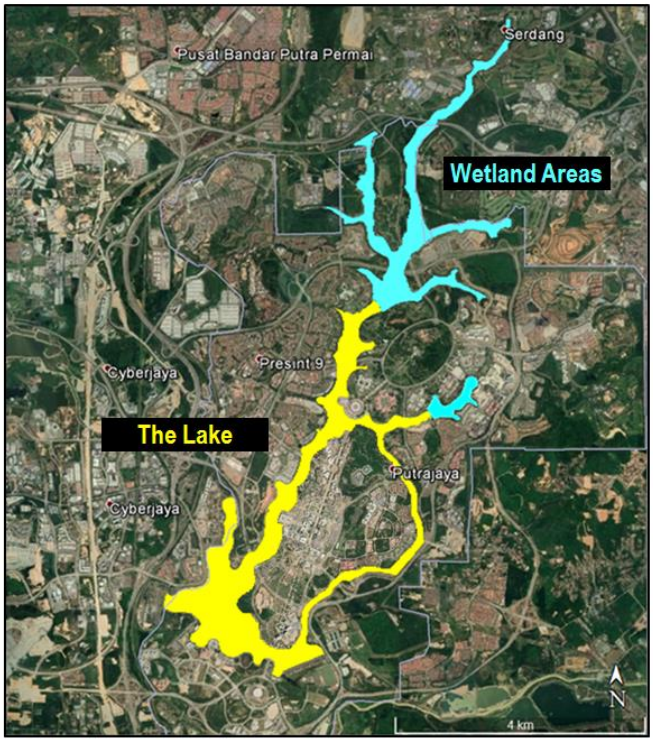

Figure 1. Overall configuration of the Putrajaya Wetland Areas and Lake.

Hydrodynamic model domain cover the main Putrajaya Lake from the Cetral Weir all the way the the dam as highlighted yellow in Figure 1. The calibarted hydrodynamic model was then used for water quality modelling.

The hydrodunamic behavious for the whole Putrajaya Lake are presented for dry, normal and wet season. Figure 2 shows the flow direction and magnitude of current during dry waether condition.

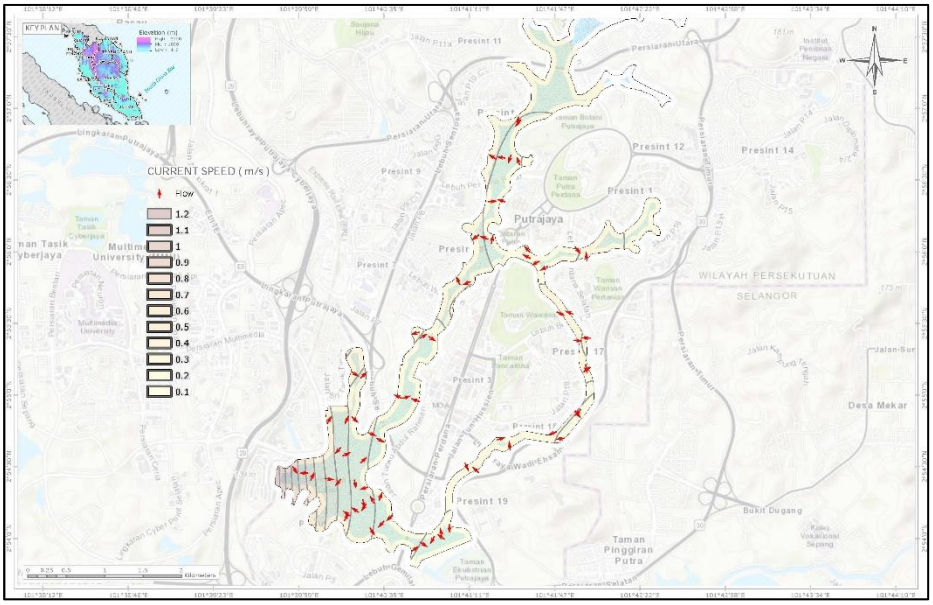

Figure 2 Overall current direction and magnitude in Putrajaya Lake during dry weather condition

The average current flow for the wet season is 0.43 m/s, which is two times faster than the current flow speed during the dry season. In fact, 93% of the POIs experienced a range of flow speed between 0.3 m/s to 0.4 m/s. Selected water quality parameters in the lake were simulated for various weather condition and presented.

Acknowledgements: The authors would like to thank Global Water Consultant Sdn Bhd for providing the data for the analysis.

References

Sharip, Z., Saman, J.M., Noordin, N., Majizat, A., Suratman, S. and Shaaban, A.J. (2016). Assessing the spatial water quality dynamics in Putrajaya Lake: a modelling approach. *Modeling Earth Systems and Environment*, 2(1), p.46.

6th International Conference and Postgraduate Colloquium for Environmental Research 2022 (POCER 2022) 9 - 11 June 2022
Langkawi, Kedah, Malaysia

PCR21042022 – 171: Multiple Solutions For Consideration? A P-graph Model For Heat Integrated Hydrogen Regeneration Networks Generation

Abdulqader Bin Sahl[a], How Bing Shen[a,*], Ákos Orosz[b], Ferenc Friedler[c]

[a]Research Centre for Sustainable Technologies, Faculty of Engineering, Computing and Science, Swinburne University of Technology, Sarawak, Malaysia

[b]Department of Computer Science and Systems Technology, University of Pannonia, 8200, Veszprém, Egyetem u. 10, Hungary

[c]Széchenyi István University, 9026 Győr, Egyetem tér 1, Hungary

*Corresponding Author E-mail: BSHow@swinburne.edu.my

Keywords: Oil Refinery; Hydrogen Network; Heat Integration; Process Optimization

Extended Abstract

Oil refineries utilize a significant amount of energy and hydrogen. They are also regarded as one of the refinery's most essential utilities. Refineries can reduce both energy and hydrogen use by performing simultaneous integration of hydrogen and heat since they coexist in most scenarios. As the hydrogen and heat exchanger network designs are interconnected, the optimization should be conducted concurrently rather than individually (Gaia et al., 2020). A hydrogen network that incorporates heat and simultaneously considers pressure and impurity limitations with a regeneration scheme during optimization is known as a heat integrated hydrogen regeneration network (HIHRN). Currently, there are very few existing works on the design of HIHRN, which are mainly performed using insight-based or mathematical programming techniques. The limitation of these techniques is the generation of a single optimal solution, which may be impractical due to the lack of consideration of certain aspects during optimization such as piping complexity, safety constraints and spatial constraints. Thus, it is imperative to provide decision-makers with several optimal and near-optimal solutions from which they can narrow down their design options based on their unique scenario. The graph-theoretic method, i.e., P-graph, is an alternative tool that can solve process network synthesis (PNS) problems by generating multiple optimal and near-optimal solutions (Friedler et al., 2019).

The research methodology framework used in this work is depicted in Figure 1. The first step refers to the data collection required for the network synthesis (i.e., the flowrate, temperature, pressure, and impurity of all hydrogen sources and sinks). In Step 2, a hydrogen regeneration network (HRN) superstructure model is constructed in P-graph. This model is capable of generating multiple optimal and near-optimal solution structures. Then, a heat cascade is implemented to transform the HRN model into a HIHRN model. It is worth noting that the introduction of heat cascade into P-graph was first introduced by Chin et al. (2019) to solve a heat integrated water regeneration problem. Such concept has been implemented for a HIHRN problem in this work. Figure 2 represents an illustrative model that incorporates heat cascade in a two source-sink hydrogen network problem. The overall external heating utility is denoted as Q_H, while the overall external cooling utility is denoted as Q_C. The temperature intervals in the heat cascade are represented by k, where the energy balance takes place for its respective temperature difference (i.e., ΔT). The last step (i.e., Step 4) includes generating the feasible HIHRN solution structures, i.e., the optimal and near-optimal structures.

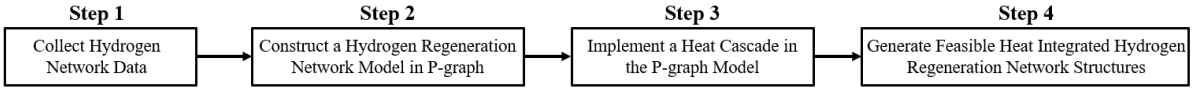

Figure 1: Research Methodology Framework

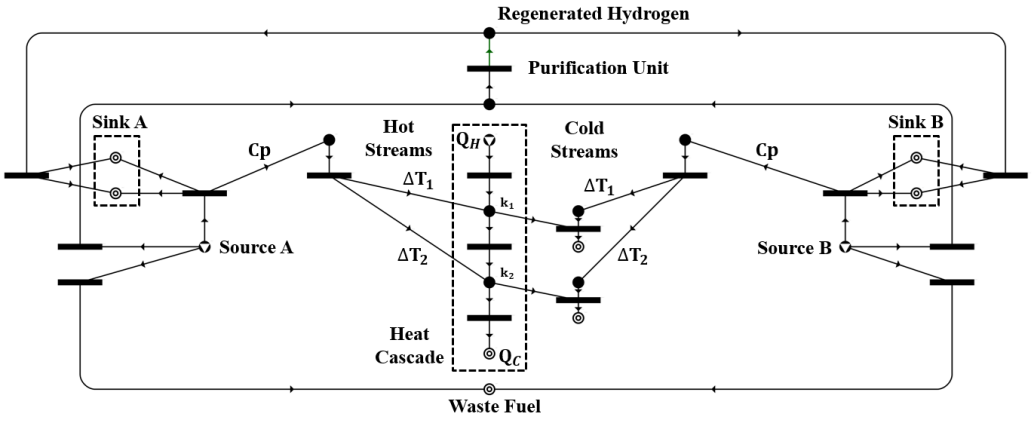

Figure 2: Two Source-Sink HIHRN Problem in P-graph

The case study adopted in this work is an oil refinery hydrogen network introduced by Hallale and Liu (2001). It consists of seven hydrogen sources, including a pressure swing absorption (PSA) unit and six hydrogen sinks. The developed HIHRN P-graph model generated more than 10,000 feasible solution structures, where a summary of the top 5 solutions is presented in **Table 1**. The total cost of production (TCOP), the fresh hydrogen consumption (F_{H_2}), and the overall required external utility (ΔQ) are

provided for each solution structure. It is worth noting that the required external utility for this problem consists of only hot utility. From Table 1, it can be observed that the optimal solution (i.e., solution 1) and near-optimal solutions (i.e., solutions 2-5) offer similar performances in terms of TCOP, F_{H_2}, and ΔQ. For instance, the percentage increase in TCOP, F_{H_2}, and ΔQ between the optimal solution and solution 5 is only 0.43%, 0.83%, and 2.62%, respectively. Therefore, the identification of these solutions are vital for decision-makers to make further analysis with considerations of other factors such as pipeline, safety, and spatial constraints.

Solution Rank	TCOP (M$/year)	F_{H_2} (MMscfd)	ΔQ (kW)
1	32.861	36.054	1122.540
2	32.870	36.060	1123.160
3	32.870	36.060	1124.770
4	33.002	36.355	1152.620
5	33.003	36.356	1152.800

Table 1: Top 5 HIHRN Structures Summary

The current work only identifies a set of feasible HIHRNs without putting much attention on the multi-solution generation for heat exchanger network (HEN) synthesis. Therefore, the authors are currently developing a systematic methodology to close this gap.

Acknowledgements: The authors thank would like to acknowledge the financial support by Ministry of Higher Educationunder Fundamental Research Grant Scheme [grant number:FRGS/1/2020/TK0/SWIN/03/3].

References

Chin, H. H., Foo, D. C. and Lam, H. L., 2019. Simultaneous water and energy integration with isothermal and non-isothermal mixing – A p-graph approach. *Resources, Conservation and Recycling.* 149, 687-713.

Friedler, F., Aviso, K. B., Bertok, B., Foo, D. C. Y. and Tan, R. R., 2019. Prospects and challenges for chemical process synthesis with P-graph. *Current Opinion in Chemical Engineering*. 26**,** 58-64.

Gaia, L., Varbanova, P. S., Klemeša, J. J. and Sunb, L., 2020. Hierarchical targeting of hydrogen network system and heat integration in a refinery. *Chemical Engineering Transactions*. 81, 217-222.

Hallale, N. and Liu, F., 2001. Refinery hydrogen management for clean fuels production. *Advances in Environmental Research*. 6, 81-98.

6th International Conference and
Postgraduate Colloquium for
Environmental Research 2022 (POCER
2022) 9 - 11 June 2022
Langkawi, Kedah, Malaysia

PCR15042022 – 172: Phase Equilibrium Measurements of Acetonitrile and Benzene with EMIM-based Ionic Liquid

Wee Jia Jun[a], Er Zhi En[a], Ong Jin Liang[a], and Ianatul Khoiroh[a*]

[a] Department of Chemical and Environmental Engineering
University of Nottingham Malaysia, Selangor, Malaysia

Corrensponsing Author E-mail: Ianatul.Khoiroh@nottingham.edu.my

Abstract

The performance of 1-ethyl-3-methylimidazolium trifluoromethanesulfonate ([EMIM][TF]) was evaluated for the extraction of acetonitrile from the binary azeotrope composed of acetonitrile and benzene. Relevant ternary phase diagram for the ternary mixture was plotted based on refractive index results, and samples were collected at 298.15K under atmospheric pressure condition. Two activity coefficient models, namely the NRTL and UNIQUAC were selected to correlate the experimental data.

Keywords: Liquid-liquid Equilibrium; Ionic Liquids; Refractive Index; Activity Coefficient.

Extended Abstract

In this work, the capacility of 1-ethyl-3-methylimidazolium trifluoromethanesulfonate ([EMIM][TF]) for the extraction of solvent in the water treatment purpose was investigated by using the cloud point method. The specific type of wastewater targeted is a sample binary azeotrope mixture of acetonitrile and water, which forms an azeotrope at 346.05 K at atmospheric pressure condition (Feng et al., 2007). The refractive index results provide the data on the mass fraction of the component in the ternary mixture. The refractive index (*n*) results, Table 1, provide the data on the mass fraction of the components, with A indicating Acetonitrile, B indicating Benzene and IL indicating the EMIM Triflate. The provided results were in mass fraction. The results appear to be promising; it was observed that good separation has occurred with the addition of the ionic liquids. The good separation that occurred produces good results that can be utilized for further industrial applications.

Table 1. Sample Component Mass Fraction and Refractive Index (*n*)

Sample No.	A Mass Frac	B Mass Frac	IL Mass Frac	*n*

1 Top	0.0424	0.9271	0.0305	1.477
1 Bottom	0.2229	0.3492	0.4279	1.4325
2 Top	0.0859	0.8793	0.0348	1.4705
2 Bottom	0.2339	0.3592	0.4069	1.432
3 Top	0.1230	0.8489	0.0282	1.465
3 Bottom	0.2657	0.3895	0.3449	1.4305

The liquid-liquid equilibrium data of the investigated ternary systems were correlated using the Non-random Two-Liquid equation (NRTL) (Renon et al., 1969) and the Universal Quasi-Chemical (UNIQUAC) (Maurer et al., 1978), respectively. The NRTL described by the following equation:

$$ln\,\gamma_i = \frac{\sum_{j=1}^{m} x_j \tau_{ji} G_{ji}}{\sum_{k=1}^{m} x_k G_{ki}} + \sum_{j=1}^{m} \frac{x_j G_{ij}}{\sum_{k=1}^{m} x_k G_{kj}} \left(\tau_{ij} - \frac{\sum_{j=1}^{m} x_j \tau_{ji} G_{ji}}{\sum_{k=1}^{m} x_k G_{ki}} \right) \quad (1)$$

$$with\ G_{ij} = exp\left(-\alpha_{ij}\tau_{ij}\right)\ and\ \tau_{ij} = \frac{\Delta g_{ij}}{RT} = \frac{g_{ij} - \Delta g_{jj}}{RT}$$

The Δg_{ij} is the energy parameter that represents the characterized interaction between the two components i and j. In this work, the non-randomness parameter of α is taken equal to 0.2 and $\alpha_{ij} = \alpha_{ji} = \alpha$. Similartly, the The UNIQUAC model equation is shown as equation (2):

$$ln\gamma_i = ln\frac{\phi_i}{x_i} + \frac{z}{2} q_i ln\frac{\theta_i}{\phi_i} + l_i - \frac{\phi_i}{x_i}\sum_{j=1}^{m} x_j l_j - q_i \ln\left(\theta_j \tau_{ji}\right) + q_i - q_i \sum_{j=1}^{m} \frac{\theta_j \tau_{ji}}{\sum_{k-1}^{m} \theta_k \tau_{kj}} \quad (2)$$

$$\text{with } \phi_i = \frac{r_i x_i}{\sum_{j=1}^{m} r_i x_i}, \theta_i = \frac{q_i x_i}{\sum_{j=1}^{m} q_j x_j}, l_j = \frac{z}{2}\left(r_j - q_j\right) - \left(r_j - 1\right) \text{ and } \tau_{ji} = \exp\left(\frac{-\Delta u_{ij}}{RT}\right)$$

The lattice coordination number z is equal to 10, and the molecular surface, q_i, and the molecular van der Waals volumes, r_i of the pure component i were calculated as the sum of the group volume and group area parameters.

The experimental data together with the correlated values is displayed in Figure 1.

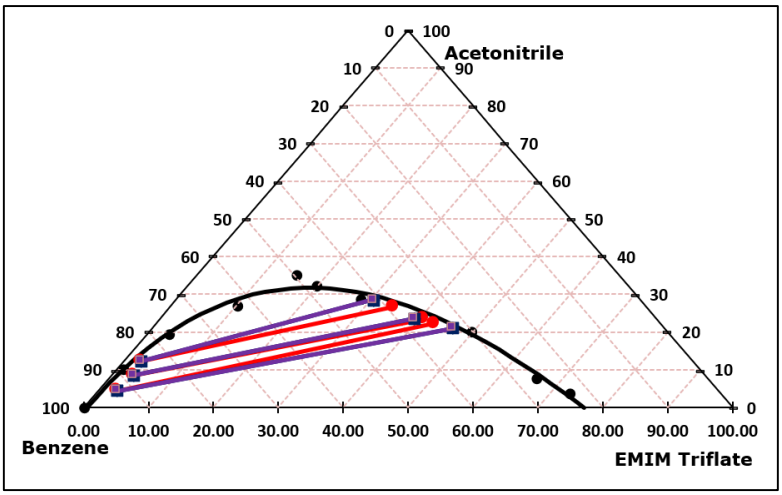

Figure 35. The NRTL and UNIQUAC correlation for ternary diagram of EMIM TF, Blue=NRTL correlation, Purple=UNIQUAC correlation, Red=Experimental Results.

From the obtained data points in red (experimental), blue (NRTL), purple (UNIQUAC), several conclusions can be made. Firstly, multiple data points were close to each other, providing indication that the data obtained by experimental procedure matches the NRTL and UNIQUAC correlation data, providing good confidence that the data possess strong reliability, and has potential to be recreated easily when followed accordingly. Next, the data points obtained provides substantial data points for future work, which further investigation on the chemical properties of the ionic liquid as well as the binary mixture azeotrope can be carried out to provide insight for industrial applications.

Acknowledgements: The authors gratefully acknowledge the financial support from the Ministry of Higher Education Malaysia under Fundamental Research Grant Scheme (FRGS) through Grant No. FRGS/1/2019/STG07/UNIM/02/3.

References

Feng, Peng, Qiu, Jiang, Tao and Lai. 2007. Synthesis of Novel Greener Functionalized Ionic Liquids Containing Appended Hydroxyl. *Synthetic Communications*. 37(16): 2671–2675.

Maurer and Prausnitz. 1978. On the Derivation and Extension of the UNIQUAC Equation. *Fluid Phase Equilibria*. 2(2): 91–99.

Renon and Prausnitz. 1969. Estimation of Parameters for the NRTL Equation for Excess Gibbs Energies of Strongly Nonideal Liquid Mixtures. *Industrial and Engineering Chemistry Process Design and Development*. 8(3): 413–419.

6th International Conference and
Postgraduate Colloquium for
Environmental Research 2022 (POCER
2022) 9 - 11 June 2022
Langkawi, Kedah, Malaysia

PCR15042022 – 173: Optimising Cost in Production of Green and Clean Hydrogen Systems

Yong Ying Loh[a], Denny K S Ng[a], Lik Yin Ng[b] and Viknesh Andiappan[a,c*]

[a] School of Engineering and Physical Sciences, Heriot-Watt University Malaysia, 62200, Putrajaya, Wilayah Persekutuan Putrajaya, Malaysia

[b] Department of Chemical & Petroleum Engineering, Faculty of Engineering, Technology and Built Environment, UCSI University (Kuala Lumpur Campus), UCSI Heights, 1, Jalan Puncak Menara Gading, Taman Connaught, 56000 Cheras, Kuala Lumpur, Malaysia.

[c] Faculty of Engineering, Computing and Science, Swinburne University of Technology, Jalan Simpang Tiga, 93350, Kuching, Sarawak, Malaysia.

- Corrensponsing Author E-mail: vamr6103@gmail.com

Keywords: Green hydrogen, Turquoise hydrogen, Renewable energies, Palm biomass, Mathematical model, Optimisation.

Extended Abstract

Energy demand in Malaysia is typically supplied from fossil fuels, leading to greenhouse gas emissions. Therefore, a new form of cleaner energy needs to be used. Hydrogen (H_2) is considered a potential resource suitable for replacing fossil fuels as the primary energy source. This is because H_2 reacts with oxygen to form water (H_2O) as the only product without producing carbon emissions. However, the implementation of a clean H_2 production process is not straightforward. Such a process suffers hurdles in the production and storage of H_2. This includes high storing costs for H_2 before being transported to the end-users, high energy consumption requirements and low H_2 production efficiency. Hence, this research presents a mathematical optimisation model to optimise clean H_2 production based on costing and energy consumption. In the optimisation model, aspects such as total annualised cost, yield and efficiency of each technology, and energy consumption of H_2 production and storage technologies, were considered. The model also screens and optimises clean H_2 technologies such as renewable energies, electrolysers, methane pyrolysis and biomass fermentation. The developed optimisation model is demonstrated using a case study with several scenarios, such as an economically feasible and clean H_2 process and optimal H_2 production and storage technologies in terms of energy consumption.

Acknowledgements: The financial support from HWUM through the EmPOWER Research Grant Scheme (Project Code: EPS/EmRGS/2021/02) is gratefully acknowledged.

6th International Conference and Postgraduate Colloquium for Environmental Research 2022 (POCER 2022) 9 - 11 June 2022
Langkawi, Kedah, Malaysia

PCR15042022 – 174: Bioelectrochemical auxiliary reactor improving the performance of horizontal anaerobic digesters

Zhengkai An[a,b], Young-Chae Song[a,b*], Keugtae Kim[c], Chae-Young Lee[c]

[a]Major of Environ. Eng., Korea Maritime and Ocean University, Busan 49112, Korea
[b]Interdisciplinary Major of Ocean Renewable Energy Engineering, Busan 49112, Korea
[c]Division of Civil, Environmental and Energy Engineering, The University of Suwon, Gyeonggi 18323, Korea

Corresponding Author E-mail: soyc@kmou.ac.kr

Keywords: Horizontal anaerobic digester; Methane production; Organic matter removal; Bioelectrochemical auxiliary reactor; Electroactive microorganisms; Direct interspecies electron transfer.

Extended Abstract

A bioelectrochemical auxiliary reactor that supplies electroactive microorganisms was studied to improve the performance of anaerobic digesters. Anaerobic reactors exposed to an electric field enrich the bulk solution with electroactive microorganisms that significantly improve methane production via direct interspecies electron transfer (DIET), called electromethanogenesis[Feng and Song, 2018]. However, applying the electromethanogenesis concept to a full-scale anaerobic reactor still has several economic and technical challenges, including the capital cost for electrode installation and maintenance, mixing the digesting slurry, and cleaning the digester. A horizontal anaerobic digester (HAD, 50L) has been operating for more than 1.5 years using a thermally hydrolyzed sludge and pulverized food waste mixture as the feed substrate. An upflow anaerobic bioelectrochemical reactor (UABE, 5L) as a bioelectrochemical auxiliary reactor was combined in the HAD. The anaerobic digestion slurry was discharged from the rear end of the HAD and pumped to the UABE. The anaerobic slurry passed through the UABE was recirculated to the HAD again. During the operation of the combined anaerobic digestion system, the enrichment of electroactive microorganisms in the UABE and the improved performance in the HAD, depending on the recirculation rate and electric field strength, were investigated. Based on the oxidation and reduction peaks of the cyclic voltammogram, the methane production and the yield, both the hydraulic retention time (HRT) and the electric field intensity

significantly affected the enrichment of electroactive microorganisms in the UABE. The appropriate HRT in the UABE was estimated to be 3 days or more, and the electric field intensity was more than 2 V/cm. The performance of HAD, including organic matter removal, methane production, and process stability, was also studied by supplying the electroactive microorganisms from the UABE. Before the assistance of the UABE, the methane production from the HAD was only 483.5 mL/L.d. Interestingly, when the recirculation rate was 1Q between the HAD and UABE, the methane production rate improved to 720.8 mL/L.d in the electric field of 2 V/cm, and it improved further 880.23 mL/L.d in the 3 V/cm.

The PCA and the path analysis demonstrate a causal relationship between the organic matter removal and methane production in the HAD and the UABE, indicating that a small bioelectrochemical reactor can improve the performance of anaerobic digesters with a big capacity. This result provides a hint for the first time that the practical application of electromethanogenesis in full-scale anaerobic digestion is possible.

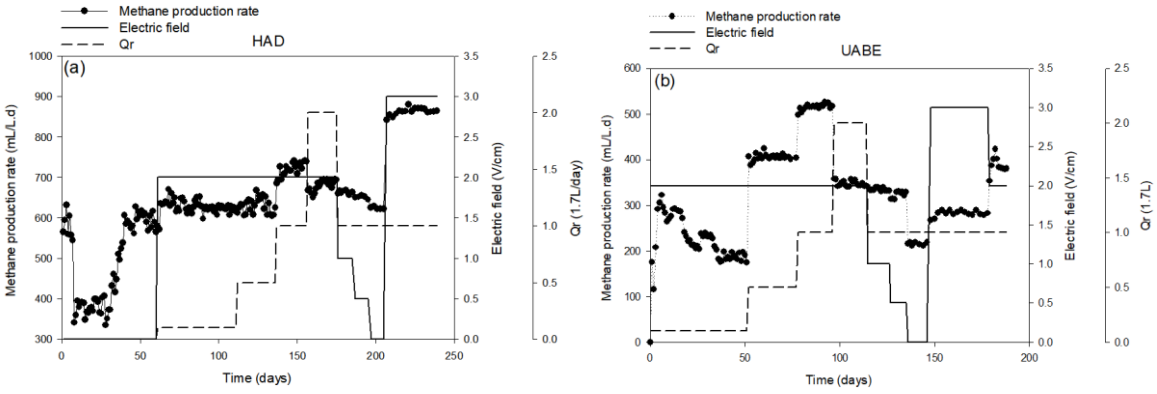

Figure 36: Methane production rate in (a) the HAD, and (b) the BEAD depending on the recirculation rate and the electric field intensity

Table 15: Summary of methane production and organic matter removal in the HAD

EF (V/cm)	Qr (1.7L)	MPR (mL CH_4/L.d)	CH_4 yield (mL/g CODr d)	COD removal (%)	VS removal (%)
0.0	0.0	483.49±13.56	258.42±4.56	52.96±6.92	57.03±7.65
2.0	0.1	623.99±2.95	335.59±11.00	54.14±1.63	57.25±4.37
2.0	0.5	623.48±14.95	316.97±6.95	59.75±3.34	64.53±2.48
2.0	1.0	720.79±16.86	324.31±3.52	69.50±5.28	64.87±2.15
2.0	2.0	680.53±13.77	307.16±4.01	72.17±2.99	72.65±2.80
1.0	1.0	663.13±4.11	293.86±1.08	72.63±3.25	77.25±3.81
0.5	1.0	650.88±3.86	285.22±1.60	73.51±2.33	77.56±1.19
0.0	1.0	624.17±2.85	273.00±2.93	71.29±2.29	71.85±1.52
3.0	1.0	882.30±16.20	339.72±9.66	76.04±1.68	78.07±4.37

Acknowledgements: The authors thank the research funds for the Ministry of Land, Infrastructure and Transport of the Korean government (22UGCP-B157945-03) and the BK21 Four program through the National Research Foundation of Korea (NRF) funded by the Ministry of Education of Korea (Center for Creative Leaders in Maritime Convergence).

References

Feng, Q., Song, Y. C., 2018. Polarized electrode enhances biological direct interspecies electron transfer for methane production in upflow anaerobic bioelectrochemical reactor. *Chemosphere*. 204: 186-192.

6th International Conference and
Postgraduate Colloquium for
Environmental Research 2022 (POCER
2022) 9 - 11 June 2022
Langkawi, Kedah, Malaysia

PCR15042022 – 175: Potential role of catechins in Indonesian seaweed for their anticancer activity against melanoma cell line

Eka Sunarwidhi Prasedya[a], Fahrurrozi[a], Ario Betha Juanssilfero[a]

[a] Bioscience and Biotechnology Research Center
University of Mataram, Mataram, Indonesia

- Corresponding Author: Eka Sunarwidhi Prasedya

Extended Abstract

Seaweeds, also known as macroalgae, are a rich source of polyphenolic compounds such as catechins, flavonols, and phlorotannins. In this study, seaweed from tropical waters of Indonesia was evaluated for their potential anticancer activity. Nine macroalgae species (*Sargassum cristaefolium, Sargassum crassifolium, Sargassum polycystum, Halimeda opuntia, Padina australis, Mastophora rosea, Hormophysa cuneiformis,* and *Galaxaura rugosa*) were collected and extracted in three solvents (ethanol, n-hexane, and ethyl acetate). Based on total phenolic content (TPC), the ethyl acetate extracts provided higher values. Significant high TPC was shown by *Mastophora rosea* ethyl acetate extract (225.40 ± 15.47 mg/g GAE) and *T. murayana* (368.81 ± 13.14 mg/g GAE). The TPC contents strongly correlates to the antioxidant activity of the macroalgae extracts. Four cancer cell lines (B16-F10, HeLa, T24, and HT-29) and normal cell line fibroblast was used for cytotoxicity activity screening of the macroalgae extracts. The ethyl acetate extract of *P.australis, M.rosea,* and *T.murayana* show strong cytotoxic activity against B16-F10 melanoma cell line with IC_{50} values < 100 μg/mL. These selected extracts also induced apoptotic features such as nuclear condensation shown by Hoechst33342 staining and increased caspase-3 expression. GCMS analyses revealed major cytotoxic compounds in these extracts such as Agmatine, Isopropyl myristate, and succinic acid. However, HPLC analyses revealed sufficient concentrations of Protocatechuic Acid and EGC in *M.rosea* and *P.australis* which potentially contributes to their strong cytotoxic activity. Current results suggest that these two extracts are potential source of novel therapeutic agent for topical treatment of melanoma.

6th International Conference and
Postgraduate Colloquium for
Environmental Research 2022 (POCER
2022) 9 - 11 June 2022
Langkawi, Kedah, Malaysia

PCR15042022 – 176: Environmental and economic analysis of renewable heating and cooling sources in Chongqing

Lulin Luo[a, b], Jinhua Chen[a, b*], Ruoen Xu[a, b], Longyue Du[a, b], Yang Pan[a, b], Yuchen Wang[a, b], and Lidi Lu[a, b]

[a] Joint International Research Laboratory of Green Buildings and Built Environments (Ministry of Education) Chongqing University, Chongqing, China

[b] National Centre for International Research of Low-carbon and Green Buildings (Ministry of Science and Technology) Chongqing University, Chongqing, China

- Corresponding Author E-mail: c66578899@126.com

Keywords: Environmental impact; Comprehensive economic cost; Renewable heating and cooling sources; LCA; LCC.

Extended Abstract

Renewable heating and cooling sources are regarded as appealing technologies to alleviate the energy crisis and environmental pollution in building sector. This study aims to quantitatively assess environmental and economic performance of renewable heating and cooling sources such as Air source heat pump (ASHP) system, Ground Source Heat Pump (GSHP), Water Source Heat Pump (WSHP) and Combined Cooling Heating and Power (CCHP) systems through a life cycle assessment coupled with life cycle costing method. Results show that impact categories of global warming and fossil depletion have significant influence on the overall environment in ASHP, GSHP, WSHP and CCHP. In a commercial building, WSHP and GSHP had the least comprehensive environmental impact index, and CCHP had the lowest economic cost. When considering the economic effects of environmental emissions, WSHP is the best choice, comprehensive economic cost of which is \$7.2/m^2.about 16% lower than the GSHP system, 35% lower than the ASHP system and 47% lower than the CCHP system. In addition, variable transmission distances and energy prices have significant impacts on the results. Recommendations on selection of renewable heating and cooling sources based on actual status quo in Chongqing could be useful for decision-makers and designers.

6th International Conference and
Postgraduate Colloquium for
Environmental Research 2022 (POCER
2022) 9 - 11 June 2022
Langkawi, Kedah, Malaysia

PCR15042022 – 177: Nuclear Trigeneration System: A Promising Sustainable Technology for Generating Simultaneous Power, Heating and Cooling Energy

Khairulnadzmi Jamaluddin[a*], Khaidzir Hamzah[a], Jasman Zainal[a], Mohsin Mohd Sies[a], Mohammad Fadil Abdul Wahab[a], Nor Afifah Basri[a], Nur Syazwani Mohd Ali[a], Muhammad Syahir Sarkawi[a], and Muhammad Arif Sazali[a]

[a] School of Chemical and Energy Engineering, Faculty of Engineering
Universiti Teknologi Malaysia, 81310 UTM Johor Bahru, Malaysia

- Corresponding Author E-mail: khairulnadzmi@utm.my

Keywords: Cogeneration system; Trigeneration System; Nuclear Reactor; desalination; district heating; process heat industry.

Extended Abstract

Energy supply is one of the prominent demands in the world nowadays. Rising energy demands enhance the increase of carbon emissions since the use of fossil fuels as a power generation is rising. Several countries are shifting the use of nuclear energy as power generation as sustainable energy sources. The nuclear reactor, however, is operating at a thermal efficiency of 30 to 40% and the rest is dissipated to the environment. Enhancement of the thermal efficiency of the nuclear reactor by recovering waste heat can reduce not only the dependency on fossil fuels but also carbon emissions. Cogeneration and trigeneration systems are technologies that can able to improve the thermal efficiency of the nuclear reactor by recovering the waste heat into useful applications such as district heating and desalination. The development studies of the nuclear cogeneration system are progressive but on the other hand, the trigeneration system in a nuclear reactor is still lagging behind. This paper reviews the various aspects of the cogeneration nuclear system, including applications on district heating, desalination and industrial process heat as well as opportunities for the implementation of the trigeneration system in the nuclear reactor. The implementation of the trigeneration system into the nuclear reactor can help not only for energy providers to increase the economics of the plant but also to provide the minimum cost for the community and industries as waste heat is reused for other applications.

A nuclear reactor has progressively developed around the world as fossil fuels are depleting and carbon emissions are increasing. As stated by International Energy Agency (2021), the total final consumptions of buildings, industry and transportation are growing on average by 1% per year and are expected to increase consistently until 2050. This has brought about the rise of carbon emissions. Hence, nuclear power reactors are demanding in the world as 454 nuclear reactors are operating which contributes more than 10% of the world's electricity and currently, 54 nuclear reactors are under construction in the world (Ho et al., 2019). The usage of nuclear reactors can reduce the dependency on fossil fuels and carbon emissions. The development of nuclear reactors allows energy providers to improve thermal efficiency. The thermal efficiency of the conventional nuclear reactors has only reached the maximum of 35% and the other thermal energy is dissipated to the environment (Khamis et al., 2013). Low thermal efficiency means most of the energy is lost that is vented as heat. Improving efficiency can translate into the reduction of emissions of all pollutants, reducing operating costs and improving energy usage. Cogeneration is one of the systems that has been proven for many decades to improve thermal efficiency by up to 80% (Lipka and Rajewski, 2020). The cogeneration system operates when the waste heat that is discarded from the conventional nuclear reactor is reused and converted for other useful applications such as desalination, district heating or cooling. However, the development of the trigeneration system in the nuclear reactor is lagging behind. This paper discusses on development of nuclear cogeneration systems in the world as well as the opportunity for the trigeneration mode to be implemented in nuclear reactors. Integration of a trigeneration system in the nuclear reactors gives benefits to the energy providers to improve the performance of the nuclear reactor by maximizing usage of the energy generation. Wu and Wang (2006) stated that implementation of the trigeneration system in the conventional power plant can improve the thermal efficiency by up to 90%, higher than cogeneration system. This can be translated into much lower operating costs and waste energy as compared with the cogeneration system.

A cogeneration system has been developed for many decades as a proven and reliable technology to provide various economic, technical and environmental advantages as compared with the heat and power separate productions. Currently, the total distributed heat and power from the nuclear cogeneration system in the world is around 5,000 MW (thermal) (International Atomic Energy Agency, 2020) and today, the applications of the nuclear cogeneration system have been widely used and operated in 13 countries for desalination, district heating, industrial process heat and non-electric applications (International Atomic Energy Agency, 2017). A further explanation of the applications on district heating, desalination and industrial process heat of the nuclear cogeneration systems is discussed in the full paper.

A trigeneration system is a technology that can able to generate electricity, heating and cooling from a single fuel, advancement from a cogeneration system through the addition of absorption chiller. As stated by (Jradi and Riffat, 2014), the implementation of the trigeneration system in a conventional power plant can improve the thermal efficiency by up to 90%, higher than the cogeneration system. The trigeneration system has been implemented in various kinds of power reactors in various industries. However, the development of the nuclear trigeneration system has been lagging behind. The studies that have been focused on trigeneration mode in the nuclear reactor are very limited. Implementing the trigeneration system into the nuclear reactor can help not only for energy providers to increase the economics of the plant but also to provide the minimum cost for the community and industries as waste heat is reused for other applications.

Nuclear reactors are producing carbon-free electricity and also a large amount of heat for district heating and cooling. The development of the nuclear cogeneration system has been extensively utilized and demonstrated in several countries. The nuclear cogeneration system is experienced the most as non-electric applications such as district heating, desalination and process heat for industry. A trigeneration system is an opportunity for the nuclear reactor to improve the thermal efficiency by up to 90%, higher than the cogeneration system. However, the study of the nuclear trigeneration mode is still lagging behind. Up to this date, studies have been done that focus on trigeneration mode in the nuclear reactor are very limited. The implementation of the trigeneration system into the nuclear reactor can help not only for energy providers to increase the economics of the plant but also to provide the minimum cost for the community and industries as waste heat is reused for other applications.

Acknowledgements: This research was funded by the Universiti Teknologi Malaysia under UTM Encouragement Research titled ‘Evaluation of Axial Distribution at the Hot Rod of the RTP Core using ANFIS Technique’ with vote number Q.J130000.3851.19J68.

References

Ho, M., Obbard, E., Burr, P. A., & Yeoh, G. (2019). A review on the development of nuclear power reactors. Energy Procedia, 160, 459-466.

International Atomic Energy Agency (2017). Opportunities for Cogeneration with Nuclear Energy, IAEA Nuclear Energy Series No. NP-T-4.1, IAEA, Vienna.

International Atomic Energy Agency (2020). Guidance on Nuclear Energy Cogeneration. International Atomic Energy Agency: France.

International Energy Agency (IEA). (2021, May). Net Zero by 2050: A roadmap for the global energy sector. Paris, France: IEA.

Jradi, M., & Riffat, S. (2014). Tri-generation systems: Energy policies, prime movers, cooling technologies, configurations and operation strategies. Renewable and Sustainable Energy Reviews, 32, 396-415.

Khamis, I., Koshy, T., & Kavvadias, K. C. (2013, August). Opportunity for cogeneration in nuclear power plants. In The 2013 World Congress on Advances in Nano, Biomechanics, Robotics, and Energy Research, Seoul.

Lipka, M., & Rajewski, A. (2020). Regress in nuclear district heating. The need for rethinking cogeneration. Progress in Nuclear Energy, 130, 103518.

Wu, D., & Wang, R. (2006). Combined cooling, heating and power: A review. progress in energy and combustion science, 32(5-6), 459-495.

6th International Conference and
Postgraduate Colloquium for
Environmental Research 2022 (POCER
2022) 9 - 11 June 2022
Langkawi, Kedah, Malaysia

PCR15042022 – 178: Impact of Biomass Burning Haze on Precipitation in Malaysia

Yixiao Chen[a], Andy Chan[a*], Teo Fang Yenn [a*], Maggie C. G. Ooi[b], Li Li[c], and Ansheng Zhu[c]

[a] Department of Civil Engineering, University of Nottingham Malaysia, Selangor, Malaysia
[b] Institute of Climate Change (IPI), National University of Malaysia (UKM) , Selangor, Malaysia
[c] School of Environmental and Chemical Engineering, Shanghai University, Shanghai 200444, China

- Corrensponsing Author E-mail: evyyc4@nottingham,edu.my; andy.chan@nottingham.edu.my; fangyenn.teo@nottingham.edu.my; chelgee.ooi@gmail.com

Keywords: Biomass Burning Haze; EOF; Percipitation; Malaysia.

Extended Abstract

Introduction

The phenomenon of haze occurs annually in Southeast Asia (SEA) for the past decade has drawn public attention as it has significant impact on the visibility, regional climate, and human health. [Admed et al., 2016]. The scale of the open biomass burning activity can be influenced by both human activity (primary) and climate patterns (secondary) [Latif et al., 2018]. 'Slash and burn' is one of the technologies used in Indonesia to clear land by fire. It is commonly used by small-scale cultivators and large-scale as it is cheap and easy to carry out the practice. Climate pattern is a secondary factor that affects open burning. During June and November in the El Niño year, the drought period is likely to extend and reduce the frequency and intensity of precipitation over the region. Therefore, fire events become harder to control and fire duration is extended under the dry environmental condition.

The annual haze episode that occurs in Malaysia can be referred to as a transboundary biomass haze from Indonesia. Monsoon plays an important role in spreading aerosol particles for a long distance to other regions in SEA [Latif et al., 2018]. The haze episode occurred between August and October 2015 in Malaysia came mainly from Sumatra Island and Kalimantan in Indonesia and was transported by the southwest monsoon. It has been indicated the trace path of aerosols travels from Indonesia to Malaysia for approximately 2 to 3 days. Prevailing wind travels in the path where across through the open field burning region at end of August and brought haze to Malaysia in the following one month in various amplitude. At end of October, airflow changed its direction from southwest to northeast, therefore reduces the aerosol concentration in Malaysia. [Admed et al. 2016]

Aerosol released from biomass burning activity can affect precipitation patterns by radiative effect and changes in the cloud composition [Rosenfeld et al., 2008]. The high concentrated human-made aerosol that suspends in the atmosphere scatters and absorbs more solar radiation in the polluted area [Ramanathan et al., 2001]. Those suspended aerosols absorb energy and heat the atmosphere. The changing temperature in the atmosphere stabilizes the low atmosphere and suppresses the convective could formation, which results in the suppression of precipitation. Aerosol also brings a big influence on precipitation patterns as it can act as cloud condensation nuclei (CCN) [Tao et al., 2007]. In the highly polluted area, precipitation is suppressed at the early stage, but increases in its intensity at the later stage, as longer time required to gather small-sized cloud droplet into larger droplet which is heavy enough to rain down.

It has been conjectured the high concentration of aerosols can affect weather patterns by creating time-lag and more intense rainfall in the future. However, there is no previous study about the specific delay time and affected range of the precipitation or storm by the server haze episode. It is important to have a clear understanding of the relationship between haze episodes and weather patterns for better planning. Therefore, this study is aimed to find the spatial-temporal relationship between haze and precipitation by analyzing the transboundary haze event that happened from 2014 to 2016 in Malaysia.

Methodology

Observational data includes Global Precipiatation Measurement, Aerosol Optical Depth are taken from Giovanni data server for analysis. Empirical orthogonal function (EOF) analysis was use to show a spatial and temporal correlation between particular aerosol and weather phenomena. By maximizing the variance of the data set, the most dominant variation mode from the dataset could be extracted. Each EOF mode represents one physical mode, and they are independent of each other. Python used to carry out the EOF analysis and visualize the metrological data in the form of map plotting.

Result and discussion

The discussion is mainly focused on the result of the first mode of EOF from AOD and precipitation, as they cover the highest percentage of the total dataset. By comparing the spatial distribution of AOD and precipitation, during the haze episode, rainfall intensity at the region with high aerosol concentration (South-East Peninsular, Sarawak) is normally lower, while rainfall occurs more around coastal areas where sir humidity is relatively higher than the mainland. Heavy precipitation has been

observed after approximately 30 days after the haze episode, and mainly concentrated at South-East Peninsular and North-East Sarawak.

After putting more attention on the Malaysia mainland and separates into East Malaysia (Peninsular) and West Malaysia (Sarawak and Sabah). Eigen-coefficient increases largely by removing the obstruction from oceanic data and produce a strong signal from the first EOF mode. In East Malaysia during 2014, high concentrated aerosols suppress the precipitation during Mid-September to Mid-October in South Sarawak. These aerosols continue to travel toward the north in the next 60 days and rain down at North-West Sarawak. 2016 is also shown with 2 months of delay in the rainfall activity. A similar movement path of aerosols has also been found in 2015 (travel from South-East to North-West), with a delay of 30 days. While in West Malaysia, aerosols are shown to arrive at South-West Sarawak during September to October and suppress local precipitation, then travel to North-East Sarawak with heavy rainfall with 60 days, 30 days, and 60 days after the haze episode in 2014, 2015, and 2016 respectively.

Acknowledgements:

I would like to express my deepest appreciation to all those who provided me the possibility to complete this work, especially to my supervisors, Professor Andy Chan and Dr Teo Fang Yenn. In addition, I would like to also thank Ms. Ooi Chel Gee (Maggie), for her patience in guiding, advising and answering my questions along this study. Her knowledge and suggestions helped to lead the direction of this study.

Reference:

1. Admed, M., Guo, X. and Zhao, X. (2016). Determination and analysis of trace metals and surfactant in air particulate matter during biomass burning haze episode in Malaysia, Atmospheric Environment 141, pp.219-229, doi: 10.1016/j.atmosenv.2016.06.066.
2. Latif, M.T., Othman, M., et al. (2018). Impact of regional haze towards air quality in Malaysia: A review, Atmospheric Environment 177, pp.28-44, doi: 10.1016/ j.atmosenv.2018.01.002.
3. Rosenfeld, D., Lohmann, U., Raga, et al., (2014). Flood or Drought: How Do Aerosols Affect Precipitation?, Science 321, 1309 (2008), doi: 10.1126/science.1160606
4. Ramanathan, V., Crutzen, P., Kiehl, J. and Rosenfeld, D. (2001). Atmosphere: Aerosols, climate, and the hydrological cycle, Science 294, pp.2119-2124, doi; 10.1126/science.1064034.
5. Wei-Kuo Tao, Xiaowen Li, Alexander Khain, Toshihisa Matsui, Stephen Lang.(2007). Role of atmospheric aerosol concentration on deep convective precipitation: Cloud-resolving model simulations, Joanne Simpson1Journal of Geophysical Research, VOL. 112, D24S18, doi:10.1029/2007JD008728, 2007

6th International Conference and
Postgraduate Colloquium for
Environmental Research 2022 (POCER
2022) 9 - 11 June 2022
Langkawi, Kedah, Malaysia

PCR16042022 – 179: Improved defluoridation and energy production using dimethyl sulfoxide modified carbon cloth as bioanode in microbial desalination cell

Sabarija A M[a], Praveena Gangadharan [a,b*], Sravan Janardhanan [c] and Abdul Rasheed P [d]

[a] Department of Civil Engineering
Indian Institute of Technology,Palakkad,Kerala,India

[b]Environmental Sciences and Sustainable Engineering Center
Indian Institute of Technology,Palakkad,Kerala,India

[c] Department of Civil Engineering
M.Dasan Institute of Technology,Kozhikode,Kerala,India

[d] Department of Biological Sciences and Engineering
Indian Institute of Technology,Palakkad,Kerala,India

- [*]Corrensponsing Author E-mail: praveenag@iitpkd.ac.in
Tel.: - 91-49-23226473 (O). Fax: - 91-49-23226301

Keywords: Microbial desalination cell; defluoridation; dimethyl sulfoxide; wastewater treatment; energy production.

Extended Abstract

Fluorides are introduced into the environment either naturally by fluoride bearing host rocks and volcanic ash, or by effluents from various industries like semiconductors, aluminium, etc. Drinking water with fluoride levels upto 1.5 mg/L is beneficial as it prevents dental decay, but concentrations > 1.5 mg/L cause dental and skeletal fluorosis. The existing efficient defluoridation techniques are energy-intensive, require chemical addition, and generate large amounts of sludge, which require further treatment prior to disposal. Recently, microbial desalination cells (MDCs) have been developed for desalination without the application of external energy. MDCs are proven technology for desalination coupled with energy production, however, its application in deflouridation has not been explored very much. In addition, the practical applicability of MDC is limited due to low energy output and costly electrode materials. Hence, in the present study: (i) MDC was applied to remove fluoride from groundwater using plain carbon cloth (CC) as an anode; and (ii) the performance of MDC for power production and deflouridation efficiency was improved by using dimethyl sulfoxide (DMSO) coated carbon cloth (CC_{DMSO}). The DMSO improves the hydrophilicity of plain carbon cloth (CC) by delivering an O atom to the surface of CC. Incorporation of O atoms onto the electrode surface increases the wettability in polar solvents and improves the effective surface area. The coating also enhances the interaction between the electrode and anolyte, thereby intensifying the electrochemical activity. Raman spectroscopic analysis revealed that the I_D/I_G ratio increased from 0.94 for CC to 1.106 for CC_{DMSO}, indicating the introduction of O functional groups onto the CC

surface. The electrochemical performance of CC_{DMSO} was investigated by cyclic voltammetry (CV) and electrochemical impedance spectroscopy (EIS). In CV analysis, CC_{DMSO} exhibited an increased current density–voltage response (1.45 mA) than CC(0.75 mA). Similarly, in EIS, the charge transfer resistance (R_{ct}) from the nyquist curve of CC_{DMSO} was found to be less (23 Ω) than CC (175 Ω). Additionally, when CC_{DMSO} was applied as an anode in MDC, the permissible level of 1.5 mg/L of F^- was achieved within 17 hrs, 48 hrs, and 96 hrs for 3 mg/L, 10 mg/L, and 20 mg/L, respectively, while the CC anode took 24 hrs, 72 hrs, and 120 hrs, respectively. Moreover, the maximum power density obtained using the CC_{DMSO} electrode was found to be 2- 2.28 times higher than that of the CC electrode in MDC. Furthermore, the anode chamber of MDC exhibited a maximum of 50% substrate degradation. The study showed that modifying CC with DMSO opens up new avenues for developing novel electrode materials for bioelectrochemical systems.

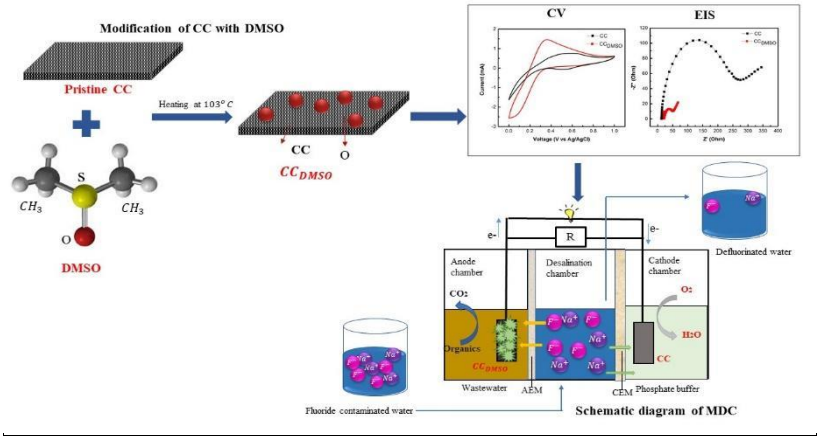

Figure 1: Graphical abstract

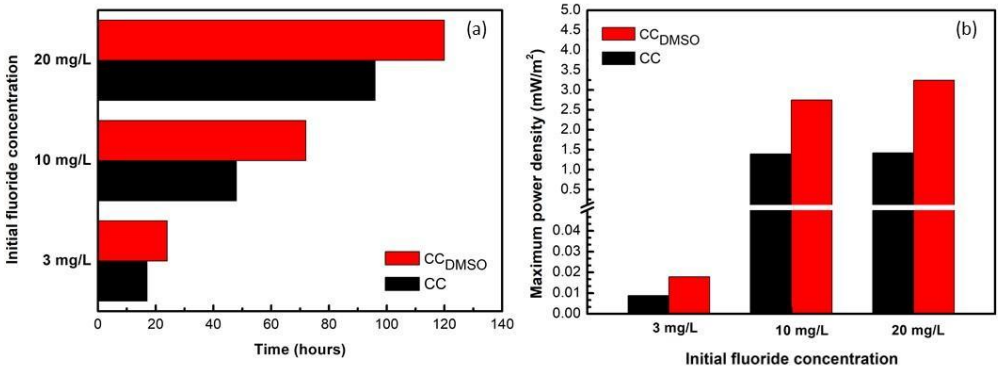

Figure 2: (a) Time taken to achieve permissible limit of 1.5 mg/L , (b) Maximum power densities obtained when CC and CC_{DMSO} was used as anode in MDC.

Acknowledgements: The authors gratefully acknowledge the financial support of the Science and Engineering Research Board (SERB) [No.EEQ/2018/000524 and ECR/2018/000601], Department of Science and Technology, Government of India in carrying out this research work.

References

Brastad, K. S. and He, Z. (2013) Water softening using microbial desalination cell technology. Desalination, 309, 32–37. [online] http://dx.doi.org/10.1016/j.desal.2012.09.015.

Cecconet, D., Sabba, F., Devecseri, M., Callegari, A., and Capodaglio, A. G. (2020) In situ groundwater remediation with bioelectrochemical systems: A critical review and future perspectives. Environment International, 137(February), 105550. [online] https://doi.org/10.1016/j.envint.2020.105550.

Hemalatha, M., Butti, S. K., Velvizhi, G., and Venkata Mohan, S. (2017) Microbial mediated desalination for ground water softening with simultaneous power generation. Bioresource Technology, 242, 28–35. [online] http://dx.doi.org/10.1016/j.biortech.2017.05.020.

Song, J. H. and Sailor, M. J. (1998) Dimethyl Sulfoxide as a Mild Oxidizing Agent for Porous Silicon and Its Effect on Photoluminescence. Inorganic Chemistry, 37(13), 3355–3360.

Xing, C., Jiang, D., Tong, L., Ma, K., Xu, Y., Xie, K., and Wang, Y. (2021) MXene@Poly(diallyldimethylammonium chloride) Decorated Carbon Cloth for Highly Electrochemically Active Biofilms in Microbial Fuel Cells. ChemElectroChem, 8(13), 2583–2589.

PCR04052022 – 180: Thermodynamic solubility modelling evaluation for the supercritical carbon dioxide extraction of palmitic and oleic acid from papaya seed oil

Rekha Ramamoorthy[a] , Yee Ho Chai[a,b*] ,Suzana Yusup[c] , and Muhammad Syafiq Hazwan Rusland[a]

a Department of Chemical Engineering, Universiti Teknologi PETRONAS, Seri Iskandar, 32610, Perak, Malaysia

b HICoE-Centre for Biofuel and Biochemical Research, Institute of Self-Sustainable Building, Universiti Teknologi PETRONAS, Seri Iskandar, 32610, Perak, Malaysia

c Biomass & Plasma Technologies, Renewable Energy & Green Technology, TNB Research Sdn. Bhd., Selangor, Malaysia d School of Chemical Engineering, College of Engineering, Universiti Teknologi MARA Shah Alam, 40450, Shah Alam, Selangor, Malaysia

• Corrensponsing Author E-mail: yeeho.chai@utp.edu.my

Keywords: Supercritical Fluid Extraction; Bio-oil Extraction; Papaya Seed Oil; Thermodynamic Solubility Modelling; Peng-Robinson; Soave-Redlich-Kwong

Extended Abstract

Supercritical fluid extraction (SFE) is a green and clean (GLEAN) extractive technique that solvates and extract phytochemical components from plant cell matrices through bulk supercritical solvent. SFE is favourable due to its unique extractive process that can operate at the absence of oxygen, contrary to conventional extraction techniques such as maceration and Soxhlet extraction, to avoid oxidation process that could potentially degrade antioxidants in the extraction process [Abbas et al., 2008].

Papaya fruit is one of the preferred fruits in the tropical region with Asia leading in the productions of papaya with 52% production globally [Ikram et al., 2015]. Papaya seed oil is reddish yellow in colour and is composed of various sources such as protein (27.3% - 28.3%), lipids (28.2% - 30.7%) and crude fibres (19.1% - 22.6%) [Malacrida et al., 2011]. In fact, the two major fatty acid composition extracted consists mainly of oleic acid and palmitic acid [Barroso et al., 2016]. Therefore, both unsaturated fatty acids was taken as a basis for the thermodynamic solubility modelling prediction of papaya seed oil solubility in supercritical carbon dioxide.

Thermodynamic modelling is often employed to predict known pure components' solubility in mixture fluids. Therefore, the only limitations of such models are restricted to the accuracy of the available thermophysical properties of solutes as these organic compounds tend to degrade at higher temperature [Martinez-Correa et al., 2010]. The determination of critical properties of organic compounds are often estimated by group contribution methods such as Joback-Reid method that utilizes functional groups from

organic compound to calculate its thermophysical properties as a function of the sum of group parameters [Joback and Reid, 1987]. The determination of $\varphi 2\ SCF$ can be derived from the equation of state coupled with classical mixing rules. In this study, two equation of states are focused: namely PengRobinson (PR) and Soave-Redlich-Kwong (SRK):

$$p = \frac{\mathrm{RT}}{v - b_m} - \frac{a_m}{v^2 + 2b_m v - b_m^2} \quad (1)$$

$$Z^3 - (1 - B)Z^2 + (A - 2B - 3B^2)Z - (AB - B^2 - B^3) = 0 \quad (2)$$

The calculated binary interaction parameters of seed oil – SCO_2 were applied to calculate and compare solubility of Carica papaya seed oil in SCO_2 against experimental solubility data. The binary interaction parameters of oleic acid and palmitic acid into the supercritical solvent system that was calculated by classical mixing rule vDW1 and vDW2 respectively. It can be observed that binary interaction parameters are closely associated with temperature where the parameters generally increase with regards to pressure. These findings are in agreement with the findings by other researchers [Lee et al., 2018].

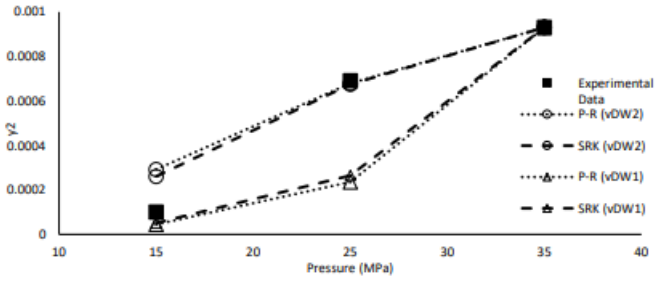

Figure 1: Thermodynamic solubility model fitting of palmitic acid at 353.15K using vDW1 and vDW2 classical mixing rule.

Peng-Robinson and Soave-Redlich-Kwong equation of states coupled with classical van der Waals mixing rules, vDW1 and vDW2, and density-based models were compared against experimental data. Solubility of Carica papaya seed oil were observed to increase with pressure and temperature where extraction of palmitic acid is more favourable compared to oleic acid. From the solubility models proposed, SRK equation of state model provided the best correlation against the experimental data obtained.

Acknowledgements: The authors would like to gratefully acknowledge the conferrment of Higher Institution Centre of Excellence (HICoE) status to Centre of Biofuel and Biochemical Research (CBBR) and the financial support by Universiti Tekologi PETRONAS (STIRF Grant Scheme – 015LA0-023) to carry out experimental work in this project.

6th International Conference and Postgraduate Colloquium for Environmental Research 2022 (POCER 2022) 9 - 11 June 2022
Langkawi, Kedah, Malaysia

PCR16042022 – 181: Mathematical Optimisation of Hydrogen Supply Chain based on Cost

Hui Xuan Oh[a], Denny K S Ng[a], Lik Yin Ng[b] and Viknesh Andiappan[a,c*]

[a] School of Engineering and Physical Sciences, Heriot-Watt University Malaysia, 62200, Putrajaya, Wilayah Persekutuan Putrajaya, Malaysia

[b] Department of Chemical & Petroleum Engineering, Faculty of Engineering, Technology and Built Environment, UCSI University (Kuala Lumpur Campus), UCSI Heights, 1, Jalan Puncak Menara Gading, Taman Connaught, 56000 Cheras, Kuala Lumpur, Malaysia.

[c] Faculty of Engineering, Computing and Science, Swinburne University of Technology, Jalan Simpang Tiga, 93350, Kuching, Sarawak, Malaysia.

- Corrensponsing Author E-mail: vamr6103@gmail.com

Keywords: Hydrogen Supply Chain, Mathematical Model, Optimisation, Decarbonisation, Storage Technologies, Transport, Distribution.

Extended Abstract

Climate change has prompted many policymakers and governments to implement strategies in establishing new solutions concerning clean renewable energy systems. In this context, hydrogen as an energy carrier has been considered an alternative towards the integration of energy sector decarbonisation. However, the access to technology and management of hydrogen (H_2) supply chains are not yet matured for deployment. As such, this study proposes to develop a mathematical decision-making model to identify the minimum cost of establishing the hydrogen supply chain. This is done by using a single objective optimisation model. The model is developed by taking into account the various echelons in the H_2 supply chain such as conditioning, storage, transportation and distribution. To demonstrate the overarching goals of this study, different scenarios were implemented to analyse the techno-economic feasibility of the supply chain. The results show that liquefied H_2 and gaseous H_2 were the most economical form of H_2 from conditioning, stroing and transporting. Lastly, distances and H_2 demand are two deciding factors on the configurations of H_2 supply chain.

Acknowledgements: The financial support from HWUM through the EmPOWER Research Grant Scheme (Project Code: EPS/EmRGS/2021/02) is gratefully acknowledged.

6th International Conference and Postgraduate Colloquium for Environmental Research 2022 (POCER 2022) 9 - 11 June 2022
Langkawi, Kedah, Malaysia

PCR16042022 – 182: Optimal Blue Hydrogen Process with Carbon Capture, Utilisation and Storage

Ti Weiee[a], Denny K S Ng[a], Lik Yin Ng[b] and Viknesh Andiappan[a,c*]

[a] School of Engineering and Physical Sciences, Heriot-Watt University Malaysia, 62200, Putrajaya, Wilayah Persekutuan Putrajaya, Malaysia

[b] Department of Chemical & Petroleum Engineering, Faculty of Engineering, Technology and Built Environment, UCSI University (Kuala Lumpur Campus), UCSI Heights, 1, Jalan Puncak Menara Gading, Taman Connaught, 56000 Cheras, Kuala Lumpur, Malaysia.

[c] Faculty of Engineering, Computing and Science, Swinburne University of Technology, Jalan Simpang Tiga, 93350, Kuching, Sarawak, Malaysia.

- Corrensponsing Author E-mail: vamr6103@gmail.com

Keywords: Blue hydrogen, carbon capture, utilisation and storage, optimisation, mathematical model.

Extended Abstract

Hydrogen (H_2) energy has high potential to become a source of sustainable future fuel to replace fossil fuel. At present, natural gas conversion is the conventional process to produce H_2. However, this process produces carbon dioxide (CO_2) emissions as a by-product. To address this issue, CO_2 capture, utilisation, and storage (CCUS) technologies can be integrated in conventional H_2 plants. By doing so, conventional H_2 plants can be retrofitted to produce cleaner H_2 called blue H_2. This work presents a mathematical model to optimise blue H_2 processes integrated with CCUS technologies. The research objectives are to determine optimal and feasible decarbonisation systems for H_2 production and optimal storage technologies for the produced H_2 with minimum cost. The developed optimisation-based model considers different grey H_2 production paths, CO_2 capture technologies, CO_2 transportation, utilisation, and storage as well as H_2 storage. The model factors aspects such as technology efficiency, costing and overall energy consumption. The developed model is demonstrated with blue H_2 production case study under different scenarios – minimum overall blue H_2 production cost, minimum overall energy consumption, and minimum CO_2 production/emissions. Three optimised blue H_2 process with CCUS are obtained with the optimisation objectives of minimising total annualised production cost and total energy consumptions.

Acknowledgements: The financial support from HWUM through the EmPOWER Research Grant Scheme (Project Code: EPS/EmRGS/2021/02) is gratefully acknowledged.

6th International Conference and
Postgraduate Colloquium for
Environmental Research 2022 (POCER
2022) 9 - 11 June 2022
Langkawi, Kedah, Malaysia

PCR16042022 – 183: Life Cycle Assessment of Organic Citrus Orchard Carbon Footprint: The Case Study of Central Taiwan

Meng-Fen Shih [a] , Xin-Yu Zeng [b] , and Chyi-How Lay [b*]

aCenter of University Social Responsibility, Feng Chia University, Taichung, Taiwan

b Master's Program of Green Energy Science and Technology, Feng Chia University, Taichung, Taiwan

• Corrensponding Author E-mail: chlay@mail.fcu.edu.tw

Keywords: Life Cycle Assessment, Carbon Footprint, Greenhouse Gas, Agriculture, Citrus Orchard

Extended Abstract

Agriculture is the largest human-managed ecosystem in the world, it relies on a large number of external resources, and large-scale monoculture is the primary method of farming. These factors cause it to increase greenhouse gas emissions when operating and most likely reduce the biodiversity of the surrounding area of the region. Organic farming is considered a solution to reducing greenhouse gas (GHG) emissions by avoiding synthetic fertilizers and pesticides in place of traditional farming systems (Viana, L.R. et al., 2022). However, in addition to the use of fertilizers, agricultural systems, whether conventional or organic, are increasingly dependent on other sectors of the economy due to the input of various agricultural practices, extensive mechanization, transportation, subsequent processing, and product distribution (Viana, L.R. et al. al., 2022). These factors also contribute to high GHG emissions from agriculture. The carbon footprint (CFP) measures the direct or indirect GHG emissions of human activities or product production in the whole life cycle. It is also one of the crucial tools for governments and businesses to reduce GHG emissions. Based on the life cycle assessment (LCA) methodology, this study investigated the CFP of organic citrus orchards in Dongshi, the vital place of fruit production in central Taiwan. In order to calculate carbon emissions and analyze emission hotspots, through on-site visits and interviews with local stakeholders, relevant information and complete data on the four steps of raw material extraction, manufacturing and processing, retail and transportation, use, and waste disposal were collected.

In the study, organic citrus orchard cultivation was based on three scenarios as analysis scenarios: (1) normal farming conditions, (2) drought due to climate change in 2021 (reduced yields during drought), and (3) conventional farming using chemical fertilizers for the carbon footprint calculation comparison and analysis. The yields of citrus orchards in Scenario 1, Scenario 2, and Scenario 3 are 6000 kg, 3600 kg, and 6000 kg, respectively. Table 1 shows the raw material extraction input in the citrus orchard farming; Table 2 shows the total CFP emissions for each scenario and the particular emissions for the four stages. Among them, it can see that the part with a significant difference in the emission of the three scenarios is the material input in the growth process. The carbon emission intensity of Scenario 1 in this part was 0.271 kg CO_2e/kg, while that of Scenario 2 was 0.452 kg CO_2e/kg, which was nearly 67% higher than that of Scenario 1. The drought in the assessment year resulted in a shortage of fruit production, making the same raw material extraction input, but getting less output was the reason. Scenario 3 also had nearly 52% higher emissions in this part than scenario 1, which was due to the use of chemical fertilizers during farming. The total emissions section

also presents these effects in Table 2. Therefore, the material input in citrus growing and farming (means raw material extraction) was the part with the most significant emission among the four stages. Figure 1 shows the hotspot analysis at this stage. It can seem that whether it is Scenario 1, 2, or 3, green manure crops were the primary source of emissions, followed by fertilizers, whether organic or chemical. It requires a deep dive into the material used in the fertilizer, the treatment process, and even the emissions that may result from its use. Notably, the fruit bagging was another emissions hotspot, reminding the industry to be more careful when using plastics. It encourages considering alternatives to other materials with the same effect but are also environmentally friendly. Hence, simply changing the farming method to organic is not a guarantee for reducing the contribution of carbon emissions in agriculture. It also needs to consider all possible activities in the agricultural production chain and the choice of materials to use. It also involves the regions of the production chain and the life behaviors of the residents. Only in this way can the factors that affect emissions be found more intuitively, and it can effectively change the impact of the production system on the environment.

Table 1: Raw material extraction input in the cirtus orchard farming

Iten	Unit	Scenario I	Scenario II	Scenario III
Green manure crop	hectare	1.2	1.2	1.2
Transportation for green manure crop	ton-kilometre	0.16	0.16	0.16
Fishing net	kg	5.7	5.7	5.7
Mineral oil	kg	52.4	52.4	52.4
Fruit bagging	kg	150	150	150
Bouillie bordelaise-$CuSO_4$	kg	6	6	6
Bouillie bordelaise-CaO	kg	6	6	6
Lime sulphur solution - Sulphur	g	144	144	144
Lime sulphur solution - Lime	g	288	288	288
Tap water	liter	2,988	2,988	2,988
BD500 horns and cow manure	g	30	30	30
BD501 horns powder	g	3	3	3
Organic fertilizer	kg	7,500	7,500	0
Urea (CN_2H_4O)	kg	0	0	192.5
Calcium superphosphate ($CaP_2H_4O_8$)	kg	0	0	96.5
Potassium chloride (KCl)	kg	0	0	144

Table 2: Carbon footprints of citrus orchard (unit: kg CO_2-e/kg per production)

Process Step	Scenario I	Scenario II	Scenario III
Distribution	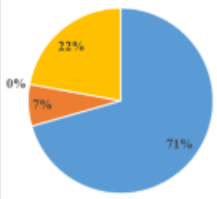	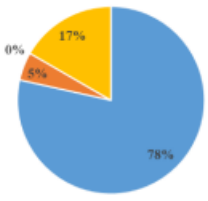	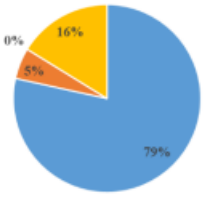
Raw material extraction	0.271	0.452	0.411
Manufacturing and processing	0.028	0.028	0.028
Retail and transportation	0	0	0 kg
Waste disposal	0.085	0.096	0.085
Total	0.376	0.568	0.516

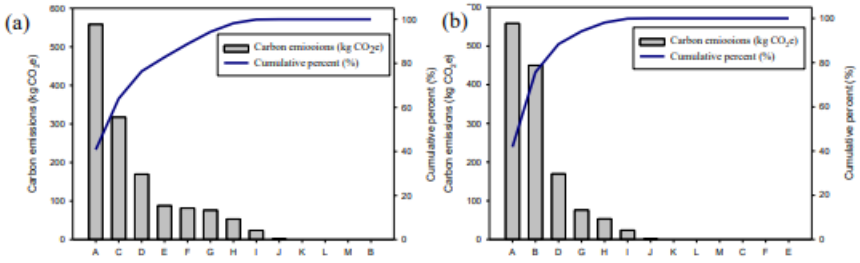

Figure 1: Hotspot analysis for the raw material extraction step in (a) Scenario I, and Scenario II and (b) Scenario III (A: Green manure crop, B: Organic fertilizer, C: Urea, D: Fruit bagging, E: Potassium chloride, F: Calcium superphosphate, G: Mineral oil, H: Fishing net, I: Bouillie bordelaise, J: Lime sulphur solution, K: Transportation for green manure crop, L: BD501 horns and silicon-powder, M: BD500 horns and cow manure)

Acknowledgements: The authors deeply appreciate the financial supports from the Ministry of Science and Technology, Taiwan (MOST 108-2221-E-035-036-MY3 and MOST 109-2221-E-035-028).

References

Viana, L. R., Dessureault, P. L., Marty, C., Loubet, P., Levasseur, A., Boucher, J. F., Paré, M. C. (2002) Would transitioning from conventional to organic oat grains production reduce environmental impacts? A LCA case study in North-East Canada. Journal of Cleaner Production. 349:131344.

6th International Conference and Postgraduate Colloquium for Environmental Research 2022 (POCER 2022) 9 - 11 June 2022
Langkawi, Kedah, Malaysia

PCR16042022 – 184: Effects of coil density in a solenoid magnetic field microbial fuel cell

Chyi-How Lay [a,b,*] , Yi-Chi Deng [a] , Chia-Min Chang [c] and Chao-Chen Hsu [b]

a Master's Program of Green Energy Science and Technology Feng Chia University, Taichung, Taiwan

b General Education Center Feng Chia University, Taichung, Taiwan

c Department of Environmental Engineering and Science Feng Chia University, Taichung, Taiwan

• Corrensponsing Author E-mail: chlay@mail.fcu.edu.tw

Keywords: microbial fuel cell, solenoid magnetic field, bioelectricity, coil density

Extended Abstract

Magnetic field has been applied to enhance simultaneously electricity generation and the pollutant remove efficiency in the bioelectrochemical system recently (Gunda et al., 2021). A long straight coil of wire can be used to generate a nearly uniform magnetic field similar to that of a bar magnet. Such coils, called solenoids, have an enormous number of practical applications. The field can be greatly strengthened by the addition of an iron core. Such cores are typical in electromagnets. The coil density is an important parameter for solenoid magnetic field (SMF).

This study would apply on the cylindrical microbial fuel cells (MFCs) to explore the effects of coil density (0, 8, 16 turns) on MFC performance. This cylindrical dual-chamber MFCs was made from acrylic and separated by a cation exchange membrane (AMI-7000, Membranes International, Ringwood, NJ) into anode with working volumn 750 mL and cathode with working volumn 300 mL. Both andic and cathodic chambers have the carbon cloth electrode (W1S1010, Ce Tech Co., Ltd, Taiwan) with the dimension of 5 cm * 3 cm and reaction surface of 30 cm^2 . An external resistance (R) of 1000 Ω connected the two electrodes by the copper wires. The seeding microorganism of granular sludge was collcected from a fructose manufactory in Central Taiwan. The granular sludge of 200 mL and the sulfate reducing bacteria medium (Lee et al. 2014) 550 mL were mixed into the anodic chamber, then the argon gas was flushed for 5 min to keep the anaerobic environment. The cathodic electrolyte was potassium ferricyanide ($K_3Fe(CN)6$) 50 mM. Both anodic and cathodic electrolytes were added 100 mM phosphate buffer saline (PBS) to maintain the stable pH to 7.5. The cylindrical MFCs were cultivated in a room temperature for 39 days.

The results showed that the peak chemical oxygen demand (COD) removal efficiency of 59.8±4.0% using 16 coil SMF which is higher than the value of 42.1±2.4% without SMF (Table 1). Gunda et al. (2021) also reported that applying the MF of 500 mV could increase the COD removal efficiency from 36.3% to 80.4% compared to the condition without MF. Moreover, the specific growth rate of SRB the in the anode of cylindrical MFC was enhanced from 9.6 mg/L-d without SMF to 10.2 to 10.2 mg/L-d while applying the SMF (Table 1). Table 2 shows the maximum bioelectricty of 521±30.4 mV was obtained while applying the SMF with 16 turns which is much higher than the 158±19.2 mV without SMF and 256±95.9 mV with 8 turns of SMF. Furthermore, the CE increases with the increase of the coil density. The coulombic efficiency (CE) from the MFC used 16 coils is 79.8±6.4%, which is significantly higher than the CE (36.5±10.2%) without current-powered MFC. The internal resistance value was evaluated by the polorization curves in Figure 1

and the peak value was 270 Ω without SMF and closer value of 253 Ω with the 8 turns of SMF. Applying the 16 turns of SMF can significantlt decreased the internal resistance to 193 Ω to enhance the bioelectricity performance of this cylindrical MFC.

Table 1: COD removal and specific growth rate at various coil density

Coil density (Number of turns)	COD removal (%)	Specific Growth Rate (mg/L-d)
0	42.1±2.4	9.6
8	55.7±3.6	10.9
16	59.8±4.0	10.2

Table 2: Electrcity performance at various coil density

Coil density (Number of turns)	Voltage (mV)	Internal resistance (Ω)	Current density (mA/m^2)	Power density (mW/m^2)	Coulombic efficiency (%)
0	158±19.2	270	41±4.9	6±1.6	30.6±1.2
8	256±95.9	253	66±24.9	19±12.2	52.6±3.1
16	521±30.4	193	135±7.8	70±8.1	62.7±2.7

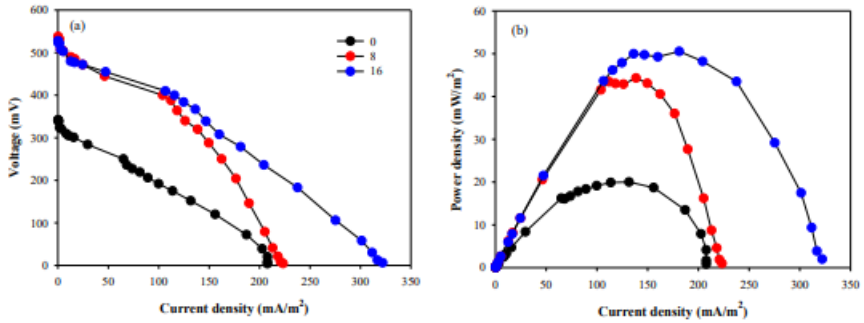

Figure 2: Polarization curves at various coil density

Acknowledgements: The authors gratefully acknowledge the financial support by Taiwan's Ministry of Science and Technology (MOST 108-2221-E-035 -036 -MY3).

References

Gunda, M., Sanath, K., Bharat, L.K., Jeevan, K.R.M., Ibrahim M.A., Riyadh, I.A. (2021). Impact of electric potential and magnetic fields on power generation in microbial fuel cells treating food waste leachate, Journal of Water Process Engineering, 40, 101841.

6th International Conference and
Postgraduate Colloquium for
Environmental Research 2022 (POCER
2022) 9 - 11 June 2022
Langkawi, Kedah, Malaysia

PCR16042022 – 185: The Effect of Non-Thermal Plasma Towards Waste Cooking Oil and Pyrolysis Oil

Danial Hakim Badrul Hisham, Muhammad Athir Mohamed Anuar, Sureiyn Nimellair and Dr. Lim Mook Tzeng

Department of Renewable Energy and Green Technology

TNB Research, Selangor, Malaysia

 Corrensponsing Author E-mail: mook.tzeng@tnb.com.my

Keywords: Waste cooking oil; Pyrolsis oil; Non-thermal plasma; Chemical properties; Treatment process.

Extended Abstract

In the effort of reducing carbon footprint, shifting the conventional energy to renewable energy is the most favourable alternative approach. Liquid fuel such as biofuel and biodiesel have been reviewed as the prime substitute for the fossil fuel as it acquire more benefits in significantly reduced the greenhouse gas, global warming, and dependancy on foreign oil (Muhammad, Shamsuddin, Danjuma, Musawa, & Dembo, 2018). The focal point of this study will be on the liquid fuel of waste cooking oil (WCO) and pyroysis oil. The global demand for cooking oil has increased significantly for the past five years. Amid the pandemic of Covid-19, the request for cooking oil displayed no adverse repercussion with an outstanding growth of 18.43% in 2020 in contrast to the average demand in 2017 to 2019 (Fortune Business Insights, 2022). In Malaysia, the consumption of cooking oil was approximately 3.37 million tons in the year 2020/2021 (Hisrchmann, 2022). However, the dumping of WCO is a hazard for health and environment, such as water or soil polution, and the clogging of sewer and drainage system (Foo, et al., 2021). In other hand, pyrolysis oil has been extensively researched as a replacement or additive towards the fossil fuel in an internal combustion engine (ICE) that operated with gasoline or diesel. From a study had revealed that pyrolysis oil has the capability to be utilised as fuel in a diesel ICE where the maximum load yielded from pyrolysis oil and diesel were 3,282 W and 3,500 W respectively (Wongkhorsub & Chindaprasert, 2013). In a flexible fuel ICE, a research demonstrated that when the pyrolysis oil is blended as an additive with ethanol, the overall engine performance will be increased (Szwaja, Chwist, Szwaja, & Juknelevicius, 2021). Therefore pyrolysis oil has proven to be one of the

most potential biofuel to replace fossil fuel.

Hanisah K et al had conducted a survey in Teluk Bahang, Penang on the WCO management, it was discovered that 84% of the repondents were discarding the WCO in drainage system, dustbin, and soil where disposing into drainage system has the highest percentage, at 60% (K, S, & AY, 2013). Recent study also justify the numbers, where 92% of the people of Pasir Gudang, Johor had improprely dump the WCO as formerly mentioned (Mat Daud, Ngadiman, & Sulaiman, 2020). This clarifies that there is a plethora of WCO that is not fully exploited. The straightforward chemical composition of WCO has become a vital chemical element for the application in lubricant products, and fuel (Mannu, Garroni, Porras, & Mele, 2020). As for raw pyrolysis oil, it is consists of various organic compound, high oxygen content, and complex water mixutres. These unfavourable chemical properties of biofuel has resulted to thermally instable, corrosiveness and high viscosity (Yang, et al., 2014). Hence, the raw pyrolysis oil is not workable for commercial application. The treatment of the raw pyrolysis oil is essential to develop a high quality biofuel. As such, it is a necessity to upgrade the biofuel by eliminating the oxygen content and refining the chemical composition from the pyrolysis oil (Lee, 2013). The objective of this study is to investigates the effect of liquid-plasma reactor powered by non-thermal plasma (NTP) on changing the properties of the liquid oils which are waste cooking oil and pyrolysis oil.

These liquid oils are treated in a different scale of plasma reactor where the cooking oil and pyrolysis oil adopted a small scale and a large scale reactor respectively. Figure 1 shows the small scale reactor setup for which was filled with 1.6L of waste cooking oil and treated for one hour. The NTP is powered by the variable AC (VARIAC) transformer at the power consumption of between 107 W to 117 W and the frequencey resonance of 28 kHz. As for the treatment of pyrolysis oil, 20L of oil was loaded in the large scale reactor for two hours. The VARIAC and frequency were set to 150 W and 25 kHz respectively. Figure 2 shows the large scale reactor.

Figure 1: The small scale of the non-thermal plasma reactor

Figure 2: The large scale of the non thermal

The WCO and pyrolysis oil were analysed using FTIR to compare the composition of the treated and untreated oil. FTIR result for the treated oil illustrated the disappearance of several peaks from the untreated oil. For WCO, the disappearance of peaks are at wavelenght range of aromatic, alkanes and alkenes group, meanwhile pyrolysis oil showed at the range of carbonyl ester and meta aromatic group. Following the treatment process, bomb calorimetry experiment was executed for pyrolysis oil which resulted to an increase of 0.3% in calorific value. Despite the slight increased in energy content, the efficiency of the plasma treatment process achieved 74%. From these results, it conveyed that by treating the liquid oils in the non-thermal plasma reactor, it able to improve the chemical properties of the WCO and upgraded the quality of pyrolysis oil. Nevertheless, further research is required to investigate the mechanism of liquid oil treatment in non-thermal plasma reactor and optimised the setting of the plasma reactor to maximise efficiency of the treatment proces.

References

Foo, W., Chia, W., Tang, D., Koay, S., Lim, S., & Chew, K. (2021). The conundrum of waste cooking oil: Transforming hazard into energy,. Journal of Hazardous Material, 417.Fortune Business Insights. (2022). Retrieved 4 10, 2022, from https://www.fortunebusinessinsights.com/cooking-oil-market-106391

Hisrchmann, R. (2022). Statista. Retrieved 4 10, 2022, from https://www.statista.com/statistics/489441/palm-oil-consumption-malaysia/

K, H., S, K., & AY, T. (2013). The Management of Waste Cooking Oil: A Preliminary Survey.

Health and Environmental Journal, 4(1), 76-81.

Lee, J. W. (2013). Advanced Biofuels and Bioproducts (1 ed.). Norfolk: Springer.

Mannu, A., Garroni, S., Porras, J., & Mele, A. (2020). Available Technologies and Materials for Waste Cooking Oil Recycling. Processes, 366(8), 1-13.

Mat Daud, M., Ngadiman, N., & Sulaiman, M. (2020). The Awareness of Recycling The Used of Cooking Oil. Journal of Critical Review, 7(8), 30-32.

Muhammad, U., Shamsuddin, I., Danjuma, A., Musawa, R., & Dembo, U. (2018). Biofuels as the

Starring Substitute to Fossil Fuels. Petroleum Science and Engineering, 2(1), 44-49.

Szwaja, M., Chwist, M., Szwaja, S., & Juknelevicius, R. (2021). Impact of Pyrolysis Oil Addition to Ethanol on Combustion in the Internal Combustion Spark Ignition Engine. Clean Technologies, 3, 450-461.

Wongkhorsub, C., & Chindaprasert, N. (2013). A Comparison of the Use of Pyrolysis Oil in Diesel Engine. Energy and Power Engineering, 5, 350-355.

Yang, H., Yao, J., Chen, G., Ma, W., Yan, B., & Qi, Y. (2014). Overview of upgrading of pyrolysis oil of biomass. Energy Procedia, 61, 1306-1309.

6th International Conference and
Postgraduate Colloquium for
Environmental Research 2022 (POCER
2022) 9 - 11 June 2022
Langkawi, Kedah, Malaysia

PCR17042022 – 186: SIMULATION OF EMPTY FRUIT BUNCH PELLET HEATING IN MICROWAVE REACTOR

Peter Nai Yuh Yek [a], Ming Chiat Law[b], Sieng Huat Kong[c], Chee Swee Wong[a], Chee Chung Wong[a], Rock Keey Liew [d] and Su Shiung Lam [e*]

[a] Centre for Research of Innovation and Sustainable Development, University of Technology Sarawak, No.1, Jalan Universiti, Sibu, Sarawak, Malaysia.

[b] Department of Mechanical Engineering, Faculty of Engineering and Science, Curtin University Malaysia Campus, CDT 250, 98009, Miri, Sarawak, Malaysia.

[c] School of Foundation Studies, University of Technology Sarawak, No.1, Jalan Universiti, 96000 Sibu, Sarawak, Malaysia.

[d] NV WESTERN PLT, No. 208B, Second Floor, Jalan Macalister, Georgetown, 10400, Pulau Pinang, Malaysia.

[e] Higher Institution Centre of Excellence (HICoE), Institute of Tropical Aquaculture and Fisheries (AKUATROP), Universiti Malaysia Terengganu, 21030 Kuala Nerus, Terengganu, Malaysia

- Correnspondsing Author E-mail: sushiung@gmail.com

Keywords: Microwave; torrefaction; Co-firing; Energy; Simulation

Extended Abstract

Simulation of microwave heating is crucial to investigate the reactor design that is able to heat the sample evenly to desire temperature. This study integrates the radio frequency and transient heat transfer modules to simulate the microwave distribution and investigate the performance of microwave heating in the cavity. The finite element analysis software of COMSOL MULTIPHYSICS predicted the temperature profile and electric field of microwave in the sample, and the simulation results were compared with the experimental results. Higher temperature distribution was observed at the bottom part and centre of the empty fruit bunch pellet bed in the reactor, showing the uniqueness of microwave heating. The simulated temperature profile obtained through specific cavity geometry and dielectric properties showed a consensus with the experimental temperature profile. The simulated temperature profile showed a logarithmic increase of 120 °C/min at the first 50 s and followed by 50 °C/min until 350 s. The experimental temperature profile showed three different heating rates before reaching 300

°C, including 78.3 °C/min (50-120 °C), 30.6 °C/min (121-250 °C) and 105 °C/min (250-300 °C). The simulation of microwave heat distribution are crucial to improve the development of microwave usage in torrefaction process.

6th International Conference and
Postgraduate Colloquium for
Environmental Research 2022 (POCER
2022) 9 - 11 June 2022
Langkawi, Kedah, Malaysia

PCR17042022 – 187: Solvothermal liquefaction of Kariba weed into value-added products

Elfina Azwar[a,b], Su Shiung Lam[b,a*]

[a] Henan Province Engineering Research Center for Biomass Value-added Products, School of Forestry, Henan Agricultural University, Zhengzhou, 450002, China

[b] Higher Institution Centre of Excellence (HICoE), Institute of Tropical Aquaculture and Fisheries (AKUATROP), Universiti Malaysia Terengganu, 21030 Kuala Terengganu, Terengganu, Malaysia

*Corrensponsing Author E-mail: lam@umt.edu.my

Keywords: Liquefaction; Aquatic weed; Biofuels; Energy

Extended Abstract

Fast growing Kariba weed (KW) creates serious issues on freshwater systems by disturbing nutrient uptake of crops, limiting sunlight penetration into freshwater system, and most likely to invade native aquatic organisms. In this work, solvothermal liquefaction (STL) of KW was performed to investigate the influences of different KW mass loading on product yield and features. The STL resulted in a KW conversion of up to 92%. The oil, char, and gas recovered were up to 33 wt%, 20 wt%, and 58 wt%, respectively. The use of lower KW mass loading (5% w/v) were found to have increase the higher heating value (HHV) of oil product up to 35 MJ/kg. On the contrary, the higher KW mass loading (10 % w/v) increased the HHV of char product (29 MJ/kg) and production of fatty acid methy ester and hydrocarbon compounds in oil product that can be used for biofuels application. This study provides useful information to promote thermochemical biorefinery of aquatic weeds rather than disposing them in landfills.

Acknowledgements: This work was supported by the Ministry of Higher Education Malaysia under Fundamental Research Grant Scheme (FRGS) [FRGS/1/2018/TK10/UMT/02/2, Vot 59512]; and Higher Institution Centre of Excellence (HICoE), Institute of Tropical Aquaculture and Fisheries (AKUATROP) program [Vot. No. 63933 & Vot. No. 56051, UMT/CRIM/2-2/5 Jilid 2 (10)].

6th International Conference and Postgraduate Colloquium for Environmental Research 2022 (POCER 2022) 9 - 11 June 2022
Langkawi, Kedah, Malaysia

PCR17042022 – 188: Conversion of shellfish waste into high value-added products by microwave pyrolysis

Yan Yang[a,b], Shin Ying Foong[a,b], and Su Shiung Lam[a,b*]

[a] Henan Province Engineering Research Center for Biomass Value-added Products, School of Forestry, Henan Agricultural University, Zhengzhou, 450002, China

[b] Higher Institution Centre of Excellence (HICoE), Institute of Tropical Aquaculture and Fisheries (AKUATROP), Universiti Malaysia Terengganu, 21030 Kuala Terengganu, Terengganu, Malaysia

- Corrensponsing Author E-mail: lam@umt.edu.my

Keywords: Shellfish Waste; Microwave Pyrolysis; Biochar; Biofuel; Value-added Products

Extended Abstract

Shellfish are rich in vitamins and minerals and are popular among consumers because of their high nutritional value and good taste. However, shellfish waste (SW) causes serious environmental pollution if it is not handled properly. In this study, three types of shellfish waste (i.e. crab shell, oyster shell and scallop shell) are recovered via pyrolysis technology and transformed into value-added products. Firstly, thermogravimetric analysis combined with Fourier transform infrared spectroscopy (TG-FTIR) and pyrolysis combined gas chromatography / mass spectrometry (Py-GC/MS) were used to determine the volatile products released from shellfish waste during pyrolysis. Shellfish waste has high carbon and oxygen content, which is suitable as pyrolysis raw materials. The shellfish waste is then subjected to microwave pyrolysis (MP) to produce biochar. TG-FTIR analysis shows that the volatile products produced by pyrolysis were mainly composed of carbon dioxide, oxygen, and light hydrocarbons such as methane. Py-GC/MS shows that pyrolysis performed at different final temperatures and heating rates recovered mainly chitin, which can potentially be used in fish feed formulation. Low calorific value (5-8 MJ/kg) and high O/C (3.2-5.2) and H/C (0.3-1.3) ratio of shellfish waste provides low chemical energy during combustion process. Thus, shellfish waste is subjected into MP to produce biochar with high calorific value (14-18 MJ/kg), which is more suitable for fuel application. Biochar produced via MP also poses high BET surface area (189.5 m^2/g), which shows the potential as an adsorbent for ammonia compounds in green crab aquaculture wastewater. These results show that biochar produced from

shellfish waste can be used as fuel and biosorbent. It is promising to transform shellfish waste into value-added products by microwave pyrolysis.

6th International Conference and Postgraduate Colloquium for Environmental Research 2022 (POCER 2022) 9 - 11 June 2022
Langkawi, Kedah, Malaysia

PCR17042022 – 189: Conversion of shrimp shell waste into high value-added products by microwave pyrolysis

Lingbo Meng[a,b], Shin Ying Foong[a,b], and Su Shiung Lam[a,b*]

[a] Henan Province Engineering Research Center for Biomass Value-added Products, School of Forestry, Henan Agricultural University, Zhengzhou, 450002, China

[b] Higher Institution Centre of Excellence (HICoE), Institute of Tropical Aquaculture and Fisheries (AKUATROP), Universiti Malaysia Terengganu, 21030 Kuala Terengganu, Terengganu, Malaysia

- Corrensponsing Author E-mail: lam@umt.edu.my

Keywords: Shrimp shell Waste; Microwave Pyrolysis; Biochar; Biofuel; Value-added Products

Extended Abstract

Shrimps are rich in nutrition, and it's delicious taste made them to be one of people's favorite seafood. However, increase consumption of shrimp has resulted in the generation of shrimp shell waste (SSW). Improper handling of this waste will create environmental problem, such as air and water pollution. In this study, thermogravimetric analysis combined with Fourier transform infrared spectroscopy (TG-FTIR) and pyrolysis gas chromatography/mass spectrometry (Py GC/MS) is used to identify the gas components produced by heating of SSW. Microwave pyrolysis with unique properties such as fast and uniform heating has been introduced to valorize SSW to produce biochar. TG-FTIR data analysis revealed that the volatile products produced by SSW pyrolysis are mainly composed of CO_2, H_2 and CH_4. Py-GC/MS indicated that pyrolysis performed at different final temperatures and heating rates mainly recovered chitin. The elemental analysis shows that the content of C and O in SSW is very high, which are (36.52 wt.%) and (46.68 wt.%), respectively. The low calorific value of SSW (15.11MJ/kg) and its high nitrogen content (10.58 wt.%) indicate that SSW is not suitable for direct combustion because it produces harmful gases such as nitrogen oxides to the environment. Alternatively, it can be a potential fertilizer or adsorbent in aquaculture wastewater treatment owing to its high nitrogen content and high BET surface area (401 m^2/g), respectively. Therefore, microwave pyrolysis is a promising, energy efficient and environmentally friendly method to valorize SSW and produces value added biochar.

6th International Conference and
Postgraduate Colloquium for
Environmental Research 2022 (POCER
2022) 9 - 11 June 2022
Langkawi, Kedah, Malaysia

PCR17042022 – 190: Microwave-assisted chemical extraction of chitosan from shellfish wastes

Shin Ying Foong[a] and Su Shiung Lam[a*]

[a] Higher Institution Centre of Excellence (HICoE), Institute of Tropical Aquaculture and Fisheries (AKUATROP), Universiti Malaysia Terengganu, 21030 Kuala Terengganu, Terengganu, Malaysia

- Corrensponsing Author E-mail: lam@umt.edu.my

Keywords: Microwave heating; Crustaceans; Molluscs; Demineralization; Deproteinization; Deacetylation

Extended Abstract

Chitin is naturally occurring biopolymer that is present in abundance in shellfish, while chitosan is the deacetylated-derivative of chitin. Chitin and chitosan have excellent biological and chemical properties, thus are widely used in applications such as adsorbent and pharmaceutical. This research work aims to extract chitosan from different shellfish waste via a fast, efficient, and easy method, by applying microwave irradiation in the extraction steps (demineralization, deproteinization and deacetylation). The physicochemical and structural properties of extracted chitosan such as the degree of deacetylation (DD%), is characterized by X-ray Diffractometry (XRD), Fourier-Transform Infrared Spectroscopy (FT-IR) and Scanning Electron Microscopy equipped with energy dispersion spectroscopy (SEM-EDS). The highest yield of chitosan is extracted from shrimp waste, with DD% of 85%. The DD% of chitosan extracted from other shellfish waste such as mussel, crab, squid pen and scallop shell are ranging from 60% to 80%. Microwave-assisted extraction has reduces the extraction time 6 folds as compared to conventional method, suggesting microwave technology can be used as an alternative to recover chitosan from shellfish waste as it is a more energy saving, efficient and environmentally friendly method.

6th International Conference and
Postgraduate Colloquium for
Environmental Research 2022 (POCER
2022) 9 - 11 June 2022
Langkawi, Kedah, Malaysia

PCR17042022 – 193: Catalytic thermal conversion of organic solid wastes to energy

Sumin Pyo[a], Hoyeon Jang[a], Hyunji Yim[a], Hyunjin Kim[a], Jihyeon Seo[a], Suhyeong Chai[a], Dongwon Chang[a], Sugyeong Jeon[a], Bo Sung Kang[a], Hoesuk Yim[a], Young-Min Kim[b], Sang Mun Jeong[c] and Young-Kwon Park[a,*]

[a] School of Environmental Engineering
University of Seoul, Seoul, Republic of Korea

[b] Department of Environmental Engineering,
Daegu University, Gyeongsan, Republic of Korea

[c] Department of Chemical Engineering, Chungbuk National University,
Chungbuk-28644, Republic of Korea

- Corrensponsing Authors E-mail: catalica@uos.ac.kr

Keywords: Microfibers; Textile laundry wastewater; Poly(ethylene terephthalate); Nylon-6; Polyacrylonitrile.

Extended Abstract

Various kinds of organic solid wastes could be converted to clean eneryg via suitable catalytic thermochemical conversion.

To do this, in this study, tandem micro-reactor-GC/MS system is constructed with two reactors online coupled with a conventional GC/MS, as shown in Fig. 1, for catalytic pyrolysis. Gas, liquid, or solid samples can be introduced into 1st reactor using a micro-syringe, micro-feeder, or inert sample cup for gas preheating, liquid vaporization, or solid pyrolysis. The product vapor emitted from 1st reactor as a results of heating or pyrolysis is transferred to 2nd reactor having catalyst bed and converted to other chemicals by the ex-catalytic reaction. If the sample and catalyst was mixed and introduced to 1st reactor, with no catalyst loading on 2nd reactor, in-situ catalytic reaction also can be performed. Final products are moved to GC and detected in MS after the separation in a capillary column in GC oven.

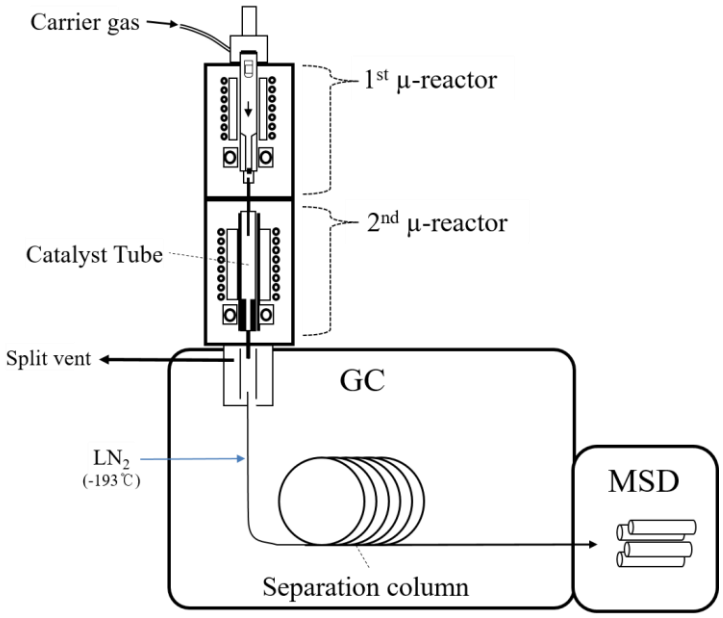

Fig. 1. Schematic diagram of tandem micro-reactor-GC/MS

Also, other catalytic thermoconversion approach, such as catalytic co-pyrolysis of biomass and plastics, catalytic hydrodeoxygenation of bio-oil, hydropyrolysis, and catalytic gasification are introduced.

Acknowledgements: This work was supported by National Reseach Foundation of Korea (NRF-2021R1A2C3011274).

6th International Conference and
Postgraduate Colloquium for
Environmental Research 2022 (POCER
2022) 9 - 11 June 2022
Langkawi, Kedah, Malaysia

PCR17042022 – 194: Effect of Nb_2O_5 and NiO/Nb_2O_5 catalyst on the degradation of polystyrene

Jihyeon Seo, Hoyeon Jang, Hyunji Yim and Young-Kwon Park*

School of Environmental Engineering
University of Seoul, Seoul, Republic of Korea

- Corrensponsing Authors E-mail: catalica@uos.ac.kr

Keywords: Pyrolysis; Catalytic Cracking; Acid catalyst ; Polystyrene; Plastic waste.

Extended Abstract

Polystyrene (PS) is the fourth most highly produced polymer worldwide and is used extensively in clear or expanded form (Inayat et al., 2021). On the other hand, polystyrene waste due to low recycling contributes up to 70% of plastic debris. Different disposal techniques are available, e.g., incineration and landfill, but the annual recycling of PS only constitutes a small portion and needs to be improved. The thermal and catalytic pyrolysis of PS are excellent techniques for recovering chemical feedstock (Ukei et al., 2000). Notably, the pyrolysis oil obtained through thermal or catalytic pyrolysis can be upgraded further using a catalytic cracking process. Many researchers have worked on the catalytic cracking of pyrolysis oil obtained using different feedstocks (Lovás et al., 2017; Gandidi et al., 2018; Rodríguez et al., 2019).

In this study, The catalytic cracking of polystyrene pyrolysis oil was investigated over a Nb_2O_5 and a NiO/Nb_2O_5 catalyst in a fixed bed reactor. First, the pyrolysis of two different polystyrene feedstock (polystyrene foam (PF) and General-purpose PS (GPPS) pellets) was carried out in a semi-batch reactor. Catalytic cracking experiments were then performed at different temperatures (350–500 °C) using Nb_2O_5 or NiO/Nb_2O_5 catalyst.

According to Figure 1(a), The GPPS pyrolysis oil was selected for the catalytic cracking reaction because of its high liquid yield (85%). Also, the catalytic pyrolysis in the semi-batch process using Nb_2O_5 as a catalyst increased the pyrolysis oil yield slightly. As shown in Figure 1 (b), gas chromatography–mass spectrometry analysis of liquid product obtained from the catalytic cracking process showed that the dimers in the pyrolysis oil were converted to monomers during the catalytic cracking process.

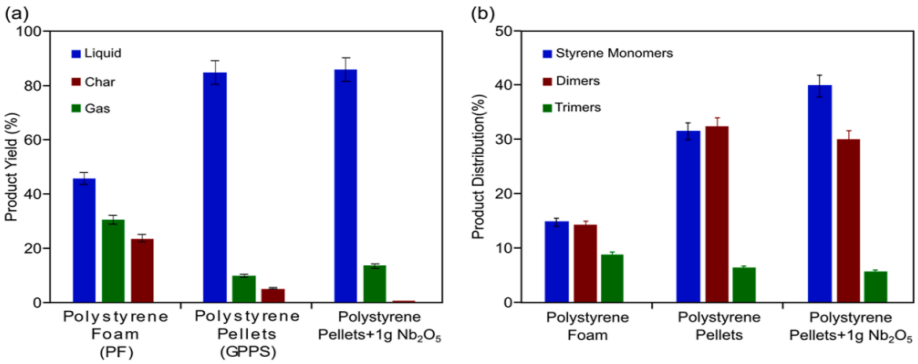

Figure 1: Thermal and catalytic pyrolysis of PS Foam (PF) and PS pellets (GPPS). (a) Product yield, (b) Liquid oil Product distribution.

Generally, the catalytic cracking process convertes the dimers present in the pyrolysis oil to monomers. Based on the Figure 2 (a,b), the Nb_2O_5 catalyst is more active towards the conversion of dimers to monomers, whereas NiO/Nb_2O_5 catalyst favored the conversion of monomers. Indeed, monomers, such as toluene, ethylbenzene, styrene, and α-methylstyrene, were further cracked over the NiO/Nb_2O_5 catalyst surface to yield a gaseous product. Overall, the highest catalytic cracking activity was observed at 400 ◦C using the Nb_2O_5 catalyst with 4% toluene, 6% ethylbenzene, 50% styrene, 13% α-methyl styrene, and only 6% of dimers in the liquid oil. The increase in temperature positively affected the yield of gases during catalytic cracking process and favored the production of H_2 and CH_4 (Figure 2 (c)).

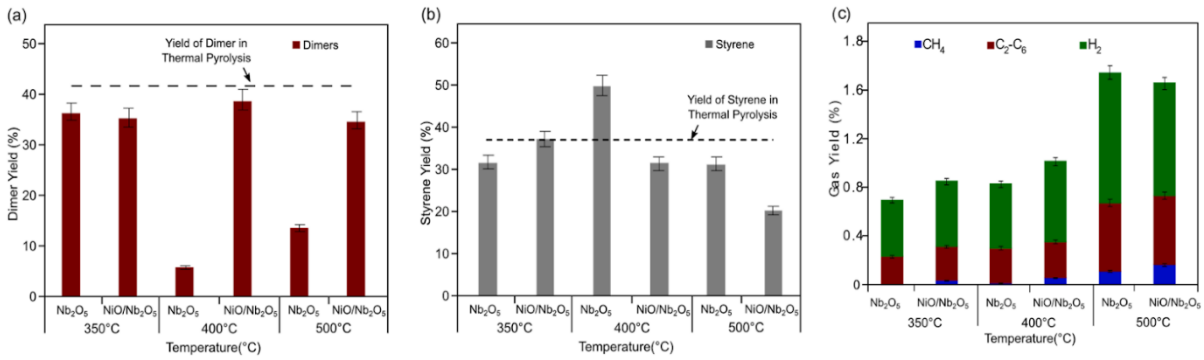

Figure 2: Effect of temperature and catalyst on the (a) dimer, (b) styrene monomer, (c) gas product composition

Acknowledgements: This work was supported by Korea Environment Industry & Technology Institute (KEITI) through Post Plastic, a specialized program of the Graduate School funded by Korea Ministry of Environment (MOE).

References

Gandidi, I.M., Susila, M.D., Mustofa, A., Pambudi, N.A., 2018. Thermal–catalytic cracking of real MSW into bio-crude oil. Journal of the Energy Institute 91, 304-310.

Inayat, A., Klemencova, K., Grycova, B., Sokolova, B., Lestinsky, P., 2021. Thermo-catalytic pyrolysis of polystyrene in batch and semi-batch reactors: A comparative study. Waste Management & Research 39, 260-269.

Lovás, P., Hudec, P., Jambor, B., Hájeková, E., Horňáček, M., 2017. Catalytic cracking of heavy fractions from the pyrolysis of waste HDPE and PP. Fuel 203, 244-252.

Rodríguez, E., Palos, R., Gutiérrez, A., Arandes, J.M., Bilbao, J., 2019. Production of non-conventional fuels by catalytic cracking of scrap tires pyrolysis oil. Industrial & Engineering Chemistry Research 58, 5158-5167.

Ukei, H., Hirose, T., Horikawa, S., Takai, Y., Taka, M., Azuma, N., Ueno, A., 2000. Catalytic degradation of polystyrene into styrene and a design of recyclable polystyrene with dispersed catalysts. Catalysis today 62, 67-75.

6th International Conference and
Postgraduate Colloquium for
Environmental Research 2022 (POCER
2022) 9 - 11 June 2022
Langkawi, Kedah, Malaysia

PCR17042022 – 195: Kinetic analysis for the catalytic degradation of polyethylene terephthalate

Dongwon Chang, Hoesuk Yim, and Young-Kwon Park*

School of Environmental Engineering
University of Seoul, Seoul, Republic of Korea

- Corrensponsing Authors E-mail: : catalica@uos.ac.kr

Keywords: Polyethylene terephthalate; Kinetic analysis; Bentonite; Pyrolysis.

Extended Abstract

Polyethylene terephthalate (PET) is known as a common plastic widely used in many industries, such as textile, packaging, and fibers manufacturing (Diaz-Silvarrey et al., 2018). The amount of waste PET bottle is also increased rapidly in recent years. Although PET bottle can be properly recycled, the considerable amount of PET wastes is still difficult to be recycled due to the co-presence of impurities, pigment, and so on, with PET (Faraca and Astrup, 2019). Pyrolysis can be the proper solution to increase the recycling efficiency of PET because the large amount of chemical and/or fuel can be produced from PET wastes (Syamsiro et al., 2014). Although the large amount of PET pyrolysis oil can be obtained by the simple pyrolysis, the high content of acids in PET pyrolysis oil is being considered as the limitation on the commercialization of PET pyrolysis process. To overcome this limitation, the catalytic pyrolysis of PET was intensively suggested.

In this study, kinetic analysis for the thermal and catalytic pyrolysis of PET (over natural zeolite (NZ), olivine, bentonite, HZSM-5, and HAl-MCM-41) was performed using a thermogravimetric (TG) and model-free kinetic analysis. Catalytic TG analysis was performed by heating PET or PET and catalyst mixture at multi-heating rates under nitrogen atmosphere. Flynn-Wall-Ozawa (Flynn and Wall, 1966) model (FWO) was applied to calculate E_a values on the thermal and catalytic pyrolysis of PET without the assumption of reaction model.

As shown in Figure 1, all catalysts revealed lower T_{max} compared to non-catalytic reaction. Although natural catalysts, NZ, olivine, and bentonite, could not lead the higher PET decomposition efficiency than synthetic zeolites, HZSM-5 and HAl-MCM-41, maximum decomposition temperatures on the differential TG (DTG) curves for the catalytic pyrolysis of PET, 436 °C over olivine, 435 °C over bentonite, and 434 °C over NZ, at 10 °C/min, were definitely lower than non-catalytic pyrolysis.

Different PET decomposition efficiency of the catalysts can be explained by catalyst acidity and pore properties. Among natural catalysts used in this study, bentonite and olivine have larger pore size, 29.8 nm and 7.9 nm respectively, than HZSM-5 (0.55 nm). NZ has the smallest pore size (0.5 nm) among the catalysts used in this study. These indicate that the diffusion limitation of reactant molecules to the pore of bentonite and olivine is lower than that of HZSM-5. Meanwhile, natural catalysts have the lower acidities around 400 °C, 0.122 mmol/g (bentonite), 0.151 mmol/g (NZ), and almost no acidity (olivine), than HAl-MCM-41 (0.553 mmol/g) and HZSM-5 (0.573 mmol/g). This suggests that the catalyst acidity is more important factor concluding PET decomposition rates.

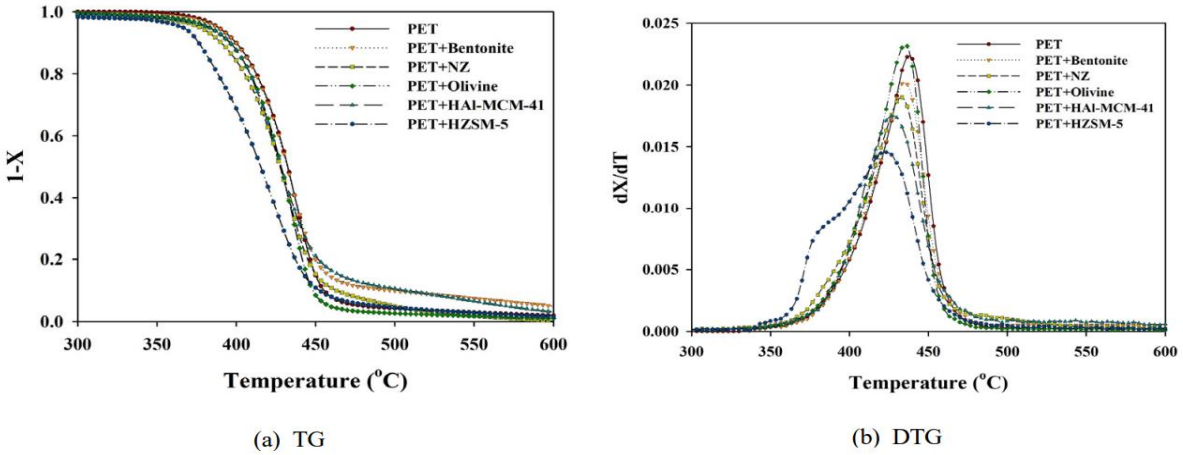

(a) TG (b) DTG

Figure 1: (a) TG and (b) DTG curves for the thermal and catalytic pyrolysis of PET at 10 °C/min.

Furthermore, according to Figure 2, calculated E_a values for the catalytic pyrolysis of PET over natural catalysts, 177 kJ/mol over olivine, 168 kJ/mol over bentonite, and 171 kJ/mol over NZ, were also not lower than those over synthetic zeolites, however, those were also much lower than the thermal decomposition, suggesting their feasibility as the proper and cost-effective catalysts on the pyrolysis of PET.

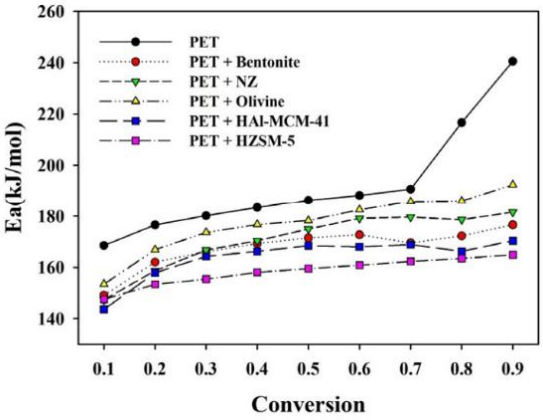

Figure 2: Activation energy values obtained from catalytic and noncatalytic TGA data.

Acknowledgements: This work was supported by Korea Environment Industry & Technology Institute (KEITI) through Post Plastic, a specialized program of the Graduate School funded by Korea Ministry of Environment (MOE).

References

Diaz-Silvarrey, L.S., McMahon, A., Phan, A.N., 2018. Benzoic acid recovery via waste poly (ethylene terephthalate)(PET) catalytic pyrolysis using sulphated zirconia catalyst. Journal of analytical and applied pyrolysis 134, 621-631.

Faraca, G., Astrup, T., 2019. Plastic waste from recycling centres: Characterisation and evaluation of plastic recyclability. Waste Management 95, 388-398.

Flynn, J.H., Wall, L.A., 1966. A quick, direct method for the determination of activation energy from thermogravimetric data. Journal of Polymer Science Part B: Polymer Letters 4, 323-328.

Syamsiro, M., Saptoadi, H., Norsujianto, T., Noviasri, P., Cheng, S., Alimuddin, Z., Yoshikawa, K., 2014. Fuel oil production from municipal plastic wastes in sequential pyrolysis and catalytic reforming reactors. Energy Procedia 47, 180-188.

6th International Conference and
Postgraduate Colloquium for
Environmental Research 2022 (POCER
2022) 9 - 11 June 2022
Langkawi, Kedah, Malaysia

PCR17042022 – 196: Selective solvent extraction and quantification of synthetic microfibers in textile laundry wastewater

Hyunjin Kim[a], Jihyeon Seo[a], Suhyeong Chai[a], Dongwon Chang[a], Sugyeong Jeon[a], Young-Min Kim[b], and Young-Kwon Park[a]

[a] School of Environmental Engineering
University of Seoul, Seoul, Republic of Korea

[b] Department of Environmental Engineering,
Daegu University, Gyeongsan, Republic of Korea

- Corrensponsing Authors E-mail: catalica@uos.ac.kr

Keywords: Microfibers; Textile laundry wastewater; Poly(ethylene terephthalate); Nylon-6; Polyacrylonitrile.

Extended Abstract

The analytical technologies for micro plastics (MPs) include visual identification, microscopy, spectroscopy, and thermal analysis (Faltynkova et al., 2021). Generally, microscopy is considered a fast and straightforward method, however, the difficulties in chemical confirmation are regarded as a limitation (Sierra et al., 2020). Fourier transform infrared (FT-IR) spectroscopy and Raman spectroscopy are typical non-destructive analysis methods, but the interference by the non-target matrix for MPs analysis is considered a limitation of these spectroscopy technologies (Dąbrowska, 2021). Various thermo-analytical technologies have been suggested to overcome the disadvantages of spectroscopy technologies on weight-based quantification, such as thermogravimetric-IR (TG-IR) (Goedecke et al., 2020), TG-mass spectrometry (TG-MS) (La Nasa et al., 2020), pyrolysis-gas chromatography/MS (PyGC/MS), and thermal extraction and desorption-GC/MS (TED-GC/ MS) (Dümichen et al., 2017).

This paper reports the selective quantification of synthetic microfibers (MFs), polyethylene terephthalate (PET), nylon-6 (N-6), and polyacrylonitrile (PAN), emitted from a textile laundry. Sequential steps consisting of filtration, MFs extraction using hexafluoroisopropanol (HFIP), TG-analysis, and PyGC/MS analysis were suggested.

After filtering the textile laundry wastewater, selective sampling of synthetic MFs excluding non-target matrices and natural fibers was achieved by extracting the filtered samples with HFIP. Figure 1 compared selected ion monitoring (SIM) chromatograms obtained from the Py-GC/MS analysis of a solid standard mixture and the solution standard mixture. MF recovery for HFIP extraction by Py-GC/MS analysis was 91.4 %, 98.5 %, and 98.8 % for PET, N-6, and PAN, respectively. This suggests that the HFIP solvent extraction of these polymers from the filtered MF sample collected after the laundry test is an efficient sample preparation step for the selective quantification of synthetic MFs emitted from a textile laundry.

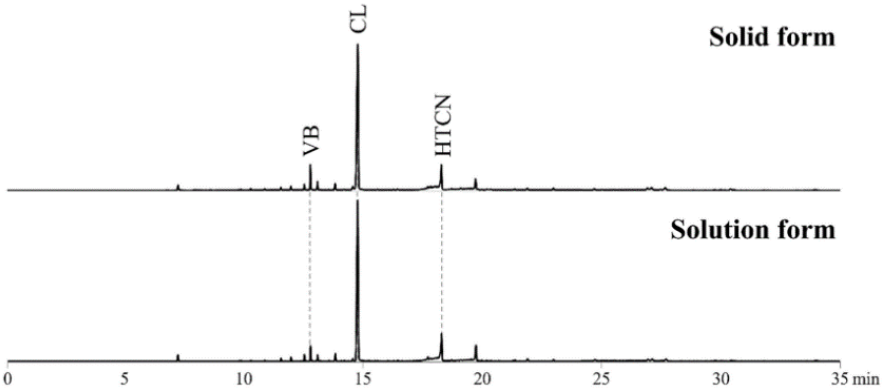

Figure 1: SIM chromatograms obtained from the pyrolysis of the solid and the solution standard mixtures. (VB: Vinyl benzoate, CL: ε-Caprolactam, HTCN: Hexane1,3,5-tricarbonitrile).

Based on the quantification results of MFs extracted from the accelerated laundering test by Py-GC/MS, the quantification results for the MFs extracted from the textile made from a single filer showed that PET, N-6, and PAN textile produced 481, 111, and 329 mg of MFs/kg textile, respectively. Compared to the single textile (PET), the blended textiles produced larger amounts of MPs, 961 mg/kg for PET/cotton and 680 mg/kg for PET/wool blended textiles, suggesting the easier formation of MFs from blended textiles during textile laundering. Although Py-GC/MS has been suggested as an appropriate quantification tool, TGA was required in the pre-analysis step before Py-GC/MS to obtain a suitable HFIP dilution factor because of the wide MF weight range from sub mg to 1,000 mg per kg textile.

Acknowledgements: This work was supported by Korea Environment Industry & Technology Institute (KEITI) through Post Plastic, a specialized program of the Graduate School funded by Korea Ministry of Environment (MOE).

References

Dąbrowska, A., 2021. Raman Spectroscopy of Marine Microplastics-A short comprehensive compendium for the environmental scientists. Marine Environmental Research 168, 105313.

Dümichen, E., Eisentraut, P., Bannick, C.G., Barthel, A.-K., Senz, R., Braun, U., 2017. Fast identification of microplastics in complex environmental samples by a thermal degradation method. Chemosphere 174, 572-584.

Faltynkova, A., Johnsen, G., Wagner, M., 2021. Hyperspectral imaging as an emerging tool to analyze microplastics: a systematic review and recommendations for future development. Microplastics and Nanoplastics 1, 1-19.

Goedecke, C., Dittmann, D., Eisentraut, P., Wiesner, Y., Schartel, B., Klack, P., Braun, U., 2020. Evaluation of thermoanalytical methods equipped with evolved gas analysis for the detection of microplastic in environmental samples. Journal of Analytical and Applied Pyrolysis 152, 104961.

La Nasa, J., Biale, G., Fabbri, D., Modugno, F., 2020. A review on challenges and developments of analytical pyrolysis and other thermoanalytical techniques for the quali-quantitative determination of microplastics. Journal of Analytical and Applied Pyrolysis 149, 104841.

Sierra, I., Chialanza, M.R., Faccio, R., Carrizo, D., Fornaro, L., Pérez-Parada, A., 2020. Identification of microplastics in wastewater samples by means of polarized light optical microscopy. Environmental Science and Pollution Research 27, 7409-7419.

6th International Conference and
Postgraduate Colloquium for
Environmental Research 2022 (POCER
2022) 9 - 11 June 2022
Langkawi, Kedah, Malaysia

PCR17042022 – 197: Effects of different Al_2O_3 support on HDPE thermal degradation using Ni-based catalysts

Behzad Valizadeh, Hyunji Yim, Sang Mun Jeong[b], and Young-Kwon Park[*]

[a] School of Environmental Engineering

University of Seoul, Seoul, Republic of Korea

[c] Department of Chemical Engineering, Chungbuk National University,

Chungbuk-28644, Republic of Korea

- Corrensponsing Authors E-mail: catalica@uos.ac.kr

Keywords: HDPE; Gasification; Nano sized alumina; Hydrogen.

Extended Abstract

The need for alternative energy resources has grown since the depletion and increasing prices of fossil fuels and their environmental footprint, hence, it is essential to find some other environmentally friendly means of energy generation. Plastic production has increased from 2 million tons per year to 381 million tons per year in 2015, which has resulted in a subsequent increase in the generation of plastic waste, such as polyethylene terephthalate (PET), polypropylene (PP) and high density polyethylene (HDPE) (Moses et al., 2002; Sancho et al., 2008). The long natural/biological degradation time for plastic waste, which accumulates in the form of landfill under the earth and oceans, poses a great threat to the environment (Moore, 2008; Chen et al., 2019). The thermochemical conversion of plastics, such as gasification, is an economical solution to the removal of plastic waste from the environment. Moreover, the use of catalysts can reduce tar generation and the operating temperature in gasification, making the process more economical compared to non-catalytic cases (Ateş et al., 2013; Saad and Williams, 2016)

This study examined the possibility of applying Ni-loaded nano-sized alumina (13 nm and < 50 nm) and m-Al_2O_3 to HDPE gasification. The catalytic gasification activities of the different Ni-loaded alumina catalysts were compared with that of the well-known Ni-loaded γ-Al_2O_3 in a laboratory scale fixed bed quartz reactor.

Based on the Figure 1, The catalysts had a significant effect on the gasification products. the catalytic activity of Ni loaded alumina was observed in the order of 13 nm-sized Al_2O_3> mesoporous Al_2O_3> (<50 nmsized Al_2O_3) > γ-Al_2O_3 for the gas yield and γ-Al_2O_3> (<50 nm Al_2O_3) > mesoporous Al_2O_3 >

13 nm Al_2O_3 for the oil yield, respectively. The product distribution showed that the nano-sized or nanostructured alumina with a nickel loading could be a suitable catalyst for obtaining a higher gas yield. However, although the maximum gas yield was observed on Ni/13 nm Al_2O_3, a detailed analysis suggested a large percentage of CO_2 and hydrocarbons (mostly CH_4).

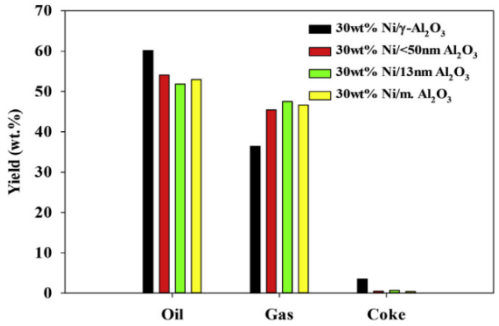

Figure 1: Yields of HDPE gasification over various catalysts.

In addition, as demonstrated in Figure 2, the production of hydrogen from Ni loaded alumina showed an increasing trend in the order of (<50 nm-sized Al_2O_3) > γ-Al_2O_3 > 13 nm-sized Al_2O_3.> mesoporous Al_2O_3. In contrast, CO showed the trend as Ni/mesoporous Al_2O_3> Ni/13 nm-sized Al_2O_3> Ni/g-Al_2O_3> (Ni/<50 nm Al_2O_3). Moreover, the maximum CO_2 generation was observed in the case of Ni/13 nm Al_2O_3 (26.90 vol%) compared to the other three, which is not recommended.

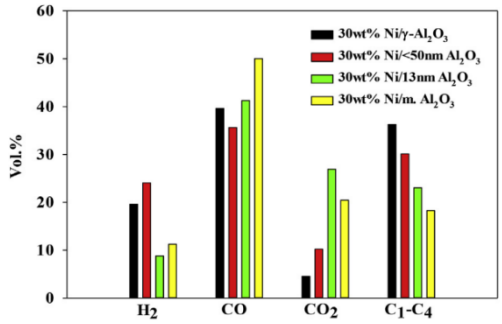

Figure 2: Gas composition from HDPE gasification over various catalysts.

Overall, the highest level of hydrogen production from the Ni/<50 nm-sized Al_2O_3 catalyst might be because of its highest Ni dispersion and surface area. Consequently, Ni/(<50 nm alumina) could be a better catalyst for enhanced hydrogen production and low CO_2 generation compared to other types of Al_2O_3 available.

Acknowledgements: This work was supported by Korea Environment Industry & Technology Institute (KEITI) through Post Plastic, a specialized program of the Graduate School funded by Korea Ministry of Environment (MOE).

References

Ateş, F., Miskolczi, N., Borsodi, N., 2013. Comparision of real waste (MSW and MPW) pyrolysis in batch reactor over different catalysts. Part I: Product yields, gas and pyrolysis oil properties. Bioresource technology 133, 443-454.

Chen, Y., Cui, Z., Cui, X., Liu, W., Wang, X., Li, X., Li, S., 2019. Life cycle assessment of end-of-life treatments of waste plastics in China. Resources, Conservation and Recycling 146, 348-357.

Moore, C.J., 2008. Synthetic polymers in the marine environment: a rapidly increasing, long-term threat. Environmental research 108, 131-139.

Moses, J.I., Zolotov, M.Y., Fegley Jr, B., 2002. Photochemistry of a volcanically driven atmosphere on Io: Sulfur and oxygen species from a Pele-type eruption. Icarus 156, 76-106.

Saad, J.M., Williams, P.T., 2016. Catalytic dry reforming of waste plastics from different waste treatment plants for production of synthesis gases. Waste management 58, 214-220.

Sancho, J.A., Aznar, M.P., Toledo, J.M., 2008. Catalytic air gasification of plastic waste (polypropylene) in fluidized bed. Part I: Use of in-gasifier bed additives. Industrial & engineering chemistry research 47, 1005-1010.

6th International Conference and
Postgraduate Colloquium for
Environmental Research 2022 (POCER
2022) 9 - 11 June 2022
Langkawi, Kedah, Malaysia

PCR17042022 – 198: Catalytic degradation of polypropylene over Ga loaded HZSM-5

Suhyeong Chai, Sumin Pyo, Bo Sung Kang, and Young-Kwon Park*

School of Environmental Engineering
University of Seoul, Seoul, Republic of Korea

- Corrensponsing Authors E-mail: catalica@uos.ac.kr

Keywords: Catalytic pyrolysis; Polypropylene; Ga/HZSM-5; Kinetic analysis; Pyrolyzer-gas chromatography/mass spectrometry.

Extended Abstract

The rapidly increased production and consumption of waste plastics are accelerating global contamination, and the microplastic issue has become an important issue worldwide (Ng et al., 2018). Among the various kinds of plastics, the use of polypropylene (PP) has increased dramatically in many applications owing to its high molecular weight, hydrophobicity, and resistance to microbial decomposition (Encarnacion et al., 2020). On the other hand, the mechanical superiority of PP makes it challenging to dispose of, and it remains in the environmental matrix for a long period when not be collected and treated appropriately. Thermal conversion processes, especially pyrolysis, can be considered a proper treatment method of organic wastes like biomass and plastics because it can decompose organic wastes in a short time and recover alternative sources of fuel or chemical feedstock (Santamaria et al., 2020). Value-added oil production on the pyrolysis of PP can be obtained through the additional use of catalysts (Kassargy et al., 2018).

In this study, the thermal and catalytic pyrolysis of PP over various catalysts (Ga/ HZSM-5 (namely GaHZ(30)), HZSM-5 with three different SiO_2/ Al_2O_3 ratios, namely HZ(SiO_2/Al_2O_3 = 30), HZ(80), HZ(280), and HY(30)) were investigated by thermogravimetric analysis (TGA) and pyrolyzer-gas chromatography/mass spectrometry (Py-GC/ MS). The apparent activation energy (E_a) on the decomposition of PP was calculated using a model-free kinetic analysis method, Ozawa-Flynn-Wall (OFW method), and the production of BTEXs was compared to determine the feasibility of GaHZ (30).

According to Figure 1 (a), The non-catalytic DTG curve of PP consisted of a single peak, indicating a single decomposition reaction. TGA result (Figure 2 (b)) indicated that HY(SiO_2/Al_2O_3; 30) is the most effective catalyst lowering PP decomposition temperature, followed by Ga/HZSM-5(30), HZSM-5(30),

HZSM-5(80), and HZSM-5 (280). So, compared to the thermal decomposition of PP, the catalytic pyrolysis of PP resulted in a different decomposition temperature, suggesting that the decomposition reaction pathway of PP was changed using the catalysts

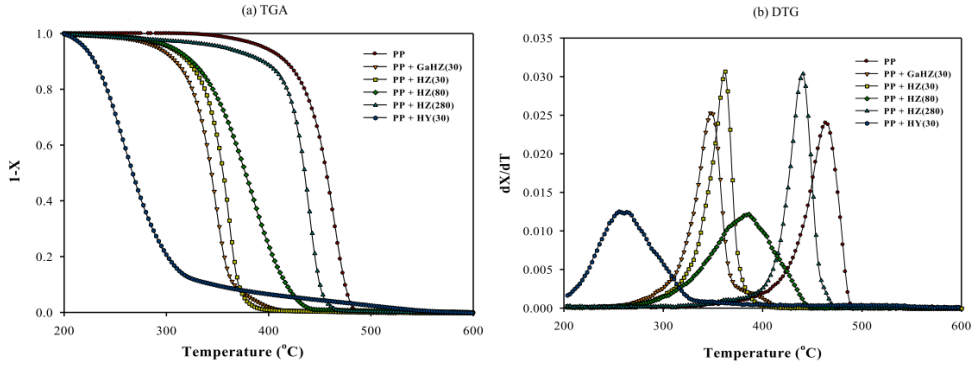

Figure 1: TGA and DTG curves for the TCP of PP at 10 C/min.

However, Ga/HZSM-5(30) revealed the lowest apparent activation energy (Ea), 110 kJ/mol, than HY(30) (159 kJ/mol), and other HZSM-5 catalysts (122 ~ 172 kJ/mol) (Figure 2 (a)), suggesting its high efficiency lowering E_a on PP pyrolysis. Moreover, as shown in Figure 2 (b), Py-GC/MS results suggested that Ga/HZSM-5 produces the largest amount of aromatic hydrocarbons, followed by HZSM-5(30), HZSM-5(80), HY(30), and HZSM-5(280). This confirms that the acceleration of PP cracking and aromatics formation was occured by the additional use of Ga with HZ.

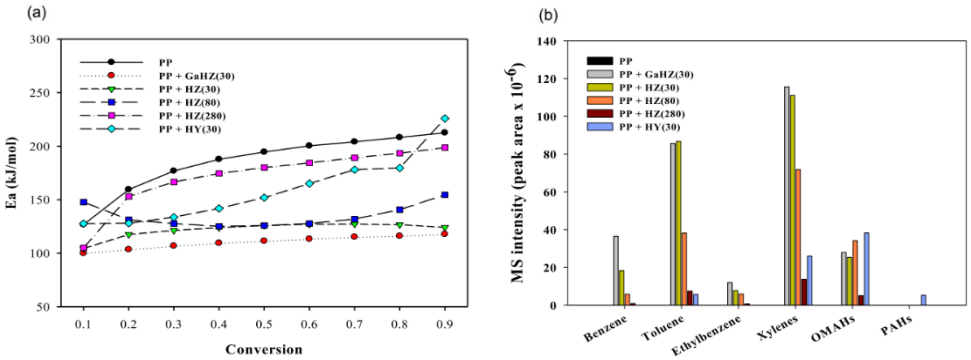

Figure 2: (a) E_a values for the TCP of PP over various catalysts from kinetic analysis, (b) Pyrolytic product materials obtained from the PP with HZ and HY catalysts.

Notably, the increase of Ga/HZSM-5(30) amount on PP pyrolysis led the further decrease of E_a value and increase of aromatics production efficiency. The cracking and aromatics formation efficiency over both HZ(30) and GaHZ(30) also increased after increasing the catalyst to PP ratio from 1/1 to 5/1.

Acknowledgements: . This work was supported by Korea Environment Industry & Technology Institute (KEITI) through Post Plastic, a specialized program of the Graduate School funded by Korea Ministry of Environment (MOE).

References

Encarnacion, J.D., Park, S.J., Ko, Y.S., 2020. Polymerization of heterophasic propylene copolymer with Me_2Si (2-Me-4-PhInd) $2ZrCl_2$ supported on SiO_2 and SiO_2-$MgCl_2$ carriers. Korean Journal of Chemical Engineering 37, 380-386.

Kassargy, C., Awad, S., Burnens, G., Kahine, K., Tazerout, M., 2018. Gasoline and diesel-like fuel production by continuous catalytic pyrolysis of waste polyethylene and polypropylene mixtures over USY zeolite. Fuel 224, 764-773.

Ng, E.-L., Lwanga, E.H., Eldridge, S.M., Johnston, P., Hu, H.-W., Geissen, V., Chen, D., 2018. An overview of microplastic and nanoplastic pollution in agroecosystems. Science of the total environment 627, 1377-1388.

Santamaria, L., Lopez, G., Arregi, A., Artetxe, M., Amutio, M., Bilbao, J., Olazar, M., 2020. Catalytic steam reforming of biomass fast pyrolysis volatiles over Ni–Co bimetallic catalysts. Journal of Industrial and Engineering Chemistry 91, 167-181.

6th International Conference and Postgraduate Colloquium for Environmental Research 2022 (POCER 2022) 9 - 11 June 2022
Langkawi, Kedah, Malaysia

PCR17042022 – 199: Effect of Nb_2O_5 on NH_4HSO_4 poisoning and thermal degradation over V_2O_5-WO_3/TiO_2 SCR Catalyst

Yoo-jin Jung[a], Jin-sun Cha[a], and Young-kwon Park[b,*]

[a]Material Technology Center, Korea Testing Laboratory, 10 Chungui-ro Jinju-si, Gyeongsangnam-do 52852, Korea

[b] School of Environmental Engineering, University of Seoul, Seoul 130-743, Korea

*Corrensponsing Authors E-mail: catalica@uos.ac.kr

Keywords: SCR; Nb_2O_5-V_2O_5-WO_3/TiO_2; De-NOx; Catalyst poisoning. Thermal regenration

Extended Abstract

Nitrogen oxides (NOx) are considered as the main air pollutants from industrial and automobile exhausts, which have caused a lot of environmental problems, such as acid rain, photochemical smog, ozone depletion and greenhouse effect(Ma et al., 2015). Currently, among the developed various techniques for NOx abatement, the selective catalytic reduction of NOx by ammonia (NH_3-SCR) is accepted to be an effective method to eliminate NOx pollutants(Wang et al., 2019). As a typical and efficient catalyst, a V_2O_5-WO_3(MoO_3)/TiO_2 catalyst used in NH_3-SCR technology has been commercialized for several decades, even though it still has some drawbacks to solve such as narrow operation temperature range, low N_2 selectivity, low thermal stability and the volatility and toxicity of vanadium oxide species(Xu et al., 2017). As a result, it is necessary to develop novel environmental friendly metal oxide NH_3-SCR catalyst which possesses excellent low-temperature deNOx activity, high N_2 selectivity and strong thermal stability in a broad operation temperature window(Zhang et al., 2021, Chen et al., 2017.)

Recently, for this reason, NbOx has attracted much attention as a promoter to improve the NH_3-SCR performance due to its unique acid property as well as excellent redox property(Sun et al., 2018). When the SCR catalyst reacts at a low temperature, NH_4HSO_4(ammonium bisulfate, ABS) would be inevitably produced through the reaction of SOx, H_2O and NH_3 in the flue gas. The as-formed ABS blocks the pore structures and covers the active sites of catalysts, which exerts a negative effect on the SCR reactions and constitutes the main barrier in commercializing low-temperature SCR systems(Ye et al., 2018, Guo et al., 2009). Thus, the key step for catalyst commercialization is to study the poisoning

properties of catalysts in the low-temperature region. Also for in-situ catalyst regeneration, it is necessary to understand the ABS decomposition behaviors.

In this study, ABS poisoning characteristics of V_2O_5-WO_3/TiO_2 and Nb_2O_5-V_2O_5-WO_3/TiO_2 catalyst at low temperature were investigated. Each catalyst was poisoned at 240℃ for 54 hours at [NH_3]=300ppm, [SO_2]=300ppm, [O_2]=5vol.%, [H_2O]=10vol.%, and the samples were characterized by elemental analysis, N_2 adsorption-desorption, XRD, FT-IR, XPS, EGA-MS method. The deNOx efficiency of each catalyst was measured at [NO]=[NH_3]=[SO_2]=300ppm, [O_2]=5vol.%, [H_2O]=10vol.%. and the interaction between ABS and Nb_2O_5 as well as the thermal decomposition of ABS over each catalyst was investigated.

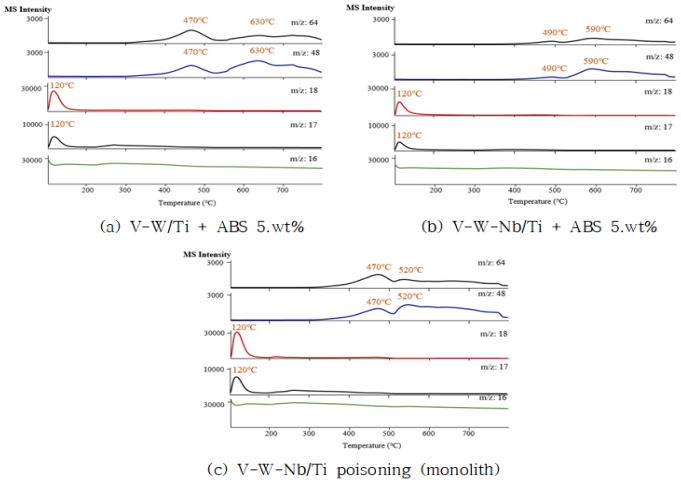

a. V-W/Ti (b) Nb-V-W/Ti

Fig. 1. EGA-MS profiles of (a) V-W/Ti (b) Nb-V-W/Ti poisoned with ABS

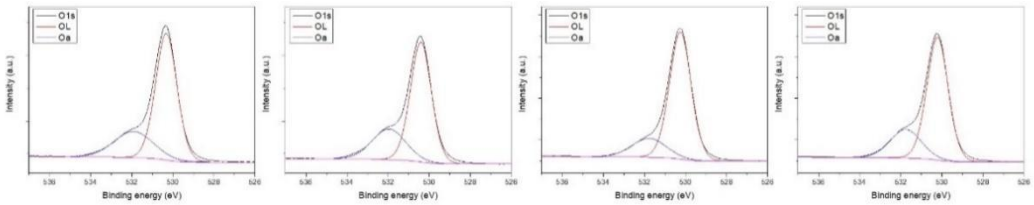

(a) V-W/Ti (b) ABS V-W/Ti (c) Nb-V-W/Ti (d) ABS Nb-V-W/Ti

Fig. 2. O1s X-ray photoelectron spectroscopy(XPS) spectra of (a) V-W/Ti (b) ABS V-W/Ti (c) Nb-V-W/Ti (d) ABS Nb-V-W/Ti

Acknowledgements: This work was supported by the Korea Ministry of Trade, Industry and Energy (MOTIE) as “Development of NOx Removal Catalyst with Wide Temperature Window (No. 20005721).”

References

Chen, H., Xia, Y., Huang, H., Gan, Y., Tao, X., Liang, C., Luo, J., Fang, R., Zhang, J., Zhang, W., Liu, X. 2017. Highly dispersed surface active species of Mn/Ce/TiW catalysts for high performance at low temperature NH_3 -SCR. Chemical Engineering Journal 330, 1195–1202.

Guo, X., Bartholomew, C., Hecker, W., Baxter, L. L. 2009. Effects of sulfate species on V_2O_5/TiO_2 SCR catalysts in coal and biomass-fired systems. Applied Catalysis B: Environmental 92(1-2), 30–40.

Ma, Z., Wu, X., Si, Z., Duan, S., Ma, J., Xu, T.,2015. Impacts of niobia loading on active sites and surface acidity in $NbOx/CeO_2–ZrO_2$ NH_3–SCR catalysts, Applied Catalysis B: Environmental, 179, 380-394.

Sun, P., Huang, S-x., Guo, R-t., Li, M-y., Liu, S-m., Pan, W-g., Fu, Z-g., Liu, S-w., Sun, X., Liu, J., 2018. The enhanced SCR performance and SO_2 resistance of Mn/TiO_2 catalyst by the modification with Nb: A mechanistic study, Applied Surface Science 447, 479–488.

Wang, X.W.; Li, L.L.; Sun, J.F.; Wan, H.Q.; Tang, C.J.; Gao, F.; Dong, L. 2019. Analysis of NOx emission and control in China and research progress in denitration catalysts. Ind. Catal., 27, 1–23

Xu, H., Lin, Q., Wang, Y., Lan, Li., Liu, S., Lin, C., Wang, C., Wang, Q., Wang, J., 2017. Promotional effect of niobium substitution on the low-temperature activity of a WO_3/CeZrOx monolithic catalyst for the selective catalytic reduction of NOx with NH_3, RSC Adv., 7, 47570-47582

Ye, D., Qu, R., Zheng, C., Cen, K., Gao, X., 2018. Mechanistic investigation of enhanced reactivity of NH_4HSO_4 and NO on Nb and Sb-doped VW/Ti SCR catalysts, Applied Catalysis A: General, 549, 310-319

Zhang, W., Tang, Y., Lu, C., Zou, J., Ruan, M., Yin, Y., Qing, M., Song, Q. 2021. Enhancement of catalytic activity in NH_3-SCR reaction by promoting dispersibility of $CuCe/TiO_2$-ZrO_2 with ultrasonic treatment. Ultrasonics Sonochemistry 72, 105466.

6th International Conference and
Postgraduate Colloquium for
Environmental Research 2022 (POCER
2022) 9 - 11 June 2022
Langkawi, Kedah, Malaysia

PCR17042022 – 200: Effect of pyrolysis temperature and KOH activation on the adsorption of formaldehyde by sludge derived biochar

Mi-jin Jeon[a,c], Jin-sun Cha[b], and Young-kwon Park[c,*]

[a] Carbon Neutral Maneuver Center, Korea Testing Laboratory, 10 Chungui-ro Jinju-si, Gyeongsangnam-do 52852, Korea

[b] Technology Center, Korea Testing Laboratory, 10 Chungui-ro Jinju-si, Gyeongsangnam-do 52852, Korea

[c] School of Environmental Engineering, University of Seoul, Seoul 130-743, Korea

*Corrensponsing Authors E-mail: catalica@uos.ac.kr

Keywords: SCR; Nb_2O_5-V_2O_5-WO_3/TiO_2; De-NOx; Catalyst poisoning, Thermal regenration

Extended Abstract

Gaseous formaldehyde is one of the major indoor VOCs pollutants, it is well-known carcinogen that causes several health isuues such as eyesm nasal and throat irritations(Salthammer et al., 2010). Several techniques have been used to contol VOCs, adsorption is an economical technique, cost effective, easy to operate, most efficient and flexble technique(Manap et al., 2017). Biochar is black carbon solid material resulting from pyrolysis of biomass under zero or low oxygen concentration and low temperature (Kong et al., 2014). Recently, biochar is used as adsorbent for organic pollutants removal. This is because there are many functional groups at the surface of biochar which affect its adsorption capacity.

In this study, the effect of biochar characteristics by pyrolysis temperature on the adsorption of formaldehyde was investigated. In addition, biochar was activated with KOH, and compare the adsorption properties of commercially available activated carbon. Sludge dereived char (SDC) was produced from fast pyrolysis of sewge sludge at 450, 500, and 550°C, respectively. To improve surface area and porosity, SDC that was generated at 450°C were activated using KOH (Fu et al., 2019).

The adsorption efficiency of formaldehyde in SDC produced from different pyrolysis temeperature was shown in Fig. 1(a), and in activated biochar(SDC-K) and activated carbon was shown Fig. 1(b). In Fig. 1(a), the formaldehyde adsorption efficiency increased as the pyrolysis temperature increased. From the specific surface area measurement results (Table 1), it can be seen that the adsorption efficiency increases as the specific surface area increases. However, activated carbon had relatively low

formaldehyde adsorption efficiency despite the high specific surface area. It can be seen that activated carbon has lower oxygen contents than other SDCs in Table 1 . From the FT-IR results in Fig. 2, it can be seen that oxygen functional groups are hardly formed in activated carbon compared to other SDCs. Yang et al. studied the effect of oxygen-containing functional groups on the adsorption of formaldehyde, and reported that the incorporation of certain oxygen-containing functional groups to the edge of the carbon surface could promote the adsorption of formaldehyde. In this study, the effect of the type of oxygen functional group on the adsorption performance of formaldehyde is to proceed.

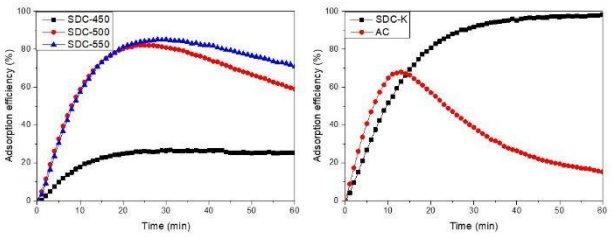

a. (b)

Fig. 1. Adsorption efficiency of formaldehyde (a) SDC produced from different pyrolysis temeperature (b) activated SDC and activated carbon

Table 1. Physico-chemical properties of SDCs, SDC-K and AC

sample	BET surface area (m^2/g)	Total pore volume(cm^3/g)	Ave. pore size(nm)	O
SDC-450	3.28	0.053	64.7	13.22
SDC-500	25.02	0.034	5.5	14.29
SDC-550	108.01	0.027	1.0	17.43
SDC-K	1,231.65	0.661	2.1	18.60
AC	1,495.06	0.775	2.0	1.03

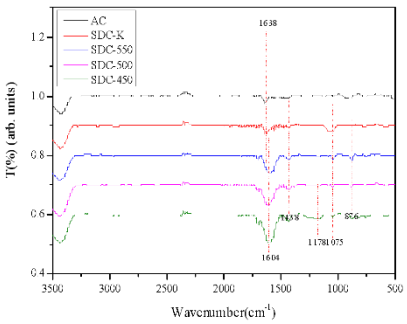

Fig. 2. FT-IR spectra of SDCs, SDC-K, and AC

Acknowledgements: This study was supported by the National Research Foundation of Korea (NRF) (2022R1A2C1013034).

References

Fu, Y., Shen, Y., Zhang, Z., Ge, X., Chen, M., 2019. Activated bio-chars derived from rice husk via one- and two-step KOH-catalyzed pyrolysis for phenol adsorption. *Sci. Total Environ.*, 646, 1567-1577.

Kong, S-H., Loh, S-K., Bachmann, R.T., Rahim, S.A., Salimon, J., 2014, Biochar from oil palm biomass: A review of its potential and challenges, *Renew. Sustain. Energy Rev*, 39, 729–739.

Manap, N.R.A., Shamsudin, R., Maghpor,M.N., Hamid, M.A.A., Jalar. A., 2018. Adsorption isotherm and kinetic study of gas-solid system of formaldehyde on oil palm mesocarp bio-char: Pyrolysis effect. *J. Env. Chem. Eng*., 6, 970-983.

Salthammer, T., Mentese, S., Marutzky, R., 2010. Formaldehyde in the indoor environment, *Chem. Rev.*, 110, 2536–2572.

Yang, X., Zhao, H., Qu, Z., He, M., Tang, Z., Lai, S., Wang, Z., 2021. The effect of oxygen-containing functional groups on formaldehyde adsorption in solution on carbon surface: A density functional theory study. *J. Env. Chem. Eng*., 9, 105987.

6th International Conference and
Postgraduate Colloquium for
Environmental Research 2022 (POCER
2022) 9 - 11 June 2022
Langkawi, Kedah, Malaysia

PCR17042022 – 201: Recycling and characterization of carbon fibers from waste CFRP with a different amine curing agent

Yong-Min Lee[a], Kay-Hyeok An[a], and Byung-Joo Kim[a*]

[a]Department of Carbon-nanomaterials Engineering
Jeonju University, JeonJu, Korea

- Corresponding Author E-mail: kimbyungjoo@jj.ac.kr

Keywords: carbon fiber-reinforced plastic, recycling, tensile properties, interfacial shear strength

Extended Abstract

Carbon fiber-reinforced plastic (CFRP) is a high-performance composite composed of carbon fiber and polymer and has high strength, high modulus, and low density. Due to these advantages, CFRP is being used in renewable energy systems, automotive parts, aerospace, and sports industries. In 2018, the global usage of CFRP was approximately 128 kilotons, and the annual global demand of CFRP is estimated to reach 199 kilotons by 2022. The increased consumption of CFRP has resulted in substantial energy and materials consumption during the production process and generates significant quantities of waste. CFRP waste was disposed of by landfilling, but landfilling is currently prohibited due to stricter regulations. To recover high-quality carbon fibers from CFRP waste, a method was used to decompose the resin. Chemical decomposition and thermal incineration were used in CFRP recycling method. Chemical decomposition uses chemical agents to decompose the resin to recover carbon fibers. Several solvents, such as acid, peroxide, supercritical alcohol, and supercritical acetone have been used as media for the chemical decomposition processing of epoxy resin. Chemical decomposition can maintain a high recovery rate and suitable strength of carbon fibers. However, the high price of chemical reagents and processes of massive harmful gases are the major drawback of recycling carbon fibers from chemical decomposition. Another method is thermal incineration. Conventional thermal incineration used N_2 and O_2 gases to decompose epoxy resin. However, it requires a high temperature of 600-1200°C to decompose the resin, so it is high price and generates low quality and harmful gases due to oxidation and adsorption. Super-heated steam was applied to the process to maintain the excellent mechanical properties of the carbon fibers. Super-heated steam is readily available water and has the characteristic that uniform heating is possible. In this study, 4,4'-diaminodiphenyl methane (DDM) and 4,4'-

diaminodiphenyl sulfone (DDS) were used as curing agents for the epoxy to prepare CFRP and pyrolyze it. CFRPs were carried out under two gas atmospheres (steam and air), and the pyrolysis temperature and time were set in the range of 500-600°C and 60-180 min, respectively. The universal testing machine measured the tensile strength, modulus, and interfacial shear strength (IFSS) of recycled carbon fibers (UTM). The functional group changes with the thermal decomposition conditions were observed by Fourier-transform infrared spectroscopy (FT-IR) and x-ray photoelectron spectroscopy (XPS). Also, the recovered decomposition product was investigated by nuclear magnetic resonance (NMR). As a result, the tensile strength, modulus, and IFSS of the recycled carbon fibers were found that all recycled carbon fibers had over 80% of the strength of as-received carbon fiber.

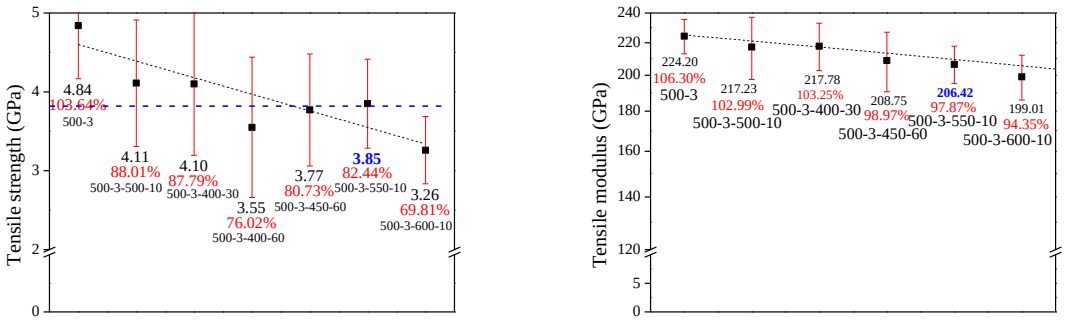

Figure 1. Tensile strength and modulus of the carbon fibers recycled in steam and air atmospheres.

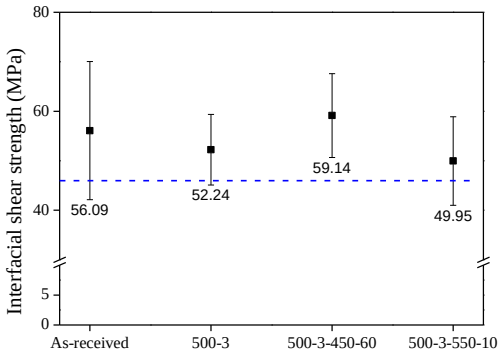

Figure 2. Interfacial shear strength of the carbon fibers recycled in steam and air atmosphere.

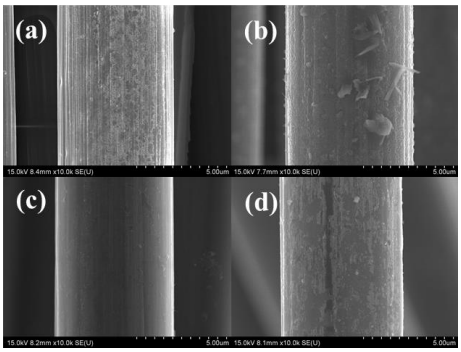

Figure 3. Surface morphologies of recycled carbon fibers; (a) 500-3-450-60, (b) 500-3-500-10, (c) 500-3-550-10, and (d) 500-3-600-10.

Acknowledgements: This work was supported by the Technology Innovation Program (20012817, The development of functional parts manufacturing technology which is costreduced more than 15% by upcycling of carbon fiber and intermediate materials) funded by the Ministry of Trade, Industry and Energy (MOTIE, Korea).

References

Kim, K.W., Lee, H.M., An, J.H., Chung, D.C., An, K.H., Kim, B.J., 2017. Recycling and characterization of carbon fibers from carbon fiber reinforced epoxy matrix composites by a novel super-heated-steam method. *J. Environ. Manage.*, 203, 872-879.

Jeong, J.S., Kim, K.W., An, K.H., Kim, B.J., 2019. Fast recovery process of carbon fibers from waste carbon fibers-reinforced thermoset plastics. *J. Environ. Manage.*, 247, 816-821.

6th International Conference and
Postgraduate Colloquium for
Environmental Research 2022 (POCER
2022) 9 - 11 June 2022
Langkawi, Kedah, Malaysia

PCR17042022 – 202: Effects of hybrid stabilization methods on textural properties of HDPE-based activated carbon fibers

Jeong-Rae Ahn [a], Kay-Hyeok An[a], and Byung-Joo Kim[a*]

[a] Department of Carbon-nanomaterials Engineering
Jeonju University, JeonJu, Korea

- Corresponding Author E-mail: kimbyungjoo@jj.ac.kr

Keywords: Polyolefin, Stabilization, Oxidation, Sulfonation, Activated carbon fiber

Extended Abstract

Activated carbon fibers (ACF) have a high specific surface area and a well-developed pore structure. Therefore, they are widely used as environmental materials. Moreover, they can possess various surface functional groups with an affinity for different adsorbates, so these features provide them with high adsorption kinetics and capacities. However, the excessively high costs of ACFs, which are mainly related to the production costs of the polyacrylonitrile (PAN) precursors used for their production, still represent a significant impediment to their widespread use.

Recently, ACF has been produced using polyethylene (PE), which is a relatively inexpensive material. PE precursors in aliphatic polymers are not stable during the carbonization process. Thermally decompose into mostly volatile aliphatic and olefinic compounds completely. Most studies have used sulfuric acid treatment at 180°C or higher to impart thermal stability to thermoplastic polyethylene. However, precursor fibers are easily broken at such high temperatures and alter the fiber's shape, making it challenging to develop a continuous process. Based on these disadvantages, a method that allows for sulfonation at temperatures that do not exceed 100°C is required.

When an electron beam and sulfonation treatment are applied to polyethylene fibers, it can accelerate sulfonation at a relatively low temperature. However, this method also does not allow sulfonation at temperatures not exceeding 100°C.

Thus, this study proposes the hybrid stabilizing method to convert high-density polyethylene (HDPE) fiber into activated carbon fiber (ACF). The stabilizing process of HDPE fiber was achieved through a hybrid treatment using electron-beam/sulfonation at 80°C/oxidation which was more effective than the traditional method. The stabilized fibers were then carbonized at 800~900°C and activated at 900°C

with different activation times. The structural characteristics and surface texture of these ACFs were observed using an X-ray diffractometer and a field-emission scanning electron microscope. The textural properties were studied using N_2/77 K adsorption isotherms. From the results, difficult to convert the HDPE fibers sulfonated at 80°C fibers because of their lower thermal stability but oxidized sulfonated fiber could be converted to activated carbon fibers because of improved thermal stability. In addition, the oxidation process was possible to control the crystallinity of the stabilized fiber by adjusting the oxidation process time.

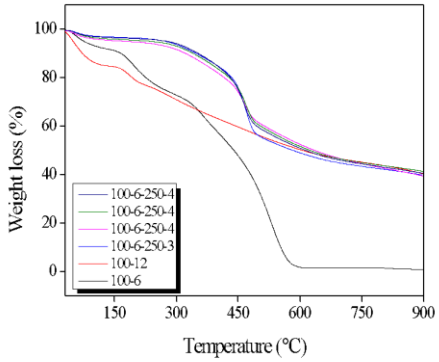

Figure 1. TGA curves of stabilized HDPE fibers as a function of various oxidation times.

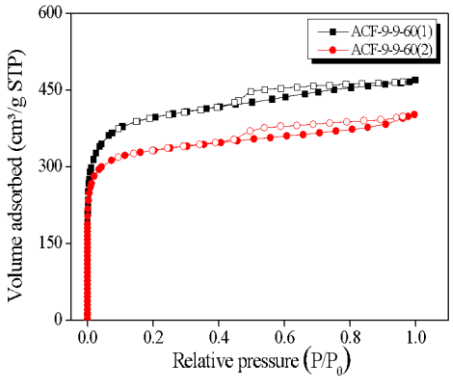

Figure 2. N_2/77K adsorption isotherm curves of HDPE-based activated carbon as a function of various oxidation times.

Acknowledgments: This research was funded by Nano-Material Technology Development Program through the National Research Foundation of Korea (NRF) funded by the Ministry of Science and ICT (NRF-2019M3A7B9071501).

References

Kang, S.-H.; Kim, K.-W.; Kim, B.-J., 2021. Carbon Fibers from High-Density Polyethylene Using a Hybrid Cross-Linking Technique. Polymers. 13, 2157.

Kim, K.-W.; Lee, H.-M.; Kang, S.-H.; Kim, B.-J., 2021. Synthesis and Characterization of Activated Carbon Fibers Derived from Linear Low-Density Polyethylene Fibers Stabilized at a Low Temperature. Polymers. 13, 3918.

6th International Conference and
Postgraduate Colloquium for
Environmental Research 2022 (POCER
2022) 9 - 11 June 2022
Langkawi, Kedah, Malaysia

PCR17042022 – 203: Effects of electron beam irradiation on DMMP adsorption behaviors of activated carbon fibers

Ju-Hwan Kim[a], Hye-Min Lee[a*], and Byung-Joo Kim[b*]

[a] Convergence Research Division
Korea Carbon Industry Promotion Agency (KCARBON), JeonJu, Korea
[b] Department of Carbon-Nanomaterials Engineering
Jeonju University, JeonJu, Korea

- Corrensponsing Author E-mail: kimbyungjoo@jj.ac.kr

Keywords: chemical protective overgarment, DMMP, activated carbon fiber, e-beam

Extended Abstract

Protection against emissions of chemical warfare agents (CWAs) is a significant social and military concern. A CWA is a chemical substance whose toxicity is used to kill, wound, or incapacitate people. sarin and soman nerve agents, a potent vesicant, has been used since World War I. Sarin and soman nerve agents are a nerve agent, interfering with normal functioning of the mammalian nervous system by inhibiting the enzyme cholinesterase. Therefore, studies on chemical protective overgarments are essential for protecting the human body from CWAs.

The Dimethyl methylphosphonate (DMMP, $CH_3PO(OCH_3)_2$) molecule is a simulant for sarin and soman nerve agents. The DMMP molecule is much less toxic, yet it has a chemical and crystal structure very similar to sulfur mustard but without one chlorine atom. Therefore, DMMP is used in the laboratory instead of sulfur mustard for research purposes because it can mimic the reactivity of sulfur mustard.

Chemical protective overgarments for protection against emissions from CWAs are classified as impermeable and permeable. Impermeable protective clothing is expected to provide excellent protection against CWAs, but it cannot be worn for a long time due to the heat load. Permeable protective clothing has been developed in which a layer of porous materials are bound between two layers of textile to reduce the heat load. The porous materials are made up of activated carbon (AC) pellets (Saratoga carbon pellet, Blucher GmbH, Germany), and the CWAs are absorbed on the AC pellets. Therefore, the shielding performance of the permeable protective clothing against CWAs is

depended on the performance of the activated carbon. AC with its excellent adsorption capacity has been studied for the long-term protection of permeable protective clothing. The adsorption rate (or speed) of activated carbon is also essential in protective systems. The adsorption capacity and rate of adsorbing media in permeable protective clothing depends on the pore structure of the adsorbent. In AC uses in protective clothing, the pores of activated carbon fiber (ACF) open directly to the outer surface, and the sizes of the pores fall within a narrow distribution. The unique pore structure of this ACF enables a higher specific surface area and faster adsorption rate than ordinary AC.

In this work, ACF were modified via e-beam irradiation at various doses for use as an adsorption material in chemical protective overgarment. The N_2 adsorption isotherm characteristics at 77K were confirmed by Brunauer-Emmett-Teller, Barrett-Joyner-Halenda and non-local density functional theory equations. The surface properties of e-beam irradiated ACF were characterized using an X-ray photoelectron spectroscopy. The DMMP adsorption capacities of the ACF were measured by breakthrough experiments in the gas phase (120 μg/mL of DMMP in N_2 flow). The textural properties of the ACF was largely unchanged by the e-beam irradiation. The DMMP adsorption capacity of the ACF treated with the e-beam at radiation doses of 200 kGy increased by 14 times compared with the untreated ACF. The enhancement of the DMMP adsorption capacity of the e-beam irradiated ACF can be attributed to a change in their surface functional group.

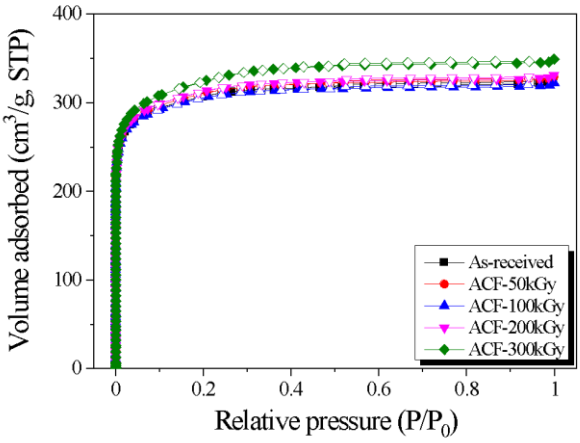

Figure 1. Nitrogen adsorption curves of electron beam-irradiated activated carbon fiber.

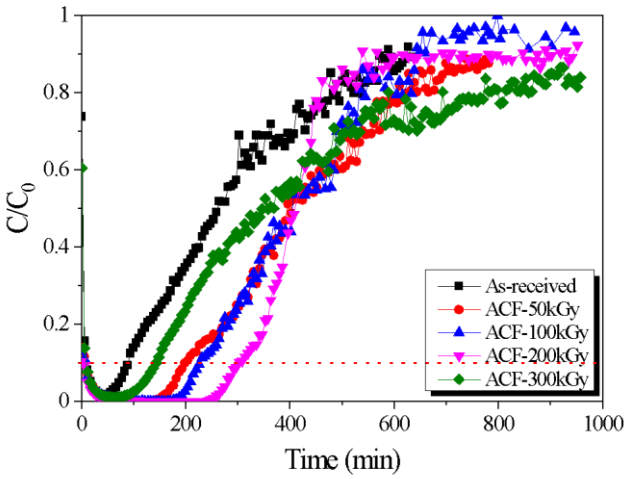

Figure 2. Breakthrough curves of electron beam-irradiated activated carbon fiber.

Acknowledgements: This work was supported by the Technology Innovation Program (20013073, Development of porous carbonbased filter materials and components) funded by the Ministry of Trade, Industry and Energy (MOTIE, Korea).

References

Lee, H.M., Lee, B.H., Park, S.J., An, K.H., Kim, B.J., 2019. Pitch-Derived Activated Carbon Fibers for Emission Control of Low-Concentration Hydrocarbon. *Nanomaterials*. 9, 1313.

Lee, H.M., Lee, B.H., Kim, J.H., An, K.H., Park, S.J., Kim, B.J., 2019. Determination of the optimum porosity for 2-CEES adsorption by activated carbon fiber from various precursors. *Carbon Lett*. 29, 649-654.

Mangun, C.L., Benak, K.R., Economy, J., Foster, K.L., 2001, Surface chemistry, pore sizes and adsorption properties of activated carbon fibers and precursors treated with ammonia. *Carbon*. 39, 1809-1820

6th International Conference and
Postgraduate Colloquium for
Environmental Research 2022 (POCER
2022) 9 - 11 June 2022
Langkawi, Kedah, Malaysia

PCR17042022 – 204: Effect of oxygen-containing functional groups on elctrochemical performance of activated carbon for EDLC

Ju-Hwan Kim[a], Hye-Min Lee[a*], Ju-Hwan Kim, Kay-Hyeok An, Byung-Joo Kim[b*]

[a] Convergence Research Division
Korea Carbon Industry Promotion Agency (KCARBON), JeonJu, Korea
[b] Department of Carbon-Nanomaterials Engineering
Jeonju University, JeonJu, Korea

- Corrensponsing Author E-mail: kimbyungjoo@jj.ac.kr

Keywords: activated carbon, oxygen functional group, supercapacitor, reduction, charge transfer resistance

Extended Abstract

As a new type of charge storage devices, supercapacitors are attracting more and more attention because of their high power density and long cyclic life compared with batteries and high energy density relative to traditional capacitors. According to the energy storage mechanism, supercapacitors can be divided into two classes, electric double-layer capacitors (EDLCs), depending on the pore structure of the electrode materials, and pseudocapacitors based on the active electrode materials, in which the Faradic redox process occurs. To develop supercapacitors with high performance, various materials have been examined as possible electrode materials. Among them, porous carbons, which have high porosity, a large surface area, and good conductivity, have been used most widely.

In general, a large surface area is considered necessary for charge accumulation for a high energy density EDLC electrode material. However, electric double-layer capacitance (CEDL) cannot be enhanced illimitably because the excessive increase of surface area causes a huge decrease of the mesoporosity, thus reducing the mass transfer capacity. Therefore, a number of approaches are under development for optimizing the specific capacitance of carbon materials while keeping a proper mesoporosity.

The oxygen functional group of the activated carbon negatively affects the charge transfer resistance of the EDLC. Oxygen-containing functional groups of activated carbon can be effectively removed by using a temperature programming method. Surface oxygen groups on carbon materials decompose upon

heating by releasing CO and CO at different temperatures. With regards to chemical properties, the effects of oxygen-containing functional groups on electric characteristics have been investigated qualitatively in terms of temperature-programmed desorption; however, there have been few quantitative investigations described in previous reports.

In this study, we investigated the correlation between the oxygen functional group of activated carbons and electrochemical characteristics. Activated carbons with reduced oxygen was prepared in various gas atmospheres for the improving the electrochemical performance of supercapacitors. Besides, the activated carbons were heat-treated at 200-900℃ for one hour under two gas atmosphere (N_2 and H_2/N_2 mixing gas). The textural properties were studied by Brunauer-Emmett-Teller, Barrett-Joyner-Halenda equations, and nonlocal density functional theory with N_2/77K adsorption isotherms. The reduction characteristics of activated carbons were investigated through Temperature Programmed Reduction (TPR) under N_2 and H_2/N_2 mixing gas atmosphere. Also, oxygen functional group changes with the heat-treated condition were observed by FT-IR and XPS. As a result, the decrease in the oxygen functional group of the activated carbon was found by the reduction step. Meanwhile, the electrochemical performance of the activated carbons was significantly enhanced after the reduction process.

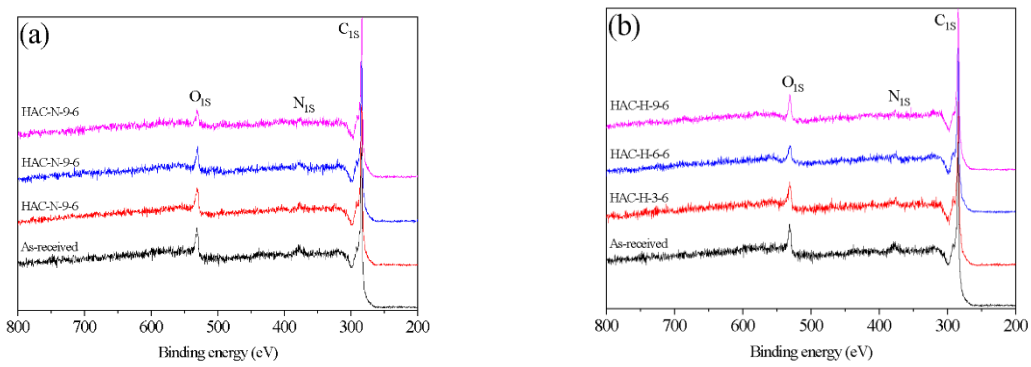

Figure 3. XPS survey spectra of reduced HAC as a function of various reduction condition by (a) N_2 atmosphere, (b) H_2 / N_2 atmosphere..

Table 1. Chemical Compositions of reduced HAC under vaious atmosphere by XPS.

Sample name	Element composition (%)			Element ratio
	O_{1S}	C_{1S}	N_{1S}	O_{1S}/C_{1S}
As-received	7.41	92.59	0.00	0.08
HAC-N-3-6	7.00	93.00	0.00	0.08

HAC-N-6-6	5.50	94.26	0.23	0.06
HAC-N-9-6	3.91	96.08	0.00	0.04
HAC-H-3-6	6.19	93.56	0.25	0.07
HAC-H-6-6	4.54	95.34	0.13	0.05
HAC-H-9-6	4.59	95.41	0.00	0.05

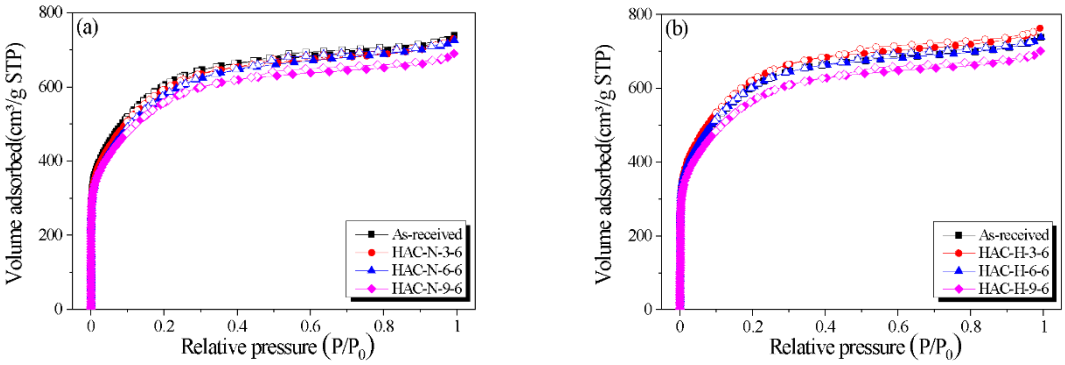

Figure 5. N_2/77K adsorption isotherm curves of reduced HAC as a function of various reduction condition by (a) N_2 atmosphere, (b) H_2 / N_2 atmosphere.

Acknowledgements: This work was supported by the Technology Innovation Program (20016795, Development of manufacturing technology independence of advanced activated carbons and application for high performance supercapacitors) funded by the Ministry of Trade, Industry and Energy (MOTIE, Korea).

References

Figueiredo, J.L., Pereira, M.F.R., Freitas, M.M.A., Órfão, J.J.M., 1999. Modification of the surface cheimstry of activated carbons. *Carbons*. 37, 1379-1389.

Oda, H., Yamashita, A., Minour, S., Okamoto, M., Morimoto, T., 2006. Modification of the oxygen-containing functional group on activated carbon fiver in electrodes of an electric double-later capacitor. *J. Power Sources*. 158, 1510-1516.

6th International Conference and Postgraduate Colloquium for Environmental Research 2022 (POCER 2022) 9 - 11 June 2022
Langkawi, Kedah, Malaysia

PCR17042022 – 205: Fabrication of Ni/TiO_2 visible light responsive photocatalyst for decomposition of Oxytetracycline

Jaegu Park[a], Sang-Chul Jung[a*]

[a] Department of Environmental Engineering, Sunchon national University, Sunchon, Republic of Korea

* Corrensponsing Author E-mail: jsc@sunchon.ac.kr

Keywords: Visible light responsive photocatalyst; antibiotics; Liquid Phase Plasma(LPP);

Extended Abstract

Worldwide antibiotic production is estimated to be about 200,000 tons per year, and tetracycline antibiotics are one of the most used antibiotics [Li et al., 2018, Vaz et al., 2016]. Among the tetracycline antibiotics, Oxytetracycline (OXY) has a low cost and high efficiency, so it is used in large amounts in agriculture and fishery industries worldwide [José Miguel et al., 2020]. Nevertheless, about 90% of OXY is not metabolized and can be excreted, which can cause environmental problems, and since OXY is chemically stable and cannot be easily treated with general wastewater treatment processes, the photofenton method for efficient removal of OXY research on AOPs and TiO_2 photocatalysts are being actively conducted [Almeida et al., 2021, Yan et al., 2018, Giler-Molina et al., 2020]. TiO_2 photocatalyst is widely used to decompose difficult-to-decompose pollutants because of its low price and high chemical stability.

In this study, a photocatalyst responsive to visible light was prepared by precipitating nickel to TiO_2 powder (P25) using the liquid phase plasma (LPP) process. The content of nickel precipitated in TiO_2 powder was increased by increasing the number of LPP processes, and the results are shown in Table 1. TNP-1 is a nickel precipitated by performing the LPP process once, and TNP-5 is a Ni/TiO_2 photocatalyst obtained by performing the LPP process five times. As the number of LPP processes increased, the nickel content in the Ni/TiO_2 photocatalyst showed a tendency to increase.

Table 16. Chemical composition of Ni/TiO_2 photocatalyst prepared by LPP process

Sample name	Ti		O		Ni	
	Wt.%	At.%	Wt.%	At.%	Wt.%	At.%
TNP-1	51.15	25.96	48.70	73.98	0.16	0.06

TNP-3	50.44	25.63	48.63	73.98	0.93	0.39
TNP-5	53.23	28.03	45.23	71.31	1.54	0.66

The band gap energy of the Ni/TiO_2 photocatalysts prepared in this study was measured using UV-VIS diffuse reflection adsorption spectra, and the results are shown in Fig. 1 along with the band gap of the bare TiO_2 photocatalyst. The band gap of the bare TiO_2 photocatalyst was measured to be 389 nm, and the band gap of the Ni/TiO_2 photocatalysts showed a larger value (406 ~ 410 nm) as the nickel content increased.

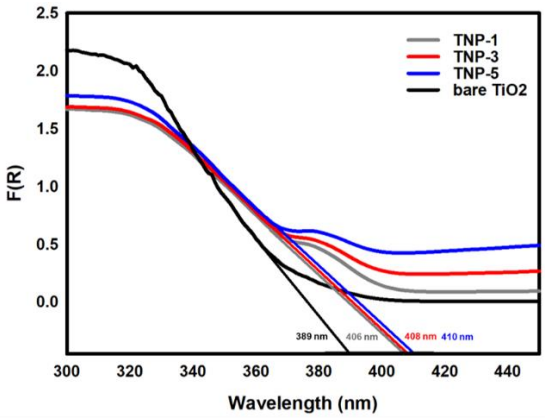

Figure 1 : UV-VIS diffuse reflection adsorption spectra of bare TiO_2 powder and TNPs.

In this study, photoactivity was compared and evaluated by performing decomposition reaction using bare TiO_2 photocatalyst and Ni/TiO_2 photocatalyst in reaction aqueous solution containing 30 ppm of antibiotic OXY to be degraded. For the decomposition reation, each of 100 UV LEDs and blue LEDs were used for UV and visible light sources, and the amount of photocatalyst powder added to the reaction was 0.2 mg/mL. In all photocatalysts, the reaction using ultraviolet light showed a faster decomposition rate than the reaction using visible light, and the photocatalyst activity of the bare TiO_2 photocatalyst was the best in the ultraviolet light source. Meanwhile, in the decomposition experiment using blue LED as a light source, the bare TiO_2 photocatalyst had the lowest activity, and the Ni/TiO_2 photocatalyst with a high nickel content showed a fast decomposition rate.

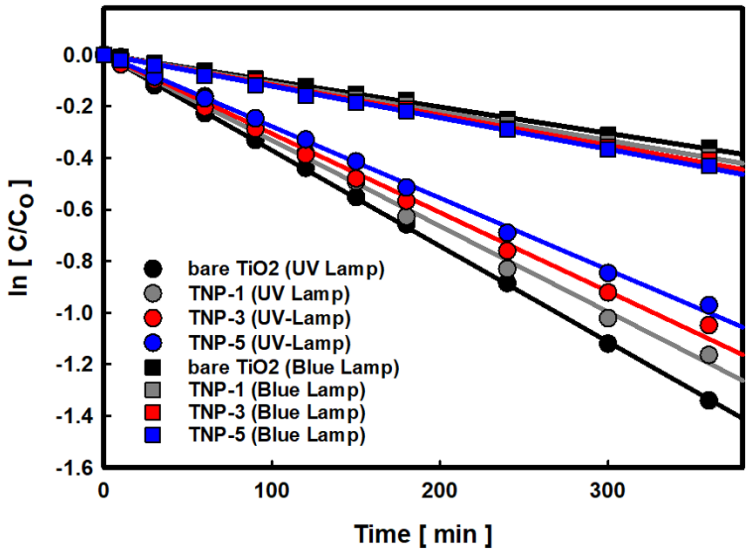

Figure 2. Rate constant of decomposition reaction using various photocatalysts with different LED Lamps.

In this study, a photocatalyst that responds to visible light was successfully prepared by precipitated nickel in TiO_2 powder using the LPP process, and the antibiotic oxytetracycline was successfully decomposed using a Ni/TiO_2 photocatalyst. These results can be applied as a new method to remove antibiotic components that cannot be treated with conventional water treatment methods.

Acknowledgements: This work was supported by the National Research Foundation of Korea(NRF) grant funded by the Korea government(MIST) (NRF-2021R1A2C1006315).

References

Almeida, A.R., Domingues, I., Henriques, I., 2021. Zebrafish and water microbiome recovery after oxytetracycline exposure. *Environ. Pollut.* 272, 116371.

José Miguel Giler-Molina, Luis Angel Zambrano-Intriago, Luis Santiago Quiroz-Fernández, Daniella Carla Napoleão, Judite dos Santos Vieira, Nelson Simões Oliveira, Joan Manuel Rodríguez-Díaz, 2020. Degradation of Oxytetracycline in Aqueous Solutions: Application of Homogeneous and Heterogeneous Advanced Oxidative Processes. *Sustainability* 12, 8807.

Li, Z., Qi, W., Feng, Y., Liu, Y., Ebrahim, S., Long, J., 2019. Degradation mechanisms of oxytetracycline in the environment. *J. Integr. Agric.* 18 (9): 1953-1960.

Vaz, S., 2016. Sorption behavior of the oxytetracycline antibiotic to two Brazilian soils. *Chem. Biol. Technol. Agric.* 3, 6.

Yan, W., Guo, Y., Xiao, Y., Wang, S., Ding, R., Jiang, J., Gang, H., Wang, H., Yang, J., Zhao, F., 2018. The changes of bacterial communities and antibiotic resistance genes in microbial fuel cells during long-term oxytetracycline processing. *Water Res.* 142, 105-114.

6th International Conference and
Postgraduate Colloquium for
Environmental Research 2022 (POCER
2022) 9 - 11 June 2022
Langkawi, Kedah, Malaysia

PCR17042022 – 206: Hydrogen production from hydrocarbons by catalytic decomposition using liquid-phase plasma

Kyong-Hwan Chung and Sang-Chul Jung*

Department of Environmental Engineering Sunchon National University, Sunchon, 57822, Rep. of Korea

*Corrensponsing Author E-mail: jsc@sunchon.ac.kr

Keywords: Hydrogen production; Liquid plasma; Carbon black; CO_2-free; Hydrocabons

Abstract

Hydrogen energy is firmly establishing as a clean future energy to replace fossil fuels. Fuel cell technology using hydrogen is also developing rapidly. However, much of the hydrogen production now depends on the way fossil fuels are used. This method has a fatal problem in emitting carbon dioxide during production. To solve this problem, a method of producing hydrogen without CO2 emission from waste hydrocarbons using plasma is presented herein. The only gaseous product was hydrogen and no CO_2 was generated. The reaction produced hydrogen as the main product and produced nano-sized carbon crystallites. Hydrogen production rate was maximized by using benzene as a reactant. The hydrogen generation rate was improved by applying transition metals loaded on zeolite as a catalyst. The carbon obtained as a solid product contained no impurities. The crystal size was very small and uniform (10 nm or less)

Introduction

In modern society, excessive use of fossil fuels has caused serious environmental problems, such as deteriorating air quality and accelerating global warming. Currently, the international community is aiming to realize a carbon-free society, and for this purpose, the ratio of renewable energy among the energy production is increasing. Hydrogen is a clean energy source that has the advantage that it can be easily converted into other compounds and can be produced in an eco-friendly way. However, since hydrogen has a small storage capacity per volume, it is expensive to store a large capacity, and that long-distance transportation is difficult.

Liquid-phase plasma (LPP) generates a large active species upon initiation (Malik et al. 2013). This active species has the function of generating hydrogen by easily decomposing organic chemicals at a

high speed (Sun et al. 2012). The lowest energy required for H_2 production by plasma discharge was found to be 0.08 kWh/m. This is more efficient than most H_2 production methods such as water electrolysis (Chung et al. 2018). Therefore, plasma discharge technology is regarded as a potential method for efficient hydrogen production. In particular, the LPP technology has the advantage of being able to produce H_2 immediately from liquefied H_2 derivatives.

Experimental

Figure 1 represents a schematic diagram of a photocatalytic reaction device for H_2 production using LPP. 100 mL of liquid hydrocarbons was used for the reaction. The reaction was carried out by directly irradiating the reactants with LPP in the photocatalytic reactor. The temperature inside the LPP reactor was controlled to 25°C by a water circulator. The generated gaseous product was measured for rate of H_2 generated by a mass flow meter for measuring H_2 gas (MFM; MFC Korea, TS- D2200). The composition of the generated gas

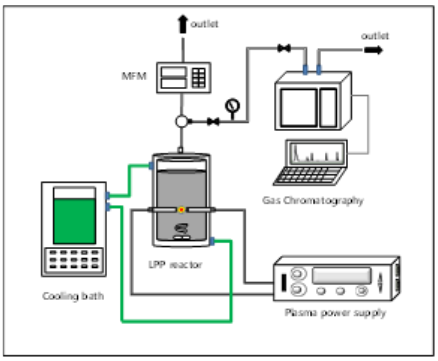

Figure 1. Schematic apparatus of photocatalytic hydrogen production using LPP device.

was analyzed by a gas chromatograph (GC; Yonglin, M600D) equipped with a TCD and Molecular sieve 5A packing column.

Plasma was emitted between the two electrodes within a double annular reactor filled with liquid benzene and a catalyst. As the electrode, a tungsten rod with a needle-shaped tip and a diameter of 4 mm was used. The plasma was discharged using a high-frequency plasma generator (Nano-Technologies, NTTI-1500). Plasma applied to the liquid benzene was discharged with a frequency of 30 kHz and a pulse width of 5 μs at 250 V.

Results and discussion

The only gaseous product was H_2 and no CO_2 was produced from n-hexane. The nano-sized carbons were produced as a solid product. The reaction produced H_2 as the main product and produced nano-

sized carbon particles contained no impurities. The crystal size was very small and uniform (10 nm or less). Figure 2. shows the amount of H_2 generated during 1 h of reaction time and the yield of nano-sized carbon black. Liquid-phase plasma decomposed liquid hydrocarbons with H_2 evolution without injecting a catalyst. When the perovskite catalyst was applied to the reaction using liquid-phase plasma, the rate of H_2 generation was increased significantly.

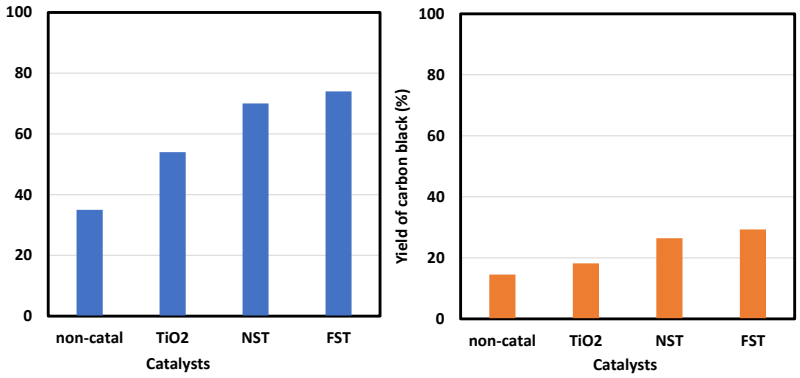

Figure 2. Amount of H_2 generated during 1 h of reaction time and the yield of carbon black.

Conclusion

Hydrogen was produced as a gaseous product in the decomposition reaction of hydrocarbons by LPP. The gaseous product was H_2, and no CO_2 was formed. This reaction produced only H_2 as a gaseous product without by-products. Simultaneously, nano-sized carbon was obtained as a solid product with hydrogen generation. Nanoscale carbon was produced as a solid product. Perovskite catalysts were applied to increase the hydrogen production efficiency. The reaction produced nano-sized carbon particles with hydrogen as the main product with no impurities. The crystal size of carbon black was very small (<10 nm) and uniform.

Acknowledgements: This research was supported by the program of Future Hydrogen Original Technology Development (NRF-2021M3I3A1084797), through the National Research Foundation of Korea (NRF), funded by the Korean government (Ministry of Science and ICT (MSIT)).

References

Malik, M.A., Hughes, D., Malik, A., Xiao, S., Schoenbach, K.H., 2013. Study of the production of hydrogen and light hydrocarbons by spark discharges in diesel, kerosene, gasoline, and methane. *Plasma Chem. Plasma Process* 33: 271-279.

Sun, B., Aye, N.N., Gao, Z., Lv, D., Zhu, X., Sato, M., 2012. Characteristics of gas-liquid pulsed discharge plasma reactor and dye decoloration efficiency. *J. Environ. Sci*. 24: 840-845.

Chung, K.-H., Park, H., Jeon, K.J., Park, Y.-K., Jung, S.-C., 2018. Irradiation of liquid phase plasma on photocatalytic decomposition of acetic acid-containing wastewater over metal oxide photocatalysts. *Catal Today* 307:131-139.

6th International Conference and
Postgraduate Colloquium for
Environmental Research 2022 (POCER
2022) 9 - 11 June 2022
Langkawi, Kedah, Malaysia

PCR17042022 – 207: Sweat electrolyte functioning on Textile supercapacitors from PEDOT:TREN/MnO_2@$MnCO_3$ composite for wearable approach

Samayanan Selvam[a,c], Kasirajan Kasinathan[a], Young-Kwon Park[b], Jin-Heong Yim[a*]

[a] Division of Advanced Materials Engineering, Kongju National University, Budaedong 275, Seobuk-gu, Cheonan-si, Chungnam 31080, South Korea

[b]Faculty of Environmental Engineering, University of Seoul, Seoul 130-743, Korea
[c]BioMe- Live Analytical Centre, Karaikudi-630003.

*Corrensponsing Author E-mail:jhyim@kongju.ac.kr

Keywords: Smart electrodes; wearable devices; supercapacitors; ionic liquid; Tris(2-aminoethyl)amine; $MnCO_3$.

Extended Abstract

We explores high flexible all solid state thin film supercapacitors integrated on textile fabric for sweat electrolyte based energy storage devices as wearable smart devices approach. The composite film electrodes fabricated using PEDOT:PTREN:MnO_2@$MnCO_3$ polymer hydrogel chelate decorated composites. The active materials made hydrothermally under $BMIMBF_4$ ionic liquid assistant. X-ray diffraction, X-ray photoelectron spectroscopy, and scanning electron microscopy examinations are used to examine physio-chemical qualities and surface morphological features. The composites's XPS outlines reveal expected peaks of Mn $2p_{1/2}$ (653.2 eV), Mn $2p_{3/2}$ (641.3 eV), N1s (401.4 eV), and C1s (285.3 eV). The mechanical and flexibility of solid state thin film supercapacitor results in a significant areal capacitance and a high energy density. After 10,000 charge-discharge cycles, these supercapacitors retain 92% of their initial performances and the biocompatibility studies also exposed good results. The textile fabricated device performed well on ionic liquid and sweat @ionic liquid dual electrolyte modes and the exhibited biocompatibility results also good. The thin film supercapacitor based supercapacitor may tenderfoot for the appropriateness to wearable smart and textile based energy storage system.

Figure 1: Schematic representation of sweat electrolyte on textile supercapacitor

To preapre MnO_2@$MnCO_3$ particles, a new method was applied. The metal oxide and carbonates were made using the hydrothermal technique using potassium permanganate, methanol, and DMF. MnO_2 and $MnCO_3$ were formed in the following way [1]. The composite preapration and incorporation on textile fabric (cotton)are schematically mentioned in Fig. 1 and 2.

$$5CH_3OH + 4MnO_4^- + 12H^+ \rightarrow 4Mn^{2+} + 11H_2O + 5HCOOH \quad (1)$$

$$(CH_3)2NCHO + MnO_4^- + 6H^+ \rightarrow (CH_3)2NH + Mn^{2+} + CO_2 + 3H_2O \quad (2)$$

$$MnO_4- + Mn^{2+} \rightarrow 2MnO_2 \quad (3)$$

$$CO_2 + H_2O \rightarrow CO_3^{2-} + 2H^+ \quad (4)$$

$$Mn^{2+} + CO_3^{2-} \rightarrow MnCO_3 \quad (5)$$

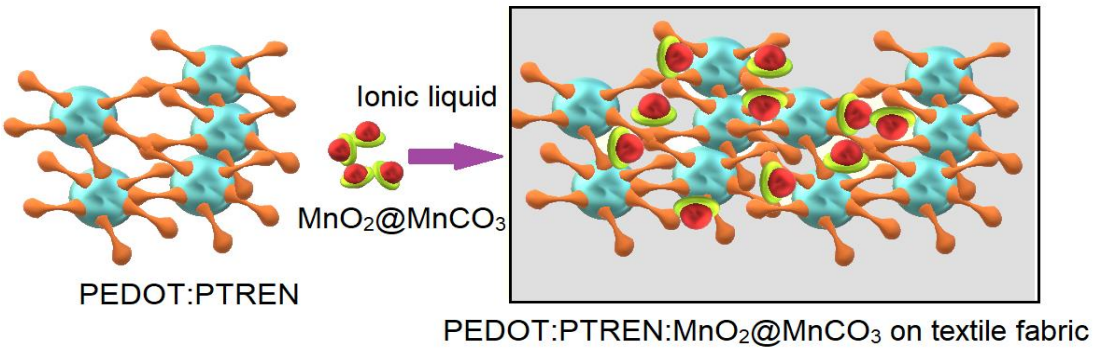

Figure 2: PEDOT:PTREN:MnO_2@$MnCO_3$ composite preaparation

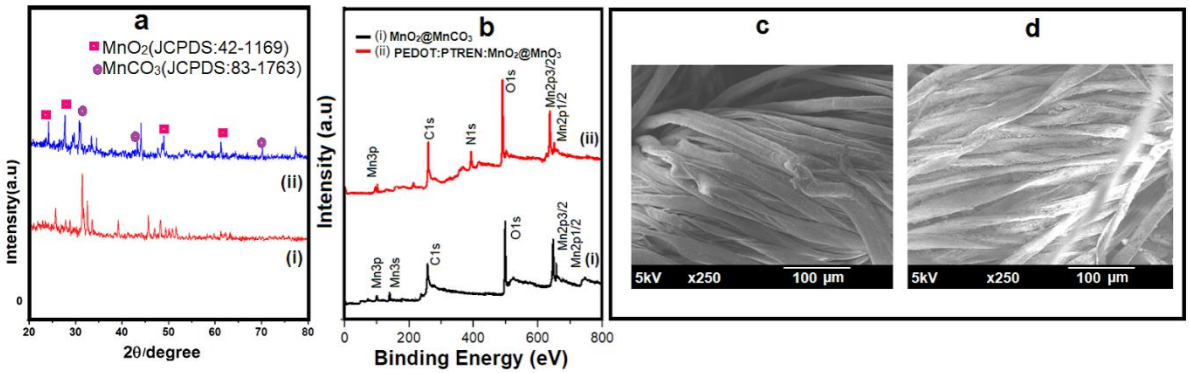

Figure 3: XRD (a), XPS (b) of MnO_2@$MnCO_3$ and PEDOT:PTREN:MnO_2@$MnCO_3$ composite and SEM images of untreated and composite treatd textile fabric (c and d)

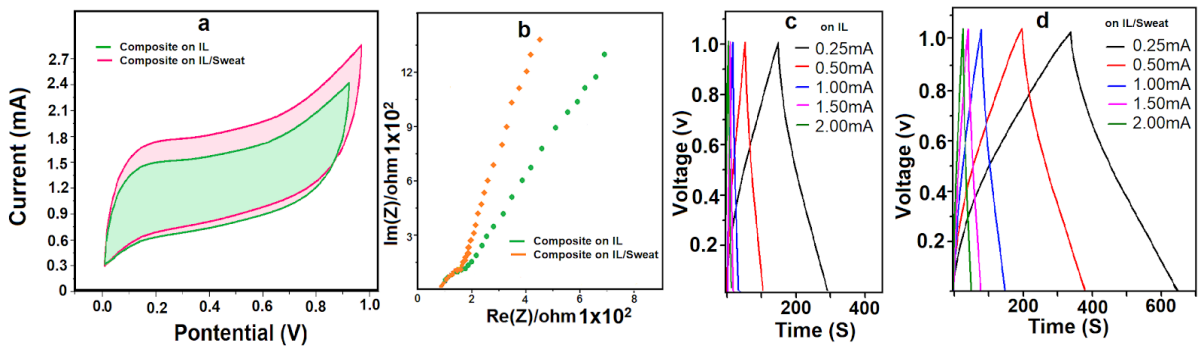

Figure 4: Cyclic voltammetry, Electrochemical impedance and galvanostatic charge discharge profile of textile supercapacitor under ionic liquid and sweat @ ionic liquid mode respectively

Acknowledgements: This research was supported by the Basic Science Research Program through the National Research Foundation of Korea (NRF) funded by the Ministry of Education (NRF-2019R1I1A3A01054826).

References

Selvam, S, Yim, J, -H, High temperature-functioning ceramic-based ionic liquid electrolyte engraved planar HAp/PVP/MnO_2@$MnCO_3$ supercapacitors on carbon cloth, J. Mater. Chem. A, 9 (2021), 14319-14330.

6th International Conference and
Postgraduate Colloquium for
Environmental Research 2022 (POCER
2022) 9 - 11 June 2022
Langkawi, Kedah, Malaysia

PCR19042022 – 208: Actual operation of direct urea fuel cells and their role in achieving the sustainable development goals

Enas T. Sayed[a,b*], Mohammad A. Abdelkareem[a,b], Nabila Shehata[c], Tabbi Wilberforce[d], Kyu-Jung Chae[e], A.G. Olabi[a,d]

[a]Sustainable Energy & Power Systems Research Centre, RISE
University of Sharjah, P.O. Box 27272, Sharjah, United Arab Emirates

[b]Chemical Engineering department, Faculty of Engineering
Minia University, Elminia, Egypt

[c]Environmental Science and Industrial Development Department,
Beni-Suef University, Beni-Suef, Egypt.

[d]Mechanical Engineering and Design
Aston University, Aston Triangle, Birmingham, B4 7ET, UK

[e]Interdisciplinary Major of Ocean Renewable Energy Engineering
Korea Maritime and Ocean University, 727 Taejong-ro, Busan 49112, Republic of Korea

*Corresponding author Email: e.kasem@mu.edu.eg

Abstract:

Securing fresh water and sustainable clean energy sources are the top priorities of human beings. Wastewater is produced daily in massive amounts and requires proper treatment before safe discharge to the environment. Traditional wastewater treatment methods are complicated and consume a large amount of energy produced from fossil fuels, accompanied by severe environmental impacts. Direct urea fuel cells (DUFCs) are novel methods that can be used for simultaneous treatment of urea contaminated wastewater and electricity generation. Recently there has been rapid progress in operating DUFCs under real operation conditions with a high power output using a complete non-precious catalyst. This work summarizes the recent progress done in the actual operation of the DUFCs, emphasizing the progress done in preparing the anode and cathode catalysts, electrolyte membrane, operation conditions, ..etc. Moreover, the role of the DUFCs in achieving the 17th development goals set by the united nations is elaborated.

Keywords:

Direct urea fuel cells (DUFC); In-situ fuel cell operation; sustainable development goals (SDGs); Indicators; wastewater treatment.

The rapid progress in the world population and the recent technological advances resulted in increased energy consumption that comes from fossil fuels. Fossil fuels are not only limited in resources

but also have severe environmental impacts (Olabi et al., 2022; Wilberforce et al., 2021a). While wastewater is daily produced in large amounts, whether domestic, municipal, or industrial, there is an apparent deficiency in freshwater resources. The conventional treatment methods of this wastewater are dependent on the aeration tanks that require a significant amount of energy and produce unsafe aerobic sludge (Wilberforce et al., 2021b). Fuel cells are efficient energy conversion devices with no or low environmental impacts (Abdelkareem et al., 2021). Direct urea fuel cells are emerging types of fuel cells that can simultaneously treat urea contaminated wastewater and produce electricity (Sayed et al., 2019). Extensive work has been done to overcome the challenges of the direct urea fuel cells, i.e., cost and low power output, through the development of efficient non-precious anode and cathode catalysts (Abdelkareem et al., 2020). Our group reported that the nanosheet structure of the metal chalcogenides (Nickel selenide), is effectively used as the anode of the DUFC and Prussian blue is used as the cathode in DUFC under real fuel cell operation, producing a high power output of 33 mW/cm^2 at room temperature, as can be seen in Figure 1 (Sayed et al., 2021). Several reports demonstrated the potential of the DUFCs in the simultaneous wastewater treatment and electricity generation under actual fuel cell operation.

All UN member states endorsed the UN 2030 Agenda for Sustainable Development in 2015, which provides "a shared blueprint for prosperity and peace for humans and the environment, either now or in the future"(Marvila et al., 2021). The 17 Sustainable Development Goals (SDGs) are at the core of this strategy as an urgent appeal for global cooperation. These SDGs have been broken down into 169 particular targets in order to attain them. Energy and water, and more especially, clean water and clean energy, are at the heart of the SDGs, with SDG 6 “clean water and sanitation” and SDG-7 "Affordable and Clean Energy" serving as key drivers of the major SDGs. The widespread use of DUFC as an energy harvester of urea contaminated wastewater significantly impacts most of the SDGs.

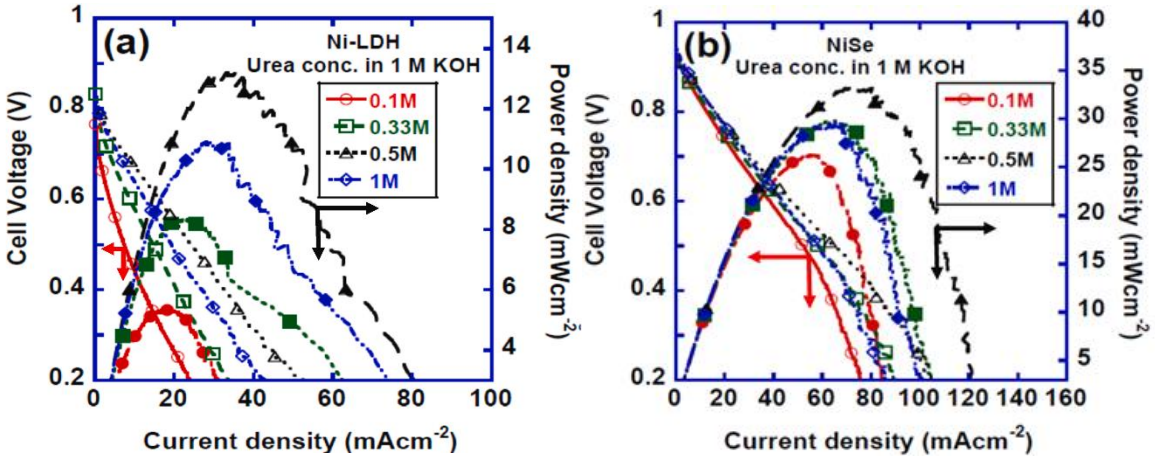

Figure 1: Actual performance, i.e., i-V and i-P, of DUFCs using (a) Ni-LDH anode and (b) Ni–Se anode. Different urea concentrations in KOH (1 M) at the anode, and H_2O_2 (2 M) in H_2SO_4 (2 M) at the cathode.

Acknowledgements: The authors thank the university of Sharjah for the support of the current work through collaborative research project No. 19020406.

References

Abdelkareem, M.A., Elsaid, K., Wilberforce, T., Kamil, M., Sayed, E.T., Olabi, A., 2021. Environmental aspects of fuel cells: A review. Science of The Total Environment 752, 141803.

Abdelkareem, M.A., Sayed, E.T., Mohamed, H.O., Obaid, M., Rezk, H., Chae, K.-J., 2020. Nonprecious anodic catalysts for low-molecular-hydrocarbon fuel cells: Theoretical consideration and current progress. Progress in Energy and Combustion Science 77, 100805.

Marvila, M.T., de Azevedo, A.R.G., de Matos, P.R., Monteiro, S.N., Vieira, C.M.F., 2021. Materials for production of high and ultra-high performance concrete: review and perspective of possible novel

materials. Materials 14, 4304.

Olabi, A.G., Obaideen, K., Elsaid, K., Wilberforce, T., Sayed, E.T., Maghrabie, H.M., Abdelkareem, M.A., 2022. Assessment of the pre-combustion carbon capture contribution into sustainable development goals SDGs using novel indicators. Renewable and Sustainable Energy Reviews 153, 111710.

Sayed, E.T., Abdelkareem, M.A., Bahaa, A., Eisa, T., Alawadhi, H., Al-Asheh, S., Chae, K.-J., Olabi, A.G., 2021. Synthesis and performance evaluation of various metal chalcogenides as active anodes for direct urea fuel cells. Renewable and Sustainable Energy Reviews 150, 111470.

Sayed, E.T., Eisa, T., Mohamed, H.O., Abdelkareem, M.A., Allagui, A., Alawadhi, H., Chae, K.-J., 2019. Direct urea fuel cells: Challenges and opportunities. Journal of Power Sources 417, 159-175.

Wilberforce, T., Olabi, A.G., Sayed, E.T., Elsaid, K., Abdelkareem, M.A., 2021a. Progress in carbon capture technologies. Science of The Total Environment 761, 143203.

Wilberforce, T., Sayed, E.T., Abdelkareem, M.A., Elsaid, K., Olabi, A.G., 2021b. Value added products

from wastewater using bioelectrochemical systems: Current trends and perspectives. Journal of Water Process Engineering 39, 101737.

PCR21042022 – 209: Glycol-based Deep Eutectic Solvent for Extractive Desulfurization of Fuel Oil

Mohd. Faridzuan Bin Majid

Extended Abstract

Separation of refractory sulfur from fuel oil is crucial to sustain a clean environment. The conventional hydrodesulfurization (HDS) could not efficiently remove sterically-hindered sulfur including dibenzothiophene (DBT). Therefore, extractive desulfurization (EDS) using deep eutectic solvent (DES) as extraction medium is recommended as it can provide a feasible process with less expensive and low-toxic materials. Four glycol-based DES were synthesized by combination of tetrabutylammonium chloride (TBAC) with glycerol (GLY), ethylene glycol (EG), tetraethylene glycol (TEG) and poly(ethylene glycol) 400 (PEG) at different mole ratios. The effect of glycols concentration, the alkyl chain and the nature of glycols towards density and viscosity was analysed at temperature ranged from 293.15 – 363.15 K. It was found that the density and viscosity of DES can be modified by changing the ratio of glycols. From the desulfurization performance, high extraction efficiency can be obtained by using glycols with longer alkyl chain at minimum concentration. The best DES was TBAC-PEG-1-2 and up to 93.89% of sulfur could be removed within three consecutive extractions at optimized conditions. Extraction temperature, DES volume ratio and mixing speed were greatly influenced the extraction efficiency. Compared to previous literature, minimum amount of DES is adequate to achieve deep desulfurization which is desirable by industrial practice. This study provides a systematic design of DES for an economical and sustainable extraction of refractory sulfur from fuel oil.

6th International Conference and Postgraduate Colloquium for Environmental Research 2022 (POCER 2022) 9 - 11 June 2022
Langkawi, Kedah, Malaysia

PCR01042022 – 210: Microfluidic synthesis of hollow microfibers for photocatalytic reduction of NOx from flue gas

Yong Ren[a,b], Zhiyu Zhang[a*]

[a] Research Group for Fluids and Thermal Engineering University of Nottingham Ningbo China, Ningbo, China b Nottingham Ningbo China Beacons of Excellence Research and Innovation Institute

• Corrensponsing Author E-mail: yong.ren@nottingham.edu.cn

Keywords: Pollution Control; Flue gas; Microfluidics; Photocatalysis

Extended Abstract

Hydrocarbon fuel combustion is the major way for energy generation in many countries. The main combustion products from the generated flue gas include water vapor and NOx (NO+NO2). If water vapor is not directly emitted but collected via condensation process to form water, it can become a considerable water source. The heat can be also recovered in the condensation process. NOx is one of the most detrimental pollutants both to the environment and human health because it is not only noxious but also acts as the precursor to form acid rain, photochemical smog, and ozone layer depletion. The catalytic membrane which combines separation and catalysis function can be applied for flue gas purification with lower energy consumption, lower pollution, and enhanced performance. The hollow fiber configuration with a thin wall and an asymmetric structure is considered as the most promising one for the industrial applications because of high permeation flux and high packing density [1]. Most of catalytic membrane are made of inorganic materials, because catalytic reactions take place under harsh conditions such as high temperature, high pressure, and the presence of corrosive gases or solutions. Among all inorganic membranes, ceramic membranes such as metal oxides (Al2O3, SiO2, ZrO2, and TiO2) have superior advantages over polymer based membranes including high chemical and thermal stability, high fouling resistance, and better mechanical strength, thus possessing properties such as lower chemical demand, lower maintenance frequency and extended lifetime [2]. Ceramic membrane structure normally include plate, tube, and hollow fiber. In particular, [3]. In spite of the recent advances in hollow fiber ceramic membranes, there remain some problems of industrial challenge and scientific interest, which have been inadequately studied and thus require investigations.

In this project, we develop a facile and cost-effective way as alternative of conventional tetra-bore spinneret to fabricate ceramic hollow fiber membranes with multichannel configurations by using microfluidic approach. The membrane also features with nanoporous surface.The ceramic hollow fiber membranes will integrate with photocatalysis function which can be activated under visible light. When the fabricated ceramic multichannel hollow fiber photocatalytic membranes are subject to flue gas, the membranes can achieve two functions: NOx from flue gas can be removed via the catalytic membranes under visible light.The membrane can be used as condenser for heat and water recovery from flue gas, the heat and mass transfer can take place simultaneously and the recovery efficiency can be enhanced by the multichannel configurations as well as the nanoporous surface structure.

Acknowledgements: This work was financially supported by Zhejiang Provincial Natural Science Foundation of China under grant No. LY19E060001 and Nottingham Ningbo China Beacons of Excellence Research and Innovation Institute.

References

[1] H. Abdallah, A review on catalytic membranes production and applications, Bulletin of Chemical Reaction Engineering & Catalysis, 2017, Vol.12(2), pp.136-156

[2] X. Dong, W. Jin, N. Xu, K. Li, Dense ceramic catalytic membranes and membrane reactors for energy and environmental applications, Chemical Communications, 2011, Vol.47(39), pp.10886- 10902

[3] G. Zhang, W. Jin, N. Xu, Design and fabrication of ceramic catalytic membrane reactors for green chemical engineering applications, Engineering, 2018, Vol.4(6), pp.848-860

6th International Conference and Postgraduate Colloquium for Environmental Research 2022 (POCER 2022) 9 - 11 June 2022
Langkawi, Kedah, Malaysia

PCR23042022 – 211: Application of LCA-WQI Approach for River Conservation

C. Hafizan[a], Z. Zainon Nur[b] , A. Aris[c], N. Hussein[d] , N. Syarmimi Zaidi[e] , N. Zaiha Arman[f]

[a,b,c,e,f] Centre for Sustainable Environment and Water Security (IPASA), Research Institute for Sustainable Environment (RISE), Universiti Teknologi Malaysia, 81310, Johor Bahru, Johor, Malaysia

[b] School of Chemical and Energy Engineering, Universiti Teknologi Malaysia, 81310 Skudai, Johor Bahru, Malaysia

[c,d,e] School of Civil Engineering, Universiti Teknologi Malaysia, 81310 Skudai, Johor Bahru, Malaysia

- Corrensponsing Author E-mail: zainurazn@utm.my

Keywords: Life Cycle Assessment; Water Quality Index; Modelling; River Conservation

Extended Abstract

Life cycle assessment (LCA) is a useful tool for not only analysing a product's environmental impact, but also for aiding with early product development prior to scaling-up costs (Moura et al., 2022). LCA studies are applied based on assumptions and scenarios about potential environmental harm and resource consumption from a specific system. When a new process or project is being verified, it may be limited in order to comply with current norms or laws. As a consequence, LCA must be combined with other criteria to demonstrate the viability of a project or process, particularly when wastewater is discharged into a river. The water quality index (WQI) provides a single number that represents the overall water quality at a given location and time. The purpose of the Water Quality Index is to interpret complex water quality data into information that the general public can understand and utilise (Moujdin and Summers, 2021). The study's goal is to use the LCA framework in combination with the Malaysia WQI to safeguard the river's water quality. In this research, the environmental impact categories' indicators, as well as the inventory data, are multiplied by characterisation factors obtained from the

Malaysia WQI (EQR, 2006). **Equation 1** is used to determine the project's or system's significance in the river basin system; the dWQI value should be greater than 0. A negative dWQI score shows that the process's present effluent is deteriorating the river class, rendering the process's current effluent undesirable and necessitating a concentration reduction.

$dWQI = WQI_i - WQI_r$ **Equation 1**

where;

WQI_i = Water quality index for mixing point when effluent mix at target river

WQI_r = Water quality index for target river

dWQI > 0; System does not degrade river class

dWQI < 0; System will degrade river class

Three scenarios were established: Scenario 1: Effluent discharge in accordance with Environmental Quality Regulations 2009 Standard A. Scenario 2: Effluent discharge in accordance with Environmental Quality Regulations 2009 Standard B. Scenario 3: The treatment system fails, resulting in the discharge of raw wastewater at the effluent outlet. The concentration in mixing point can be generated through projected pollution dispersion analysis. **Figure 1** illustrates the scenario build up in the river basin area.

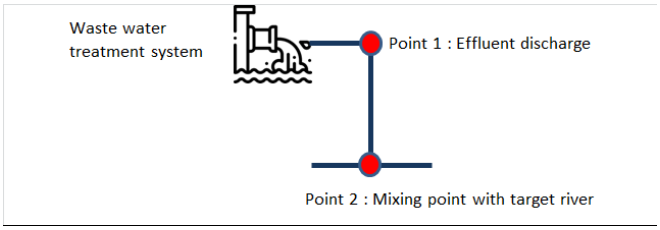

Figure 1: Scenario builds up in the river basin area

The dWQI result for each scenario using Class II river as the baseline is shown in **Table 1**. Scenario 1's dWQI value is greater than zero, suggesting that the new maximum concentration from effluent to the target river will not lower the river class, indicating that the wastewater treatment system is feasible. Scenario 2 (which is based on Standard B) may degrade target river water quality to Class III, while Scenario 3 can degrade target river water quality to Class IV. The findings suggest that the procedure is straightforward and repeatable for determining effluent requirement from wastewater treatment system. Furthermore, the approach assesses the feasibility of the study using dissolved oxygen and pH as metrics, which has limits in terms of its usage in life cycle impact assessment methodology. The approach might also be utilised as a mean of project viability verification, such as in an environmental impact assessment study.

Table 1: The dWQI value for each scenario

Scenario	dWQI
1	5.31
2	-9.33
3	-33.06

Acknowledgements: This work was supported by the Water Security and Sustainable Development Hub funded by the UK Research and Innovation's Global Challenges Research Fund (GCRF) [grant number: ES/S008179/1] and UTM High Impact Research with the centre number (Q.J130000.2451.09G03).

References

Environmental Quality Index (EQR), 2006. Available online at https://enviro2.doe.gov.my/ekmc/wp-content/uploads/2016/08/1403318138-Environmental_Quality_Report_(EQR)_2006.pdf. Retrieved date:7.4.2022

Moujdin, I.A. and Summers, J.K., 2021. Promising Techniques for Wastewater Treatment and Water Quality Assessment.

Moura, B., Monteiro, H., Mata, T. M., Iten, M., & Martins, A. A. (2022). Environmental life cycle assessment of early-stage development of ergosterol extraction from mushroom bio-residues. Journal of Cleaner Production, 131623.

6th International Conference and
Postgraduate Colloquium for
Environmental Research 2022 (POCER
2022) 9 - 11 June 2022
Langkawi, Kedah, Malaysia

PCR23042022 – 212: Thermal, Physical and Acid Pretreatment Of Napier Grass For Lignin Extraction

Syazmi Zul Arif Hakimi Saadon[a] , Noridah Binti Osman[a*] , and Leong Yung Syuen[b]

a Department of Chemical Engineering, Universiti Teknologi PETRONAS, Bandar Seri Iskandar, 32610 Perak, Malaysia

b HICOE – Center for Biofuel and Biochemical Research, Institute of Self-Sustainable Building, Universiti Teknologi PETRONAS, Bandar Seri Iskandar, 32610 Perak, Malaysia

• Corrensponsing Author E-mail: noridah.osman@utp.edu.my

Keywords: Lignin, Pretreatment, Napier grass, Thermal pretreatment, Acid Pretreatment

Extended Abstract

Lignin is one of the most abundant natural compounds in all plants. Its properties such as fibrous structure and good combustion value has called for its utilization in various application especially in fuel industry. This study will explore on the pretreatment of lignin from Napier grass using thermal, physical, and chemical means as well as determine the optimum condition for the feedstock pretreatment. In thermal pretreatment, the drying temperature and time are varied from 45-135 °C and 5-25 hours, respectively while for physical pretreatment, a comparison between grinding and ball milling is done. Acid pretreatment is done by varying the stem: leaf ratio, concentration, and soaking duration. Moisture analysis, FTIR spectroscopy, XRD analysis and Klason lignin are done to analyze the moisture, functional group, and crystallinity of sample. Moisture content of sample after physcial and thermal pretreatment are found to be inversely proportional to the drying conditions. The FTIR result showed that higher conditions produce lower peak intensity with higher drying condition while ball-milling also shows less reduction of peak intensities as compared to grinding. Acid pretreatment produces higher peaks signifying lignin concentration. Crystallinity only slightly affected by physical and thermal pretreatment while the sulfuric acid causes it to increase. Higher total lignin is obtained after physical and thermal pretreatment as compared to acid pretreated sample. Optimization is done by evaluating the statistical significance of each effect of the pretreatments. 15 hours, 75 °C and ball milling onto leaf sample are found to produce most lignin for thermal and physical pretreatment while 4.0M for 150 minutes onto 75:25 stem:leaf ratio produce most lignin for acid pretreatment. This findings can be used for further optimize the extraction of lignin from biomass sources especially grass-type biomass.

Acknowledgements: The authors would like to acknowledge the funding support from the Ministry of Higher Education (MOHE) Malaysia through the HICoE grant to CBBR (cost centre: 015MA0-052) and supported by the Department of Chemical Engineering (ChE), Universiti Teknologi PETRONAS.

References

[1] Malaysia Energy Commission, Malaysia Energy Statistics Handbook 2017, Energy Comm. (2017) 1–174. http://www.statcan.gc.ca/pub/57-601-x/57-601-x2012001-eng.pdf%5Cnpapers2://publication/uuid/792EFC7D-A6CF-40B5-A139-8FA59714AA41.

[2] H.E. Schoemaker, K. Piontek, On the interaction of lignin peroxidase with lignin, Pure Appl. Chem. 68 (1996) 2089–2096. doi:10.1351/pac199668112089.

[3] N. Osman, Chemistry of Hot-Pressing Hybrid Poplar Wood, University of Idaho, 2010.

[4] A.K. Kumar, S. Sharma, Recent updates on different methods of pretreatment of lignocellulosic feedstocks: a review, Bioresour. Bioprocess. 4 (2017). doi:10.1186/s40643-017-0137-9.

[5] J. Baruah, B.K. Nath, R. Sharma, S. Kumar, R.C. Deka, D.C. Baruah, E. Kalita, Recent trends in the pretreatment of lignocellulosic biomass for value-added products, Front. Energy Res. 6 (2018) 1–19. doi:10.3389/fenrg.2018.00141.

[6] T.P. Houghton, D.M. Stevens, P.A. Pryfogle, C.T. Wright, C.W. Radtke, The effect of drying temperature on the composition of biomass, Appl. Biochem. Biotechnol. 153 (2009) 4–10. doi:10.1007/s12010-008-8406-x.

[7] J.S. Lupoi, S. Singh, R. Parthasarathi, B.A. Simmons, R.J. Henry, Recent innovations in analytical methods for the qualitative and quantitative assessment of lignin, Renew. Sustain. Energy Rev. 49 (2015) 871–906. doi:10.1016/j.rser.2015.04.091.

[8] D. Ciolacu, F. Ciolacu, V.I. Popa, Amorphous cellulose - Structure and characterization, Cellul. Chem. Technol. 45 (2011) 13–21.

[9] T.A. Lloyd, C.E. Wyman, Combined sugar yields for dilute sulfuric acid pretreatment of corn stover followed by enzymatic hydrolysis of the remaining solids, Bioresour. Technol. 96 (2005) 1967–1977. doi:10.1016/j.biortech.2005.01.011.

[10] L.M.F. Pardo, J.G.S. Mendoza, J.E.L. Galán, Influence of pretreatments on crystallinity and enzymatic hydrolysis in sugar cane residues, Brazilian J. Chem. Eng. 36 (2019) 131–141. doi:10.1590/0104-6632.20190361S20180093.

[11] I.Y. Mohammed, Y.A. Abakr, F.K. Kazi, S. Yusup, I. Alshareef, S.A. Chin, Comprehensive characterization of Napier grass as a feedstock for thermochemical conversion, Energies. 8 (2015) 3403–3417. doi:10.3390/en8053403.

6th International Conference and
Postgraduate Colloquium for
Environmental Research 2022 (POCER
2022) 9 - 11 June 2022
Langkawi, Kedah, Malaysia

PCR25042022 – 213: Energy and exergy analysis of R-134a operated large scale vapor compression refrigeration (VCR) cycle for district cooling (DC) application

Muhammad Saad Khan[a#], Bhajan Lal[a,b*], Faiz Ahmed[c], Khalik M Sabil[d], Khor Siak Foo[b,e] and Quah Chong Jin[f]

[a] CO_2 Research Center
Universiti Teknologi PETRONAS, Perak, Malaysia

[b] Chemical Engineering Department
Universiti Teknologi PETRONAS, Perak, Malaysia

[c] Mechanical Engineering Department
Universiti Teknologi PETRONAS, Perak, Malaysia

[d] PETRONAS Research Sdn Bhd, Bangi, Salangor, Malaysia

[e] PTTEP, Petronas Twin Towers, Kuala Lumpur, Salangor, Malaysia

[f] Numit Enterprise, Seri Kembangan, Salongor, Malaysia

- Corrensponsing Author E-mails: #muhammad.saad@utp.edu.my
  *bhajan.lal@utp.edu.my

Keywords: COP; District cooling; Energy analysis; Exergy analysis; R134a; VCR.

Extended Abstract

District Cooling Systems (DCS) are a sustainable method of consuming energy used for refrigeration and delivering chilled water to end-users via chillers and distribution networks (Khan et al., 2021a, 2022). DCS, generally operated with vapor compression refrigeration (VCR) chillers, is superior to conventional air conditioning as it helps to reduce energy consumption and protect the environment by reducing carbon dioxide emissions (S. Kadam et al., 2021; S. T. Kadam et al., 2022; Khan et al., 2021b). The advantages of the district cooling plant can further be improved by carefully optimizing the VCR operating parameters (S. T. Kadam et al., 2022; Khan et al., 2021a). Although thermodynamic assessments of VCR cycles are available in the open literature, most studies have been conducted for cooling capacity well below the actual DCS requirement (less than 500 kW)(S. Kadam et al., 2021; Khan et al., 2021b). As a result, this work aims to investigate the energy and exergy analysis of a large-

scale VCR cycle operating on 1,1,1,2-tetrafluoroethane (R134a) refrigerant for a cooling capacity of approximately 4300 kW and to assess the influence of several operating parameters on cycle performance. Figure 1 represents the process flow diagram of the R134a operated VCR cycle. Different parameters such as evaporator operating pressure (10.5-12.5 atm), chilled water inlet temperature (280-284 K), isentropic efficiency of a compressor (0.60-0.96), compressor pressure (10-12.5), condenser temperature (315-340 K), cooling output (4300-4700 kW), cooling water inlet temperature (307-310.5 K) and chilled water temperature (282.15-285.15 K) are varied in the parametric investigations. The 2nd law (exergy destruction) analysis of the cycle's components is also included in the study. Overall, the COP and Exergy efficiency of the R134a cycle was observed up to (6.27) and (65%). The exergy destruction analysis of individual components suggested that maximum exergy loss was found in the compressor section, whereas minimum loss was observed in the evaporator unit. In addition, the VCR system is optimized based on the R134a operated VCR cycle. For large-capacity district cooling systems, optimal operating conditions were established for various parametric situations. As a result, the findings will serve as a road map for designing and optimizing large-scale DCS systems in Malaysia that run on VAR cycles.

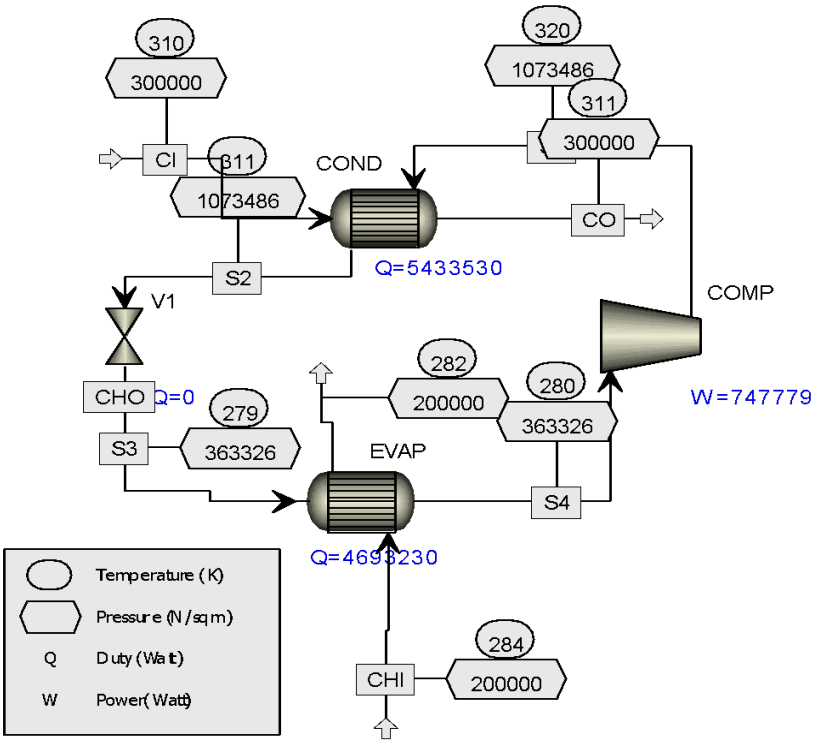

Figure 1: ASPEN Plus generated process flow sheet for R134a operated large scale VCR system.

Acknowledgements: The authors would like to thank the Yayasan UTP for the YUTP project of 015LC0-399.

References

Kadam, S., Khan, M. S., Kyriakides, A.-S., Papadopoulos, A. I., Hassan, I., Rahman, M. A., & Seferlis, P. (2021). Thermodynamic, Environmental and Cost Evaluation of Compression-Absorption Parallel and

Cascade Refrigeration Chiller. *ASME 2021 International Mechanical Engineering Congress and Exposition*, 1–7. https://doi.org/10.1115/imece2021-70886

Kadam, S. T., Kyriakides, A. S., Khan, M. S., Shehabi, M., Papadopoulos, A. I., Hassan, I., Rahman, M. A., & Seferlis, P. (2022). Thermo-economic and environmental assessment of hybrid vapor compression-absorption refrigeration systems for district cooling. *Energy*, *243*, 122991. https://doi.org/10.1016/j.energy.2021.122991

Khan, M. S., Kadam, S. T., Kyriakides, A.-S., Hassan, I., Papadopoulos, A. I., Rahman, M. A., & Seferlis, P. (2021a). Comparative Energy and Exergy Analysis of Large Capacity Ammonia-Water and Water-Lithium Bromide Vapor Absorption Refrigeration (VAR) Cycles. *ASME 2021 International Mechanical Engineering Congress and Exposition*, 1–8. https://doi.org/10.1115/imece2021-71084

Khan, M. S., Kadam, S. T., Kyriakides, A.-S., Hassan, I., Papadopoulos, A. I., Rahman, M. A., & Seferlis, P. (2021b, August 10). Modified Operating Parameter-Based Iyer Correlation for the Coefficient of Performance (COP) Prediction of Different Fluid Pairs in Double-Effect Vapor Absorption Refrigeration (VAR) Cycles. *ASME 2021 Fluids Engineering Division Summer Meeting*. https://doi.org/10.1115/FEDSM2021-65709

Khan, M. S., Kadam, S. T., Kyriakides, A., Papadopoulos, A. I., Hassan, I., Azizur, M., & Seferlis, P. (2022). A new correlation for performance prediction of small and large capacity single-effect vapor absorption refrigeration systems. *Cleaner Energy Systems*, *1*(January), 100002. https://doi.org/10.1016/j.cles.2022.100002

.

6th International Conference and
Postgraduate Colloquium for
Environmental Research 2022 (POCER
2022) 9 - 11 June 2022
Langkawi, Kedah, Malaysia

PCR25042022 – 214: An estimation method of watershed-scale water environmental capacity supported by machine learning

Xin Wang[a,b], Rong Li[c], Yong Tian[b], and Chongxuan Liu[b,*]

[a] School of Environment, Harbin Institute of Technology, Harbin, China

[b] Department of Environmental Science and Engineering
University of Southern University of Science and Technology, Shenzhen, China

[c] Department of Environment and Energy
University of South China University of Technology, Guangzhou, China

- Corresponding Author E-mail: Chongxuan Liu (liucx@sustech.edu.cn)

Keywords: Water environmental capacity; Artificial neural network; Optimization; Maozhou River watershed; Water quality standard; Modelling.

Extended Abstract

The water environmental capacity (WEC) is an important index for implementing the management of the water environment in river watershed and water area (e.g. river, lake, estuary, sea). The WEC is defined as the maximum number of contaminants that a water body can take without producing unacceptable environmental impacts[Li *et al*., 2010]. In this study, a WEC estimation method that incorporated the machine learning approach and process-based model was developed. A process-based model was used to simulate contaminant concentrations at monitoring or critical river locations in response to contaminant inputs in the watershed, while an artificial neural network (ANN) as a machine learning method was trained to link the contaminant inputs in the watershed with the contaminant concentrations at the critical locations. From the linkages, a global optimization method called "The Shuffled Complex Evolution method developed at the University of Arizona algorithm (SCE-UA)" was used to find the a watershed-scale WEC that meets the targets of the water quality at critical locations[Duan *et al*., 1994; Hubbard *et al*., 2020]. Maozhou River watershed at Shenzhen City, Southeast China, a typical rapidly urbanized zone was used as an example to illustrate the approach with ammonium as an example contaminant under different water quality standards with two different

scenarios. Scenario 1 represents those watersheds with the fixed ratio between contaminant inputs, while scenario 2 represents those watersheds under design to optimize flux inputs. In scenario 1, the inflow concentration ratios of contaminant at different branches were fixed, and the WEC can be easily estimated by iterative running of the process-based model. The estimation results of the WEC of ammonium were 361.71 t yr^{-1} and 483.66 t yr^{-1} under the water constraints of Class IV and Class V standards. However, with less water quality data availability, the constraint of input concentration ratios at each branch is difficult to be determined. In scenario 2, the WEC was estimated without priori information of these pollutant concentration ratios. In this case, the WEC estimation results ranged from 766.84 t yr^{-1} to 880.90 t yr^{-1} with an average value of 815.44 t yr^{-1} under the water constraints of Class IV standard and 1118.10 t yr^{-1} to 1129.88 t yr^{-1} with an average value of 1123.38 t yr^{-1} under the water constraints of Class V standard. The optimization step generated several different solutions to approach the maximum WEC. In these solutions, the values of estimated WECs were very close to each other but the spatial distribution of local WEC in each sub-domain showed significant difference. The results from this study have strong implications for the environmental management and water quality control in the Maozhou River watershed in eliminating contaminant sources or re-distributing contaminant sources by taking the advantage of WEC. In addition, comparing with the traditional processed-based model approach, the estimation method proposed in this study is more applicable and effective for the problems limited by the river network complexity and water quality data availability.

Acknowledgements: This research is supported by Key-Area Research and Development Program of Guangdong Province (2019B110205005). Additional support was National Natural Science Foundation of China (project No. 41830861) and from the Guangdong province project (2017ZT07Z479). The authors also thank the support by Center for Computational Science and Engineering of Southern University of Science and Technology.

References

Duan, Q. Y., Sorooshian, S., Gupta, V. K., 1994. Optimal use of the SCE-UA global optimization method for calibrating watershed models. *Journal of Hydrology*. 158(3-4), 265-284.

Hubbard, S. S., Varadharajan, C., Wu, Y., Wainwright, H., Dwivedi, D., 2020. Emerging technologies and radical collaboration to advance predictive understanding of watershed hydrobiogeochemistry. *Hydrological Processes*, 34(15), 3175-3182.

Li, Y. X., Qiu, R. Z., Yang, Z. F., Li, C. H., Yu, J. S., 2010. Parameter determination to calculate water environmental capacity in Zhangweinan Canal Sub-basin in China. *Journal of Environmental Sciences*. 22(6): 904-907.

6th International Conference and Postgraduate Colloquium for Environmental Research 2022 (POCER 2022) 9 - 11 June 2022
Langkawi, Kedah, Malaysia

PCR26042022 – 215: The adsorption of antibiotics by the solid particles in the aquifer by intraparticle diffusion

Cheng Zhang[a], Chongxuan Liu[a*], Rong Li[b], Dongfang Ke[a], Hongri Suo[a], Lili Zhang[c],

[a] State Environmental Protection Key Laboratory of Integrated Surface Water-Groundwater Pollution Control, School of Environmental Science and Engineering, Southern University of Science and Technology, Shenzhen, People's Republic of China

[b] The Key Lab of Pollution Control and Ecosystem Restoration in Industry Clusters, Ministry of Education, School of Environment and Energy, South China University of Technology, Guangzhou 510006, People's Republic of China

Shenzhen Key Laboratory of Environmental Chemistry and Ecological Remediation,College of Chemistry and Environmental Engineering, Shenzhen University,Shenzhen 518060,China

* Corrensponding Author E-mail: liucx@sustech.edu.cn

Keywords: Antibiotics; Adsorption Kinetic; Intraparticle Diffusion; Quartz Sand; Clay

Extended Abstract

The prevalence of antibiotics (ATs) in aquifers causes potential public risks, owing to their transfer possibility to drinking water [Ben et al., 2020] and their ability to induce resistance genes even at low concentrations [Zhang et al., 2019]. Unlike traditional pollutants (POPs and heavy metal pollutant), the environmental concentration of ATs is lower, which may lead to less chance of being removed by adsorption. In addition, in the natural aquatic environment, ATs generally present a variety of charged ionic states (cationic, anionic, and zwitterionic species) [Qin, Liu, Wang, Weng, & Li, 2014], and the special functional group structure of most ATs is easily complexed with divalent cations into stable complexation states [Wang, Yao, Sun, Li, & Huang, 2016]. However, the transfer mechanisms of ATs in aquifers is still remained unclear.

In this study, batch experiments were performed to understand the adsorption behavior of two frequently detected ATs Tetracycline (TC) and levofloxacin (LEV) on the solid particles in the aquifer with 50 mg/L initial concentration. Results indicated that the adsorption kinetics of TC and LEV were well fitted with intraparticle diffusion model (Figure 1). This was supported by the scanning electron microscope equipped with electron backscatter diffraction (SEM-EDS) and confocal laser scanning fluorescence microscopy (CLSM) results that the ATs were observed to diffuse into the micropores/fractures inside of the quartz sands (Figure 2); and also supported by the X-ray powder diffraction (XRD) result that the ATs could diffuse into the clay layer.

Correlation analysis found that the adsorption of LEV had a strong correlation with the surface physical parameters, while the adsorption behavior of TC was significantly related with the pore parameters. In addition, the irreversible strong bonding inhibited the desorption of adsorbed antibiotics in the pores. Therefore, antibiotics could easily diffuse into the micropores or interlayers of the solid particles in the aquifer, but hardly desorb into solution again. These results shed light on understanding the fate of ATs in aquifers.

Acknowledgements: This work was supported by the Department of Science and Technology of Guangdong Province [grant number 2017ZT07Z479].

References

Ben, Y., Hu, M., Zhang, X., Wu, S., Wong, M. H., Wang, M., and Zheng, C., 2020. Efficient detection and assessment of human exposure to trace antibiotic residues in drinking water. *Water Research*, 175, 115699.

Qin, X., Liu, F., Wang, G., Weng, L., & Li, L., 2014. Adsorption of levofloxacin onto goethite: effects of pH, calcium and phosphate. *Colloids and Surfaces B: Biointerfaces*, 116, 591-596.

Wang, H., Yao, H., Sun, P., Li, D., & Huang, C. H., 2016. Transformation of tetracycline antibiotics and Fe (II) and Fe (III) species induced by their complexation. *Environmental Science & Technology*, 50(1): 145-153.

Zhang, C., Xue, J., Cheng, D., Feng, Y., Liu, Y., Aly, H. M., & Li, Z., 2019. Uptake, translocation and distribution of three veterinary antibiotics in Zea mays L. *Environmental Pollution*, 250, 47-57.

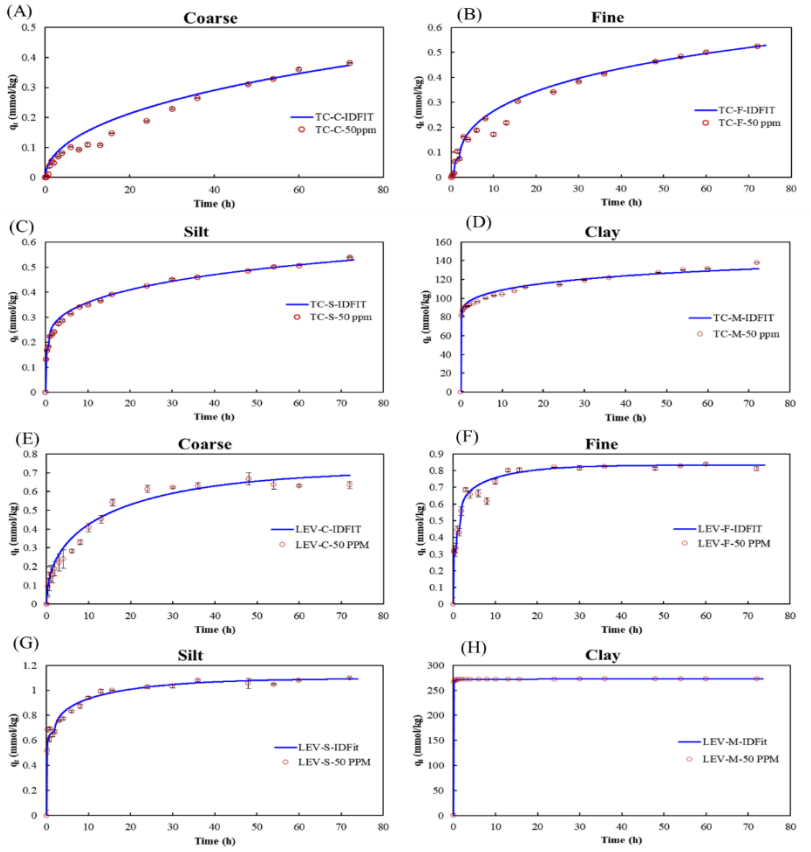

Figure 1 The fitting results of intraparticle diffusion compared with the observed concentration of TC and LEV adsorbed on the solids.

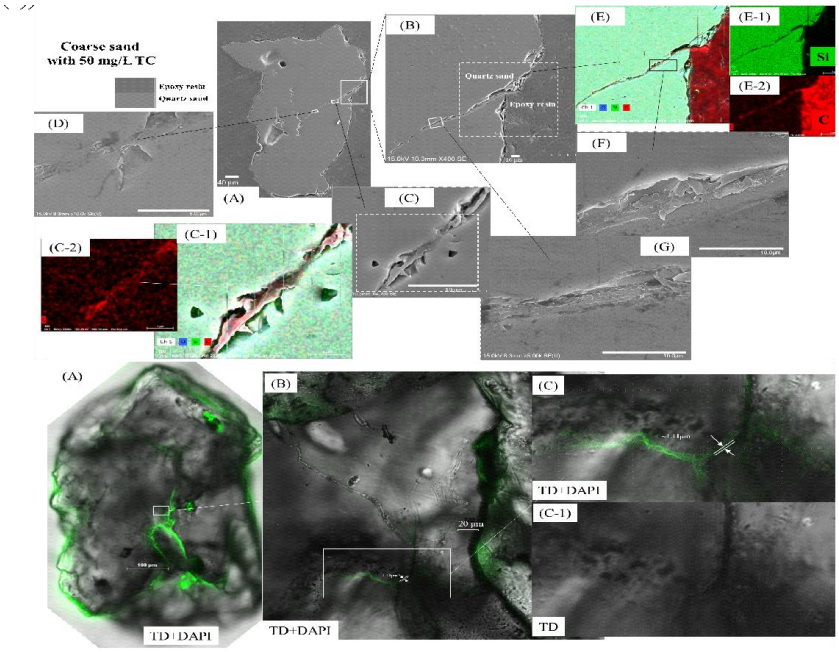

Figure 2 The SEM-EDS (I) CLSM (II) images of the profiles of the sand with adsorption of TC

6th International Conference and
Postgraduate Colloquium for
Environmental Research 2022 (POCER
2022) 9 - 11 June 2022
Langkawi, Kedah, Malaysia

PCR27042022 - 216 : [Bmim]acetate Pretreatment of Giant Reed Triggering Yield Improvement of Biohydrogen Production via Photo-fermentation

Quanguo Zhanga, Xuenan Shuia, Tian Zhanga, Jiabin Yanga, Zhou Chena, Tingzhou Leib, Caihong Zouc, and Danping Jianga*

a Key Laboratory of New Materials and Facilities for Rural Renewable Energy of Ministry of Agriculture and Rural Affairs of China Henan Agricultural University, Zhengzhou 450002, PR China

b Changzhou University, Changzhou 213164, PR China

c College of Mechanical and Electrical Engineering Henan Agricultural University, Zhengzhou 450002, PR China

Corresponding Author E-mail: JIANGDANPING@HENAU.EDU.CN

Keywords: [Bmim]acetate; Pretreatment; Hydrogen Production; Photo-fermentation.

Extended Abstract

The study aimed to evaluate the effect of [Bmim]acetate pretreatment of giant reed on hydrogen yield improvement via photo-fermentation. Different concentrations (3 g/L, 6 g/L, 12 g/L, 24 g/L), different temperatures (60 °C, 70 °C, 80 °C, 90 °C) and different time (1 h, 2 h, 3 h, 4 h) of [Bmim]acetate pretreatment were carried out to check the effectiveness. Giant reed pretreated by 6g/L of [Bmim]acetate at 70 °C for 4 h achieved the maximum sugar yield of 9.5 g/L during the enzymatic hydrolysis. Additionally, the maximum hydrogen production of 361.6 mL was also obtained from giant reed pretreated by 6g/L of [Bmim]acetate at 70 °C for 4 h. Moreover, Ternary analysis was employed to demonstrate the effect of [Bmim]acetate pretreatment on delignification、sugar yield and hydrogen yield. The results of this study would help in understanding the photo-fermentative hydrogen yield improvement of giant reed via [Bmim]acetate pretreatment.

6th International Conference and
Postgraduate Colloquium for
Environmental Research 2022 (POCER
2022) 9 - 11 June 2022
Langkawi, Kedah, Malaysia

PCR27042022 – 217: Effects of AM Fungi on Selenium Accumulation and Utilization Efficiency in Winter Wheat (*Triticum aestivum* L.) under Different Fertilization Time

Jiao Li[a,b*], Mukesh Kumar Awasthi[a], and Fuyong Wu[a,b]

[a] College of Natural Resources and Environment
Northwest A&F University, Yangling, Shaanxi Province 712100, PR China

[b] Key Laboratory of Plant Nutrition and the Agri-environment in Northwest China
Ministry of Agriculture, Yangling 712100, Shaanxi, China

- Corresponding Author E-mail: LIJIAO0829@126.COM

Keywords: Mycorrhizae; Selenate; Rhizosphere Soil; Se Speciation; Winter Wheat.

Extended Abstract

Arbuscular mycorrhizal fungi (AMF) are ubiquitous in the soil that can form symbiotic associations with roots of the majority of plant species. In the present study, we investigated the effects of mycorrhizal inoculation on the distribution, transformation of selenium (Se) fractions in the rhizosphere soil, and the accumulation and availability of Se in each part of winter wheat. A pot experiment was conducted using different concentrations of exogenous selenate (0.1, 0.25 and 0.5 mg Se kg^{-1} soil) at different growth stages in wheat (before sowing, jointing stage, heading stage). The results demonstrated that inoculation with AMF had no significant effect either on wheat biomass or grain yield ($p < 0.05$). Se distribution in different parts of wheat plant ranked decline as grain > leaf > husk >stem > root with selenate treatment. The inoculation of AMF significantly increased available Se (SOL–Se + EXC−Se) content by 0.34 -6.80 times, respectively, compared with the control. In addition, the dominant Se fraction in all treatments was EXC–Se, accounting for 34.46%-56.23%. The results indicated that the availability of Se in rhizosphere soil was influenced by mycorrhizal inoculation. The results indicated that inoculation with AMF significantly ($p < 0.05$) increased Se accumulation in grain when selenium fertilizer was added at heading stage. Mycorrhizal inoculation effectively improved Se absorption by activating soil available Se. AMF has the potential to increase the Se content in wheat grain and would be a new strategy improves the dietary of residents living on wheat as a staple food.

6th International Conference and
Postgraduate Colloquium for
Environmental Research 2022 (POCER
2022) 9 - 11 June 2022
Langkawi, Kedah, Malaysia

PCR27042022 – 218: Enhancing Performance of a Groove-type Flat Panel Bio-reactor using Immobilized Photosynthetic Bacteria for Continuous Photo-fermentative Hydrogen Production

Yi Wang[a], Abdolhamid Akbarzadeh[b], Nadeem Tahir[a], and Mukesh Kumar Awasthi[c*]

[a] MOA Key Laboratory of New Materials and Facilities for Rural Renewable Energy
Henan Agricultural University, Zhengzhou, 450002, China

[b] Department of Bioresource Engineering
McGill University, Montreal, QC, H9X 3V9, Canada

[c] College of Natural Resources and Environment
Northwest A&F University, Taicheng Road 3#, Yangling, Shaanxi, 712100, China

- Corresponding Author E-mail: MUKESH_AWASTHI45@YAHOO.COM

Keywords: Photofermentative Hydrogen Production; Flat Panel Bio-reactor; Bio-film; Mass Transfer; Response Surface Methodology (RSM).

Extended Abstract

To strengthen the process of continuous photofermentative hydrogen production, a novel groove-type flat panel bio-reactor (GFPR) with higher surface-to-volume ratio was proposed in this study. With the specific geometric structure of wavy grooves, both cell-immobilization and continuous-flow operation mode were achieved simultaneously to ensure the steady performance of hydrogen production to be maintained. Key factors associated with hydrogen production and substrate degradation were regulated to optimize the bioprocess using response surface methodology (RSM). Desirable hydrogen production rate of 28.81 mL/h/L was attained under the light intensity of 44.3 μE/m^2/s, inlet substrate concentration of 55.6 mmol/L and flow rate of 928.1 mL/h.

6th International Conference and
Postgraduate Colloquium for
Environmental Research 2022 (POCER
2022) 9 - 11 June 2022
Langkawi, Kedah, Malaysia

PCR27042022 – 219: Effect of Biochar Supplement on the Dynamics of Antibiotic Resistant Fungi during Pig Manure Composting

Yuwen Zhou[a], and Mukesh Kumar Awasthi[a*]

[a] College of Natural Resources and Environment
Northwest A&F University, Taicheng Road 3#, Yangling, Shaanxi, 712100, China

- Corresponding Author E-mail: MUKESH_AWASTHI45@YAHOO.COM

Keywords: Coconut Shell Biochar; Bamboo Biochar; Fungi Dynamics; Pig Manure Composting.

Extended Abstract

The purpose of this study is to investigate fungi dynamics in pig manure composting assisted by coconut shell biochar (CSB) and bamboo biochar (BB). Three different treatments (blank, 10% CSB and 10% BB) were designed to put into pig manure and indicated with T1, T2 and T3. 16S rDNA high-throughput sequencing and β diversity analysis were elected to analyze the evolution of antibiotic resistant fungi (ARF) communities during composting. The experimental results declared that the number of fungi in composting environment is scarce but three dominant phyla were *Ascomycota*, *Basidiomycota* and *Mucoromycota*. There were significant differences in the relative abundance and diversity of fungi among 3 treatments. Moreover, the participation of biochar regulated the fungal community. Compared with the control group, the abundance of fungi was significantly positively mobilized, and especially in some aspects, bamboo biochar showed a better effect. These findings offer insight into potential strategies to understand the succession of ARFs during PM reutilize. Conclusively, biochar which can inhibit the dynamics and degrade of antibiotic resistant fungi is a promising additive for improved composting, which provide inspiration for modern agricultural management.

6th International Conference and Postgraduate Colloquium for Environmental Research 2022 (POCER 2022) 9 - 11 June 2022
Langkawi, Kedah, Malaysia

PCR27042022 – 220: Enhancement of anaerobic fermentation with corn straw by sludge-corn stalk mixed biochar

Youzhou Jiao[a,b,c], Ninglu Zhang[a,b,c], Chao He[a,b,c], Xiaoran Ma[a,b,c], Xinxin Liu[a,b,c], Liang Liu[a,b,c], Tingting Hou[a,b,c], Xiaohui Pan[a,b,c,*]

[a] Key Laboratory of New Materials and Facilities for Rural Renewable Energy of Ministry of Agriculture and Rural Affairs, College of Mechanical & Electrical engineering, Henan Agricultural University, Zhengzhou 450002, China.

[b] Henan International Joint Laboratory of Biomass Energy and Nanomaterials, Henan Agricultural University, Zhengzhou 450002, China.

[c] Henan Collaborative Innovation Center of Biomass Energy, Henan Agricultural University, Zhengzhou 450002, China

- Corrensponsing Author E-mail: panxiaohui1987@163.com

Keywords: Sludge-corn stalk mixed biochar; Anaerobic fermentation; Corn straw; Methane production.

Extended Abstract

In order to realize the efficient resource utilization of straw and sludge, this study used sludge and corn straw as raw materials to prepare sludge-corn straw mixed biochar at different carbonization temperatures, raw material ratios, holding times and heating rates. As an additive for anaerobic fermentation, the effect of sludge-corn straw mixed biochar on the anaerobic fermentation performance of corn straw was investigated, and the correlation between the physicochemical properties of biochar and anaerobic fermentation performance was established. The results showed that when the preparation conditions of biochar were as follows: carbonization temperature of 600℃, raw material ratio of 1, holding time of 90 min, and heating rate of 20℃/min, the cumulative methane production of corn stalk by anaerobic fermentation exhibited the highest value of 269.23 mL/g VS, which was 47.1% higher than the blank control group. The specific surface area and pore structure of biochar only affect methane production in a certain range. This study provides a theoretical basis for further research on the

mechanism relationship between the properties of biochar materials and methane production by anaerobic fermentation.

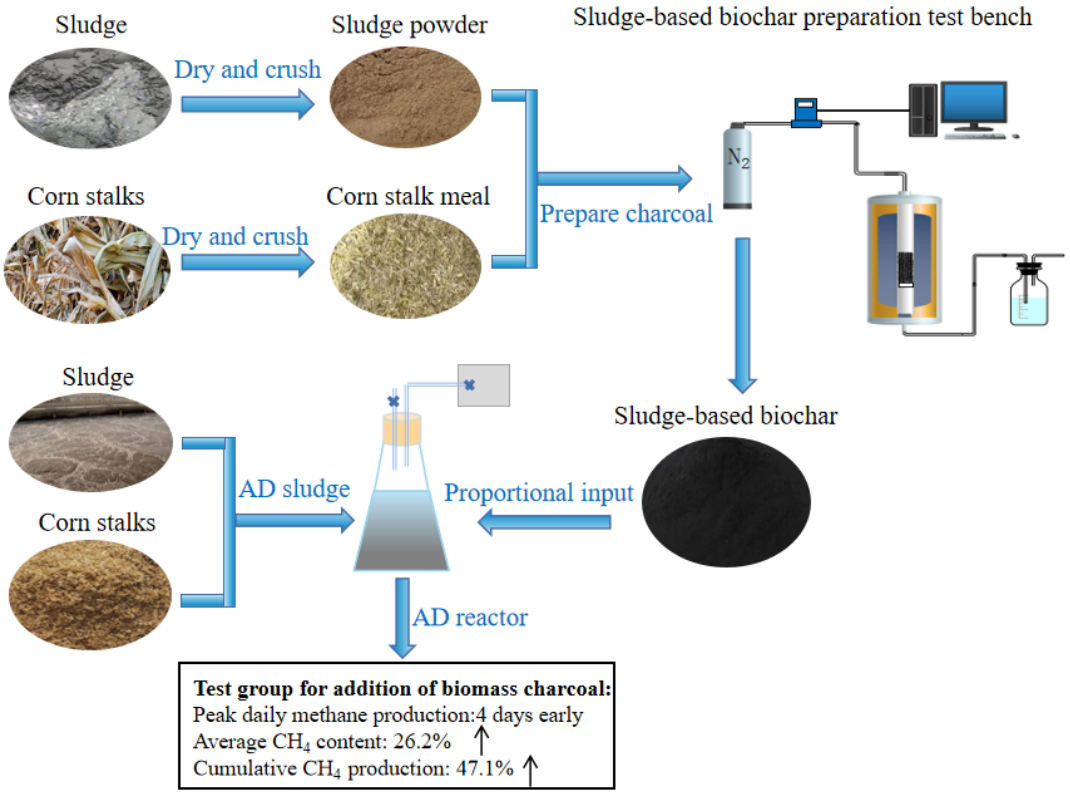

Acknowledgements: The authors thank the National Key Research and Development Program of China (2018YFE0206600), National Natural Science Foundation of China (52176184), Key Scientific Research Projects of Henan Higher Education Institutions(No. 21A416008).

6th International Conference and Postgraduate Colloquium for Environmental Research 2022 (POCER 2022) 9 - 11 June 2022
Langkawi, Kedah, Malaysia

PCR27042022 – 221: Effect of Polyethylene Glycol 4000 and Ammonium Polyphosphate on Photo-fermentative Hydrogen Production of Corncob

Zigang Wang[a,b], Chao He[a,b], Xinxin Liu[a,b], Liang Liu[a,b], XiaoRan Ma[a,b], Zhiping Zhang[a,b], Quanguo Zhang[a,b], and Youzhou Jiao[a,b*]

[a] Key Laboratory of New Materials and Facilities for Rural Renewable Energy, Ministry of Agriculture and Rural Affairs, College of Mechanical & Electrical Engineering
Henan Agricultural University, Zhengzhou 450002, China

[b] Henan International Joint Laboratory of Biomass Energy and Nanomaterials
Henan Agricultural University, Zhengzhou 450002, China

- Corresponding Author E-mail: JIAOYOUZHOU@HENAU.EDU.CN

Keywords: Photo-fermentative Hydrogen Production; Corncob; Polyethylene Glycol 4000; Ammonium Polyphosphate.

Extended Abstract

The addition of surfactant or fillers can change the interfacial state and viscosity of the hydrogen-production material liquid, which facilitates the escape rate of hydrogen bubbles. Therefore, the performance of the photofermented biohydrogen production system with the addition of surfactants and fillers was evaluated in the work. The cumulative hydrogen production, pH value, reducing sugar concentration and hydrogen production kinetics are analyzed under different concentrations of polyethylene glycol 4000 and ammonium polyphosphate using corncob as hydrogen production substrate. The results showed that the addition of polyethylene glycol 4000 and ammonium polyphosphate effectively increased the cumulative hydrogen production. The highest cumulative hydrogen production was achieved when 1.5 g/L polyethylene glycol 4000 and 1.0 g/L ammonium polyphosphate were added, with 397.30 mL and 365.38 mL, respectively, which were 50.39% and 38.79% higher than the control group. The maximum energy conversion efficiencies reached 5.47% and 5.04%, which were 50.27% and 38.46% higher, respectively. The results of hydrogen production kinetic properties showed that both the appropriate amount of polyethylene glycol 4000 and ammonium polyphosphate could improve the maximum hydrogen production potential and maximum hydrogen

production rate. In addition, the flow index of the hydrogen production stream was reduced by the appropriate amount of polyethylene glycol 4000 and ammonium polyphosphate. This study can provide a reference for the biohydrogen production process of straw-based biomass photofermentation.

Acknowledgements: The authors thank the National Key Research and Development Program of China (2018YFE0206600), National Natural Science Foundation of China (51706063), Henan Provincial Science and Technology Research Project (222102240099).

6th International Conference and Postgraduate Colloquium for Environmental Research 2022 (POCER 2022) 9 - 11 June 2022
Langkawi, Kedah, Malaysia

PCR27042022 – 222: Determination of Physicochemical Properties of Stingless Bee (*Geniotrigona thoracica* and *Heterotrigona itama*) Honey

Nashratul Shera Mohamad Ghazali[a], Yus Aniza Yusof[ab*], Chin Nyuk Ling[a], Siti Hajar Othman[a] and Syahrul Anis Hazwani Mohd Baroyi[a]

[a] Department of Process and Food Engineering, Faculty of Engineering, Universiti of Putra Malaysia, 43400, UPM Serdang, Selangor, Malaysia

[b] Laboratory of Halal Science Research, Halal Products Research Institute, Universiti Putra Malaysia, 43400, UPM Serdang, Selangor, Malaysia

[*]Correnspoinsing Author E-mail: yus.aniza@upm.edu.my

Abstract

Stingless bee honey contains greater health benefits over regular honey that lead to the increase of awareness among people to consume it. However, no international standard for stingless bee honey is available due to the lack of knowledge of its composition. This study aims to evaluate the physicochemical properties of Malaysian stingless bee honey that was produced by *Geniotrigona thoracica* and *Heterotrigona itama* stingless bee. These stingless bee honeys were harvested from the same geographical origin which was at an orchard in Universiti Putra Malaysia. The data from this study suggested to be useful in determining quality patterns for these stingless bee honeys from Malaysia.

Keywords: *Geniotrigona thoracica*; *Heterotrigona itama*; Honey; Physicochemical; Stingless bee honey

1. Introduction

Stingless bees or locally known as kelulut, belong to the family Apidae, order Hymenoptera, with sub-family level of Meliponinae (Michener, 2013). In Malaysia, two common stingless bees can be found are *Heterotrigona itama and Geniotrigona throacica*. Stingless bee honey usually contains higher moisture content compared to *Apis mellifera* honey (Alvarez-Suarez et al., 2018). Stingless bee honey contains greater health benefits over honey produced by honey bee, *A. mellifera*, that lead to the increase of awareness among people to consume it. However, the production of stingless bee honey is limited when compared to the production of *A. mellifera* honey due to the absence of quality control standards in relation to stingless bee honey, limited knowledge about the product, and low levels of industrial production. There is no international standard for stingless bee honey is available. Furthermore, international standard for honey quality, i.e. International Honey Commission (IHC), only focused on quality of honey bee honey and sometimes are not suitable for stingless bee honey. Therefore,

the objective of this study was to evaluate the physicochemical properties of Malaysian stingless bee honey that was produced by *Geniotrigona thoracica* and *Heterotrigona itama* stingless bee.

2. Methodology

Stingless bee (*G. thoracica* and *H. itama*) honey were harvested pots in the log hives placed in Orchard 10, Universiti Putra Malaysia (UPM), Serdang, Malaysia. Moisture content, total soluble solids (TSS) content, ash content, pH and free acidity of honey samples were analysed according to the methods recommended by the Association of Official Analytical Chemists (AOAC, 2005). Colour intensity of the honey was measured based on the honey industry's Pfund scale, an overall honey colour score. The sugar compositions (glucose, fructose and maltose) and hydroxymethylfurfural (HMF) content were determined using method described in the IHC (2009) using HPLC using a Waters Alliance 2695 (Waters Corp., Milford, MA, USA) system.

3. Results and discussions

The physicochemical properties of *G. thoracica* honey and *H. itama* honey were presented in Table 1. The results showed that the moisture content of the honey was ranging from 25.8–26.4 g/100 g which revealed that the *G. thoracica* honey contained higher moisture than *H. itama* honey. The obtained value of moisture content for both honey was higher than the limit of < 20% set by IHC. Similar findings that found moisture content of *G. thoracica* honey was higher than *H. itama* honey were reported for stingless bee honey from different states in Malaysia (Johor and Malacca) (Abu Bakar et al., 2017). As a results due to the high moisture content of *G. thoracica* honey, the TSS content in *G. thoracica* honey (72.2 ± 0.3 °Brix) lower than TSS content in *H. itama* honey. This is owing to the fact that the value of TTS content of honey relates the water and sugar content in honey (Ghazali et al., 2020).

The ash content of the honey samples ranged from 0.06 to 0.11 g/100 g of honey.it is reported that the ash content value affected by the amount of minerals present in the nectar (Nordin et al., 2018). Both honey was found to be acidic with pH value ranging between 3.11–3.44 and free acidity value of 85–172 mEq/kg. The free acidity of *G. thoracica* honey was found higher compared to *H. itama* honey due to its more acidic in pH. The high free acidity value of honey was attributed by the presence of organic acids in honey (Nordin et al., 2018). The value of colour intensity of all honey samples ranged between 132–165.1 mmPfund, with *G. thoracica* honey being the darkest colour. For sugar compositions, *G. thoracica* honey had higher maltose content, and lower glucose and fructose content than *H. itama* honey. Based on Table 1, both honey contained higher value of glucose than fructose. The variations in sugar content of these stingless bee honeys might be due to the diverse floral sources utilised by the bees during foraging activities, where larger body size of stingless bee (*G. thoracica*) can wander further when foraging. The HMF content was not detected in both honey indicating that the honey was fresh and proved that no additional treatment, e.g. heating treatment, was applied.

Table 1: Physicochemical properties of *G. thoracica* honey and *H. itama* honey

Physiochemical properties	***Geniotrigona thoracica* honey**	***Heterotrigona itama* honey**
Moisture content (g/100 g)	26.4 ± 0.3	25.82 ± 0.03
TTS content (°Brix)	72.2 ± 0.3	72.64 ± 0.03
Ash content (g/100 g)	0.055 ± 0.014	0.11 ± 0.01
pH	3.11 ± 0.01	3.44 ± 0.01
Free acidity	172.0 ± 1.4	85 ± 2.8
Colour intensity (mmPfund)	165.1 ± 1.5	132 ± 2.1
Glucose content (g/100 g)	10.98 ± 0.08	25.98 ± 0.04
Fructose content (g/100 g)	9.47 ± 0.01	19.56 ± 0.04
Maltose content (g/100 g)	55.70 ± 0.19	21.67 ± 0.14
HMF content (mg/kg)	nd	nd

4. Conclusions

Based on the results obtained, different type of stingless bees exhibited differences in some of the physicochemical properties. This study will provide information on stingless bee honey to add up to the current knowledge as well as for future research on the development of nutrient–rich food products.

Acknowledgements: The authors would like to thank the Ministry of Education Malaysia for the Transdisciplinary Research Grant Scheme (TRGS/1/2016/UPM/ 01/5/3) for the research funding.

References

Abu Bakar, M.F., Sanusi, S.B., Abu Bakar, F.I., Cong, O.J., & Mian, Z. (2017). Physicochemical and antioxidant potential of raw unprocessed honey from Malaysian stingless bees. *Pakistan Journal of Nutrition*, 16, 888–894.

Alvarez-Suarez, J. M., Giampieri, F., Brenciani, A., Mazzoni, L., Gasparrini, M., González-Paramás, A. M., … Battino, M. (2018). Apis mellifera vs Melipona beecheii Cuban polifloral honeys: A comparison based on their physicochemical parameters, chemical composition and biological properties. *LWT - Food Science and Technology*, 87, 272–279. https://doi.org/10.1016/j.lwt.2017.08.079.

AOAC (1990). Official methods of analysis (15th ed.). Arlington, VA, USA: Association of Official Analytical Chemists.

Ghazali, N. S. M., Yusof, Y. A., Ghazali, H. M., Othman, S. H., Manaf, Y. N. A., Chang, L. S., & Baroyi, S. A. H. M. (2020). Effect of surface area of clay pots onphysicochemical and microbiological properties of stingless bee (*Geniotrigona thoracica*) honey. *Food Bioscience*, 40, 100839. https://doi.org/10.1016/j.fbio.2020.100839.

International Honey Commission (2009). Harmonised methods of the international honey commission. Forschungsanstalt fuer Milchwirtschaft, Bern (p. 63). Switzerland: Swiss.

Nordin, A., Sainik, N.Q.A.V., Chowdhury, S.R., Saim, A.B., & Idrus, R.B.H. (2018). Physicochemical properties of stingless bee honey from around the globe: A comprehensive review. *Journal of Food Composition and Analysis*, 73, 91–102.

6th International Conference and
Postgraduate Colloquium for
Environmental Research 2022 (POCER
2022) 9 - 11 June 2022
Langkawi, Kedah, Malaysia

PCR27042022 – 223: Co-pyrolysis of food waste and wood bark to produce hydrogen with minimizing pollutant emissions

Heesue Lee[a], Chanyeong Park[a] and Jechan Lee[ab*]

[a] Department of Energy Systems Research,
University of Ajou, Suwon, 16499, Republic of Korea

[b] Department of Energy Systems Research,
University of Ajou, Suwon, 16499, Republic of Korea

- Corrensponsing Author E-mail: jlee83@ajou.ac.kr

Keywords: Co-pyrolysis, Food waste, Lignocellulosic biomass, Waste-to-energy, Waste valorization

Extended Abstract

In this study, the co-pyrolysis of food waste with lignocellulosic biomass (wood bark) in a continuous-flow pyrolysis reactor was considered as an effective strategy for the clean disposal and value-added utilization of the biowaste. To achieve this aim, the effects of major co-pyrolysis parameters such as pyrolysis temperature, the flow rate of the pyrolysis medium (nitrogen (N2) gas), and the blending ratio of food waste/wood bark on the yields, compositions, and properties of three-phase pyrolytic products (i.e., non-condensable gases, condensable compounds, and char) were investigated. The temperature and the food waste/wood bark ratio were found to affect the pyrolytic product yields, while the N2 flow rate did not. More non-condensable gases and less char were produced at higher temperatures. For example, as the temperature was increased from 300 °C to 700 °C, the yield of non-condensable gases increased from 6.3 to 17.5 wt%, while the yield of char decreased from 63.6 to 30.6 wt% for the co-pyrolysis of food waste and wood bark at a weight ratio of 1:1. Both the highest yield of hydrogen (H2) gas and the most significant suppression of the formation of phenolic and polycyclic aromatic hydrocarbon (PAH) compounds were achieved with a combination of food waste and wood bark at a weight ratio of 1:1 at 700 °C. The results suggest that the synergetic effect of food waste and lignocellulosic biomass during co-pyrolysis can be exploited to increase the H2 yield while limiting the formation of phenolic compounds and PAH derivatives. This study has also proven the effectiveness of co-pyrolysis as a process for the valorization of

biowaste that is produced by agriculture, forestry, and the food industry, while reducing the formation of harmful chemicals.

Acknowledgements: This work was supported by the National Research Foundation of Korea (NRF) grant funded by the Government of Republic of Korea (Ministry of Science and ICT) (No.2020R1C1C1003225).

6th International Conference and Postgraduate Colloquium for Environmental Research 2022 (POCER 2022) 9 - 11 June 2022
Langkawi, Kedah, Malaysia

PCR29042022 – 224: Biochemical Compositions and Prediction of Chlorophyll Content in Microalgae for Potential Therapeutic Applications

Doris Ying Ying Tang [a], Xuefei Tan [b], Kit Wayne Chew [c,d], Shir Reen Chia [e], Huong-Yong Ting [f], Yuk-Heng Sia [f], Francesco G. Gentili [g], Pau Loke Show [a,*]

[a] Department of Chemical and Environmental Engineering, Faculty of Science and Engineering, University of Nottingham Malaysia, Jalan Broga, 43500 Semenyih, Selangor Darul Ehsan, Malaysia
[b] College of Materials and Chemical Engineering, Heilongjiang Institute of Technology, Harbin, 150050, PR China; State Key Laboratory of Urban Water Resource and Environment, School of Environment, Harbin Institute of Technology, Harbin, 150090, PR China; Dalian SEM Bio-Engineering Technology Co., Ltd., Dalian, 116620, PR China
[c] School of Energy and Chemical Engineering, Xiamen University Malaysia, Jalan Sunsuria, Bandar Sunsuria, 43900 Sepang, Selangor Darul Ehsan, Malaysia
[d] College of Chemistry and Chemical Engineering, Xiamen University, Xiamen 361005, Fujian, China
[e] Institute of Sustainable Energy, Universiti Tenaga Nasional (UNITEN), Jalan IKRAM-UNITEN, 43000 Kajang, Selangor, Malaysia
[f] School of Computing and Creative Media, University College of Technology Sarawak, Sarawak, Malaysia
[g] Department of Forest Biomaterials and Technology (SBT), Swedish University of Agricultural Sciences (SLU), 901 83, Umeå, Sweden

- Corrensponsing Author E-mail: PauLoke.Show@nottingham.edu.my

Keywords: RGB colour model; Antioxidant; Fatty acids; Polysaccharides; Microalgae

Extended Abstract

Microalgae are well known to produce bioactive compounds such as proteins, fatty acids, polysaccharides and antioxidants, which can be adapted by pharmaceutical industries as a promising alternative for therapeutic application (Tang et al., 2020). In this study, the biochemical composition of mixed microalgae species, *Desmodesmus* sp. and *Scenedesmus* sp. was studied to explore its pharmaceutical potential and revealed that the biomass consisted of varied concentration of

carbohydrates, protein and lipids. Phenolic compounds and antioxidant activity was high, at 60.22 mg/L of phenolic compounds and 90.69% scavenging activity respectively.

Next, artificial intelligence system was utilized to estimate the chlorophyll content in microalgae on total 40 samples for each extractant solvent with one dependent variable (concentration) and one independent variable (colour index). Through the regression analysis, methanol exhibited the strongest linear relationship with colour index whereas ethanol showed the weakest linear relationship. All the extractant solvents, except ethanol, showed the significant result in determining chlorophyll concentration. Regression models that are statistically significant should theoretically have a high R-squared value. Lower R-squared value in this study were due to the high variability around the regression line due to the given datasets. Hence, for future studies, the sample size of dataset can be increased to train the machine learning system, for example, input of minimum 100 datasets instead of 40 datasets only or application of multiple models to get the colour index. Nonetheless, R-squared value does not convey the reliability of a model and cannot be used to determine whether the regression model fits adequately to the data set (Frost, 2017; Parveen et al., 2019). Further works are required into this area including more data sets and application of various machine learning techniques. This will enable a more reliable relationship between the concentration of chlorophyll and colour index as well as the development of a model for the purpose of recognizing the chlorophyll concentration of microalgae. Overall, this research study holds the promise in a machine learning approach to estimate chlorophyll in microalgae species at industrial scale.

Acknowledgements: The authors thank Fundamental Research Grant Scheme, Malaysia [FRGS/1/2019/STG05/UNIM/02/2] and MyPAIR-PHC-Hibiscus Grant [MyPAIR/1/2020/STG05/UNIM/1]. The financial support of Vinnova (2017-03301) was greatly appreciated. We thank Calle Niemi (Department of Forest Biomaterilas and Technology Swedish University of Agricultural Sciences) for assistance in microalgae freeze-drying.

References

Tang DYY, Khoo KS, Chew KW, et al., 2020. Potential utilization of bioproducts from microalgae for the quality enhancement of natural products. Bioresour Technol, 304: 122997. https://doi.org/10.1016/j.biortech.2020.122997

Parveen S, Duddela V, Narravula R, et al. , 2019 Effect of various solvents on chlorophyll and carotenoid extraction in green algae: Chlamydomonas reinhardtii and chlorella vulgaris. Ann Plant Sci, 21: 341-345.

Frost J. 2017. How to interpret regression models that have significant variables but a low r-squared.

6th International Conference and
Postgraduate Colloquium for
Environmental Research 2022 (POCER
2022) 9 - 11 June 2022
Langkawi, Kedah, Malaysia

PCR29042022 – 225: Inhibition Effect of Pure Diethylene Glycol , Glycine and their mixture on CO_2 Gas Hydrate: An Experimental Study

Adeel ur Rehman [a], Bhajan Lal [a*], Dzulkarnain B Zaini [a]

a Department of Chemical Engineering

Universiti Teknologi of PETRONAS

Bandar Seri Iskandar,32610, Perak, Malaysia

- Corresponding author email: bhajan.lal@utp.edu.my

Keywords: CO_2 Hydrates; Glycol amines; Thermodynamic Inhibition

Extended Abstract

In flow assurance, line losses and commotions caused by pipeline bottlenecks can pose a major safety concern while also depressing the production economy (Sloan Jr & Koh, 2007). CO_2 concentrations in some Malaysian offshore gas fields range from 70 to 80 percent. In a deep-water situation, higher CO2 concentrations pose issues in terms of gas production and delivery (E. Dendy Sloan & Koh, 2008). Gas hydrates are formed when high pressures and low temperatures are combined, trapping gas molecules in the cage molecules of frozen water (Koh, 2002). Water removal, heating, depressurization, and chemical inhibition are four fundamental approaches for preventing hydrate formation in deep seawater environments (Khan et al., 2018). The hydrate vapor-liquid equilibrium was changed by these THIs (HLVE). Chemical inhibitors, on the other hand, are usually the only viable option for hydrate inhibition in offshore gas pipelines. Methanol and glycol amines, which are traditional thermodynamic hydrate inhibitors, are utilized at much higher concentrations, sometimes up to 50% (Nasir et al., 2014). Diethlyene glycol (DEG) and glycine (Gly) combinations are shown to inhibit the production of carbon dioxide hydrate by shifting phase boundaries to the lower temperature side in this experimental investigation. DEG and Gly in a 1:1 ratio was examined at concentrations of 5% weight percent and pressures ranging from 2.5 to 4.0 MPa. The impact of the suggested mix on the CO_2 hydrate was evaluated using a T-cycle method to determine the dissociation temperature, as shown in Figure 1. In comparison to the 5 wt. % of pure chemicals, the results demonstrate that 5 wt. % DEG and Gly mixture has a very good inhibitory impact as compared to the pure components.

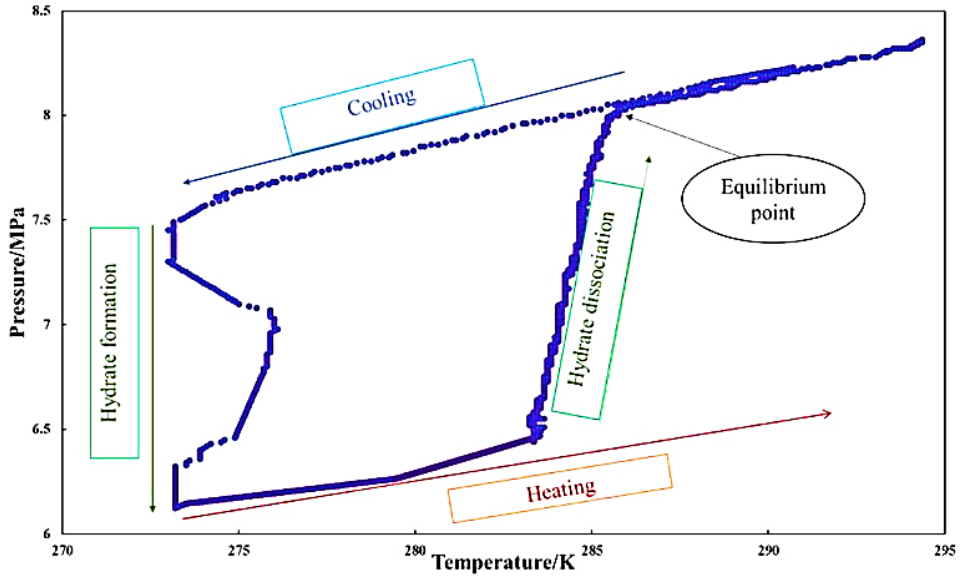

Figure 1 T-Cycle method to measure the equilibrium point.

Acknowledgements: The authors would like to express their gratitude to the Chemical Engineering Department, Universiti Teknologi PETRONAS (UTP) Malaysia, for providing financial support and experimental facilities for the study.

References

E. Dendy Sloan, & Koh, C. A. (2008). *Gas Hydrates of Natural Gases* (E. D. Sloan & C. A. Koh (eds.); third). CRC Press LLC, 2000 Corporate Blvd., N.W., Boca Raton, FL 33431, USA Orders from the USA and Canada (only) to CRC Press LLC.

Khan, M. S., Yaqub, S., Manner, N., Karthwathi, N. A., Qasim, A., Mellon, N. B., & Lal, B. (2018). Experimental equipment validation for methane (CH4) and carbon dioxide (CO2) hydrates. *IOP Conference Series: Materials Science and Engineering*, *344*(1), 12025.

Koh, C. a. (2002). Towards a fundamental understanding of natural gas hydrates. *Chemical Society Reviews*, *31*(3), 157–167. https://doi.org/10.1039/b008672j

Nasir, Q., Lau, K. K., & Lal, B. (2014). Enthalpies of dissociation of pure methane and carbon dioxide gas hydrate. *World Academy of Science, Engineering and Technology*, *8*(8).

Sloan Jr, E. D., & Koh, C. A. (2007). *Clathrate hydrates of natural gases*. CRC press.

6th International Conference and
Postgraduate Colloquium for
Environmental Research 2022 (POCER
2022) 9 - 11 June 2022
Langkawi, Kedah, Malaysia

PCR29042022 – 226: Modification and innovative utilization of straw biomass

Shiyu Zhang[a], Jishuang Chen [a*], Yue Qiu[a,b] and Yuyang Hou[a]

[a] Instute of Bioresource Engineering ,College of Biotechnology and Pharmaceutical Engineering
Nanjing Tech University, Nanjing, 211816, Jiangsu, China
[b] Dafeng marine Industry Research Institute
Nanjing Tech University,Yancheng ,224100,Jiangsu,China

- Corrensponsing Author E-mail: biochenjs@njtech.edu.cn

Keywords: Biomass; Modification; Straw; Straw-Plastic Composites ; Puffing.

Extended Abstract

Through the investigation, analysis and summary of the resource reserve, various modification methods and industrial application of biomass straw, this paper summarizes the main utilization ways of waste straw, new modification treatment methods and technical barriers that need to be overcome. It is clear that new straw plastic materials are the key direction of comprehensive utilization and high-value utilization of crop straw, and straw modification is the difficulty of material research. At the same time, the development trend of innovative utilization of straw is pointed out, which provides a reference for efficient utilization of crop straw and energy conservation and emission reduction.

Table 1: Utilization ways and proportion of straw biomass

Utilization way	Energy	Material	Feed	Fertilizer	Stroma
Proportion	43%	4%	31%	21%	1%

As a huge amount of renewable resources, the development of industrial utilization still needs efforts. Among many application ways, straw as a material is the most efficient utilization way. Adding the modified straw powder into plastic can not only significantly enhance the toughness and tensile strength of the composite, but also increase the friendliness of the material to the environment.

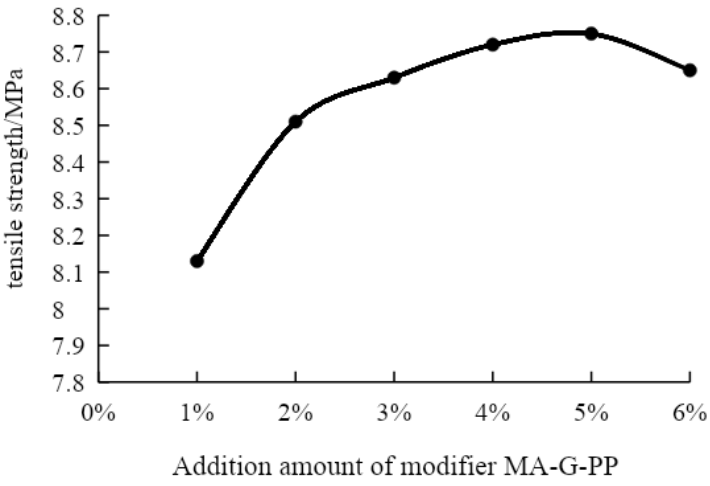

As shown in the above figure, through the selection of different modification methods and contents of straw, new Straw-Plastic Composites with various excellent properties can be obtained. In addition, straw can also be modified and added into geopolymer cementitious materials to prepare new lightweight thermal insulation wall materials. The expansion of straw for papermaking can reduce the pollution in the production process. The key lies in the modification method of straw, which is still the focus of current research.

Acknowledgements: The authors acknowledge Dr Jishuang Chen, Professor of the Nanjing Tech University, for his help in interpreting the significance of the results of this study。

References

Lu, Xiang'an,Liu, Yiliang,Ni, Yufan,Dai, Yifan,Yang, Ning,Zhu, Shiqiang,Duns, Gregory Joseph,Chen, Jishuang. (2017).Study on the Folding of Imitation Rattan with Wheat Straw Fibers. Journal of Biobased Materials and Bioenergy.11(4).

Liu Yiliang,Bekele Lemma Dadi,Lu Xiangan,Zhang Wentao,Yu Chunhan,Duns Gregory Joseph,Jin Leilei,Chen Jishuang. (2017). The Effect of Lignocellulose Filler on Mechanical Properties of Filled-High Density Polyethylene Composites Loaded with Biomass of an Invasive Plant Solidago canadensis. Journal of Biobased Materials and Bioenergy.11(1).

Zhang Wentao, Chen Jishuang .(2016).Research and industrial prospect of straw plastic composites ,Science and Technology Bulletin.32 (01): 97-101

Chen Jishuang, Liu Yiliang .(2015).Industrial utilization of straw biomass and new straw plastic materials , Journal of Jiangsu Normal University (NATURAL SCIENCE EDITION), 33 (03): 31-35

Yu Chunhan,Zhang Wentao,Bekele Lemma Dadi,Lu Xiang'an,Duns Gregory Joseph,Jin Leilei,Jia Qi,Chen Jishuang. (2018)Characterization of Thermoplastic Composites Developed with Wheat Straw and Enzymatic-hydrolysis Lignin[J]. BioResources.13(2).

Bekele, Lemma Dadi,Zhang, Wentao,Liu, Yiliang,Duns, Gregory Joseph,Yu, Chunhan,Jin, Leilei,Li, Xiaofei,Chen, Jishuang. (2017)Impact of Cotton Stalk Biomass Weathering on the Mechanical and Thermal Properties of Cotton Stalk Flour/Linear Low Density Polyethylene (LLDPE) Composites. Journal of Biobased Materials and Bioenergy.11(1).

Bekele Lemma Dadi,Zhang Wentao,Liu Yiliang,Duns Gregory Joseph,Yu Chunhan,Jin Leilei,Li Xiaofei,Jia Qi,Chen Jishuang. (2017) Preparation and Characterization of Lemongrass Fiber (Cymbopogon species) for Reinforcing Application in Thermoplastic Composites. BioResources.12(3).

6th International Conference and
Postgraduate Colloquium for
Environmental Research 2022 (POCER
2022) 9 - 11 June 2022
Langkawi, Kedah, Malaysia

PCR29042022 – 227: Treatment of oily wastewater from gas condensate field by chemical demulsification approach

Habineswaran Rajan[a] , Nur'aini Raman Yusuf [a] , and Dzeti Farhah Mohsim[a] , Nor Hadhirah Bt Halim[b]

a Department of Petroleum Engineering
Universiti Teknologi PETRONAS, 32610, Seri Iskandar, Perak, Malaysia

b PETRONAS Research Sdn Bhd
Jln Ayer Hitam, Kawasan Institusi Bangi, 43000 Bandar Baru Bangi, Selangor

• Corrensponsing Author E-mail: dzetifarhah.mohshim@utp.edu.my

Keywords: Emulsion; Produced water; Demulsifier; Demulsification; , Oil-in-water content (OIW); OA-KX

Extended Abstract

Oily wastewater or also known as produced water is one of inseparable hydrocarbon waste in the petroleum industry and their existing in the form of severe oil-in-water emulsion results in costly impact to the petroleum industry. In order to break up oil-in-water emulsion into crude oil and water, the industry aims to look for profoundly effective, speedy and low-cost demulsifying materials. Thus, in this paper, several types of demulsifiers such as cationic polyamine, resin alkoxylate, EO/PO block copolymers and a non-ionic surfactant are used to treat emulsion of gas condensate field. Based on the initial screening, a novel demulsifier was developed by adding appropriate weight percentage ratio of resin alkoxylate and non-ionic surfactant. The demulsification efficiency (De) of 95.5 % based on turbidity measurement was achieved after the treatment of OA-KX demulsifier at a dosage of 7 ppm.. To further conclude the efficiency of the demulsifier, oil-in-water content (OIW) of the produced water after the treatment of OA-KX demulsifier was measured. The developed OA-KX demulsifier was able to reduce the oil content of oily wastewater from 1008.3 ppm to 97.1 ppm under 15 mins at a dosage of 7 ppm and achieved the oil removal efficiency up to 90.37%.

Introduction: In today's world, various crises are being faced including environmental pollution, a high demand for fresh water, and the discovery of new energy sources. As a consequence, during oil/gas exploration and development, an excessive amount of water will be produced, which must be properly handled in order to protect the environment from contamination. Produced water can be in the form of oil-

in-water emulsion where it can be contaminated with the crude oil and it needs to be treated before discharged into the sea. An emulsion is a mixture of two incompatible liquid phases in which one is dispersed into the other [Tadros, 2013]. Demulsification is the breaking of a crude oil emulsion into oil and water phases. One of the common methods to accomplish this process is through chemical method by adding demulsifiers to enhance the process of emulsion breaking [Razi et al., 2011]. The main function of chemical additives is to neutralize the stabilizing effect of emulsifying agents [Daniel-David et al., 2018]. In this paper, various types of demulsifier such as cationic polyamine, resin alkoxylate, EO/PO block copolymers and a non-ionic surfactant have been tested to treat the oily wastewater. The effect of these demulsifiers were studied on the oil-in-water emulsion.

Materials and Methods: The produced water and condensate from a Miri oilfield were provided from PETRONAS Research Sdn. Bhd. (PRSB). Several types of chemicals such as demulsifier HF, KX, BS1, BS2 and OA are industrial grade and were obtained from PETRONAS Research Sdn. Bhd. (PRSB) for the treatment of oily wastewater.

Preparation of emulsion: The emulsion is prepared at a ratio of 85:15 of the produced water and condensate crude oil. 34 ml of produced water is poured into 100 ml beaker and 6 ml of condensate added as well. The mixture is then stirred at 4000rpm for 10 mins using IKA Ultra-Turrax T-50 Homogenizer to form a stable oil-in-water emulsion

Zeta potential and Interfacial Tension (IFT) of the emulsion: The zeta-potential of produced water sample without any addition of chemicals additives was measured using Malvern Zetasizer NanoZSP. Interfacial tension of two immiscible fluids which are oil and produced water phase can be determined by using Du Nuoy ring method.

Bottle test screening: The prepared emulsion is then transferred to a bottle and placed in water bath at a temperature of 60 °C for 30 mins. Once the injection of demulsifier done, the bottles was shaken 100 times by hand for the demulsifier to evenly distribute in the emulsion. Then, the bottles were placed in the water bath for 15 mins to allow the sample to settle. . The turbidity and oil concentration of the water sample were measured.

Turbidity measurement: The measurement of emulsion turbidity was performed using a HACH 2000 turbidimeter with a highest sensitivity of 0.001 NTU. 2.6 Oil-in-water (OIW) concentration measurement: The TD-500D Handheld Oil in Water Analyser from HMA INSTRUMENTATION was used to measure the OIW concentration of the sample.

Results and Discussion:

Zeta potential and Interfacial Tension (IFT) of the emulsion: The sample recorded a pH of 3.7 which is quite acidic condition and has a zeta potential measurement of -23.7 mV that indicates a stable emulsion.. The interfacial behavior of interfaces between produced water and condensate is 24.72 mN/m.

Effect of demulsifier on turbidity of produced water: The bottle test screening was performed on the prepared emulsion. A concentration of 7ppm, 10ppm and 20 ppm was injected into the emulsion sample. The demulsifier OA and KX exhibited much higher reduction of turbidity compared to the blank sample.

Addition of demulsifier KX showed a continuous reduction of turbidity as the concentration of dosage increased from 7ppm to 20ppm. Demulsifier OA recorded the lowest turbidity (181 NTU) at a concentration of 7ppm.

Development of novel demulsifier (OA-KX): A novel demulsifier for treatment was developed based on the weight percentage ratio of OA and KX demulsifier. The novel demulsifier, OA-KX was then tested at 7ppm, 10ppm and 20 ppm for the treatment of emulsion. Based on the results, at a dosage of 7 ppm, the OA-KX was able to reduce the turbidity of produced water to 45 NTU which is lower than than results obtained by the addition of demulsifier OA (181 NTU).

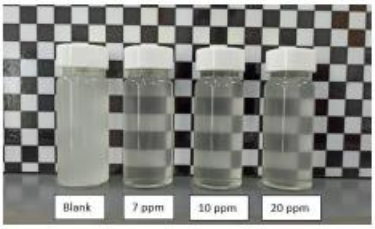

Figure 1 : Produced water after the addition of OA-KX

Effect of demulsifier OA-KX on OIW concentration: The lowest reading of OIW content (97.1 ppm) was recorded at the dosage of 7ppm of OA-KX. The OIW content of the blank sample without any chemical injection was 1008.3 ppm. The results show a significant result in the reduction of OIW content when the novel demulsifier, OA-KX was added at an oil removal efficiency of 90.37 %. A gradual increase of OIW content was recorded as the dosage of demulsifier was increased. 4.0

CONCLUSION: The optimum dosage of OA-KX demulsifier was obtained at 7ppm under a settling temperature of 60 °C for 15 mins. The oil content of the produced water from gas condensate was able to reduce from 1008.3 ppm to 97.1 ppm under 15 mins which is an oil removal efficiency of 90.37%.

Acknowledgements: The authors would like to acknowledge Department of Petroleum Engineering for funding of this project (015MD0-066) under Universiti Teknologi PETRONAS.

References

Tadros, T. F. (2013). Emulsion formation, stability, and rheology. Emulsion formation and stability, 1, 1-75.

Razi, M., Rahimpour, M. R., Jahanmiri, A., & Azad, F. (2011). Effect of a different formulation of demulsifiers on the efficiency of chemical demulsification of heavy crude oil. Journal of Chemical & Engineering Data, 56(6), 2936-2945.

Daniel-David, D., Le Follotec, A., Pezron, I., Dalmazzone, C., Noik, C., Barre, L., & Komunjer, L. (2008). Destabilisation of water-in-crude oil emulsions by silicone copolymer demulsifiers. Oil & Gas Science and Technology-Revue de l'IFP, 63(1), 165-173.

6th International Conference and
Postgraduate Colloquium for
Environmental Research 2022 (POCER
2022) 9 - 11 June 2022
Langkawi, Kedah, Malaysia

PCR30042022 – 228: Extraction and separation of lipids from municipal sewage sludge for biodiesel production: A sustainable approach

Alyaa Abdulhussein Alsaedi[a], Md. Sohrab Hossain[a*], Venugopal Balakrishnan[b], Nor Afifah Khalil[c], Ahmad Naim Ahmad Yahaya[c], Norli Ismail[a]

[a] Environmental Technology Division, School of Industrial Technology, Universiti Sains Malaysia, Penang, Malaysia.

[b] Institute for Research in Molecular Medicine (INFORMM), Universiti Sains Malaysia, Penang 11800, Malaysia.

[c] Universiti Kuala Lumpur, Malaysian Institute of Chemical and Bioengineering Technology (MICET), Alor Gajah, Malacca, Malaysia

- Corrensponsing Author E-mail: sohrab@usm.my

Keywords:

Extended Abstract

There is increasing attention worldwide on biodiesel production as an alternative to commercial diesel because of its growing demand, rapid depletion, and environmental pollution concerns. However, the high feedstock price for biodiesel production has made it less completive to commercial diesel. Therefore, studies are conducted to determine renewable biomass as a viable feedstock for biodiesel production. The municipal sewage sludge (MSS) could be a viable feedstock for biodiesel production due to its high lipids content, abundance availability, and low cost. In the present study, lipids were extracted from MSS with a solvent extraction method using methanol as a solvent with varying temperature (40 -80 oC), treatment time (1 -5 h), and sludge to the solvent (S/L) ratio. It was found that the lipids extraction was influenced by the temperature, treatment time, and S/L ratio. About 26.62±1.2% of lipids were extracted from MSS at a temperature of 70 ℃, treatment time of 3 h, and S/L ratio of 1: 10. Subsequently, the biodiesel was produced from the extracted lipids via the catalytic transesterification process using methanol as a solvent. The highest, about 84% of biodiesel was produced from MSS lipids at lipids to methanol molar ratio 1:12, catalyst concentration of 5 wt %, temperature of 60 ℃, and time of 4 h. Several analytical methods were employed to determine physicochemical and fatty acids properties of the extracted lipids and biodiesel. The physicochemical properties of the produced biodiesel comply with the ASTM D6751 and EN 14214 standards. The findings of the present study reveal that the MSS could be utilized as a potential feedstock for biodiesel production. Besides, the utilization of the MSS as a biodiesel feedstock will enhance the sustainable utilization of waste materials while minimizing negative environmental impacts.

6th International Conference and
Postgraduate Colloquium for
Environmental Research 2022 (POCER
2022) 9 - 11 June 2022
Langkawi, Kedah, Malaysia

PCR30042022 – 229: Effect of quorum sensing molecules on bio-hydrogen production in an anaerobic CSTR

Nguyen Tang Thau[a], Parthiban Anburajan[a,b], You Mit Prohim[a], Sungmi Kim[a], and Hyun-Suk Oh[a,b*]

[a] Department of Environmental Engineering, Seoul National University of Science & Technology, Seoul, South Korea

[b] Institute of Environmental Technology, Seoul National University of Science and Technology, Seoul, South Korea

- Corresponding Author E-mail: hyunsukoh@seoultech.ac.kr.

Keywords: Bio-hydrogen; Dark fermentation; Quorum sensing; Continuous stirred tank reactor (CSTR); *N*-acyl homoserine lactone (AHL); Microbial community.

Extended Abstract

Dark fermentation is one of the propitious ways for bio-hydrogen production using a mixture of various microorganisms present in anaerobic sludge from a wastewater treatment plant (WWTP). The mixture of microorganisms will break down different types of organic substances during fermentation and convert them to hydrogen in the absence of light and oxygen. Most studies on bio-hydrogen production using dark fermentation have been focused on the effects of various substrates and operating conditions and on hydrogen production, but little attention has been paid to communication within the complex microbial community.

Quorum sensing (QS) is cell-to-cell communication based on population density and organizes group behaviors using signaling molecules known as auto-inducers, which are produced and recognized by microorganisms. By activating social behaviors through QS signaling molecules in diverse microbial populations during fermentation, the formation of biofilms or granules by hydrogen-producing microorganisms might be accelerated, resulting in an increased hydrogen production thanks to improved stability in adverse environmental conditions. However, little has been studied about the role of QS signaling in the biohydrogen production process.

In this study, we investigated the effect of QS molecules of *N*-acyl homoserine lactone (AHL), on hydrogen production in a lab-scale continuous anaerobic reactor. A continuously stirred tank reactor (CSTR) with a working volume of 2.9 L was operated. The pre-treated anaerobic suspended sludge immobilized in sodium alginate beads was used as an inoculum for the CSTR system, and the reactor was continuously fed with a Modified Endo medium with a concentration of 15 g/L glucose at an HRT of 6 h. Once the system has started to generate stable bio-hydrogen production, various types of AHLs mixed as a cocktail (C4-, C6-, C8-, and C10-HSL) were added into the system with a final concentration of 20 µM to observe the impact of the QS signaling molecules in the hydrogen production.

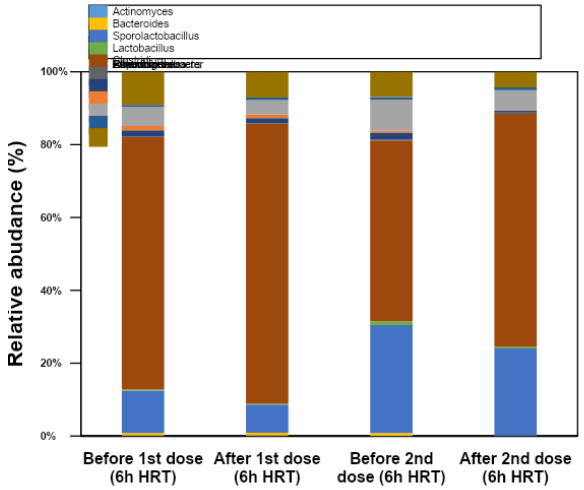

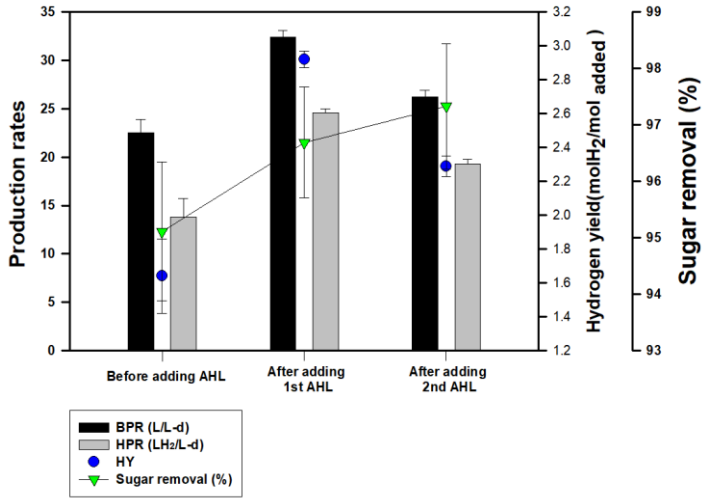

Figure 1: A) Biogas production rate (BPR), hydrogen production rate (HPR), and hydrogen yield (HY) change when AHL is added to the system, B) Taxonomic composition of the microbial community at genus level revealed by illumina Miseq of 16S rRNA.

The addition of the AHL cocktail resulted in an increased hydrogen production rate (24.6 ± 0.4 and 19.3 ± 0.5 L H_2/L-d after the first and the second dosage, respectively) compared to before the addition (13.8 ± 1.9 L H_2/L-d) (figure 1, A). Analysis of the microbial community revealed that the addition of AHLs increased the abundance of *Clostridium* genus known as hydrogen-producing bacteria (figure 1, B), which appears to have played an important role in increasing hydrogen production. We also observed increased biofilm formation after the addition of AHL cocktails. These results demonstrated that the QS molecules may have an impact on the hydrogen-producing bacterial community, thereby altering the biofilm in the system as well as the bio-hydrogen production rate. Therefore, this study suggests that QS signaling plays an important role in biological hydrogen production and that it may be possible to increase hydrogen production through its regulation.

Acknowledgements: This work was supported by the Basic Science Research Program through the National Research Foundation of Korea (NRF) funded by the Ministry of Education (NRF-2020R1A6A1A03042742 and 2021R1I1A1A01060274)

References

Anburajan, P., Park, J.H, Sivagurunathan, P., Pugazhendhi, A., Kumar, G., Choi, C.S, Kim, SH., 2017. Mixed-culture H_2 fermentation performance and the relation between microbial community composition and hydraulic retention times for a fixed bed reactor fed with galactose/glucose mixtures. *Journal of Bioscience and Bioengineering*. 124, 339-345.

Oh, H.S., Lee, CH., 2018. Origin and evolution of quorum quenching technology for biofouling control in MBRs for wastewater treatment. *Journal of Membrane Science*. 554, 331–345.

Sivagurunathan, P., Anburajan, P., A., Kumar., Kim, SH., 2016, Effect of hydraulic retention time (HRT) on biohydrogen production from galactose in an up-flow anaerobic sludge blanket reactor. *International Journal of Hydrogen Energy*. 41, 21670-21677.

Yan, H., Li, H., Meng, J., Li, J., Jha, A.K., Zhang, Y., Fan, Y., Wang, X., 2021. Effects of reflux ratio on the anaerobic sludge and microbial social behaviors in an expanded granular sludge bed reactor: From the perspective of acyl-homoserine lactones-mediated quorum sensing. *Bioresource Technology*. 337, 125360

6th International Conference and Postgraduate Colloquium for Environmental Research 2022 (POCER 2022) 9 - 11 June 2022
Langkawi, Kedah, Malaysia

PCR30042022 – 230: Effect of quorum quenching in anaerobic digestion for biomethane recovery

You Mit Prohim[a], Roent Dune A. Cayetano[a,b], Parthiban Anburajan[a,b], Nguyen Tang Thaua , Sungmi Kima , and Hyun-Suk Oh[a,b*]

a Department of Environmental Engineering, Seoul National University of Science & Technology, Seoul, South Korea

b Institute of Environmental Technology, Seoul National University of Science and Technology, Seoul, South Korea

• Corresponding Author E-mail: hyunsukoh@seoultech.ac.kr

Keywords: Anaerobic digestion, Biomethane, Quorum Sensing (QS), Quorum Quenching (QQ)

Extended Abstract

Anaerobic digestion (AD) is a low-cost biological wastewater treatment method that employs a diverse array of bacteria and archaea to break down organic matter into biomethane in three stages: hydrolysis, acidogenesis, and methanogenesis. Biomethane recovered in AD is a renewable, sustainable, and costeffective alternative energy that could help meet the community's rising energy demands. Hydrolysis is thought to be the rate-limiting step in the AD process, influencing the activity of substrate-dependent methanogenic archaeons and, as a result, biomethane production. Treatment success in AD reactors depends on the synergy of essential microorganisms and the control of competitive microbes that contribute to excessive cell aggregation, which can hinder the efficient treatment process. It is then imperative to promote/control certain microbial interactions while ensuring the retention of an active and robust microbial community which is essential for biomethane recovery.

Quorum sensing (QS) is a chemical signaling system that allows microorganisms to communicate with each another. It is important for activating social behaviors in microbial populations and controlling group activities including biofilm formation and virulence factor production. Recently, quorum quenching (QQ), which disables QS systems, has been reported as an effective strategy to mitigate unwanted group behaviors, such as biofilm formation, in anaerobic membrane bioreactors (An-MBRs) as well as aerobic MBRs. However, the effect of QS and QQ on methanogenesis in AD has been rarely explored. The main objective is to develop an understanding regarding the effects of QS/QQ within the AD system during efficient biomethane recovery. In this study, various concentrations of AHL cocktails (C6-, C8-, C10-, and 3oxo-C6-HSL) and a facultative QQ bacteria (*Bacillus sp.)* were introduced into a sealed batch anaerobic mixed culture with 2 g/L of glucose as a substrate to determine the role of QS and QQ in anaerobic systems, respectively. The changes in biogas and extracellular polymeric substances, aggregation formation, and particle size distribution were analyzed. Furthermore, with AD treatment, changes in microbial composition were observed.

Table 1: Methane monitoring parameters as predicted by Modified-Gompertz Model

Samples	Max methane production (mL)	Methane yields ($mLCH_4/gCOD$)	Methanogenic activity (mL/g-VSS/d)	Lag phase (d)	R^2
Control	67.45	278.7	25.21	4	0.99
AHL-2 µM	72.89	305.65	25.62	3.45	0.99
AHL-20 µM	78.18	330.43	35.24	2.86	0.99
QQ-1%	72.71	306.13	28.09	3.77	0.99
QQ-3%	78.03	328.97	33.29	4.55	0.99
QQ-5%	79.23	337.16	39.13	4.82	0.99

The addition of 20 µM AHLs resulted in the highest average methane yield of 330 mL CH4/g-COD, which increased methane production by 14% when compared to the control (without AHL addition) (table 1). It also reduced the lag phase of the systems by 28%. It seems that activating QS systems by adding exogenous AHLs could promote the methanogenesis pathway. In addition, the composition of EPS was elevated following dosing with the AHL cocktail (figure 1, A). Furthermore, adding AHLs promotes floc formation and particle size, which is a key factor in enhancing biomethane production by increasing the microbial population. QQ bacteria, on the other hand, had a considerable negative impact on EPS synthesis, as seen by lower PS concentrations. As a result of the lowered EPS production, the addition of QQ bacteria reduced the average floc diameters. Nevertheless, surprisingly, adding QQ bacteria also increased methane output, with 5% of QQ bacteria resulting in the highest methane production (337.16 ml CH4/gCOD) (table 1). The hydrolysis activity of QQ bacteria itself was investigated to see how it influenced the biomethane recovery of the mixed community of AD system. As shown in Figure 1, B, the QQ bacteria used in this experiment had high hydrolysis activity, which might result in more available food for methanogenesis and thus increased methane productivity.

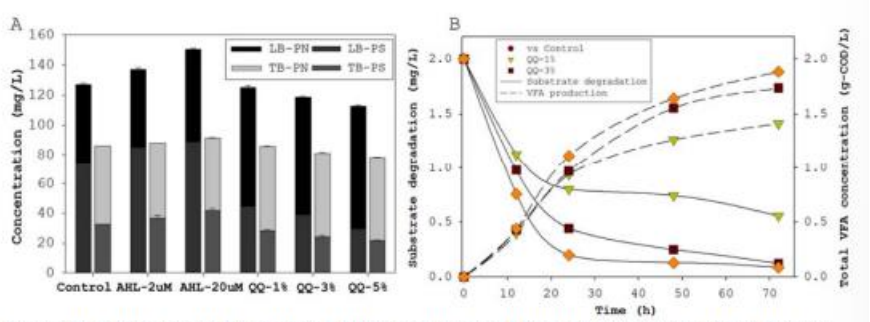

Figure 1: A) Impact of QS and QQ on EPS production and B) hydrolysis profile of QQ bacteria depicting substrate degradation and VFA production

The results of this study demonstrate that the QS mechanism plays an important role in the methanogenesis efficiency of AD systems. (1) QS has the potential to boost methanogenesis activity as well as microbial regulation and EPS generation. This could be useful in AD systems where microbial wash-out is a problem, as it increases microbial retention through improved flocculation. (2) QQ application may interfere with effective methane production by lowering EPS production and inhibiting floc formation, but increased hydrolysis by QQ bacteria can rather boost overall methane production.

Acknowledgments: This work was supported by the National Research Foundation of Korea (NRF) grant funded by the Ministry of Science and ICT (NRF-2020R1C1C1012755) and the Ministry of Education (NRF-2021R1I1A1A01060274).

6th International Conference and
Postgraduate Colloquium for
Environmental Research 2022 (POCER
2022) 9 - 11 June 2022
Langkawi, Kedah, Malaysia

PCR30042022 – 231: Optimization of Deep Eutectic Solvent Pretreatment for Bioethanol Production from Napier Grass

Elizabeth Jayex Panakkal[a], Marttin P. Gundupalli[a], Santi Chuetor[b], Atittaya Tandhanskul[c], Kraipat Cheenkachorn[b] and Malinee Sriariyanun [a*]

[a] Biorefinery and Process Automation Engineering Center, Department of Chemical and Process Engineering, TGGS, King Mongkut's University of Technology North Bangkok, Bangkok, Thailand

[b] Department of Chemical Engineering, Faculty of Engineering,
King Mongkut's University of Technology North Bangkok, Bangkok, Thailand

[c] Department of Food Technology, Faculty of Biotechnology, Assumption University, Bangkok, Thailand

*Corresponding Author E-mail: macintous@gmail.com

Keywords: Deep eutectic solvent; Enzymatic hydrolysis; Fermentation; Pretreatment; Biorefinery

Extended Abstract

The growing demands of fossil fuel consumption led to the depletion of fossil fuels, and global warming problem. Sustainable development has thus become a necessity in the current scenario. Lignocellulose with its rich carbon source is considered as an alternative for fossil fuels to produce biofuels and several platform chemicals. Napier grass has been identified as an important energy crop due to its high growth rate, and carbohydrate content (Nantasaksiri et al., 2021). This study aimed to enhance conversion of Napier grass to bioethanol by pretreatment with acidic deep eutectic solvent (DES) , choline chloride: lactic acid (ChCl/LA).

The physical properties of the synthesized ChCl/LA were also determined in this study (pH of 0.15, density of 1.04 g/ml, and viscosity of 125 mPa). The pH for ChCl, varying in composition from 1:1 to 1:9 was reported within the range of 1.50 to 0.47 (Kumar et al., 2018). The change in pH is due to the difference in the molar ratio of components along with temperature (Fanali et al., 2021). In addition to this, the change in viscosity for increasing temperature was also determined. This trend could be due to the altered nature of DES by the thermal expansion of the structure (Fanali et al., 2021).

Even though several studies are carried out using different types of DESs, until now these studies could not confirm the best DES type or any optimized process conditions (Xu et al., 2020). However, optimized pretreatment conditions are necessary to maximize sugar yield from biomass. Therefore, the pretreatment conditions for choline chloride: lactic acid (1:4) were optimized using Box Behnken Design (BBD) of Response Surface Methodology (RSM). The optimization study has considered three factors namely, biomass loading (1:5 to 1:20, w/w), pretreatment temperature (80 to 130 ℃) and pretreatment time (0.5 to 5 h) and sugar concentration (mg/mL) after enzymatic hydrolysis was considered as the response. The model could predict the optimal pretreatment condition as biomass loading of 15.30% (w/w), pretreated at 80 ℃ for 5 h. Pretreatment at optimal conditions was predicted to provide a sugar yield of 4.140 mg/mL. Also, the BBD model could reveal the factors and their interaction effect on pretreatment. The study obtained maximum sugar yield at either lower temperature and longer pretreatment time or higher temperature and shorter pretreatment time suggesting that pretreatment temperature and time as influential factors in pretreatment (Figure 1). Under optimized pretreatment conditions, there were significant changes in the biomass composition, which confirms the positive effect of pretreatment (Table 2). The pretreatment with DES has contributed to the removal of lignin and enhancing cellulose content after pretreatment.

Further studies conducted to analyze the inhibitor formation in the pretreatment hydrolysate after pretreatment under optimized conditions. However, only acetic acid could be detected in the hydrolysate, which could be formed from the acetyl group of the hemicellulose. Fermentation studies were also conducted

to evaluate the bioethanol production from the biomass. The pretreated Napier grass could produce 96.3% of the theoretical ethanol yield. Overall, this study provides optimized pretreatment conditions for choline chloride: lactic acid (1:4) for pretreating Napier grass and demonstrates the potential of Napier grass for producing bioethanol.

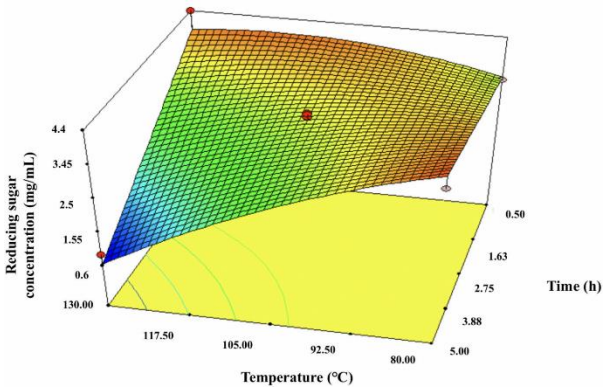

Figure 37: Effect of pretreatment temperature and time on reducing sugar concentration

Table 2: Biomass composition of Napier Grass

Biomass	Biomass Composition (%)		
	Glucan	Xylan	Lignin
Untreated Napier Grass	22.315 ± 0.07	7.754 ± 0.18	19.309 ± 0.43
Pretreated Napier Grass	31.635 ± 0.02	12.550 ± 0.28	10.986 ± 2.43

Acknowledgments: The authors would like to thank King Mongkut's University of Technology North Bangkok for providing all facilities and financial support (Grant Contract no: KMUTNB-FF-65-37, KMUTNB-PHD-64-02) for conducting the research.

References

Fanali, C., Gallo, V., Posta, S. Della, Dugo, L., Mazzeo, L., Cocchi, M., Piemonte, V., & De Gara, L. (2021). Choline chloride–lactic acid-based NADES as an extraction medium in a response surface methodology-optimized method for the extraction of phenolic compounds from hazelnut skin. *Molecules*, *26*(9). https://doi.org/10.3390/molecules26092652

Kumar, A. K., Shah, E., Patel, A., Sharma, S., & Dixit, G. (2018). Physico-chemical characterization and evaluation of neat and aqueous mixtures of choline chloride +lactic acid for lignocellulosic biomass fractionation, enzymatic hydrolysis and fermentation. *Journal of Molecular Liquids*, *271*, 540–549. https://doi.org/10.1016/j.molliq.2018.09.032

Nantasaksiri, K., Charoen-Amornkitt, P., & Machimura, T. (2021). Land potential assessment of napier grass plantation for power generation in thailand using swat model. Model validation and parameter calibration. *Energies*, *14*(5). https://doi.org/10.3390/en14051326

Xu, H., Peng, J., Kong, Y., Liu, Y., Su, Z., Li, B., Song, X., Liu, S., & Tian, W. (2020). Key process parameters for deep eutectic solvents pretreatment of lignocellulosic biomass materials: A review. *Bioresource Technology*, *310*. https://doi.org/10.1016/J.BIORTECH.2020.123416

6th International Conference and
Postgraduate Colloquium for
Environmental Research 2022 (POCER
2022) 9 - 11 June 2022
Langkawi, Kedah, Malaysia

PCR30042022 – 234: In-situ Condensation of Furans to Diesel Precursors during the Acidic Saccharification of Lignocellulose

Hyeonmin Jo[ab], Hyemin Yang[ab], Jae-Wook Choi[a], Dong Jin Suh[a], Chun-Jae Yoo[a], Hyunjoo Lee[ac], Kwang Ho Kim[ac], Chang Soo Kim[ac], Kyeongsu Kim[a], Jungkyu Choi[b] and Jeong-Myeong Ha[ac*]

[a] Clean Energy Research Center
Korea Institute of Science and Technology, Seoul, Republic of Korea

[b] Department of Chemical and Biological Engineering
Korea University, Seoul, Republic of Korea

[c] Division of Energy and Environment Technology
Korea University of Science and Technology, Seoul, Republic of Korea

- Corrensponsing Author E-mail: jmha@kist.re.kr

Keywords: Acidic saccharification; Furfural; 2-Methylfuran; Condensation; Diesel.

Extended Abstract

The acidic saccharification of lignocellulose has been a potentially feasible method to mass produce sugars, particularly glucose, from the inedible biomass for the further conversion to alcohols and fine chemicals [Wijaya *et al.*, 2014]. Although this process has successfully produced the sugars from lignocellulose, the degradation of sugars to furans and other compounds occurred in the presence of strong acids significantly reducing the yields of sugars. The furan byproducts can inhibit the fermentation of sugars. In addition, the formation of polymeric resins from furans can also occur to reduce the carbon yields of process.

In this study, we propose the in-situ production of diesel precursors from the unwanted byproduct furans obtained during the acidic saccharification of lignocellulose. Furfural byproduct prepared by acidic dehydration of xylose can be converted to the C15 hydrocarbons as diesel precursors [Kwon *et al.*, 2019]. For converting furfural to the C15 compounds, the acidic saccharification using an aqueous sulfuric acid was performed in the presence of extracting solvent (Figure 1). 2-Methylfuran (2-MF), which can be obtained by the selective hydrogenation of furfural [Park *et al.*, 2020], was dissolved in

the extracting solvent, cyclopentyl methyl ether (CPME) in this study, for the condensation with furfural prepared in the aqueous phase.

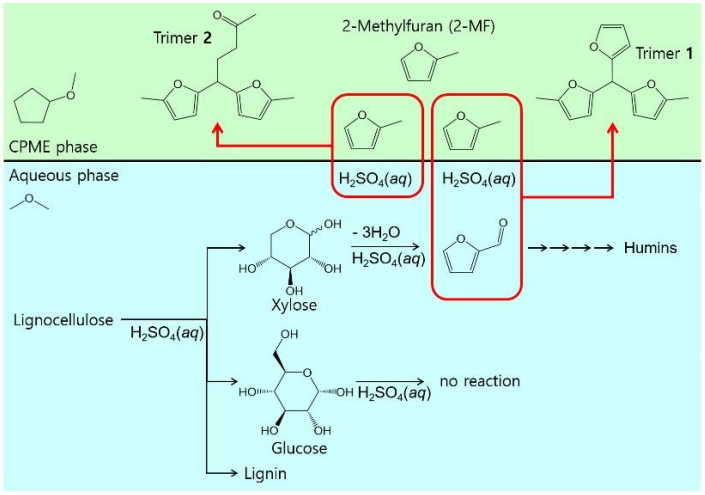

Figure 38: Production of C15 compounds from furfural during the acidic saccharification of lignocellulose

The goal of this study is (i) to suppress the carbonization of furfural and xylose to humins by the in-situ transfer of prepared furfural from acid-containing aqueous phase to organic extracting solvent, and (ii) to remove the fermentation-inhibiting furans for purifying glucose in the aqueous phase.

Two-step acidic saccharification was performed using *M. giganteus*: the decrystallization of cellulose fraction was performed followed by the dehydration and condensation. For the first step decrystallisation of *M. giganteus*, the dispersion of *M. giganteus* in the aqueous sulfuric acid (75 wt% in the DI water) was prepared in the closed batch reactor. For the second step reaction using the decrystallised mixture, DI water was added to the mixture to reduce the concentration of sulfuric acid to 10–30 wt%. NaCl was added to the mixture, and then CPME was added to achieve (CPME)/(aqueous solution) = 0.2–2 (v/v). 2-MF (~1 M) was added to the biphasic mixture mixture, and N_2 was added to reach 4 bar at room temperature. The reaction mixture was heated to 80–120 °C, and for 1 h. After the reaction, the reaction mixture was quenched to the cold water for 1 h. The prepared mixture was filtered using the glass filter followed by the weighing and the further characterization.

When the reaction was performed, the production of C15 compounds from the intracondensation of 2-MF and furfural was observed, which reduced the production of furfural-based carbons reserving the lignocelluose-derived sugars.

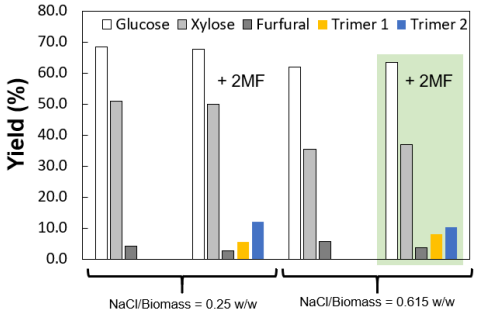

Figure 2: In-situ condensation of furfural during the acidic saccharification

Acknowledgements: This research was supported by the Technology Development Program to Solve Climate Changes (2020M1A2A2079798) through the National Research Foundation of Korea (NRF) funded by the Ministry of Science and ICT.

References

Kwon, J. S., Choo, H., Choi, J.-W., Jae, J., Jin Suh, D., Young Lee, K., Ha, J.-M., 2019. Condensation of pentose-derived furan compounds to C_{15} fuel precursors using supported phosphotungstic acid catalysts: Strategy for designing heterogeneous acid catalysts based on the acid strength and pore structures. *Applied Catalysis A: General*. 570, 238-244.

Park, S., Kannapu, H. P. R., Jeong, C., Kim, J., Suh, Y.-W., 2020. Highly Active Mesoporous Cu−Al_2O_3 Catalyst for the Hydrodeoxygenation of Furfural to 2-methylfuran. *Chemcatchem.* 12, 105-111.

Wijaya, Y. P., Putra, R. D. D., Widyaya, V. T., Ha, J.-M., Suh, D. J., Kim, C. S., 2014. Comparative study on two-step concentrated acid hydrolysis for the extraction of sugars from lignocellulosic biomass. *Bioresource Technology*. 164, 221-231.

6th International Conference and Postgraduate Colloquium for Environmental Research 2022 (POCER 2022) 9 - 11 June 2022
Langkawi, Kedah, Malaysia

PCR30042022 – 237: Enhancing the production of fermentative bioH_2 from lignocellulosic biomass through manipulated photo nanocatalysts

Nadeem Tahir[a], Faiqa Nadeem[a], Quanguo Zhang[a], Zhang Zhiping[a]

[a] Collaborative Innovation Center of Biomass Energy, Henan Agricultural University, Zhengzhou 450002, China

- Correnspondsing Author E-mail: ntahir@henau.edu.cn

Keywords: nanocatalyst; lignocellulosic biomass; photofermentation; biohydrogen; oxygen vacancies.

Extended Abstract

The quests for the alternative energy resources with environmentally friendly and renewable sources have already been started. Hydrogen is a clean fuel with no CO2 emission and has high-energy yield of 122 kJ/g, which is 2.75 times higher than hydrocarbon fuel can be potential candidate to reduce our dependence on fossil fuels which are serious threat for global warming. China has abundance of agricultural residues according to statistics, which is estimated to approximately 5.0×10^9 tons per year, so it is certainly worth studying biomass conversion technology. Through biological route, the low efficiency of hydrogen production is the main bottleneck for its realization. The processes of biohydrogen production are strongly related with change in electron donor types, redox potential, substrate type and microorganism helping to the flow of charges. Thus, electrons and protons play crucial role in regulating biohydrogen through internal enzyme reaction. Semiconducting photo nanocatalysts have attracted massive research interest since it has been regarded as one of the most promising solution to deal with the biomass conversion to energy. It has been shown that altering nanomaterials through surface defects engineering (creation of oxygen vacancies) can be possible route to enhance the hydrogen production from agricultural residue of corn stover. Surface defects of oxygen vacancies in SnO_2 nanoparticles were controlled through subsequent annealing in various environments such as oxygen (O), air and reducing gas (Ar95%+$H_2$5%). In relation to control group, nanoparticles annealed in reducing and air environment showed increase in hydrogen production rate and accumulated hydrogen production of 25.64% (147mL/h), 23.636% (345mL) and 16.24% (136mL/h), 11.83% (312mL) respectively. Reducing environment helped to generate more oxygen vacancies (confirmed through various characterizations) which enhances charge transfer mechanism, and

eventually increases the metabolic rate to enhance the hydrogen production. Furthermore, in extrinsic defect engineering process, excessive electrons were fed to the fermentative medium through charge compensation mechanism by Zn doping in SnO_2. Maximum hydrogen yield of 335mL is observed at 8%Zn doped SnO_2 nanocatalysts with concentration of 150 mg/L, almost 47% higher as compare to standard sample (228 mL). Zn doping in SnO_2 nanocatalysts not only helped to reduce the lag time (24 h from 48) but also increased the hydrogen production rate (77 mL/h observed for 8%Zn at 24 h). The maximum decrease in total amount of byproducts (2.52 g/L from 4.28 g/L) by 8% Zn doping suggests increase in bacterial metabolism which leads to decrease in volatile fatty acids (VFAs). Maximum change in oxidation reduction potential (-525 mV) is observed at 24 h for 8%Zn. The charge compensation through Zn doping provides excessive electrons to the fermentative medium which help the bacteria to transfer electron faster during redox reaction which leads to enhance the enzymatic process, eventually hydrogen production considerably. Current study highlight the novel route through which tailored nanocatalysts can be implied to regulate biohydrogen production.

6th International Conference and
Postgraduate Colloquium for
Environmental Research 2022 (POCER
2022) 9 - 11 June 2022
Langkawi, Kedah, Malaysia

PCR30042022 – 238: AI-autonomous ventilation control for smart indoor air quality and energy management in a subway station: Offline reinforcement learning approach

Sangyoun Kim[a], Kijeon Nam[b], Sungku Heo[a], Taeyong Woo[a], JuinYau Lim[a], ChangKyoo Yoo[a]

[a]Integrated Engineering, Dept. of Environmental Science and Engineering, College of Engineering, Kyung Hee University, 1732 Deogyeong-daero, Giheung-gu, Yongin-si, Gyeonggi-do, 17104, Republic of Korea

[b]Smart Factory group, Innovation center, Samsung Electronics Device Solutions, 129, Samsung-ro, Yeongtong-gu, Suwon-si, Gyeonggi-do, 16677, Republic of Korea

- Corresponding Author E-mail: ckyoo@khu.ac.kr

Keywords: Autonomous control, Ventilation system, Offline reinforcement learning, Indoor air quality, Smart energy management, Particulate matter 10 (PM_{10})

Extended Abstract

Hazardous risk of particulate matter (PM) on public human health evokes the awareness in alleviation of indoor air quality (IAQ). Mechanical ventilation system has been employed to maintain the IAQ of subway stations, which are especially located undergroud, as a healthy level. However the conventional ventialtion system is operated by the fixed schedule of inverter frequency without considering the IAQ level; it is reported that 50% of total energy consumption is caused by the exaggerated operation of ventilation [J.E. Son, K.H. Lee, 2016]. Hence, trade-off between improving IAQ and saving energy should be solved through the innovative operation of ventilation system for sustainable development in transportation and building sector.

Numerous investigations were devoted to developing the smart and efficient operation of ventilation system specialized to the subway station. Most of the precious studies aimed to maintain the IAQ while minimizing energy consumption. However, they were limited by inaccurate modeling of IAQ dynamics and cannot deal with the unexpected events including a disturbances from the outdoor air quality, and required an assistances of human expert to perform a superior operation of ventilation system. Remarkably, Heo *et al.*, (2019) suggested a novel ventilation control system utilized Deep-Q-Network (DQN), which is a kind of on-line reinforcement learning. Herein, DQN is one of the machine learning technique which train the agent through interaction of virtual environment. This method can reduce

14% of energy consumption while maintaining IAQ and identifying the IAQ dynamics such as rush-hour and dinural trends without human intervention. However, the DQN agent of a proposed ventilation control system should be trained as an on-line manner, which the agent trained by controlling the real ventilation system in real subway station directly. It is difficult to be implemented in real world due to exploration that is property of on-line reinforcement learning; hence, further innovative and smart autonomous ventilation control system should be developed.

In this manner, an off-line reinforcement learning (OffRL)-based ventilation control system was developed for smart IAQ management in subway system while overcoming the limitaitons of previous studies. OffRL can be trained as the data-driven approach from the bigdata which is collected by experts' experiences without interacting with the real environment. To maintain IAQ as healthy level while saving energy, the proposed OffRL-driven ventilation system was trained to search the optimal inverter frequency considering the IAQ dynamics from outdoor air quality(OAQ) variation, train schedule, and passangers.

Figure 1. represented the step-by-step development of proposed OffRL-based ventilation control system. First of all, IAQ bigdata in a confined subway station in Seoul, South Korea, was collected including OAQ, subway schedule, and number of passengers. Then, advantage weighted actor-critic(AWAC) algorithm, which is a kind of OffRL [Levine *et al.*, 2018], was candidated to develop autonomous ventilation control system for smart IAQ management. To train the AWAC agent, we considered that the previous trained DQN agent as an expert which learned the IAQ dynamics and theirs interaction with ventilation system. For this, we gathered the experience dataset of ventilation control form the DQN agent from the previous study done by [S.K. Heo *et al.*, 2019]; the dataset was utilized to train the proposed AWAC-based ventilation control system. The control performance was validated by considering scenarios as moderate OAQ levels.

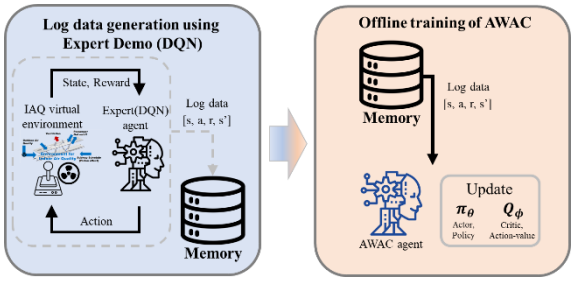

Figure. 1 Framework for a proposed autonomous ventilation control system using AWAC algorithm of OffRL approach

The control performance of proposed AWAC-based ventilation system was graphically represented in **Figure 2.** As shown in the **Figure 2(a)**, the AWAC agent could be trained better rather than DQN agent

of previous study by obtaining higher rewards. Furthermore, **Figure 2(b)** indicated that the proposed AWAC agent could highly reduce the energy consumption by minimizing inverter freqeuncy of ventilation system, while maintaining the indoor PM10 concentrations under the control limit(i.e., 150 $\mu g/m^3$). Comparing to the DQN agent, the proposed AWAC-based ventilation system can reduce the energy consumption by 21% . Hence, this study was verified that the proposed novel AWAC-based ventilation control system could be adopted to accomplish the sustainable operations in subway station to compromise the trade-off between energy consumption and IAQ without human intervention.

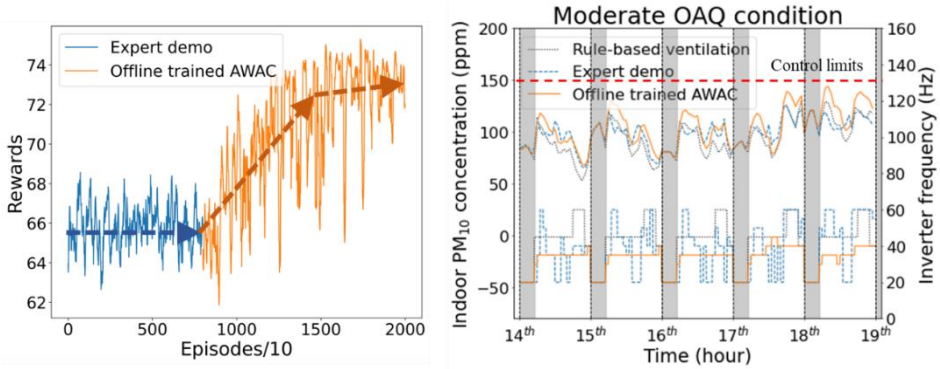

Figure. 2 Comparisons of DQN-based expert demo and AWAC-based OffRL agent (a) the average reward profiles and (b) the ventilation control performances of indoor PM_{10} concetration and inverter frequency.

Acknowledgements: This research was supported by a grant from the National Research Foundation of Korea (NRF) funded by the Korean government (MSIT) (No. 2021R1A2C2007838), and the Subway Fine Dust Reduction Technology Project of the Ministry of Land Infrastructure and Transport from the Republic of Korea (22QPPW-C152457-04).

References

Son, Jeong Eun, and Kwang Ho Lee., "Cooling energy performance analysis depending on the economizer cycle control methods in an office building.", *Energy and Buildings*, 120, (2016), 45-57.

Heo, SungKu, et al., "A deep reinforcement learning-based autonomous ventilation control system for smart indoor air quality management in a subway station.", *Energy and Buildings*, 202 (2019), 109440.

Nair, Ashvin, et al., "Awac: Accelerating online reinforcement learning with offline datasets.", *arXiv preprint arXiv*,2006.09359, (2020).

PCR30042022 – 239: Interpretable Soft Sensor Development for Total Nitrogen and Total Phosphorus Concentrations Using eXplainable Deep AI Models with Hybrid Feature Selection

Abdulrahman H. Ba-Alawi[a], Amir Saman Tayerani Charmchi[a], Mohammad Moosazadeh[a], TaeYong Woo[a], SungKu Heo[a], SangYoun Kim[a], JuinYau Lim[b], MinHan Kim[b], DongChan Won[b] and ChangKyoo Yoo[a]*

[a] Integrated Engineering, Department of . of Environmental Science and Engineering Kyung Hee University, Deogyeong-daero, Giheung-gu, Yongin-si, Gyeonggi-do, 17104, Republic of Korea.

[b]H-KORBI, Co., Ltd., Strategic Business Division, Republic of Korea

*Corrensponsing Author E-mail: ckyoo@khu.ac.kr

Keywords: Interpretable AI soft sensor; Multivariate calibration; Hybrid feature selection; X-AI analysis; Total nitrogen (TN); Total phosphorus (TP).

Extended Abstract

Waterbodies should maintain excellent ecological and chemical conditions to protect the water supply and safeguard ecosystems. Monitoring nutrient concentrations is essential to assess the water quality and significantly reduce eutrophication (Viviano et al., 2014). However, crucial nutrient variables such as total nitrogen (TN) and total phosphorus (TP) concentrations are always difficult to measure online due to the high costs, dynamism, uncertainties, and the time lag associated with real-time monitoring. Data-driven models based soft sensors can afford a reliable online TP and TN estimation using in-situ data of easy-to-measure variables. However, due to the nonlinearity and the autocorrelations of water system datasets, conventional methods cannot effectively provide an interpretable and high prediction of the TN and TP parameters simultaneously.

This study aims to develop a new explainable artificial intelligence (XAI)-soft sensing model for estimating TN and TP concentrations in rivers based on a deep neural network (DNN) with hybrid statistical-AI feature selection (HFS). The deep XAI-based soft sensor (XAI-DNN) model development can effectively capture complex dynamic relationships among water quality parameters and provide superior prediction and interpretability using the explainable SHapley Additive exPlanations (SHAP). The XAI-DNN soft sensor framework contains mainly five steps as illustrated in **Figure 39**. Firstly, data acquisition includes preprocessing, data cleansing, outliers detection, and data interpolation, as shown in **Figure 40 (a)**. Data were collected from a real catchment in a river at Yongsan, S. Korea

containing biological-chemical variables including turbidity (Turb), dissolved oxygen (DO), and pH. In the second step (**Figure 41 (b)**), a multivariate calibration (MC) analysis was conducted to provide an explanation and quantification of TN and TP by relating multiple independent variables. Also, principal component analysis (PCA) was performed as an exploratory analysis (Viviano et al., 2014). In the third step (**Figure 42 (c)**), a hybrid feature selection technique was utilized to select the important features for TN and TP estimation. The fourth step (**Figure 43 (d)**) included the development of the explainable deep neural network (DNN) structure and fine-tuning the associated hyperparameters based on a grid search followed by the online prediction of TN and TP applying the test set. Then, X-AI analysis was applied by computing the SHAP values considering global and local interpretability to provide a clear explanation of the model behavior (Samek et al., 2017). In the fifth step (**Figure 44 (e)**), a comparison analysis was conducted to show outperformance from the XAI-DNN deep of estimating the TN/TP. For the evaluation, three matrices were used, including mean absolute error (MAE), root mean squared error (RMSE), and coefficient of determination (R^2).

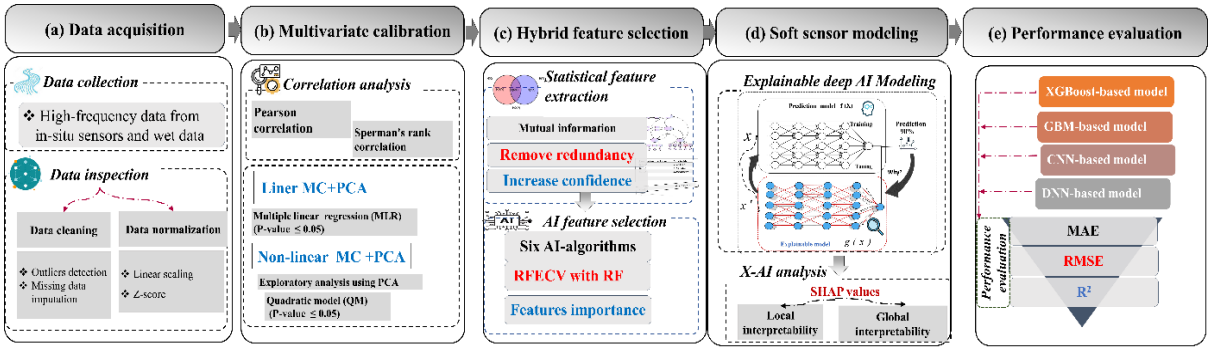

Figure 45: **Schematic framework of developing an explinable deep AI-soft sensor.**

The results of AI-HFS showed that NO3-N, NH3-N, TOC, PO4-P, DO, and EC were the most significant input predictors for the explainable DNN model (**Figure 46 (a)**). For the online prediction of the TN and TP concentrations, superior performance was achieved by the explainable DNN model-based soft sensor (MAE=0.0465, 0.0316 mg/L) (**Figure 47 (b)**). This high performance was interpreted using X-AI analysis considering global and local interpretability to show how much each feature has increased or decreased the predicted TN/TP. For example, increasing the NH4-N feature value increases the SHAP values leading to a higher predicted TN (**Figure 48 (c)**).

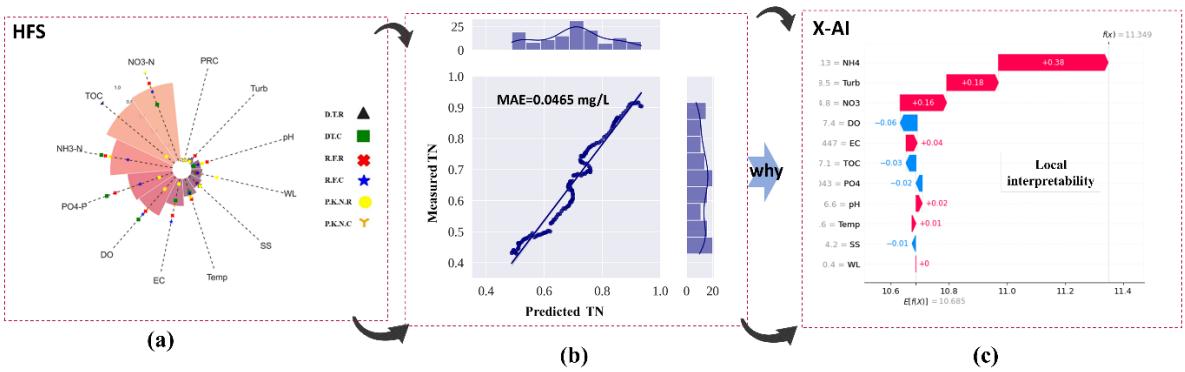

Figure 49: Performance of XAI-DNN based soft sensor (a) HFS (b) prediction (c) XAI analysis.

The developed XAI-DNN based soft sensor can offer a worthy tool to monitor the waterbodies' status in an online fasion with a reliable and explainable prediction, avoiding the expensive acquisition and uncertainty of measuring TN and TP. This developed XAI-DNN could be useful for the decision-makers to assess the quality of waterbodies and to control and reduce the eutrophication risk.

Acknowledgements: This research is funded by the BK21 FOUR program of National Research Foundation of Korea (NRF) and by the Korean government (MSIT) (No. 2021R1A2C2007838), Korea Ministry of Environment as “Prospective green technology innovation project (2020003160009), and project for Collabo R&D between Industry, Academy, and Research Institute funded by Korea Ministry of SMEs and Startups in 2021.(Project No.S3105519).

References

Samek, W., Wiegand, T., Müller, K.-R., 2017. Explainable Artificial Intelligence: Understanding, Visualizing and Interpreting Deep Learning Models. https://doi.org/10.48550/arxiv.1708.08296

Viviano, G., Salerno, F., Manfredi, E.C., Polesello, S., Valsecchi, S., Tartari, G., 2014. Surrogate measures for providing high frequency estimates of total phosphorus concentrations in urban watersheds. Water Res. 64, 265–277. https://doi.org/10.1016/J.WATRES.2014.07.009

6th International Conference and Postgraduate Colloquium for Environmental Research 2022 (POCER 2022) 9 - 11 June 2022
Langkawi, Kedah, Malaysia

PCR30042022 – 240: Spatial-temporal pattern analysis of long-term particulate matter distributions with land use information and an optimum sensor network placement in Mega-city urban environments

Roberto J. Chang Silva[a], Shahzeb Tariq[a], Taeyong Woo[a], Sangyoun Kim[a], Sungku Heo[a], JuinYau Lim[b], ChangKyoo Yoo[a]

[a]Integrated Engineering, Dept. of Environmental Science and Engineering, College of Engineering, Kyung Hee University, 1732 Deogyeong-daero, Giheung-gu, Yongin-si, Gyeonggi-do, 17104, Republic of Korea

- Corresponding Author E-mail: ckyoo@khu.ac.kr

Keywords: Spatial-temporal analysis; Land Use; Particulate matter; Urban morphology; Sensor placement.

Extended Abstract

In today's industrialized and overpopulated world, exposure to particulate matter (PM) in the air threatens human health and contributes to morbidity and mortality (Dominski et al. 2021). PM is closely related to the development of chronic pulmonary disease (COPD), congestive heart failure (CHF), and mortality (Xing et al. 2016). Constant exposure to air pollutants in intensive land use areas may cause adverse health effects on the respiratory and cardiovascular systems in the short and long term. Zones with high human interaction led to higher levels of air pollution than regions with lower human activity. Furthermore, active monitoring and in-depth analysis of outdoor PM dynamics and its sensor network are critical for planning strategies that prioritize human well-being and deploy mechanisms for pollution prevention.

This study focuses on the long-term registered measurements of PM_{10} and $PM_{2.5}$ and their relationship with intensive land use in Pyeongtaek, South Korea. **Figure 1** shows a schematic view of the methodology used for this study. A total of three installed monitoring stations in the region were selected for the statistical analysis. The air quality monitoring data are installed in urban and industrial areas. The hourly concentrations (µg/m3) of PM_{10} and $PM_{2.5}$ were collected from AirKorea from 2014 to 2021 and from 2018 to 2021, respectively. Land use (LU) data were collected from the environmental

space information service, and the sensor coverage radius considered is 3 Km. The land classes are divided into residential, commercial facilities, industrial, public facilities, vegetation, cropland, body of water, and barren land areas for 2014 and 2018. Then a spatial-temporal descriptive statistical analysis is conducted to understand the behavior of the site in terms of particulate matter and land use. Here, the seasonal, monthly, and yearly variations are considered. Moreover, the relationship between PM and LU was analyzed. This study determines the relationship between the behavior of the land use occupation and the amount of particulate matter in each zone. Finally, considering the urban patterns, an RL-based sensor network placement methodology is suggested.

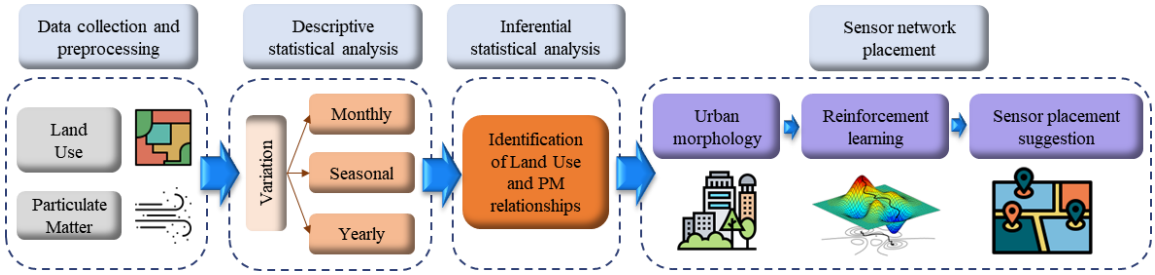

Figure. 1 Schematic view of methodology

The results reveal that PM_{10} and $PM_{2.5}$ mean levels in intensive industrial regions in Pyeongtaek differed significantly from residential domains, as shown in **Figure 2**. The median PM levels in the industrial zone (PM_{10}=46 µg/m3, $PM_{2.5}$=20) are considerably higher than in the residential (PM_{10}=39 µg/m3, $PM_{2.5}$=20) (Dunn's test: Z=(-26,36,-4.12), p=(0.00,0.00) considering the changes in the land use during this time and its use. PM concentrations have decreased except for 2021, which suffered an increment. However, despite the decreasing global trend, the levels remain above the recommended levels. PM levels reach the highest levels between winter and spring.

Because understanding the behavior of air pollution patterns aids in understanding global and local policy actions aimed at reducing air pollution, the early detection of hazardous pollutant levels and effective monitoring in urban areas give a broad perspective to policymakers on the better identification of air pollution control strategies. Besides, spatial and detailed analysis of pollutant concentrations opens a new paradigm to identify national, regional, and local air quality status to develop specific policies based on industrial and population growth. Due to these findings, a novel RL-based methodology for sensor network placement will be proposed as future work considering urban morphology.

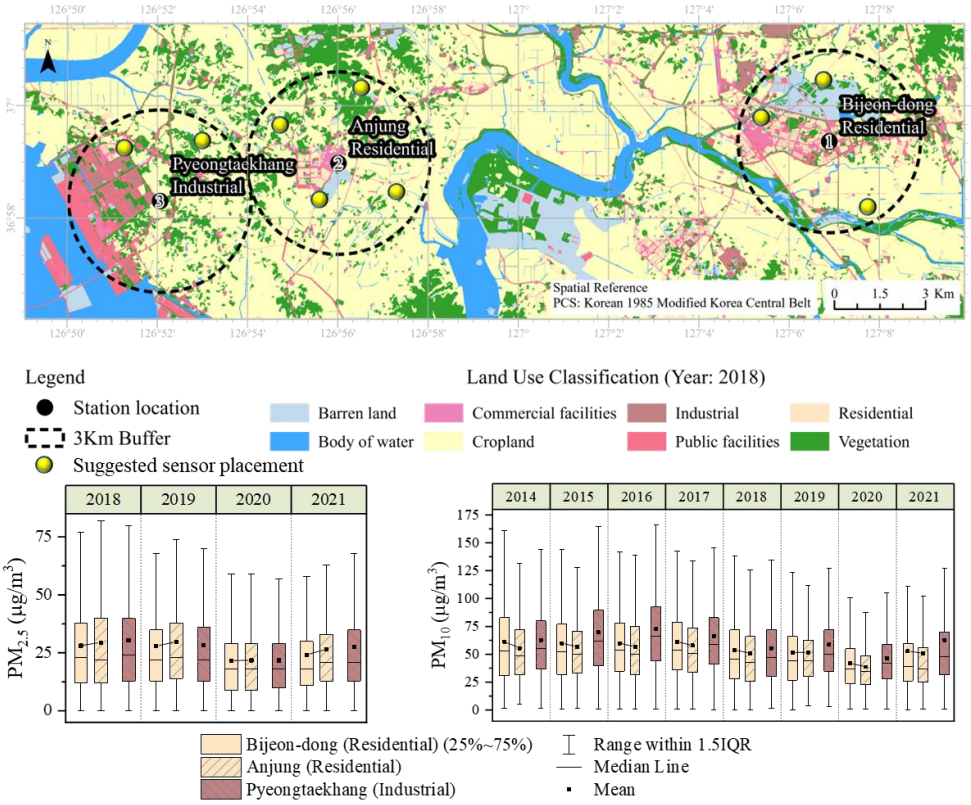

Fig. 2 Spatial temporal distributions ofparticulate matter (PM) considering urban and industrial spaces for three air quality monitoring stations of Pyeongtaek.

Acknowledgements: This research was supported by a grant from the National Research Foundation of Korea (NRF) funded by the Korean government (MSIT) (No. 2021R1A2C2007838), the Subway Fine Dust Reduction Technology Project of the Ministry of Land Infrastructure and Transport from the Republic of Korea (22QPPW-C152457-04), and the Ministry of Education of the Republic of Korea and the National Research Foundation of Korea (NRF-2019S1A5A2A03049104).

References

Dominski, Fábio Hech et al. 2021. "Effects of Air Pollution on Health: A Mapping Review of Systematic Reviews and Meta-Analyses." *Environmental Research* 201: 111487.

Xing, Yu Fei, Yue Hua Xu, Min Hua Shi, and Yi Xin Lian. 2016. "The Impact of PM2.5 on the Human Respiratory System." *Journal of Thoracic Disease* 8(1): E69–74. https://jtd.amegroups.com/article/view/6353/html (November 24, 2021).

6th International Conference and Postgraduate Colloquium for Environmental Research 2022 (POCER 2022) 9 - 11 June 2022
Langkawi, Kedah, Malaysia

PCR30042022 – 241: Development of a biowaste-driven carbon-negative multigeneration system using a circular integration approach

Mohammad Moosazadeh[a], Amir Saman Tayerani Charmchi[a], Pouya Ifaei[a], SungKu Heo [a] and ChangKyoo Yoo[a]*

[a] Department of Environmental Science and Engineering Kyung Hee University, Deogyeong-daero, Giheung-gu, Yongin-si, Gyeonggi-do, 17104, Republic of Korea.
*Corresponding Author E-mail: ckyoo@khu.ac.kr

Keywords: Biowaste-based multigeneration, Carbon capture and storage, Climate Change mitigation, Cryptocurrency, Multi-objective optimization.

Extended Abstract

Keeping global warming below 1.5 degrees Celsius by the middle of the century would necessitate multi-faceted efforts to reduce carbon emissions in the energy sector for net-zero emission. Meeting the Paris Agreement would require a combination of CO_2 capture and widespread adoption of renewable energy in the industrial sector, resulting in neutral or further net-negative emissions. Using appropriate renewable energy sources to attain carbon neutrality has long been a mature topic that brings a zero CO_2 emission. Given the efforts and investments in green energy systems and technological advancement, the viability of present technologies is still questioned. Besides, CO_2 capture, utilization, and storage (CCUS) is a sustainable solution to some of the world's most challenging problems, including global warming, climate change, and reaching net negative CO_2 emissions. CO_2 capture modules in the industry have been thoroughly investigated. However, high energy demand and process costs have hindered the implementation on the commercialization scale. While different methods for CO_2 capture have been developed, maximizing energy recovery and reducing implementation costs remains a significant difficulty. To reduce operational cost and fill the energy demand and supply gap during CO_2 capture, it is imperative to address its high energy requirement through novel energy optimization.

Process integration (PI) is a viable technique widely used to overcome the high energy demand and increase system efficiency. Hence, efficient integration of multi-carrier and multi-product networks also helps sustainable growth and justifies green system funding as a consequence of analyzing new era products and assessing their benefits and drawbacks in cross markets. Furthermore, PI is a mature approach to engineering system design and sustainable management that has effectively addressed a

wide range of sustainability challenges in various industries. PI has been highlighted by retrofitting existing facilities with new technology to reduce energy demands and costs. Harkin et al. (2009) investigated the integration of the CCS module with a coal power plant and demonstrated that the energy penalty could be reduced from 39% to 24% by employing the process integration associated with lower energy consumption. Novotny et al.(2017) studied the energy and cost benefits of integrating waste heat recovery systems with CCS power plants. Based on the results, the economic impact was positive in different CCS plants, including pre-combustion and post-combustion. Aside from all of the benefits of PI, this approach focuses just on energy recovery. However, circular integration (CI) considers the circular economy, industrial ecology, and process integration. Ifaei et al. (2022), proposed a utility-free circular integration approach for optimal multigeneration from biowaste streams and showed the proposed system could increase the system efficiency while minimizing the environmental impact. While the large-scale integration of CCS with industries has been extensively investigated, a small-scale net negative profitable multigeneration system integrating with CCS is scarce, with literature highlighting technological and economic challenges.

A multigeneration system can generate different products and add value to overcome economic challenges, depending on the application and demands. The energy-intensive crypto products (CPs) and Hydrogen are growing in the market, which have the inherent potential to increase the system's profitability and sustainability. Although liquidity is a big benefit for CPs, the prices are subject to variations. In addition, the literature focuses on the feasibility of using the wealth generated through the products trading, neglecting the sustainable development goals. Furtheremore, the market for H_2 as a bridge to the future energy is still infant level and limited. According to the literature, these two highly valuable products can assure the system's profitability; however, a multigeneration system including CPs and H_2 has received little attention while considering their carbon impact.

Taking into account the aforementioned research gaps, this study proposes a novel system of the systems by integrating biogas-based green multi-product technologies, a capturing module for reducing CO_2 emissions, crypto products (CPs) and H_2 to secure the system's profitability. The configuration of the proposed system is schematically shown in **Figure 50**, in which the biogas, water, energy, and closed-cycle streams are shown in gray, blue, red, and black, respectively. Furthermore, a comprehensive evaluation of the techno-economic performance regarding CO_2 capture cost and net profit of life cycle was performed for the proposed system to obtain the system performance and feasibility. Finaly, a novel multi-objective optimization model is developed for maximizing profitability and waste recovery to obtain the optimal design of the net negative carbon emission process considering the water-exergy-carbon-cost nexus.

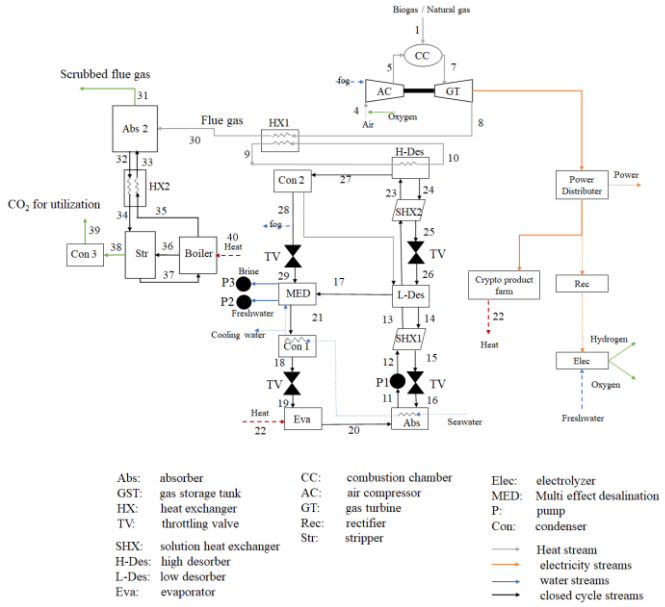

Figure 50: Schematic representation of the modeled multi-carrier and multi-product network

Our findings indicated that the proposed integrated system could provide sustainable electricity, water, hydrogen, and value-added cryptocurrencies while improving energy usage and waste recovery. The results showed that the CI approach reduced the energy penalty in the integrated system by employing heat recovery in the carbon capture module, and the system was capable of producing products with negative CO_2 emissions, resulting in a high level of sustainability. Furthermore, the results demonstrated that revenue from CPs and H_2 could ensure the system's profitability while accounting for CCS costs.

Acknowledgments: This work was supported by the National Research Foundation of Korea (NRF) grant funded by the Korean government (MSIT) (No. 2021R1A2C2007838), the Korea Ministry of Environment (MOE) as a Graduate School specialized in Climate Change and Korea Ministry of Environment as "Prospective green technology innovation project (2020003160009)"

References

Harkin, T., Hoadley, A., Hooper, B., 2009. Process integration analysis of a brown coal-fired power station with CO2 capture and storage and lignite drying, in: Energy Procedia. Elsevier, pp. 3817–3825. https://doi.org/10.1016/j.egypro.2009.02.183

Ifaei, P., Charmchi, A.S.T., Vilela, P., Safder, U., Yoo, C.K., 2022. A new utility-free circular integration approach for optimal multigeneration from biowaste streams. Energy Convers. Manag. 254, 115269. https://doi.org/10.1016/j.enconman.2022.115269

Novotny, V., Vitvarova, M., Kolovratnik, M., Hrdina, Z., 2017. Minimizing the Energy and Economic Penalty of CCS Power Plants Through Waste Heat Recovery Systems, in: Energy Procedia. Elsevier, pp. 10–17. https://doi.org/10.1016/j.egypro.2016.12.184

6th International Conference and
Postgraduate Colloquium for
Environmental Research 2022 (POCER
2022) 9 - 11 June 2022
Langkawi, Kedah, Malaysia

PCR30042022 – 242: An effectiveness guidance of deploying solar and wind energy alongside with microalgae-based biofuel in a nationwide scale: A case study of South Korea

Juin Yau Lim[a,1], Roberto Chang[a,1], and Chang Kyoo Yoo[a*]

[a] *Integrated Engineering, Dept. of Environmental Science and Engineering, College of Engineering, Kyung Hee University, 1732 Deogyeong-daero, Giheung-gu, Yongin-Si, Gyeonggi-do, 17104, Republic of Korea*

[1] Both the authors contributed equally in this research.

- [*]Corrensponsing Author E-mail: ckyoo@khu.ac.kr

Keywords: Renewable energy; Energy policy; Multi-period optimization; Game theory; System reliability.

Extended Abstract

Energy droughts is a critical issue which confronted by most of the countries in this modern era with the drastically growth of population. An urge on identifying alternatives apart from current dominant energy source especially fossil fuel is essential to address the climate change. Yet, unforeseen circumstances (i.e., sudden withdrawal of certain party from initial plan) might occur with the participation of multiple parties that will lead to unstable energy supply. This study has proposed an explicit insights on a preliminary approach targeting nationwide planning scheme for sustainable renewable generation with the aid of game theory. The strategic actions involved by the decision makers is assessed to ensure an optimal tradeoff considering economics and environmental aspects. A total of 14 provinces in South Korea is used as a case study to demonstrate the peer-to-peer (P2P) energy trading scheme between multiple regions. Due to the feasible weather condition across different season, a great mixture of the solar and wind energy will be considered. Upon the deployment of hybrid renewable energy system (HRES) from each region considered, the hydrogen is generated by utilizing excessive electricity via proton-exchange membrane electrolyzer. Apart from that, an incorporation of the microalgae based biorefinery is considered with the great potential of deployment. A study by Rhee *et al.*, (2020) has reported a viable approach on a local deployment of microalgae biorefinery in Incheon

which integrated with energy-recovery system from livestock manure. The capacity of both the renewable energy configuration aforementioned in the study is in accordance with the study reported by Lim *et al.*, (2020) which is shown in **Figure 1**.

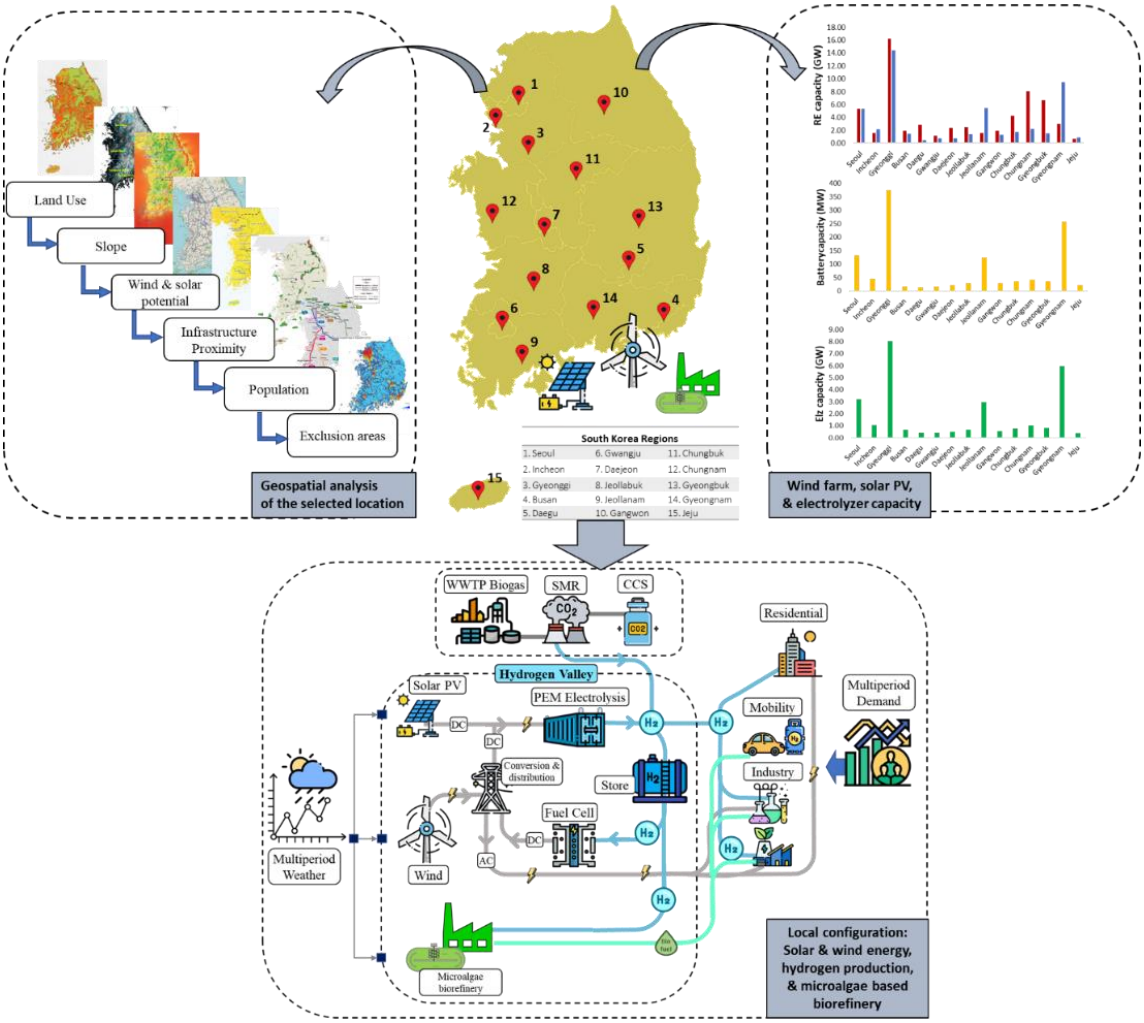

Figure 1: Renewable energy configuration deployment of 14 different provinces in South Korea considering solar, wind, and microalgae based biorefinery (Lim *et al.*, 2020)**.**

In prior of deployment, a comprehensive geospatial analysis on all the locations are performed with the aid of geographic information system (GIS) to identify the potential location for installing the relative infrastructure. A multi-period optimization approach formulating in mixed-integer linear programming (MILP) is developed based on the framework proposed in an one-year timeframe. Such optimization problem is targeted to minimizing the total annual cost required for overall regions to ensure a competitive cost of energy including the renewable electricity, hydrogen, and microalgae-based biofuel generated. The model will be further evaluated in the perspective of game theory with the involvement

of multiple agents considered in the study. Agents (players) that considered in this framework are supply agent, market agent, demand agent, and utilities agent. As a demonstration, the supply agents are the regions considered for the deployment of HRES to generate renewable electricity; the demand agent represent the energy required as of each regions. Wherein the market agent is considered as the centralized distribution that collect the renewable electricity generated from each region and distribute accordingly. In the circumstance that are unfavorable (i.e., low renewable electricity generation and high spikes of demand), the utilities agent which supply electricity from main grid will takes place to ensure the optimal deployment policy.

Acknowledgements: The authors thank the support by National Research Foundation (NRF) grant funded by the Korea government (MSIT) (No. 2021R1A2C2007838), Korea Ministry of Environment (MOE) as Graduate School specialized in Climate Change, and Korea Ministry of Environment as "Prospective green technology innovation project (2020003160009).

References

Lim, J. Y. *et al.* (2020) 'Nationwide sustainable renewable energy and Power-to-X deployment planning in South Korea assisted with forecasting model', *Applied Energy*, p. 116302. doi: https://doi.org/10.1016/j.apenergy.2020.116302.

Rhee, G. *et al.* (2020) 'Evaluation of an integrated microalgae-based biorefinery process and energy-recovery system from livestock manure using a superstructure model', *Journal of Cleaner Production*, p. 125325. doi: https://doi.org/10.1016/j.jclepro.2020.125325.

6th International Conference and
Postgraduate Colloquium for
Environmental Research 2022 (POCER
2022) 9 - 11 June 2022
Langkawi, Kedah, Malaysia

PCR30042022 – 243: Artificial Neural Network modeling for prediction of weight average molecular weight, number average molecular weight and the Polydispersity Index of Polycaprolactone synthesized using enzymatic polymerization

Mohammad Asad Tariq[a], and Senthil Kumar Arumugasamy[b*]

[a] Chemistry Department, Army Public College and School System, 158 Iqbal Shaheed Rd, Karachi, Sindh 74400, Pakistan

[b] Department of Chemical and Environmental Engineering
University of Nottingham Malaysia, Jalan Broga, 43500 Semenyih, Selangor Darul Ehsan, Malaysia

- Corrensponsing Author E-mail: Senthil.Arumugasamy@nottingham.edu.my

Keywords: Aritificial Neural Network; Enzymatic Polymerization; Polycaprolactone; Polymers

Extended Abstract

Polycaprolactone (PCL) is one of the environmentally friendly polymers that has gained attention in recent times due to its vast application in the field of drug delivery system and tissue engineering. It has lots of salient features like low cost, biodegradability, being compatible with many polymers, can be fabricated to a lots of shapes and structures and most importantly high thermal stability lead to easy melting process (Dhanasekaran et al. 2022). PCL in recent times are sythesized using enzymatic catalysts and this method is called as “enzymatic polymerization”. A variety of bacterial, fungal enzymes have proven to produce PCL of high molecular weight and among these *Candida Antarctica* lipase B (CALB) has been the most successful and popular enzyme (Pakalapati et al., 2019). In enzymatic polymerization, operating conditions like reaction temperature, reaction time, type of solvent, mixing speed, enzyme-solvent ratio have had significant impact on the PCL molecular weight (Kumar et al., 2000). There is a need for a modeling technique which can help in understanding the relationship between these operating conditions and polymer molecular weight. Also, these models can predict the polymer molecular weight which can help in reducing the operating cost of research by carrying out fewer trials.

Artificial neural network is one such modeling technique which has gained popularity in recent times and the field of polymers is no exception. Recent research include modeling to determine the effect of

reaction temperature and reaction time on PCL molecular weight using FANN and ANFIS models using CALB enzyme via enzymatic polymerization (You et al. 2020). In this study an Artificial Neural Network (ANN) model was developed using the data from enzymatic polymerization process with weight average molecular weight (M_w), number average molecular weight (M_n) and the Polydispersity index (PDI) are the experimental results optimised by manipulating the inputs reaction time (s), reaction temperature (^oC), mixing speed (RPM) and enzyme-solvent ratio (Volume) (Pakalapati et al., 2019).

An ANN model consists of a network of neurons which works as a function that replicates the processing of a biological neuron in the human brain. The neurons are connected with weight coefficients to form a neural network. An ANN works by passing message through and along neurons in different layers. A typical ANN usually consists of three layers, namely, the input, hidden and output layers. The network developed in this paper consists of one input layer with 4 inputs, one hidden layer (1 to 20 hidden neurons) and an output layer with three outputs. The number of hidden neurons that gave best results in terms of performance criterion was chosen. The entire architecture of the neural network was made through Matlab™ (R2017a). A transfer function in a neural network is a differentiable function that is applied to the input of each neuron to produce its output. One transfer function each for hidden layer and output layer is used in the network architecture. Four transfer functions were tested in this study namely Log-sigmoidal (Logsig), Tan-sigmoidal (Tansig), Radial basis (Radbas) and linear transfer function (Purelin). The procedure used to alter the weights and biases in the hidden neurons to fit the data trend in the training process in an ANN is called a training algorithm. Four training algorithms were tested namely, Levenberg-Markquardt (LM), Bayesian Regularization (BR), Resilient Backpropagation (RP) and Scaled Conjugate Gradient (SCG). For each training algorithm the hidden neurons are optimized based on the performance criterions. Out of the total amount of data, 40 % of it is used to train the network, 40 % is used for training and the last 20 % is used to validate the network. So that It can accurately predict the output of any input parameter.

Results and Discussion:

After analysing the results from all the possibilities, it was found that Tan-Sigmoidal transfer function in the hidden and output layer gives the best performance. While, Levenberg-Marquardt (LM) training algorithm used for the training of the network at 7 hidden neurons gave the best results. With Mean Squared Error (MSE), Mean absolute error (MAE), mean absolute percentage error (MAPE) and R-squared values of M_n being 331971.6015, 322.058, 0.142486, 0.95 respectively, for M_w being 774719.7, 492.6551, 0.15965, 0.95 respectively and PDI being 0.001395, 0.017323, 0.01234, 0.98 respectively. It

can be clearly seen that the prediction accuracy of the network is much stronger with PDI than it is with M_n or M_w.

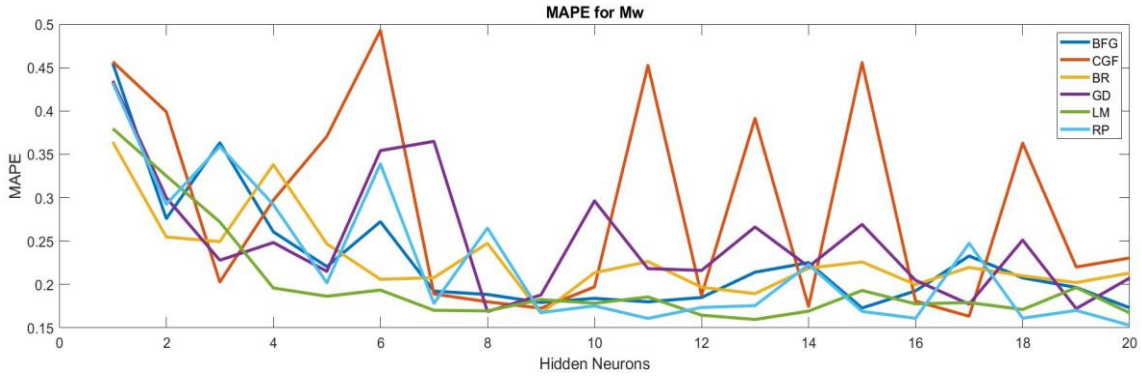

Figure 1: Figure showing the plot for MAPE of Mw for all training algorithms.

Conclusion:

Artificial Neural Network (ANN) model was developed using the data from enzymatic polymerization process with reaction time, reaction temperature, mixing speed and enzyme-solvent ratio as inputs and weight average molecular weight (M_w), number average molecular weight (M_n) and the Polydispersity index (PDI) as outputs. The best training algorithm determined for this ANN is Levenberg-Marquardt algorithm.

References

Kumar A, Gross RA (2000) Candida antarctica Lipase B Catalyzed Polycaprolactone Synthesis: Effects of Organic Media and Temperature. Biomacromolecules 1:133-138.

Pakalapati H, Tariq MA, Arumugasamy SK (2019) Optimization and modeling of enzymatic polymerization of ε-caprolactone to polycaprolactone using Candida Antarctica Lipase B with response surface methodology and artificial neural network. Enzyme Microb Technol 122:7–18.

N.P.D. Dhanasekaran, K.S. Muthuvelu, S.K. Arumugasamy, Recent Advancement in Biomedical Applications of Polycaprolactone and Polycaprolactone-Based Materials Reference Module in Materials Science and Materials Engineering, 2022

6th International Conference and
Postgraduate Colloquium for
Environmental Research 2022 (POCER
2022) 9 - 11 June 2022
Langkawi, Kedah, Malaysia

PCR30042022 – 244: Cultivation of Chlorella vulgaris using food waste compost as an organic nutrient source

Silvanir[a], and Kit Wayne Chew[a,b,*]

[a] School of Energy and Chemical Engineering, Xiamen University Malaysia, Jalan Sunsuria, Bandar Sunsuria, 43900 Sepang, Selangor Darul Ehsan, Malaysia

[b] College of Chemistry and Chemical Engineering, Xiamen University, Xiamen, 361005, Fujian, China

- Corresponding Author E-mail: silvanirtioe12@gmail.com

Keywords: Microalgae; Biomass; *Chlorella*; Food waste compost; Organic medium; Cultivation

Extended Abstract

Transformation of food waste into a value-added product such as compost through biological means is an effective and environmentally friendly organic waste management. [Cerda et al., 2018]. Compost produced from food waste is rich in humic substances and organic components (e.g., carbohydrates, proteins, lipids, and organic acid), making it suitable to produce organic fertilizer and cultivate microorganisms [Zeng et al., 2018; Zhou et al., 2016]. Microalgae is a promising biomass feedstock that has high growth rates, less competition with terrestrial crops, and wide distribution. It also has the potential to produce multiple valuable products and a wide range of functional ingredients that spark interest in various industries. A large quantity of freshwater and high-cost nutrients are essential to the commercialization and scaling up of microalgae production for biomolecules extraction. Wastewater has been used to cultivate microalgae given its benefit in purifying the wastewater, but the uncertainties of wastewater content affect the growth of microalgae. Food waste is an alternative nutrient medium for the cultivation of microalgae that is rich in ammonium and phosphate concentration. These pollutants can be significantly reduced while simultaneously growing the microalgae [Cerda et al., 2018]. Integration of food waste compost medium and inorganic medium could potentially substitute the major nutrients such as nitrate and phosphate that are crucial in microalgae cultivation, leading to a more sustainable approach to microalgae cultivation.

The goal of this study was to see if food waste compost could be used as a nutrient source for *Chlorella vulgaris* FSP-E culture. Using different ratios of food waste compost mixture, the algal biomass accumulation and the viability of substituting inorganic fertilizers with organic fertilizers for microalgae culture were investigated. The biochemical components of microalgae, such as lipid, protein, and carbohydrate contents, were isolated from the microalgae biomass to assess biomass productivity. The results obtained showed that substitution of 25% of compost mixture yielded higher biomass concentration (11.1%) and better lipid (10.1%) and protein (2.0%) content as compared to the microalgae cultivated in a fully inorganic medium. These findings showed that mixing an inorganic medium with an organic food waste compost medium can effectively lower microalgae cultivation costs while also increasing biochemical content in the grown microalgae.

Table 1. Food waste compost (FWC) composition.

Medium	BG11 (%)	Compost solution (%)
100C	100	0
85C	85	15
75C	75	25
65C	65	35
50C	50	50
25C	25	75
100F	0	100
75F	25 (H_2O)	75

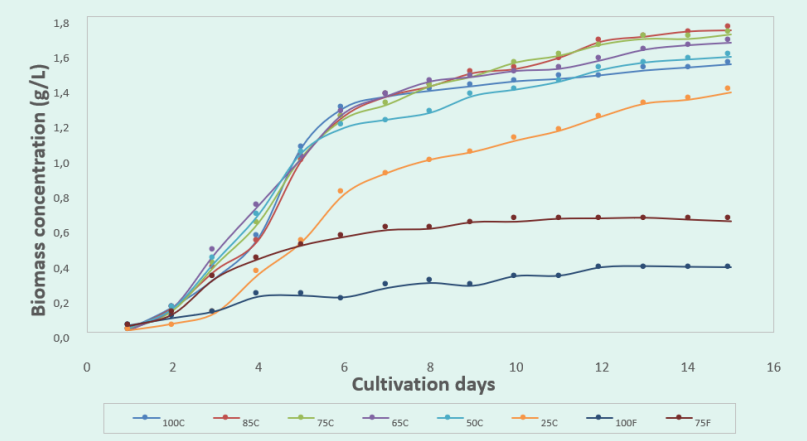

Figure 1: Growth curve of *Chlorella vulgaris* cultivated in BG11 and various food waste compost medium combinations.

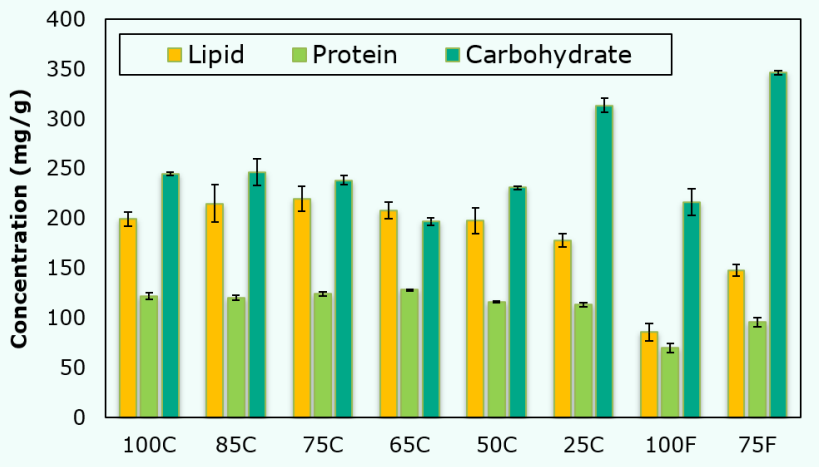

Figure 2: Lipid, protein and carbohydrate content in *Chlorella* vulgaris cultivated in BG11 and various food waste compost medium combinations.

Acknowledgements: This work is supported by Xiamen University Malaysia Research Fund (Grant number: XMUMRF/2021-C7/IENG/0033) and Hengyuan International Sdn. Bhd.

References

Cerda, A., Artola, A., Font, X., Barrena, R., Gea, T., & Sánchez, A. (2018). Composting of food wastes: Status and challenges. Bioresource technology, 248, 57-67.

Chew, K.W., Chia, S.R., Show, P.L., Yap, Y.J., Ling, T.C. and Chang, J.S., 2018. Effects of water culture medium, cultivation systems and growth modes for microalgae cultivation: A review. Journal of the Taiwan Institute of Chemical Engineers, 91, pp.332-344.

Chew, K.W., Chia, S.R., Show, P.L., Ling, T.C., Arya, S.S. and Chang, J.S., 2018. Food waste compost as an organic nutrient source for the cultivation of Chlorella vulgaris. Bioresource technology, 267, pp.356-362.

Zeng, Y., Xie, T., Li, P., Jian, B., Li, X., Xie, Y., & Zhang, Y. (2018). Enhanced lipid production and nutrient utilization of food waste hydrolysate by mixed culture of oleaginous yeast Rhodosporidium toruloides and oleaginous microalgae Chlorella vulgaris. Renewable Energy, 126, 915-923.

Zhou, Y., Selvam, A., & Wong, J. W. (2016). Effect of Chinese medicinal herbal residues on microbial community succession and anti-pathogenic properties during co-composting with food waste. Bioresource Technology, 217, 190-199.

6th International Conference and
Postgraduate Colloquium for
Environmental Research 2022 (POCER
2022) 9 - 11 June 2022
Langkawi, Kedah, Malaysia

PCR30042022 – 245: Biorefinery of *Chlorella vulgaris* via Ultrasound-Assisted Three Phase Partitioning

Sherlyn Sze Ning Koay[a], Wei Han Foo[a], Kit Wayne Chew[a,b*]

[a] School of Energy and Chemical Engineering
Xiamen University Malaysia, Selangor, Malaysia

[b] College of Chemistry and Chemical Engineering
Xiamen University, Xiamen 361005, Fujian, China

- Corresponding Author E-mail: kitwayne.chew@xmu.edu.my

Keywords: Ultrasound; Three phase partitioning; Protein extraction; Microalgae; Bio-separation.

Extended Abstract

The unceasing growth of the human population every year has indicated that the supply growth of food production is crucial to minimise the proportion of global hunger. It was claimed that protein, which is one of the macronutrients, will be having shortages in the near future which requires an alternative protein source to cope with the growing human population. Microalgae is well-known as a viable source of biological components such as carbohydrates, lipids, pigments, vitamins, and polyphenols, especially proteins [Chia, 2018]. In fact, the protein quality in microalgae is claimed to be identical to those traditional protein sources like milk, meat and egg. Hence, the use of microalgae as the main protein source contributed to several benefits such as rapid growth rate, high productivity and required low cultivation effort [Chew, 2018]. Three phase partitioning (TPP) as a green alternative to conventional extraction technique is advantageous in several aspects, including the ease of operation, scalable, low energy consumption, high efficiency, along with the non-toxic and cheap solvent [Qiu et al., 2019]. In most studies, the TPP system uses tert-butanol and salt to form a three-layers mixture, in which the lipids will be found at the upper layer, whereas protein precipitate will be obtained at the middle phase and bottom layer is the aqueous layer [Chia et al., 2019]. On the other hand, the mass transfer of targeted biomolecules is intensified with the utilisation of sonication technique. Ultrasound-assisted extraction utilised high-intensity ultrasonic waves which transmit the liquid molecules and resulting in the formation of microbubbles around the cells. Thus, the cell wall is shattered when shockwaves are released due the bursting of the bubbles [Khoo et al., 2020]. Ultrasound-assisted TPP (UATPP) was

used in the present study to extract proteins from *Chlorella vulgaris* and the feasibility of the enhanced technique was investigated. In the proposed technology, several operating parameters were studied and optimised comprehensively including the types and concentration of salt, slurry to tert-butanol ratio, ultrasonic frequency and power, irradiation time, duty cycle and microalgae biomass loading. Table 17 summarises the studied operating parameters and their optimised values after the investigation. The results showed that high separation efficiency and yield were achieved using the UATPP technique with the optimal conditions as follow: ammonium sulphate with concentration 50% and tert-butanol as UATPP medium, ratio of slurry to tert-butanol 1:2, sonication power 100%, irradiation time 10 minutes, ultrasonic frequency 35 kHz, ultrasonic duty cycle 80%, as well as microalgae biomass loading 0.75 wt%. Under the optimised conditions, the separation efficiency was found to be 74.59 ± 0.45% with a protein recovery yield of 56.57 ± 3.70%. Figure 51 shows the FESEM images of microalgae cells before and after sonication treatment. It was observed that the microalgae surfaces after sonication treatment were smooth with round-shape cells that are clumped on the surface. The structure of the microalgae cell was more severely altered, and became flat and more shrunken which indicated that UATPP can deal more disruptive damage to the microalgae cell. In consequence, UATPP was declared to be very effective in disrupting the microalgae cells and leads to the enhancement of protein extraction.

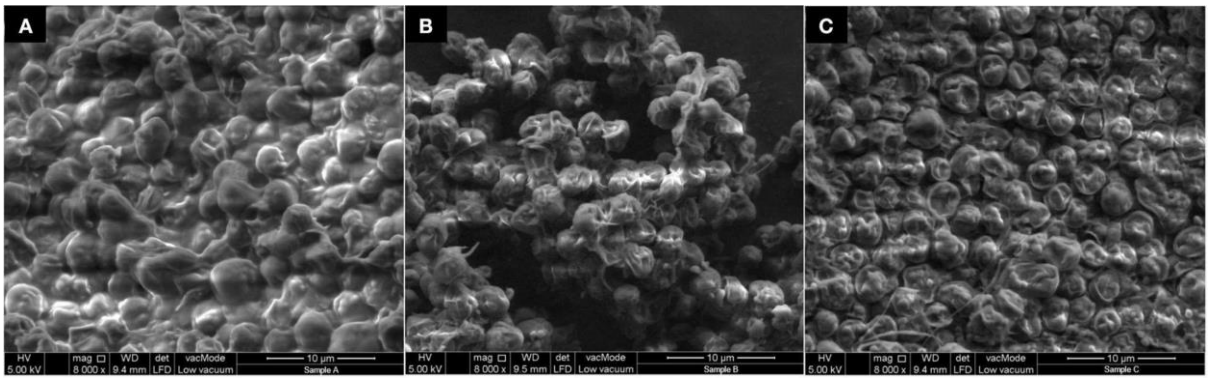

Figure 51: FESEM images of microalgae cells (A) before sonication treatment; (B) after ultrasound with water as medium; (C) after ultrasound with UATPP medium

Table 17: Summary of operating parameters investigated and the respective optimal condition

Parameter	Variables	Optimal condition
Types of salt	Na_2SO_4 $MgSO_4$ $(NH_4)_2SO_4$	$(NH_4)_2SO_4$

	K_2HPO_4	
Salt concentration	20% to 60%	50%
Slurry to tert-butanol ratio	1:0.5 to 1:2.5	1:2
Ultrasonic power	20% to 100%	100%
Irradiation time at 35 kHz	2.5 minutes to 12.5 minutes	10 minutes
Irradiation time at 130 kHz	2.5 minutes to 12.5 minutes	NIL
Duty cycle	20% to 100%	80%
Microalgae biomass loading	0.25 wt% to 1.25 wt%	0.75 wt%

Acknowledgements: This work was supported by the Ministry of Higher Education, Malaysia and the grants are as follows: Fundamental Research Grant Scheme, Malaysia [FRGS/1/2019/STG05/UNIM/02/2] and MyPAIRPHC-Hibiscus Grant [MyPAIR/1/2020/STG05/UNIM/1].

References

Chew, K. W., Chia, S. R., Show, P. L., Yap, Y. J., Ling, T. C., & Chang, J. S. (2018). Effects of water culture medium, cultivation systems and growth modes for microalgae cultivation: A review. *Journal of the Taiwan Institute of Chemical Engineers*, *91*, 332-344.

Chia, S. R., Chew, K. W., Show, P. L., Yap, Y. J., Ong, H. C., Ling, T. C., & Chang, J. S. (2018). Analysis of economic and environmental aspects of microalgae biorefinery for biofuels production: a review. *Biotechnology journal*, *13*(6), 1700618.

Chia, S. R., Chew, K. W., Zaid, H. F. M., Chu, D. T., Tao, Y., & Show, P. L. (2019). Microalgal protein extraction from Chlorella vulgaris FSP-E using triphasic partitioning technique with sonication. *Frontiers in bioengineering and biotechnology*, *7*, 396.

Khoo, K. S., Chew, K. W., Yew, G. Y., Leong, W. H., Chai, Y. H., Show, P. L., & Chen, W.-H. (2020). Recent advances in downstream processing of microalgae lipid recovery for biofuel production. *Bioresource technology*, *304*, 122996.

Qiu, C., He, Y., Huang, Z., Li, S., Huang, J., Wang, M., & Chen, B. (2019). Lipid extraction from wet Nannochloropsis biomass via enzyme-assisted three phase partitioning. *Bioresource technology*, *284*, 381-390.

6th International Conference and Postgraduate Colloquium for Environmental Research 2022 (POCER 2022) 9 - 11 June 2022
Langkawi, Kedah, Malaysia

PCR30042022 – 247: Semi-batch *Chlorella vulgaris* cultivation: Artificial Intelligence model for biomass growth monitoring

Angela Paul Peter [a]

[a] Department of Chemical and Environmental Engineering, Faculty of Science and Engineering, University of Nottingham Malaysia, Jalan Broga, 43500 Semenyih, Selangor Darul Ehsan, Malaysia

• Corrensponsing Author E-mail: angelapaulpeter@gmail.com

Keywords: Semi batch; culture medium recycling; cultivation; colour model; biomass growth

Extended Abstract

Microalgae biomasses are emerged as a novel, sustainable, and clean energy source for the synthesis of third-generation biofuels [1]. According to the US Energy Information Administration [2], nonrenewable energy resources such as petroleum are expected to reach maximum output in 2019, followed by a downward trend, particularly for crude oil supply. Gielsen et al., (2019), reported that the energy consumption has risen dramatically, with global energy demand expected to rise by more than 85% by 2040 [3]. Hence, alternate energy sources were constantly studied based on the existing climate, as the rising global population, industrialization and increasing need for transportation occurred. Biodiesel was recognized as one of the most promising alternative fuels. Biodiesel was described as mono-alkyl esters produced from vegetable oils, animal fats, or waste cooking oil that have a long chain of fatty acids [4]. As compared to conventional petroleum-based diesel, biodiesels are characterized as biodegradability with higher Cetane number, higher flash point, and lower exhaust pollutants [5]. However, the production of biodiesel from crops has a major controversy due to the food vs fuel competition.

To address these issues, microalgae-based biomass is proposed as a possible feedstock for the generation of sustainable and renewable biodiesel. Omar et al., (2021) discovered that microalgae with high biomass productivity and lipid content, are favorable for biodiesel generation [6]. From an environmental standpoint, microalgae growth combined with CO_2 fixation and wastewater biotreatment could develop the cultivation system into a viable green energy generator without competing food crops for arable land and water [7]. Based on areal productivity, microalgae species such as *Botryococcus*, *Chlamydomonas*, and *Chlorella* could generate 15-300 times more oil for biodiesel generation than conventional crops [8]. Microalgae also have short harvesting cycle (ranging from 1- 10 days depending on the culture condition), allowing continuous harvests with higher biomass yield as compared to traditional crops that are harvested once or twice a year [9]. Hence, microalgae cultivation is recognized as a modern biotechnologist advancement and it is projected that by 2036, the global market for microalgae-based biomass would have the capacity to produce 5000 tons of dry biomass per year with a revenue of USD 1250 million [10].

For large scale microalgae cultivation process, photo-bioreactor is the most preferred system as it saves land area and allow the culture to grow in a closed environment with less exposure to external contamination [11]. Nevertheless, the capital and operational costs for photo-bioreactors are significantly high due to the fabrication of high-volume tank and control system for nutrient medium, carbon supply, and light source [12]. Hence, growing microalgae in a semi-continuous culture mode is the most cost-effective cultivation

system compared to batch mode for large biomass output within a short period of time. The semi - batch culture mode is preferred as it prevents the downtime at the end of the culture, and also minimizes the limitation in terms light penetration during stationary phase. However, excessive addition of fresh culture medium may result in a rise in medium osmotic pressure, which may damage the photosynthetic mechanism of microalgae [13]. Thus, in this study *Chlorella vulgaris* cultivation was cultivated in semi-batch mode with nutrient recycling and the fresh medium supply ratio was optimized.

Moreover, industrial revolution 4.0 can break down traditional barriers and allow for sustainable growing conditions with quick testing on biomass growth. In previous years, photo-bioreactors are widely investigated on its design structure, in terms of sustainable and economical aspects [4]. The emerging of technology onto photo-bioreactors has developed a constant maximum biomass yield by monitoring microalgae growth with an array of interconnected sensors, adjusting conditions as needed, and identifying ideal growth parameters through machine learning [14]. However, implementation of artificial intelligence able to overcome the tough challenge, by identifying the best time to harvest the algae before it degraded. The current UV- Vis's methods are too tedious, costly and time consuming which prevents stake holders in venturing into large scale algae growth. Hence, this study also includes the application of custom vision service in monitoring the algae growth via image classifiers.

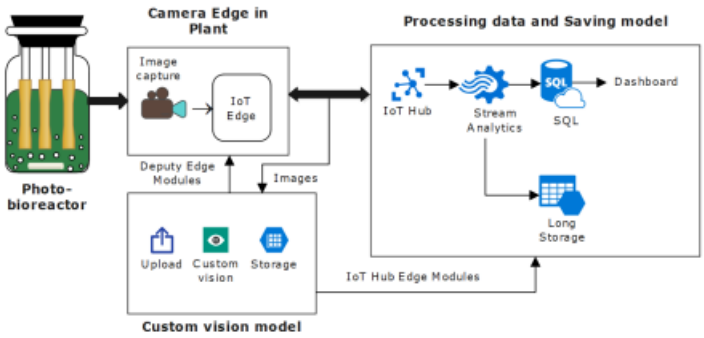

Figure 1: Digital architecture system of Algae growth monitoring.

Acknowledgements: Author would like to acknowledge the Fundamental Research Grant Scheme, Malaysia [FRGS/1/2019/STG05/UNIM/02/2] and MyPAIR-PHC-Hibiscus Grant [MyPAIR/1/2020/STG05/UNIM/1]

References

[1] Peter AP, Khoo KS, Chew KW, Ling TC, Ho SH, Chang JS, et al. Microalgae for biofuels, wastewater treatment and environmental monitoring. Environ Chem Lett 2021;19:2891–904. https://doi.org/10.1007/s10311-021-01219-6.

[2] Birol F. Southeast Asia Energy Outlook 2019 – Analysis. Int. Energy Agency, 2019, p. 199.

[3] Gielen D, Boshell F, Saygin D, Bazilian MD, Wagner N, Gorini R. The role of renewable energy in the global energy transformation. Energy Strateg Rev 2019;24:38–50. https://doi.org/10.1016/j.esr.2019.01.006.

[4] Peter AP, Koyande AK, Chew KW, Ho SH, Chen WH, Chang JS, et al. Continuous cultivation of microalgae in photobioreactors as a source of renewable energy: Current status and future challenges. Renew Sustain Energy Rev 2022;154:111852. https://doi.org/10.1016/j.rser.2021.111852.

[5] Kaya T, Kutlar OA, Taskiran OO. Evaluation of the Effects of Biodiesel on Emissions and Performance by Comparing the Results of the New European Drive Cycle and Worldwide Harmonized Light Vehicles Test Cycle. Energies 2018;11. https://doi.org/10.3390/en11102814.

[6] ElFar OA, Chang CK, Leong HY, Peter AP, Chew KW, Show PL. Prospects of Industry 5.0 in algae: Customization of production and new advance technology for clean bioenergy generation. Energy Convers Manag X 2021;10:100048. https://doi.org/10.1016/j.ecmx.2020.100048.

[7] Ali S, Paul Peter A, Chew KW, Munawaroh HSH, Show PL. Resource recovery from industrial effluents through the cultivation of microalgae: A review. Bioresour Technol 2021;337:125461. https://doi.org/10.1016/j.biortech.2021.125461.

[8] Rahul S M, Sundaramahalingam MA, Shivamthi CS, Shyam Kumar R, Varalakshmi P, Karthikumar S, et al. Insights about sustainable biodiesel production from microalgae biomass: A review. Int J Energy Res 2021;45:17028–56. https://doi.org/10.1002/er.6138.

[9] Dragone G, Fernandes BD. Third generation biofuels from microalgae Third generation biofuels from microalgae. Appl Microbiol Microb Biotechnol 2010:1355–66.

[10] Biloria N, Thakkar Y. Integrating algae building technology in the built environment: A cost and benefit perspective. Front Archit Res 2020;9:370–84. https://doi.org/10.1016/j.foar.2019.12.004.

[11] M. K Egbo, A. O Okoani IEO. Photobioreactors for microalgae cultivation – An Overview. Int J Sci Engeering Res 2018;9:65–74.

[12] Schädler T, Thurn AL, Brück T, Weuster-Botz D. Continuous production of lipids with microchloropsis salina in open thin-layer cascade photobioreactors on a pilot scale. Energies 2021;14. https://doi.org/10.3390/en14020500.

[13] Wu M, Du M, Wu G, Lu F, Li J, Lei A, et al. Water reuse and growth inhibition mechanisms for cultivation of microalga Euglena gracilis. Biotechnol Biofuels 2021;14:1–15. https://doi.org/10.1186/s13068-021-01980-4.

[14] Thor ESJ, Schoeters F, Spit J, Miert S Van. Photobioreactors Using Nephelometry. Processes 2021;9.

6th International Conference and
Postgraduate Colloquium for
Environmental Research 2022 (POCER
2022) 9 - 11 June 2022
Langkawi, Kedah, Malaysia

PCR30042022 – 248: Polyhedral Oligomeric Silsesquioxane as hydrophobic support for heterogenous catalysis: CO_2 hydrogenation to methanol

Yanet Rodriguez Herrero[a], and Amn Ullah[a*]

[a] Department of Agricultural, Food and Nutritional Science
University of Alberta, Edmonton, Canada

- Corrensponsing Author E-mail: **ullah2@ualberta.ca**

Keywords: carbon dioxide; methanol; catalysis; hydrophobicity; silsesquioxane; hydrogenation

Abstract

Every year over 60 000 deaths are caused by weather-related natural disasters as a consequence of global warming. The rise of the global temperature on 0.85°C in the last 130 years is attributed to the excess of greenhouse gases (GHG) produced by human activities. Among these gases, 41 billion tons of carbon dioxide (CO_2) are generated yearly with 91% of global contribution only from the fossil fuel and cement industry (Friedlingstein et al. 2020). If this increasingly annual production of CO_2 is not reduced, humanity is in jeopardy. To keep the rise of global temperatures within acceptable limits, the industries would need to cut emissions to zero, which is unfeasible. However, removing half of the current emissions from the atmosphere to store or convert them to value-added products would be a reasonable option.

Hydrogenation of CO_2 has been one of the major approaches to chemically convert CO_2 into oxygenated compounds like methanol, formic acid, and dimethyl ether. The hydrogenation of CO_2 to methanol has been the center of great number of research due to the low number of hydrogens needed and growing demand of methanol as fuel and energy storage. A major challenge to convert CO_2 is the requirement of a catalyst that is stable, highly active, selective, and able to function at low temperatures and pressures.

The commercial path for the production of methanol employs a syngas feed catalyzed by $Cu/ZnO/Al_2O_3$ at 493-573 K and a pressure of 5-10 MPa (Olah, Goeppert, and Prakash 2018). When the syngas feed

is replaced by CO_2 (reactions 1 and 2), the water produced as a by-product, act as inhibitor when it binds to the active metal site, reducing the surface area and the catalytic activity. Further, the hydrophilic property of the Al_2O_3 favor the production of $ZnAl_2O_4$ disrupting the synergistic effect of Cu/ZnO, which is reported as responsible for the conversion. Thus, the repulsion of the water away from the catalytic sites turns out to be an essential issue to improve the catalytic activity and the system efficiency.

$$CO_2 + 3H_2 \rightleftarrows CH_3OH + H_2O \qquad \Delta H°=-49.5\ kJmol^{-1} \qquad (1)$$

$$CO_2 + H_2 \rightleftarrows CO + H_2 \qquad \Delta H°=+41.2\ kJmol^{-1} \qquad (2)$$

Carbon materials as carbon nanotubes, activated carbon, and reduced graphene oxide (Deerattrakul et al. 2016) have been studied as supports as a result of their high surface area and high thermal stability. Another alternative to overcome the deactivation of the catalyst is using polyhedral oligomeric silsesquioxane (POSS) as hydrophobic support. POSS has received a lot of attention in research for its well-defined organic/inorganic hybrid constituents and its unique rigid cage-like molecular structure connected by Si-O-Si bonds. (Sangtrirutnugul et al. 2017) POSS are characterized by high thermal stability (>350°C) and fully tunable solubility. The irregularity of molecular shapes for some POSS molecules inhibits crystallization by preventing good packing. Hydrophobic groups attached to the cage could potentially prevent catalyst deactivation by water effect.

In this research, we investigated the Cu/ZnO impregnation onto the hydrophobic nPhenyl-POSS (n=8,12) via incipient wetness impregnation for the hydrogenation of CO_2 to methanol. We report the activities of the catalysts at different metal loadings (10, 20, and 30%) on O-POSS and D-POSS. The catalysts were characterized using SEM, TEM, EDX, BET, FT-IR, TGA, XRD, and XPS. The catalytic acitivity was tested in batch reactors in the CO_2 hydrogenation to methanol at 2 MPa in a temperature range 200-270°C. The products of the hydrogenation were analyzed using GC-TCD/FID.

Results and Discussion

Figure 1-A shows the the XRD pattern of Cu/ZnO-modified D-POSS. At a low loading of metals on the support, the diffraction peaks are practically not visible as a result of a high dispersion of the metals oxide on the surface of the D-POSS. When the ratio of metals:support was increased, the metals oxide peaks corresponding to CuO and ZnO were clearly visible in agreement with the high resolution XPS for O1s, where there is a broadeinging of the total peak as a result of CuO and ZnO. There is change in the shape of the peak at $2\theta = 7.41°$ which started broading as the load of metals increases. This could

be as a result of metals covering the surface of the silsesquioxane cages causing pores blockings in agreement with the BET results suggesting that the surface area of the catalysts decreased with increasing metal loading on the surface of the support. The size distribution from BET corresponds to mesoporous catalyts with a range between 2-5 nm. The catalytic activity of the modified catalysts was explored using mini batch reactors. Figure 1-B shows that the methanol yield increases as the metal loading increases on the support probing a succesful nanoimbobilization of the metals on the surface of 3D hydrophobic cages.

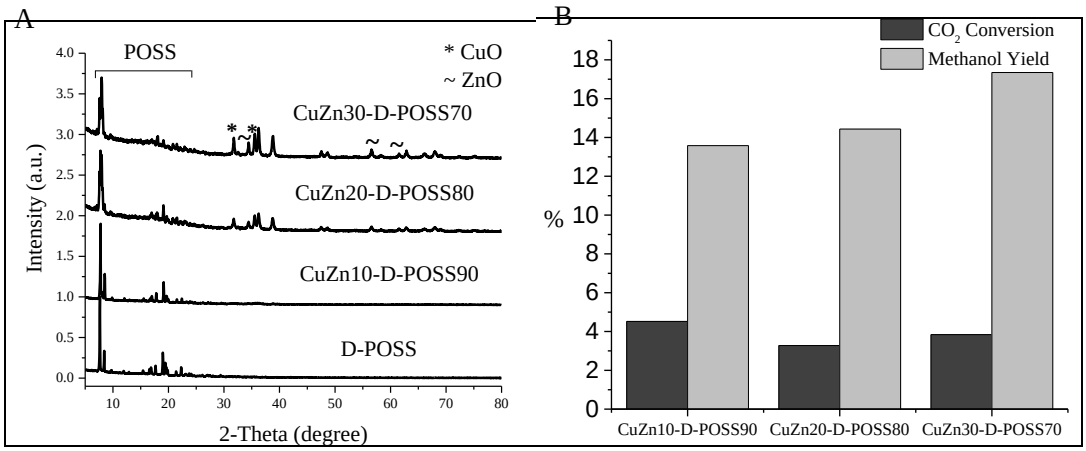

Figure 52: A) XRD of Cu/ZnO-modified D-POSS. B) The catalytic activity of CuZnX-D-POSSY in the CO_2 hydrogenation to methanol at 220°C, 2MPa, and 18 hr.

References

Deerattrakul, Varisara, Peerapan Dittanet, Montree Sawangphruk, and Paisan Kongkachuichay. 2016. "CO2 Hydrogenation to Methanol Using Cu-Zn Catalyst Supported on Reduced Graphene Oxide Nanosheets." *Journal of CO2 Utilization* 16: 104–13.

Friedlingstein, Pierre et al. 2020. "Global Carbon Budget 2020." *Earth System Science Data* 12(4): 3269–3340. https://essd.copernicus.org/articles/12/3269/2020/ (April 28, 2022).

Olah, George A, Alain Goeppert, and G K Surya Prakash. 2018. *Beyond Oil and Gas: The Methanol Economy*. John Wiley & Sons.

Sangtrirutnugul, Preeyanuch et al. 2017. "Tunable Porosity of Cross-Linked-Polyhedral Oligomeric Silsesquioxane Supports for Palladium-Catalyzed Aerobic Alcohol Oxidation in Water." *ACS applied materials & interfaces* 9(14): 12812–22.

PCR03052022 – 249: Enhancement of anaerobic fermentation with corn straw by sludge-corn stalk mixed biochar

Youzhou Jiao[a,b,c], Ninglu Zhang[a,b,c], Chao He[a,b,c], Xiaoran Ma[a,b,c], Xinxin Liu[a,b,c], Liang Liu[a,b,c], Tingting Hou[a,b,c], Xiaohui Pan[a,b,c,*]

[a] Key Laboratory of New Materials and Facilities for Rural Renewable Energy of Ministry of Agriculture and Rural Affairs, College of Mechanical & Electrical engineering, Henan Agricultural University, Zhengzhou 450002, China.

[b] Henan International Joint Laboratory of Biomass Energy and Nanomaterials, Henan Agricultural University, Zhengzhou 450002, China.

[c] Henan Collaborative Innovation Center of Biomass Energy, Henan Agricultural University, Zhengzhou 450002, China

- Corrensponsing Author E-mail: panxiaohui1987@163.com

Keywords: Sludge-corn stalk mixed biochar; Anaerobic fermentation; Corn straw; Methane production.

Extended Abstract

In order to realize the efficient resource utilization of straw and sludge, this study used sludge and corn straw as raw materials to prepare sludge-corn straw mixed biochar at different carbonization temperatures, raw material ratios, holding times and heating rates. As an additive for anaerobic fermentation, the effect of sludge-corn straw mixed biochar on the anaerobic fermentation performance of corn straw was investigated, and the correlation between the physicochemical properties of biochar and anaerobic fermentation performance was established. The results showed that when the preparation conditions of biochar were as follows: carbonization temperature of 600℃, raw material ratio of 1, holding time of 90 min, and heating rate of 20℃/min, the cumulative methane production of corn stalk by anaerobic fermentation exhibited the highest value of 269.23 mL/g VS, which was 47.1% higher than the blank control group. The specific surface area and pore structure of biochar only affect methane production in a certain range. This study provides a theoretical basis for further research on the

mechanism relationship between the properties of biochar materials and methane production by anaerobic fermentation.

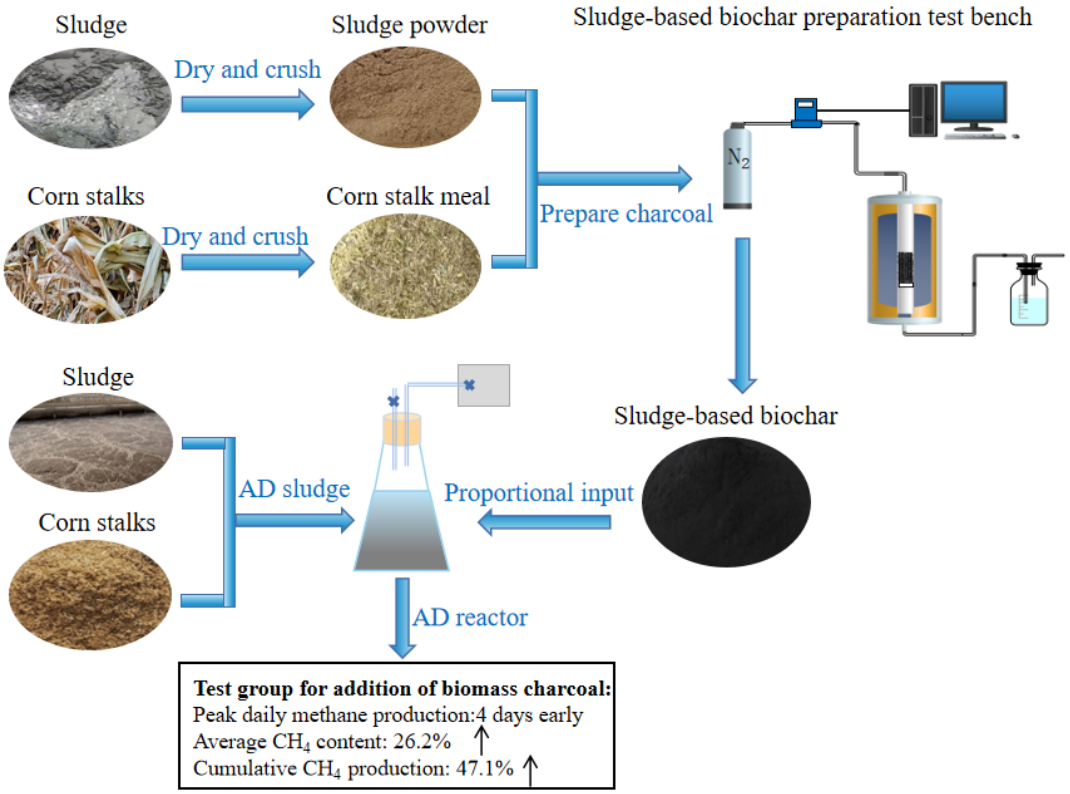

Acknowledgements: The authors thank the National Key Research and Development Program of China (2018YFE0206600), National Natural Science Foundation of China (52176184), Key Scientific Research Projects of Henan Higher Education Institutions(No. 21A416008).

6th International Conference and Postgraduate Colloquium for Environmental Research 2022 (POCER 2022) 9 - 11 June 2022
Langkawi, Kedah, Malaysia

PCR03052022 – 250: Structure-performance correlation of high surface area and hierarchical porous biochars as chloramphenicol adsorbents

Gaihong Wang[a], Xiaoyu Yong[a], Liwen Luo[b], Jonathan W.C. Wong[b], Jun Zhou[a*]

[a] Bioenergy Research Institute, College of Biotechnology and Pharmaceutical Engineering, Nanjing Tech University, Nanjing, Jiangsu 211816, China

[b] Institute of Bioresource and Agriculture, Hong Kong Baptist University, Hong Kong Special Administrative Region

- Corrensponsing Author E-mail: zhoujun@njtech.edu.cn

Keywords: High surface area; Hierarchical porous biochar; Structure-performance; Chloramphenicol adsorption; Alkaline modification.

Extended Abstract

Biochars have attracted widespread attention as a low-cost adsorbent for antibiotic removal. High surface area and hierarchical porous biochars (HHBCs), originating from five types of feedstocks, were prepared via simple carbonization and alkaline activation route and tested for chloramphenicol removal from the water environment. All biochars showed a maximum adsorption capacity of over 300 mg/g at room temperature, with a large specific surface area of 1687-2003 m^2g^{-1}. Adsorption isotherms and kinetics adhered well to Langmuir and pseudo-first-order models. The structure-performance correlation was analyzed to explore the effects of adsorbents' physical properties, morphology, and functional groups on adsorption performance. The pseudo-first-order kinetic constant, representing the adsorption rate, was strongly correlated with the external surface area and mesoporous pore volume. The maximum monolayer adsorption capacity, calculated by the Langmuir model, was strongly correlated with the microporous surface area and pore volume. A higher proportion of graphite and stronger hydrophilicity decreased the adsorption capacity. The primary adsorption mechanism appears to be physical adsorption through micropore filling, along with π-π electron donor-acceptor, electrostatic and hydrophobic interactions. Thus, a key factor influencing adsorption performance is the ratio of the microporous and mesoporous pore volume of adsorbents. To simultaneously enhance the adsorption rate and capacity, it is crucial to regulate the ratio of microporous and mesoporous pores of

biochars. Establishing this relationship could have important implications for regulating the adsorbent structure and improving adsorption behaviour.

Acknowledgements: The authors thank supports by the Jiangsu Agriculture Science and Technology Innovation Fund (SCX(21)2175), the Key Research and Development Technology of Ningxia Hui Autonomous Region (special project for foreign science and technology cooperation, 2019BFH02008), the Graduate Research and Innovation Project of Jiangsu Province (KYCX21_1166), and the Jiangsu Synergetic Innovation Center for Advanced Bio-Manufacture (XTD2204).

6th International Conference and
Postgraduate Colloquium for
Environmental Research 2022 (POCER
2022) 9 - 11 June 2022
Langkawi, Kedah, Malaysia

PCR03052022 – 251: Effects of biochar and biogas slurry reflux on methane production by mixed anaerobic digestion of cow dung and corn straw

Ye Yang[a], Mengyao Wang[a], Su Yan[b], Jun Zhou[a*]

[a] Bioenergy Research Institute, College of Biotechnology and Pharmaceutical Engineering
Nanjing Tech University, Nanjing, Jiangsu 211816, China

[b] Bioenergy Research Institute, School of Environmental Science and Engineering
Nanjing Tech University, Nanjing, Jiangsu 211816, China

- Corresponding Author E-mail: zhoujun@njtech.edu.cn

Keywords: Anaerobic digestion; Cow dung; Corn straw; Biochar; Biogas slurry; Microbial community

Extended Abstract

Recently, renewable energy has received a lot of attention as a promising means to address global energy needs and provide multiple environmental benefits due to the environmental problems caused by fossil fuels and the rise of energy security concerns. Biogas from anaerobic digestion represents a renewable and sustainable energy technology, in which methane can be used as alterative to fossil fuel. At present, crop straw and livestock and poultry manure are the main raw materials for biogas production in China. The aim of this work was to enhance methane production of mixed anaerobic digestion of cow dung and corn straw by adding biochar and biogas slurry reflux. Biochar was made of biogas residue as raw material, and biogas slurry was added instead of water in anaerobic digestion system. The biochar prepared from biogas residue is made according to the method in the previous work and characterized by X-ray photoelectron spectroscopy, fourier transform infrared spectroscopy and Scanning electron microscope. Biogas slurry was taken from 300 m^3 anaerobic biogas digester of Nanjing Tech University and added to the experimental group instead of water to realize biogas slurry reflux. In addition to the monitoring of daily biogas production and methane production in different experimental groups, the properties of digestive juices in different experimental stages were determined, such as pH, COD, ammonia nitrogen, VFAs, microbial diversity and microbial community analysis.

The characterization of biochar materials not only reveals that it can provide attachment for the growth of microorganisms, but also has abundant surface functional groups. Cyclic voltammetry showed that DIET mediated by surface oxygen-containing functional groups increased the yield of methane. Overall, pH in the experimental group decreased at first and then increased, which is consistent with the phenomenon observed in other studies. The total biogas production (14153 mL) of the experimental group with biochar and biogas slurry reflux was 36.98% higher than that of the blank group (10332 mL), and the total methane production (6149 mL) was 34.30% higher than that of the blank group (4575 mL). While the degradation rate of COD in the experimental group with biochar and biogas slurry reflux reached 46.75%. Affected by the original composition of biogas slurry, the system showed a high initial ammonia nitrogen value. However, the addition of biochar could promote its adsorption, which not only eliminates the inhibitory effect of high ammonia nitrogen on methanogenic bacteria, but also ensures high methane production under biogas slurry reflux. Alpha diversity showed that compared with the blank group, both the addition of biochar and biogas slurry reflux increased the Ace and Chao index. Microbial community analysis revealed that *Methanobacterium* and *Methanobrevibacter* were the dominant methanogens, while *Methanomassiliicoccus* appeared only at the late period of each system.

This work not only provides a promising method for the efficient operation of mixed anaerobic digestion, but also provides a new idea for the treatment of biogas residue and biogas slurry.

Acknowledgements: The authors thank supports by the Jiangsu Agriculture Science and Technology Innovation Fund (SCX(21)2175), and the Jiangsu Synergetic Innovation Center for Advanced Bio-Manufacture (XTD2204).

6th International Conference and Postgraduate Colloquium for Environmental Research 2022 (POCER 2022) 9 - 11 June 2022
Langkawi, Kedah, Malaysia

PCR03052022 – 252: Remediation of Cd and Zn contaminated soil by zero valent iron (Fe^0): a field trial

Ping Wang[a], Feng Shen[a], Ronghua Li[a], Di Guo[a], Wen Liang[a], Tao Liu[a], Zengqiang Zhang[a*]

[a] College of Natural Resources and Environment, Northwest A&F University, Yangling, Shaanxi Province 712100, PR China

- Corrensponsing Author E-mail: zhangzq58@126.com

Keywords: Zero valent iron; Field trial; Soil remediation; Cadmium; Zinc.

Extended Abstract

Remediation of contaminated soil is a long-term challenge faced by human beings. The in-situ remediation was carried out using zero valent iron (Fe^0) with the rotation pattern of soybean-rape the near a smelter influenced by atmospheric subsidence. The results showed that the total contents of Cd and Zn in rhizosphere soils with Fe^0 treatment were lower than that in the control. The biomass of soybean and rape increased by 55.4 ~ 64.9% and 6.2 ~ 42.8%, respectively with the addition of Fe^0. And Fe^0 decreased the availability of Cd and Zn and the accumulation of Cd and Zn in plant roots. The Cd and Zn contents of the iron-rich substances separated from soil were much high, reaching 155.8 mg/kg and 29525 mg/kg, respectively and the total Cd and Zn in the remaining soil decreased by 28.5% and 44.6%, respectively. XRD and XPS analysis of the separated substance implied that the new production of iron oxides (γ-FeOOH and γ-Fe_2O). The existence of CdO and CdS were obversed and the main forms of Zn were ZnS, ZnO and $ZnCO_3$ through the immobilization of iron oxides. This work suggested the feasibility of Fe^0 in the contaminated soil. Using retrievable materials from soil to remove permanently pollutants should be considered in the future remediation practice.

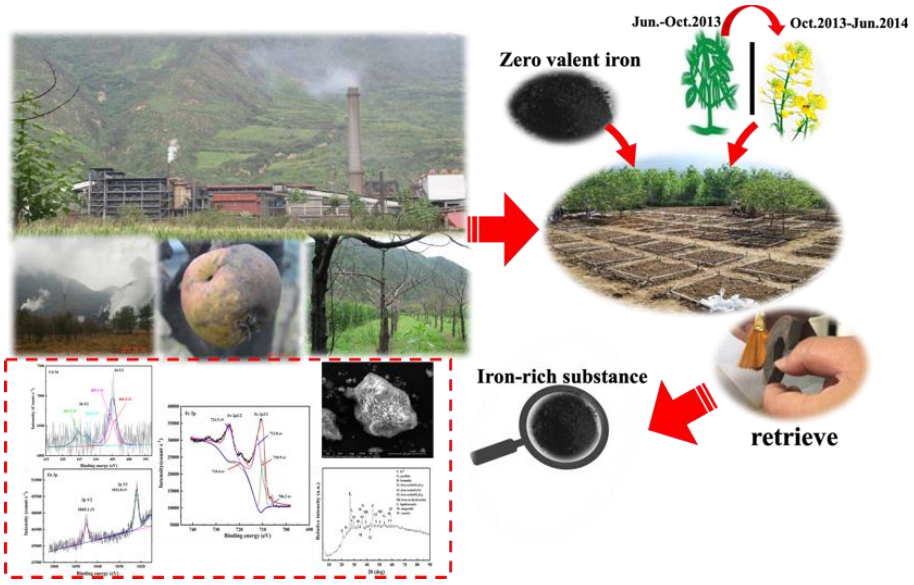

Figure 53: The graphical abstract of the experiment

6th International Conference and
Postgraduate Colloquium for
Environmental Research 2022 (POCER
2022) 9 - 11 June 2022
Langkawi, Kedah, Malaysia

PCR03052022 – 253: The application of mineral additive in mitigating pollutant during the composting process

Xiuna Rena[a], Minna Jiao[a], Zengqiang Zhanga[a]*

[a] College of Natural Resources and Environment, Northwest A&F University, Yangling, Shaanxi Province 712100, PR China

- Correnspoonsing Author E-mail:

Keywords: Zero valent iron; Field trial; Soil remediation; Cadmium; Zinc.

Extended Abstract

The livestock manure, dominant component of agricultural waste, is abundant in nutrients, estimating to attain 0.23 billion tons of nitrogen equivalents in 2030 all over the world. If treated improperly, it would not only waste resources, but also result in environmental pollution. Recently, aerobic composting is widely accepted as an eco-practical way to recycle organic waste, which could convert degradable organic substances into high-value fertilizers through a series of chemical-biological reactions. Meanwhile, the application of organic fertilizer into farmlands is beneficial for improving soil structure and accelerating plant growth. However, some disadvantages occur in the traditional composting, which restrict the development of composting technology, including long period, greenhouse gases emission, nitrogen loss and low humification. These aforementioned issues not only affect adversely quality of end products and reduce its agricultural value, but also damage to ecological environment, and thereby restricting the development of composting technology. Recently, among of all methods, adding exogenous mineral additive has caused more attention due to its easy operability, high availability and special characteristics including huge specific surface area, porosity and strong absorb capacity. And it has been confirmed that Zeolite, Bentonite, Medical stone, Clay, Diatomite, Black tourmaline, Biochar and others play a positive effect on GHGs reduction, nitrogen conservation and humification increasement by buffering pH variation, increasing oxygen diffusion, immobilizing more nitrogen and improving microbial succession. While considering the engineering practicability, effective composting process and economic benefits, it is supposed to search more minerals amendment in the future. Besides, metagenomics and metabonomics are used to investigate the mechanisms and pathways of how mineral additive affect composting process deeply.

6th International Conference and Postgraduate Colloquium for Environmental Research 2022 (POCER 2022) 9 - 11 June 2022
Langkawi, Kedah, Malaysia

PCR03052022 – 254: Enhancing the performance of microbial fuel cells with a Fe-CN catalyst modified bioanode

Xiao-Long Cheng[a], Qian-Wen Yang[b], Qiang Xu[a], Jun Zhou[a], Xiao-Yu Yong[a*]

[a] College of Biotechnology and Pharmaceutical Engineering, Bioenergy Research Institute, Nanjing Tech University, Nanjing, 211816, China

[b] School of Environmental Science and Engineering, Nanjing Tech University, Nanjing 211816, China

- Corrensponsing Author E-mail: yongxiaoyu@njtech.edu.cn

Keywords: MFCs; Extracellular electron transfer; Fe-CN catalyst; Modified anode

Extended Abstract

Microbial fuel cells (MFCs) have gained tremendous attention as a novel platform for simulataneous wastewater treatment and electricity generation through microbial anaerobic metabolic ability [1]. Although some impressive progress in terms of the efficiency of MFCs has obtained in recent years, the relatively low voltage output and power density compare with other technologies limit their industrial application. Here, Fe-CN catalyst was prepared by one-pot pyrolysis of $FeCl_3$ and urea at 550°C (Fe-CN0: pure $FeCl_3$, Fe-CN1: 0.5 g $FeCl_3$ and 3 g urea) were further adhered onto the surface of carbon paper with Nafion solution for the fabrication of composite MFCs anodes (MFC0: carbon paper anode, MFC1: modified anode with Fe-CN0, MFC2: modified anode with Fe-CN1).

Performance of MFCs

All MFCs had a similar trend of voltage output in all run processes, which implied the matured formation of eletroactive biofilms on anodes. MFC0 had a long lag time of about 100 h before obvious voltage production, while MFC1 and MFC2 had faster voltage output at the beginning of inoculation (especially in MFC2), indicating that the modified electrode increased the oxidation of carbon source and the production of electrons. Moreover, MFC1 and MFC2 achieved the higher maximum voltage output of 792.76 mV and 711.89 mV than that of MFC1 (616.39 mV), which demonstrated a better biocompatibility of the modified anodes for bacterial attachment [2].

Electrochemical activity of electroactive biofilms

CV experiment results showed that modified anodes changed the exotracellular electron transfer pathway of eletroactive biofilm, since there were two pairs of redox peaks in MFC1 and MFC2, while only one pair of redox peaks in MFC0. In addition, higher catalytic current was achieved in MFC1 (0.58 mA) and MFC2 (0.97 mA) than that of MFC0 (0.45 mA) at the scan rate of 10 mV/s. When the scan rate was increased from 10 mV/s to 200 mV/s, the peak current also increased simultaneously. The peak current of all MFCs exhibited a good line relation with the scan rates, which suggested that the electrochemical reactions in all anodes were the typical surface-controlled processes [3]. The EIS experiment showed that the Rct in MFC1 (29.59 Ω) and MFC2 (26.54 Ω) were greatly lower than that of in MFC0 (36.24 Ω), suggesting that the modified anode decreased the Rct and thus increased extracellular electron transfer [4].

Microbial communities in different anodes

The high-throughput squencing results showed that *Geobacter* was the domaint exoelectrogens in all MFCs. Moreover, higher proportion of *Geobacter* appeared in MFC2, which demonstrated Fe-CN catalyst modified anode could enrich exoelectrogens for higher voltage output than carbon paper anode. In addition, the concentration of sodium acetate was detected in the end of expriment. The results showed that sodium acetate was almost consumed in MFC0, while there was many surplus in MFC1 and MFC2. This result indicated that other functional microorganism competed with *Geobacter* for carbon source in MFC0, which resulted in lower voltage output.

This work provied a facile approch for the development of bioanode with high voltage output in MFCs that is promising for practical applications.

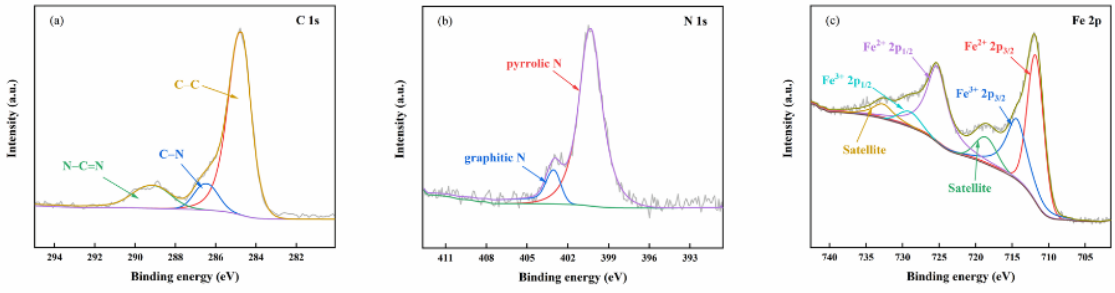

Figure 1: XPS diagram C1s (a), N1s (b), and Fe 2p (c) of Fe-CN catalyst

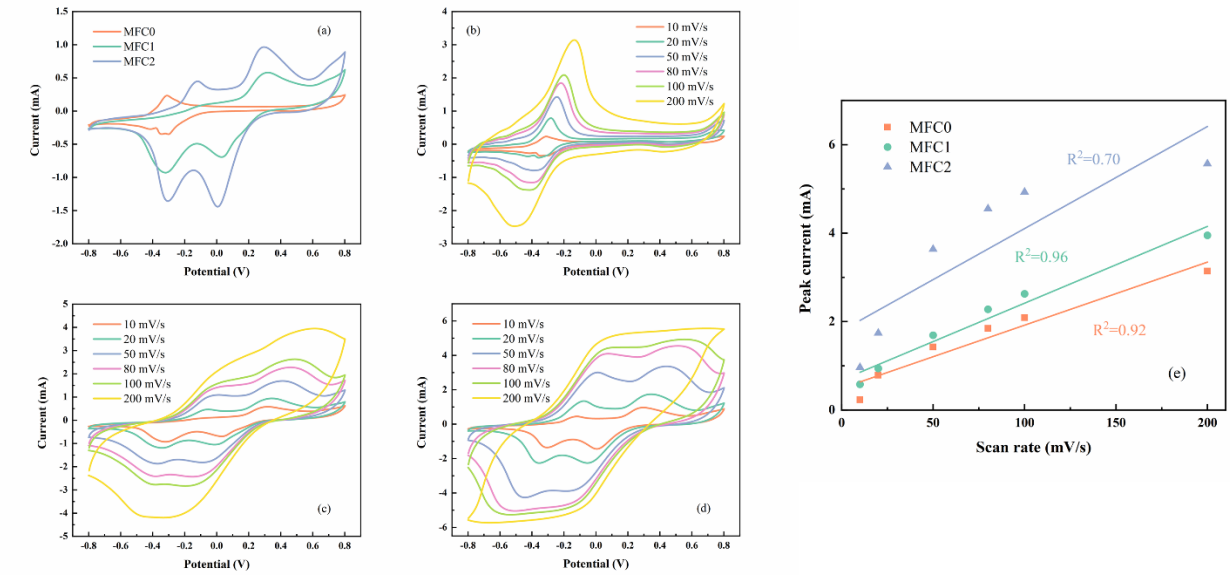

Figure. 2: CV at 10 mV/s of all MFCs (a). Scan rate-dependent CV of MFC0 (b), MFC1 (c), and MFC2 (d). Plots of current peak versus scan rate achieved from the CV curves (e).

Acknowledgements: The authors thank supports by The National Key Research and Development Program of China (Project No. 2021YFA0910400), and The Jiangsu Synergetic Innovation Center for Advanced Bio-Manufacture (Project No. XTD2216).

References

Li, B., et al., *Coordinated response of Au-NPs/rGO modified electroactive biofilms under phenolic compounds shock: Comprehensive analysis from architecture, composition, and activity.* Water Res, 2021. **189**: p. 116589.

Li, Y., et al., *Tailoring spatial structure of electroactive biofilm for enhanced activity and direct electron transfer on iron phthalocyanine modified anode in microbial fuel cells.* Biosens Bioelectron, 2021. **191**: p. 113410.

Li, Y., et al., *Enhanced electricity generation and extracellular electron transfer by polydopamine–reduced graphene oxide (PDA–rGO) modification for high-performance anode in microbial fuel cell.* Chemical Engineering Journal, 2020. **387**.

Munjal, M., et al., *An insight of bioelectricity production in mediator less microbial fuel cell using mesoporous Cobalt Ferrite anode.* International Journal of Hydrogen Energy, 2020. **45**(22): p. 12525-12534.

6th International Conference and
Postgraduate Colloquium for
Environmental Research 2022 (POCER
2022) 9 - 11 June 2022
Langkawi, Kedah, Malaysia

PCR03052022 – 255: Caproic acid production from anaerobic fermentation of organic waste – Pathways and microbial perspective

Wenjian Dong[a], Chao Liu[a], Lin Luo[a], Binghua Yan[a]*

[a] College of Resources and Environment, Hunan Agricultural University, Changsha 410128, China

Extended Abstract

Ever increasing organic waste production is threatening our environmental sustainability and simultaneously wasting organic resources and nutrients. Anaerobic fermentation is widely accepted as one of the promising technologies for organic waste conversion, through which both waste disposal and resources recovery can be achieved. Caproic acid is an important platform chemical, the value of which is much higher than short chain volatile fatty acids. During anaerobic fermentation, it is generally believed that microbial synthesis of caproic acid is a chain elongation process of carboxylic acid (i.e., reverse β oxidation reaction.), in which ethanol and lactate are common electron donors. The oxidation of electron donor provides energy, reduction equivalent and acetyl-CoA for the reverse β oxidation reaction (a cyclic process), during which acetate(C2) is elongated to butyrate(C4) and then to caproate(C6). Microbes play a crucial role in anaerobic caproic acid production, pure bacteria with ability of caproic acid production was screened in this work and their performance was compared with mixed culture. The main factors, such as pH, temperature, electron donor and acceptor, hydrogen partial pressure, and competition between microorganisms were summarized. Facing with the immature caproic acid separation technology, muti-methods were compared from the prospect of application and proposed that electrodialysis technology might be the mainstream technology of caproic acid separation. Targeting on a large scale caproic acid production through anaerobic fermentation, it is also necessary to strengthen the research on the synergy and competition between microorganisms in the process of anaerobic fermentation, and to establish a complete set of caproic acid separation technology. This will be expected to contribute to the goal of global carbon peaking and carbon neutrality.

6th International Conference and
Postgraduate Colloquium for
Environmental Research 2022 (POCER
2022) 9 - 11 June 2022
Langkawi, Kedah, Malaysia

PCR03052022 – 256: Effect of water regime on the emission of free ammonia during high solid anaerobic digestion of pig manure

Jian Su[a], Wenjuan Lv[a], Liheng Ren[a], Xiaoliang Kong[a], Binghua Yan[a]*

[a] College of Resources and Environment, Hunan Agricultural University, Changsha 410128, China

Keywords: pig manure, biogas, ammonia inhibition, water adding frequency, free ammonia

Extended Abstract

This study intends to investigate the effects of different initial solid content and water adding frequency on high solid anaerobic digestion of pig manure. With equal amount of water addition, the four treatments were set with varied adding frequencies, i.e. once but at different time in treatments TI and T2, twice in T3 while it was three times in treatment T4. Results show that the whole methanogenic process ran smoothly with the biogas production rate maintaining at 191.1 L CH_4/Kg·VS_{added}. The pH was in a range of 6.8-7.5, which basically fell in the ideal methanogenic range and the effluent COD was maintained at a low level of 1500-1700 mg/L. Although the gas production rate of T1 is 217.4 LCH_4/Kg·VS_{added}, the initial solid content and water addition frequency of one time led to higher potential ammonia nitrogen inhibition. The cumulative release of free ammonia was 188.79 mg/L in T1, and the fraction of free ammonia in ammonia balance is the largest. The lowest gas production rate of T4 is 172.2 LCH_4/KgVS_{added}, and the cumulative release of free ammonia is 173.6 mg/L, which was lower than T1 but higher than T2 and T3, indicating that the high frequency of water addition is not conducive to gas production and alleviating the inhibition of ammonia nitrogen. The gas production rate and the accumulation of free ammonia of T2 and T3 is similar, which were ~186.75 LCH_4/KgVS_{added} and ~155.45 mg / L, respectively. It is inferred that the tendency of ammonia nitrogen inhibition in high solid anaerobic digestion of pig manure can be reduced through low-frequency dilution.

6th International Conference and Postgraduate Colloquium for Environmental Research 2022 (POCER 2022) 9 - 11 June 2022
Langkawi, Kedah, Malaysia

PCR03052022 – 257: Interfacing Biosyntheic CdS with Engineered *Rhodopseudomonas palustris* for Efficient Visible Light-Driven CO_2-CH_4 Conversion

Yulei Qian[a], Jun Zhou[a*]

[a] Bioenergy Research Institute, College of Biotechnology and Pharmaceutical Engineering, Nanjing Tech University, Nanjing, Jiangsu 211816, China

- Corrensponsing Author E-mail: zhoujun@njtech.edu.cn

Keywords: Semi-artificial photosynthesis; CO_2 biomethanation; Biohybrid system; Photoelectron transfer.

Extended Abstract

Semi-artificial photosynthesis, bundling specific biocatalysts with highly efficient photosensitizers, revolutionizes existing photosynthetic systems for solar-to-chemical (S2C) conversion.In this work, we refined the design for the two key elements involved: 1) a model anoxygenic phototroph *Rhodopseudomonas palustris* was selected due to its diverse metabolic pathways and light-driven ATP genaration. Simple means of genetic engineering made it possible to achieve one-step sustainable CO_2 biomethanation relying on a remodeled [MoFe]-nitrogenase (N_2ase*) under irradiation. 2) CdS nanoparticles (CdS NPs) with excellent biocompatibility and visible light absorption property were precipitated on the surface of cell membrane in the facile self-assembling form. As experted, the photo-driven CH_4 yield in *R. palustris* (N_2ase*)-CdS biohybrid system biohybrid system reached 155 nmol/mL, which was 13.4 folds of the pure bacteria. Higher electrical conductivity and generated photocurrent in response to irradiation were observed when bacteria was intimately coupled with biogenic CdS NPs. The transcriptome profiles reavealed that gene expression related to electron transfer chain (ETC), nitrogenase, nanofilaments and redox stress defendence was activated. Thus, the greatly enhanced CO_2 biomethanation process in biohybrid system was attributed to the remarkable increase of intracellular reducing power and the stronger rigidity of the cells with the assistance of photoexcited electrons from CdS NPs.Our discovery encourages a novel insight and promising strategy for the improvemnet of the current CO_2-CH_4 biomanufacturing system.

Acknowledgements: The authors thank supports by the Jiangsu Agriculture Science and Technology Innovation Fund (SCX(21)2175), the Key Research and Development Technology of Ningxia Hui Autonomous Region (special project for foreign science and technology cooperation, 2019BFH02008),

the Graduate Research and Innovation Project of Jiangsu Province (KYCX21_1166), and the Jiangsu Synergetic Innovation Center for Advanced Bio-Manufacture (XTD2204).

6th International Conference and
Postgraduate Colloquium for
Environmental Research 2022 (POCER
2022) 9 - 11 June 2022
Langkawi, Kedah, Malaysia

PCR10052022 – 258: Waste biorefinery for renewable energy and valuable bioproducts production

Shams Forruque Ahmed[a*], Fatema Tuz Zuhara[a], Maliha Kabir[a], Aanushka Mehjabin[a], Samiya Ahmed[a], Samiha Mannan[a], M. Mofijur[b, c], Anh Tuan Hoang[d*], M.A. Kalam [b, e], T.M.I. Mahlia[b, e]

[a] Science and Math Program
Asian University for Women, Chattogram 4000, Bangladesh

[b] Centre for Technology in Water and Wastewater
School of Civil and Environmental Engineering, University of Technology Sydney, Ultimo, NSW 2007, Australia

[c] Mechanical Engineering Department
Prince Mohammad Bin Fahd University, Al Khobar, 31952, Saudi Arabia

[d] Institute of Engineering
HUTECH University, Ho Chi Minh City, Viet Nam

[e] Department of Mechanical Engineering
College of Engineering, Universiti Tenaga Nasional, Selangor, Malaysia.

- Corresponding Author E-mail: shams.ahmed@auw.edu.bd; shams.f.ahmed@gmail.com (Shams Forruque Ahmed); hatuan@hutech.edu.vn (Anh Tuan Hoang)

Extended Abstract

Global energy shortages and the issues they will pose in the future, as well as a current climate calamity wreaking havoc around the world and a massive amount of food waste filling our landfills, are all factors to consider. As a result, putting the ideas of circular bioeconomy and bioconversion of food waste into practise appears to be not only a good idea but also one that is urgently needed. However, the existing relevant research did not place a strong emphasis on technological advancement and circular bioeconomy in the context of bioconversion of food waste, even though this is an important topic. This article assesses how food waste generated in large quantities can be converted into valuable bioproducts

through bioconversion processes such as solventogenesis, anaerobic fermentation, and oleaginous metabolism, which are gaining popularity due to their sustainable and efficient procedure as well as their resource recycling. It also discusses biorefinery approaches that are connected with the economy to construct a circular bioeconomy, as well as the problems that must be overcome while exploring various techno-economic, environmental, and life cycle scenarios. By looking at the technological, economic, and environmental effects, it is clear that biorefinery of food waste can be a profitable business if certain paths are kept. It has also been found that bioconversion methods for making useful bioproducts have a much smaller effect on the environment than traditional methods. Integrating the bioconversion processes makes the process even more efficient and helps recover resources in a sustainable way. To create a circular bioeconomy, a biorefinery strategy with an integrated approach needs to be adapted.

6th International Conference and
Postgraduate Colloquium for
Environmental Research 2022 (POCER
2022) 9 - 11 June 2022
Langkawi, Kedah, Malaysia

PCR11052022 – 259: Resource recovery and biorefinery potential of apple orchard waste in the circular bioeconomy

Yumin Duan, Mukesh Kumar Awasthi

College of Natural Resources and Environment, Northwest A&F University, Yangling, Shaanxi Province 712100, China

***Corresponding author:**

Dr. Mukesh Kumar Awasthi

College of Natural Resources and Environment,

Northwest A&F University, Yangling,

Shaanxi Province 712100, PR China

E. mail address: mukesh_awasthi45@yahoo.com (M.K. Awasthi)

Abstract

Huge quantities of apple orchard waste generated which regarded as a promising alternative energy source for biofuel and biomaterial production. Biorefinery emerged as a sustainable approach and recognized promising transformation platforms for products, to achieve circular bioeconomy which focuses on the biomass efficient and sustainable valorization, promotes resource regeneration and restorative. The emerged biowaste biorefinery has proved as sustainable approach for integrated bioproducts further applied in industrial, commercial, agricultural and energy sectors. Based on carbon neutral sustainable development, this review comprehensive explained the apple orchard waste as renewable resource generation and resource utilization technologies from the perspective of energy, nutrient and material recovery in the concept of biorefinery. Integrate biorefinery concepts into apple orchard waste management is promise for conversion into value-added materials and contribute as driving force to cope with resource scarcity, climate changes and huge material demand in circular bioeconomy.

Keywords: Apple orchard waste; Biorefinery; Bioeconomy; Sustainability; Perspectives

6th International Conference and Postgraduate Colloquium for Environmental Research 2022 (POCER 2022) 9 - 11 June 2022
Langkawi, Kedah, Malaysia

PCR14052022 – 260: Graphene Oxide-based Dendritic Thin Film Nanocomposite Membrane for Improved Flux and Antifouling Properties

Siew Fen Chua[a], Alireza Nouri[a], Kar Mun Lam[a], Wei Lun Ang[a,b]*, Ebrahim Mahmoudi[a,b], Woei Jye Lau[c], Abdul Wahab Mohammad[a,b]

[a]Department of Chemical and Process Engineering, Faculty of Engineering and Built Environment, Universiti Kebangsaan Malaysia, 43600, Bangi, Selangor, Malaysia

[b]Centre for Sustainable Process Technology (CESPRO), Faculty of Engineering and Built Environment, Universiti Kebangsaan Malaysia, 43600, Bangi, Selangor, Malaysia

[c]Advanced Membrane Technology Research Centre (AMTEC), Universiti Teknologi Malaysia, 81310 Skudai, Johor, Malaysia

- Corrensponsing Author E-mail: wl_ang@ukm.edu.my

Keywords: GO-PDMAEMA; Thin film nanocomposite membrane; POME; Nanofiltration; Antifouling

Extended Abstract

The main issues that are often faced by membrane filtration technology and restrict its application are membrane fouling and also the trade-off effect between membrane permeability and rejection selectivity. Tremendous of researches and efforts have been done in order to improved the membrane properties without sacrificing the membrane selectivity. This research mainly focus on nanofiltration. Conventionally, thin film composite (TFC) membrane is fabricated by interfacial polymerization (IP) to form a polyamide (PA) layer on top of a porous support membrane. In order to overcome the main drawbacks mentioned, the incorporation of nanomaterials into diamine monomer aqueous solution is often employed. This has proven improved the membrane filtration and antifouling performance by enhancing the membrane properties. GO that has great hydrophilicity due to its abundant of oxygen functional groups is decorated with dendrimer poly(2-(dimethylamino)) ethyl methacrylate (PDMAEMA) which is rich in amine groups. These amine groups on the dendrimer branch could aid in the IP process. GO-PDMAEMA is dispersed into amine aqueous solution with different loading

concentration (0-0.020 wt%) during the IP process. In this research, the performance of six different sets of thin film nanocomposite membranes with different GO and GO-PDMAEMA loadings, which are TFC (0 wt%), TFNG-1 (GO-0.010 wt%), TFNG-P1 (GO-PDMAEMA-0.005 wt%), TFNG-P2 (GO-PDMAEMA-0.010 wt%), TFNG-P3 (GO-PDMAEMA-0.015 wt%) and TFNG-P4 (GO-PDMAEMA-0.020 wt%), have been tested and analyzed. The filtration experiments were performed using a cross-flow filtration system. The membrane permeability increased upon the loading of GO and GO-PDMAEMA into the amine aqueuous layer. This is because of the hydrophilicity nature of both GO and GO-PDMAEMA. As the loading of GO-PDMAEMA increase from 0-0.010 wt%, the membrane permeability increased, the highest at 9.75 LMH. The membrane permeability decreased slightly when the GO-PDMAEMA loading increased from 0.015 – 0.020 wt%. Nevertheless, the membrane permeability for all TFN membranes fabricated is found higher than unmodified TFC membrane. This could be attributed to the incorporation of GO and GO-PDMAEMA. Besides the hydrophiliciy, for GO decorated PDMAEMA, PDMAEMA could increase the interlayer spacing in between GO in which also aid in water molecules diffusion through GO layer. Thus, the improvement of water flux and permeability could be observed for all TFN membranes. For salt rejection, especially the divalent salt rejection, Na_2SO_4, for all the TFN membrane fabricated, the percentage of rejection are more than 95% with TFNG-P2 shows the highest rejection percentage, 98.2%, where as for TFC, the rejection percentage is the lowest, 93%. In order to evaluate the anti-fouling performance of TFN membranes fabricated, fouling test was carried out for 3 cycles, 5 hours for each cycle. Palm oil mill effluent (POME) which could cause severe environmental problems and pollution is utilized as foulant in this experiment. In each cycle, the test is begun with pure water filtration then followed by 5 hours of POME filtration. Upon completing 1 cycle, the membrane is washed. The flux recovery rate (FRR) for both TFNG-1 and TFNG-P2 membrane showed improvement as compared to TFC after completing 3 cycles of fouling test. This is due to the hydrophilic nanomaterials, GO and GO-PDMAEMA that able to form a protective layer and reduce the interaction between the membrane surface and foulants. This in a way minimize the deposition of foulants on membrane surface and hence improved the antifouling properties of the modified thin film nanocomposite membrane. In conclusion, the incorporation of GO-PDMAEMA into PA layer has proven to enhance membrane permeability and antifouling properties without sacrificing the membrane selectivity ability.

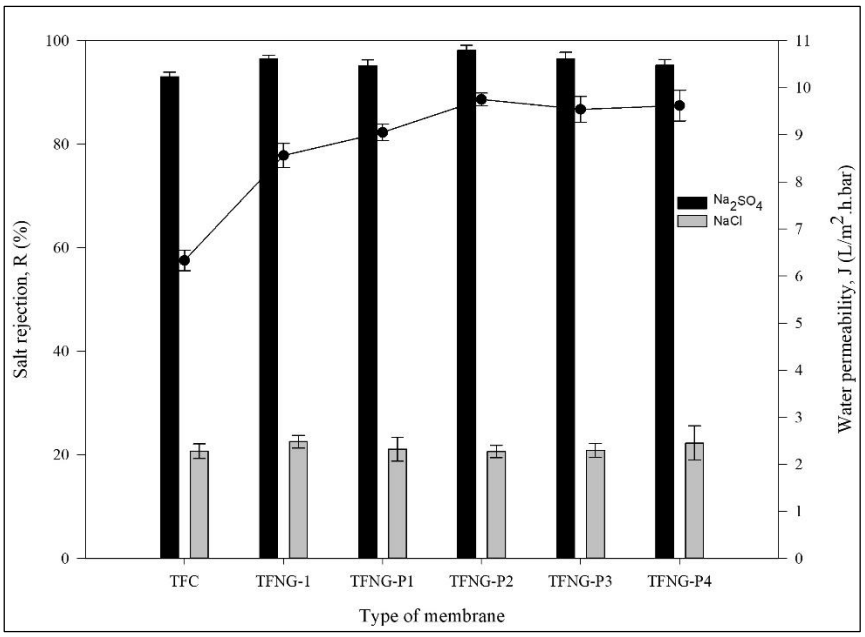

Figure 1: Salt Rejection and Water Permeability of TFC, TFNG and TFNG-P membranes

Table 1: FRR after 3 cycles of fouling

Membrane	FRR (%)
TFC	79.3
TFNG-1	84
TFNG-P2	86.5

Acknowledgement: The authors would like to thank the financial support given by Universiti Kebangsaan Malaysia (UKM) under the research project with Grant no.: DIP-2020-016.

6th International Conference and
Postgraduate Colloquium for
Environmental Research 2022 (POCER
2022) 9 - 11 June 2022
Langkawi, Kedah, Malaysia

PCR16052022 – 261: Novel Carbon Aerogel from Pineapple Leaf-based Microfibrillated Cellulose for Removal of Oil and Organic Solvent

Luon Tan Nguyen[a,b], Thuan Nguyen Ngoc[a,b], Nga H.N. Do[a,b], Huong L.X. Doan[a,b], Phong Thanh Mai[a,b], Kien A. Le[c] and Phung Kim Le[a,b*]

[a] Refinery and Petrochemical Technology Research Centre
Ho Chi Minh City University of Technology (HCMUT), 268 Ly Thuong Kiet Street, District 10, Ho Chi Minh City, Vietnam

[b] Vietnam National University Ho Chi Minh City
Linh Trung Ward, Thu Duc District, Ho Chi Minh City, Vietnam

[c] Institute for Tropical Technology and Environmental Protection, 57A Truong Quoc Dung Street, Phu Nhuan District, Ho Chi Minh City, Vietnam

- Corresponding Author E-mail: phungle@hcmut.edu.vn

Keywords: Carbon Aerogel; Microfibrillated cellulose; Oil absorption; Organic solvent absorption.

Extended Abstract

Oil and chemical spills kill a myriad of marine animals, destroy aquatic habitats, and pollute the food chains. Carbon aerogels from natural polymers like cellulose have enormous potential for oil and solvent removal due to their porous structure, hydrophobic surface, and eco-friendliness. For the first time, carbon aerogels from pineapple leaf-derived microfibrillated cellulose (MFC) were effectively and economically fabricated for dealing with oil and organic solvent pollution. MFC was first synthesized by using mild acidic hydrolysis and high-speed homogenization on the pineapple leaf pulp. Polyamide amine-epichlorohydrin (PAE) was then utilized to crosslink the MFC chains to produce cellulose-based aerogels that were further pyrolyzed to create carbon aerogels. The effects of inner gas flow rate and heating speed on characteristics of carbon aerogels were comprehensively studied. The developed aerogels were extremely lightweight (28.0-29.5 mg/cm^3) and hydrophobic. Those aerogels exhibited excellent absorption capacity of 22.4-24.2 and 22.1-28.5 g/g for 5w30 oil and toluene, respectively. It was found that the nitrogen flow rate had an insignificant impact on the aerogel structure and removal efficiency, whereas the slow heating rate made the aerogels denser, thus leading to their

lower absorption capacity. Based on the results, our carbon aerogels are a promising candidate for environmental protection because of their ability to manage effectively oil and organic solvent-contaminated water.

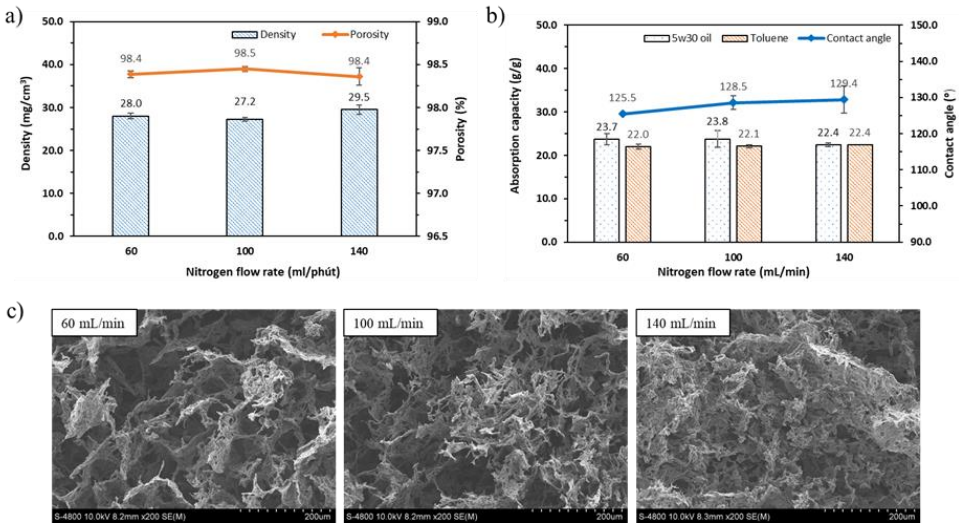

Figure 1: Density and porosity (a), contact angle and absorption capacity (b), and SEM images (c) of MFC carbon aerogel as a function of nitrogen flow rate.

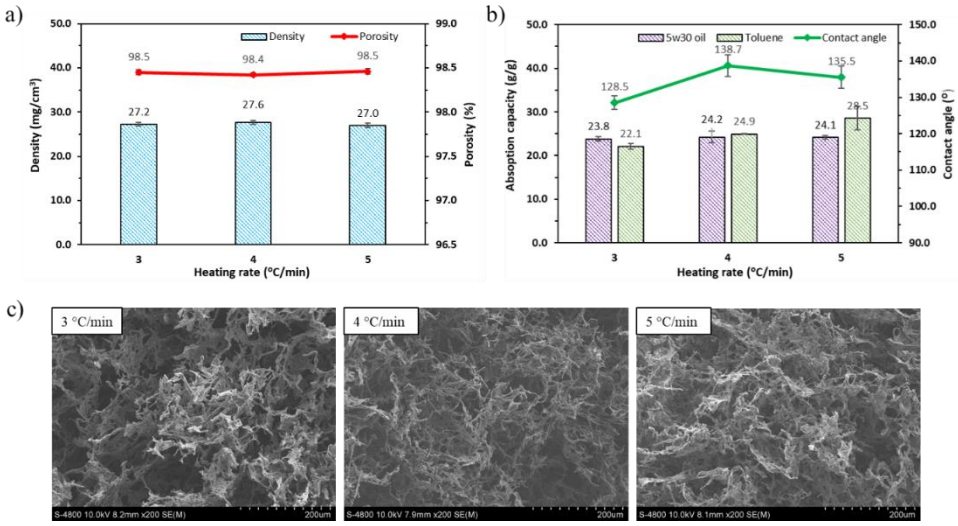

Figure 2: Density and porosity (a), contact angle and absorption capacity (b), and SEM images (c) of MFC carbon aerogel as a function of heating rate.

Acknowledgements: This work was funded by Vingroup Joint Stock Company and supported by Vingroup Innovation Foundation (VINIF) under project code VINIF.2020.NCUD.DA112. We also acknowledge the support of time and facilities from Ho Chi Minh City University of Technology (HCMUT), VNU-HCM for this study.

References

Wang, M., Shao, C., Zhou, S., Yang, J., & Xu, F, 2017. Preparation of carbon aerogels from TEMPO-oxidized cellulose nanofibers for organic solvents absorption. *RSC advances*. 7(61): 38220-38230.

Wang, H., Gong, Y., Wang, Y. 2014. Cellulose-based hydrophobic carbon aerogels as versatile and superior adsorbents for sewage treatment. *RSC Advances*. 4(86): 45753-45759.

Huang, P., Zhang, P., Min, L., Tang, J., Sun, H., 2020. Synthesis of cellulose carbon aerogel via combined technology of wet ball-milling and TEMPO-mediated oxidation and its supersorption performance to ionic dyes. *Bioresource Technology*. 315: 123815.

Zhang, S., Feng, J., Feng, J., Jiang, Y., Ding, F., 2018. Carbon aerogels by pyrolysis of TEMPO-oxidized cellulose. *Applied Surface Science*. 440: 873-879.

Meng, Y., Young, T. M., Liu, P., Contescu, C. I., Huang, B., Wang, S., 2015. Ultralight carbon aerogel from nanocellulose as a highly selective oil absorption material. *Cellulose*. 22(1): 435-447.

PCR17052022 – 262: Al-impregnated biochar derived from Korean pine residue and Alum sludge for phosphorus removal

Tuan Van Truong, Jongbeom Kim, Youngjin Kim and Dong-Jin Kim*

Department of Environmental Sciences and Biotechnology & Institute of Energy and Environment, Hallym University, 1 Okcheon, Chuncheon, Korea, 24251

* Corresponding author: Dong-Jin Kim (dongjin@hallym.ac.kr)

Keywords: Metals-impregnated biochar; Korean pine residue; Alum sludge; Phosphate adsorption, Phosphate desorption.

Extended Abstract

Al extract recovered from Al sludge in water treatment plant was utilized as an alternative Al source to impregnate biomass for biochar product. Korean pine residue biochar impregnated with the Al extract was used as a phosphate adsorbent and its adsorption performance was compared with reagent Al-impregnated Korean pine residue biochars. Phosphate adsorption kinetics and capacity of Al extract-impregnated biochar was close to that of the best reagent Al-impregnated biochar. The optimal pH for phosphate adsorption by Al extract-impregnated Korean pine residue biochar was around 6. The co-existence of HCO_3^- had a great influence on phosphate adsorption by Al extract-impregnated Korean pine residue biochar. The optimal dose of Al extract impregnated Korean pine residue biochar for

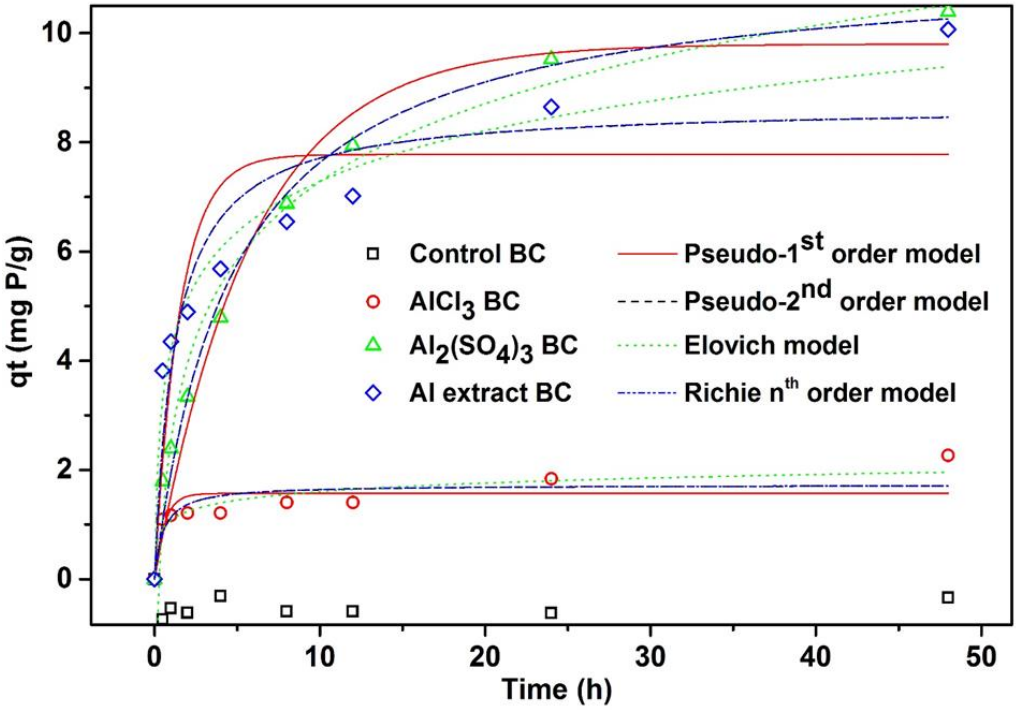

phosphate removal was 5 g/L. P adsorbed Al extract-impregnated Korean pine residue biochar showed a high phosphate desorption (nearly 65%) and low Al release (about 15%) under citric acid condition.

Figure 1: Phosphate adsorption kinetics of Korean pine residue biochars

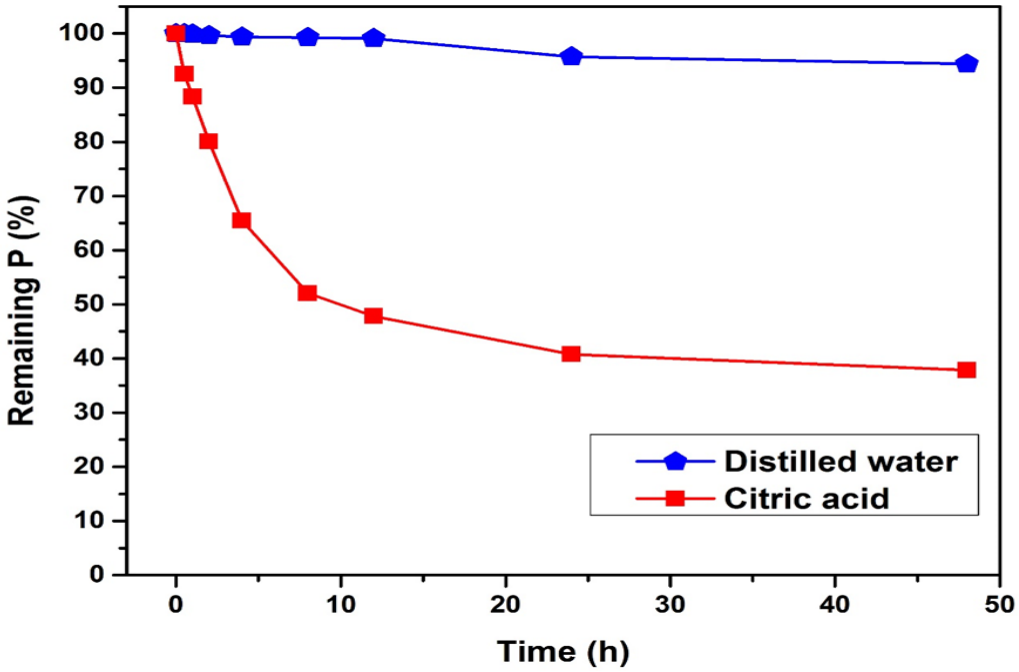

Figure 2: Phosphate desorption of Al extract-impregnated Korean pine residue biochar in distilled water and citric acid

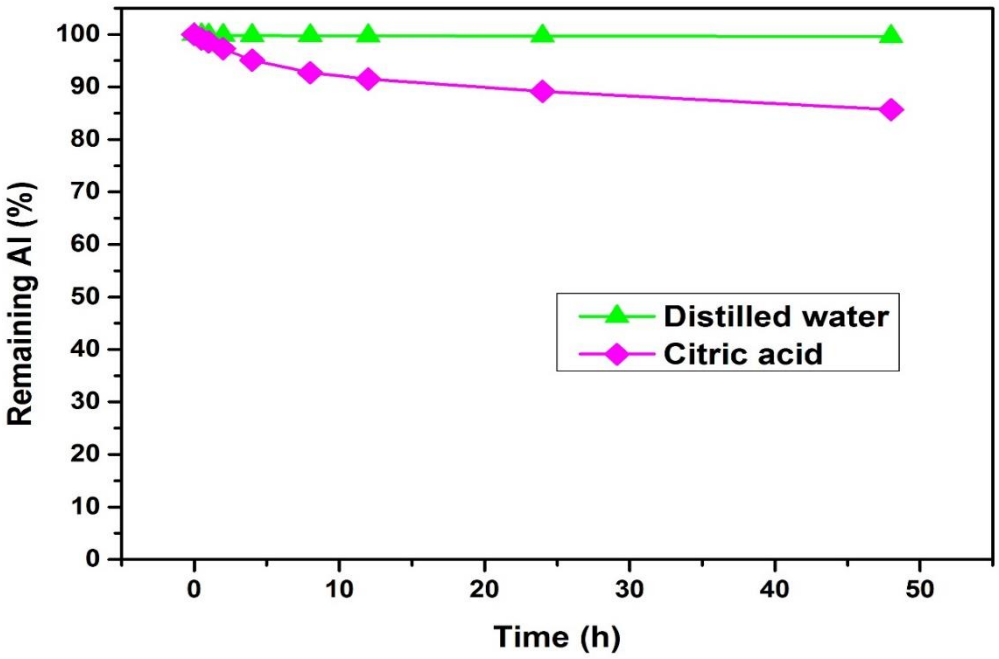

Figure 3: Al release of Al extract-impregnated Korean pine residue biochar in distilled water and citric acid

References

Truong, T. Van, Tiwari, D., Mok, Y.S., Kim, D.J., 2021. Recovery of aluminum from water treatment sludge for phosphorus removal by combined calcination and extraction. *Journal of Industrial and Engineering Chemistry*. 103, 195–204.

6th International Conference and Postgraduate Colloquium for Environmental Research 2022 (POCER 2022) 9 - 11 June 2022
Langkawi, Kedah, Malaysia

PCR17052022 – 263: Evalution of Waste Oxy-fuel Combustion with Indirect Supercritical Carbon Dioxide Cycle

Seung Seok Oh[a1], Hyun Jun Park[a1], Chul Seung Jung[b], Han Saem Park[b], Jester Jie Lih Ling[b], Sang Mun Jeong[c], Young-Kwon Park[d], and See Hoon Lee[a, b*]

[a] Department of Environment and Energy, Jeonbuk National University, Jeonju, Republic of Korea

[b] Department of Mineral Resources and Energy Engineering, Jeonbuk National University, Jeonju, Republic of Korea

[c] Department of Chemical Engineering, Chungbuk National University, Chungbuk, Republic of Korea

[d] Department of Environmental Engineering, University of Seoul, Seoul, Republic of Korea

- Corrensponsing Author E-mail: donald@jbnu.ac.kr

[1]these authors equally contributed to this study.

Keywords: Waste; sCO_2 cycle; Oxy-fuel Combustion; Gas Recirculation; Carbon Nuetral;

Extended Abstract

Recetly carbon neutrality is considered as one of energy policy basis in ther world since anthropogenic activities such as production, transportation, agriculture, and deforestation have inevitably generated huge greenhouse gases which contribute to climate change(Wet et al. 2020). As a result, various novel processes and technologies are being designed and tested in energy fields in order to minimize the emission of greenhouse gases and the change of global climate. Though oxy-fuel combustion regarded as promising and economical carbon capture technologies have been developed and commercially tested, high energy penalties from air separation unit (ASU) and carbon dioxide processing unit (CPU) still remain as biggest hurdle which must be solved. Therefore, supercritical carbon dioxide cycle (sCO_2 cycle) may become a practical solution because sCO_2 cycle can increase power generation efficiency due to higher density, the reduction of work necessary for compression, and low expansion ratio. In this study, waste oxy-fuel combustion composed of ASU, circulating fluidized bed boiler, gas recirculatin

unit, sCO_2 cycle, CPU and related auxillary equipments was designed and simulated with ASPEN PLUS shown in Figure 1(Ling et al. 2021).

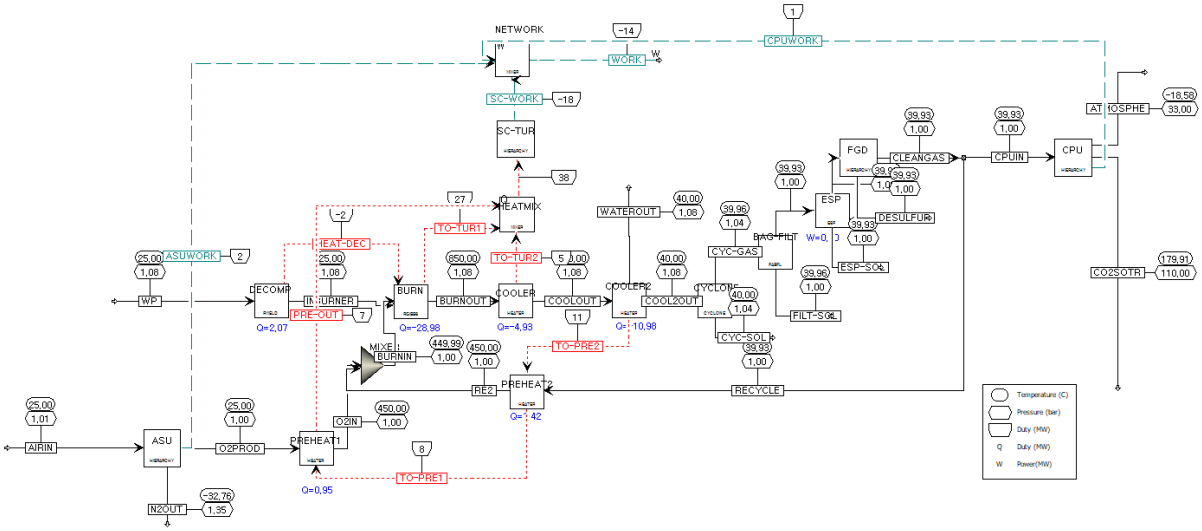

Figure 1: Waste Oxy-fuel Combustion with indirect sCO_2 cycle

For the evaluation of this novel process, wastes generated in Korea as a raw material is used to invesitgate the effect of operation values such as excess oxygen ratio, flue gas recirculation ratio, wet or dry recirculation, and oxygen concentration on overall conversion efficiency, CO_2 concentration and gas concentrations. The 200ton/day oxy-fuel combustor was assumed to be a RGibbs reactor and was operated at 850°C. The operating conditions of the sCO_2 cycle were applied at 760°C and 300bar. In addition, the recirculation ratios were between 0.60 and 0.80, and the oxygen concentration discharged from the ASU was set to 95 vol%. Since this novel process eliminates the neccessity of flue gas separation for CO_2 capture, environmental facilities can be reduced, less compression work is consumed through recompression in the sCO_2 cycle, and NOx and SOx can be simultaneously removed at high temperatures. Although the components of biomass are highly volatile, it was found that net efficiency was close to 35%. In addition, higher efficiency resulted from sCO_2 cycle can compensate high power consumption generated from the ASU and CPU.

Acknowledgements: This work was supported by a grant from the National Research Foundation of Korea, which was funded by the Ministry of Education, Science and Technology (NRF-2020R1I1A3A04037715).

References

Ling, J.L.J., Kim, HW., Go, ES., Oh, SS., Park, H.J., Jeong, C.S., Lee, S.H., 2022. Analysis of operational characterisitcs of biomass oxygen fuel circulating fluidized bed combustor with indirect supercritical carbon dioxide cycle. *Energy Conv Manag.* 259:115569.

Wei, X., Manovic, V., Hanak, DP., 2020. Techno-economic assessment of coal-or biomass-fired oxy-combustion power plants with supercritical carbon dioxide cycle. *Energy Conv Manag.* 221:113143.

PCR18052022 – 264: Evaluation of gut microbiome community in Jeju-Black Swine under the effect of *Rhodobacter sphaeroides using* longitudinal dynamics

Thi-My-Le Nguyen[1], Seung-Moon Park[2*]

[1,2] Department of BioEnvironmental Chemistry, College of Agricultural and Life Sciences, Jeonbuk National University, Jeonju 54896, Korea

Tel: (+82) 063-270-2542 Fax: (+82) 063-270-2550

ABSTRACT

Longitudinal studies are considered a pressing need that investigates the stability of the swine gut microbiota in Jeju-Black Swine. In this study, we examined the bacterial composition of the healthy swine fed with the feed additive containing *Rhodobacter sphaeroides,* and a normal diet was applied as a control. The *R. sphaeroides* was continuously supplemented every day for 2 weeks and were alternated by the additional dairy diet without feed additive every day for 2 next weeks. The fecal samples were harvested after every 2 weeks to assess variation of microbiome diversity. High throughput sequencing of 16S rRNA genes was proceeded to address the significant changes in the microbiota community before and after treatment. The obtained results revealed that *Firmicutes*, *Bacteroidetes*, *Spirochaetes*, and *Proteobacteria* were observed as the four most predominant phyla at initial, 2 weeks, and 4 weeks time points of collected fecal samples. The α-diversity comparison showed there was no significant difference in the total number of species in each group at initial, 2 weeks, and 4 weeks. However, the β-diversity analysis statistically identified the strong varieties. Genus *Coenonia* was unique present at an initial time while family *Sphingobacteriaceae* was only identified as a biomarker at 2 weeks of *R. sphaeroides*-fed group. Interestingly, the family *Sphingobacteriaceae* has been reported in improving egg production, egg quality, and eliminate fecal ammonia of laying hens as a probiotic role. *R. sphaeroides*-supplemented swine enhanced the lipid metabolism and biosynthesis of siderophore group nonribosomal peptides after 2 weeks of treatment and improved 21 significant metabolisms after 4 weeks. Furthermore, thirty-five crucial connectors and one module hub were achieved at 2 weeks after feeding with *R. sphaeroides*. This knowledge on Jeju-Black Swine study has been not discovered yet. Therefore, a longitudinal study is a necessary approach to address the gap information on microbiome challenges under the effects of the feed additive containing *R. sphaeroides*.

References

1. Wagner Mackenzie et al., “Longitudinal study of the bacterial and fungal microbiota in the human sinuses reveals seasonal and annual changes in diversity,” Sci. Rep., vol. 9, no. 1, pp. 1–10, 2019.

2. J. Y. Jacela et al., “Feed additives for swine: Fact sheets prebiotics and probiotics, and phytogenics,” J. Swine Heal. Prod., vol. 18, no. 3, pp. 132–134, 2010.

3. Z. Liu, A. Ma, E. Mathé, M. Merling, Q. Ma, and B. Liu, “Network analyses in microbiome based on high-throughput multi-omics data,” Brief. Bioinform., vol. 22, no. 2, pp. 1639–1655, 2021.

6th International Conference and
Postgraduate Colloquium for
Environmental Research 2022 (POCER
2022) 9 - 11 June 2022
Langkawi, Kedah, Malaysia

PCR20052022 – 265: Binding Sites Interaction between MOF and Ionic Liquids from Molecular Docking Simulation

Nor Ain Fathihah Abdullah[a], Khairulazhar Jumbri[a*]

[a] Department of Fundamental and Applied Science
University of Petronas, Perak, Malaysia

- Corrensponsing Author E-mail: khairulazhar.jumbri@utp.edu.my

Keywords: Binding energies, molecular docking, metal organic framework, ionic liquid, adsorbent

Extended Abstract

Utilizing high surface area adsorbents such as MOFs is an appealing choice for the evacuation of heavy metals from wastewater. However, the stability and selectivity of MOFs for wastewater treatment are still a questionable challenge as the structure MOF may collapse upon exposure to the water [Li *et al.*, 2019, Rivera *et al.*, 2016, Wang *et al.*, 2015]. Recent research has shown that the hybridization of MOF with another component might give new materials that have similar characteristics with both the host MOF and material added. This combination could enhance the host MOF properties and may lead to a new type of designer hybrid material in various applications. These hybrid MOF has shown promising results in various application [Aijaz *et al.*, 2014, Huang *et al.*, 2017]. The consolidation of IL interior MOF has been demonstrated could enhance the performance of pristine MOF in terms of stability and reusability depending on its application [Kavak *et al.*, 2019], however, the studies of the interaction between MOF framework and IL at molecular level still scarce. The fundamental interactions between the MOFs and ILs moiety (cation and anion molecules), especially the types of interaction play an important role in determining the stability, compatibility, and selectivity of this hybrid material. In this research, molecular docking calculation was carried out to identify the binding energy (ΔG_{bind}) and binding affinity between UIO66 with TFSI-imidazole (EMIM, PMIM, BMIM) and TFSI-pyridinium ILs (BPYDM, EMPYDM, PMPYDM, BMPYDM). The binding energies were calculated using AutoDock software to find specific binding sites of IL toward MOF. The initial 3D structures were prepared using the default parameter in Autodock software. The IL was docked consecutively into the MOF cavity inside the gridbox (x, y, z) dimension to identify binding sites of MOF. From the results, both TFSI-imidazole and TFSI-pyridinium IL exhibited good interaction with MOF with binding

energy of -4.12 to -8.60 kcal mol^{-1} (Table 2). In the case of TFSI-imidazole, the addition of alkyl chain decrease the binding energy, meanwhile inconsistent ΔG_{bind} value was observed in TFSI-pyridinium system when alkyl chain was added to pyridinium cation. In terms of binding affinity, the PMPYDM/TFSI has shown superior performance toward UIO66 with ΔG_{bind} of -8.60 kcal mol^{-1}. From docking structures, both anion and cation preferred to bind at the corner of the MOF pore which is in accordance with the previous study. *Abbreviations—1-ethyl-3-methylimidazolium [EMIM], 1- propyl-3-methylimidazolium [PMIM], 1-butyl-3-methylimidazolium [BMIM], 1-butylpyridinium [Bpydm], 1-ethyl-4-methylpyridinium [EMPYDM], 1-propyl-4-methylpyridinium [PMPYDM], 1-butyl-4-methylpyridinium [BMPYDM], bis((trifluoro)sulfonyl)imide [TFSI],*

Table 18: Binding energies of TFSI-imidazole and TFSI-pyridinium for UIO66

MOF	ILs	Binding Energies (kcal mol^{-1})
UIO66	EMIM/TFSI	-4.25
	PMIM/TFSI	-4.18
	BMIM/TFSI	-4.18
	BPYDM/TFSI	-4.23
	EMPYDM/TFSI	-4.12
	PMPYDM/TFSI	-8.60
	BMPYDM/TFSI	-4.19

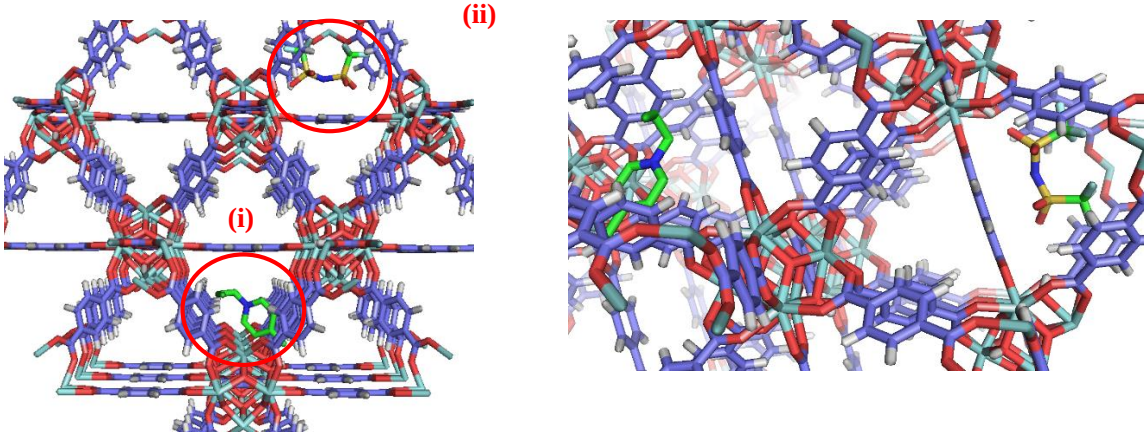

Figure 54: The molecular docking structure of PMPYDM/TFSI-UIO66 (i) PMPYDM cation, (ii) TFSI anion

Acknowledgements: The authors thank the Ministry of Education for the Fundamental Research Grant Scheme to carry out this project.

References

Aijaz, A., Xu, Q., 2015. Catalysis with metal nanoparticles immobilized within the pores of metal–organic frameworks. *The Journal of Physical Chemistry Letters*. 5 (8): 1400-1411.

Wang, C., Liu, X., Chen, J. P., Li, K., 2016. Superior removal of arsenic from water with zirconium metal-organic framework UiO-66. *Scientific reports*. 5: 16613-16613.

Rivera, J. M., Rincón, S., Youssef, C. B., Zepeda, A., 2016. Highly efficient adsorption of aqueous Pb(II) with mesoporous metal-organic framework-5: An equilibrium and kinetic study. *Journal of Nanomaterials*. 2016: 1-9

Kavak, S., Polat, H. M., Kulak, H., Keskin, S., Uzun, A., 2019. MIL-53(Al) as a versatile platform for ionic-liquid/MOF composites to enhance CO2 selectivity over CH4 and N2. *Chemistry - An Asian Journal*. 14 (20): 3655-3667.

Huang, W., Li, S., Cao, X., Hou, C., Zhang, Z., Feng, J., 2017. Metal–organic framework derived iron sulfide–carbon core–shell nanorods as a conversion-type battery material. *ACS Sustainable Chemistry & Engineering*. 5 (6): 5039-5048.

Li, X., Wang, B., Cao, Y., Zhao, S., Wang, H., Feng, X., Zhou, J., Ma, X., 2019. Water Contaminant Elimination Based on Metal–Organic Frameworks and Perspective on Their Industrial Applications. *ACS Sustainable Chemistry & Engineering*. 7 (5): 4548-4563.

6th International Conference and
Postgraduate Colloquium for
Environmental Research 2022 (POCER
2022) 9 - 11 June 2022
Langkawi, Kedah, Malaysia

PCR22052022 – 266: Bioremediation Potential of *Chlorella Vulgaris* in the treatment of Restaurant Wastewater: An approach contributing towards Green Circular Bioeconomy

Imran Ahmad[a], Norhayati Abdullah[a*], Iwamoto Koji[a], AliYuzir[a], Shaza Eva Mohamad[a], Paul Loke Show[b*]

[a] Malaysia-Japan International Institute of Technology, Universiti Teknologi Malaysia, Jalan Sultan Yahya Petra, 54100, Kuala Lumpur, Malaysia.

[b]Department of Chemical and Environmental Engineering, Faculty of Science and Engineering, University of Nottingham Malaysia Campus, Jalan Broga, Semenyih 43500, Selangor Darul Ehsan, Malaysia.

- Corrensponsing Author E-mail: norhayati@utm.my; PauLoke.Show@nottingham.edu.my

Keywords: Restaurant Wastewater;*chlorella vulgaris*; biomass production; pollutants; bioremediation

Extended Abstract

Abstract

The overwhelming situation of complex energy demand, environmental pollution and risk to sustainability have led to the advent of microalgae. Microalgae may be grown in varying environments (i.e., pH, nutrients, temperature), non-arable land with less water footprint. Moreover, by capturing light through photosynthesis, microalgae produce larger quantities of oxygen, rich biomass and helps to mitigate CO_2. Standing out in the list of most investigated microalgal species, there are the green microalga designated as *Chlorella vulgaris*. *Chlorella vulgaris (size=2-10 µm)* is a spherical, single-celled, green, eukaryotic, and freshwater microalgae containing chloroplasts, cell wall and mitochondria and is known for its potential in biomass production, biofuel production and wastewater treatment. The strain of *chlorella vulgaris* is obtained from National institute of Environmental studies, Japan (NIES-1269). *Chlorella vulgaris* NIES-1269, that is extensively being used as microalgae-based wastewater treatment processes. This study aims to couple cultivation freshwater species of microalgae with the RWW at bench scale There is no study reported till date using freshwater species of microalgae to evaluate their potential in the removal of pollutants, nutrients, and FOG in RWW and this study provides the opportunity for experimental application at UTM Residensi. While *chlorella vulgaris* was cultivated using AF6 under the optimized conditions of aeration (Air=2-3 L/min/CO2=2%) and illumination of 24:0 (light: dark) with a 80-110 µmol photons m^{-2} s^{-1} irradiance (artificial fluorescence

light) the growth of *chlorella vulgaris* is high. The paper will provide the details of growth, biomass concentration, productivity, pollutant removal and nutrient uptake potential of *chlorella vulgaris*. The study involves 2 conditions *chlorella vulgaris* grown with raw RWW and grown with RWW+AF6, with the control being the *Chlorella vulgaris* grown with AF6. The results shown below signifies that *chlorella vulgaris* has immense potential in the treatment of RWW.

Pollutants Removal						Nutrients uptake			
COD	BOD	FOG	TSS	TDS	Co	AN	K	TP	TN
94±4%	96±3%	92±5%	97±2%	80±5%	75±5%	95±4%	86±4%	98±2%	88±6%

1.Introduction

The physical and chemical treatment technologies usually employed for the treatment of RWW are difficult to install at the site, uneconomic, inefficient and are not environmentally friendly (Chen et al., 2002, Dubeski et al., 2001) (Sastrawidana and Sukarta, 2018) Therefore, this study shall provide an alternate/potential solution for overcoming the issues associated with FOG generated alongside the RWW from the eateries situated at UTM Residensi. Hence, the usage microalgae may be a possible milestone in the treatment of RWW as it has been already used efficiently for the treatment of textile mill wastewater, petroleum wastewater, palm oil mill effluent (Hodaifa et al., 2017, Takáčová et al., 2015). Nutrient supply is a constraint on microalgae production and sustainability at the same time microalgae cultivation can be water-intensive. These limitations will be overcome by the current study.

2.Materials and Methods

The wastewater sample (Restaurant wastewater) is collected periodically from the UTM Residensi complex periodically. The source of the collection is the central Gravity Grease Interceptor.*Chlorella vulgaris* is grown using AF6 medium in different conditions subjected for the treatment of RWW.The cultivation is carried out in 500ml vessel flasks. The optical density (OD) at 750 nm and dry cell weight concentration were used to assess microalgal growth. A UV–Vis spectrophotometer (UV-1900, Shimadzu, Japan) was used to measure the OD750nm of a 1 mL microalgae culture every alternate day. Biological Oxygen Demand (BOD), chemical oxygen demand (COD), potassium, ammoniacal nitrogen (NH3–N), total nitrogen (TN), and total phosphorus (TP) concentrations were all evaluated in wastewater. The Standard Method for the Examination of Water and Wastewater (APHA, 2012) was used for all analyses.

3.Results and Discussion

The biomass productivity in terms of dry cell weight shows that the maximum biomass is obtained when *chlorella vulgaris* is grown with AF6+RWW that is about 580 mg/l as compared to 540 mg/l when it is grown with RWW. The values of removal are shown in the table above. The growth of *chlorella vulgaris* (control) is shown with the pre and post treatment samples of RWW(Figure 1).

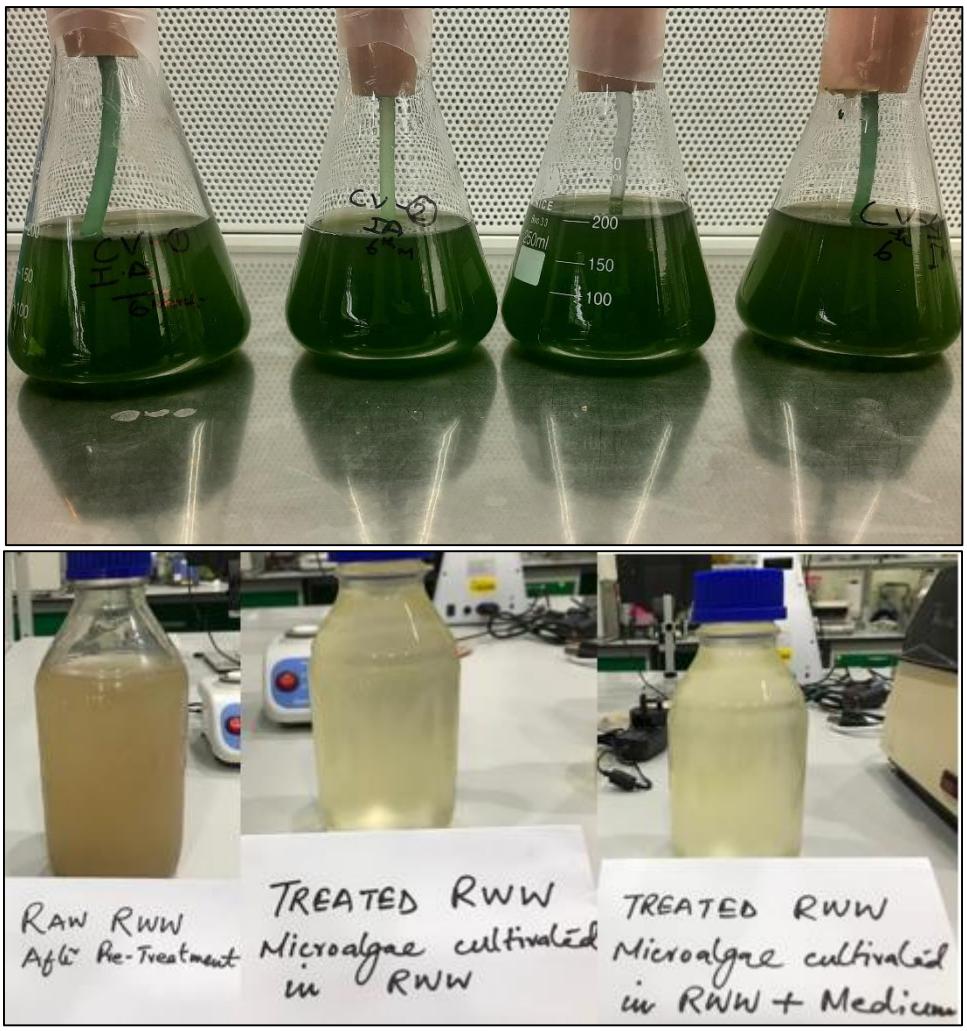

Figure 1: Growth conditions of *chlorella vulgaris* and RWW (Pre and Post Treatment)

Conclusion

The consequences related to the management and discharge of RWW containing FOG are severe and require utmost attention, sustainable management, and efficient treatment. The bioremediation of restaurant wastewater using microalgae will provide a novel study in the evaluation of the potential of

chlorella vulgaris in the treatment of pollutants and uptake of nutrients. The study will contribute significantly to circular bioeconomy as it will reduce the cost of nutrients and requirement of water for the bioremediation. The study will also contribute to 3 SDGs:clean water and sanitation, sustainable cities and communities and climate action.

Acknowledgements: The authors thank the Algae and Biomass Research Laboratory for providing the setup for the experiments

References

Chen, X., Chen, G. & Yue, P. L., 2002. Novel electrode system for electroflotation of wastewater. Environmental science & technology, 36**,** 778-783.

Dubeski, C. V., Branion, R. M. & Lo, K. V., 2001. Biological treatment of pulp mill wastewater using sequencing batch reactors. Journal of Environmental Science and Health, Part A, 36**,** 1245-1255.

Hodaifa, G., Romero, A. M., Halioui, M. & Sánchez, S. Combined Process for Olive Oil Mill Wastewater Treatment Based in Flocculation, Photolysis, Microfiltration and Microalgae Culture. Euro-Mediterranean Conference for Environmental Integration, 2017. Springer, 1127-1129.

Sastrawidana, I. D. K. & Sukarta, I. N., 2018. Indirect Electrochemical Oxidation with Multi Carbon Electrodes for Restaurant Wastewater Treatment. Journal of Ecological Engineering, 19.

Takáčová, A., Smolinská, M., Semerád, M. & Matúš, P., 2015. DEGRADATION OF BTEX BY MICROALGAE Parachlorella kessleri. Petroleum & Coal, 57.

6th International Conference and Postgraduate Colloquium for Environmental Research 2022 (POCER 2022) 9 - 11 June 2022
Langkawi, Kedah, Malaysia

PCR26052022 – 267: Hydrogen-Rich Gas Production from Steam Reforming of Ethanol over Ni-Based Catalysts: Effect of Re Addition

Peat Khemnarong[a], Suwimol Wongsakulphasatch[b], Worapon Kiatkittipong[a*], Pattaraporn Kim-Lohsoontorn[c,d], Navadol Laosiripojana[e], Jun Wei Lim[f], Izumi Kumakiri[g], and Suttichai Assabumrungrat[c,d]

[a] Department of Chemical Engineering, Faculty of Engineering and Industrial Technology, Silpakorn University, Nakhon Pathom 73000, Thailand

[b] Department of Chemical Engineering, Faculty of Engineering, King Mongkut's University of Technology North Bangkok, Bangkok 10800, Thailand

[c] Center of Excellence in Catalysis and Catalytic Reaction Engineering, Department of Chemical Engineering, Faculty of Engineering, Chulalongkorn University, Bangkok 10330, Thailand

[d] Bio-Circular-Green-economy Technology & Engineering Center, BCGeTEC, Department of Chemical Engineering, Faculty of Engineering, Chulalongkorn University, Bangkok 10330, Thailand

[e] The Joint Graduate School of Energy and Environment, King Mongkut's University of Technology Thonburi, Bangkok 10140, Thailand

[f] Department of Fundamental and Applied Sciences, HICoE-Centre for Biofuel and Biochemical Research, Institute of Self-Sustainable Building, Universiti Teknologi PETRONAS, Seri Iskandar 32610, Perak Darul Ridzuan, Malaysia

[g] Graduate School of Sciences and Technology for Innovation, Faculty of Engineering, Yamaguchi University, 2-16-1 Tokiwadai Ube, Yamaguchi 755-8611, Japan

- Corrensponsing Author E-mail: kiatkittipong_w@su.ac.th

Abstract

Supported Ni catalysts widely used in ethanol steam reforming (ESR); however, it was seriously suffered by rapid deactivation due to coke deposition and high methane formation. In this study, the effects of Re addition on the catalyst activity and stability for hydrogen production from ESR is

evaluated. Small amount of rhenium (Re) promoted on Ni/Al_2O_3 catalysts is prepared by wetness impregnation method and characterized by various techniques such as N_2 physisorption (BET method), and XRD. The characterization results show both Re and Ni particle are highly dispersed on the catalysts surface without any sign of aggregation. The experimental results indicate that $3\%Re\text{-}Ni/Al_2O_3$ catalyst provides considerably high reforming activity and excellent resistance towards carbon deposition in comparison with Ni/Al_2O_3. Promoting a small proportion of Re (3 wt.%) on Ni/Al_2O_3 causes a significant influence by greatly reduced CO formation from ca. 20% to less than 10% throughout the reaction time. High stability of the catalyst is observed as the reaction can perform over 60 h time-on-stream without any deactivation.

Keywords: Ethanol Steam reforming; Hydrogen; Re-Ni catalyst; Anti-coke formation

1. Introduction

Nowadays, much effort has been devoted for developing clean and highly active energy, which is motivated largely by a demand for solving energy crisis and environmental problems (Ahmad and Zhang, 2020). Hydrogen energy is of interest because hydrogen is the most common element in nature. Hydrogen has high calorific value (1.4×10^5 kJ/kg) compare with other fossil fuels, chemical fuels and biological fuels (Dömök & Baán et al., 2008). Hydrogen is an ideal energy carrier for the sustainable energy development as when it burns cleanly without emitting any environmental pollutants (Mazloomi and Gomes, 2012). At present, the production of hydrogen from liquid organic compounds has been proven to be an effective and successful synthetic strategy (Abdalla & Hossain et al. 2018). Among the candidates for hydrogen production, ethanol offers some advantages such as being easily produced by fermentation of biomass, low toxicity, and ease for transportation (Contreras & Salmones et al., 2014). It is also known that the application of ethanol for the production and the use of H_2 as an energy is CO_2 neutral and does not result in any net emission of NO_x, SO_x, and others toxic compound (Fatsikostas, Kondarides et al. 2002). Therefore, ethanol steam reforming (ESR) is of interest for hydrogen production.

$$CH_3CH_2OH_{(g)} + 3H_2O(g) \rightarrow 6H_2 + 2CO_2 \qquad \Delta H^o_{298\ K} = 174.2\ kJ/mol \qquad (1)$$

Ethanol conversion by steam reforming consists of several reaction steps that require catalytic formulations: (i) ethanol dehydrogenation, (ii) C-C bonds breaking of surface intermediates to produce CO and CH_4 and (iii) water reforming from C1 products to hydrogen. The type of active phase and support has a significant impact on the reaction pathway and the product distribution. The yield of H_2

and the stability of the catalyst also depend on the control of these products. Therefore, the well-designed of the catalyst is a crucial for the future development of hydrogen production technology.

Among the numerous active phases, noble metal group (Rh, Pd, Pt, and Ru) exhibits an outstanding result by showing high activity and selectivity of hydrogen in the ESR (Palma, Castaldo et al. 2014). Nevertheless, the high cost of noble metal catalysts made it far from commercial use. Therefore, the most researched catalysts for hydrogen production via the ESR route which are much cheaper and widely available are Ni- and Co-based materials (de la Peña O'Shea, Nafria et al. 2008). The Ni-based catalyst was very well known for its high activity for C-C bond cleavage and high performance in H_2 production (Mathure, Ganguly et al. 2007). Comas et al. (2004) studied the ESR on Ni/γ-Al_2O_3 catalyst at temperatures between 573 and 773 K. The result showed that selectivity of 91% was found, however, large amount of carbon monoxide was also produced from the reaction. Nickel also seriously suffered from rapid deactivation due to coke formation and also the sintering of Ni particles (Sehested 2006). There was evidenced that the addition of Re could enhance the catalytic activity, selectivity, and long-term stability in various reactions by raising the metal dispersion, which results in preventing agglomeration of particles and also facilitate water dissociation leading to improving the water gas shift activity (Pongsiriyakul, Kiatkittipong et al. 2021). In the present work, Re was promoted to the Ni/Al_2O_3 catalyst to perform the hydrogen production from ESR to investigate the effects of Re addition on the catalyst properties along with the evaluation of catalytic performance, activity, and stability.

2. Experimental

2.1. Catalyst preparation

The Re-Ni/Al_2O_3 catalysts used in this experiment were prepared through wetness impregnation method. Prior the preparation, commercially γ-alumina support was preheated in water bath at 80 ^oC then impregnated with the aqueous solution containing a theoretical amounts of nickel (II) nitrate hexahydrate ($Ni(NO_3)_2$,$6H_2O$) and ammonium perrhenate (NH_4ReO_4). After evaporate the remaining water, the catalysts were dried overnight at 105 ^oC and then calcined at 600 ^oC in the presence of air to achieve 1, 3 and 5% Re-Ni/Al_2O_3 catalysts.

2.2. Catalyst characterization

The catalysts were characterized by various techniques such as N_2 physisorption (BET method), XRD, SEM-EDX, and H_2-TPR.

2.3. Catalyst evaluation

Steam reforming experiments were performed at ambient pressure in a fixed-bed quartz reactor (6 mm i.d., 500 mm length) placed in a temperature-controlled oven. Prior to the reaction, 100 mg of each catalyst was reduced with a mixed stream of 20% H_2 in N_2 (70 ml/min) at 500 ^oC for 150 min. After purging the reactor with N_2 flow (55 ml/min) for 60 min, the temperature was then ramp to the reaction

temperature. A liquid mixture of ethanol/water (1.5 ml/h, 1:3 molar ratio) was introduced into the system by a syringe pump (NE-300 Just Infusion™). Inlet line was heated at 140 °C to vaporize the liquid mixture with N_2 flow as carrier gas (55 ml/min). The condensable products were trapped with ice-salt cold trap, the dry gasses (non-condensable gas products) were then analyzed using an on-line gas chromatography (SRI-8610 C, USA) equipped with two columns (Molecular Sieve 5A and Silica Gel) and a thermal conductivity detector (TCD).

3. Results and discussion

3.1. Physicochemical Characterization

Table 1 demonstrates physical properties of support and Re-Ni/Al_2O_3 catalysts. All catalysts exhibites type-IV isotherms of a mesoporous structure. A significant drop of surface area (S_{BET}) from 164.25 m^2/g to 125.91 m^2/g is observed upon loading Ni to the alumina support. The surface area is further slightly decreased after Re was introduced to the catalysts. This result might cause from partial blocking of the mesoporous structure by the added up metal species.

Table 1: BET surface area, average particle size, mean pore diameter and crystalline size of the catalysts.

Catalysts	BET Surface area (m^2/g)	Average pore diameter (nm)	Crystalline size (nm)	Reducibility (%)
Al_2O_3	164.25	5.98	-	-
10Ni/Al_2O_3	125.91	6.32	8.26	71.87
1Re-10Ni/Al_2O_3	128.14	6.06	6.09	92.77
3Re-10Ni/Al_2O_3	119.70	6.55	6.29	95.87
5Re-10Ni/Al_2O_3	115.38	6.38	6.50	95.43

The XRD patterns of the samples are reported in Figure 1. The XRD spectra shows the diffraction peaks at 2θ = 37.4°, 46.07°, and 66.9°, corresponding to (311), (400), and (440) crystal planes of γ-Al_2O_3 with low crystallinity (JCPDS 29-0063), respectively (Andraos, Abbas-Ghaleb et al. 2019). The diffraction peaks located at 37.4° and 43.5° originated from NiO (111) and NiO (200) crystal planes (JCPDS 44-1159) (Profeti, Dias et al. 2009). However, by introducing Re to the system, the positions of the characteristic diffraction peaks are remained unchanged and rhenium oxide does not observe in

any rhenium doped samples. This result might be a high dispersion of rhenium species over the surface of alumina or rhenium phase id amorphous. Similar results have been reported in the Re-based catalysts over Al_2O_3 support, where no rhenium oxides was observed (Baranowska, Okal et al. 2014). Scherrer equation was further applied to estimate the crystalline size as shown in Table 1. The results reveal that bare Ni on alumina shows the crystalline size of 8.26 nm and by doping Re the crystalline size slightly decreases to 6.09 nm then slightly increases along with the Re amount loaded into the catalysts for up to 6.50 nm at 5% Re.

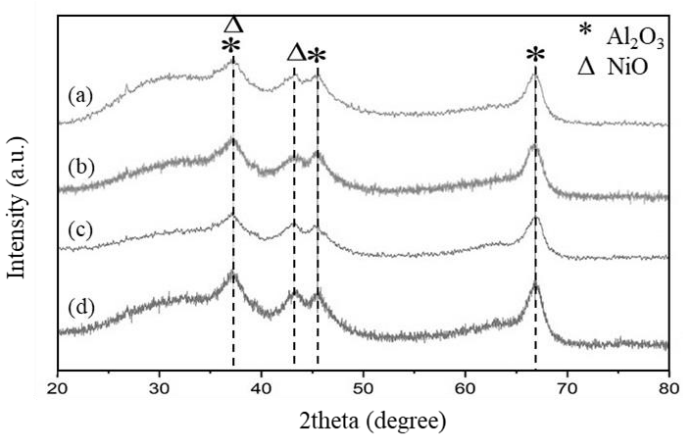

Figure 1: XRD diffraction patterns of (a) 5% Re-Ni/Al_2O_3, (b) 3% Re-Ni/Al_2O_3, (c) 1% Re-Ni/Al_2O_3, and (d) 10% Ni/Al_2O_3

3.2. Catalytic activity and stability

The catalytic activity of different amounts of Re loading (0, 1, 3, and 5 wt.% Re) on Ni/Al_2O_3 catalyst was evaluated at ambient pressure with the temperature of 650 °C. The complete conversion is found for all catalyst loading. Figure 2 shows product distribution of 10%Ni/Al_2O_3 in ESR at 650 °C. H_2, CO, CO_2, and CH_4 are the major product during the entire reaction process. The H_2 concentration is maintained at ca. 63% with a high amount of CH_4 and CO. It is suggested that carbon-containing compounds are formed by additional reactions during the steam reforming of ethanol, which could be attributed to CH_4 reforming ($CH_4 + 2H_2O \rightarrow CO_2 + 4H_2$) (Zanchet, Santos et al. 2015). Interestingly results is found upon performing ESR with the Re-containing catalysts. Figure 3 illustrates the product distribution of 3%Re-Ni/Al_2O_3 in ESR at 650 °C. Although the major products formed are similar to the bare Ni catalyst, the CO concentration was considerably suppressed to less than 9%. This could be attributed to the higher reactivity of the water-gas shift reaction ($CO + H_2O \rightarrow H_2 + CO_2$) enhanced by the facilitative water dissociation of Re species (Kunkes, Simonetti et al. 2008). Moreover, a more

consistent flow of H_2 with a concentration of up to 75% is detected for over 60 h on steam without any sight of deactivation, indicating long-term stability of the catalyst.

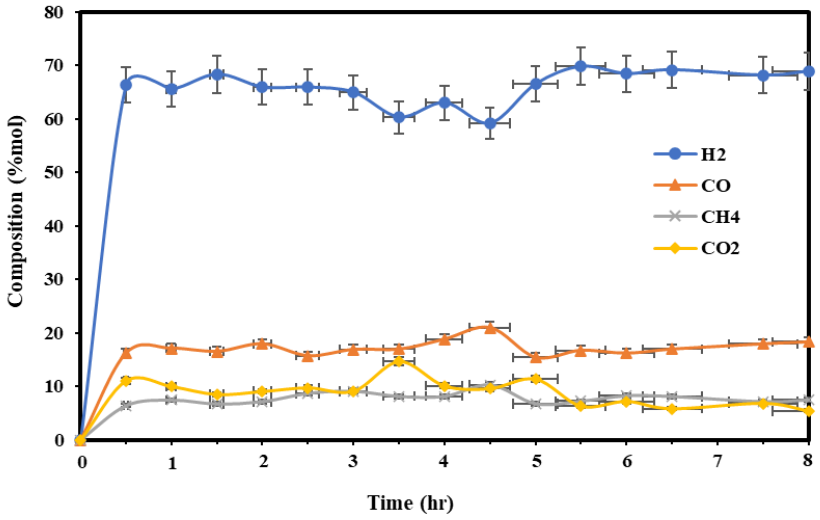

Figure 2: Product distribution of 10%Ni/Al_2O_3 in ethanol steam reforming reaction at 650 ºC

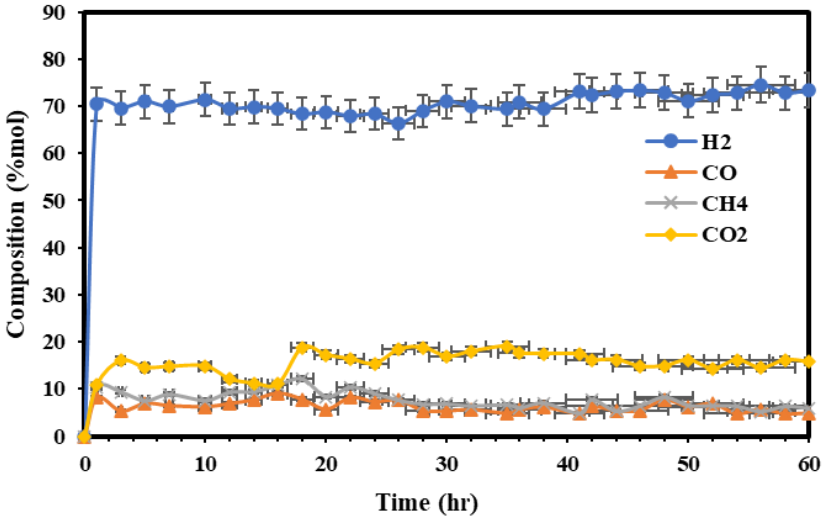

Figure 3: Product distribution of 3%Re-Ni/Al_2O_3 in ethanol steam reforming reaction at 650 ºC for 60 hr.

4. Conclusions

In this study, the bimetallic Re-Ni/Al_2O_3 catalysts were prepared by the wetness impregnation method to investigate the influence of Re addition on the catalytic performances of Ni/Al_2O_3 for ethanol

steam reforming reaction. The catalysts were characterized by numerous techniques including BET and XRD. The characterization results could confirm that Re-Ni/Al_2O_3 catalysts were successfully synthesized with a high dispersion of active metals over the catalyst surface. The presence of Re in bimetallic Re-Ni/Al_2O_3 catalyst caused the beneficial effect by significantly promoting the ESR reactivity from the suppression of CO formation during the reaction thus, increases the selectivity towards CO_2 and H_2. It is suggested that, during reaction, the NiO particles on the Al_2O_3 support are stabilized and the sintering process is effectively suppressed by the incorporation of Re. Moreover, the additional of a small amount of Re could facilitate the water dissociation resulting in higher WGS reactivity as well as promoting long-term stability with up to 60 h without any deactivation observed. It could be concluded that, with sufficient NiO sites, the collaborative effect of Ni–Re, and brilliant stability contribute to the excellent catalytic performance of Ni–Re/Al_2O_3 catalysts for the steam reforming of ethanol.

Acknowledgements: The financial support from Office of National Higher Education Science Research and Innovation Policy Council, Program Management Unit for Human Resources & Institutional Development, Research and Innovation (PMU-B) (Network Strengthening Fund) is gratefully acknowledged. The authors also would like to acknowledge the Research Chair Grant supported by the National Science and Technology Development Agency (NSTDA).

References

Abdalla, A. M., S. Hossain, O. B. Nisfindy, A. T. Azad, M. Dawood and A. K. Azad (2018). "Hydrogen production, storage, transportation and key challenges with applications: A review." *Energy Conversion and Management* 165: 602-627.

Ahmad, T. and D. Zhang (2020). "A critical review of comparative global historical energy consumption and future demand: The story told so far." *Energy Reports* 6: 1973-1991.

Andraos, S., R. Abbas-Ghaleb, D. Chlala, A. Vita, C. Italiano, M. Laganà, L. Pino, M. Nakhl and S. Specchia (2019). "Production of hydrogen by methane dry reforming over ruthenium-nickel based catalysts deposited on Al2O3, MgAl2O4, and YSZ." *International Journal of Hydrogen Energy* 44(47): 25706-25716.

Baranowska, K., J. Okal and N. Miniajluk (2014). "Effect of Rhenium on Ruthenium Dispersion in the Ru–Re/γ-Al2O3 Catalysts." *Catalysis Letters* 144(3): 447-459.

Comas, J., F. Mariño, M. Laborde and N. Amadeo (2004). "Bio-Ethanol Steam Reforming on Ni/Al2O3 Catalyst." *Chemical Engineering Journal* 98: 61-68.

Contreras, J. L., J. Salmones, J. A. Colín-Luna, L. Nuño, B. Quintana, I. Córdova, B. Zeifert, C. Tapia and G. A. Fuentes (2014). "Catalysts for H2 production using the ethanol steam reforming (a review)." *International Journal of Hydrogen Energy* 39(33): 18835-18853.

de la Peña O'Shea, V. A., R. Nafria, P. Ramírez de la Piscina and N. Homs (2008). "Development of robust Co-based catalysts for the selective H2-production by ethanol steam-reforming. The Fe-promoter effect." *International Journal of Hydrogen Energy* 33(13): 3601-3606.

Dömök, M., K. Baán, T. Kecskés and A. Erdőhelyi (2008). "Promoting Mechanism of Potassium in the Reforming of Ethanol on Pt/Al2O3 Catalyst." *Catalysis Letters* 126(1): 49-57.

Fatsikostas, A. N., D. I. Kondarides and X. E. Verykios (2002). "Production of hydrogen for fuel cells by reformation of biomass-derived ethanol." *Catalysis Today* 75(1): 145-155.

Kunkes, E., D. Simonetti, J. Dumesic, W. Pyrz, L. Murillo, J. Chen and D. Buttrey (2008). "The Role of Rhenium in the Conversion of Glycerol to Synthesis Gas Over Carbon Supported Platinum-Rhenium Catalysts." *Journal of Catalysis* 260: 164-177.

Mathure, P. V., S. Ganguly, A. V. Patwardhan and R. K. Saha (2007). "Steam reforming of ethanol using a commercial nickel-based catalyst." *Industrial and Engineering Chemistry Research* 46(25): 8471-8479.

Mazloomi, K. and C. Gomes (2012). "Hydrogen as an energy carrier: Prospects and challenges." *Renewable and Sustainable Energy Reviews* 16(5): 3024-3033.

Palma, V., F. Castaldo, P. Ciambelli and G. Iaquaniello (2014). "CeO2-supported Pt/Ni catalyst for the renewable and clean H2 production via ethanol steam reforming." *Applied Catalysis B: Environmental* 145: 73-84.

Pongsiriyakul, K., W. Kiatkittipong, S. Adhikari, J. W. Lim, S. S. Lam, K. Kiatkittipong, A. Dankeaw, P. Reubroycharoen, N. Laosiripojana, K. Faungnawakij and S. Assabumrungrat (2021). "Effective Cu/Re promoted Ni-supported γ-Al2O3 catalyst for upgrading algae bio-crude oil produced by hydrothermal liquefaction." *Fuel Processing Technology* 216: 106670.

Profeti, L. P. R., J. A. C. Dias, J. M. Assaf and E. M. Assaf (2009). "Hydrogen production by steam reforming of ethanol over Ni-based catalysts promoted with noble metals." *Journal of Power Sources* 190(2): 525-533.

Sehested, J. (2006). "Four challenges for nickel steam-reforming catalysts." *Catalysis Today* 111(1-2): 103-110.

Zanchet, D., J. B. O. Santos, S. Damyanova, J. M. R. Gallo and J. M. C. Bueno (2015). "Toward Understanding Metal-Catalyzed Ethanol Reforming." *ACS Catalysis* 5(6): 3841-3863.

6th International Conference and
Postgraduate Colloquium for
Environmental Research 2022 (POCER
2022) 9 - 11 June 2022
Langkawi, Kedah, Malaysia

PCR30052022 – 268: Response Surface Methodology and Docking Simulation for Optimization of MCPA Removal onto MIL-101(Cr) Metal-organic Framework

Hamza Ahmad Isiyaka[a,b], Khairulazhar Jumbri[a,b*], and Nonni Soraya Sambudi[c]

[a] Department of Fundamental and Applied Sciences
Universiti Teknologi PETRONAS, 32610 Seri Iskandar, Perak, Malaysia

[b] **Centre of Research in Ionic Liquid, (CORIL), Institute of Contaminant Management, Universiti Teknologi PETRONAS,** 32610 Seri Iskandar, Perak, Malaysia

[c] **Department of Chemical Engineering**
Universiti Teknologi PETRONAS, 32610 Seri Iskandar, Perak, Malaysia
Corrensponsing Author E-mail: khairulazhar.jumbri@utp.edu.my

Abstract

Pollutant of emerging concerned such as 4-chloro-2-methylphenoxyacetic acid (MCPA) is carcinogenic, recalcitrant and persistent herbicide in the environment. Efficient removal, optimization and the binding interaction by metal-organic framework (MOF), response surface methodology (RSM) and molecular docking simulation are presented. The MOF was characterized using Fourier transformed infrared spectroscopy (FTIR) before and after adsorption. The FTIR show that the MOF maintained a stable crystalline after adsorption. The MIL-101(Cr) show high adsorption capacity and efficiency of 233.576 mg/g and 97.05% within 25 minutes of equilibration time at optimized conditions due to the porous nature of the MOF. The RSM provided minimum number of significant experimental runs using 3D graphical representations. The binding orientation and affinity of the MCPA and MOF show that the molecule is better adsorbed within the internal pore of the MOF. The findings show that the MIL-101(Cr) form a stable complex and good selectivity with the MCPA molecule and the experimental design can be used for efficient wastewater treatment process.

Keywords: Pollution Control; Optimization; Modelling; Adsorption; Metal-organic framework Response surface methodology.

1. Fourier transformed infrared spectroscopy (FTIR)

Figure 1 describe the FTIR spectra for MIL-101(Cr) before and after adsorption of MCPA

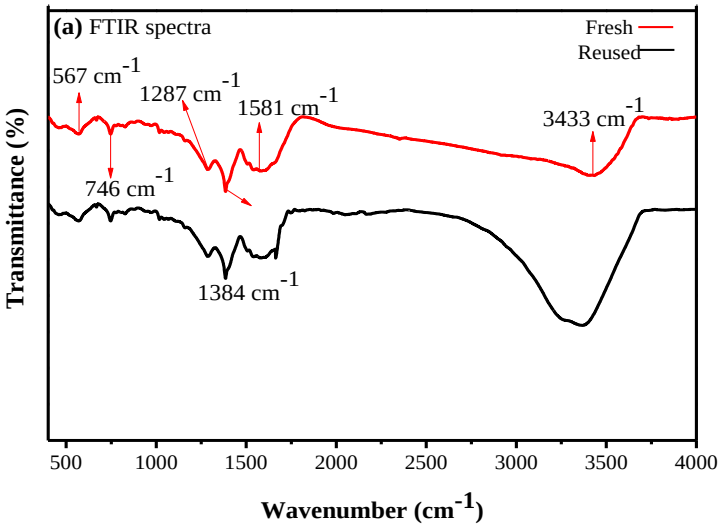

Figure 1: FTIR Spectra of MIL-101(Cr) before and after adsorption

The broad peaks at 3433/3367 cm^{-1} (Figure 1) is attributed to the stretching vibrations of OH group due to the presence of residual water molecules in the MOFs (Gao et al., 2018). The existence of intense peaks at 1621 cm^{-1} and 1581 cm^{-1} denotes the C=O and C-O stretching of the terephthalic acid in the MOFs (Liu et al., 2013).

2. 3D interactive surface plot

The MCPA adsorption by MIL-101(Cr) is described by the 3D graph showing the simultanous interaction of all parameters at a time. The curvatures of the plot (Figure 2(a)) depict the presence of multivariate interaction during the adsorption process. The optimized condition for the efficient adsorption capacity were gotten at contact time ~ 25 minutes, initial concentration 50 mg/L, adsorbent dosage 20 mg, pH 4 and temperature 40°C. The contour lines that show points of identical responses in two dimensional planes are presented in Figure 2(b)

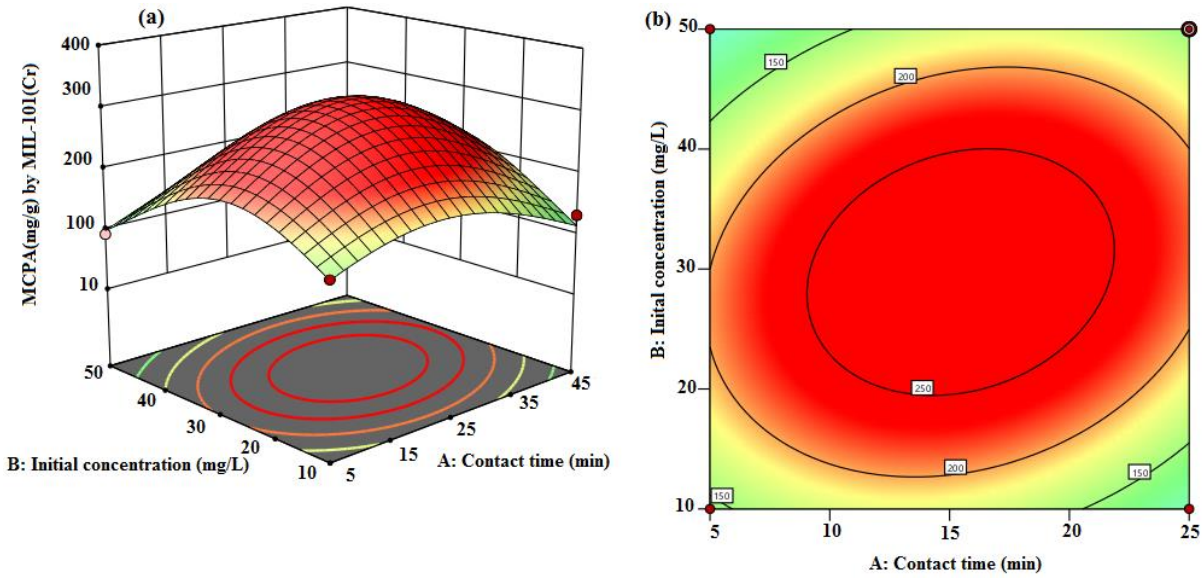

Figure 2: (a) 3D interactive plot (b) contour lines showing optimum adsorption capacity

Acknowledgements: The authors thank the Ministry of Science, Technology and Innovation and the Universiti Teknology Petronas for the FRGS (015MA0-127) research grant.

References

Gao, Y., Liu, K., Kang, R., Xia, J., Yu, G., Deng, S., 2018. A comparative study of rigid and flexible MOFs for the adsorption of pharmaceuticals: Kinetics, isotherms and mechanisms. J. Hazard. Mater. 359, 248–257. https://doi.org/10.1016/j.jhazmat.2018.07.054

Liu, Q., Ning, L., Zheng, S., Tao, M., Shi, Y., He, Y., 2013. Adsorption of Carbon Dioxide by MIL-101(Cr): Regeneration conditions and influence of flue gas contaminants. Sci. Rep. 3, 1–6. https://doi.org/10.1038/srep02916

6th International Conference and
Postgraduate Colloquium for
Environmental Research 2022 (POCER
2022) 9 - 11 June 2022
Langkawi, Kedah, Malaysia

PCR31052022 – 269: Structural, Electrical and Magnetic Properties in $Pr_{0.67}Ba_{0.33}MnO_3$

Asmira Amaran[a], and Zakiah Mohamed[a*]

[a] Faculty of Applied Sciences
University Teknology MARA,UiTM, Selangor, Malaysia

- Corrensponsing Author E-mail: zakiah626@uitm.edu.my

Keywords: X-ray, perovskite manganite, structural, electrical, magnetic

Extended Abstract

We report here the results of structural, electrical and magnetic properties in the $Pr_{0.67}Ba_{0.33}MnO_3$ (PBMO) perovskite manganite which was prepared by solid state method. Structural, morphology and chemical composition were examined by x-ray diffraction, rietveld structure refinement, scanning electron microscopy and EDX analyses. The compound exhibit a single phase with orthorhombic perovskite structure with Pnma space group without any impurities. In addition, fourier transform infrared spectroscopy (FTIR) reveals that the Mn-O bonds appear at 600 cm^{-1}. Electrical resistivity measurements showed a transition from metallic behavior to insulating behavior with two peaks of metal-insulator at T_{p1}=193 K and T_{p2}=158 K as the temperature was increased. In addition, magnetic susceptibility versus temperature measurements showed ferromagnetic (FM) to paramagnetic (PM) transition with Curie temperature, T_C=212 K.

6th International Conference and
Postgraduate Colloquium for
Environmental Research 2022 (POCER
2022) 9 - 11 June 2022
Langkawi, Kedah, Malaysia

PCR31052022 – 270: Structural, Optical and Electronic Studies of Sr_2NiTeO_6 and Sr_2ZnTeO_6 Double Perovskite by Experimental and First-Principle DFT–LDA+U Calculation

F.I.H. Alias[a], M.H. Ridzwan[a], M.K. Yaakob[a], C. W. Loy[b] and Z. Mohamed[a*]

[a] Faculty of Applied Sciences
Universiti Teknologi MARA, 40450 Shah Alam, Selangor, Malaysia

[b] ARC Training Centre for Automated Manufacture of Advanced Composites
University of New South Wales, Sydney NSW 2052 Australia

- Corrensponsing Author E-mail: zakiah626@uitm.edu.my

Keywords: Double perovskite; Density functional theory; Electronic band structure; Hubbard U; Absorbance

Abstract

The structural, electronic and optical properties of Sr_2NiTeO_6 and Sr_2ZnTeO_6 double perovskites have been studied using combined experimental and first principle approaches. X-ray diffraction patterns showed that both samples were crystallized in monoclinic symmetry with *I*2/*m* space group. Rietveld refinement analysis revealed that the unit cell volume were higher in Zn-substitution structure. The morphological scanning electron microscopy reported that the grain sizes decreased as Zn was present in the structure. The UV-vis diffuse reflectance spectroscopy conducted for both samples found that the optical band gap energy, E_g, for Sr_2NiTeO_6 and Sr_2ZnTeO_6 were 3.71 and 4.14 eV, respectively, where the range of E_g is classified as wide band gap semiconductor. For first principles calculation, the Hubbard U parameter for the treatment of highly strong Coulomb repulsion among electrons in 3d/4f orbitals was included in LDA+U functional. The U values were set at 8 eV at Ni 3d orbital only. The calculated crystal volume structures for Sr_2NiTeO_6 and Sr_2ZnTeO_6 samples were 247.813 and 247.841 $Å^3$, respectively, which consistent with the XRD data, the calculated crystal volume higher for Zn substitution. Besides, the calculated electronic band structure reported that the electronic E_g were 1.723 and 0.757 eV for Sr_2NiTeO_6 and Sr_2ZnTeO_6, respectively. The electronic properties were further investigated by density of states of Sr_2NiTeO_6 and Sr_2ZnTeO_6 double perovskite compound and showed

that there was a significant effect on hybridization of Ni 3d and O 2p states at the conduction and valence band, respectively.

6th International Conference and Postgraduate Colloquium for Environmental Research 2022 (POCER 2022) 9 - 11 June 2022
Langkawi, Kedah, Malaysia

PCR31052022 – 271: Investigating the magnetic structures of LiM1-xZnxPO4 (M= Fe, Mn) cathode materials for lithium-ion batteries by neutron powder diffraction Preparation

Z. Mohamed[a*], and Chris. D Ling[b]

[a] Faculty of Applied Sciences
Universiti Teknologi MARA, 40450 Shah Alam, Selangor, Malaysia

[b] School of Chemistry,
University of Sydney, NSW2006, Sydney, Australia

- Corrensponsing Author E-mail: zakiah626@uitm.edu.my

Keywords: Magnetic; Cathode Materials; Neutron Powder Diffraction.

Abstract

A series of Li$M_{1-x}Zn_xPO_4$ (M= Fe, Mn) compounds with x= 0, 0.1 and 0.2 for lithium-ion batteries have been synthesized by solid state reaction and their structures have been characterized using XRD, NPD and magnetic susceptibility measurement. All samples are single phase and indexed to an orthorhombic structure with *Pnma* space group. The unit cell volume decreased with increasing substitution of Zn^{2+} ranging between 291.391 $Å^3$ to 293.136 $Å^3$ for Li$Fe_{1-x}Zn_xPO_4$ and 300.727 $Å^3$ to 304.503 $Å^3$ for Li$Mn_{1-x}Zn_xPO_4$. The magnetic susceptibility measurements show that the $1/\chi_m$-χ_o decreases corresponding to the influence of non-magnetic Zn^{2+} doped in M-site. All samples exhibit AFM ordering below the T_N which decreased at higher Zn^{2+} doping. The magnetic structures of Li$Fe_{1-x}Zn_xPO_4$ and Li$Mn_{1-x}Zn_xPO_4$ compounds were characterized using propagation vector k= (0 0 0) indexed with *Pnma'* and *Pn'm'a'* space groups, similar to magnetic structures of undoped samples.

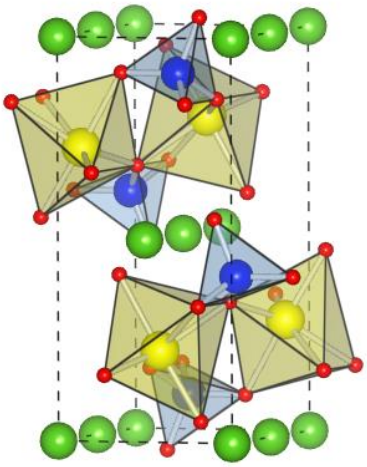

Figure 55: Structure of olivine type $LiFePO_4$ viewed along the *b*-axis. The FeO_6 octahedra are show in yellow colour , PO_4 tetrahedra in blue colour, Li atoms in green and O atoms in red.

References

[1] K. Kim, Y.-H. Cho, D. Kam, H.-S. Kim, J.-W. Lee, Journal of Alloys and Compounds, 504 (2010) 166-170.

[2] M. Gaberscek, R. Dominko, M. Bele, M. Remskar, D. Hanzel, J. Jamnik, Solid State Ionics, 176 (2005) 1801-1805.

[3] K.S. Park, K.T. Kang, S.B. Lee, G.Y. Kim, Y.J. Park, H.G. Kim, Materials Research Bulletin, 39 (2004) 1803-1810.

[4] S.Y. Chung, J.T. Bloking, Y.M. Chiang, Nature materials, 1 (2002) 123-128.

[5] Y. Wang, Z. Liu, S. Zhou, Electrochimica Acta, 58 (2011) 359-363.

[6] L. Chen, Y.-Q. Yuan, X. Feng, M.-W. Li, Journal of Power Sources, 214 (2012) 344-350.

[7] S.T. Song, P.H. Ma, S.Y. Li, X.C. Deng, C.Y. Yan, Chinese Chemical Letters, 19 (2008) 337-341.

[8] Y.C. Yourong Wang, Siqing Cheng, and Liangnian He, Korean J.Chem. Eng, 28(3) (2011) 964-968.

6th International Conference and
Postgraduate Colloquium for
Environmental Research 2022 (POCER
2022) 9 - 11 June 2022
Langkawi, Kedah, Malaysia

PCR31052022 – 272: Synthesis and Study on the Effect of Ca^{2+} Doping on the Structural, Optical and Dielectric Properties of Tungstate Based Double Perovskite $Sr_{2-x}Ca_xNiWO_6$

Nur Amira Farhana Mohamed Saadon[a] and Zakiah Mohamed[a*]

[a] Faculty of Applied Sciences
Universiti Teknologi MARA, 40450, Shah Alam, Selangor, Malaysia

- Corrensponsing Author E-mail: zakiah626@uitm.edu.my

Keywords: Double Perovskite; Structural; Optical; Dielectric

Extended Abstract

In this paper, $Sr_{2-x}Ca_xNiWO_6$ (x=0, 0.02, 0.04, 0.06) were synthesized using a solid state reaction method and the crystal structure, optical and dielectric properties of the compounds were studied using X-ray diffraction (XRD), UV-vis diffuse reflectance spectroscopy (UV-vis) and electrochemical impedance spectroscopy (EIS) respectively. The Rietveld refinement of XRD confirmed that the compounds crystallized in a tetragonal structure with a space group I4/m. The UV-Vis analysis revealed that the band gap energy of the compounds decreased from 3.17 to 3.13 eV as the amount of doping increased from x=0 to x=0.06. The dielectric characterization showed that the dielectric constant (ε') and dielectric loss (tan δ) for all compounds possessed a similar trend where it was higher in low frequency area (~1 Hz) and dropped instantaneously with the enhancement of frequency up to 1 MHz until it reached constant values. The increase in ε' values from ~550 to ~845 from x=0 to x=0.06 could be attributed to the decrease in crystallite size of the compounds. In addition, compound with x=0.06 exhibited the lowest dielectric loss at low frequency region approximately at 6.

6th International Conference and
Postgraduate Colloquium for
Environmental Research 2022 (POCER
2022) 9 - 11 June 2022
Langkawi, Kedah, Malaysia

PCR31052022 – 273: Influence of Ag Substitution on Electrical Properties of $NdMnO_3$

Nurul Atiqah Azhar[a] and Zakiah Mohamed[a]

[a] Faculty of Applied Sciences

University Teknologi MARA (UiTM) Shah Alam, Selangor, Malaysia

- Corrensponsing Author E-mail: zakiah626@uitm.edu.my

Keywords: electrical properties, manganite, resistivity, x-ray diffraction

Extended Abstract

Pure and Ag-doped $NdMnO_3$ were synthesized using the conventional solid-state reaction route to investigate the structural and electrical properties of both samples. The crystal structural, morphological, and optical properties of both samples were determined using X-ray diffraction (XRD), Fourier Transform Infrared spectroscopy (FTIR), and four-point probe. The Rietveld refinement showed that the compounds crystallized in orthorhombic structure, with the decrease in volume from 233.50 (x = 0) to 231.03 (x = 0.3) with the increase of lattice parameter b from 5.56 to 5.69, respectively. FTIR spectra showed that absorption bands were located within the range of 580 - 600 cm−1, which corresponded to the Mn–O stretching vibration. The resistivity curve shows a decrease when Ag was doped into the sample. Under external magnetic field of 0.8 T, the value of resistivity of undoped sample decrease, while the value of resistivity of doped sample remains unchanged. The insulator region of the resistivity curves was fitted well using variable range hopping (VRH) and small polaron hopping (SPH) models. The hopping distance, R_h and energy hopping, E_h at 150 K were decrease due to the distortion of the MnO_6. Other than that, the values of activation energy, E_a decrease as Ag was doped, and when external magnetic were applied, indicating that the delocalization of charge carrier was increased for this system.

Acknowledgements: The authors would like to thank the Faculty of Applied Sciences, Universiti Teknologi MARA for XRD, FTIR,and 4 point-probe measurements. This research was financially supported by the Ministry of Education Malaysia (MOE) and Universiti Teknologi MARA, grant number 600-RMC/YTR/5/3 (008/2020).